

*Samarkand State University named after Sharof Rashidov*



**Samarkand International  
Symposium on Magnetism**

**2 – 6 July, 2023**

**BOOK OF  
ABSTRACTS**  
of  
Samarkand International  
Symposium on Magnetism  
**SISM-2023**

**Samarkand, Uzbekistan  
2023**

*Samarkand State University named after Sharof Rashidov*



**Samarkand  
International Symposium  
on Magnetism**

**2 – 6 July, 2023**

# Book of Abstracts

## **Main Topics**

Spintronics, Magnonics, Magnetotransport  
Magnetophotonics (linear and nonlinear magneto-optics, magnetophotonic crystals)  
High Frequency Properties and Metamaterials  
Diluted Magnetic Semiconductors and Oxides  
Magnetic Nanostructures and Low Dimensional Magnetism  
Magnetic Soft Matter (magnetic polymers, complex magnetic fluids and suspensions)  
Soft and Hard Magnetic Materials  
Magnetic Shape-Memory Alloys and Magnetocaloric Effect  
Multiferroics  
Topological Insulators  
Magnetism and Superconductivity  
Theory  
Magnetism in Biology and Medicine  
Miscellaneous

**Samarkand 2023**

УДК 537.6  
ББК 22.334

ISBN: 978-5-00202-320-2

**Samarkand International Symposium on Magnetism**  
**2 – 6 July 2023, Samarkand**

**Book of Abstracts**

The text of abstracts is printed from original contributions.

**Editors:** N. Perov  
A. Granovsky  
A. Kharlamova  
L. Makarova  
Yu. Alekhina

© SISM – 2023

**Organizing Committee**

## Chairman of the National organizing committee:

R. I. Xalmuradov – *Rector of Samarkand State University  
named after Sharof Rashidov*

**Chairmen:** A. Granovsky  
N. Perov

**Scientific  
secretaries:** M. Salakhitdinova  
Yu. Alekhina

## International Advisory Committee

S. Caprara	<i>Italy</i>	S. Ovchinnikov	<i>Russia</i>
M. Farle	<i>Germany</i>	S. Parkin	<i>Germany</i>
D. Fiorani	<i>Italy</i>	R. Pisarev	<i>Russia</i>
E. Hristoforou	<i>Greece</i>	Th. Rasing	<i>Netherlands</i>
M. Inoue	<i>Japan</i>	K.-H. Shin	<i>South Korea</i>
S. Keshri	<i>India</i>	V. Ustinov	<i>Russia</i>
N. Mushnikov	<i>Russia</i>	M. Vazquez	<i>Spain</i>
S. Nikitov	<i>Russia</i>	A. Vedyayev	<i>Russia</i>
A. Nugroho	<i>Indonesia</i>	A. Zvezdin	<i>Russia</i>

## National Advisory Committee

*Chairman:*

R. I. Xalmuradov – *Rector of Samarkand State University named after Sharof  
Rashidov*

H. Khushvaktov – *Vice rector for scientific works and innovations of Samarkand  
State University named after Sharof Rashidov*

A. Akhatov – *Vice rector for international cooperation of Samarkand State  
University named after Sharof Rashidov*

A. Yarmukhamedov – *Director of Engineering Physics Institute of Samarkand State  
University named after Sharof Rashidov*

- R. Rajabov – *Head of General Physics department of Engineering Physics Institute of Samarkand State University named after Sharof Rashidov*
- O. Kuvandikov – *Professor at Engineering Physics Institute of Samarkand State University named after Sharof Rashidov:*
- K. Mukimov – *National University of Uzbekistan*
- U. Valiev – *National University of Uzbekistan*
- E. Ibragimova – *Institute of Nuclear Physics Academy of Science Republic of Uzbekistan*
- M. Sharipov – *Bukhara institute of engineering and technology*
- D. Djuraev – *Bukhara state university*
- U. Usarov – *Samarkand Architectural and Construction Institute*
- A. Eshkulov – *Tashkent State Technical University*

## **Program Committee**

*Chairman:* A. Granovsky

*Vice Chairman:* A. Kimel

*Vice Chairman:* A. Pyatakov

*Secretaries:* M. Salakhitdinova, Yu. Alekhina

B. Aronzon	<i>Moscow</i>	K. Rozanov	<i>Moscow</i>
N. Bebenin	<i>Yekaterinburg</i>	A. Semisalova	<i>Diusburg</i>
V. Belotelov	<i>Moscow</i>	V. Shavrov	<i>Moscow</i>
E. Ibragimova	<i>Tashkent</i>	S. Streltsov	<i>Krasnoyarsk</i>
A. Kalashnikova	<i>Saint-Petersburge</i>	A. Smirnov	<i>Moscow</i>
V. Khovailo	<i>Moscow</i>	L. Tagirov	<i>Kazan</i>
A. Kirilyuk	<i>Nijmegen</i>	U. Usarov	<i>Samarkand</i>
V. Koledov	<i>Moscow</i>	A. Vasiliev	<i>Moscow</i>
G. Kurlyandskaya	<i>Yekaterinburg</i>	A. Vinogradov	<i>Moscow</i>
O. Kuvandikov	<i>Samarkand</i>	A. Zhukov	<i>San Sebastian</i>
K. Mukimov	<i>Tashkent</i>	M. Zhuravlev	<i>Moscow</i>
A. Murtazaev	<i>Makhachkala</i>	K. Zvezdin	<i>Moscow</i>
L. Panina	<i>Moscow</i>		
Yu. Pastushenkov	<i>Tver</i>		
N. Pugach	<i>Moscow</i>		
Yu. Raikher	<i>Perm</i>		
V. Rodionova	<i>Kaliningrad</i>		

## Local Committee

*Chairmen:* O. Kuvandikov, M. Salakhitdinova, A. Granovsky

E. Arzikulov	N. Hamraev	D. Imamnazarov	B. Amonov
I. Subkhankulov	S. Akhrorov	Z. Shodiev	G. Sharipov
Z. Mirtoshev	S. Eshmamatov	Z. Ruzimuradov	R. Eshburiev
N. Eshkobilov			
K. Abdurakhmanova	A. Kharlamova	R. Makarin	Z. Rakhmonov
J. Akhtamov	K. Khasanov	L. Makarova	B. Shamsiev
Yu. Alekhna	B. Khayrullaev	U. Mardonov	K. Shermatova
R. Berdiev	E. Khudaigulova	U. Mayinova	E. Shipkova
Y. Dzhuraev	A. Komlev	F. Nazarov	M. Toshboev
S. Eshkuvatov	G. Kulmatova	A. Norkulov	R. Usanov
N. Khamraeva	Y. Kushbakova	N. Perova	K. Zoirova

## CONTENT

<b>JULY 2</b> .....	<b>6</b>
PLENARY LECTURES .....	6
ORAL SESSIONS I .....	9
<i>Spintronics and magnetotransport</i> .....	9
<i>Soft and Hard Magnetic Materials</i> .....	13
<i>Topological Insulators</i> .....	17
ORAL SESSIONS II .....	21
<i>Magnetic Soft Matter (magnetic polymers, complex magnetic fluids and suspensions)</i> .....	21
<i>Heusler Alloys and Phase Transitions</i> .....	29
<i>Theory</i> .....	37
POSTER SESSIONS .....	44
<i>Spintronics and Magnetotransport</i> .....	44
<i>Soft and Hard Magnetic Materials</i> .....	68
<i>Magnetic Soft Matter, Magnetism in Biology and Medicine</i> .....	85
<i>Magnetic Nanostructures and Low Dimensional Magnetism</i> .....	97
<b>JULY 3</b> .....	<b>125</b>
PLENARY LECTURES .....	125
ORAL SESSIONS I .....	128
<i>Magnonics</i> .....	128
<i>Magnetophotonics</i> .....	133
<i>Magnetism and Superconductivity</i> .....	137
ORAL SESSIONS II .....	141
<i>Spintronics and Magnetotransport</i> .....	141
<i>Magnetophotonics</i> .....	148
<i>Magnetism and Superconductivity</i> .....	155
POSTER SESSIONS .....	162
<i>Magnetophotonics</i> .....	162
<i>Magnetic Shape Memory Alloys and Magnetocaloric Effect</i> .....	175
<i>Magnetism and Superconductivity</i> .....	186
<i>Multiferroics</i> .....	192
<i>Diluted Magnetic Semiconductors and Oxides</i> .....	201
<i>Magnetic materials. High Frequency Properties</i> .....	215
<i>Miscellaneous</i> .....	225
<b>JULY 4</b> .....	<b>236</b>
PLENARY LECTURES .....	236
ORAL SESSIONS I .....	240
<i>Spintronics and magnetotransport</i> .....	240
<i>Magnetic Nanostructures and Low Dimensional Magnetism</i> .....	246
<i>Magnetism in Biology and Medicine</i> .....	251
ORAL SESSIONS II .....	256
<i>Magnetic Soft Matter (magnetic polymers, complex magnetic fluids and suspensions)</i> .....	256
<i>Magnetic Nanostructures and Low Dimensional Magnetism</i> .....	263
<i>Magnetic Materials. High Frequency Properties</i> .....	270
<b>JULY 5</b> .....	<b>277</b>
PLENARY LECTURES .....	277
ORAL SESSIONS I .....	280
<i>Magnetic Nanostructures and Low Dimensional Magnetism</i> .....	280
<i>Magnetism and Superconductivity</i> .....	289
<i>Multiferroics</i> .....	296
<i>Soft and Hard Magnetic Materials</i> .....	302
ORAL SESSIONS II .....	311
<i>Miscellaneous</i> .....	311
<i>Magnetism and Superconductivity</i> .....	318
<i>Multiferroics</i> .....	324
<b>AUTHOR INDEX</b> .....	<b>328</b>

July 2

9:15 - 10:45

Sunday

PLENARY  
LECTURES

## CHIRAL SPINTRONICS

*Parkin S.S.P.*

Max Planck Institute of Microstructure Physics, Halle (Saale), Germany  
stuart.parkin@mpi-halle.mpg.de

Spintronics is a field of research that harnesses the electron's spin to create novel materials with exotic properties and devices especially those for storing digital data that is the lifeblood of many of the most valuable companies today. Spintronics has already had two major technological successes with the invention and application of spin-valve magnetic field sensors that allowed for more than a thousand-fold increase in the storage capacity of magnetic disk drives that store ~70% of all digital data today. Just recently, after almost a 25-year exploration and development period, a high performance nonvolatile Magnetic Random Access Memory, that uses magnetic tunnel junction memory elements, became commercially available. A novel spintronics memory-storage technology, Magnetic Racetrack Memory is on track to become the third major success of spintronics. Racetrack Memory is a novel, non-volatile memory in which data is encoded in mobile chiral domain walls that are moved at high speeds by current induced spin-orbit torques to and thro along synthetic antiferromagnetic racetracks. Chiral domain walls are just one member of an ever-expanding family of nano-scopic chiral spin textures that are of great interest from both a fundamental as well as a technological perspective. A zoology of complex spin textures have been discovered including, anti-skyrmions, elliptical Bloch skyrmions, two-dimensional Néel skyrmions, and fractional anti-skyrmions. Finally, I will discuss some of our recent work in superconducting spintronics that could lead to a very low energy-consuming cryogenic racetrack memory that is needed for advanced quantum computing systems.

## ULTRAFAST OPTO-MAGNONICS IN THE CENTER AND AT THE EDGE OF THE BRILLOUIN ZONE

*Kalashnikova A.M.*

Ioffe Institute, St. Petersburg, Russia  
kalashnikova@mail.ioffe.ru

Magnonics studies generation, propagation, control, and detection of spin waves, as well as the corresponding media and structures for efficient spin wave transducers, waveguides etc. Magnon wavelengths range from tens of microns to nanometers, while their frequencies range from giga- to terahertz, and their propagation can proceed without accompanying Joule losses. Therefore, magnonics is considered as a promising direction for development of a component base for fast, miniature and energy-efficient information processing devices [1]. However, magnonics faces several challenges, including fundamental ones. Among them are the problem of generating waves with large wave vectors and frequencies, the problem of controlling their propagation, and the problem of compatibility of magnonic elements with components of electronics or photonics.

In this talk, we show how femtosecond laser pulses can facilitate development of magnonics by tackling some of these challenges. We present a brief overview of femtomagnetic phenomena [2] leading to the generation of spin waves, discuss limitations for their frequencies and wavevectors [3], and show how features of the interaction of short laser pulses with magnetic materials can be used to control the properties of spin waves [4].

Specifically, we consider laser-induced generation of magnetostatic waves in anisotropic magnetic metals [3-5] - spin waves near the centre of the Brillouin zone, which are already used in magnonics as information carriers. We also suggest implementation of a tuneable source of magnetostatic packets [6] and of waves with unidirectional propagation [7].

We also consider the laser-induced excitation of coherent two-magnon modes characterized with highest possible wavevectors and frequencies at the edge of the Brillouin zone. We analyse how such excitation is related to the ultrafast control of the exchange interaction [8,9]. We show in particular that such spin dynamics, although not manifested as macroscopic magnetization dynamics, can be detected optically. This raises an interesting question on the possibility of using such spin excitations at the edge of the Brillouin zone for ultrafast information processing.

Author is extremely grateful to the members of the Ferroics Physics Laboratory at Ioffe Institute for fruitful collaboration. Support by RFBR grant No. 19-52-12065 is acknowledged.

- [1] A. Barman et al., *J. Phys.: Condens. Matter*, **33** (2021) 413001.
- [2] N. E. Khokhlov et al., *Tech. Phys. Lett.*, **67** (2022) 2335.
- [3] N. E. Khokhlov et al., *Phys. Rev. Appl.*, **12** (2019) 044044.
- [4] Ia. A. Filatov et al., *Appl. Phys. Lett.*, **120** (2022) 112404.
- [5] L. A. Shelukhin et al., *Phys. Rev. Appl.*, **14** (2020) 034061.
- [6] N. E. Khokhlov et al., *J. Magn. Magn. Mater.*, **534** (2021) 168018.
- [7] P. I. Gerevenkov et al., *Phys. Rev. Appl.*, **19** (2023) 024062.
- [8] A. E. Fedianin et al., *Phys. Rev. Appl.*, **107** (2023) 144430.
- [9] F. Formisano et al., arXiv:2303.06996.

**July 2**

11:15 - 12:30

Sunday

ORAL  
SESSIONS I

Section A

**Spintronics and  
magnetotransport**

2IT-A-1

**SPIN-TO-CHARGE CONVERSION IN Ag/Bi BILAYER REVISITED***Jin X.*

Fudan university, Shanghai, China

xfjin@fudan.edu.cn

The spin-to-charge conversion of the Ag/Bi interface is studied in a device in which a spin current can be injected from either side selectively. The charge voltages generated by the two counterpropagating spin currents show opposite signs, that is consistent with the inverse spin Hall effect rather than the well accepted inverse Rashba-Eldestein effect in the Ag/Bi bilayer. Femtosecond laser is further employed to generate the spin-current-induced terahertz signal in a Ag/Bi bilayer, which shows no evidence for the inverse Rashba-Eldestein effect, either. This work provides a clear-cut method to identify the spin-to-charge mechanism in a Rashba electronic state and delivers new understanding for the relevant spin-transport phenomena.

## CHIRAL MAGNETS WITH DZYALOSHINSKII-MORIYA INTERACTION

*Laliena V.<sup>1</sup>, Campo J.<sup>2</sup>*

<sup>1</sup> Department of Applied Mathematics, University of Zaragoza, Zaragoza, Spain

<sup>2</sup> Aragon Nanoscience and Materials Institute (CSIC-University of Zaragoza) and Condensed Matter Physics Department, University of Zaragoza, Zaragoza, Spain  
Javier.Campo@csic.es

Chiral magnets are very promising building blocks to design new spintronic devices since they can host magnetic textures protected by topology that can be controlled by magnetic fields or electric currents, which made of them excellent candidates for a new generation of a smart and more efficient spintronics. On the other hand, besides the applications to spintronics, chiral magnets are interesting from a fundamental point of view because the chiral symmetry, and its breaking and restoration, are ubiquitous phenomena appearing virtually in any domain of science, from particle physics to astrophysics, and including chemistry, biology, and geology.

The Dzyaloshinskii-Moriya (DM) interaction, present in non-centrosymmetric magnetic materials, often originates canted or helimagnetic structures depending on the DM vector ( $\sim D_{ij}$ ) and the dimensionality of the interactions. In helical monoaxial magnets, for which the strong magnetic anisotropies fix the helical axis along an unique crystallographic axis, several magnetic structures (chiral soliton lattices, helical, conical) can appear depending on the orientation of the applied magnetic field respect to the helical axis. In cubic DM magnets also skyrmionics phases have been found.

Here we will summarize several results obtained by our research group concerning the phase diagram of the monoaxial chiral helimagnet as a function of temperature  $T$  and magnetic field with components perpendicular ( $H_x$ ) and parallel ( $H_z$ ) to the chiral axis. Also, the stability of the skyrmion textures and the role of the thermal fluctuations in cubic helimagnets has been theoretically investigated by our group. It is show that a skyrmionic “A-phase” might exist as a stable, or metastable, state at low temperatures. We also predicted that a new state (“B-phase”), different from the typical hexagonal skyrmionic phase, might emerge in the low temperature region of the phase diagram.

This talk also will show that chiral solitons in monoaxial helimagnets can be stabilized with external magnetic fields. Once created, the soliton moves steadily in response to a polarized electric current, provided the induced spin-transfer torque has a dissipative (nonadiabatic) component. We show that using spin-polarized currents chiral solitons in the chiral soliton lattice can be pushed against each other and it is possible to annihilate the solitons one-by-one in a controlled way.

Finally, we will talk about our recent results concerning magnonics. It is a subject of much interest in recent years since it is a promising field that could transform the design of devices for information technology by replacing electric currents by spin waves as information carriers. Focusing on the isolated solitons of monoaxial helimagnets, it is shown that the spin waves scattered (reflected and transmitted) by the soliton suffer a lateral displacement analogous to the Goos-Hänchen effect of optics.

- [1] V. Laliena, J. Campo, Y. Kousaka, *Phys. Rev. B*, **95** (2017) 224410.
- [2] V. Laliena, J. Campo, *Phys. Rev. B*, **96** (2017) 134420.
- [3] V. Laliena, G. Albalate, J. Campo, *Phys. Rev. B*, **98** (2018) 224407.
- [4] V. Laliena, S. Bustingorry, J. Campo, *Sci. Rep.*, **10** (2020) 20430.
- [5] V. Laliena, J. Campo, *Adv. Electron. Mater.* **8(3)** (2021) 2100782.

## MAGNETIZATION DYNAMICS IN Co/IrMn AND Co/FeMn STRUCTURES

*Dzhan I.O.<sup>1</sup>, Chechenin N.G.<sup>1,2</sup>*

<sup>1</sup> SINP Lomonosov Moscow State University, Moscow, Russia

<sup>2</sup> Faculty of Physics, Lomonosov Moscow State University, Moscow, Russia  
nchechenin@yandex.ru

Exchange-biased ferromagnet (F)/antiferromagnet (AF) structures are of great interest due to their application in spintronic devices such as spin diodes based on the giant magnetic resistance effect. In the past few years, due to the discovery of the spin Hall effect in metallic AFs and spin transfer in some AFs, studies of the dynamics of magnetization in two-layer F/AF structures have again aroused interest. Here, the temperature dependence of the ferromagnetic resonance linewidth and the resonance field in two-layer Co/FeMn and Co/IrMn structures with an exchange bias have been studied. We present the results of studying the dynamics of magnetization by the ferromagnetic resonance (FMR) method in these binary structures. The main features of the dynamics of magnetization in F/AF samples at low temperatures are a decrease in the resonance field and a broadening of the FMR line, which characterizes the damping coefficient of spin precession.

It is shown that the free F-layer is characterized by a slight decrease in the resonance field by 25 Oe as the temperature decreases from 300 K to 115 K. At room temperature, the Co/IrMn and Co/FeMn samples are characterized by higher resonance fields than the free layer. As the temperature decreases, a sharp decrease in the resonance field is observed in the Co/IrMn sample, which is characterized by an insignificant anisotropy along and perpendicular to the easy magnetisation axis (EMA) of the sample. In the Co/FeMn sample, a sharply anisotropic temperature dependence of the resonant field is observed: in the direction along the field applied during the deposition of the sample, an insignificant decrease in the resonant field is observed with decreasing temperature, while in the antiparallel direction, a significant increase in the resonant field is observed.

It was observed that at room temperature, the width of the FMR line for the Co/IrMn and Co/FeMn samples is greater than for the free F layer, which may be a manifestation of negative rotational anisotropy [1]. With decreasing temperature, broadening of the FMR line is observed both for the free F layer and for the F/AF structures. In contrast to the shift of the resonant field, the broadening is isotropic over the entire temperature range studied, except for a temperature of 115 K, at which an anisotropy of the FMR linewidth is observed for the free Co layer and the Co/FeMn sample, which is explained in terms of the two-magnon scattering mechanism on structural defects of the F layer and small domains of the AF layer at the interface between the layers [2], the influence of which becomes more significant at low temperatures due to a decrease in surface anisotropy [3].

The temperature dependence of the magnetization dynamics of the free layer is described in terms of the slow relaxation process [4], while the additional contribution to the broadening of the FMR line and the shift of the resonant field for F/AF structures with decreasing temperature is caused by a combination of mechanisms for the inclusion of small grains and the mosaic structure of the AF structure.

[1] R. L. Rodríguez-Suarez et al., *J. Appl. Phys.*, **123** (2018) 043901.

[2] R.A. Gallardo, R.L. Rodríguez-Suarez, P. Landeros, *J. Appl. Phys.*, **120** (2016) 223904.

[3] M. Diaz de Sihues et al., *J. Magn. Magn. Matter*, **316** (2007) e462–e465.

[4] V. L. Safonov and H. N. Bertram, *J. Appl. Phys.*, **94** (2003) 529-538.

**July 2**

11:15 - 12:30

Sunday

ORAL  
SESSIONS I

Section B

**Soft and Hard  
Magnetic Materials**

## DEVELOPMENT OF AMORPHOUS MICROWIRES WITH GRADED MAGNETIC ANISOTROPY

*Zhukov A.*<sup>1,2,3,4</sup>, *Corte-Leon P.*<sup>1,2</sup>, *Blanco J. M.*<sup>2,3</sup>, *Ipatov M.*<sup>1,2</sup>, *Zbukova V.*<sup>1,2</sup>

<sup>1</sup> Dept. Polym. Adv. Mater., Univ. Basque Country, UPV/EHU, San Sebastian, Spain

<sup>2</sup> Dept. Appl. Phys., EIG, Univ. Basque Country, UPV/EHU, San Sebastian, Spain

<sup>3</sup> EHU Quantum Center, University of Basque Country, UPV/EHU, Spain

<sup>4</sup> IKERBASQUE, Basque Foundation for Science, Bilbao, Spain  
arkadi.joukov@ehu.es

Soft magnetic materials are demanded for numerous applications [1,2]. Magnetic softness is main interest for such applications, however the combination of mechanical properties (ductility, high tensile strength, elastic moduli, hardness...), corrosion resistance and size reduction are other important characteristics for industrial applications [2]. Studies of magnetic wires have attracted great interest owing to outstanding magnetic properties, like the giant magnetoimpedance (GMI) or the magnetic bistability and related single domain wall (DW) propagation. These properties make them quite attractive for a number of technological applications [1,2]. An important advantage of the glass-coated magnetic microwires prepared using the Taylor-Ulitovsky technology is that the wire diameter can be significantly reduced (an order of magnitude). Another advantages of such microwires are better corrosion resistance and mechanical properties. Therefore, such microwires are suitable for emerging applications including biomedicine, non-destructive control of external stimuli (stress, temperature) in smart composites, magnetic memories and logics, magnetic and magnetoelastic sensors or electronic surveillance [2,3].

Recently we observed that, the hysteresis loops Fe-rich microwires are substantially affected by the stress-annealing conditions (temperature or stress). In Co-rich microwires even conventional annealing at different temperatures produce similar modification of the hysteresis loops [2]. Therefore, we proposed simple method to prepare glass-coated microwires with graded magnetic anisotropy by annealing at variable temperature [2]. Previously, graded magnetic anisotropy was obtained by rather sophisticated method involving modification of the chemical composition during the sample preparation [4]. Magnetic materials with a graded magnetic anisotropy presenting controllable spatial distribution of the magnetic anisotropy can show unusual magnetic properties, like controllable nucleation or pinning of domain walls [2,5].

We have studied the magnetic properties and domain wall dynamics in Fe-rich and Co-rich microwires subjected to stress-annealing. For the wires stress-annealed at variable temperatures we obtained a graded magnetic behavior with local hysteresis loops shapes and properties (coercivity, remanent magnetization) changing along the sample length. In the samples subjected to local stress-annealing we created an artificial source of DW injection allowing the manipulation of the DW dynamics. The observed stress-induced anisotropy could be related to the internal stresses relaxation after annealing and the interplay of compressive “back-stresses” arisen after stress annealing and axial internal stresses.

[1] K. Mohri et.al, *IEEE Trans.Magn.*, **Mag-26** (1990) 1789-1781.

[2] A. Zhukov et.al., *J. Phys. D: Appl. Phys.*, **55** (2022) 253003.

[3] M.H. Phan, H.X. Peng, *Progr. Mater. Sci.*, **53** (2008) 323-420.

[4] C.L. Zha et.al., *J. Appl. Phys. Lett.*, **97** (2010) 182504.

[5] R. Skomski, T.A. George, D.J. Sellmyer, *J. Appl. Phys*, **103** (2008) 07F531.

2IT-B-2

## MAGNETIZATION PROCESSES AND MAGNETOIMPEDANCE IN LOW-CURIE TEMPERATURE MICROWIRES

*Panina L.V.<sup>1,2</sup>, Alam J.<sup>1</sup>, Yudanov N.A.<sup>1</sup>, Nemirovich M.<sup>1</sup>, Morchenko A.T.<sup>1</sup>, Kostishin V.G.<sup>1</sup>*

<sup>1</sup> National University of Science and Technology “MISIS”, Moscow, Russia

<sup>2</sup> Immanuel Kant Baltic Federal University, Kaliningrad, Russia

drlpanina@gmail.com

Amorphous ferromagnetic microwires have gained significant attention for their potential in sensor development. This paper explores the utilization of microwires with low Curie temperatures ( $T_c=40-70$  °C) as temperature sensors and investigates two fundamental effects near  $T_c$ : the generation of higher frequency harmonics of the voltage pulse induced during re-magnetization and magnetoimpedance (MI).

In many sensing applications, temperature stability is crucial, necessitating the use of materials with high Curie temperatures. However, for ambient temperature measurements, low- $T_c$  materials are desired. Microwires composed of amorphous CoFe-based alloys with higher additions of Cr or Ni exhibit reduced  $T_c$  values, which can be further modified through annealing treatments. Near  $T_c$ , magnetic properties such as saturation magnetization, magnetostriction, and anisotropy undergo significant variations, leading to modifications in magnetization reversal and MI as  $T_c$  is approached.

This study focuses on microwires with two compositions:  $\text{Co}_{27.4}\text{Fe}_5\text{B}_{12.26}\text{Si}_{12.26}\text{Ni}_{43.08}$  and  $\text{Co}_{64.82}\text{Fe}_{3.9}\text{B}_{10.2}\text{Si}_{12}\text{Cr}_9\text{Mo}_{0.08}$ , which possess different easy anisotropy. The microwires of the first composition exhibit axial easy anisotropy due to positive magnetostriction. Such anisotropy is crucial for achieving fast re-magnetization, which occurs even near  $T_c$ . The voltage signal generated during re-magnetization contains higher harmonics of the excitation frequency, and their amplitudes decrease significantly as  $T_c$  is approached. Utilizing lock-in techniques, high-frequency signals can be detected with excellent sensitivity, enabling the development of miniature and wireless sensing elements. The axial anisotropy also facilitates temperature-dependent MI, although observing a monotonic drop in impedance with increasing temperature towards  $T_c$  requires relatively high frequencies in the range of hundreds of megahertz. In contrast, microwires of the second composition possess negative magnetostriction and circumferential easy anisotropy. In this case, achieving substantial changes in impedance with temperature necessitates using a dc bias field, as the transverse permeability is small at zero fields for any temperature.

Precise control over the compositional adjustment of  $T_c$  within a narrow range is challenging but can be achieved through annealing, leading to microscopic atomic re-arrangements. Typically,  $T_c$  variations are less than 10%, but in absolute values, they can be within 10-15 degrees, which is sufficient to meet specific requirements for the considered temperature range.

Overall, this research demonstrates the potential of low- $T_c$  microwires as temperature sensors by analyzing higher harmonics generation and magnetoimpedance near  $T_c$ . The study provides insights into the unique magnetic properties of different microwire compositions and their suitability for specific sensing applications.

Support by «Priority 2030» (project K6-2022-043).

## MAGNETIC STATES IN QUASI-TWO-DIMENSIONAL $\text{Fe}_y\text{Ti}(\text{S},\text{Se})_2$ INTERCALATION SYSTEMS

*Baranov N.V.<sup>1,2</sup>, Selezneva N.V.<sup>2</sup>, Sherokalova E.M.<sup>2</sup>*

<sup>1</sup> M.N. Mikheev Institute of Metal Physics UB of RAS, Yekaterinburg, Russia

<sup>2</sup> Ural Federal University, Yekaterinburg, Russia

baranov@imp.uran.ru

In transition metal ( $T$ ) dichalcogenides  $\text{TX}_2$  ( $X = \text{chalcogen}$ ) with a layered crystal structure of the NiAs-type, the metal layers are sandwiched between full-filled layers of chalcogen. The weak van der Waals-type (vdW) bonds between the  $X-T-X$  hexagonal packed tri-layers ( $X = \text{chalcogen}$ ,  $T = \text{transition metal of IV-VI groups}$ ) in dichalcogenides  $\text{TX}_2$  makes it possible to exfoliate such structures and obtain graphene-like two-dimensional systems, but also allows intercalation of other atoms or molecules into the so-called vdW gap between  $X-T-X$  sandwiches, thus generating a wide class of new materials with unique physical properties which have the potential for practical applications. In the case of intercalation with 3d-transition metal ( $M$ ) atoms having magnetic moments, structures with alternating layers of magnetic and non-magnetic atoms can be obtained. The magnetic properties of the  $M_x\text{TX}_2$  intercalated compounds are controlled by combination of reduced dimensionality, ordering effects, magnetocrystalline anisotropy, and exchange interactions of different types. The  $M_x\text{TX}_2$  compounds demonstrate a rich variety of magnetic states; spin-glass, cluster-glass magnetic states and three-dimensional long-range magnetic orderings of various types are observed depending on the kind and concentration of intercalated  $M$  atoms, and on the type of the  $\text{TX}_2$  matrix. Thus, spin-cluster glass state, antiferromagnetic (AFM) and ferrimagnetic orderings are found to exist in the  $\text{Fe}_x\text{TiS}_2$  system at various Fe concentrations [1].

Comprehensive studies by using X-ray and neutron diffraction, the measurements of the magnetization in steady and pulsed magnetic fields and magnetoresistance have been performed for the titanium dichalcogenides  $\text{Fe}_x\text{TiS}_{2-y}\text{Se}_y$  intercalated with iron in order to reveal how the changes in the Fe content and replacement of sulfur by selenium affect the magnetic state of these compounds. Sulfur-rich  $\text{Fe}_x\text{TiS}_{2-y}\text{Se}_y$  compounds with the Fe concentrations  $x \geq 0.25$ , except for compounds with  $x = 0.33$ , behave at low temperatures as antiferromagnets (AFMs), exhibiting spin-flip transitions to a metastable ferromagnetic (FM) state. The  $\text{Fe}_{0.33}\text{TiS}_2$  compound exhibits the magnetization and magnetoresistance behaviors typical of cluster glass due to the formation of a triangular network of Fe atoms located between S-Ti-S tri-layers and frustrations of exchange interactions of different signs. An increase in the selenium content in antiferromagnetic (AF) compounds  $\text{Fe}_{0.5}\text{TiS}_{2-y}\text{Se}_y$  leads to the change from the spin-flip to spin-flop type transitions and a near tenfold increase in the critical transition field is ascribed to decrease in the energy of the magnetocrystalline anisotropy owing to the crystal lattice expansion caused by substitution. The formation of a metastable field-induced FM state  $\text{Fe}_{0.25}\text{TiS}_2$  and  $\text{Fe}_{0.5}\text{TiS}_{2-y}\text{Se}_y$  compounds ( $y < 0.5$ ) is accompanied by a large remnant magnetoresistance; and the irreversibility of the AFM-FM transition in these compounds is confirmed by neutron diffraction measurements [2]. Along with the Ising character of Fe ions, magnetoelastic interactions can be responsible for the formation of the metastable field-induced high-coercive FM state in  $\text{Fe}_x\text{TiS}_{2-y}\text{Se}_y$ .

This work was supported by the Russian Science Foundation (Grant No 22-13-00158).

[1] N.V. Baranov et al., *Phys. Rev. B*, **100** (2019) 024430.

[2] N.V. Selezneva et al., *Phys. Rev Materials*, **7** (2023) 014401.

**July 2**

11:15 - 12:30

Sunday

ORAL  
SESSIONS I

Section C  
**Topological  
Insulators**

2IT-C-1

## INTRINSIC MAGNETIC TOPOLOGICAL INSULATORS OF THE $\text{MnBi}_2\text{Te}_4$ FAMILY

Otrokov M.M.<sup>1,2</sup>

<sup>1</sup> Centro de Física de Materiales (CFM-MPC), Donostia-San Sebastián, Spain

<sup>2</sup> IKERBASQUE, Basque Foundation for Science, Bilbao, Spain

mikhail.otrokov@gmail.com

Magnetic topological insulators (MTIs) are narrow gap semiconductor materials that combine non-trivial band topology and magnetic order. They host a number of exotic phenomena having potential applications. Previously, MTIs were only created by means of doping nonmagnetic TIs such as  $(\text{Bi}_{1-x}\text{Sb}_x)_2\text{Te}_3$  with Cr or V atoms, however such an approach leads to strongly inhomogeneous magnetic and electronic properties of these materials, restricting the observation of important effects to very low temperatures. Recently, a stoichiometric compound  $\text{MnBi}_2\text{Te}_4$  was theoretically predicted and then experimentally confirmed to be the first intrinsic antiferromagnetic TI (AFMTI) [1-4].

The discovery of  $\text{MnBi}_2\text{Te}_4$  opens a new field that focuses on intrinsically magnetic stoichiometric compounds: several  $\text{MnBi}_2\text{Te}_4$ -derived MTIs were synthesized right away [5,6], such as  $(\text{MnBi}_2\text{Te}_4) \cdot n(\text{Bi}_2\text{Te}_3)$ ,  $\text{MnBi}_{2-x}\text{Sb}_x\text{Te}_4$ ,  $(\text{MnSb}_2\text{Te}_4) \cdot n(\text{Sb}_2\text{Te}_3)$ ,  $\text{Mn}_2(\text{Bi,Sb})_2\text{Te}_5$ , and  $\text{MnBi}_2\text{Se}_4$ , that will also be discussed in the talk. As a result,  $\text{MnBi}_2\text{Te}_4$  has been predicted to be a platform for realizing high-order topological insulator and superconductor states, Weyl semimetal phase, skyrmions, quantized magnetoelectric coupling, and Majorana fermions. Moreover,  $\text{MnBi}_2\text{Te}_4$ -based systems are predicted and/or observed to show 11 different types of Hall effect, some of them are fundamentally new, such as the layer Hall effect [7]. In  $\text{MnBi}_2\text{Te}_4/\text{hBN}$  van der Waals heterostructures, a stack of  $n$   $\text{MnBi}_2\text{Te}_4$  films with  $C = 1$  intercalated by hBN monolayers gives rise to a high Chern number state, characterized by  $C = n$  chiral edge modes [8], this number being as large as allowed by the van der Waals heterostructures growth technology.

Concerning current challenges of this field, we will discuss in detail the issue of the Dirac point gap in the  $\text{MnBi}_2\text{Te}_4$  topological surface state that caused a lot of controversy [9,10]. While the early experimental measurements reported on large Dirac point gaps, in agreement with ab initio calculations, a number of further studies claimed to observe a gapless dispersion of the  $\text{MnBi}_2\text{Te}_4$  Dirac cone. A number of possible theoretical explanations of this unexpected behavior have been put forward, which we will discuss in the context of the available experimental data.

- [1] M.M. Otrokov et al., *Nature*, **576** (2019) 416.
- [2] M.M. Otrokov et al., *Phys. Rev. Lett.*, **122** (2019) 107202.
- [3] Y. Deng et al., *Science*, **367** (2020) 895.
- [4] C. Liu et al., *Nature Mater.*, **19** (2020) 522.
- [5] I.I. Klimovskikh et al., *npj Quantum Mater.*, **5** (2020) 54.
- [6] H. Deng et al., *Nature Phys.*, **17** (2021) 36.
- [7] A. Gao et al., *Nature*, **595** (2021) 521.
- [8] M. Bosnar et al., *npj 2D Mater. Appl.*, **7** (2023) 33.
- [9] Y. Hao et al., *Phys. Rev. X*, **9** (2019) 041038.
- [10] M. Garnica et al., *npj Quantum Mater.*, **7** (2022) 7.

**DISORDER IN MAGNETIC TOPOLOGICAL INSULATORS***Ernst A.*<sup>1,2</sup><sup>1</sup> Johannes Kepler University, Linz, Austria<sup>2</sup> Max Planck Institute of microstructure physics, Halle, Germany  
Arthur.Ernst@jku.at

It is a well known fact that a magnetic field can break the time reversal symmetry and therewith can destroy a topologically protected surface state in topological insulators. However, the interplay between magnetism and topological order can yield a number of interesting phenomena such as the quantum anomalous Hall effect, a topological magneto-electric effect, and quantised Kerr- or Faraday rotation. This motivates researcher for a search of new magnetic topological insulators and for an intensive study on their electronic and magnetic properties. In my talk, I'll give an overview of our first-principles investigations on this class of materials focusing on the impact of disorder effects. In the first part, I'll present a method and approximations used in our simulations and then talk about several examples of magnetic topological insulators, studied in our group within the last three years. First of all, I'll discuss topological insulators doped with magnetic impurities, which can imply various magnetic order in *these* materials. A special attention will be devoted to the exchange interaction between magnetic impurities and to the impact of electron-magnon interaction on the electronic structure in some doped topological systems. As next, I'll demonstrate how some defects or impurities without magnetic moments can induce magnetism in topological insulators and discuss the main features of magnetic interactions in these systems.

## TEMPERATURE-RESOLVED SPIN-PUMPING IN $\text{MnBi}_2\text{Te}_4/\text{NiFe}$ HETEROSTRUCTURES

*Pakhomov A.S.<sup>1,2</sup>, Yurlov V.V.<sup>1</sup>, Skirdkov P.N.<sup>1,3</sup>, Chernov A.I.<sup>2</sup>, Zvezdin K.A.<sup>1,3</sup>*

<sup>1</sup> “New Spintronic Technologies” LLC, Moscow, Russia

<sup>2</sup> Moscow Institute of Physics and Technology, Dolgoprudnyy, Russia

<sup>3</sup> Prokhorov General Physics Institute RAS, Moscow, Russia

a.pakhomov@nst.tech

Strong spin-orbit coupling makes topological insulators (TIs) to be very attractive and promising material for use in future spintronic devices. One of such materials is the recently discovered topological insulator  $\text{MnBi}_2\text{Te}_4$ , which demonstrates antiferromagnetic properties at low temperatures.

In this work, we performed cryogenic FMR experiment to study the heterostructures composed by the  $\text{MnBi}_2\text{Te}_4$  and thin film of permalloy. The permalloy thickness was 20 nm and 10 nm, and the TI thickness was 10 nm, which corresponds to 7 SL (septuple layer). The Gilbert damping constant of these samples was studied at different temperatures. Anomalous behavior of the damping parameter was investigated. At temperatures about 70 K anomalous peak was observed and associated with magnetization reorientation and amplified with effective spin-pumping from NiFe to TI and effective Gilbert damping constant is 3 times higher than in pristine NiFe films [1]. In addition, the voltage of the inverse spin Hall effect (ISHE) was measured for the same samples at the same temperatures, but at a frequency of 6 GHz. Anomalous behavior has been detected. The Gilbert damping parameter has a maximum value at  $\sim 70\text{K}$  while the ISHE voltage has a minimum at the same temperature, and at  $\sim 140\text{K}$  the Gilbert damping has a minimum and the voltage has a maximum. Such behavior was observed in both heterostructures. We associate such behavior with anomalous Nernst effect, which adds another voltage to the measured ISHE voltage.

Support by RSF №22-12-00367 is gratefully acknowledged.

[1] Y. Zhao, Q. Song, S.H. Yang et al., *Sci. Rep.*, **6** (2016) 22890.

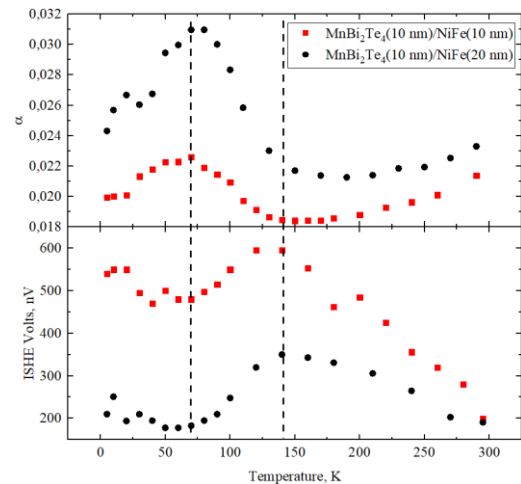


Figure 1. Temperature dependence of the ISHE voltage and Gilbert damping constant for  $\text{MnBi}_2\text{Te}_4(10\text{ nm})/\text{NiFe}(20\text{ nm})$  and  $\text{MnBi}_2\text{Te}_4(10\text{ nm})/\text{NiFe}(10\text{ nm})$ .

**July 2**

Sunday

16:00 - 18:15

ORAL  
SESSIONS II

Section A

**Magnetic Soft Matter**  
(magnetic polymers,  
complex magnetic fluids  
and suspensions)

## NONLINEAR OPTICAL PROPERTIES OF MAGNETIC NANOFLUIDS

*Figueiredo Neto A.M.*

University of São Paulo, Institute of Physics, São Paulo, Brazil

afigueiredo@if.usp.br

Magnetic colloids are an interesting class of materials to investigate nonlinear optical properties of nanoparticles. The external magnetic field can be employed to orient single particles and impose the formation of different types of aggregates, from linear chains to bundles. In these conditions, the electric field (e.g., from light) can be oriented parallelly and perpendicularly to the external magnetic field, to investigate anisotropies on the nonlinear response of the particles alone or in clusters. One of these parameters is the first-order hyperpolarizability ( $\beta_H$ ), which is present in the energy ( $U$ ) of a dipole ( $\mathbf{P}$ ) in the presence of an external electric field ( $\mathbf{E}$ ):  $U=U_0-P_iE_i-\alpha_{ij}E_iE_j-\beta_{Hijk}E_iE_jE_k$ . Assuming, now, an ensemble of dipoles in the magnetic colloid, the third-order electric susceptibility ( $\chi^{(3)}$ ) is present in the expression of the electric polarization:  $P=\chi^{(1)}E+2\chi^{(2)}EE+3\chi^{(3)}|E|^2$ . The first-order hyperpolarizability  $\beta$  of magnetite nanoparticles in colloidal dispersion was measured in the presence and absence of an external magnetic field of magnitude  $H = 800$  G. For that, the (linear) attenuation spectrum was measured, and the nonlinear properties were obtained through the hyper-Rayleigh scattering technique. The attenuation spectrum is the same, regardless of the external magnetic field, indicating that large aggregates of nanoparticles were not formed on our system. The first-order hyperpolarizability, on the other hand, increased when the incident laser-beam polarization was parallel to the magnetic field, and decreased when the directions were orthogonal. This is due to the alignment of the crystallographic planes of the material when nanoparticles rotate, in order to align their individual magnetic momentum with respect to the external field. For the parallel case,  $\beta_{H\parallel}=9.8(2)\times 10^{-28}\text{cm}^5/\text{esu}$ , while for the perpendicular configuration,  $\beta_{H\infty}=8.1(1)\times 10^{-28}\text{cm}^5/\text{esu}$ . Defining the x axis of the particle reference frame parallel to the  $\langle 111 \rangle$  crystallographic direction, which corresponds to the direction of easy magnetization,  $\beta_{H\parallel}=\beta_{Hxxx}$ , and  $\beta_{H\infty}$  corresponds to an average from  $\beta_{Hyyy}$ , and  $\beta_{Hzzz}$ . The Real and Imaginary parts of  $\chi^{(3)}$  of magnetite nanoparticles were also measured by using, now, the Z-Scan technique. The nonlinear index of refraction and absorption are of the order of  $-14\times 10^{-14}\text{cm}^2/\text{W}$  and  $1.5\text{ cm}/\text{GW}$ , respectively. An anisotropy was also observed in the  $\chi^{(3)}$  measurements, as observed in the measurements of  $\beta_H$ .

Support by FAPESP, CNPq, CAPES, INCT-Complex Fluids.

2IT-A-5

## DYNAMIC SUSCEPTIBILITY AND MAGNETIC HYPERTHERMIA IN A SYSTEM OF INTERACTING FERROPARTICLES

*Zubarev A. Yu.*

Ural Federal University, Yekaterinburg, Russia  
A.J.Zubarev@urfu.ru

We present results of theoretical study of effect of magnetic interparticle interaction on dynamic magnetic susceptibility and magnetic hyperthermia in systems of single-domain ferromagnetic particles, immobilized in a host medium. These systems can model ferrogels, biological tissues with embedded particles, solidified ferrofluids and other similar materials.

Two kinds of the materials are considered – the systems with homogeneous (gas-like) spatial distribution of the particles and the ones with the simplest heterogeneous internal structures (dimers, consisting of two particles). It is supposed that the energy of the internal magnetic anisotropy of the particles is significantly more than the thermal energy of the system. This is typical, for instant, for the magnetite particles with diameter about and more than 17-18nm, which can provide significant response of the system on an alternating magnetic field.

Analysis is based on the solution of the Fokker-Planck equation for the distribution function (density of probability) of a given orientation of magnetic moments of the interacting ferroparticles. For the systems with their gas-like spatial distribution, this equation has been solved in the frames of the well-known pair approximation. For the both considered systems the equation's solution have been obtained in the frames of mathematically rigorous Kramers method; any intuitive or heuristic hypothesis have not been used. As a result, simple linear differential equations for the statistically mean (measurable) magnetic moment of the particle have been obtained. Note that these equations differ from the phenomenological Debye equations, very often used for the analysis of the relaxation phenomena.

Our results show that increase of the applied magnetic field (its amplitude) decreases the characteristic time of the Neel remagnetization of the particles. If the field amplitude is small (the Langevin parameter of the particle interaction with the field is less than one), magnetic interparticle interaction increases the time of relaxation. For the homogeneous spatial distribution of the magnetite particles with the diameter 17-18 nm, this increase is about 20-30 per cent. For the clusters of the particles this increase can achieve 2-4 orders of magnitude. This means that clustered particles will be excluded from the dynamic response of the systems on the fields oscillating with the period, comparable with the time of relaxation of the single particle. In the opposite case of the strong external field, this interaction decreases this relaxation time (about a few tens of per cent for the noted particles with volume concentration about several per cent). Thus, effect of the inter particle interaction on the rate of the remagnetization is determined by the applied field amplitude.

The equilibrium mean magnetic moment of the particle increases due to the interparticle interaction both for the clustered and homogeneously distributed particles. Effect of these factors on the intensity of the heat production under the oscillating magnetic field (magnetic hyperthermia) is discussed.

## INERTIAL FERROFLUID SENSORS: PHYSICAL AND ENGINEERING ASPECTS

*Ivanov A.S., Somov S.A., Koskov M.A.*

Institute of Continuous Media Mechanics UB RAS, Perm, Russia  
lesnichiy@icmm.ru

Inertial sensors (IS) are used in a wide variety of measuring devices: accelerometers, inclinometers, seismographs, vibration meters and others. As a rule, the size and weight of IS are larger than those of MEMS and capacitive sensors, but their production technology is much simpler and cheaper, while the accuracy is about the same. However, there is one type of IS that is still modern and promising – the ferrofluid (FF) sensor, which demonstrates one more advantage over capacitive sensors – the higher (by one order of magnitude) sensitivity [1]. This useful feature results from the construction of the sensor: the inertial mass (permanent magnet) levitates in a vessel filled with FF, thus it doesn't exhibit dry friction that usually coarsens the sensitivity threshold. The only serious problem of such devices is magnetophoresis – the drift of colloidal particles in FF into the region with highest field intensity (to the inertial mass). This natural and unavoidable process is very harmful, because the measuring circuit of such sensors is based on magnetic measurements [1], and even the usage of negative feedback amplifiers doesn't improve the situation. A lot of different constructions were proposed [2] since the first patents were registered [1], but the main disadvantage remained the same.

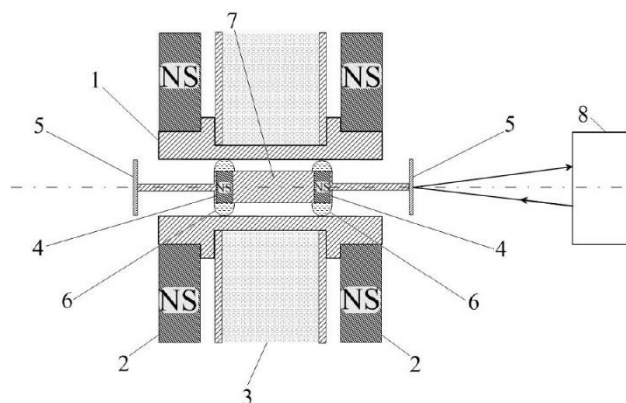


Figure 1. The sensor [3]: 1 – nonmagnetic housing, 2, 4 – permanent magnets, 3 – correcting coil, 5, 7 – nonmagnetic rods, 6 – FF drops, 8 – optical (laser) displacement meter.

We propose a new design of the FF inertial sensor (see Figure 1) with three distinguishing engineering solutions [3]: first, the FF in our sensor doesn't fill the whole volume of the sensor housing, - it is used only as a lubricant; second, the magnetic system of the sensor is constructed to get the linear return force [4] acting on the inertial mass; third, we separate the magnetic subsystem of the sensor that restores the zero position of the inertial mass and the subsystem of the sensor that measures its current position. The latter subsystem is proposed to be optical, i.e. independent of the internal magnetophoresis process in FF and very accurate at the same time. These

engineering solutions are now being supported by our investigations of the FF hydrodynamic flow in the coaxial gap between the inertial mass and the sensor housing. The viscous friction force acting on the inertia mass plays an important role in case of dynamic measurements (accelerometers and vibration sensors).

The work was supported by Russian Science Foundation (Project No. 23-21-00100).

[1] R.L. Bailey, *J., Magn. Magn. Mater.*, **33** (1983) 178-182.

[2] L. Qian, D. Li, *J., Sensors*, **2014** (2014) 9.

[3] A.S. Ivanov, M.A. Koskov, RF patent no. 2788591 C1 (2022) 10.

[4] M.A. Koskov, A.S. Ivanov, *Vestnik IGEU*, **6** (2022) 26-36.

## PVDF-BASED COMPOSITES FOR BIOMEDICAL APPLICATIONS: COMBINING THE INCREASED MAGNETOELECTRIC EFFECT AND BIOCOMPATIBILITY

*Omelyanchik A.<sup>1,2</sup>, Antipova V.<sup>1</sup>, Sobolev K.<sup>1</sup>, Kolesnikova V.<sup>1</sup>, Alekhina Yu.<sup>3</sup>, Makarova L.<sup>3</sup>, Rodionov V.<sup>1</sup>,  
Ershev P.<sup>1</sup>, Levada E.<sup>1</sup>, Rodionova V.<sup>1</sup>*

<sup>1</sup> Immanuel Kant Baltic Federal University, Kaliningrad, Russia

<sup>2</sup> Department of Chemistry and Industrial Chemistry (DCIC), University of Genova, Genova, Italy

<sup>3</sup> Lomonosov Moscow State University, Moscow, Russia

<sup>4</sup> Institute of Structure of Matter–CNR, Rome, Italy

<sup>5</sup> Amirkhanov Institute of Physics of Dagestan Federal Research Center, Russian Academy of  
Sciences, Makhachkala, Russia

vvrodionova@kantiana.ru

Magnetolectric (ME) effect is concluded in the mutual control of magnetic and electrical properties of a single material or composite. The polymeric ME composites are promising classes of materials for different applications in biomedicine to due to their mechanical flexibility, ease of fabrication, and biocompatibility. This work is devoted to the 0-3 type composites consisted of PVDF or PVDF-TrFE piezopolymers with included magnetic nanoparticles (MNPs) [1, 2]. The ME coupling in such materials is due to the stress induced in the piezopolymeric matrix by the rotation and/or magnetostatic attraction of the MNPs when a magnetic field is applied. The ME effect in composites based on the PVDF-TrFE was higher because of the higher piezoelectric  $\beta$ -phase content. The MNPs were produced by the sol-gel autocombustion method which allows producing large amount of material with the high magnetic anisotropy and saturation magnetisation which can be tuned by chemical composition. In this way, two systems of spinel ferrites MNPs with compositions of  $\text{CoFe}_2\text{O}_4$  (CFO) and  $\text{Zn}_{0.25}\text{Co}_{0.75}\text{Fe}_2\text{O}_4$  (ZCFO) were synthesized. The effective magnetic anisotropy constant of CFO MNPs ( $1.6 \times 10^6$  erg/cm<sup>3</sup>) was higher compared to ZCFO MNPs ( $0.95 \times 10^6$  erg/cm<sup>3</sup>) while a value of the saturation magnetisation of  $\sim 74$  emu/g was slightly higher in ZCFO MNPs. The resonance field of ME effect was tuned by changing the magnetic anisotropy constant. Further steps to increase the ME effect were the alignment of MNPs by polymerisation under magnetic field and the inclusion of the ferroelectric  $\text{BaTiO}_3$  (BTO) particles. Alignment of magnetic particles allowed increasing ME effect trough modulating of the magnetostatic dipolar interactions. The inclusion of BTO particles increased the electric polarization of the polymer and lead to a further increase of ME effect. The highest ME coefficient  $\alpha_{33}$  of  $18.5 \text{ mV} \times \text{cm} \cdot 10^{-1} \text{ Oe}^{-1}$  was found in the aligned sample with 5 wt.% of BTO particles and 15 wt.% of CFO MNPs. The resulting samples were then tested to be used as scaffolds to remotely control the electrical microenvironment of the cells and thus control their fate. Experiments on stem cell cultures have shown the possibility of using such materials as a bioactive surface for differentiation and enhancement of stem cell proliferation.

The work was supported by the Russian Science Foundation No. 21-72-30032.

[1] A. Omelyanchik et al., *Nanomaterials*, **11** (2021) 1154.

[2] K. Sobolev et al., *Polymers*, **14**(22) (2022) 4807.

## INFLUENCE OF FIELD AMPLITUDE AND DIPOLAR INTERACTIONS ON THE DYNAMIC RESPONSE OF IMMOBILIZED MAGNETIC NANOPARTICLES

*Elfimova E.A., Ambarov A.V., Zverev V.S.*

Ural Federal University, Yekaterinburg, Russia  
Ekaterina.Elfimova@urfu.ru

The dynamic magnetic properties of an ensemble of interacting immobilized magnetic nanoparticles with aligned easy axes in an applied ac magnetic field are considered. The nanoparticles are distributed randomly within an implicit solid matrix, but the easy axes of the particles are aligned parallel or perpendicular to the ac magnetic field (Figure 1). The system models soft, magnetically sensitive composites synthesized from liquid dispersions of the magnetic nanoparticles in a strong static magnetic field, followed by the carrier liquid's polymerization. After polymerization, the nanoparticles lose translational degrees of freedom; they react to an ac magnetic field via Néel rotation, when the particle's magnetic moment deviates from the easy axis inside the particle body. Based on a numerical solution of the Fokker-Planck equation for the probability density of the magnetic moment orientation, the dynamic magnetization, frequency-dependent susceptibility, and relaxation times of the particle's magnetic moments are determined. It is shown that the system's magnetic response is formed under the influence of competing interactions, such as dipole-dipole, field-dipole, and dipole-easy axis interactions. The contribution of each interaction to the magnetic nanoparticle's dynamic response is analyzed. The obtained results provide a theoretical basis for predicting the properties of soft, magnetically sensitive composites, which are increasingly used in high-tech industrial and biomedical technologies.

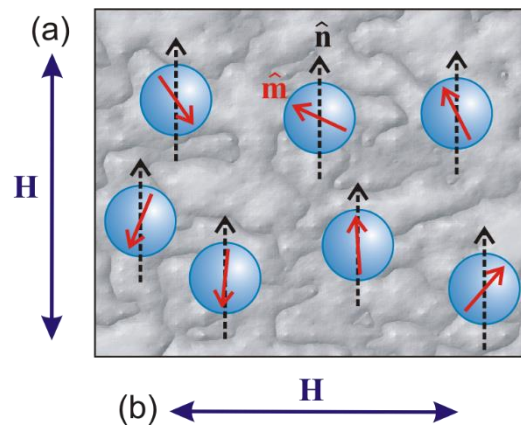


Figure 1. Sketch of the sample considered here: a frozen configuration of magnetic nanoparticle positions and easy axis orientations. The dashed black arrows show the easy axis direction  $\hat{\mathbf{n}}$ , while the solid red arrows represent the magnetic moment orientation  $\hat{\mathbf{m}}$ ; the ac magnetic field  $\mathbf{H}$  is directed (a) parallel or (b) perpendicular to the easy magnetization axes.

Support by the Ministry of Science and Higher Education of the Russian Federation (Ural Federal University project within the Priority 2030 Program) is acknowledged.

## DYNAMICS OF COMPOSITE MAGNETIC FLUID SYSTEMS UNDER THE INFLUENCE OF A MAGNETIC FIELD

*Ryapolov P.A., Sokolov E.A., Kaluzhnaya D.A., Shel'deshova E.V.*

Southwest State University, Kursk, Russia

r-piter@yandex.ru

We propose a new technique for creating active bubbles and drops with a nonmagnetic core and a coating formed by a magnetic fluid [1, 2]. The hydrodynamics of these systems is considered in various channels under the influence of an inhomogeneous magnetic field. Magnetic fluids are a colloidal solution of magnetic nanoparticles coated with a surfactant, dispersed in a carrier fluid.

The process of formation of active bubbles and drops consists in the introduction of a non-magnetic phase into the magnetic one, which is held by the inhomogeneous magnetic field of a combined source that combines a ring magnet and an electromagnet. We have investigated various regimes leading to various active bubbles and drops, and the influence of the magnetic field on the size, speed and acceleration of active droplets formed has also been investigated. It is shown that active bubbles change their trajectory under the action of a constant magnetic field, and also decay under the action of a pulsed one. This provides a new mechanism for controlling drops and bubbles using a magnetic field. Unlike the flow focusing method, which is one of the main methods in drip microfluidics, non-magnetic drops and bubbles detach from a levitating non-magnetic volume rather than from a capillary. In this case, the levitating gas cavity acts as a receiver, making it possible to stabilize the size of the detached bubbles and increase the range of adjustment, in contrast to the data of [3], in which the detachment of bubbles in a magnetic fluid occurred in a uniform magnetic field.

This creates the prerequisites for the development of liquid multilayer capsules controlled by a magnetic field, which can be concentrated in a certain place and destroyed under impulse action. The results obtained can be applied to create drop-based microfluidics systems in which a non-uniform magnetic field can be used to focus drop and bubble flows in a ferrofluid.

Samples with different physical parameters are considered, and the dependence of the magnetoviscous effect is studied. It was shown that the microstructure of the sample and the presence of large magnetic particles have the greatest effect on the dynamics of a magnetic fluid subjected to vibrational-shear and magnetic-viscous effects. The results can be used to develop a method for rapid testing of magnetic fluid samples and to develop acceleration and vibration sensors using magnetic fluids.

The microfluidic part of research was supported by the Russian Science Foundation grant No. 22-22-003113 <https://rscf.ru/project/22-22-003111/>, the magnetoviscous effect has been researched within the part of the implementation of the Russian Federation State task (No 0851-2020-0035).

[1] E. Sokolov et al., *Fluids*, **8**(2) (2023).

[2]. P.A. Ryapolov, E.A. Sokolov, E.B. Postnikov, *J. Magn. Magn. Matter*, **594** (2022) 169067.

[3]. H. Yamasaki et al., *J. Magn. Magn. Matter*, **501** (2020) 166446.

## DEFORMATION OF A MAGNETIC FLUID DROPLET WITH AN IMMERSSED MAGNETIZABLE BODY UNDER UNIFORM MAGNETIC FIELDS

*Sogomonyan K.L.<sup>1</sup>, Vinogradova A.S.<sup>2</sup>, Sharova O.A.<sup>1,2</sup>, Pelevina D.A.<sup>1,2</sup>, Naletova V.A.<sup>2</sup>*

<sup>1</sup> Faculty of Mechanics and Mathematics, Lomonosov Moscow State University, Moscow, Russia

<sup>2</sup> Institute of Mechanics, Lomonosov Moscow State University, Moscow, Russia  
alexandra.vinogradova@imec.msu.ru

The potential of magnetic fluid (MF) droplets to be used as miniature reconfigurable soft robots and actuators for a range of biomedical, microfluidic, and lab-on-a-chip applications has been widely explored, e. g. [1-2]. Such robots, capable of controlled movement, can also engulf/transport or push/manipulate particles. Since position and shape control of MF droplets by the magnetic field gradient, direction, and magnitude has been well studied, we focus on combined shape control of a droplet and position control of an immersed body by uniform fields.

The effect of a uniform applied magnetic field on the deformation of a MF droplet with an immersed magnetizable ball is investigated numerically and compared with experimental data. A droplet is placed on a horizontal plane, and a ball takes its equilibrium position in the droplet at a certain levitation height above the plane under a uniform tilted field (see Figure 1). Spherical shape of the body is chosen for ease of calculating due to a known expression for the magnetic field near the surface of the ball being magnetized in a uniform applied field, but bodies of other shapes are also considered in the experiment. In the noninductive approximation, an analytic expression is obtained for the force exerted by MF on the body. We develop a 3D model to predict the deformation of the droplet under uniform fields of different directions and magnitudes. The levitation of a ball in a droplet is demonstrated experimentally and theoretically. It is shown that the ball levitation height increases with an increase in MF volume, magnitude and tilt angle of the applied field. It is found that there are minimum and maximum volumes of MF, and a minimum field magnitude required for body levitation. Given these results, we conclude that the droplet shape and the ball position could be controlled by tuning the tilt angle and magnitude of the field.

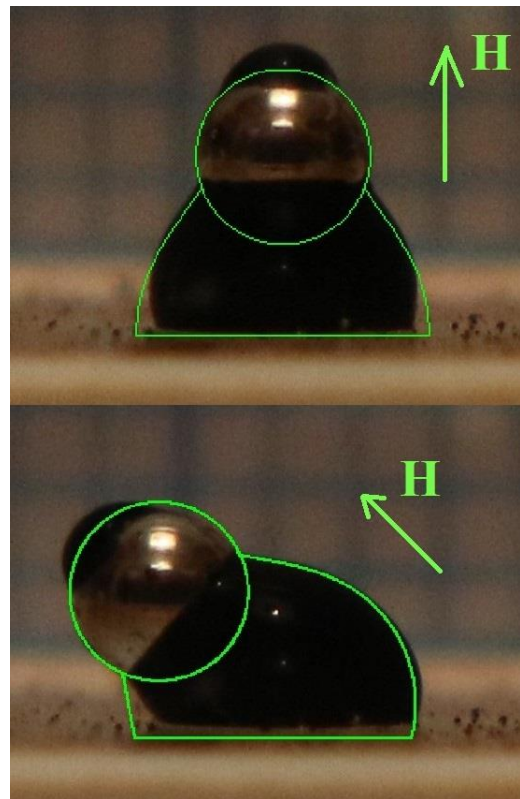


Figure 1. Experimental and calculated profiles of the MF droplet with an immersed magnetizable ball under the uniform field of different directions.

Support by RSF Grant 20-71-10002-P is acknowledged.

[1] R. Ahmed et al., *Soft Robotics*, **8** (2021) 687-698.

[2] L. Yang et al., *IEEE/ASME Transactions on Mechatronics*, **3** (2023) 1-11.

**July 2**

16:00 - 18:15

Sunday

ORAL  
SESSIONS II

Section B

**Heusler Alloys  
and Phase Transitions**

## ***AB INITIO* INVESTIGATION THE PROPERTIES OF MN<sub>2</sub>-BASED HEUSLER ALLOYS UNDER EXTERNAL PRESSURE**

*Buchelnikov V.D., Sokolovskiy V.V., Zagrebin M.A., Baigutlin D.R.*

Chelyabinsk State University, Chelyabinsk, Russia

buche@csu.ru

Half-metallic ferro- and ferrimagnetic alloys are the most interesting class of materials, since in them one spin direction has a metallic behaviour, while the other one shows a semiconductor character. In this regard, electrons with one kind of spin participate in the electron transport properties and exhibit 100% spin polarization at the Fermi level. This suggests the possibility of creating such an electronic device, in which not only the charge, but also the electron spin can play an important role in signal transmission and, thus, it is free from ohmic dissipation. Among the expected benefits of spintronics technologies are non-volatile data storage with high density and low power consumption, fast data transfer, as well as devices based on tunnelling and giant magnetoresistance [1]. In recent years, Mn<sub>2</sub>-based Heusler alloys are especially attractive due to their interesting half-metallic properties and potential applications in the fields of spintronics and spin caloritronics. They can be used as spin injectors for magnetic random-access memory and the spin-transfer torque devices [2]. The interest to Mn<sub>2</sub>-based Heusler family is caused by the presence of two Mn sublattices aligned ferrimagnetically with the resulting small total magnetization and high Curie temperature. As a result, the reducing of stray flux and energy compensation can be achieved.

In this work the structural, magnetic, and electronic properties of Mn<sub>2</sub>YSn (Y = Sc, Ti, and V) Heusler alloys under applied hydrostatic pressure are studied by the first-principles calculations in VASP program package [3] and the GGA PBE exchange correlation approximation [4] and Monte Carlo simulations. We find that as in case of the SCAN exchange correlation functional [5,6] two magnetic reference states with low and high magnetic moment at the low and high crystal lattice volume, respectively, can coexist together due to the almost equal energy under applied pressure of 3.4, -2.9 and -3.25 GPa for Mn<sub>2</sub>ScSn, Mn<sub>2</sub>TiSn, and Mn<sub>2</sub>VSn, correspondingly. The positive/negative pressure correspond to the uniform lattice contraction/expansion. We show that for all compounds, the low magnetic state (LMS) is characterized by the almost half-metallic behaviour, and it is maintained against hydrostatic pressure. However, the electronic structure of the high magnetic state (HMS) takes on a metallic character. For HMS, the magnetic exchange parameters and Curie temperatures are found to be sufficiently larger values as compared to those of LMS.

To identify stable phases at given pressures, the phase diagrams are constructed.

The pressure-induced switching mechanism between almost half-metallic and metallic states with different magnetization is proposed.

This work was supported by the Russian Science Foundation and the Government of Chelyabinsk Region, grant No. 22-12-20032.

- [1] S. Bhatti et al., *Materials Today*, **20** (2017) 530.
- [2] V.V. Marchenkov et al., *Phys. Metals Metallogr.*, **119** (2018) 1321.
- [3] H. Ebert et al., *Rep. Progr. Phys.*, **103** (2021) 054414.
- [4] J.P. Perdew et al., *Phys. Rev. Lett.*, **77** (1996) 3865.
- [5] V. Buchelnikov et al., *Phys. Rev. B*, **59** (1999) 1758.
- [6] J. Sun et al., *Phys. Rev. Lett.*, **115** (2015) 036402.

## UNDERSTANDING HEUSLER ALLOYS FOR MAGNETOCALORIC APPLICATIONS USING DIFFRACTION TECHNIQUES

*Ari-Gur P.<sup>1</sup>, Madiligama A.<sup>2</sup>, Koledov V.<sup>3</sup>, Shavrov V.<sup>3</sup>*

<sup>1</sup> Western Michigan University, Kalamazoo, MI, USA

<sup>2</sup> Penn State University DuBois, DuBois, USA

<sup>3</sup> Kotelnikov IRE RAS, Moscow, Russia

pnina.ari-gur@wmich.edu

Heusler alloys may demonstrate unique combinations of properties, such as, ferromagnetism (sometimes even when the alloy is made of non-magnetic elements), antiferromagnetism, and superconductivity. Their properties critically depend on their crystalline structures, chemical order, structural phase transformations, and crystallographic texture. A combination of diffraction techniques is essential for the understanding of their properties and behavior. A major contribution to the giant magnetocaloric effect is the entropy change during the structural phase transformation from austenite (typically cubic L2<sub>1</sub>) to a lower symmetry martensite. Its magnitude depends on the structure and the modulation of the martensite. Heusler alloys studied for the magnetocaloric effect are of non-stoichiometric composition. The site occupancy determines the chemical order and hence, the exchange interaction between atoms and, as a result, the magnetic nature of the phase. The chemical order is studied by a combination of x-ray and neutron diffraction because the sensitivity of each technique to different atoms is different.

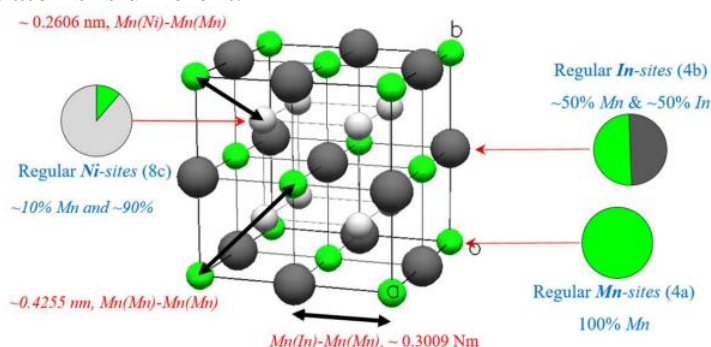


Figure 1. Austenitic L2<sub>1</sub> ( $a = 0.6018$  nm) of Ni<sub>45</sub>Mn<sub>43</sub>In<sub>12</sub> (314 K, 4 T). Site occupancies of the Mn (green), In (black), and Ni (silver) and the interatomic distances between different crystallographic sites are shown.

Neutron diffraction confirmed the antiferromagnetic phase in Heusler alloy Ni<sub>44.9</sub>Mn<sub>43</sub>In<sub>12.1</sub>. The crystallographic phase (monoclinic *7M* & *5M* martensite) is best determined by synchrotron diffraction, then neutron diffraction reveals an extra peak, (115 magnetic in this case).

Crystallographic texture often results from the processing route used to make the device. In magnetic materials it affects the direction of the magnetization easy axis in the sample. That will play an important role in the magnetocaloric effect. Both synchrotron and neutron diffraction techniques are efficient tools for analyzing the texture and the resulting magnetic anisotropy.

Support by several NSF grants, the Department of Energy, Office of Science (Advanced Photon Source) under Contract DE-AC02-06CH1137 and Los Alamos National Laboratory, operated by Triad National Security, LLC, for the National Nuclear Security Administration of the U.S. Department of Energy under contract number 89233218NCA000001 are acknowledged.

## COLLAPSE OF THE INVERSE MAGNETOCALORIC EFFECT IN HEUSLER ALLOYS IN CYCLIC MAGNETIC FIELDS

*Gamzatov A.G., Batdalov A.B., Aliev A.M.*

Amirkhanov Institute of Physics, DFRC, RAS, Makhachkala, Russia  
gamzatov\_adler@mail.ru

Despite the fact that the process of creating solid-state magnetic refrigerators is entering the practical plane, the technology of magnetic cooling has faced many problems that require further scientific research. It is known that the prototypes of magnetic refrigerating machines created to date operate at relatively low frequencies (1–20 Hz) [1]. Therefore, the traditional requirements for magnetocaloric materials (large magnetocaloric effect (MCE), convenient operating temperatures and high cooling power) are insufficient conditions for identifying suitable materials for magnetic cooling technology [2-4]. To them should be added such properties as the independence of the above parameters from the frequency of change of the magnetic field, as well as temporal and mechanical stability under long-term cyclic exposure to a magnetic field.

This paper presents the results of direct measurements ( $\Delta T_{ad}$ ) of the MCE in Heusler alloys in cyclic magnetic fields of 1.2 T (at frequencies  $1 < f \leq 25$  Hz) and 1.8 T (at frequencies  $f = 0.2$  Hz). It has been shown that the value of the inverse MCE in Heusler alloys in cyclic magnetic fields depends on a number of parameters, such as the number of on/off cycles of the magnetic field (frequency of the cyclic magnetic field), and the rate of temperature scanning [2–4]. In a cyclic magnetic field of 1.8 T with a frequency of 0.2 Hz, the value of the inverse MCE in the  $Ni_{47}Mn_{40}Sn_{13}$  alloy depends on the temperature scan rate. The higher the scanning rate, the higher the value of the inverse effect [2, 3]. In cyclic magnetic fields of 1.2 T, as the frequency increases from 1 to 30 Hz in a field of 1.2 T, the value of  $\Delta T_{ad}$  for the  $Ni_{47}Mn_{40}Sn_{13}$  sample near  $T_C$  decreases from 0.78 K to 0.35 K, i.e., more than 2 times. Near the magnetostructural phase transition at  $f \geq 1$  Hz, the inverse MCE almost does not appear and does not depend on the temperature scanning rate, i.e. the reverse MCE collapses in cyclic magnetic fields [4].

The observed effect is explained by irreversible phase transition, induced by a magnetic field, from a low-symmetry martensitic phase to a high-symmetry austenitic phase. Moreover, it is observed only within the temperature hysteresis loop of the magnetostructural phase transition. Such materials, despite the considerable MCE values under a single application of the magnetic field, are unpromising due to a strong change in the magnetocaloric properties in cyclic magnetic fields.

The study was supported by the Russian Science Foundation grant No. 22-19-00610 (<https://rscf.ru/en/project/22-19-00610/>).

- [1] B. Yu et al., *International Journal of Refrigeration*, **33** (2010) 1029.
- [2] A.G. Gamzatov et al., *Appl. Phys. Lett.*, **113** (2018) 172406.
- [3] A.G. Gamzatov et al., *J. Mater. Sci.*, **56** (2021) 15397.
- [4] A.G. Gamzatov et al., *J. Mater. Sci.*, **58** (2023) 8503.

## MAGNETIC PROPERTIES OF Fe<sub>3</sub>(Al, Ga) ALLOYS: *AB INITIO* STUDY

*Matyunina M.V., Zagrebin M.A., Sokolovskiy V.V., Buchelnikov V.D.*

Chelyabinsk State University, Chelyabinsk, Russia

miczag@mail.ru

Intermetallic Fe-based phases have attracted a lot of attention owing to their unusual mechanical, electrical and magnetic properties [1]. Fe-Al alloys are well-known materials that exhibit a good oxidation and sulfidation resistance, excellent resistance to abrasive wear and erosion, high strength, relatively low density and high magnetic permeability [2]. The Fe-Ga alloys are successful magnetostrictive materials, which demonstrated two peaks of saturation magnetostriction  $\lambda_{001}$  and make it possible to consider these materials as an alternative to high-magnetostriction rare-earth magnets [1,2]. After the discovery of giant magnetostriction in Fe-Ga alloys in the early 2000s other Fe-based alloys particular Fe-Al have been investigated in more detail. Compared with pure Fe, the tetragonal magnetostriction  $\lambda_{001}$  of these alloys increases fivefold as the Al content [2]. Nevertheless, the  $\lambda_{001}$  values for Fe-Al are smaller compared to the Fe-Ga system. The magnetic properties and phase diagram of Fe-(Ga Al) [1, 2] alloys have been studied by many investigators, however despite 20 years of efforts, the reasons for the formation of giant magnetostriction, for example, in Fe-Ga alloys, remain not fully understood and explained. In this work, magnetic properties are studied using various approaches and exchange-correlation functionals in the framework of the density functional theory.

To perform *ab initio* calculations, the projected augmented wave and Korringa-Kohn-Rostoker (KKR) methods implemented in the VASP [3] and SPR-KKR [4] codes were employed. For the exchange-correlation functional, the generalized gradient approximation (GGA) in the scheme of Perdew, Burke, and Ernzerhof [5] and meta-GGA SCAN [6] were applied. Magnetic exchange constants  $J_{ij}$  were calculated with the help of two approaches. The first is based on the KKR Green's function method implemented in SPR-KKR code, and the second one is based on the Green's function method with the local rigid spin rotation treated as a perturbation. To do this, the maximally-localised Wannier functions were firstly calculated by the Wannier90 code [7]. As you can see from Figure 1 obtained results for Fe<sub>3</sub>Ga in L1<sub>2</sub> phase in good agreement with each other.

This work was supported by the Ministry of Science and Higher Education of the Russian Federation within the framework of the State Assignment under contract No. 075-01493-23-00.

- [1] I.S. Golovin et al., *Phys. Metals Metallogr.*, **121** (2020) 851-893.
- [2] A.M. Balagurov and I.S. Golovin, *Phys.-Usp.*, **64** (2021) 702.
- [3] G. Kresse and D. Joubert, *Phys. Rev. B*, **59** (1999) 1758.
- [4] H. Ebert et al., *Rep. Progr. Phys.*, **74** (2011) 096501.
- [5] J.P. Perdew et al., *Phys. Rev. Lett.*, **77** (1996) 3865.
- [6] J. Sun et al., *Phys. Rev. Lett.*, **115** (2015) 036402.
- [7] G. Pizzi et al., *J. Phys. Condens. Matter*, **32** (2020) 165902.

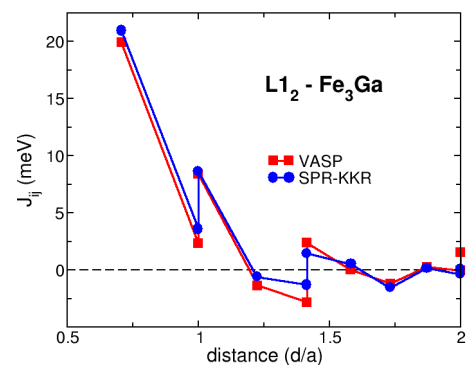


Figure 1. Magnetic exchange constants of Fe<sub>3</sub>Ga in L1<sub>2</sub> phase as function of distance, obtained via different methods.

## THE METAMAGNETIC PHASE TRANSITION EVOLUTION IN FeRh SYSTEM

*Komlev A.S.<sup>1</sup>, Makarin R.A.<sup>1</sup>, Seleznev M.S.<sup>1</sup>, Vashchenkova A.R.<sup>1</sup>, Ilina T.S.<sup>2</sup>, Chirkova A.M.<sup>3</sup>, Kulesh N.A.<sup>4</sup>,  
Volegov A.S.<sup>4</sup>, Zverev V.I.<sup>1</sup>, Kiselev D.A.<sup>2</sup>, Perov N.S.<sup>1</sup>*

<sup>1</sup> Lomonosov Moscow State University, Moscow, Russia

<sup>2</sup> National University of Science and Technology “MISiS”, Moscow, Russia

<sup>3</sup> TU Darmstadt, Institute for Materials Science, Darmstadt, Germany

<sup>4</sup> Ural Federal University, Yekaterinburg, Russia

komlev.as16@physics.msu.ru

Materials with first-order magnetostructural phase transitions exhibit complex transition mechanisms due to the interdependence of magnetic, structural, and electronic properties. Understanding the driving forces behind these transitions can be challenging. However, the correlation between physical properties in such materials leads to anomalous effects like giant magnetocaloric effect, colossal magnetoresistance, and giant magnetostriction. These effects have practical applications in refrigeration, spintronics, energy harvesting, medicine, and information recording [1,2]. The origin of these effects remains unresolved, hindering their full exploration. At the moment, it is necessary to study in detail the various features of the first-order magnetic phase transitions in order to step by step draw up a complete picture.

The binary FeRh alloy, with a near-equiatomic stoichiometric composition, serves as a fascinating model for analyzing first-order magnetic phase transitions. This alloy undergoes an antiferromagnetic-ferromagnetic phase transition around room temperature, maintaining cubic symmetry in its crystal lattice throughout the transition. FeRh alloys have demonstrated exceptional values for various effects, facilitating experimental results and accurate interpretation. Notably, the long-term magnetization relaxation near the phase transition temperature has attracted significant attention [2], highlighting its importance in understanding the system.

This study focuses on investigating the phase transition evolution from the antiferromagnetic to the ferromagnetic state in the FeRh alloy. The objects of study include alloys with varying volume content of the paramagnetic gamma phase and thin films, which experience different mechanical stresses that significantly influence the growth of the magnetic phase during the transition [3]. The research reveals distinct stages of ferromagnetic phase nucleation and growth: (I) primary nucleation, (II) surface nucleation and growth, (III) growth and merging of ferromagnetic clusters, and (IV) pinning of the antiferromagnetic phase near the localization of the gamma phase. Additionally, the study differentiates between the surface and bulk growth stages of the ferromagnetic phase within the bulk sample. The reliability of the findings is supported by consistent results from vibrational magnetometry, Kerr and magnetic force microscopy. However, further investigation is required to explore the detailed mechanisms of the phase transition and the dynamics of ferromagnetic phase nucleation for alloys with different compositions.

The authors acknowledge support from Russian Ministry of Science and Education grant No. 075-15-2021-1353. Komlev A.S. thanks the BASIS Foundation for scholarship support.

[1] F. Albertini et al., *Energy Procedia*, **142** (2017) 1288–1293.

[2] A.S. Komlev et al., *JALCOM*, **874** (2021) 159924.

[3] L.I. Vinokurova, A.V. Vlasov, M. Pardavi-Horváth, *Phys. Stat. Sol. (b)*, **78** (1976) 353–357.

## ELECTRONIC STRUCTURE AND MAGNETIC PROPERTIES OF Fe<sub>2</sub>Cr<sub>0.5</sub>Ti<sub>0.5</sub>X (X = Al, Ga) HEUSLER ALLOYS

*Murtaẓin A.A.<sup>1</sup>, Inerbaev T.M.<sup>1,2</sup>, Bogach A.V.<sup>3</sup>, Abuona A.<sup>2</sup>, Seredina M.A.<sup>1</sup>, Chatterjee R.<sup>4</sup>, Khovaylo V.V.<sup>1</sup>*

<sup>1</sup> National University of Science and Technology “MISIS”, Moscow, Russia

<sup>2</sup> L.N. Gumilyov Eurasian National University, Astana, Kazakhstan

<sup>3</sup> Prokhorov General Physics Institute, Russian Academy of Sciences, Moscow, Russia

<sup>4</sup> Indian Institute of Technology Delhi, New-Delhi, India  
khovaylo@misis.ru

Half-metallic materials are predicted to exhibit a high (reaching 100%) spin polarization at the Fermi level. Among the variety of such materials exhibiting the half-metallic behavior is the family of Heusler alloys with general formula X<sub>2</sub>YZ (X, Y are transition metals, Z is an s-p element). The use of such materials in spintronic devices makes it possible to increase the recording density and, at the same time, to reduce the size of devices. Among such materials, compensated ferrimagnets represent a new class of materials, perspective for the applications in the field of spintronics.

Theoretical calculations suggest that it is possible to obtain the half-metallic materials based on X<sub>2</sub>YZ Heusler alloys which obey the Slater-Pauling rule; - namely, when the total magnetic moment  $M_t$  is related to the number of valence electrons  $N_V$  as  $M_t = N_V - 24$ . This approach implies that the Heusler compounds with  $N_V = 24$  should have zero magnetic moment.

Considering Fe<sub>2</sub>-based Heusler alloys, this rule is valid for Fe<sub>2</sub>VAl, which is a well-known thermoelectric materials [1]. In order to extend this approach for another representatives of the Fe<sub>2</sub>-based Heusler alloys, we performed theoretical and experimental study of Fe<sub>2</sub>Cr<sub>0.5</sub>Ti<sub>0.5</sub>X (X = Al, Ga) alloys, which satisfy the  $N_V = 24$  condition.

Results of the first-principles calculations have shown that, indeed, the electronic structure of the Fe<sub>2</sub>Cr<sub>0.5</sub>Ti<sub>0.5</sub>X (X = Al, Ga) Heusler alloys resembles the electronic structure of a gapless semiconductor with zero magnetic moment. Experimentally studied magnetic properties of these alloys confirmed the absence of a long-range magnetic ordering down to 4.2 K, which is in a sharp contrast with the well-defined ferromagnetism of the parent Fe<sub>2</sub>CrX compounds, whose Curie temperature  $T_C$  exceeds 300 K [2]. However, a deviation of the inverse magnetic susceptibility curve of the studied Fe<sub>2</sub>Cr<sub>0.5</sub>Ti<sub>0.5</sub>X alloys from the Curie-Weiss law suggests that short-range magnetic correlations make a significant contribution to magnetic properties of these compounds. Hence, it can be concluded that the degree of the L2<sub>1</sub> superstructural ordering can strongly modify magnetic properties of the Fe<sub>2</sub>Cr<sub>0.5</sub>Ti<sub>0.5</sub>X Heusler alloys.

Support by Russian Science Foundation (grant No. 21-42-00035) is acknowledged.

[1] I. Galanakis, *In Heusler Alloys: Properties, Growth, Applications* (Springer, 2016).

[2] R.Y. Umetsu et al., *Jalcom*, **528** (2012) 34-39.

## SEARCH FOR THE NEW APPROACHES TO NEW GENERATION OF CRYOGENIC AND SUPERCONDUCTING TECHNOLOGY BASED ON PHASE TRANSITIONS IN MAGNETIC FIELDS

*Shavrov V.G.<sup>1</sup>, Bychkov I.V.<sup>2</sup>, Koledov V.V.<sup>1</sup>, Kamantsev A.P.<sup>1</sup>, Karpukhin D.A.<sup>1</sup>, Kolesov K.A.<sup>1</sup>,  
Kosbikid'ko Yu.S.<sup>1</sup>, Kuznetsov A.S.<sup>1</sup>, Kuzmin D.A.<sup>2</sup>, Mashirov A.V.<sup>1</sup>, Petrov A.O.<sup>1</sup>, Prokunin A.V.<sup>1</sup>,  
Suslov D.A.<sup>1</sup>, Taskaev S.V.<sup>2</sup>, Utarbekova M.V.<sup>2</sup>*

<sup>1</sup> Kotelnikov IRE RAS, Moscow, Russia

<sup>2</sup> Chelyabinsk State University, Chelyabinsk, Russia

shavrov@cplire.ru

Nowadays, the research on the magnetocaloric effect (MCE) has gained wide acceptance around the world due to its potential application as solid-state magnetic materials for highly efficient cooling at room temperature. Recently, the authors of the report proposed a new concept for the study and application of magnetocaloric materials, which involves the creation and study of advanced solid-state magnetic cooling systems for maintaining high-efficiency superconducting sources of a strong magnetic field. It is proposed to study in strong magnetic fields, in a wide temperature range, magnetic and magnetostructural phase transitions and magnetocaloric properties of new materials based on alloys based on 3d and 4f metals and permanent superconducting magnets based on high-temperature superconductors. Based on new knowledge about the properties of these materials in strong magnetic fields, magnetic cooling cycles should be experimentally reproduced and studied, and strong magnetic fields and superconductivity should be maintained by cryogenic solid-state magnetic cooling technology using the studied functional materials. The new principles of magnetic solid state cooling are also very promising for creating low temperatures and strong magnetic fields for microelectronics, medicine, energy, magnetic transport, and many other areas.

This report will review the current results of the search for a solutions to the problem of efficient conversion of thermal energy into other forms using the so-called solid-state caloric materials, in which strong effects of temperature and entropy changes in external fields are observed: MCE, electrocaloric, elastocaloric and others, in order to achieve an extremely high level of the coefficient of conversion of thermal energy into other forms and vice versa. In particular, the new experimental methods for studying magnetocaloric cooling processes in strong magnetic fields up to 10 T and new solid-state elements and refrigerator systems in the cryogenic temperature range will be presented.

The main scientific and engineering problems along this path will be discussed: the relatively low magnetic-field-induced temperature changes even of the best solid-state magnetocaloric materials, which leads to the use of multi-stage systems, the limitations of the maximum frequency of solid-state refrigeration cycles associated with the maximum achievable cooling capacity, the design of a variable superconducting strong magnetic sources, the poor efficiency heat exchange systems at cryogenic temperatures etc.

This work was supported by the Russian Science Foundation, grant No. 20-19-00745-P.

**July 2**

16:00 - 18:15

Sunday

ORAL  
SESSIONS II

Section C  
**Theory**

## THE JAHN-TELLER EFFECT IN CASE OF HEAVY TRANSITION METAL IONS

*Streltsov S.V.<sup>1</sup>, Temnikov F.<sup>1</sup>, Kugel K.I.<sup>2</sup>, Khomskii D.I.<sup>3</sup>*

<sup>1</sup> M.N. Mikheev Institute of Metal Physics UB of RAS, Yekaterinburg, Russia

<sup>2</sup> Institute for Theoretical and Applied Electrodynamics, Moscow, Russia

<sup>3</sup> University of Cologne, Cologne, Germany

streltsov.s@gmail.com

The Jahn-Teller effect is one of the most fundamental phenomena important not only for physics but also for chemistry and material science. Solving the Jahn-Teller problem and taking into account strong electron correlations we show that quantum entanglement of the spin and orbital degrees of freedom via spin-orbit coupling strongly affects this effect. Depending on the number of  $d$ -electrons, it may quench (electronic configurations  $t^2_{2g}$ ,  $t^4_{2g}$ , and  $t^5_{2g}$ , partially suppress  $t^1_{2g}$ , or, in contrast, induce ( $t^3_{2g}$ ) Jahn-Teller distortions. Moreover, in certain situations, interplay between the Jahn-Teller effect and spin-orbit coupling promotes formation of the “Mexican hat” energy surface facilitating various quantum phenomena [1,2]. We will also discuss Jahn-Teller physics in various different classes of material including, but not restricting to 1D chain-like structures, double and quadrupolar perovskites etc. [3,4]

Support by Russian Science Foundation 23-12-00159 is acknowledged.

[1] S.V. Streltsov, D.I. Khomskii, *Phys. Rev. X*, **10** (2020) 031043.

[2] S.V. Streltsov et al., *Physical Review B*, **105** (2022) 205142.

[3] G.S. Thakur et al., *Angewandte Chemie*, **60** (2021) 16500.

[4] S.V. Streltsov unpublished.

## OVERHAUSER EFFECT AND SOLID EFFECT IN AS AND P DOPED SILICON IN STRONG MAGNETIC FIELDS AND LOW TEMPERATURES

*Grabar V.A., Lifshits M.B., Averkiev N.S.*

Ioffe Institute, St.-Petersburg, Russia  
averkiev@les.ioffe.ru

Dynamic nuclear spin polarization (DNP) of single impurities occurs in crystals under EPR conditions. Depending on the type of excited transitions, the Overhauser effect and the solid effect are distinguished. The excitation of allowed transitions with electron spin flip and nuclear spin conservation leads into the Overhauser effect. While pumping transitions with a simultaneous change in the projections of the spins of the nucleus and electron (flip-flop transitions) gives the solid effect. The emergence of a nonequilibrium, but stationary, polarization of nuclei is possible due to the presence of a superfine interaction between the spin of the impurity nucleus and the spin of the charge carrier localized on it. A significant difference in the times of the charge carrier spin-lattice relaxation and the flip-flop transition is also required. The hyperfine interaction is leading to the splitting of the EPR lines in a magnetic field. Without considering flip-flop transitions, states with different spin projections of nuclei in a magnetic field are occupied equally, since the dependence of their occupation on the external magnetic field may be neglected due to the small value of the nuclear Bohr magneton. In the presence of flip-flop transitions, the Boltzmann factor determines the occupation of states with different projections of the electron and nuclear spins. In an external alternating field under stationary conditions, the occupation of states with various nuclear spin projections changes and, consequently, changes the equilibrium occupation of nuclear sublevels.

A feature of the considered DNP effect is the magnitude of the external dc magnetic field and temperature. Under standard EPR conditions, magnetic fields and temperature ensure that the various spin sublevels of a charge carrier are roughly equally occupied, and then the magnitude of the nuclear polarization is small, and a high pump intensity is needed to reach it. In recent experiments [1,2] on silicon crystals doped with P and As a large value of nuclear polarization was observed at temperatures below 1K. We have analyzed the results of these experiments and found the characteristic relaxation times. It is shown that the time of a stationary nuclear polarization establishment is determined by the flip-flop transition time, but at low temperatures these times differ by two orders of magnitude. Considering the difference in the times of spin-lattice relaxation and flip-flop transitions, the equations of nuclear dynamics for these impurities are compiled, it is revealed that the main mechanism of flip-flop transitions is the modulation of the electron g-factor by acoustic phonons. The reason for spin-lattice relaxation is the deformation interaction of a localized electron with longitudinal and transverse acoustic phonons. These conclusions are made based on the analysis of the temperature and field dependences of the EPR signals for different lines and excitation conditions.

The work was supported by the Russian Science Foundation (project 22-12-00139).

[1] W. Knap et al., *Terahertz enhancement of dynamic nuclear polarization in semiconductors*, in: *RJUSE-TeraTech-2021*.

[2] J. Järvinen et al., *Applied Magnetic Resonance*, **48** (2017) 473–483.

## MAGNETIC SUSCEPTIBILITY AND SHORT-RANGE ORDER IN METALS ABOVE THE CURIE TEMPERATURE: A DSFT STUDY

*Melnikov N.B.<sup>1</sup>, Gulenko A.S.<sup>1</sup>, Reser B.I.<sup>2</sup>*

<sup>1</sup>Lomonosov Moscow State University, Moscow, Russia

<sup>2</sup>M.N. Mikheev Institute of Metal Physics UB of RAS, Yekaterinburg, Russia

melnikov@cs.msu.ru

Experiment in ferromagnetic metals shows that near the Curie point the inverse paramagnetic susceptibility  $\chi^{-1}(T)$  deviates from the linear Curie–Weiss law [1]. In models with *localized* spins, this deviation is explained by the cluster formation above the Curie temperature  $T_C$ . In metals, most of the first-principles calculations produce almost no deviation of the inverse susceptibility from the Curie–Weiss law.

We present results in the dynamic spin-fluctuation theory (DSFT) [2], which takes into account both quantum nature and nonlocal character of spin fluctuations (Figs.1 and 2). We show that the susceptibility and correlation radius have a power-law behavior at temperatures up to 1.1–1.15  $T_C$ , which gives an estimate for the region of critical temperatures in metals. The critical exponents for Fe, Co and Ni obtained in the DSFT give an appreciable improvement compared to the predictions

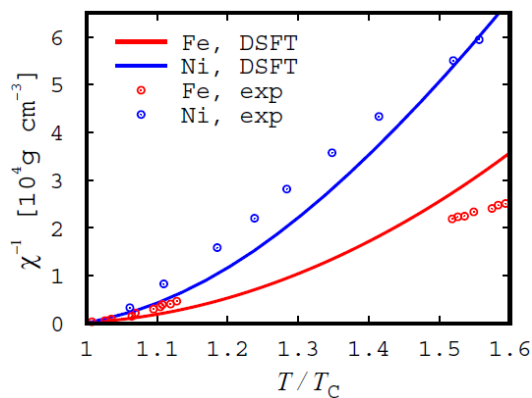


Figure 1. Inverse paramagnetic susceptibility  $\chi^{-1}(T)$  of Fe and Ni calculated in the DSFT.

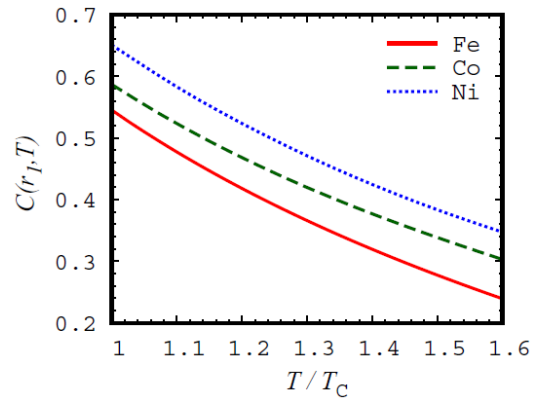


Figure 2. Correlation function  $C(r_l, T)$  for the nearest-neighbor atoms in Fe, Co and Ni as a function of reduced temperature.

of the Ginzburg–Landau theory and are in reasonable agreement with experiment [3]. As for the DSFT correlation function  $C(r, T)$ , near  $T_C$  it is close to the Ornstein–Zernike function and can be used to describe small-angle critical neutron scattering. At higher temperatures,  $C(r, T)$  gives a good description of the spin correlations at interatomic distances and allows us to estimate the magnetic short-range order in metals above  $T_C$  [4,5].

The research was carried out within the state assignment of Ministry of Science and Higher Education of the Russian Federation (theme “Electron” No. 122021000038-7).

[1] U. Köbler, *J. Magn. Magn. Matter*, **453** (2018) 17-29.

[2] N.B. Melnikov, B.I. Reser, *Dyn. Spin Fluct. Theory of Met. Magn.* (Berlin: Springer, 2018).

[3] N.B. Melnikov, A.S. Gulenko, B.I. Reser, *JETP*, **136** (2023) 26-30.

[4] N.B. Melnikov, B.I. Reser, *J. Magn. Magn. Matter*, **397** (2016) 347-351.

[5] N.B. Melnikov, G.V. Paradezhenko, B.I. Reser, *J. Magn. Magn. Matter*, **525** (2021) 167559.

## MAGNETIC PROPERTIES OF BROADENED LANDAU LEVELS AT THE SADDLE POINT ENERGY OF TWO-DIMENSIONAL LATTICE

*Nikolaev A.V.<sup>1</sup>, Zhuravlev M.Ye.<sup>2</sup>*

<sup>1</sup> SINP Lomonosov Moscow State University, Moscow, Russia

<sup>2</sup> St. Petersburg State University, St. Petersburg, Russia

nikolaev@srd.sinp.msu.ru

Studying the magnetic characteristics of the two dimensional (2D) lattice (hexagonal, graphene-like [1,2] and the square one [3]) by solving numerically the exact system of discrete equations, which fully describes the broadening of Landau levels, we have found that the energy spectrum of the Landau level at the energy of the saddle point (which is also known as a Van Hove peak) is principally continuous, so that even in a very small magnetic field this Landau level is always broadened in a miniband. In contrast to that, at other energies in a weak magnetic the spectrum of Landau levels is discrete. At the energy of the saddle point of the Brillouin zone the corresponding density of states  $N(EF)$  is formally infinite ( $N(EF) \rightarrow +\infty$ ).

We then consider the 2D square lattice [3], used as a prototype electron system in which the Fermi level lies exactly at the Van Hove peak. According to the electron band treatment this could lead to a formally divergent paramagnetic susceptibility and an infinite electron contribution to the specific heat at zero temperature. Our accurate analysis shows that both values remain finite. Taking into account the electron spin polarization and the obtained numerical solution, we reproduce the temperature dependence of the induced magnetic moment proportional to the magnetic susceptibility, and the electron contribution to the specific heat. Both plots demonstrate unusual dependencies reflecting the “metal”-like or “insulator”-like structure of the Landau minibands in the neighborhood of the Fermi energy. At low temperatures all quantities display oscillatory behavior. We also prove rigorously that the fully occupied electron band has no contribution to the diamagnetic susceptibility and specific heat [1,2,3].

[1] A.V. Nikolaev, *Phys. Rev. B*, **104** (2021) 035419.

[2] A.V. Nikolaev, *Phys. Rev. B*, **105** (2022) 039902.

[3] A.V. Nikolaev, M.Ye. Zhuravlev, *JMMM*, **560** (2022) 169674.

## EFFECTIVE SPIN FILTERING IN CORRELATED SEMICONDUCTOR NANOSTRUCTURES

*Mantsevich V.N.<sup>1</sup>, Maslova N.S.<sup>1</sup>, Frolov D.S.<sup>2</sup>, Rozhansky I.V.<sup>2</sup>, Averkiev N.S.<sup>2</sup>*

<sup>1</sup> Lomonosov Moscow State University, Moscow, Russia

<sup>2</sup> Ioffe Institute, St-Petersburg, Russia

vmantsev@gmail.com

Nowadays spin-polarized electron transport in semiconductor nanostructures attracts great attention [1,2]. Among the major problems of general interest is the possibility of spin injection and spin filtering. The rapidly growing research field of spin electronics or spintronics covers various spin-dependent phenomena of both fundamental and practical importance. The most important and promising application of spin selectivity is the possibility to construct small size and denser universal memory with high speed and low power consumption. Two possible technologies for that are magnetic memory [3] and spin memory [4].

Here we come up with a new theoretical concept of an electrically controllable single-electron spin filter (polarizator) based on the exchange interaction in the system of interacting quantum dots or impurity atoms. The sign of the spin polarization of the current flowing through the device can be effectively controlled in two ways (i) by changing the applied bias and (ii) by tuning the tunnel coupling via an external gate.

The minimal realization involves three bound state levels coupled to the contact leads. One of these levels is occupied by a single electron with a certain spin and the two-electron occupation is prohibited by a strong on-site Coulomb repulsion. An exchange interaction is present in the system and is considered between the occupied energy level and one of the levels involved in the spin transport. Interestingly, while the spin polarization of this state is fixed, the sign of the single-electron current spin polarization flowing between the contacts through two consistent bound state levels can be switched.

The proposed system allows to tune the ration between the tunneling amplitude  $T$  and exchange energy  $J$ . It can be realized experimentally by means of the gate voltage (see Figure 1), so one can control the spin dependent tunneling and switch it from spin up to spin down by changing the coupling between the energy levels. It means that the considered system allows to realize an effective spin filtering. Moreover, tunneling currents flowing in the tunneling contact leads become spin-polarized.

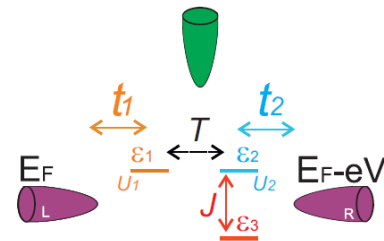


Figure 1. Scheme of the considered system.  $T$  is the tunneling transfer amplitude between single electron energy levels;  $U_{1(2)}$  is the on-site Coulomb repulsion;  $J$  is the exchange interaction between electrons localized in the energy levels 1 and 3.

Support by Russian Science Foundation # 22-12-00139.

- [1] D.D. Awschalom, D. Loss, N. Samarth, *Semiconductor Spintronics and Quantum Computation: Nanoscience and Technology* (Berlin: Springer, 2002).
- [2] I. Zutic, J. Fabian, S. Das Sarma, *Rev. Mod. Phys.*, **76** (2004) 323.
- [3] W. J. Gallagher, S. S. P. Parkin, *IBM J. Res. Dev.*, **50** (2006) 5.
- [4] Y. Huai, *AAPPS Bull.*, **18** (2008) 33.

## A TOY MODEL OF INDIRECT EXCHANGE INTERACTION IN DILUTED MAGNETIC SEMICONDUCTORS BEING IN INSULATING PHASE

*Kokurin I.A.*<sup>1,2</sup>, *Averkiev N.S.*<sup>1</sup>

<sup>1</sup> Ioffe Institute, Saint-Petersburg, Russia

<sup>2</sup> Mordovia State University, Saransk, Russia  
ivan.a.kokurin@gmail.com

At present, the question of the nature of the exchange interaction in dilute magnetic semiconductors (DMS) seems to be resolved. In  $\text{Ga}_{1-x}\text{Mn}_x\text{As}$  with  $x$  about a few percent, it is generally accepted that the indirect exchange is mediated by free holes in the spirit of the RKKY model [1]. However, now, DMS being at the insulating side of the metal-insulator transition (concentration of the magnetic constituent about  $10^{18}$ - $10^{20}$   $\text{cm}^{-3}$ ) are of great interest. In this case, weak ferromagnetism (Curie temperatures of the order of Kelvin) is mediated by holes localized at acceptors and is associated with a weak overlap of a hole wave functions. Such DMS are of interest at the creation of ferromagnet–superconductor hybrid structures [2], and the low temperature is not so critical, since it is also necessary for the transition to the superconducting state.

As in any problem of magnetism, we begin by considering the pairwise interaction of magnetic moments. For this purpose, a simplified model of two interacting magnetic centers is considered: one or two electrons are bound by the field of two paramagnetic ions (the magnetic analogues of the molecular hydrogen ion  $\text{H}_2^+$  and the hydrogen molecule  $\text{H}_2$ ). For simplicity, we consider the case of donors near the edge of a simple band with a scalar effective mass and paramagnetic ion with a minimum spin of  $1/2$ .

Both spectral problems can be solved analytically. The set of envelopes for the ground and first excited states of nonmagnetic complexes  $\text{D}_2^+$  and  $\text{D}_2^0$ , obtained by analogy with the molecular orbital method [3], is used as the initial basis. Further, the pair exchange interaction  $H_{ij} = -J(\mathbf{r}_i - \mathbf{R}_j) \mathbf{s}_i \mathbf{s}_j$  of each carrier ( $i=1$  or  $i=1,2$ ) with the magnetic shell of each center ( $j=A,B$ ) is taken into account. In both cases, problems  $16 \times 16$  can be diagonalized taking into account the conservation of the total spin (of 3 or 4 particles) projection onto the intercenter axis.

Depending on the sign of the one-center exchange constant, different spin structures of the ground state of the  $\text{D}_2^+$  and  $\text{D}_2^0$  magnetic complexes are possible. The dependences of the energy levels of the complexes on the intercenter distance  $R$  have been studied. These dependences demonstrate significantly different behavior for  $\text{D}_2^+$  and  $\text{D}_2^0$  magnetic complexes. Based on these dependences, estimates of the effective indirect exchange constants (Curie temperatures) and their dependence on the concentration of the magnetic component are obtained for both cases. Nevertheless, the presence of compensation in real samples [1] implies the simultaneous presence of both types of alignment (as in  $\text{D}_2^+$  and  $\text{D}_2^0$ ). This means that in order to find the Curie temperature, it is necessary to solve a many-body problem in the spirit of the Heisenberg model, taking into account the implementation of both types of two-center alignment and with the appropriate averaging over possible configurations. It should be also noted, that multicenter impurity complexes can manifest themselves in the optical properties of semiconductors [4].

Support from the Russian Science Foundation (Grant No. 22-12-00139) is acknowledged.

[1] T. Dietl and H. Ohno, *Rev. Mod. Phys.*, **86** (2014) 187.

[2] J. Linder and J.W.A. Robinson, *Nat. Phys.*, **11** (2015) 307.

[3] I.N. Levine, *Quantum chemistry, 4th ed.* (Prentice Hall, New Jersey, 1991).

[4] I.A. Kokurin, N.S. Averkiev, *Phys. Rev. B*, **107** (2023) 125208.

**July 2**

18:15 - 20:00

Sunday

POSTER  
SESSIONS

Section L1

**Spintronics and  
Magnetotransport**

## EQUIVALENT MODEL OF A FERRIMAGNET FOR MICROMAGNETIC SIMULATION

*Bazrov M.A., Antonov V.A., Namsaraev Zh.Zh., Letushev M.E., Ognev A.V., Samardak A.S., Steblyi M.E.*  
Far Eastern Federal University, Vladivostok, Russia  
steblyme@gmail.com

Ferrimagnetic media are promising candidates for the development of spintronics due to their high stability and efficiency of current-induced action [1,2]. One of the important tools of spintronics is micromagnetic simulation, which allows, on the one hand, to compare the results of experiments and simulations to analyze processes at the micromagnetic level, and, on the other hand, to predict possible processes. This approach has shown its usefulness in studying systems based on ferromagnets, but in the case of ferrimagnets, it is generally not applicable.

This work proposes an equivalent model that makes it possible to simulate ferrimagnets in standard software packages for ferromagnets. The applicability of the model is tested by comparing the simulation results with various experimental studies, which gives a qualitative agreement.

Using MuMax<sup>3</sup> software [3], three experiments typical for ferrimagnets were carried out: 1) the dependence of the resulting magnetization on the mutual concentration of atoms; 2) the dependence of the resulting magnetization on temperature; 3) the magnetic hysteresis loop in high fields. In the first case, to simulate the change in concentration, the saturation magnetization of the layers varies interdependently, which will allow us to define the standard dependence of the resulting magnetization passing through the compensation point.

The third experiment shows the simulation of the hysteresis loop in high fields. In small fields, the magnetization in the sublattices switches to the opposite direction, as a result, a rectangular loop is observed in the central part of the dependence. With a further increase in the field, the magnetic structure is in a stationary state: a sublattice with a large magnetic moment is aligned along the field, with a smaller one, in the opposite direction due to the antiferromagnetic exchange interaction. However, at a certain value, the external field becomes larger than the effective field of the exchange interaction, and the collinear ordering is violated in the system: the magnetization in the sublattice with a smaller magnetic moment begins to rotate smoothly along the field. The proposed two-layer model of a ferrimagnet makes it possible to qualitatively repeat the experimental dependences.

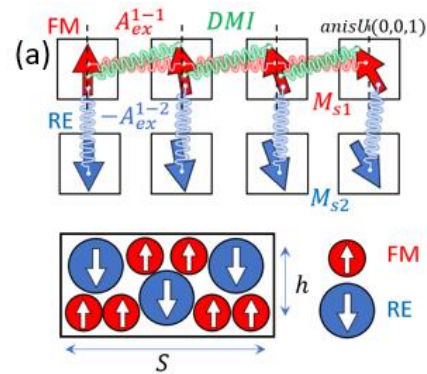


Figure 1. Schematic representation of the parameters taken into account for ferrimagnetic media.

This work was supported by the Russian Ministry of Science and Higher Education (State Task No. FZNS-2023-0012).

[1] G. Sala, P. Gambardella, *Adv. Mater. Interfaces*, **9** (2022) 2201622.

[2] K. Cai, Z. Zhu, H. Yang, *Nat. Electr.*, **3(37)** (2020).

[3] “The design and verification of mumax3”, *AIP Advances*, **4** (2014),107133.

2PO-L1-2

## SUBSTRATE INFLUENCE ON TERAHERTZ GENERATION IN FeCo THIN FILMS

*Bezvikonnyy N.<sup>1</sup>, Buryakov A.<sup>1</sup>, Andeev P.<sup>1</sup>, Tiercelin N.<sup>2</sup>, Mishina E.<sup>1</sup>, Preobrazhensky V.<sup>3</sup>*

<sup>1</sup> Department of Nanoelectronics, MIREA—Russian Technological University, Moscow, Russia

<sup>2</sup> Univ. Lille, CNRS, Centrale Lille, Univ. Polytechnique Hauts-de-France, UMR 8520 -IEMN, France

<sup>3</sup> Prokhorov General Physics Institute of RAS, Moscow, Russia  
bezvikonnyj@mirea.ru

In our study [1], we explored THz generation using a series of FeCo films with varying thicknesses and substrates. We determined a significant influence of the substrate type on the emitted THz radiation. Notably, we observed a significant increase in THz amplitude when utilizing a Si substrate. This relationship can be attributed to the pronounced disparity in refractive indexes between glass and Si substrates within the THz region.

Additionally, the two-temperature model of ultrafast demagnetization was utilized to study the system's out-of-equilibrium spin dynamics. This part was vital for validating the assumption about the linear relationship between THz amplitude and electron-spin system relaxation time, as posited in work [2].

However, during this research, we have discovered a non-linear dependency in the thin samples (5 nm and 10 nm) on Si substrates, specifically within the low optical fluence region. This observation can be elucidated by positing the presence of two distinct mechanisms of THz generation within thin structure. Under certain conditions, one of these mechanisms prevails over the other, which provides a plausible explanation for this non-linear dependency. For possible explanation to this phenomena we need to study mechanisms of generation and their parameters.

In order to gain a comprehensive understanding of the underlying mechanisms involved in THz generation, it is imperative to delve deeply into the generation of out-of-equilibrium spin states and their subsequent transformation into spin currents. Through the use of temperature models that account for ultrafast demagnetization, we can gain critical insights into these processes, thereby fostering the development of highly efficient spintronic emitters.

The study was supported by a grant from the Russian Science Foundation № 21-79-10353, <https://rscf.ru/en/project/21-79-10353/>.

[1] A. Buryakov et al., *Nanomaterials*, **13** (2023) 1710.

[2] R. Rouzegar et al., *Phys. Rev. B*, **106** (2022) 144427.

## DYNAMICS OF MAGNETIC VORTICES IN A SPIN-TRANSFER NANOOSCILLATOR

*Filippova V.V.<sup>1</sup>, Antonov G.I.<sup>1</sup>, Zvezdin K.A.<sup>2</sup>, Ekomasov E.G.<sup>1</sup>*

<sup>1</sup> Ufa University of Science and Technology (former Bashkir state university), Ufa, Russia

<sup>2</sup> General Physics Institute A.M. Prokhorov RAS, Moscow, Russia

EkomasovEG@gmail.com

The structure and dynamics of magnetization in a vortex spin-transfer nanooscillator (STNO), which is a three-layer spin-valve magnetic nanopillar, is studied during the passage of a spin-polarized current and the presence of an external magnetic field [1]. Using micromagnetic simulation in nanopillar with a small diameter, we studied the dynamic change in the vortices structure, the formation of the C-structure vortex state and edge vortices, the trajectory of movement and the time it takes to reach different dynamic modes [2]. The time needed for the vortices to reach different dynamic modes was found. The possibility of the dynamic generation of radial edge vortices without the presence of a Dzyaloshinsky field or an external inhomogeneous magnetic field is shown. We demonstrate that a vortex in a thick magnetic layer can be a generator of spin waves in a thin magnetic layer with an adjustable oscillation frequency. The effect of the thickness of a nonmagnetic layer on the coupled dynamics of two magnetic vortices in a spin torque nano-oscillator has been studied [3]. The thick permalloy magnetic layer has a thickness of 15 nm, the middle non-magnetic layer has a thickness in the first case of 12.5 and in the second 15 nm, and the thin permalloy magnetic layer has a thickness of 4 nm. Numerical calculation of the dynamics of magnetostatically coupled vortices was carried out using the software package SpinPM for micromagnetic modeling. The features of the vortex motion dynamic are studied for different thicknesses of the nonmagnetic interlayer. It is shown that in all cases of thickness of the nonmagnetic interlayer, three regimes of vortex dynamics are observed: the oscillations of magnetic vortices damped over time, the mode of stationary coupled oscillations of magnetic vortices, and regime, when vortices “leave” the edge of the disk. It is found that increasing in the thickness of the nonmagnetic layer leads to decreasing in the values of the first, second, and third critical currents.

For a STNO of large diameter, the effect of a large spin polarized current on the coupled dynamics of vortices in spin-transfer nanooscillators 400 nm in diameter has been studied. The effect of the appearance of new regions of stationary regimes of coupled oscillations of P- and AP-vortices has been discovered. A diagram of dependences of the frequency of stationary coupled oscillations of magnetic vortices on the spin of the polarized current has been constructed. The found effect can be used to increase the operating frequencies of spin-transfer nanooscillators of large diameters.

Support by assignment of Russian Federation for the implementation of Scientific Research by laboratories (#075-03-2021-193/5 30.09.2021) is acknowledged.

[1] K.A. Zvezdin, E.G. Ekomasov, *Phys. Metals Metallogr.*, **123** (2022) 201.

[2] S.V. Stepanov et al., *JMMM*, **562** (2022) 169758.

[3] V.V. Mukhamadeeva et al., *Letters on Materials*, **12** (4) (2022) 327-331.

## MICROWAVE SPIN-PUMPING FROM AN ANTIFERROMAGNET FEBO<sub>3</sub>

*Gabrielyan D.A.<sup>1,2</sup>, Volkov D.A.<sup>1,2</sup>, Safin A.R.<sup>1,2</sup>, Kalyabin D.V.<sup>1</sup>, Strugatsky M.B.<sup>3</sup>, Nikitov S.A.<sup>1,4,5</sup>*

<sup>1</sup> Kotelnikov IRE RAS, Moscow, Russia

<sup>2</sup> National Research University “MPEI”, Moscow, Russia

<sup>3</sup> V.I. Vernadsky Crimean Federal University, Simferopol, Russia

<sup>4</sup> Moscow Institute of Physics and Technology, Dolgoprudny, Moscow Region, Russia

<sup>5</sup> Saratov State University, Russia

davidgabrielyan1997@gmail.com

Recently, magnetic resonance-driven spin-pumping has been considered to be an excellent experimental technique for detecting spin currents in magnet-nonmagnet heterostructures. Firstly, demonstrated for ferromagnetic metals, this measurement technique has been extended to magnetic insulators and alloys [1]. More recently, with the extensive progress of high-frequency microwave technologies and great interest in antiferromagnets (AFMs), subterahertz spin-pumping has been demonstrated for different materials, such as Cr<sub>2</sub>O<sub>3</sub> [2], MnF<sub>2</sub>[3], and NiO [4]. In contrast, ways to generate spin-pumping voltage from noncollinear AFMs have not been widely considered yet.

In this paper, we explore experimentally spin-pumping in noncollinear AFM – iron borate FeBO<sub>3</sub> [5] with a strong Dzyaloshinskii-Moriya interaction (DMI) induced canting and capped with a heavy metal platinum layer. The induced inverse-spin Hall effect voltage is caused by the conversion of the spin current into a charge current in the platinum layer, which has a high spin-orbit interaction. Figure 1 shows the results of the measured ISHE voltage normalized by the actual RF power acting on the sample, taking into account the influence of irregularities in the amplitude-frequency characteristics of the microwave path. Our measurements show the presence of a resonance-type ISHE voltage signal, similar to those measured earlier on hematite [6,7], but with an order of magnitude smaller spectral linewidth.

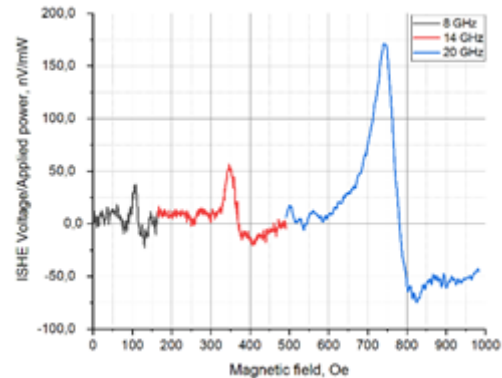


Figure 1. ISHE Voltage normalized by the actual RF power at various frequencies: 8, 14 and 20 GHz.

Experimental measurements were done by supporting the Russian Science Foundation grant No. 21-79-10396, and the processing of measurement results was supported by the Russian Science Foundation grant No. 23-79-00016.

- [1] V. Baltz et al., *Rev. Mod. Phys.*, **90** (2018) 015005.
- [2] J. Li et al., *Nature*, **578** (2020) 70.
- [3] P. Vaidya et al., *Science*, **368** (2020) 160.
- [4] P. Stremoukhov et al., *arXiv:2211.00353v1* (2022).
- [5] E. A. Mashkovich, *Phys. Rev. Lett.*, **123** (2019) 157202.
- [6] I. Boventer et al., *Phys. Rev. Lett.* **126** (2021) 187201.
- [7] H. Wang et al., *Phys. Rev. Lett.* **127** (2021) 117202.

## ELECTRIC-FIELD CONTROLLED SPINTRONIC THz EMITTER BASED ON A TWO-DIMENSIONAL SEMICONDUCTOR

*Gorbatova A.V.<sup>1</sup>, Buryakov A.M.<sup>1</sup>, Andeev P.Yu.<sup>1</sup>, Lebedeva E.D.<sup>1</sup>, Sapozhnikov M.V.<sup>2,3</sup>, Pasbenkin I.Y.<sup>2,3</sup>,  
Mishina E.D.<sup>1</sup>*

<sup>1</sup> MIREA - Russian Technological University, Moscow, Russia

<sup>2</sup> Institute for Physics of Microstructures RAS, Nizhny Novgorod, Russia

<sup>3</sup> Lobachevsky State University, Nizhny Novgorod, Russia  
gorbatova.anastasiya@mail.ru

Semiconductor spintronics represents a novel branch of spintronics devoted to the development of hybrid devices that combine semiconductor-based transistor logic and magnetic recording in a single architecture, and could perform several basic operations at once, such as logic, communication, storage and recording [1]. Efficient injection of spins from ferromagnetics into semiconductors constitutes a significant step towards the realization of semiconductor spintronic [2] and optospintronic [3] devices.

Among optospintronic applications, the most promising is the development of THz spintronic emitters [4]. Excitation a ferromagnetic/nonmagnetic material (metal or semiconductor) interface by ultrashort laser pulses leads to the generation of THz radiation [4,5]. In the case of a semiconductor, the charge current is formed only by high-energy spin-polarized electrons with an energy sufficient to overcome the band gap energy [5]. Moreover, the application of an electric field to a ferromagnetic/semiconductor heterostructure can be used to reduce the Schottky barrier and effectively modulate the spin current and THz radiation. A similar approach was first demonstrated in [6] in geometry with a planar electric field.

This manuscript introduces a study of the emission characteristics of THz radiation in the Co/WSe<sub>2</sub> heterostructure. Our results confirm the presence of spin current injection into a layer of an atomically thin semiconductor. We also demonstrate possibility of electric-field controlled amplitude modulation of THz signal. The observed effect exceeds 10%. In addition, our results are of high value for the development of spintronic THz generators based on heterostructures consisting of materials with spin-orbit interaction of Rashba type, such as two-dimensional semiconductor transition metal dichalcogenides (MoS<sub>2</sub>, WSe<sub>2</sub>, etc.).

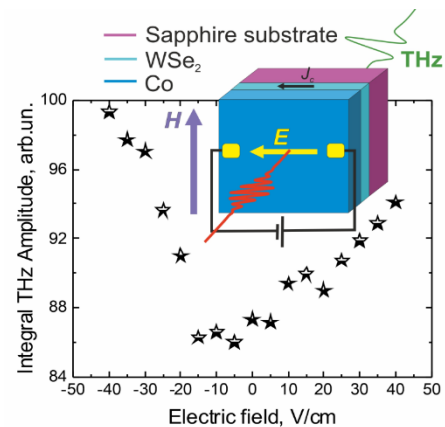


Figure 1. Electric field-controlled modulation of the THz amplitude in the Co/WSe<sub>2</sub> structure.

The study was supported by the Russian Science Foundation grant No. 23-19-00849 and the Ministry of Science and Education of RF (Project No.075-15-2022- 1131).

- [1] D.D. Awschalom and M. E. Flatté, *Nat. Phys.* **3** (2007) 153.
- [2] D. Bercioux and P. Lucignano, *Reports Prog. Phys.* **78** (2015) 106001.
- [3] V.I. Safarov et al., *Phys. Rev. Lett.* **128** (2022) 057701.
- [4] T.S. Seifert (Dictoral thesis, FU Berlin, 2017).
- [5] L. Cheng et al., *Nat. Phys.* **15** (2019) 347.
- [6] M. Chen et al., *Adv. Opt. Mater.* (2018) 1801608.

## VOLTAGE-CONTROLLED TOPOLOGICAL TRANSITIONS OF SPIN WAVES IN MAGNONIC CRYSTAL/PZT STRUCTURE

*Grachev A.A.<sup>1</sup>, Gorlach M.A.<sup>2</sup>, Beginin E.N.<sup>1</sup>, Sadovnikov A.V.<sup>1</sup>*

<sup>1</sup> Saratov State University, Saratov, Russia

<sup>2</sup> ITMO University, Saint Petersburg, Russia

Stig133@gmail.com

Systems based on semiconductor transistors are commonly used to generate, transmit, and process information signals. However, they have limitations that can be overcome by magnonics, a new trend in condensed matter physics based on the effects of electron spin transfer rather than charge transfer. This opens up new possibilities for the application of spin waves (SW) as elements of microwave and terahertz information processing, transmission, and storage devices [1,2]. Monocrystals and single-crystal films of yttrium iron garnet (YIG) are known to have very low attenuation constants and have long been used for experimental studies of spin-wave phenomena and the fabrication of spin-wave magnonic devices [3,4]. Arrays of YIG microstructures can be used to build magnonic networks for signal processing. In these networks, information is distributed through SW waveguides, and logical operations are based on the principles of spin-wave interference.

To develop more efficient magnonic devices, it is important to be able to control the transmission of spin waves by both electric and magnetic fields [5]. Synthetic multiferroic structures with two-dimensional deformations in the form of mechanically coupled magnetostrictive and piezoelectric layers are of particular interest for magnon straintronics [5,6].

This work will investigate the regularities of changes in the spin wave excitation spectrum in planar magnonic crystals under the influence of elastic deformations. Experimental and numerical methods will be used to determine the mechanisms controlling the electric field of the spatial and transmission properties of dipole spin waves in a single magnonic crystal with a piezoelectric layer.

The study will experimentally and numerically demonstrate the possibility of tuning the frequency band in the spectrum of spin waves due to distributed elastic deformations occurring at the interface between a magnonic crystal and a piezoelectric layer.

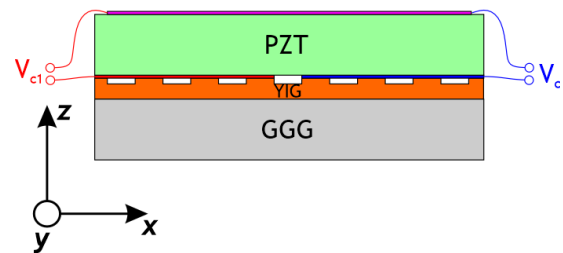


Figure 1. Scheme of magnonic crystal with piezoelectric layer.

This work was supported by a grant from the Russian Science Foundation (Project No. 23-79-30027).

- [1] A. Barman et al., *Journal of Physics: Condensed Matter*, **33(41)** (2021) 413001.
- [2] A.V. Chumak et al., *IEEE Transactions on Magnetics*, **58(6)** (2022) 1-72.
- [3] T. Goto et al., *Physical Review Applied*, **11(1)** (2019) 014033.
- [3] H. Qin, S. van Dijken, *Applied Physics Letters*, **116(20)** (2020) 202403.
- [4] A.A. Grachev, A.V. Sadovnikov, S.A. Nikitov, *Nanomaterials*, **12(9)** (2022) 1520.
- [5] A.A. Grachev et al., *Applied Physics Letters*, **118(26)** (2021) 262405.

## SPIN CURRENT AT THE INTERFACE OF $\text{La}_{0.7}\text{Sr}_{0.3}\text{MnO}_3$ EPITAXIAL FILM AND $\text{TbCo}_2\text{FeCo}$ NANOSTRUCTURE

*Klimov A.*<sup>1,2</sup>, *Volkov D.*<sup>1</sup>, *Gabrielyan D.*<sup>1</sup>, *Tiercelin N.*<sup>3</sup>, *Kalyabin D.*<sup>1</sup>, *Safin A.*<sup>1,4</sup>, *Nikitov S.*<sup>1,5</sup>

<sup>1</sup> Kotel'nikov Institute of Radioengineering and Electronics RAS, Moscow, Russia

<sup>2</sup> Russian University of Technology - MIREA, Moscow, Russia

<sup>3</sup> IEMN (CNRS UMR 8520), PRES Univ. Lille Nord de France, France

<sup>4</sup> National Research University "MPEI", Moscow, Russia

<sup>5</sup> Moscow Institute of Physics and Technology, Dolgoprudny, Moscow Region, Russia

Structures in which spin current generation is observed usually consist of two layers: a ferromagnetic (or ferroelectric) in which ferromagnetic resonance (FMR) is excited and a non-magnetic metal with strong spin-orbit interaction. The spin current is detected using the inverse spin Hall effect (ISHE) in the non-magnetic metal by converting it into a conduction current [1,2]. However, not only non-magnetic metals can be used as ISHE spin current detectors. In a number of papers, it has been shown that alloys such as permalloy  $\text{Ni}_{81}\text{Fe}_{19}$  as well as metals Fe, Co, Ni are also capable of converting spin current to a charge current [3-5].

Previously, we have presented the results of experimental studies of magnetoresistance (GMR) and ferromagnetic resonance (FMR) in uniaxial (EA) layered nanostructure  $\text{TbCo}_2\text{FeCo}/\text{La}_{0.7}\text{Sr}_{0.3}\text{MnO}_3$  [6]. The magnetic interaction between  $\text{La}_{0.7}\text{Sr}_{0.3}\text{MnO}_3$  and  $(\text{Tb}_2\text{CoFeCo})$  indicated an antiferromagnetic nature. In the  $\text{TbCo}_2\text{FeCo}/\text{Y}_3\text{Fe}_5\text{O}_{12}$  structure [7], the energy of exchange interaction between the layers has been determined, and the spin current flowing through their boundary has been recorded at the FMR frequency 9.0 GHz.

This report presents the results of measurements of the FMR spectrum and spin current characteristics in the  $\text{TbCo}_2\text{FeCo}/\text{La}_{0.7}\text{Sr}_{0.3}\text{MnO}_3$  heterostructure on an NGO substrate in the frequency range up to 20 GHz. Using the magneto-optical Kerr effect (MOKE), the direction of the hard magnetization axis (HA) along which the bias magnetic field was applied in subsequent high-frequency measurements was determined. The FMR was excited using a microstrip transmission line. The sample was placed on top of the line and pressed onto contact pads located on either side of the microstrip line [7]. A voltage proportional to the spin current was taken from the two contact pads.

The measured voltage is the sum of two components: the first appears due to the detection of an FMR signal from the sample at the contacts, and the second is due to the inverse spin Hall effect, which converts the spin current into an electric current. To separate these two contributions, voltage measurements were made at two oppositely directed external magnetic fields. Details of the measurement method and prospects for the use of the  $\text{TbCo}_2\text{FeCo}$  nanostructure in spintronics elements will be presented.

This work was supported by the Russian Science Foundation grant № 23-79-00016.

- [1] M.I. Dyakonov, V.I. Perel, *Phys. Lett. A*, **35** (1971) 459.
- [2] E. Saitoh, M. Ueda, H. Miyajima, G. Tatara, *Appl. Phys. Lett.*, **88** (2016) 182509.
- [3] B.F. Miao S.Y. Huang, D. Qu, C.L. Chien, *Phys. Rev. Lett.*, **111** (2013) 066602.
- [4] P. Hyde et al., *Phys. Rev. B*, **89** (2014) 180404(R).
- [5] F. Yang, P.C. Hammel, *J. Phys. D*, **51** (2018) 253001.
- [6] A.S. Grishin et al., *J. El. Mater.*, **47**(2018) 1595-1600.
- [7] T. A. Shaikhulov et al., *Physics of the Solid State*, **62** (2020) 1653–1658.

2PO-L1-8

## MAGNETIC AND STRUCTURAL PROPERTIES OF Pd(111)/Co/Pd AND Pd(100)/Co/Pd THIN FILMS

*Kuznetsova M.A., Turpak A.A., Kozlov A.G.*

Far Eastern Federal University, Vladivostok, Russia  
kuznetcova.mal@dvfu.ru

The main purpose of this study is to compare the magnetic characteristics of Pd/Co/Pd three-layer films grown on Si(111) and Si(100) monocrystal silicon substrates of different orientations. The study may be relevant due to the occurrence of spin-orbit interaction in the system with two heavy metal/ferromagnet interfaces. Such systems are characterized by the presence of interface effects, for example, the Dzyaloshinskii-Moriya effect, a strong SOT effect, etc. and can be used for the magnetic recording devices.

The source of the perpendicular magnetic anisotropy in the Pd(111)/Co(111)/Pd(111) system grown on the Si(111) substrate is the stress at the interface caused by the mismatch between the Pd and Co lattices and electronic effects at the interfaces [1]. In this study the epitaxy of follow layers grown on a Si(100) substrate was study. The high-speed electron diffraction was used. We observed that the perpendicular magnetic anisotropy is grow with the roughness of the Pd(100) layer on Cu(10ML)/Si(100). The roughness was observed by a scanning tunneling microscope. Previous studies have shown three main steps in the growth process of palladium on a buffer layer: surface alloying (strains relaxation), layer-by-layer and 3D island strains growth [2]. But we a expect that the growth processes will be different for 7x7 and 2x1 surfaces.

The samples were grown in ultra-high vacuum system by Omicron Nanotechnology (vacuum value is about 10–8 Torr). The samples have a variable thickness of the palladium seed layer and a constant thickness of cobalt and top palladium layers. The thicknesses were controlled by a quartz thickness monitor. The magnetic properties of the films were measured by the vibrating sample magnetometer in two directions of the magnetic field. The dependences of the magnetic characteristics on the thickness of the ferromagnetic layer in order to determine the contribution to the effective magnetic anisotropy (surface and volume).

This work was supported by the Russian Ministry of Science and Higher Education (State Task No. FZNS-2023-0012)

[1] A.V. Davydenko et al., *Physical Review B*, **95(6)** (2015) 064430.

[2] A.V. Davydenko et al., *Applied Surface Science*, **384** (2016) 406-412.

## DEVELOPMENT AND TESTING OF A MAGNETIC TUNNEL JUNCTION COMPACT MODEL IN VERILOG-A TO USE IN CAD SYSTEM

*Lobkova M.D.<sup>1</sup>, Skirdkov P.N.<sup>1,2</sup>, Zvezdin K.A.<sup>1,2</sup>*

<sup>1</sup>New Spintronic Technologies, Moscow, Russia

<sup>2</sup> Prokhorov General Physics Institute of RAS, Moscow, Russia

m.shkanakina@nst.tech

The rapid industrial development of spintronic devices based on magnetic tunnel junctions (MTJ) dictates the need to create behavioral simulation model, that makes it possible to co-design hybrid spintronic-electronic circuits. In this work, we present a compact model of magnetic tunnel junction in Verilog-A language, which allows to simulate various spintronic devices such as TMR-sensors [1], MRAM (STT-MRAM) [2], nanogenerators and spin-torque diodes [3]. Compatibility of the compact model with computer-aided design (CAD) systems and scalability to various technological nodes will allow circuit designers to combine and analyze the operation of complementary metal-oxide-semiconductor (CMOS) transistors with spintronics cells.

In the simple case magnetic tunnel junction consists of two ferromagnetic layers, separated by an isolator. The bottom ferromagnetic layer has a fixed magnetization and is usually referred as a polarizer, and the top ferromagnetic layer with variable magnetization is called a free layer. The compact model (Figure 1) of such device simulates the magnetization dynamics as a function of the external field, device anisotropy, magnetostatic field, spin-transfer-torque (STT) and thermal induced fields. The developed model is based on the macrospin approximation [4] of the stochastic Landau-Lipschitz-Gilbert-Slonczewski equation and allows to convert the magnetization dynamics properties of MTJ to electrical characteristics using the tunnel magnetoresistance (TMR) module.

To verify the model, several tests were developed and performed in simulation platform Cadence Virtuoso, corresponding to the main operating modes of MTJ: switching, generation, and rectification.

This work was supported by Russian Science Foundation (grant # 19-12-00432).

- [1] J. Lenz, A. Edelstein, *IEEE Sens. J.*, **6** (2006) 631–649.
- [2] S. I. Kiselev et al., *Nature*, **425** (2003) 380.
- [3] A. Tulapurkar et al., *Nature*, **438** (2005) 339.
- [4] J. C. Slonczewski, *J. Magn. Magn. Mater.* **159** (1996) L1.

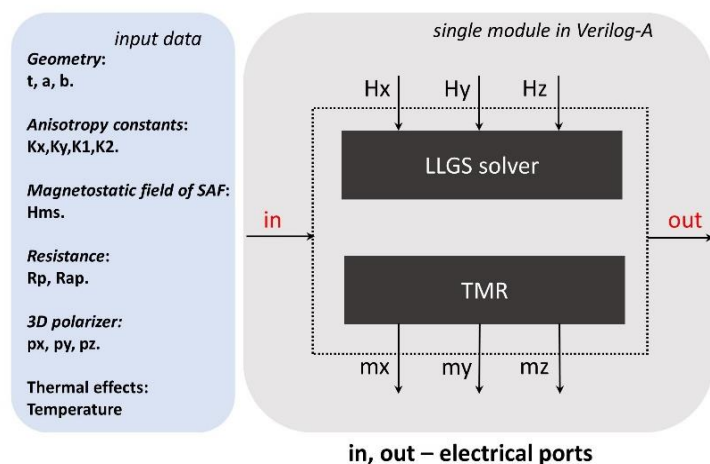


Figure 1. MTJ modeling framework.

## EVOLUTION OF THE SKYRMION LATTICE IN MnGe-BASED COMPOUNDS UNDER HIGH PRESSURE

*Skanchenko D.O.<sup>1,2</sup>, Altynbaev E.V.<sup>1,2,3</sup>, Heinemann A.<sup>4</sup>, Martin N.<sup>5</sup>, Grigoriev S.<sup>1</sup>, Tsvyashchenko A.<sup>2</sup>*

<sup>1</sup> NRC «Kurchatov Institute» - PNPI, Gatchina, St-Petersburg, Russia

<sup>2</sup> Institute for High Pressure Physics, Troitsk, Moscow, Russia

<sup>3</sup> Saint-Petersburg State University, Saint Petersburg, Russia

<sup>4</sup> Helmholtz Zentrum Geesthacht, Geesthacht, Germany

<sup>5</sup> Laboratoire Leon Brillouin, CEA Saclay, Gif-sur-Yvette Cedex, France

skanchenko\_do@pnpi.nrcki.ru

We have grown  $Mn_{1-x}Fe_xGe$  compounds with  $x = 0.1$  and  $0.3$  using high pressure synthesis [1]. The appearance of the skyrmion lattice (SkX) in MnGe-based compounds with Fe-replacement of Mn atoms was observed under external magnetic field within the wide field range at temperatures far below  $T_C$  [2]. The increase of the field range of its presence is accompanied by the linear increase of the DMI in  $Mn_{1-x}Fe_xGe$  with increase of Fe concentration [3-5]. The temperature range of the presence of the SkX is most likely connected to the intrinsic instability of the magnetic structure found for MnGe and Fe-doped compounds [6].

Here we report on the evolution of the magnetic system of the  $Mn_{1-x}Fe_xGe$  compounds with  $x = 0.1$  and  $0.3$  under external magnetic field and quasi-hydrostatic pressure up to 1.0 GPa. As the result the (H-T) phase diagram has been plotted for each compound.

With pressure increase all of the critical fields increases at low temperatures for both compounds, while the ordering temperature decreases. The temperature and field ranges of the existence of the SkX decreases with pressure increase. We believe that these facts are connected to the stabilization of the magnetic structure of MnGe-based compounds under pressure. This process is opposite to the Fe-replacement of Mn atoms despite the fact that the lattice constant continues to decrease.

Support by the Russian Scientific Foundation (Grant No 22-12-00008).

[1] A. V. Tsvyashchenko, *J. Less-Common Met.*, **99** L9 (1984).

[2] E. Altynbaev et al., *Physical Review B*, **101** (2020) 100404.

[3] T. Koretsune et al., *Sci. Rep.*, **5** (2015) 13302.

[4] J. Gayles et al., *Phys. Rev. Lett.*, **115** (2015) 036602.

[5] T. Kikuchi et al., *Phys. Rev. Lett.*, **116** (2016) 247201.

[6] E. Altynbaev et al., *Physical Review B*, **94** (2016) 17.

[7] D. Skanchenko et al., *Jallcom*, **865** (2021) 158606.

## BROADBAND RECTIFICATION EFFECT IN SPIN-TORQUE DIODES

*Skirdkov P.N.<sup>1,2</sup>, Kichin G.A.<sup>1</sup>, Zvezdin K.A.<sup>1,2</sup>*

<sup>1</sup> New Spintronics Technologies, Moscow, Russia

<sup>2</sup> Prokhorov General Physics Institute of RAS, Moscow, Russia  
petr.skirdkov@gmail.com

Spin-torque diodes (STDs), formed by magnetic tunnel junctions (MTJ) consisting of a free ferromagnetic layer and a pinned ferromagnetic layer separated by a dielectric tunnel barrier, after numerous design improvements already surpass existing semiconductor technology in several key parameters. The rectification in STDs occurs due to the free layer's (FL) magnetization oscillations (and corresponding resistance changes) caused by the spin-transfer torque effect under radio frequency (RF) current injection. In this case a direct-current (DC) voltage across the structure interface appears. This phenomenon was firstly observed by Tulapurkar et al. [1]. Although, the RF detection sensitivity in this first work [1] (about 1.4 mV/mW) was more than three orders lower than that in the case of semiconductor Schottky diode detectors, recent works demonstrated more than competitive performance with sensitivity more than 4500 mV/mW [2] without DC bias and more than 200 000 mV/mW with DC bias [3].

All above mentioned STDs operate in the resonant mode and can effectively rectify input RF current only near the resonant frequency of one to several gigahertz order. Recently, a new type of broadband rectification regime has been theoretically reported [4]. The rectified voltage was observed in a very wide frequency range and did not have a resonant character. A necessary condition for this is a significant out-of-plane (OOP) component of the magnetization, which has been originally proposed to be created using perpendicular magnetic field bias [4]. However, recent findings have shown that it is possible to create an OOP magnetization component and therefore to achieve broadband rectification using interfacial PMA [5,6,7]. Up today, through free layer proper interface PMA engineering, the maximum bandwidth of the broadband STD detection was reported to be up to 3 GHz [7]. Although the mentioned results on broadband rectification are very promising from the applied point of view, the required fine tuning of the perpendicular magnetic anisotropy increases the technical complexity of their implementation.

In this work we report a new type of non-resonant broadband RF rectification mechanism in STDs with in-plane magnetization of the free layer and no external out-of-plane magnetic field. Using spin-torque FMR (ST-FMR) method we show that spin-torque driven response exhibits a RF rectification over a very wide frequency range reaching the record-breaking 6 GHz. We compare the experimental results with micromagnetic calculations and theoretical analysis to explain the results and reveal the role of turned in-plane magnetic field and free layer inhomogeneous. Our work paves the way towards improved energy efficiency of wireless microwave energy harvesting applications.

Financial support by the Russian Science Foundation, Project No. 19-12-00432 is acknowledged.

- [1] A.A. Tulapurkar et al., *Nature*, **438** (2005) 339–342.
- [2] A. Buzdakov, P.N. Skirdkov, K.A. Zvezdin, *Phys. Rev. Appl.*, **15** (2021) 054047.
- [3] L. Zhang et al., *Appl. Phys. Lett.*, **113** (2018) 102401.
- [4] O. Prokopenko et al., *J. Appl. Phys.*, **111** (2012) 123904.
- [5] B. Fang et al., *Phys. Rev. Appl.*, **11** (2019) 014022.
- [6] M. Tarequzzaman et al., *Appl. Phys. Lett.*, **112** (2018) 252401.
- [7] L. Zhang et al., *ACS Appl. Mater. Interfaces*, **11** (2019) 29382.

## EXCHANGE BIAS IN Pd/Co/CoO FILMS WITH DIFFERENT Co OXIDATION TIMES AND THE NUMBER OF REPETITIONS OF [Pd/Co/CoO]<sub>n</sub> BILAYERS

*Tarasov E.V.<sup>1,2</sup>, Turpak A.A.<sup>1</sup>, Tkachenko I.A.<sup>2</sup>, Kozlov A.G.<sup>1</sup>*

<sup>1</sup> Laboratory of spin-orbitronics, Far Eastern federal university, Vladivostok, Russia

<sup>2</sup> Institute of Chemistry FEB RAS, Vladivostok, Russia  
tarasov.ev@dvfu.ru

The article presents the results of studying the exchange bias in ultrathin epitaxial Pd/Co/CoO films with perpendicular magnetic anisotropy as a function of the oxidation time of the cobalt layer and the number of repetitions of [Pd/Co/CoO]<sub>n</sub> bilayers. Studies of the magnetic properties, carried out using the Vibration Magnetometer system for measuring physical properties, showed an increase in the exchange bias with an increase in the oxidation time (Figure 1a). It was also found that the dependence of the exchange bias on the number of repetitions of bilayers is complex (Figure 1b).

Exchange bias is one of the phenomena associated with the exchange anisotropy that occurs at the interface between ferromagnetic (FM)/antiferromagnetic (AFM) materials [1].

The samples were obtained by molecular beam epitaxy on an Omicron ultrahigh vacuum complex. The epitaxial layers were grown on single crystal Si(111) substrate at an operating pressure of 10<sup>-10</sup> Torr.

Figure 1a shows that with an increase in the oxidation time, the temperature at which the exchange bias effect manifests itself increases, which is associated with an increase in the thickness of the cobalt oxide layer. For a sample oxidized for 5 minutes, the exchange bias begins to appear at 100K, and for a sample oxidized for 1 minute, the bias appears at 25K.

The possibility of the existence of an exchange bias perpendicular to the film plane during Pd/Co/CoO epitaxy structures with varying degrees of Co and [Pd/Co/CoO]<sub>n</sub> oxidation, which are characterized by perpendicular the magnetic anisotropy is shown. It was found that the exchange bias depends on the oxidation parameters and on the number of bilayers.

The authors thank the Russian Ministry of Science and Higher Education for state support of scientific research conducted under the supervision of leading scientists in Russian institutions of higher education, scientific foundations, and state research centers (075-15-2021-607).

[1] J. Nogues, I.K. Schuller, *J. Magn. Magn. Mater.*, **192** (1999) 203-232.

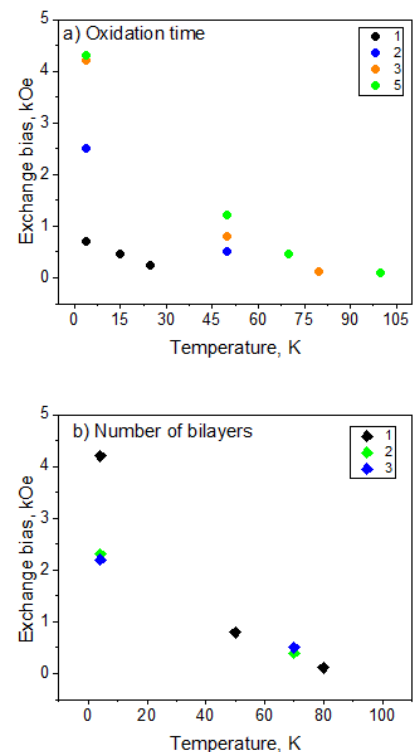


Figure 1. Dependences of the exchange bias on temperature: a) at different oxidation times, b) random repetition of [Pd/Co/CoO]<sub>n</sub> bilayers.

## MUTUALLY SYNCHRONIZED SPIN HALL NANO-OSCILLATORS BY A COMMON CURRENT

*Tsyrlnikova L.A.<sup>1,2</sup>, Safin A.R.<sup>1,2</sup>*

<sup>1</sup> Kotel'nikov Institute of Radioengineering and Electronics, Russian Academy of Sciences, Moscow, Russia

<sup>2</sup> Moscow Power Engineering Institute, Moscow, Russia  
mila.tsyrlnikova@gmail.com

Recently, considerable attention has been paid to the design of spintronic nano-oscillators (SO), which are used to implement the hardware implementation of neuromorphic network computing. The connection of many COs ( $N = 100..1000$ ) allows you to set the output power by  $N$  times and reduce the width of the spectral line inversely proportional to  $N$  [1]. An important task in building a network is their synchronization, which can be achieved through magneto-dipolar coupling, coupling through the radiation of propagating spin waves or a common current coupling [2].

The purpose of this work is to quantify the impact of various communication mechanisms on CO synchronization. The model studied in the work is two ferromagnetic nanopillars connected by a common layer of platinum, through which a constant electric current is passed (Figure 1).

In this work, on the basis of the Hamiltonian formalism [2], a theoretical model is constructed that describes the dynamics of magnetization in a system of bound COs (Figure 1) and allows one to quantitatively calculate the range of parameters at which synchronization occurs.

Dependence of the coefficients of connection by the common current, magneto-dipolar coupling and coupling through the radiation of propagating spin waves on the distance between the oscillators was received.

The common current coupling coefficient, unlike other types of couplings, does not depend on the distance between the oscillators and increases with increasing current passing through the platinum layer.

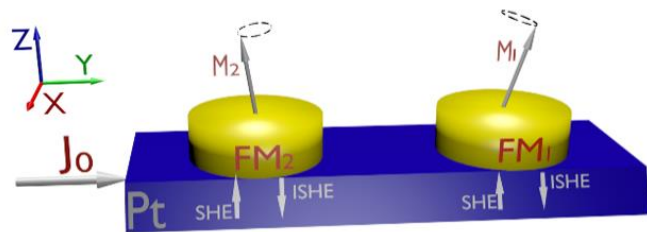


Figure 1. Two spin Hall nano-oscillators coupled by a spin current. Two ferromagnets ( $FM_{1,2}$ ) are located on a layer of heavy metal - platinum (Pt).  $J_0$  is the electric current flowing through the platinum layer.  $M_{1,2}$  - magnetization vectors. SHE - spin Hall effect, ISHE - inverse spin Hall effect.

Support by RSF 21-79-10396 is acknowledged.

[1] M. Zahedinejad et al., *Nat. Nanotechnol.*, **15** (2020) 47–52.

[2] A. Slavin, V. Tiberkevich, *IEEE Tran. on Magn.*, **45** (2009) 1875 - 1918.

## MAGNETOTRANSPORT AND ELECTRICAL PROPERTIES OF COBALT MONOCRYSTAL AT LOW TEMPERATURES

*Kuvandikov O.K.<sup>1</sup>, Usarov U.T.<sup>2</sup>*

<sup>1</sup> Samarkand State University named after Sharof Rashidov, Samarkand, Uzbekistan

<sup>2</sup> Samarkand State University of Architecture and Civil Engineering, Samarkand, Uzbekistan  
quvandikov@rambler.ru

This paper presents the results of studies of the magnetotransport and electrical properties of cobalt single crystals at low temperatures in strong magnetic fields in order to elucidate the topological features of the Fermi surface.

For this purpose, potentiometric setup was assembled [1]. The magnetic field was created by a superconducting solenoid. The measurements were carried out for various orientations of the magnetic field relative to the hexagonal axis ( $\varphi = 0, 20, 30, 45, 60,$  and  $90^\circ$ , where  $\varphi$  is the angle between the direction of the magnetic field and the hexagonal axis of the crystal). The obtained experimental results are explained on the basis of theoretical works on galvanomagnetic phenomena in metals [2], the band structure of cobalt [3–5], and the electrical resistance of ferromagnetic metals.

Experimental results show that at  $\varphi = 90^\circ$ , when  $\vec{j} \parallel c.$ , the electrical resistance curve in strong magnetic fields increases according to quadratic law, which indicates the existence of open sections in planes parallel to the C axis, in the case of  $\varphi = 30^\circ$ , the electrical resistance curve tends to saturation with increasing H in high fields. The results obtained confirm the theoretical conclusions on the Fermi surface of cobalt.

On the basis of experimental studies of electrical resistance, the following were estimated: current carriers at temperatures  $T < 50$  K are scattered on impurities and defects, at temperatures  $T > 50$  K on phonons. Baber scattering is highly dependent on the anisotropy of the Fermi surface.

[1] O.K. Kuvandikov, U.T. Usarov, *Scientific Bulletin of SamSU* (2023).

[2] I.M. Lifshitz, M.Ya. Azbel, M.I. Kaganov, *Electronic Theory of Metals* (Moscow, 1971).

[3] E.I. Kondorsky, *Zone theory of magnetism* (Moscow State University, 1976).

[4] S. Wakon, I. Yamashita, *J. phys. Soc. Japan*, **28** (1970) 1151.

[5] F. Batallam, J. Rosenman, *Proc. Intern. Conf. Low. Temp. phys.* (Tokyo, 1971).

## SPIN-POLARIZED CONDUCTANCE IN MAGNETIC TUNNEL JUNCTION WITH MULTIFERROIC BiFeO<sub>3</sub>

*Useinov N.Kh.<sup>1</sup>, Useinov A.N.<sup>2</sup>*

<sup>1</sup> Kazan Federal University, Kazan, Russia

<sup>2</sup> National Yang-Ming Chiao-Tung University, Hsinchu, Taiwan ROC

nuseinov@mail.ru, artu@nycu.edu.tw

Utilization of the multiferroic (MF) material such as BiFeO<sub>3</sub> with antiferromagnetic properties as a functional barrier for a magnetic tunnel junction (MTJ) is challenging problem. It assumes a new degree of the device functionality, which is not available in conventional MTJs. From one hand, switching of the ferroelectric (FE) polarization changes the potential barrier geometry and related conductance, leading to the tunnelling electro-resistance effect; from other hand, latter one coexists with tunnelling magneto-resistance [1]. At the same time, FE switching is one of energy effective (low power) event, and device reliability is good enough for applications [2].

In present work, tunneling transport model is developed for the MF MTJ (MFTJ), consisting two ferromagnetic electrodes (FMs), which are separated by a few nm thick BiFeO<sub>3</sub> barrier. The complexity of the model includes approximation of free electrons in the framework of the ballistic spin-resolved point contact model and noncollinear orientation of magnetizations in semi-infinite FMs. The expression for the potential barrier is defined, using the spin-dependent Thomas-Fermi screening approximation [1,3], which includes also the magnitude and orientation of the magnetizations [4].

Calculation of the components of the spin-polarized conductances is executed vs integration by transmission coefficients, accounting the applied voltage, the rotation of the quantization axis and the conservation law of the wave vector's components at the Fermi level. The voltage dependence of the conductance is considered without and with screening effect, modifying the barrier on the FE/FM interfaces, for example:  $G_{\lambda=0}^{AP} = G_{\uparrow}^{AP} + G_{\downarrow}^{AP}$  and  $G_{\leftrightarrow}^{AP} = G_{\uparrow, \leftrightarrow}^{AP} + G_{\downarrow, \leftrightarrow}^{AP}$  are shown in Figure 1 for antiparallel (AP) magnetic alignment of FMs;  $\leftrightarrow$  refers to the positive (negative) FE polarization of the barrier,  $\uparrow\downarrow$  are the spin components. It can be seen that the screening effect (with a screening length  $\lambda = 0.9 \text{ \AA}$ ) significantly modifies the spin-polarized conductance in MFTJ.

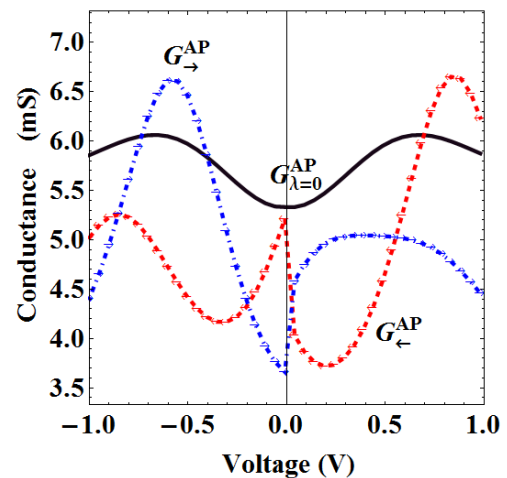


Figure 1. The bias-voltage dependences for  $G_{\lambda=0}^{AP}$  and  $G_{\rightarrow}^{AP}$ ,  $G_{\leftarrow}^{AP}$  evaluated at  $\lambda = 0.9 \text{ \AA}$ .

Supported by NSTC 111-2221-E-A49-120-

[1] M.Y. Zhuravlev, S. Maekawa, E.Y. Tsymbal, *Phys. Rev. B.*, **81** (2010) 104419.

[2] J.T. Heron, D.G. Schlom, R. Ramesh, *Appl. Phys. Rev.*, **1** (2014) 021303.

[3] A. Useinov, M. Chshiev, A. Manchon, *Phys. Rev. B.*, **91** (2015) 064412.

[4] N.Kh. Useinov, A.P. Chuklanov et al., *Phys. of the Solid State*, **62** (2020) 1706.

## APPEARANCE OF UNIDIRECTIONAL ANISOTROPY IN THE HETEROSTRUCTURE $\text{SrMnO}_3/\text{La}_{0.7}\text{Sr}_{0.3}\text{MnO}_3$ AT ROOM TEMPERATURE

*Shaikhbulov T.A.<sup>1</sup>, Temiryazeva M.P.<sup>2</sup>, Sizov V.E.<sup>2</sup>, Demidov V.V.<sup>1</sup>, Matveev A.A.<sup>1</sup>, Volkov D.A.<sup>1,3</sup>, Tlegenov R.<sup>1,4</sup>, Safin A.R.<sup>1,3</sup>, Logunov M.V.<sup>1</sup>, Kalyabin D.V.<sup>1</sup>, Nikitov S.A.<sup>1,4</sup>*

<sup>1</sup> Kotelnikov IRE RAS, Moscow, Russia

<sup>2</sup> Kotelnikov IRE RAS, Fryazino Branch, Fryazino, Russia

<sup>3</sup> National Research University MPEI, Moscow, Russia

<sup>4</sup> Moscow Institute of Physics and Technology, Dolgoprudny, Moscow Region, Russia  
shcaihulov@hitech.cplire.ru

The epitaxial heterostructures of mixed-valence manganites open up possibilities to create devices based on magnetic phenomena and competing interface interactions. One of the interfacial phenomena is the appearance of additional unidirectional anisotropy. Its occurrence is explained by the exchange interaction between ferromagnetic (FM) and antiferromagnetic (AFM) spins at the interface. Film  $\text{SrMnO}_3$  (SMO) belongs to the  $\text{La}_{1-x}\text{Sr}_x\text{MnO}_3$  families. SMO polymorphs have the G-type antiferromagnetic insulator properties with a Neel ( $T_N$ ) temperature, that varies from 260 to 278K [1]. Figure 1 confirms the antiferromagnetic state of the SMO at the room temperature. In AFM/FM heterostructure instead of uniaxial anisotropy (two equivalent easy configurations in opposite directions) magnetization in AFM/FM systems has only the one easy direction, often referred to as unidirectional anisotropy. The antisymmetric peaks in the angular dependence of the resonant field indicate the appearance of unidirectional anisotropy in heterostructure, which is explained by the appearance of an exchange interaction at the AFM/FM interface [2].

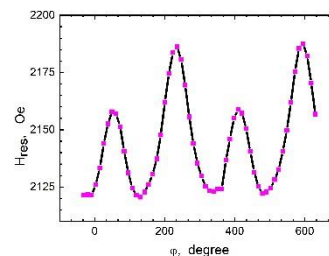


Figure 1. Angular dependence of the resonance field of  $\text{SrMnO}_3/\text{La}_{0.7}\text{Sr}_{0.3}\text{MnO}_3$  heterostructure (magenta squares), at  $T = 300$  K.

Work was supported by the Russian Science Foundation grant No. 21-79-10396

[1] R. Søndena et al., *Phys. Rev.*, **74** (2006) 144102.

[2] J. Nogues, K. I. Schuller, *J. Magn. Magn. Mater.*, **192** (1999) 203.

## APPEARANCE OF THE INTERFACIAL PERPENDICULAR MAGNETIC ANISOTROPY IN $\text{La}_{0.7}\text{Sr}_{0.3}\text{MnO}_3$ FILM-BASED HETEROSTRUCTURES

*Shaikhulov T.A.<sup>1</sup>, Temiryazeva M.P.<sup>2</sup>, Safin A.R.<sup>1,3</sup>, Kalyabin D.V.<sup>1</sup>, Nikitov S.A.<sup>1,4</sup>*

<sup>1</sup> Kotelnikov IRE RAS, Moscow, Russia

<sup>2</sup> Kotelnikov IRE RAS, Fryazino Branch, Fryazino, Russia

<sup>3</sup> National Research University MPEI, Moscow, Russia

<sup>4</sup> Moscow Institute of Physics and Technology, Dolgoprudny, Moscow Region, Russia  
shcaihulov@hitech.cplire.ru

Perovskite manganites show a wide range of various interesting physical phenomena, including colossal magnetoresistance, high Curie temperature, phase separation, and an interaction between electrons. Magnetic thin films are interesting due to their potential use in information technology and spintronics. For such applications, among many different properties, the most important are those that determine the magnetization reversal process and the stability of the magnetic configuration. Extensive studies of the ferromagnet (FM)/heavy metal (HM) show that HM layers at FM/HM interfaces induce strong perpendicular magnetic anisotropy [1]. These effects can also be induced using antiferromagnetics (AFM) [2]. This possibility can be used to stabilize skyrmions at room temperature without external magnetic fields [3]. The exchange bias effect caused by FM coupling with AFM may be especially important for domain wall pinning, which is necessary for stabilizing and optimizing domain wall movement. Figure 1 shows  $\text{La}_{0.7}\text{Sr}_{0.3}\text{MnO}_3$  film-based heterostructures in which interfacial perpendicular anisotropy appeared due to additional layers of an antiferromagnet ( $\text{SrMnO}_3$ ) and a material with a heavy metal ( $\text{SrIrO}_3$ ).

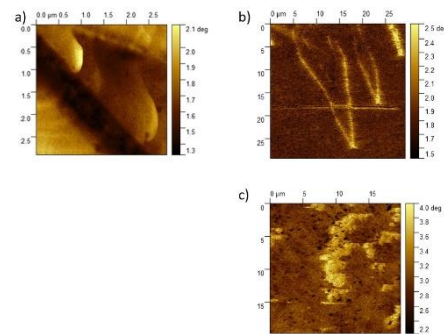


Figure 1. MFM images of a) 30nm  $\text{La}_{0.7}\text{Sr}_{0.3}\text{MnO}_3$  films on  $\text{NdGaO}_3(110)$  substrates, b)  $\text{SrMnO}_3/\text{La}_{0.7}\text{Sr}_{0.3}\text{MnO}_3$ , c)  $\text{SrIrO}_3/\text{La}_{0.7}\text{Sr}_{0.3}\text{MnO}_3$  without an external field.

Work was supported by the Russian Science Foundation grant No. 23-79-00016

[1] V.V. Demidov, T.A. Shaikhulov, *J. Magn. Magn. Mater.*, **566** (2023) 170299.

[2] F. Li et al., *Sci. Rep.*, **5** (2015) 16187.

[3] Y. Guang et al., *Nat. Commun.*, **11** (2020) 1–6.

## ORTHOGONAL MAGNETIC STRUCTURES OF $\text{Fe}_5\text{O}_6$ : REPRESENTATION ANALYSIS AND DFT CALCULATIONS

*Zhandun V.S., Kazak N.V.*

Kirensky Institute of Physics - Federal Research Center “Krasnoyarsk Science Centre”, SB RAS,  
Krasnoyarsk, Russia  
jvc@iph.krasn.ru

Iron oxides are attracting a lot of attention due to their complex structural properties and fundamental aspects from the point of view of the natural sciences and industrial applications [1,2]. In the last decade, studies at high temperatures and high pressures have revealed the existence of new binary iron oxides with unusual stoichiometry, such as  $\text{Fe}_4\text{O}_5$  [3] and  $\text{Fe}_5\text{O}_6$  [4]. The discovery of new classes of systems motivated the study of their physical properties and potential for innovative applications [2]. While structural information and some properties of the new oxides at atmospheric pressure are available, information on their electronic and magnetic properties under extreme pressure-temperature conditions is very limited. Knowledge of these properties is important for both solid state physics and the earth sciences. We have applied a combination of irreducible representation analysis and density-functional theory plus Hubbard U (DFT + U) calculations to analyze the ground magnetic state of  $\text{Fe}_5\text{O}_6$  at ambient pressure (Figure 1). For the parent space group  $Cmcm$  (#63), the total energies of the different spin configurations involving iron ions at all symmetry non-equivalent sites have been calculated. The spin structures with  $k = (0, 0, 0)$  propagation vectors can be realized. The ground state magnetic configuration corresponds to orthogonal structures with Fe spins in the 1D chains directed along the  $b$  axis and spins in the slabs aligned along the  $c$  axis. The evolution of magnetic moments under high pressure was studied and a site-dependent spin-state crossover was found.

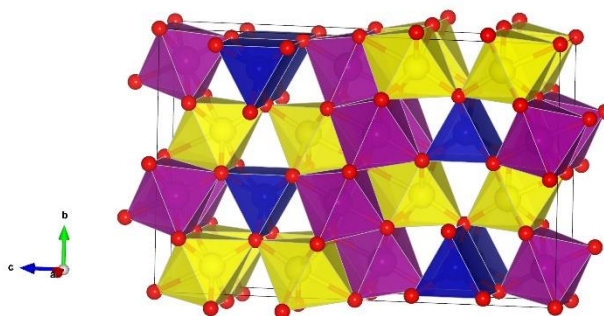


Figure 1. The crystal structure of  $\text{Fe}_5\text{O}_6$ . The symmetry distinct iron sites are highlighted in purple (Fe1), yellow (Fe2), and blue (Fe3).

This research is funded by the Russian Foundation for Basic Research (project no. 21-52-12033).

- [1] C. Delacotte et al., *Solid State Chem.*, **247** (2017) 13–19.
- [2] S. V. Ovsyannikov et al., *Nat. Commun.*, **9** (2018) 4142.
- [3] B. Lavina et al., *Proc.Natl.Acad.Sci. U.S.A.*, **108** (2011) 17281–5.
- [4] B. Lavina, Y. Meng, *Sci. Adv.*, **1** (2015) e1400260–e1400260.

## LINEAR MAGNETORESISTANCE IN $(\text{Bi}_{1-x}\text{Eu}_x)_2\text{Se}_3$ TOPOLOGICAL INSULATOR

*Aronzon B.A.<sup>1</sup>, Mekbiya A.B.<sup>1</sup>, Oveshnikov L.N.<sup>1</sup>, Davydov A.B.<sup>1</sup>, Prudkoglyad V.A.<sup>1</sup>,  
Rodionov Ya.I.<sup>2</sup>, Kugel K.I.<sup>1,2</sup>, Selivanov Yu.G.<sup>1</sup>*

<sup>1</sup> P.N. Lebedev Physical Institute, RAS, Moscow, Russian

<sup>2</sup> Institute for Theoretical and Applied Electrodynamics, RAS, Moscow, Russia  
aronzon@mail.ru

We investigated the change in the properties of 2D topological insulators  $(\text{Bi}_{1-x}\text{Eu}_x)_2\text{Se}_3$  doped by Eu at concentrations  $x = 0-0.21$ . It follows from the symmetry that the magnetoresistance ( $\text{MR} = 100\% \cdot (R_{xx}(B) - R_{xx}(0))/R_{xx}(0)$ , where  $R_{xx}$  is the electrical resistance) is an even function of the magnetic field  $B$ . However, in high magnetic fields, a linear dependence of the magnetoresistance (LMR) can be observed. The LMR turns out to be especially pronounced at low-temperatures in samples with magnetic impurities such as Eu at a high Eu content. In our samples, the dopants are concentrated within platelet-like Eu-rich inclusions.

We want to emphasize that in all materials under study, the characteristic magnetic field range (from  $B_{max}$  to  $B_{min}$ ), where the LMR manifests itself, shifts toward higher fields with an increase in  $x$  ( $B_{max}$  it is the field, up to which LMR still exists, and  $B_{min}$  it is the field, up to which the weak localization still exists). Note that in the case of  $B_{max}$ , it increases only up to 15 T. If the number of inclusions exceeds some threshold value, this leads to the formation of a partially amorphous structure due to an overlap of inclusions. In this case, the LMR begins to disappear, and  $B_{max}$  decreases. As far as the LMR slope is concerned, it more or less reminds the temperature dependence of the dephasing length ( $T^{-1/2}$ ).

General LMR theories can be divided into two main groups – classical and quantum. Classical models (Parish–Littlewood) [1] basically assume that the LMR arises due to the mixing of the Hall contribution when the current wraps around islands with low mobility and partially flows perpendicular to the direction of the electric field. Quantum models suggest that LMR can occur in the ultraquantum limit (i.e. in a high magnetic field when only one Landau level is occupied) (the Abrikosov model) [2]. In recent years, additional considerations have been made about the phenomenon of LMR in topological systems. It has been suggested that due to the absence of gaps in the spectrum of topological materials, relatively low disorder can cause the formation of pools of electrons and holes, which act as islands with low mobility in the Parish–Littlewood model. On the other hand, it was assumed [3] that the Abrikosov model remains applicable even below the ultraquantum limit in topological systems.

It is difficult for us to choose one of the two proposed models, but it seems to us that they both correctly describe the situation and both have the right to exist depending on the parameters. In this work, we present a certain discussion of these issues, but note that the Abrikosov model has more chances, especially when taking into account two features that we have discovered recently.

The work was supported by the Russian Science Foundation, Grant No. 21-12-00254 (<https://rscf.ru/en/project/21-12-00254/>).

[1] M. M. Parish and P. B. Littlewood, *Nature*, **426** (2003) 162.

[2] A. A. Abrikosov, *Phys. Rev. B*, **58** (1988) 2788.

[3] Ya. I. Rodionov *et al*, *Phys. Rev. B*, **107** (2023) 155120.

## ELASTICITY OF THE CHIRAL SOLITON LATTICE IN $\text{Cr}_{1/3}\text{NbS}_2$

*Tereshchenko A.A.<sup>1</sup>, Ovchinnikov A.S.<sup>1,2</sup>, Sinitsyn V.I.E.<sup>1</sup>, Bostrem I.G.<sup>1</sup>*

<sup>1</sup> Ural Federal University, Yekaterinburg, Russia

<sup>2</sup> M.N. Mikheev Institute of Metal Physics UB of RAS, Yekaterinburg, Russia  
alexey.tereshchenko@urfu.ru

The study of the magnetic properties of monoaxial chiral helimagnets, in which the helical magnetic order is due to the antisymmetric Dzyaloshinskii–Moriya exchange interaction, is one of the promising areas of modern magnetism. In view of potential application in spintronics, these systems are attractive due to easily control of their magnetic order by external influences. For example, by applying an external magnetic field perpendicular to the helicoidal axis, the magnetic chiral soliton lattice (CSL) is formed [1]. The period of the magnetic structure increases with a growth of the external magnetic field. A recent study has proven the existence of the CSL at room temperature, which brings the use of such a magnetic structure in real spintronic devices much closer [2].

Tensile or compressive elastic strains applied to the CSL can also deform this spatially inhomogeneous magnetic structure whenever the single-ion magnetoelastic interaction is relevant. Deformations of the CSL in the layered chromium dichalcogenide  $\text{Cr}_{1/3}\text{NbS}_2$  have been analyzed by us and it was proven that the double sine-Gordon (dSG) model describes well the deformed CSL [3]. This model predicts the existence of two different phases: the phase in which magnetization mostly retains along the magnetic field, and the packed structure phase, where magnetization is predominantly directed at an angle to the magnetic field. Comparison of the theory with experimental data obtained by the Lorentz microscopy evidences that the first case does take place in  $\text{Cr}_{1/3}\text{NbS}_2$  samples subjected by tensile stress.

Previously, it was demonstrated that distortions of the skyrmion lattice in cubic helimagnets may be described in terms of the theory of elasticity [4], whenever Hooke's law is valid for deformations of the magnetic structure. In our work, we realize this idea for the soliton lattice arising in the helimagnets of hexagonal symmetry.

More specifically, we consider weak distortions of the CSL as solutions of the dSG model at given magnetic field. The elastic deformations lead to increase of a period of the deformed magnetic configuration that makes possible to introduce the effective elastic deformation tensor  $u_{zz}$ , which is directly proportional to the real elastic strains. In addition, a difference between the energy of the deformed CSL and that of non-deformed CSL turns out to be quadratic in  $u_{zz}$ . This suggests a Hooke's law regime for small deformations and allows us to calculate the corresponding elasticity constant  $c_{33}$ . Remarkably, this elasticity constant decreases monotonically with increasing of the magnetic field. These results demonstrate relevance of elasticity theory to describe deformations of magnetic soliton lattice by external forces.

This work was supported by the Russian Science Foundation (Grant No. 22-13-00158).

- [1] Y. Togawa et al., *Phys. Rev. Let.*, **108** (2012) 107202.
- [2] R. Brearton et al., *Advanced Physics Research*, (2023) 2200116.
- [3] G.W. Paterson et al., *Phys. Rev. B.*, **101** (2020) 184424.
- [4] S.P. Kang et al., *Journal of Applied Physics*, **121** (2017) 203902.

## NONLINEAR FREQUENCY SHIFT OF THE MAGNETIZATION PRECESSION IN THIN MAGNETIC FILMS UNDER THE ACTION OF SPIN-POLARIZED CURRENT IN THE PRESENCE OF AN EXTERNAL MAGNETIC FIELD

*Matveev A.A.<sup>1</sup>, Safin A.R.<sup>1,2</sup>, Nikitov S.A.<sup>1,3</sup>*

<sup>1</sup> Kotel'nikov Institute of Radioengineering and Electronics RAS, Moscow, Russia

<sup>2</sup> Moscow Power Engineering Institute, Moscow, Russia

<sup>3</sup> Moscow Institute of Physics and Technology, Dolgoprudny, Russia  
maa.box@yandex.ru

The study of the nonlinear dynamics of magnetic films is of scientific interest since they can be implemented in spintronics devices - from spin-transfer nanooscillators to non-volatile memory devices and magnetic logic elements [1]. It has been shown that the dynamics of a homogeneously magnetized film can be successfully described within the framework of the Hamiltonian formalism [2]. This formalism allows to reduce the Landau-Lifshitz-Gilbert (LLG) equation with additional spin-transfer torque to a nonlinear differential equation for complex amplitude  $c$ . Form of this equation is typical for self-oscillating systems

$$\frac{dc}{dt} = -i\omega(|c|^2)c - \Gamma_+(|c|^2)c + \Gamma_-(|c|^2)c. \quad (1)$$

Here  $\omega(|c|^2) = \omega_0 + N|c|^2$  is the frequency of the magnetization precession;  $\omega_0$  is the eigenfrequency;  $\Gamma_+(|c|^2)$  is the damping, that arises from the Gilbert term in LLG;  $\Gamma_-(|c|^2)$  is the pumping due to the spin-polarized current. The change in the frequency with an increase in the amplitude of the precession of magnetization is determined by the coefficient  $N$ . In this work, we use micromagnetic simulations in MUMAX [3] and numerical calculations to determine the critical out-of-plane angle  $\theta_{0c}$  of the  $\mathbf{H}_{ext}$  at which  $N = 0$ . The results for permalloy are presented in Figure 1. We show that this angle decreases with increasing of the external magnetic field modulus and cannot surpass a certain minimum angle  $\theta_{min}$ . For example, the derived expression for this minimum angle for permalloy has the form

$$\theta_{min} = \frac{1}{2} \arccos\left(\frac{1}{3}\right) \approx 35^\circ \quad (2)$$

Support by RSF 21-79-10396 is acknowledged.

[1] Q. Shao et al., *IEEE TMAG*, **57**(7) (2021) 1-39.

[2] A. Slavin and V. Tiberkevich, *IEEE TMAG*, **44**(7) (2008) 1916-1927.

[3] A. Vansteenkiste et al., *AIP Advances*, **4** (2014) 107133.

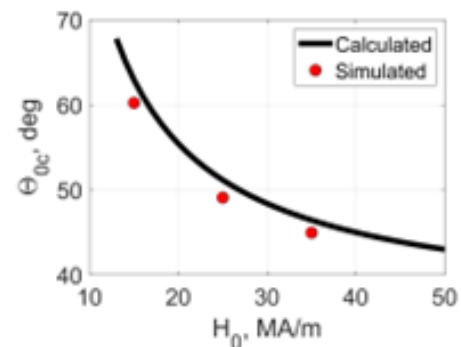


Figure 1. The dependence of the critical angle of the external magnetic field on the modulus of this field  $H_0$  for permalloy  $Ni_{80}Fe_{20}$ . Red circles show the results obtained using micromagnetic simulations and a solid black line indicates the numerical solution of the equation  $N = 0$ .

## FINITE-ELEMENT-BASED MICROMAGNETIC MODEL OF THE EFFECT OF NONLINEAR GIANT MAGNETOIMPEDANCE IN AN AMORPHOUS FERROMAGNETIC SHELL WITH A DIELECTRIC SPACER

*Demin G.D., Fedina A.D., Djuzhev N.A.*

National Research University of Electronic Technology (*MIET*), Moscow, Russia  
gddemin@gmail.com

At present, the actual direction of spintronics is devoted to the development of highly sensitive and compact magnetoresistive sensors capable of detecting ultra-low magnetic fields. The main attention in this area is paid to the design of tunnel magnetoresistive (TMR) sensors based on magnetic tunnel junctions (MTJ), which have a high magnetoresistance (MR) ratio (from 150% to 604%), good sensitivity (about 10%/Oe), a suitable measurement range of magnetic fields (from hundreds of pT to several nT) and the ability to scale down up to 10 nm. However, the technology of MTJ fabrication is quite complex (high uniformity and quality of layers with thicknesses of a few nm is required) and uses materials based on expensive transition metals (such as Ir, Ru, Pt), which have a limited supply and greatly increase the final cost of devices. Anisotropic magnetoresistive (AMR) sensors, which are simpler in design, inexpensive and widely used in the industry, do not have similar characteristics – the MR ratio does not exceed 3-4%, and the minimum detected fields do not go beyond a few nT.

In contrast to the above TMR and AMR sensors, sensors based on the non-linear giant magneto-impedance (GMI) effect, demonstrating a noticeable change in the complex resistance of amorphous ferromagnetic (FM) structures in an alternating magnetic field (up to 700% and higher) and sensitivity at the level of several hundred %/Oe, combine ease of fabrication (inexpensive materials and simple design) and a wide operating range (from 0.1 pT to 0.1 mT), which makes it possible to measure weak magnetic fields. One of the promising types of GMI sensor is based on a thin-film structure with a dielectric spacer separating the metal conductor with an alternating current (AC) from the FM shell surrounding it [1].

Unlike GMI multilayers without a spacer, it has no effect of eddy currents on the output signal at high frequencies and is more technologically advanced for the integration into CMOS technology. However, when designing such a GMI sensor, it is important to take into account the features of field-induced spin dynamics arising from the film roughness, as well as those associated with the shape of the FM shell and the magnetic field distribution, which requires a complex approach to simulate the output signal. In this work, we propose a model of a GMI sensor based on micromagnetic simulation of the spin dynamics in an arbitrary-shaped FM shell with a dielectric spacer in a non-uniform AC magnetic field. The results show the predominance of the second harmonic of the output signal (Figure 1). The signal amplitude varies from 0.01 to 17.36 mV when the field varies from 0 to 5 Oe (at a frequency of 10 MHz). This approach can be used to predict the impact of the fabrication process on the geometry and performance of the GMI sensor. The work is supported by the RF Ministry of Science and Higher education (#075-15-2021-1350).

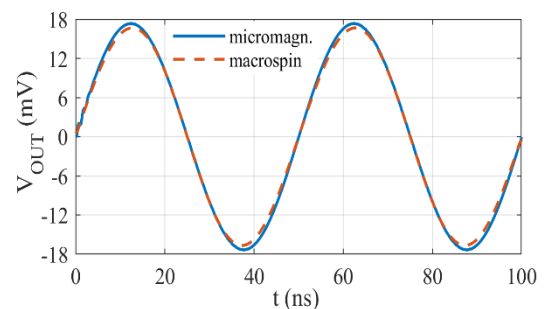


Figure 1. The output signal of the thin-film GMI sensor at field of 5 Oe and a frequency of 10 MHz.

[1] T. Morikawa et al., *IEEE Trans. Magn.*, **32** (1996) 4965-4967.

# FIRST-PRINCIPLES STUDY OF THE SPIN-TRANSFER-TORQUE EFFECT IN COTB-MGO-COTB FERRIMAGNETIC TUNNEL JUNCTIONS

Demin G.D., Djuzhev N.A.

National Research University of Electronic Technology (MIET), Moscow, Russia  
gddemin@gmail.com

The MgO-based magnetic tunnel junctions (MTJs), which demonstrate a high value of magnetoresistance and excellent scalability, have found a wide range of practical applications - from highly sensitive magnetoresistive sensors, microwave detectors to non-volatile magnetoresistive memory (STT-MRAM) devices [1]. An important role in the energy consumption and performance of such spintronic devices is played by the choice of the material of the magnetic electrodes, which determines the spin polarization, the spin-precession time, and the magnetic anisotropy constants. Soft magnetic materials (Co, CoFe, CoFeB) have a low switching speed (at the level of several ns), which limits the use of MTJs based on them for ultra-dense scaling of STT-MRAM cells or creating a new element base for THz range spintronic devices. In turn, compensated ferrimagnets, which have a strong exchange coupling between oppositely polarized magnetic moments of sublattices, low Gilbert damping parameter ( $\sim 10^{-3}$ ), and high magnetic anisotropy, provide ultrafast magnetic dynamics [2]. In particular, alloys of rear-earth (RE) and transition metal (TM) elements, in which there is an exchange interaction between the d- and f-electrons of RE and TM atoms, exhibit suitable ferrimagnetic properties. The compensation point of such alloys, at which the magnetization is equal to zero, can be controlled by changing their component composition (the ratio of the atomic fractions of the RE and TM), which is promising for the high-speed nanoelectronics based on ferrimagnetic tunnel junctions (FMTJ) and for the development of the future generation of STT-MRAM. It was found in [3] that FMTJs with CoTb alloy as the electrode material have a number of advantages – high thermal stability, picosecond switching time, and energy efficiency 25 times higher than MgO-based MTJs. However, the features of spin-transfer torque (STT) effect in such FMTJs are still poorly studied, which plays a key role in the spin dynamics of the free CoTb layer.

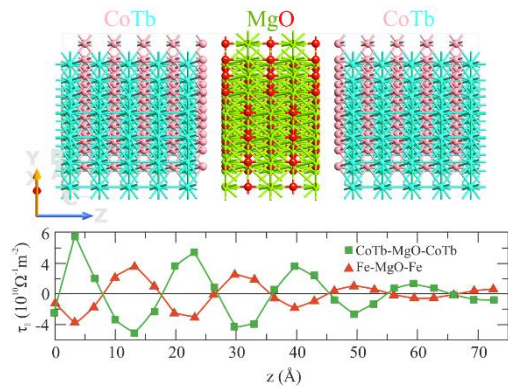


Figure 1. The crystal structure of CoTb-MgO-CoTb FMTJ and calculated in-plane component of STT acting on the Co sublattice. The thickness of the MgO layer is equal to about 5 monolayers.

In this work, using the density functional theory (DFT) and the nonequilibrium Green's function (NEGF) method, we perform first-principles calculation of the STT in the CoTb-MgO-CoTb MTJ (Figure 1). It was shown that the spatial oscillation of in-plane STT in a free CoTb layer is resistant to changes in the thickness of the layers and the bias voltage. For a hyper-thin MgO barrier, the STT can even exceed values obtained in the Fe-MgO-Fe MTJ.

The work is supported by the RF Ministry of Science and Higher education (#075-15-2021-1350).

- [1] Z. Guo, J. Yin et al., *Proceedings of the IEEE*, **109** (2021) 1398.
- [2] D.-H. Kim, T. Okuno, S.K. Kim et al., *Phys. Rev. Lett.*, **122** (2019) 127203.
- [3] S. Smidstrup et al., *J. Phys.: Condens. Matter*, **32** (2020) 015901.

**July 2**

18:15 - 20:00

Sunday

POSTER  
SESSIONS

Section L2

**Soft and Hard  
Magnetic Materials**

## INFLUENCE OF SYNTHESIS CONDITIONS ON MICROWAVE PROPERTIES OF FINE IRON POWDERS OBTAINED VIA ULTRASONIC SPRAY-PYROLYSIS

*Artemova A.V., Maklakov S.S., Shiryayev A.O., Osipov A.V., Komarov I.V., Petrov D.A., Rozanov K.N., Lagarkov A.N.*

Institute of Applied and Theoretical Electrodynamics RAS, Moscow, Russia  
avometras@gmail.com

For metal ferromagnetic powders, new insights into the complex relationships between microwave properties and chemical condition, i.e., chemical purity, opens new possibilities for the production and design of materials for electromagnetic compatibility solutions. The ultrasonic spray-pyrolysis technique allows for the solid particles in an unreserved range of chemical compositions to be produced from liquid solutions. Principally, atomized aerosol particles solidify under high temperatures with diffusion and crystallization of dissolved metal solids near the surface. The characteristics of the final product depend on synthesis parameters. The ability to produce complex structures, such as, hollow [1], that are of special interest for microwave applications, or nanostructured microspheres, are the advantages of the technique. Post-annealing of the as-prepared metal oxide in a hydrogen atmosphere allows metal particles to be produced. Annealing in an H<sub>2</sub> flow at temperatures lower than 600 °C [2] makes it possible to finely control the reduction degree, i.e., composition, of the final product.

The nanostructured spherical iron particles were synthesized by a two-stage process involving ultrasonic spray-pyrolysis from aqueous solution Fe(NO<sub>3</sub>)<sub>3</sub> (10 and 20 wt. %) at 1000 °C and reduction in H<sub>2</sub> at 350 – 500 °C temperature range [2]. The dependence between the microwave permeability of the ferromagnetic iron powders and synthesis conditions, including H<sub>2</sub>-annealing and concentration of the solution, was investigated.

Increase in the reduction temperature from 350 to 500 °C produced iron powders with the chemical purity of the  $\alpha$ -Fe phase up to 95 %, which was established using X-ray diffraction and simultaneous thermal analysis. The reduction temperature did not change the shape and size of the particles (the average sizes were 0.5 and 0.7  $\mu$ m, proportionally to solution concentration), governing microwave permeability and permittivity. But a porous, mesh structure, consisting of iron grains was formed due to losses of weight and volume in decomposition of  $\alpha$ -Fe crystalizes from initial iron oxide. Noticeably, that reduction at 400 °C allows a smooth surface with distinct porous particles to obtain. The further increase caused partial destruction of particles.

Measurements of microwave properties of composites with paraffin matrix showed the dependence of permeability on the chemical purity of iron. An increase in the chemical purity increased the value of the Acher's parameter, which is the quantitative characteristic of the dynamic magnetic performance of a material. Also, an increase in the chemical purity of iron increased the amplitude of both the real and imaginary parts of the permeability and shifted magnetic loss peaks to lower frequencies. Among other samples, powders obtained at 400 °C demonstrated high chemical purity, low porosity, high Acher's parameter, and high magnetic losses at around 15 GHz frequency range.

The results obtained enhance understanding of the relationship between the chemical condition of iron and the dynamic magnetic properties of iron-based composite materials.

This research was funded by the Russian Science Foundation (RSF), grant number 21-19-00138.

[1] A. Artemova et al., *Sensors*, **22**(8) (2022) 3086.

[2] A. Artemova et al., *Magnetism*, **3**(2) (2023) 90-101.

## PERMANENT MAGNET UNDULATORS FOR SYNCHROTRON RADIATION FACILITY

*Kilmetova I.V., Kulevov T.V., Skachkov V.S., Sergeeva O.S.*

National Research Centre “Kurchatov Institute,” Moscow, Russia  
irina.kilmetova@yandex.ru

The fourth-generation synchrotron radiation source is considered to create at National Research Centre “Kurchatov Institute” [1]. SILA source (a fourth-generation SR source with an X-ray free-electron laser) is a multi-user interdisciplinary system of megascience class for many research and applications in physics, chemistry, crystallography, materials science, biology, and medicine. Sources of this type are also in demand in imaging tasks, for spectroscopy and the development of nanodiagnostics methods with resolution on atomic level.

The accelerator facility under development exceeds the currently existing electron storage rings in its characteristics. It assumes an extremely low horizontal beam emittance of  $\sim 75$  pm-rad at energy of 6 GeV. With the bunch length of 3.4 mm, it will provide the smallest size of SR source with spatial coherence and high brightness whereas divergence is of 1  $\mu$ rad.

Several dozens of research stations and laboratories will be arranged in the experimental area of the SILA source. The basic types of foreseen for experimental stations sources will be permanent magnet undulators with period length of 27–45 mm. Some stations require *in-vacuum* undulators with small period of 14–18 mm as well as wigglers with high magnetic field and special short bending magnets. The main parameters of the basic type of permanent magnet undulators are specified in Table 1.

Table 1. SILA source: main characteristics of U-27 undulator.

Material type	Structure period length, mm	Period number	Structure length, mm	Max magnetic field, T	Radiation energy, keV
Nd-Fe-B	27	59	1593	0.556	6.386

Possible designs of permanent magnet undulator structure with variable field are discussed. The Nd-Fe-B alloy was chosen as the material, which has a significantly higher residual magnetization compared to the Sm-Co alloy and is capable of providing increased coercivity. Among the most effective designs, beside hybrid dipole magnet, it is preferable to use both the sector and rod type of implicit multipole, as well as QSM [2] technique (Figure 1).

Each of these systems has advantages and disadvantages. The sector design requires a lot of magnetization orientations relative to the magnetic element faces, while the rod design uses elements with unique geometry. On the other hand, the former ones are easier mounting and precise adjustment of their position, while the latter ones require a holder in the form of a key pair and, in addition, have a slightly lower fill factor. Due to the significant discreteness of the magnetization distribution in the longitudinal direction, in addition to the fundamental field harmonic, high order harmonics are also appeared in the Fourier expansion.

The paper presents the spectra of the longitudinal field distribution in the regular part of various undulator structures.

[1] M.V. Kovalchuk et al., *J. Cryst.*, **67** (2022) 676-683.

[2] V.S Skachkov, *NIM A*, **500** (2003) 43-54.

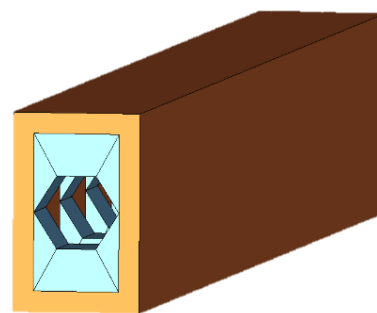


Figure 1. Structure with QSM dipole

## AMORPHIZATION OF THIN SUPERMALLOY FILMS $\text{Ni}_{79}\text{Fe}_{17}\text{Mo}_4$ WITH OXYGEN DURING MAGNETRON SPUTTERING

*Maklakov S.S.<sup>1</sup>, Naboko A.S.<sup>1</sup>, Maklakov S.A.<sup>1</sup>, Bobrovskii S.Y.<sup>1</sup>, Polozov V.I.<sup>1</sup>, Zezyulina P.A.<sup>1</sup>, Osipov A.V.<sup>1</sup>, Ryzhikov I.A.<sup>1</sup>, Rozanov K.N.<sup>1</sup>, Filimonov D.F.<sup>2</sup>, Pokholok K.V.<sup>2</sup>, Lagarkov A.N.<sup>1</sup>*

<sup>1</sup> Institute of Applied and Theoretical Electrodynamics RAS, Moscow, Russia

<sup>2</sup> Lomonosov Moscow State University, Moscow, Russia

squirrel498@gmail.com

Soft ferromagnetic materials, including thin films, core-shell structures, and fine ferromagnetic powders of different structure, recently showed high potential in electromagnetic interference applications in microwave range [1-6]. Further fundamental studies on structure-property relationship between dynamic magnetic performance and structure of thin ferromagnetic films are of high interest.

Reactive sputtering of permalloy typically reduces crystallite size in films, if the concentration of reactive gas is low. This advances magnetic properties: decreases coercivity and increases good in-plane magnetic anisotropy. But oxygen is rarely applied for this purpose. Here, peculiar deposition conditions, including the geometry of the vacuum deposition system and large polymer substrate, allowed for the deposition of supermalloy with unusually high admixture of oxygen. Evolution of both static and dynamic magnetic properties with an increase in oxygen concentration proved to be dealt with the balance between grain size, surface structure, disordering of atomic structure and internal stresses. The critical concentration when supermalloy shows indications of oxidation is 5% of  $\text{O}_2$ . Coercivity, resistivity, roughness and ferromagnetic resonance frequency are the parameters that are most sensitive to oxidation [7].

More specifically, reactive sputter deposition of  $\text{Ni}_{79}\text{Fe}_{17}\text{Mo}_4$  with unusually high admixture of oxygen to a large polymer substrate resulted in the amorphization of the film. Grain size, surface structure, defects concentration and stresses non-monotonically changed with oxygen concentration. (Here and after:  $\{x\%\text{O}_2\}_i$  - samples notation;  $\sigma$  - internal stress in a volume of a supermalloy film;  $S_a$  - mean surface roughness;  $R$  - resistivity;  $H_c$  - coercivity.) This produced three types of strongly anisotropic films: *high  $H_c$  - high  $R$  - high  $\sigma$  ( $\{0\%\text{O}_2\}$ )*, *low  $H_c$  - low  $R$  - low  $\sigma$  ( $\{1\%\text{O}_2\}$  and  $\{2\%\text{O}_2\}$ )* and *high  $H_c$  - high  $R$  - low  $\sigma$  ( $\{5\%\text{O}_2\}$ )*. First traces of oxidation were detected only at 5 vol% of oxygen admixture. This increased  $H_c$  and  $R$  and decreased  $S_a$ . This also caused a blueshift in ferromagnetic resonance frequency and suppressed magnetoelastic effect. An interesting extension could be an attempt to turn easy axis or eliminate in-plane magnetic anisotropy within the studied films.

This research was funded by the Russian Science Foundation (RSF), grant number 21-19-00138.

- [1] A.V. Artemova et al., *Sensors*, **22** (2022) 3086.
- [2] A.V. Dolmatov et al., *Sensors*, **14** (2021) 4624.
- [3] V.I. Polozov et al., *Phys. Status Solidi A*, **2017** (2020) 2000452.
- [4] V.I. Polozov et al., *Phys. Rev. B.*, **101** (2020) 214310
- [5] V.I. Polozov et al., *IOP Conf. Ser. Mater. Sci. Eng.*, **848** (2020) 012073.
- [6] A.V. Kosevich (Artemova) et al., *Coatings*, **10** (2020) 995.
- [7] S.S. Maklakov et al., *Jallcom*, **763** (2018) 558.

## ADDITIVE MANUFACTURING OF R-Fe-B TYPE PERMANENT MAGNETS

*Maltseva V., Urzhumtsev A., Andreev S., Volegov A.*  
Ural Federal University, Yekaterinburg, Russia  
viktorija.maltseva@urfu.ru

Hard magnetic materials and permanent magnets made from them are widely used in modern technical devices and in electronic devices that surround us every day. Because of the desire to reduce the size of devices in general, there is a need to significantly optimize permanent magnets and magnetic systems. Technologies that have been developed over the years for obtaining magnets are not always able to maintain the same magnetic characteristics when the magnets are reduced in size, or the magnets cannot be configured as required when the magnets are miniaturized. One option for creating magnets of complex shapes without losing their magnetic hysteresis characteristics is the use of additive manufacturing technologies [1]. The aim of this work is to establish the relationship between the magnetic hysteresis properties of samples of single-layer permanent magnets of the *Nd-Fe-B* system and the conditions of their synthesis by selective laser sintering.

Magnetic hysteresis properties were measured on printed single-layer samples. Samples look like squares and have a linear dimension about 10x10 mm and width less than 1 mm. A mechanical mixture of two powders was used for 3D – printing: MQP-B (manufactured by Magnequench Int.) and a eutectic alloy of  $\text{Pr}(\text{Nd})_{75}(\text{Cu}_{0,25}\text{Co}_{0,75})_{25}$  in proportion 80% – 20% wt. The alloys were milled in alcohol in a ball mill. A powder fraction with a particle size of up to 100  $\mu\text{m}$  was used. The particle size was determined by sieving through several sieves after drying the obtained powder. Process of 3D-printing was made with use Orlas Creator RA. For the printing process, a brass platform is inserted into the build chamber, on which powder is evenly distributed in a 1 mm indentation. The brass provides sufficient heat dissipation for sintering the samples, but prevents the fused powder from sticking to the platform. Process of 3D-printing was made with use Orlas Creator RA. During the printing process, parameters such as the number of laser passes over the powder (*N*), laser power (*P*, *W*), hatch (*h*,  $\mu\text{m}$ ), laser beam speed (*v*, mm/s), laser beam direction ( $\alpha$ , deg), beam expander (*d*,  $\mu\text{m}$ ) were varied to achieve improved hysteresis properties. All magnetic hysteresis properties were measured  $T = 300\text{ K}$  by a PPMS DynaCool T9. The possibility of obtaining the coercivity of 19.5 kOe on single-layer magnets without the use of heavy rare-earth metals was shown.

The report will present the results in more detail and suggest ways to carry out further research.

Support by grant RSF № 21-72-10104 is acknowledged.

[1] A.S. Volegov et al., *Acta Materialia.*, **188** (2020) 733-739.

## CRYSTAL STRUCTURE AND MAGNETIC PROPERTIES OF $\text{Fe}_{0.25}\text{TaSe}_2$

*Nosova N.M.*<sup>1</sup>, *Volegov A.S.*<sup>1</sup>, *Selezneva N.V.*<sup>1</sup>, *Baranov N.V.*<sup>1,2</sup>

<sup>1</sup> Ural Federal University, Yekaterinburg, Russia

<sup>2</sup> M.N. Mikheev Institute of Metal Physics UB of RAS, Yekaterinburg, Russia  
toporova.natalia@urfu.ru

The transition metal dichalcogenides (TMDCs) and their intercalates have been the subject of increasingly active study in the fields of physics, chemistry, and materials science due to their intriguing physical and chemical properties and potential applications. In particular, the incorporation of 3d transition metal atoms into TMDC structure results in the onset of various magnetic states and properties which can be tuned by the intercalant concentration, the choice of intercalated atoms, and the host lattice. For example, the magnetic properties of the ferromagnetic compound  $\text{Fe}_x\text{TaS}_2$  with  $x \sim 0.25$  are found to substantially depend on the sample preparation procedure and heat treatments as well as on the small changes in the Fe content [1]; in particular, the value of the Curie temperature  $T_C$  in compounds with  $0.25 \leq x < 0.29$  varies from 70 K to 160 K.

The aim of the present work is to synthesize the  $\text{Fe}_{0.25}\text{TaSe}_2$  samples by using two types of methods and different heat treatments and cooling procedures, determine the features in the crystal structure and magnetic properties. Three polycrystalline samples of  $\text{Fe}_{0.25}\text{TaSe}_2$  were prepared by solid-phase reactions at 700°C using two types of routes: S1-sample synthesized by a one-stage method with subsequent cooling by removing the ampoule from the furnace to air; SC-sample (two-stage method with slow cooling in the furnace after it was turned off) and Q-sample (two-stage method with quenching of the ampoule with the sample in ice water). The X-ray certification was carried out by using a Bruker D8 Advance diffractometer. The magnetization was measured by using a SQUID-magnetometer at temperatures from 2 K to 350 K and in magnetic fields up to 70 kOe.

According to the X-ray diffraction measurements, the crystal structure of all three samples was identified as the hexagonal structure (space group  $P6_3/mmc$ ). It was found that the different methods and heat treatments do not have a strong influence on the crystal structure and lattice parameters of the main phase in the samples. The  $\text{Fe}_{0.25}\text{TaSe}_2$  samples show wide hysteresis loops with coercive field up to 65 kOe at 2 K, which is characteristic of anisotropic ferromagnets. The temperature dependence of the magnetization measured on the S1-sample in an applied magnetic field  $H = 1\text{kOe}$  and FC/ZFC regimes have revealed a pronounced anomaly of the magnetization at  $T \approx 60\text{ K}$ , which can be associated with the Curie temperature. Different heat treatments dramatically affect the peak position, and the value of the critical magnetic temperature is determined to be 38 K and 33 K for the SC-sample and the Q-sample, respectively. A substantially reduced value of  $T_C$  for the quenched sample compared with the slow-cooled sample can be attributed to the difference in the distribution of Fe atoms over the lattice. Supposedly, this difference is due to the partial mixing of tantalum and iron atoms in the Q-sample, which leads to the placement of iron atoms both in the tantalum layer and between Se-Ta-Se tri-layers, where the Fe atoms, according to previous studies [2], have different spin states.

The research funding from the Ministry of Science and Higher Education of the Russian Federation (Ural Federal University Program of Development within the Priority-2030 Program) is gratefully acknowledged.

[1] Y.J. Choi et al., *Europhysics Letters.*, **86** (2009) 37012.

[2] M. Eibschütz et al., *Phys. Rev. B.*, **15** (1977) 103-114.

## FABRICATION AND MAGNETIC CHARACTERIZATION OF 3D PRINTED COMPOSITES FROM FERRITE PARTICLES AND POLY(LACTIC ACID) POLYMER

*Amirov A.<sup>1</sup>, Omelyanchik A.<sup>1</sup>, Murzin D.<sup>1</sup>, Kolesnikova V.<sup>1</sup>, Vorontsov S.<sup>1</sup>, Musov I.<sup>2</sup>, Musov Kb.<sup>2</sup>,  
Khashirova S.<sup>2</sup>, Rodionova V.<sup>1</sup>*

<sup>1</sup> REC SMBA, Immanuel Kant Baltic Federal University, Kaliningrad, Russia

<sup>2</sup> Progressive Materials and Additive Technologies Center, Kabardino-Balkarian State University  
Named after H.M. Berbekov, Nalchik, Russia  
ASOmelyanchik@kantiana.ru

The advent of 3D printing technology has revolutionized the field of personalized medicine, allowing for the production of customized medical devices such as implants and scaffolds [1,2]. By incorporating functional inclusions, such as magnetic micro- and nanoparticles, additional properties can be added to these materials. The magnetic properties of such materials, in particular, can be exploited for drug trigger release or hyperthermic therapy [3,4]. In this study, we prepared composite magnetic filaments for 3D printing with tunable magnetic properties using a thermoplastic polylactic acid (PLA) polymer and magnetic ferrite particles of varying size and chemical composition [5]. Specifically, we utilized cobalt ferrite  $\text{CoFe}_2\text{O}_4$  nanoparticles, a mixture of  $\text{CoFe}_2\text{O}_4$  and zinc-substituted cobalt ferrite  $\text{Zn}_{0.3}\text{Co}_{0.7}\text{Fe}_2\text{O}_4$  nanoparticles (<20 nm), and barium hexaferrite  $\text{BaFe}_{12}\text{O}_{19}$  microparticles (<40  $\mu\text{m}$ ). Our results indicate that the filament sample containing 5 wt% barium hexaferrite microparticles exhibits the maximum coercivity field  $H_C = 1.6 \pm 0.1$  kOe, while the minimum  $H_C$  was found for a filament with a mixture of cobalt and zinc-cobalt spinel ferrites. Furthermore, we demonstrated the ability of the FDM 3D printing process to produce parts with simple (ring) and complex geometric shapes (honeycomb structures) using the magnetic composite filament. These findings offer promising implications for the development of personalized magnetic medical devices with tailored magnetic properties.

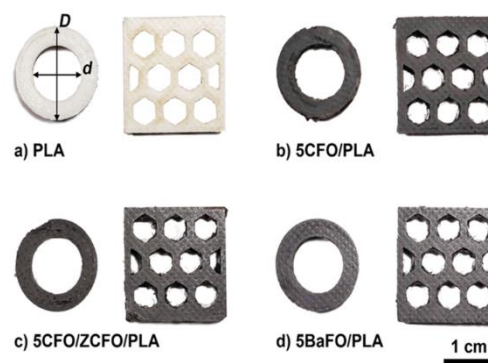


Figure 1. Pictures of objects printed with a 3D printer from the pure and composite PLA-based filament: a) pure PLA; b) 5CFO/PLA, c) 5CFO/ZCFO/PLA and d) 5BaFO/PLA composites. Reprinted from ref.[5].

This work was supported by the Russian Science Foundation under grant no 21-72-30032.

- [1] G. Giammona and F.C. Emanuela, *Molecules*, **23(4)** (2018) 980.
- [2] A. Gregor et al., *Journal of biological engineering*, **11(1)** (2017) 1-21.
- [3] J. Tang et al., *Extreme Mechanics Letters*, **46** (2021) 101305.
- [4] A. Makridis et al., *Phys. D: Appl. Phys.*, **56** (2023) 285002
- [5] A. Amirov et al., *Processes*, **10(11)** (2022) 2412.

## MAGNETIC PROPERTIES OF SUBSTITUTED FERRITES BASED ON Ni, Zn AND Co

*Perov N.S.<sup>1</sup>, Shipkova E.D.<sup>1</sup>, Vinnik D.A.<sup>2,3</sup>, Sherstyuk D.P.<sup>2</sup>*

<sup>1</sup> Lomonosov Moscow State University, Moscow, Russia

<sup>2</sup> South Ural State University, Chelyabinsk, Russia

<sup>3</sup> Moscow Institute of Physics and Technology, Dolgoprudny, Russia

Shipkova.ed17@physics.msu.ru

Ferrites include two classes of materials – magnetically hard and magnetically soft, which gives them a wide range of magnetic properties and applications. Their primary field of application is in microwave devices - phase shifters, antenna systems, circulators. Their promising application include masking of flying objects, anechoic chambers and in medicine, where they can be used for targeted drug delivery and as contrast agents in MRI [1]. It is known that by directionally doping of a material with atoms of other chemical elements, it is possible to change the magnetic properties of the material quite significantly changing it from a magnetically hard state to a magnetically soft state and vice versa [2]. Of particular interest are those materials whose magnetic properties can be tuned to specific requirements using a double or more degree of substitution. The additional possibility of using a small step in the doping concentration allows the magnetic properties of the material to be adjusted smoothly, thereby increasing its functionality [3,4].

In this work, spinel ferrites with a triple degree of substitution have been studied. The samples were divided into three series, in each of which the concentration of Co was fixed, and the concentrations of the other two elements Ni/Zn varied within certain limits:  $\text{Co}_{0.1}\text{Zn}_{0.9-x}\text{Ni}_x\text{Fe}_2\text{O}_4$ ,  $\text{Co}_{0.2}\text{Zn}_{0.8-x}\text{Ni}_x\text{Fe}_2\text{O}_4$ ,  $\text{Co}_{0.4}\text{Zn}_{0.6-x}\text{Ni}_x\text{Fe}_2\text{O}_4$ .

The samples are powders obtained by solid-phase synthesis by colleagues from the South Ural State University in the Crystal Growth Laboratory. Based on the data obtained as a result of element analysis (Jeol JSM 7001F, INCA X-max 80 electron microscope), it can be concluded that the given and actual formulas are in a good agreement. The surface morphology of the samples is a set of microcrystallites characteristic of the cubic system. The samples phase compositions were studied on a powder diffractometer Rigaku Optima IV. All the observed peaks correspond exactly to the JCPDS 74-2397 related to ferrite with space group  $\text{Fd}\bar{3}\text{m}$ .

Measurements of hysteresis loops were carried out on a LakeShore 7407 series vibration sample magnetometer (VSM) at different temperatures: 100, 300 and 420 K. From them the main magnetic parameters were obtained – saturation magnetization ( $M_s$ ) and coercive force ( $H_c$ ). Also, for each series, the dependence of magnetization on the temperature  $M(T)$  was measured in the general temperature range from 100 to 1000 K, from which the Curie temperatures ( $T_c$ ) were obtained. The concentration dependences of the main magnetic parameters ( $M_s$  and  $H_c$ ) for a series of samples  $\text{Co}_{0.1}\text{Zn}_{0.9-x}\text{Ni}_x\text{Fe}_2\text{O}_4$  are shown in Figures 1 and 2.

The behaviour of  $M_s(x)$  is shown in Figure 1. Irrespective of the measurement temperature, it has a general form: increases, reaches a maximum and decreases. This can be explained by the distribution of the cations along tetrahedral and octahedral spinel positions. It is known that  $\text{Zn}^{2+}$  ions prefer to occupy tetrahedral positions (A), while  $\text{Ni}^{2+}$  and  $\text{Co}^{2+}$  ions tend to occupy octahedral positions (B). According to these preferences and the mechanism of distribution of cations in A and B positions, the magnetic moment of the sublattice A increases, and that of the sublattice B decreases. Then, in accordance with the Neel model, there is an increase in  $M_s(x)$  in Figure 1. The further decrease of  $M_s(x)$  can't be explained by Neel's model. Probably, another model should be used to explain the  $M_s(x)$  dependence. As the measurement temperature decrease for a fixed concentration, the  $M_s$  value increases, which can be explained by a decrease in thermal fluctuations.

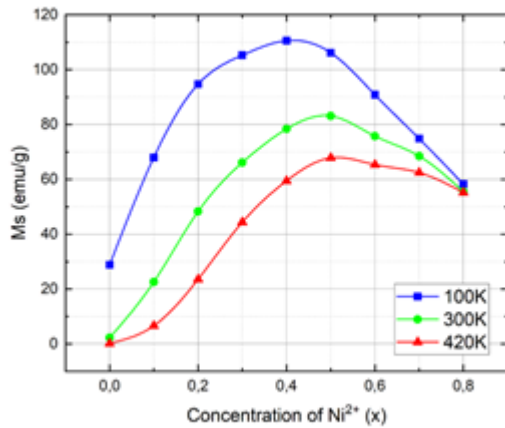


Figure 1. Concentration dependence of saturation magnetization, 16kOe.

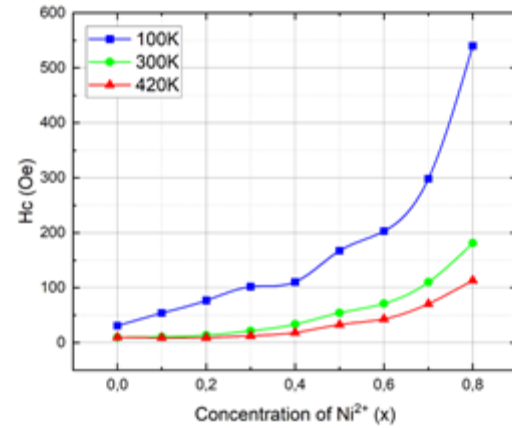


Figure 2. Concentration dependence of coercive force, 16kOe.

The general growth trend of the  $H_c(x)$  dependencies, shown in Figure 2, can be explained by an increase in magnetic anisotropy.

For random samples, four for each series, Curie temperatures were obtained. They increase with increasing concentration of doped  $Ni^{2+}$ . This can be explained by the increasing exchange interlattice AB-interaction.

- [1] Z. Shi et al., *JMMM*, **498** (2020) 166222.
- [2] M. Kurian, S. Thankachan, *Open Ceram.*, **8** (2021) 100179.
- [3] D.A. Vinnik et al., *Ceram. Int.*, **48** (2022) 18124-18133.
- [4] D.P. Sherstuk et al., *Ceram. Int.*, **47** (2021) 12163-12169.

## INFLUENCE OF LOAD ANNEALING ON MAGNETIC PROPERTIES AND STRUCTURE OF $\text{Fe}_{68.5}\text{Cr}_5\text{Si}_{13.5}\text{B}_9\text{Nb}_3\text{Cu}_1$ NANOCRYSTALLINE RIBBONS

*Kharlamova A.M.<sup>1</sup>, Kozhevnikova P.Y.<sup>1</sup>, Kaminskaya T.P.<sup>1</sup>, Larrañaga A.<sup>2</sup>, Kurlyandskaya G.V.<sup>3</sup>, Shalygina E.E.<sup>1</sup>*

<sup>1</sup> Lomonosov Moscow State University, Moscow, Russia

<sup>2</sup> SGIKER, The Basque Country University UPV/EHU, Leioa, Spain

<sup>3</sup> Ural Federal University, Yekaterinburg, Russia

anna-h-m@mail.ru

New alloys based on the so-called FINEMET class of materials were created by changing the composition in order to acquire excellent soft magnetic properties, requested by different applications. The addition of Cr and as a consequence Fe reduction led to an increase in the temperature of crystallization and corrosion resistance of the ribbons [1]. In this work the results of the influence of load annealing on the structure and magnetic properties of  $\text{Fe}_{68.5}\text{Cr}_5\text{Si}_{13.5}\text{B}_9\text{Nb}_3\text{Cu}_1$  ribbons are presented. The ribbons were obtained by rapid quenching from the melt and then annealed at a temperature of 520°C for 2 hours without load (FM-AN) and under the load of 150 MPa (FM-SA). Two ribbons of different width,  $c$ , 0.88 mm (FM1 and FM4) and 0.60 mm (FM2 and FM3) were produced in each series (FM-AN and FM-SA). According to XRD data, the ribbons had a nanocrystalline structure and the size of crystallite is of the order of 15 nm. AFM data showed that for the samples FM-AN the average surface roughness,  $R_a$ , is about 20 nm, and the deviation of the surface profile,  $\Delta Z$ , is about 100 nm and for FM-SA -  $R_a \approx 10$  nm and  $\Delta Z \approx 20$  nm. During magnetic measurements the external magnetic field,  $H$ , was applied in the plane of the ribbons. The holder rotated around its axis from 0° to 360° in increments of 10°. At  $\theta=0^\circ$   $H$  was parallel to the long side of the ribbon. The volume magnetic characteristics obtained by the vibration magnetometer (VSM) (Figure 1a, 1b) indicate the effect of load annealing: the hysteresis loops become more sloped as a result of the induction of transverse magnetic anisotropy; the values of  $H_C$  and  $H_S$  increases and values of  $M_S$  decrease. Reducing the width of the ribbon leads to a decrease in the values of  $M_S$  and an increase in the values of  $H_C$ . The magnetic field behavior of the samples depends on the  $\theta$ . The oscillating dependence  $H_S(\theta)$  (Figure 1b) confirms the presence of uniaxial magnetic anisotropy.

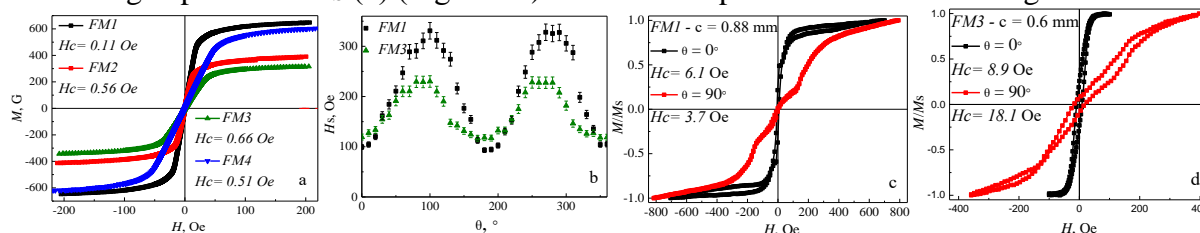


Figure 1. Hysteresis loops measured by VSM (a) and  $H_S(\theta)$  dependence (b); hysteresis loops and DS images, for FM1 (c) and FM3 (d) measured by MOKE.

The surface hysteresis loops and simultaneous visualization of the changes of domain structure (DS) were measured using a magneto-optical Kerr magnetometer (MOKE) by means of the meridional Kerr effect (Figure 1c, 1d). The surface hysteresis loops have a more complex shape and the magnetization reversal at  $\theta=90^\circ$  occurs in two stage. The near-surface values of  $H_C$  increase with a decrease in the width of the ribbons, and are also an order of magnitude greater than the volume values. The angular dependence of the magnetization is analysed.

[1] G.V. Kurlyandskaya et al., *J. of Alloys and Compounds*, **566** (2013) 31-36.

## AMORPHOUS RIBBONS FOR EPOXYCOMPOSITE DETECTION

*Pasynkova A.A.<sup>1,2</sup>, Timofeeva A.V.<sup>1</sup>, Mel'nikov G.Yu.<sup>2</sup>, Lukshina V.A.<sup>1</sup>, Kurlyandskaya G.V.<sup>2</sup>*

<sup>1</sup> M.N. Mikheev Institute of Metal Physics UB RAS, Yekaterinburg, Russia

<sup>2</sup> Ural Federal University, Yekaterinburg, Russia

pasynkova\_a@imp.uran.ru

Magnetic biodetection is a hot topic of recent decades [1]. The important aim in this area is detection of magnetic particles in polymer matrix using a sensitive element. At the first stages, it is optimal to choose polymer matrix that both non-interacting with the sensitive element and easy to handle in a physical laboratory. These qualities are satisfied by solid composites based on epoxy resin [2]. Sensing elements based on the giant magnetoimpedance effect (GMI) effect stand out due to the extremely high dependence of the impedance of the conductor through which the alternating current flows, when an external magnetic field is applied [1]. The influence of the interdependence of the shape parameters of both composites with microparticles and amorphous ribbons will be studied in this work.

Composites based on epoxy resin and commercial microparticles Alfa Aesar were studied, the sample had the shape of a cylinder with a diameter of 5 mm and a height of 4 mm. For this experiment sample with epoxy composite with 0% concentration (control, B) with a concentration of 30% (C) were selected. A sample based on the  $\text{Fe}_3\text{Co}_{67}\text{Cr}_3\text{Si}_{15}\text{B}_{12}$  alloy (A) after thermomechanical treatment at 250 MPa, 1 hour, that is, at the parameters at which the GMI effect of up to 250 % was previously obtained [3]. A sample with geometric parameters of  $45 \times 0.8 \times 0.024 \text{ mm}^3$  was studied. An amorphous ribbon was fixed to a microstrip line using silver glue and then attached on a measuring complex based on an Agilent impedance analyzer. The GMI ration was calculated as follow  $\Delta Z/Z = 100 \% \times (Z(H) - Z(H_{\text{max}})) / Z(H_{\text{max}})$ , where  $H_{\text{max}} = 130 \text{ Oe}$ . A cylindrical sample was placed in the center of the ribbon and above it. As can be seen, the influence of the composite is about  $\Delta Z/Z = 12 \%$ , and the largest contribution is observed in the field region of 4.8 Oe, without a significant shift in the position of the maximum of the field dependence (Figure 1). Based on this, we can conclude that influence of the epoxycomposite on an amorphous ribbon of this length falls mainly the transverse component of stray fields (along the short side of the GMI element).

Comparative analysis of ribbons of different lengths, as well as mathematical modeling of the system "amorphous ribbon + epoxycomposite with microparticles" will be presented in the report.

This work was supported by the Grant of the President of the Russian Federation MK-2080.2022.1.2.

[1] H.T. Huang et al., *SPIN*, **09(02)** (2019) 1940002.

[2] G.Yu. Mel'nikov et al., *Phys. Met. Metallogr.*, **123(11)** (2022) 1075-1083.

[3] A.A. Pasynkova, A.V. Timofeeva, V.A. Lukshina, *SPIN*, (2022) online ready.

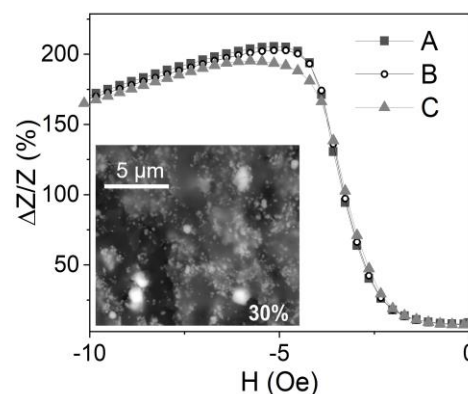


Figure 1. Field dependence of magnetoimpedance ratio of the total impedance at frequency 37 MHz. SEM images of the surface of epoxy composites with mass concentrations of FeOx microparticles of 30 wt. % in the inset.

## MAGNETISATION REVERSAL PROCESSES IN PERMANENT MAGNETS Nd-Fe-B AND Sm(Co, Fe, Zr, Cu)<sub>z</sub> TYPE

*Urzhumtsev A.N.<sup>1,2</sup>, Maltseva V.E.<sup>1</sup>, Volegov A.S.<sup>1</sup>*

<sup>1</sup> Ural Federal University, Yekaterinburg, Russia

<sup>2</sup> POZ-Progress Ltd., Verkhnyaya Pyshma, Russia

andrei.urzhumtsev@urfu.ru

Rare-earth permanent magnets (PM) are the main part of devices for electrical energy conversion. The efficiency of such devices as electric motors and generators is mainly limited by the maximum energy of the PM used in them. For further development of PMs, a fundamental understanding of the processes of changing their magnetic state in the process of magnetization and demagnetization is necessary.

The most common PM grades were chosen for the study: N35, N48 and N48SH based on the Nd<sub>2</sub>Fe<sub>14</sub>B phase and Sm(Co, Fe, Zr, Cu)<sub>6.63</sub> based on the Sm<sub>2</sub>Co<sub>17</sub> phase, provided by POZ-Progress Ltd. Their microstructure was studied by SEM and EDX analysis on a Tescan Mira3 LMU microscope. Magnetic measurements were carried out on measuring complexes MPMS XL 7 and DynaCool in the fields up to 7 and 9 Tesla, respectively. Magnetization curves  $\sigma(H)$  and  $\sigma_r(H)$ , reversible magnetic susceptibility curves  $\chi(H)$  and  $\chi_r(H)$ , reversible magnetization contribution curves  $(\sigma - \sigma_r)(H)$  from the thermal demagnetized state, as well as partial hysteresis loops and angular dependences of coercivity  $H_c(\theta)$  on the angle of the demagnetizing field application to the magnet texture axis were obtained and analyzed.

The study of the microstructure of PM showed that in N35 the presence of oxide-based phases both in the grain volume and grain boundary phase is observed, in N48 their presence in the boundaries was noted, in N48SH no phases in connection with oxygen were found. In Sm(Co, Fe, Zr, Cu)<sub>6.63</sub> the traces of oxides are slightly present as local inclusions in the structure of sintered particles.

Magnetic analysis techniques show that magnetization from the thermo-demagnetized state proceeds more easily, in the samples with the least presence of oxide phases. The reversible magnetic susceptibility curves for N35 and N48 exhibit a response from the unfixed domain walls during demagnetization, which is practically not observed in N48SH. The analysis of the angular dependences of the coercive force shows that the curves for N35 and N48 within the magnetostatic interactions approximation correspond to the pinning model [1].

In the Sm(Co, Fe, Zr, Cu)<sub>z</sub> magnets, a response from the unbound domain walls in the thermo-magnetized state was found, which is not observed in the samples demagnetized by the field. The magnetization and demagnetization processes in the Sm(Co, Fe, Zr, Cu)<sub>z</sub> PMs were found to be qualitatively similar to those in the Nd-Fe-B N48SH grade and indirectly indicate the predominance of nucleation-type mechanisms.

The results show that within the same class of permanent magnets, depending on their microstructure, both the nucleation mechanism and the pinning mechanism can prevail. It is shown that the superposition of the remagnetization mechanisms leads to a violation of the monotonicity on the partial hysteresis loops.

The paper analyzes the results based on magnetometric techniques that can be used to determine the role of the nucleation and pinning mechanism in the remagnetization processes of a wide range of PM samples.

This work was financially supported by RSF grant № 21-72-10104.

[1] A.N. Urzhumtsev et al., *Phys. Metals Metallogr.*, **123** (2022) 1054-1060.

## TRANSPORT PHENOMENA OF CRYSTALLINE AND AMORPHOUS ALLOYS OF TRANSITION METALS

*Imamnazarov D.H.*

Samarkand State University named after Sharof Rashidov, Samarkand, Uzbekistan  
davronimamnazarov@gmail.com

The work presents the results of calculations of the electrical resistivity  $\rho$ , the Hall effect coefficient  $R$ , and the magnetoresistance  $\Delta\rho/\rho_0$  of crystalline and amorphous transition metal alloys with unoccupied d-states. In this case, we use the expressions we obtained earlier in the framework [1] of the generalized s-d model of the single-site of the coherent potential approximation (CPA), in which the partial contributions to the kinetic effects of the s- and d-states, the hybridization contributions of both intraband and interband current carriers.

It is shown that the hybridization contributions are significant for explaining the values of  $\rho$  and  $R$ , the change in the sign of the Hall coefficient  $R$  with a change in the concentration composition of the alloy.

Using the examples of model calculations with semi-elliptic form of the density of states and calculations with a realistic form of the density of states for PdAg, PdAu, and AuAg alloys, it was found that the contribution of d states to the conductivity dominates at the position of the Fermi level near the edge of the d peak; under certain conditions, the contribution associated with hybridization is not small and can lead to significant change in the sign of  $R$  from negative to positive with change in the concentrations of one of the alloy components. The significant deviation from the Nordheim law is determined for the concentration dependence of  $\rho$  for highly resistive alloys depending on strong scattering and hybridization. It is shown that when the Fermi level lies inside the d-band, the smearing of the effective density of states by the electron-phonon interaction leads to a temperature-independent  $\rho$ , and when the Fermi level is located near the maximum density of d-states, then  $\rho(T)$  can decrease with increasing temperature, which is consistent with Muji's rule of thumb about the correlation between the temperature coefficient of resistance (TCR) and the density of states. In contrast to  $\rho$ , the Hall coefficient has opposite temperature dependences and can be determined by analogy with the Muji criterion on the correlation between the TCR and the temperature dependence of the Hall coefficient.

In the case of amorphous alloys, the single-site Green's function of the alloy is first calculated in the CPA taking into account the off-diagonal disorder, in which the jump integral of the s-d model takes a continuous series of values corresponding to the pair distribution function of the atoms of the amorphous alloy. The electronic structure of the amorphous alloy determined in this way is then used to calculate the kinetic effects based on the Kubo formula using a procedure similar to that developed in the CPA for crystalline alloys. It is shown that amorphization leads to significant changes in the electronic structure and transport phenomena. The calculated concentration and temperature dependences of  $\rho$  and  $R$  for CuZr, CuTi, NiZr, and FeZr amorphous alloys are in good agreement with the available experimental data.

The results of calculations of the magnetoresistance of disordered alloys within the framework of the PKP are also presented. The analysis of the resulting general expression shows that, in the limiting case of weak scattering, the transverse magnetoresistance vanishes in accordance with the classical theory, and taking into account the first nonvanishing corrections for the spreading of the Fermi surface leads to a deviation from the classical expression. It is also shown that as the scattering intensity increases, the magnetoresistance increases in proportion to the spreading of the Fermi surface.

[1] D.H. Imamnazarov, A.B. Granovsky, *Moscow Uni. Phys. Bull.*, **75(3)** (2020) 230-236.

## MAGNETIC PROPERTIES OF ALLOYS OF THE SYSTEM $\text{Fe}_{85-x}\text{Cr}_x\text{B}_{15}$ ( $x=8\div 15$ ) IN AMORPHOUS AND LIQUID STATES

*Kuvandikov O.K.<sup>1</sup>, Usarov U.T.<sup>2</sup>, Suleimanov O.A.<sup>3</sup>, Usanov Sh.<sup>4</sup>*

<sup>1</sup> Samarkand State University named after Sharof Rashidov, Samarkand, Uzbekistan

<sup>2</sup> Samarkand State University of Architecture and Civil Engineering, Samarkand, Uzbekistan

<sup>3</sup> Uzbek-Finnish Pedagogical Institute of SSU, Samarkand, Uzbekistan

<sup>4</sup> State inspection for supervision of education quality at the CM RUz, Uzbekistan  
quvandikov@rambler.ru

Among the many different types of magnetic ordering, antiferromagnets make up numerous class that includes more than thousand elements, compounds and alloys. In recent years, dozens of oxide compounds have been added to them.

The purpose of this work is high-temperature studies of the magnetic properties of  $\text{Fe}_{85-x}\text{Cr}_x\text{B}_{15}$  alloys in amorphous and liquid states, synthesis and analysis of research objects. Study of the influence of the concentration of chromium atoms in the studied objects on magnetic phase transitions. The magnetic susceptibilities of alloys of the  $\text{Fe}_{85-x}\text{Cr}_x\text{B}_{15}$  system in the amorphous and liquid states were measured on high-temperature setup using the Faraday differential method [1].

The temperature dependence of the paramagnetic susceptibility of alloys of the  $\text{Fe}_{85-x}\text{Cr}_x\text{B}_{15}$  system in the amorphous and liquid states is described by the Curie-Weiss formula:

$$\chi = \frac{N\mu_B^2 S^2}{3k(T \pm \theta_N)}$$

With an increase in the concentration of chromium in amorphous  $\text{Fe}_{85-x}\text{Cr}_x\text{B}_{15}$  alloys, a shift in temperature  $\theta_N$  towards low temperatures is observed; at a concentration of chromium  $\text{Fe}_{85-x}\text{Cr}_x\text{B}_{15}$ , a ferromagnet-antiferromagnet transition is observed. When extrapolating the temperature dependences ( $\chi^{-1}$ ), the asymptotic Curie temperatures  $\theta_A$  of alloys of the  $\text{Fe}_{85-x}\text{Cr}_x\text{B}_{15}$  system in the liquid state were found. At the melting point, the susceptibility noticeably increases, after which the linear dependence  $\chi^{-1}(T)$  is again fulfilled.

The value of  $\theta_N$  for the liquid phase changes towards negative values, the constant C also changes, it becomes somewhat smaller than for the solid phase.

Table 1. Parameters of magnetic properties of the samples

Alloy	Amorphous state				Liquid state			
	$\theta_C, \text{K}$	$\theta_N, \text{K}$	$C, 10^{-2}$	$\mu_{eff}, \mu_B$	$\theta_N, \text{K}$	$\theta_A, \text{K}$	$C, 10^{-2}$	$\mu_{eff}, \mu_B$
1. $\text{Fe}_{77}\text{Cr}_8\text{B}_{15}$	440	-	3,42	4,3	-	-1910	7.27	5.36
2. $\text{Fe}_{75}\text{Cr}_{10}\text{B}_{15}$	400	-	2,48	3,5	-	-1200	5.07	4.45
3. $\text{Fe}_{73}\text{Cr}_{12}\text{B}_{15}$	350	-	2,78	3,8	-	-880	4.32	4.11
4. $\text{Fe}_{70}\text{Cr}_{15}\text{B}_{15}$	-	300	2,54	3,7	-	-1138	4.27	4.08

For liquid state  $\theta_n$  and the energy of exchange interaction decreases with an increase in temperature. The reduction in the energy of exchange interaction is understandable, if only because with an increase in temperature the distance between atoms increases and, therefore, the integral of the overlapping of d-functions decreases. Since the alloys of the  $\text{Fe}_{85-x}\text{Cr}_x\text{B}_{15}$  are antiferromagnets, they are in the area of the negative values of the exchange integral. For the investigated  $\text{Fe}_{85-x}\text{Cr}_x\text{B}_{15}$  amorphous systems,  $\text{Fe}_{77}\text{Cr}_8\text{B}_{15}$ ,  $\text{Fe}_{75}\text{Cr}_{10}\text{B}_{15}$ ,  $\text{Fe}_{73}\text{Cr}_{12}\text{B}_{15}$  alloys behave like ferromagnets, while  $\text{Fe}_{70}\text{Cr}_{15}\text{B}_{15}$  alloys behave like an antiferromagnet. In the liquid state, these alloys are antiferromagnets.

[1] O.K.Kuvandikov. *Magnetic and kinetic properties of condensed alloys and compounds based on transition and rare earth metals.* (Tashkent: Fan, 2009)

## MAGNETIC PROPERTIES AND HALL EFFECT OF COMPENSATED FERRIMAGNET $\text{Mn}_{1.5}\text{Co}_{0.75}\text{V}_{0.75}\text{Al}$

*Seredina M.A.<sup>1</sup>, Bogach A.V.<sup>2</sup>, Gorsbenkov M.V.<sup>1</sup>, Karpenkov D.Yu.<sup>1,3</sup>, Kolesnikov E.A.<sup>1</sup>, Taskaev S.V.<sup>4</sup>, Kbovaylo V.V.<sup>1</sup>*

<sup>1</sup> National University of Science and Technology “MISIS”, Moscow, Russia

<sup>2</sup> GPI RAS, Moscow, Russia

<sup>3</sup> Lomonosov Moscow State University, Moscow, Russia

<sup>4</sup> CSU, Chelyabinsk, Russia

nmseredina@gmail.com

Compensated ferrimagnets of Heusler alloys with a high Curie temperature have attracted considerable interest recently due to the prospects in applications of spintronics. In some compensated ferrimagnets, for example, in a tetragonal  $\text{Mn}_{2.3}\text{Pd}_{0.7}\text{Ga}$  [1], the emergence of the topological Hall effect has been observed. Here we report on the similar features which we found in a compensated cubic ferrimagnet  $\text{Mn}_{1.5}\text{Co}_{0.75}\text{V}_{0.75}\text{Al}$  in the form of melt spun ribbons.

Ribbons were synthesized by melt spinning technique. Preliminarily the ingot was prepared by an arc melting method in argon atmosphere. XRD analysis revealed that ribbons were single-phase (space group  $F\bar{4}3m$ ) with lattice parameter  $a = 0.5823$  nm. The results of transmission electron microscopy showed the presence of antiphase domains in the samples. Real composition of samples determined by energy dispersive X-ray spectroscopy was found to be  $\text{Mn}_{1.51}\text{Co}_{0.76}\text{V}_{0.69}\text{Al}_{1.04}$ . Magnetic and galvanomagnetic properties were measured in a temperature range 4.2 – 600 K and in magnetic field up to 80 kOe.

The experimentally determined Curie temperature was  $T_C = 495$  K, while the compensation temperature was  $T_{comp} \sim 396$  K. In the samples, the dominant role of hole conductivity was observed in temperature range 4.2 – 420 K. Near the compensation point in weak magnetic fields, the Hall resistivity curves demonstrated an additional contribution, similar to the topological Hall effect (Figure 1). The normal Hall coefficient, carrier concentration and Hall mobility were on the order of  $10^{-2}$ - $10^{-3}$   $\text{cm}^3/\text{C}$ ,  $10^{20}$ - $10^{21}$   $\text{cm}^{-3}$  and  $10^1$   $\text{cm}^2/(\text{V}\cdot\text{sec})$ , respectively.

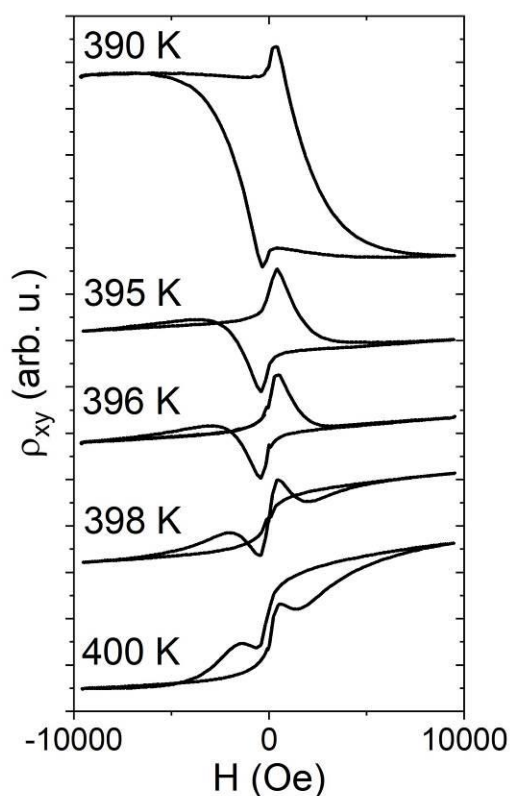


Figure 1. Magnetic field dependencies of Hall resistivity for  $\text{Mn}_{1.5}\text{Co}_{0.75}\text{V}_{0.75}\text{Al}$  at different temperatures near the compensation point.

This work was supported by Russian Science Foundation (grant No. 21-42-00035).

[1] W.-Y. Choi, W. Yoo, M.-H. Jung, *NPG Asia Materials*, **13** (2021) 79.

2PO-L2-14

## NON-COLLINEAR PHASE IN RARE EARTH FERRITE GARNET FILMS AT THE COMPENSATION POINT

*Suslov D.A.<sup>1</sup>, Vetoshko V.V.<sup>1</sup>, Mashirov A.V.<sup>1</sup>, Taskaev S.V.<sup>3</sup>, Polulyakb S.N.<sup>2</sup>, Berzhansky V.N.<sup>2</sup>  
Shavrov V.G.<sup>1</sup>*

<sup>1</sup> Kotel'nikov IRE RAS, Moscow, Russia

<sup>2</sup> V.I. Vernadsky Crimean Federal University, Simferopol, Russia

<sup>3</sup> Chelyabinsk State University, Chelyabinsk, Russia  
sda\_53@mail.ru

The experimental discovery of the suppression effect of the non-collinear phase in strong magnetic fields near the compensation point in ferrimagnetic structures has been made. The observations were carried out using the magneto-optical method by creating a lateral temperature gradient in the plane of the epitaxial films of ferrite garnets. The non-collinear phase arises in the vicinity of the compensation point in magnetic fields exceeding some critical value  $H_{c1}$ . As the magnetic field is increased, the region of existence of the non-collinear phase expands to the value of the magnetic field  $H_{c2}$  and disappears at the critical field  $H_{c3}$ . The effect of the occurrence and suppression of the non-collinear phase is demonstrated on samples of two types of ferrite garnet films with two and three magnetic sublattices. Phase diagrams of magnetic states in the vicinity of the critical point are constructed, and it is shown that the region of existence of the non-collinear phase in a two-sublattice magnet is smaller than in a three-sublattice one.

The research was carried out with the support of the Russian Science Foundation, project No. 22-22-00754, <https://rscf.ru/project/22-22-00754/>.

## HIGH COERCIVITY AND EXCHANGE BIAS EFFECT IN $\text{Fe}_2\text{CrSe}_4$

*Selezneva N.V.<sup>1</sup>, Komarova V.A.<sup>1</sup>, Mozgovykh S.N.<sup>1</sup>, Sherokalova E.M.<sup>1</sup>, Volegov A.S.<sup>1</sup>, Baranov N.V.<sup>1,2</sup>*

<sup>1</sup> Ural Federal University, Yekaterinburg, Russia

<sup>2</sup> M.N. Mikheev Institute of Metal Physics UB of RAS, Yekaterinburg, Russia  
N.V.Selezneva@urfu.ru

Among other transition metal chalcogenides, the  $\text{Fe}_3\text{Se}_4$  compound is considered as a promising platform for creating rare-earth-free permanent magnets [1, 2]. The  $\text{Fe}_3\text{Se}_4$  composition lies in an intermediate position in the series of transition metal ( $M$ ) chalcogenides  $M_{1-z}X$  ( $X = \text{chalcogen}$ ) between  $MX$  with the NiAs structure and  $MX_2$  with the  $\text{CdI}_2$  structure. Due to the ordering of vacancies and the monoclinic crystal structure, the  $\text{Fe}_3\text{Se}_4$  compound has a high magnetocrystalline anisotropy, which is associated with the spin-orbital interaction and the influence of the crystal electric field. The substitution of chromium for iron in  $\text{Fe}_{3-x}\text{Cr}_x\text{Se}_4$  leads to significant changes in the magnetic and transport properties [3]. Data on the magnetic behavior of  $\text{Fe}_2\text{CrSe}_4$  are scarce.

This work aims to study how the replacement of one third of the iron atoms in the ferrimagnet  $\text{Fe}_3\text{Se}_4$  by chromium atoms affects the crystal structure and magnetic behavior with temperature and in magnetic fields. Taking into account that the distribution of iron and chromium atoms in and between cation layers can affect the exchange interaction and the formation of the resulting magnetization in  $\text{Fe}_2\text{CrSe}_4$ , attention is paid to the effect of heat treatment and cooling conditions on the structure and magnetic hysteresis in this compound at different temperatures. The results obtained, we hope, will help to better understand the mechanisms responsible for the formation of the magnetic properties of layered chalcogenide materials and find ways to control these properties.

A polycrystalline as-synthesized  $\text{Fe}_2\text{CrSe}_4$  sample (AS-sample) and a sample after subsequent additional heat treatment and quenching (Q-sample) were studied in the present work by means of x-ray diffraction and magnetization measurements. The crystal structure of the AS-sample was refined in the monoclinic syngony using three models. It was found that the AS-sample of  $\text{Fe}_2\text{CrSe}_4$  below the Neel temperature  $T_N \sim 300$  K exhibits the behavior characteristic of a ferrimagnet with a compensation point  $T_{\text{comp}} \sim 140$  K, and has a large magnetic hysteresis (hysteresis loop half-width up to 15 kOe) and a significant exchange bias effect ( $H_{\text{EB}}$  up to 6.6 kOe at 2 K). The temperature change in the half-width of the hysteresis loop is quite complex; it can be described as a superposition of exponential decay of  $H_c$  with increasing temperature and a nonmonotonic temperature dependence of  $H_c$  with two peaks at temperatures below and above  $T_{\text{comp}}$ . The exchange bias effect in  $\text{Fe}_2\text{CrSe}_4$  is ascribed to the inhomogeneity of the magnetic state of this compound arising from the inhomogeneous distribution of chromium atoms replacing iron atoms in cationic layers and the possible coexistence of regions with different atomic orderings. Meanwhile, our data on the effect of additional annealing and quenching confirm the importance of the distribution of chromium and iron atoms and vacancies in the formation of the properties of  $\text{Fe}_2\text{CrSe}_4$  and the exchange bias. The Q-sample obtained by an additional heat treatment and subsequent rapid cooling of the AS-sample was found to exhibit an increased by 13% magnetic ordering temperature, no compensation for sublattice magnetizations, and a significant decrease in the exchange bias.

This work was supported by the Russian Science Foundation (Grant No. 22-13-00158).

[1] D. Li et al., *J. Magn. Magn. Mat.*, **469** (2019) 535-544.

[2] Z. Shao et al., *Nanoscale Advances.*, **2** (2020) 4341-4349.

[3] G. J. Snyder et al., *Phys. Rev. B.*, **62** (2000) 10185.

**July 2**

Sunday

18:15 - 20:00

POSTER  
SESSIONS

Section L3

**Magnetic Soft Matter,  
Magnetism in  
Biology and Medicine**

2PO-L3-1

## MOLECULAR DYNAMICS SIMULATIONS OF MAGNETIC ELASTOMERS FILLED WITH ANISOTROPIC SHAPED PARTICLES

*Aleksandrov I.A.<sup>1</sup>, Dobroserdova A.B.<sup>1</sup>, Kantorovich S.S.<sup>2</sup>*

<sup>1</sup> Ural Federal University, Yekaterinburg, Russia

<sup>2</sup> University of Vienna, Vienna, Austria

alla.dobroserdova@urfu.ru

Magnetic elastomers are systems consisting of magnetizable particles embedded in a non-magnetic elastomer matrix. They have a wide range of applications, from technical applications to medicine. Magnetic elastomers are used in the design of magnetically controlled adaptive damping devices, stiffness tunable mounts, vibrational absorbers, force sensors and artificial muscles, soft actuators and micromanipulators [1]. The basis of their practical application lies in the fact that the mechanical and rheological behaviour of such materials, their shape and physical properties can be controlled using an applied external magnetic field. It is important to note that, in contrast to natural soft magnetic materials, in the case of magnetic elastomers, rather weak fields can be used, which is an undoubted advantage of such systems.

In this work, we focus on the study of magnetic elastomers using molecular dynamics simulations. We model magnetic elastomers filled with magnetic particles with shape anisotropy. To model such complex particles, we create a special shape that resembles flakes. To do this, the magnetic particle must be surrounded by non-magnetic particles, which will move and rotate together with the magnetic one. We also plan to complicate the modeling of such a particle by giving dipole moments not only to the central particle, but also to several others. Thus, it will be possible to simulate particles with a distributed dipole moment. After that, it is necessary to simulate an elastic matrix, which will contain magnetic particles with shape anisotropy. To do this, we use four harmonic springs to limit translational and rotational motion. The base of such a particle can be considered an ellipse. Two harmonic springs will hold the extreme non-magnetic particles located on the major axis of the ellipse, the rest – the extreme non-magnetic particles on the minor axis.

Further, it is interesting to compare the magnetic energies of two systems: with the point and distributed dipoles. There is an assumption that in such systems distributed dipoles will contribute to a decrease in magnetic energy.

RSF 19-12-00209 is acknowledged.

[1] G. Filipcsei, *In Oligomers – Polymer Composites – Molecular Imprinting* (Berlin, 2007).

[2] P.A. Sanchez et al., *Soft Matter*, **14** (2018) 2170–2183.

[3] Extensible Simulation Package for Research on Soft matter systems. – Mode of access <http://espressomd.org>.

## MATHEMATICAL MODEL OF MAGNETICALLY ACTIVE ELASTOMER DEFORMATION

*Ignatov A.A.<sup>1</sup>, Stolbov O.V.<sup>2</sup>, Rodionova V.V.<sup>1</sup>*

<sup>1</sup> Immanuel Kant Baltic Federal University, Kaliningrad, Russia

<sup>2</sup> Institute of Continuum Mechanics, Ural Branch of the RAS, Perm, Russia

artem.ignatov98@gmail.com

In the last few years, there has been an increased interest in “smart” materials based on a polymer with magnetic inclusions [1]. Numerical methods are used to study the quantitative properties of such materials [2]. This work is devoted to the calculation of deformations in an external field of a structured magnetically active elastomer with magnetically hard inclusions in a 2D formulation by the finite element method using the FEniCS package.

In this work, deformations of a representative volume of a composite were studied. In the initial state of the composite, the particles (Figure 1) were located at the nodes of a 4 by 4 rectangular grid with square cells and had a “checkerboard” orientation of magnetic moments—any neighboring particles in a “vertical” or “horizontal” row have an antiparallel orientation of magnetic moments.

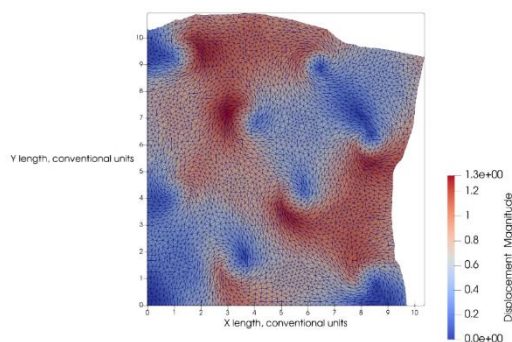


Figure 1. Deformation of an elastic matrix with hard magnetic particles.

The Neo-Hooke potential [3] was used to describe the hyperelastic matrix material. In modeling, the shape of the particles was assumed to be an ideal circle, and the particles themselves were considered to be single-domain. Also, during the simulation, the possibility of destruction of the matrix-particle boundary was excluded, i.e. full adhesion of particles and matrix was assumed.

As a result, the deformations of the material were calculated depending on the initial orientation of the magnetization of the particles and the magnitude of their magnetic moments.

The project was supported by the Ministry of Science and Higher Education of the Russian Federation (agreement no. 075-02-2023-934)

[1] A. Allue et al., *Comp.Part A: Appl. Sci. and Man.*, **120** (2019) 12-20.

[2] G. Sossou et al., *Materials and Design*, **181** (2019) 108074.

[3] A.I. Lurie, *Theory of elasticity* (Nauka, 1970).

## SIMULATION OF FIELD-CONTROLLED MASS TRANSPORT IN MAGNETIC NANOENSEMBLES

*Kuznetsov A.A.<sup>1</sup>, Zverev V.S.<sup>2</sup>, Kantorovich S.S.<sup>1</sup>*

<sup>1</sup> University of Vienna, Vienna, Austria

<sup>2</sup> Ural Federal University, Yekaterinburg, Russia  
andrey.kuznetsov@univie.ac.at

Magnetophoresis is a motion of magnetic particles under the action of a nonuniform (gradient) magnetic field. This phenomenon is the basis for many applications of magnetic nanoparticles (MNPs) in biotechnology and medicine (including targeted drug delivery and magnetic cell separation). Quite often, theoretical treatment of magnetophoretic mass-transport in ferrofluids is highly idealized – MNP dispersion is considered as an ideal gas of non-interacting dipoles. Even the non-linear magnetization behaviour, one of the key hallmark of superparamagnetism, is sometimes neglected.

In this contribution, we propose a new transport equation for an ensemble of interacting MNPs. It is derived within the LFE theory by Elfimova et al. [1]. The equation accurately takes into account steric, dipolar and hydrodynamic interparticle interactions and does not impose any restrictions on values of the field gradient. To test the new equation, we consider the problem of a MNP redistribution in the vicinity of a current-carrying cylindrical conductor. Particle concentration profiles and relaxation times are determined in wide ranges of current values, dipolar coupling constants and net particle volume fractions. Theoretical results are critically compared with the results of Langevin dynamics simulations and predictions of other transport equations available in the literature [2].

In addition, we briefly discuss several alternatives to a traditional magnetophoretic transport. This includes the motion of catalytic nanoswimmers with embedded magnetic nanoparticle in a static magnetic field [3] and the self-propulsion of asymmetric magnetic particles in a rotating magnetic field [4].

[1] E.A. Elfimova, A.O. Ivanov, P.J. Camp., *PRE*, **88** (2013) 042310.

[2] A.F. Pshenichnikov, E.A. Elfimova, A.O. Ivanov, *JCP*, **134** (2011) 184508.

[3] M. Kaiser et al., *JML*, **304** (2020) 112688.

[4] K. I. Morozov et al., *PRFluids*, **2** (2017) 04420.

2PO-L3-4

## MORPHOLOGICAL SIGNATURE IN MAGNETIC AND HYDRODYNAMIC RESPONSE OF A MAGNETIC NANOGELS' SUSPENSION

*Novikau I.S.<sup>1</sup> and Kantorovich S.S.<sup>1,2</sup>*

<sup>1</sup> University of Vienna, Vienna, Austria

<sup>2</sup> Ural Federal University, Yekaterinburg, Russia

ivan.novikau@univie.ac.at | vanadiuz.github.io

Hydrogels are soft materials that have attracted solid interest over the last six decades and are widely used in chemical, biomedical, and even civil engineering applications. Today, at the forefront of the gels' realm, stand out nanogels, often additionally functionalized, for instance, by magnetic nanoparticles - so-called magnetic nanogels (MNGs).

Understanding the dynamics and internal structure of MNGs is crucial for their applications, for example, in targeted drug delivery. Based on the experimentally obtained dynamic magnetic susceptibility ( $\chi$ ) of the system [1], we developed a numerical model of MNG [2], which was further used in molecular dynamics (MD) simulations in conjunction with the Lattice-Boltzmann (LB) scheme in order to describe how the MNG internal structure manifests itself in magnetic and rheological properties on the suspension scale.

We study in detail how  $\chi$  is affected by the distribution of crosslinkers: uniform, with a Gaussian distribution from the center to the periphery, and reverse. We examine as well how  $\chi$  depends on MNGs concentration, size and way of magnetic nanoparticles coupling to polymer matrix. Finally, we analyse viscoelastic properties in the case of mixed response, when an external magnetic field and a hydrodynamic shear flow are simultaneously applied to the suspension of MNGs.

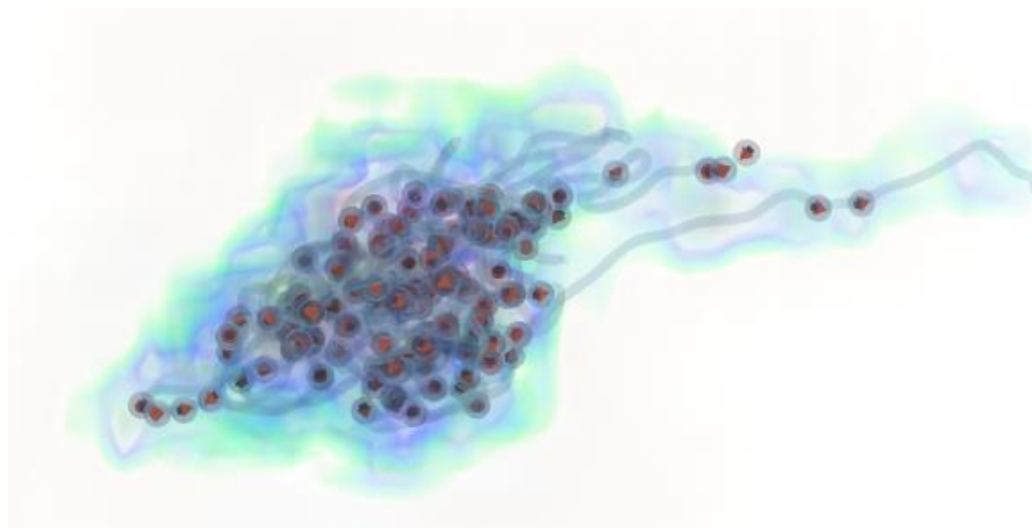


Figure 1. MNG under shear flow and velocity modulus of perturbed hydrodynamic field around the gel.

[1] S. Witt et al., *Soft Matter*, **18** (2022) 1089-1099.

[2] I. Novikau et al., *Journal of Molecular Liquids*, **346** (2022)118056.

## LEVITATION OF A SPHERICAL MAGNET IN A MAGNETIC FLUID DROP ON A HORIZONTAL PLANE

*Pelevina D.A., Sharova O.A., Turkov V.A., Naletova V.A.*  
Lomonosov Moscow State University, Moscow, Russia  
pelevina.daria@gmail.com

It is known that magnetizable bodies and magnets can levitate in vessels with magnetic fluid (MF) [1]. In this paper, a heavy spherical magnet levitating due to magnetic forces in a MF drop on a horizontal plane is investigated theoretically and experimentally.

Two cases are considered: without an applied magnetic field and with applied vertical uniform field (Fig 1). In the experiments, the height of the magnet levitation is measured depending on the MF volume. In the first case (without magnetic field), in contrast to [2, 3] where the magnetic moment of the magnet is perpendicular to the bottom, here we obtain that the magnet in the MF orients its magnetic moment horizontally, parallel to the plane. In the second case, even a small magnetic field orients the magnetic moment vertically, along the direction of the field.

Theoretically, we determine the MF shape, calculate the force acting on the magnet and find the height of the magnet levitation. In theory, the experimentally measured nonlinear dependence of the MF magnetization on the magnetic field is taken into account.

In both cases, the magnet levitates high enough (at a distance nearly equals to a magnet radius from the horizontal plane). This is very different from the case of a magnetizable spherical body: it levitates high enough in an applied vertical field [4], and it does not levitate in a horizontal field [5].

The levitation height increases with an increase in the MF volume both in theory and in experiment. It is shown that the theoretical solution proposed here describes the experiment better than the theory with constant magnetic permeability proposed previously [4,5].

The research was supported by the RSF grant (project No. 20-71-10002-P).

- [1] R. E. Rosensweig, *Nature*, **210** (1966) 613–614.  
 [2] S. Kvitantsev, V.A. Naletova, V.A. Turkov, *Fluid Dyn.*, **37(3)** (2002) 361 - 368.  
 [3] D. Pelevina et al., *EPJ Web Conf.*, **185** (2018) 09008.  
 [4] D.A. Pelevina et al., *J. Magn. Magn. Mater.*, **494** (2020) 165751.  
 [5] O.A. Sharova et al., *JETP*, **136(1)** (2023) 14-23.

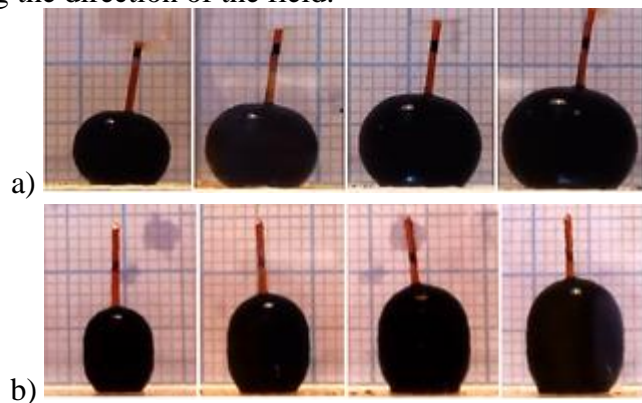


Figure 1. Magnet levitation in a MF drop on a horizontal plane (side view, various MF volumes): a) without applied field, b) in vertical uniform magnetic field 2 kA/m.

## THEORETICAL STUDY OF THE PROPERTIES OF POLYDISPERSE MAGNETOPOLYMER COMPOSITES WITH AN ANISOTROPIC ORIENTATIONAL STRUCTURE OF THE MAGNETIC FILLER

*Radushnov D.I., Solovyova A.Yu., Elfimova E.A.*

Ural Federal University, Yekaterinburg, Russia

Dmitry.Radushnov@urfu.ru

The work is devoted to a theoretical study of the effect of the polydispersity on the magnetic properties of an ensemble of immobilized ferroparticles, taking into account the interparticle dipolar interactions and orientational anisotropy. The model is based on the following assumptions. Before the polymerization of a liquid medium, magnetic nanoparticles moved freely due to Brownian motion; therefore, the magnetic moments and easy magnetization axes could change their orientation along with the rotation of the particle body. Under the influence of an external magnetic field of polymerization  $h^p$  which is directed parallel to the  $O_z$  axis and interparticle interactions, the ferroparticles are ordered into a certain orientational structure, after which the system polymerizes. The further reaction of the polymerized composite with immobilized magnetic nanoparticles to a magnetic field  $h$  which  $h \parallel h^p$  is superparamagnetic in nature, the change in the orientation of the magnetic moment occurs inside the nanoparticle body according to the Neel mechanism due to the deviation of the magnetic moments from the magnetic anisotropy axis of the particles.

An analytical expression for the magnetization of a polymerized ferrocomposite was obtained using a virial expansion up to the first order in the concentration of fractions of dipole particles and the intensity of dipole-dipole interactions. The influence of various fractions on the structural and magnetic properties of the system is analyzed. An independent computer simulation by the Monte Carlo (MC) method was carried out in the broad range of system parameters. The results obtained by the MC method are turned out in good agreement with the theoretical results.

Figure 1 shows the magnetization of the ferrocomposite and ferrofluid. In both samples the volume concentration of the magnetic filler is  $\varphi = 0.125$ . To assess the effect of polydispersity on the magnetization of the samples, a bidisperse (BD) system with a fraction of small particles  $v_s = 0.8$  is shown. In weak fields, the ferrocomposite magnetizes better than the ferrofluid because the orientation texture formed in the ferrocomposite contributes to its magnetization. At  $h = h^p$  the magnetization of the composite and the ferrofluid are the same. At  $h > h^p$ , the magnetization of the ferrocomposite is less than that of the ferrofluid.

Support by Russian Science Foundation (Project No. 23-12-00039) is acknowledged.

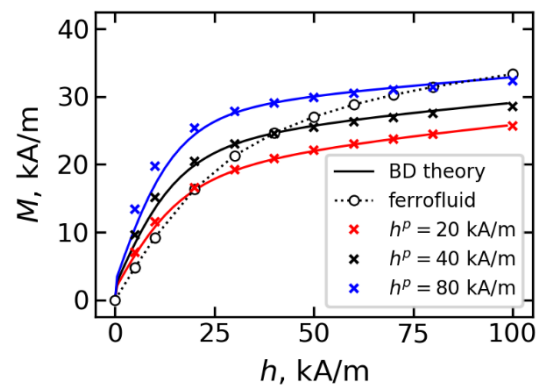


Figure 1. Comparison of the magnetization of the ferrocomposite and ferrofluid with the same disperse composition:  $\varphi = 0.125$  and  $v_s = 0.8$ . Solid lines show theoretical results, symbols indicate MC simulation data. The unfilled dots show the results of simulation of ferrofluid magnetization before polymerization, and the crosses show MC data for the ferrocomposite. Different colors correspond to different values of the  $h^p$ .

## LINEAR AND CUBIC MAGNETIC SUSCEPTIBILITY OF CONCENTRATED FERROFLUID IN AC FIELD OF ARBITRARY AMPLITUDE

*Rusanov M.S., Elfimova E.A., Zverev V.S.*  
Ural Federal University, Yekaterinburg, Russia  
rusanoff.mixail@yandex.ru

In this work we study the magnetic response of ferrofluid to an AC magnetic field of arbitrary amplitude. In the AC magnetic field  $H \cos(\omega t)$  with an amplitude  $H$  and a frequency  $\omega$  a ferrofluid is magnetized and its dynamic magnetization  $M(t)$  can be written as a series of periodic functions:

$$M(t) = \sum_{k=1}^{\infty} M'_k \cos(k\omega t) + M''_k \sin(k\omega t),$$

where  $t$  is time. The coefficients  $M'_k$  and  $M''_k$  depend on the AC field amplitude and determine the  $k$ -th harmonic of the susceptibility:  $\chi_k = \chi'_k + i\chi''_k$  ( $\chi'_k = M'_k/H^k$ ,  $\chi''_k = M''_k/H^k$ ). In this work, we study linear  $\chi_1$  and cubic  $\chi_3$  susceptibility theoretically. Analytic expressions for  $\chi_1$  and  $\chi_3$  are known for several limiting cases. For example, in the case of small amplitudes of the AC field in the single-particle approximation the linear susceptibility is described by the classical Debye theory; the analytical formula for the third harmonic is proposed in [1]; the impact of the AC field amplitude on the linear and cubic susceptibility in the single-particle approximation is studied in [2]; the dipole-dipole interaction in the linear susceptibility of ferrofluid in the weak AC field is considered in [3]. The focus of our study is to investigate how the amplitude of the AC field and interparticle interactions impact the dynamical properties, on  $\chi_1$  and  $\chi_3$ . For that, the ferrofluid is modeled as an ensemble of interacting moving particles. It is assumed that the relaxation of particle magnetic moments occurs only according to the Brownian mechanism. The linear and cubic susceptibilities are determined using the numerical solution of the Fokker-Planck equation. Numerical solution allowed us to obtain  $\chi_1$  and  $\chi_3$  for various values of field amplitude, particle concentration and intensity of dipole-dipole interactions. Based on the numerical results, simple approximate formulas for  $\chi_1$  and  $\chi_3$  are obtained using the least squares method. The results for the linear susceptibility can be found in [4].

Support by Russian Science Foundation (Project No. 23-12-00039) is acknowledged.

- [1] Y.L. Raikher, V.I. Stepanov, *Advances in Chemical Physics*, **129** (2004) 88-90.
- [2] T. Yoshida, K. Enpuku, *Japanese Journal of Applied Physics*, **48** (2009) 127002.
- [3] A.O. Ivanov, V.S. Zverev, S.S. Kantorovich, *Soft Matter*, **12** (2016) 3507-3513.
- [4] M.S. Rusanov, E.A. Elfimova, V.S. Zverev, *Physical Review E*, **104** (2021) 044604.

## ORIENTATION TEXTURING OF SMALL MULTI-CORE PARTICLE

*Solovyova A.Yu., Sokolsky S.A., Eljimova E.A., Ivanov A.O.*

Ural Federal University, Yekaterinburg, Russia

Anna.Soloveva@urfu.ru

The different spatial arrangement of the core-nanoparticles inside the multi-core particle (MCP) leads to the peculiarities of its response to an applied magnetic field. The prediction of these features is extremely important for the development of the methods of magnetic resonance imaging, magnetic particle imaging, cell tracking and cell cultivation. In the case of a small number of superparamagnetic particles (SPPs) in the MCP, the continuous medium approximation is not applicable because it is impossible to apply statistical methods to small ensembles of particles. Therefore, the problem of direct analysis of the small-scale MCP structure arises. We study the influence of the spatial arrangement of SPPs on the features of the magnetization of small MCPs. We focus on the analysis of the properties of the MCPs containing 7 and 8 SPPs, which are located randomly or at the nodes of a simple cubic lattice, as it is shown in Figure 1. For all MCPs an external magnetic field is applied along laboratory Oz axis.

By means of the Monte Carlo computer simulations we investigate the orientation probability

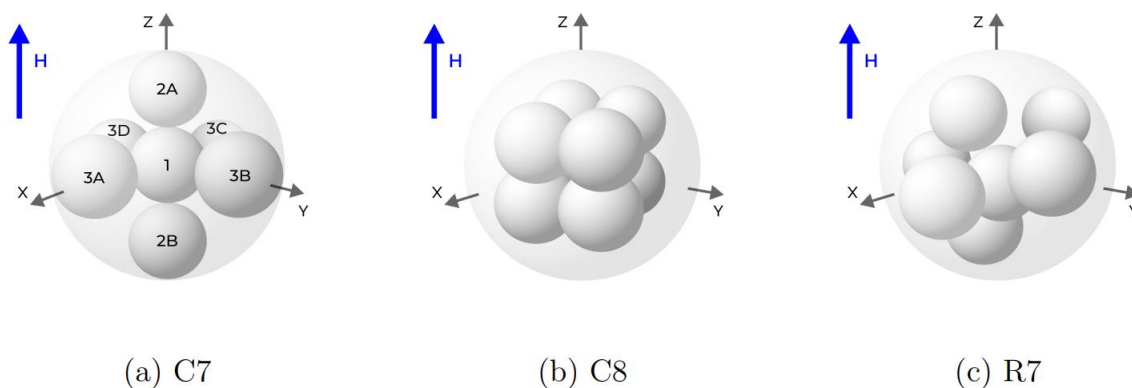


Figure 1. The internal structure of the MCPs under study. (a) Structure C7; the SPP, marked as 1, is placed at the center of the MCP; other six SPPs are positioned as the nearest neighbors in a cubic lattice. (b) Structure C8; eight SPPs are immobilized at the vertices of the cube, the center of which coincides with the center of the spherical MCP. (c) Structure R7 represents the random displacement of seven SPPs inside the spherical MCP.

density for the SPP magnetic moments, and we discovered the different orientation behavior for the SPPs located in various parts of the MCP C7 and C8. We suggest the rough classification, namely, the 'tip', the 'internal' and the 'surface' SPPs, according their reaction to the field. The simulated orientation probability densities for ten independent realization of structure R7 demonstrate that each classification type of SPPs can be identified for each random MCP configuration.

Support by the Ministry of Science and Higher Education of the Russian Federation (Ural Federal University project within the Priority 2030 Program) is acknowledged.

2PO-L3-9

## DYNAMICAL PROPERTIES OF AN ENSEMBLE OF CORRELATING ELLIPSOID-SHAPED MAGNETIC NANOPARTICLES IN A LIQUID CARRIER

*Zverev V.<sup>1</sup>, Pyanzina E.<sup>1</sup>, Novak E.<sup>1</sup>, Kantorovich S.<sup>2</sup>*

<sup>1</sup> Ural Federal University, Yekaterinburg, Russia

<sup>2</sup> University of Vienna, Vienna, Austria

vladimir.zverev@urfu.ru

Magnetic fluids typically consist of magnetic nanoparticles that are spherical in shape. However, various other particle shapes, including fibers, rods, spheroids, plates, and their aggregation clusters, have also been investigated for their usefulness in various modern technological applications. It should be noted that the magnetic nanoparticles produced during the synthesis of magnetic fluids are not completely spherical. In addition, magnetic particles can form aggregates in chain. In both cases, ellipsoidal shape can be used as an approximation of geometrical form. Ellipsoidal magnetic nanoparticles are useful by itself and can lead to anisotropic magnetic behavior, which can be used in various applications.

The focus of our study is to investigate dynamical properties of an ensemble of ellipsoidal magnetic nanoparticles in a liquid carrier when an alternating magnetic field is applied. Particles are modelled as elongated ellipsoids with different orientations of the magnetic moment inside each particle, namely, along and perpendicular to the main axis of revolution. The ellipsoid might be simply diffusing due to Brownian motion or additionally self-propelling. It is assumed that the relaxation of the magnetic moments of ferroparticles occurs only through Brownian mechanism. In case of simple diffusion the rotational motion of the magnetic moment of a random ferroparticle is determined from the solution of the corresponding Fokker-Planck equation. Interparticle dipole-dipole interactions are considered at the level of the modified first order mean field theory by means of an additional term to the energy of the system [1]. The data obtained from computer simulation shows a good agreement with theoretical results for moderately concentrated ferrofluids.

The work was supported by RSF 19-72-10033.

[1] A.O. Ivanov, V.S. Zverev, S.S. Kantorovich, *Soft Matter*, **12(15)** (2016) 3507-3513

2PO-L3-10

## STAR-SHAPED Au@Fe<sub>3</sub>O<sub>4</sub> NANOPARTICLES FOR BIOMEDICAL APPLICATIONS

*Pshenichnikov S.E.<sup>1</sup>, Motorzhina A.V.<sup>1</sup>, Anikin A.A.<sup>1</sup>, Belyaev V.K.<sup>1</sup>, Albino M.<sup>2,3</sup>, Panina L.V.<sup>1,4</sup>, Rodionova V.V.<sup>1</sup>, Sangregorio C.<sup>2,3</sup>, Levada K.V.<sup>1</sup>*

<sup>1</sup> REC SMBA, Immanuel Kant Baltic Federal University, Kaliningrad, Russia.

<sup>2</sup> Institute of Chemistry of Organometallic Compounds – C.N.R, Sesto Fiorentino, Italy

<sup>3</sup> Department of Chemistry ‘Ugo Schiff’ & INSTM, University of Florence, Sesto Fiorentino, Italy

<sup>4</sup> National University of Science and Technology ‘MISIS’, Moscow, Russia  
spshnikov@gmail.com

Application of nanosized hybrid materials provides wide opportunities for development of novel biomedical techniques. Possibility of combining several characteristics in the same nanostructure, e.g. high magnetic susceptibility, magnetic-plasmonic effects, biocompatibility and controllable cytotoxicity, provide paths manufacturing multifunctional instruments for theranostics. In current research we propose star-shaped Au@Fe<sub>3</sub>O<sub>4</sub> nanoparticles (GN) as a prospective instrument for antitumor photothermal therapy (PTT). GN were synthesized and characterized according to protocols described in the previous publication [1]. GN are Au@Fe<sub>3</sub>O<sub>4</sub> core@shell structures with highly uniform star-like morphology. GN possess combined plasmonic and magnetic properties. GN applicability for PTT was evaluated using laser heating setup, based on ThorLabs L808P500MM laser diode at 0.6 W output optical power and 815 nm wavelength. Suspensions of GN with different concentrations showed overheating of experimental solutions in comparison with distilled water (Figure 1A). Cytotoxicity of GN was evaluated using WST-1 assay. Human hepatocarcinoma cells (Huh7) were cultivated according to the manufacturer’s protocols. GN induced cytotoxic effects in Huh7 cells at 1, 5, 10 µg/ml (Figure 1B) and 50, 100 µg/ml (data not shown). On the next step cell morphology was analyzed using the Cell-IQ® v2 MLF integrated platform. Analysis showed overstressed round-shaped Huh7 cells after 24 h treatment with GN at concentration 100 µg/ml. In further experiments suspensions at concentration 10 µg/ml of GN (and lower) will be used to evaluate the PTT efficiency against tumor cells in *in vitro* conditions.

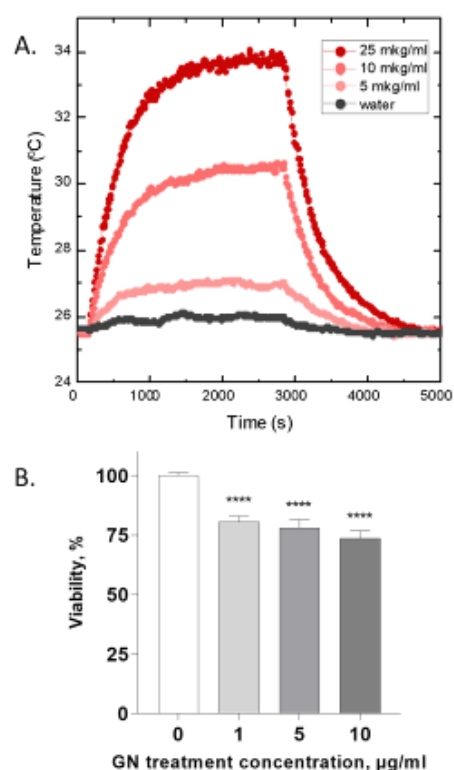


Figure 1. GN inhibit Huh7 cell viability: A – heating of experimental solutions under laser irradiation, B – viability of hepatocarcinoma cells after 24 h treatment with GN.

This research was funded by RSF, grant number 21-72-20158.

[1] B. Muzzi et al., *ACS Applied Materials and Interfaces*, **14** (2022) 29087.

## SLOW RELAXATION OF THE MAGNETIZATION OF A FERROFLUID WITH INTERNAL STRUCTURES

*Chirikov D.N., Zubarev A.Yu.*

Ural Federal University (*UrFU*), Yekaterinburg, Russia  
d.n.chirikov@urfu.ru

The first theories of ferrofluids kinetics of magnetization deal with extremely dilute media, in which any interactions of particles can be neglected. Magnetic interparticle interaction was considered in [1–3] under the assumption of the homogeneous spatial disposition of the particles. The physical mechanism of the magnetization relaxation in these works is explained by the finite time of the particles reorientation after the applied field alternation. The estimated characteristic relaxation time for the typical ferrofluids was about  $10^{-6} - 10^{-4}$  sec.

As is known, particles in ferrofluids can form chains and other heterogeneous aggregates. The appearance of such structures significantly changes the physical, including magnetic, properties of the fluids. However, the time of formation and destruction of these structures is much longer than the time of the particles reorientation. Therefore, this mechanism can lead to much lower relaxation phenomena than the reorientation effects.

We propose a model of kinetics of the chains evolution in ferrofluids, as well as effect of this process on their macroscopic magnetization. We consider a ferrofluid consisting of identical nano-sized ferromagnetic particles combined into the chain aggregates. To simplify the calculations as much as possible, we neglect other possible types of aggregates (for example, drops). A mathematical model is proposed for the evolution of an ensemble of the chains after the field alternation. The model is based on the Smoluchowski kinetic equations for the distribution function  $g_n$  over the number  $n$  of the particles in the chain. Their "chain-chain" association, as well as the thermal disintegration, is considered. The dependence of  $g_n$  on time  $t$  after the magnetic field change has been determined. Using the determined function  $g_n(t)$  and the results for the average magnetization of the chain with a given number  $n$  of the particles, we have considered kinetics of the magnetization relaxation after stepwise increase and decrease of the applied field. Calculations have shown that the characteristic relaxation time can be on the order of 2–3 seconds, which is several orders of magnitude more than the relaxation time corresponding to the particles reorientation. Therefore, the evolution of ensemble of the internal aggregates in ferrofluids must lead to a much slower relaxation of its magnetization, than that provided by the particle reorientation.

[1] D.V. Berkov, L.Yu. Iskakova, A.Yu. Zubarev, *Phys. Rev. E*, **79** (2009) 021407.

[2] A.O. Ivanov, O.B. Kuznetsova, *Phys. Rev. E*, **64** (2001) 041405.

[3] E.A. Elfimova, L.Yu. Iskakova, A.Yu. Solovyova, A.Yu. Zubarev, *Phys. Rev. E*, **00** (2021) 004600.

**July 2**

Sunday

18:15 - 20:00

POSTER  
SESSIONS

Section L4

**Magnetic Nanostructures and  
Low Dimensional Magnetism**

## CLUSTER STRUCTURE OF $(\text{FeCoZr})_x(\text{MgF}_2)_{100-x}$ NANOCOMPOSITES BY GISAXS

*Baulin R.A.<sup>1</sup>, Pripechenkov I.M.<sup>1</sup>, Ganshina E.A.<sup>1</sup>, Andreeva M.A.<sup>1</sup>, Sitnikov A.V.<sup>2</sup>*

<sup>1</sup> Lomonosov Moscow State University, Moscow, Russia

<sup>2</sup> Voronezh State Technical University, Voronezh, Russia

baulin.roman@physics.msu.ru

Magnetic nanocomposites (NC) of metal-dielectric type have a number of unique physical properties that are promising for their use in spintronics. Recently, in composites with oxygen-free matrices (with Fe or  $\text{Fe}_{51}\text{Co}_{49}$  alloy distributed in the  $\text{MgF}_2$  dielectric matrix) a giant magnetoresistance was found at room temperature [1]. The phase structural transition of  $\text{CoFeZr}$  nanocrystals in  $\text{MgF}_2$  matrix from a HCP to a BCC structure at  $x = 38$  at.% on the glass substrates has been observed, this feature was supported by the spectral dependences of TKE [2]. For the glass-ceramic substrate this transition is shifted to the larger concentrations.

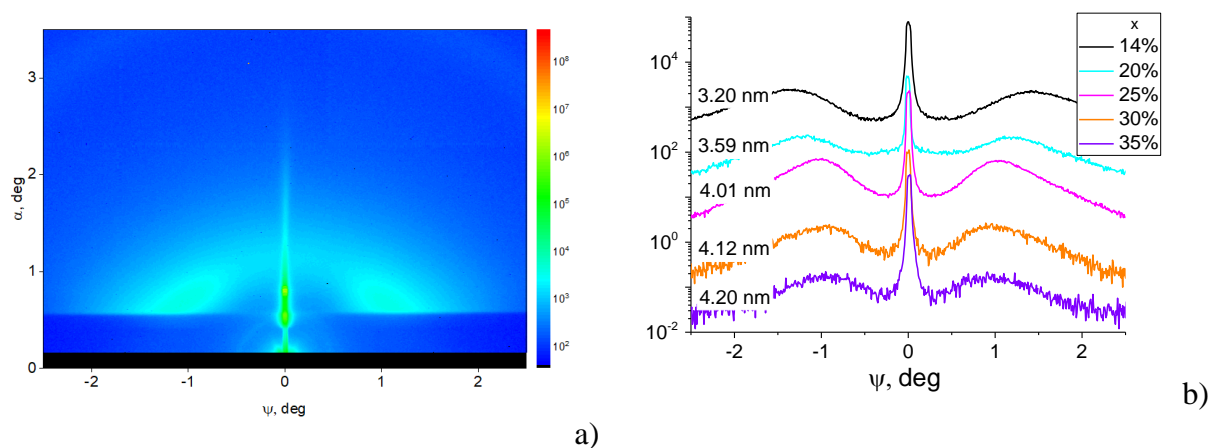


Figure 1. (a) Typical experimental GISAXS pattern (for one of the samples with  $x=25$  at.%). (b) Horizontal cross sections of GISAXS patterns at  $\alpha=0.7^\circ$  for samples with different FeCoZr concentration  $x$ . The obtained cluster separations are pointed for each curve.

Investigations of  $(\text{FeCoZr})_x(\text{MgF}_2)_{100-x}$  NC have been performed by GISAXS (Grazing Incidence Small Angle X-ray Scattering) method [3, 4] at Kurchatov Synchrotron (Figure 1). The observed wings confirm the existence of FeCoZr nano clusters having short order, which separation depend on the FeCoZr concentrations. The larger separation means the enlargement of their size. It is surprising that not so essential change of cluster sizes leads to radical change of shape of TKE spectra [2]. For the glass-ceramic substrate GISAXS patterns of  $(\text{FeCoZr})_x(\text{MgF}_2)_{100-x}$  show more complicated behavior.

The authors are grateful to M.M. Borisov and E.Kh. Mukhamedzhnov (NRC “Kurchatov Institute”, Moscow, Russia) for help with the experiment.

[1] N. Kobayashi et al., *J. Appl. Phys.*, **90** (2001) 4159–4162.

[2] E. A. Ganshina et al., *Nanomaterials*, **11** (2021) 1666.

[3] D.-M. Smilgies, *J Polym Sci.*, **60** (2021) 1–19.

[4] R.A. Baulin et al., *Materials Science & Engineering B*, **291** (2023) 1163.

2PO-L4-2

## EXCHANGE-COUPLED SULFUR AND MANGANESE COMPLEXES IN SILICON

*Askarov S.<sup>1</sup>, Sharipov B.<sup>1</sup>, Mavlyanov A.<sup>2</sup>, Saliyeva Sh.<sup>1</sup>, Ibragimova B.<sup>1</sup>*

<sup>1</sup> Tashkent State Technical University, Tashkent, Uzbekistan

<sup>2</sup> Semiconductor Physics and Microelectronics Research Institute, Mirzo Ulugbek NUU, Tashkent, Uzbekistan  
microelectronics74@mail.ru

It is known that in the process of heat treatment of silicon crystals, that were diffusional doped with sulfur and one of the elements of the transition group, in a certain temperature range, there is an intense interaction between these centers, accompanied by electrical neutralization of both impurity centers.

In order to find out how such complexes appear in the course of such an interaction, the present work is devoted to the study of the spectra of EPR of silicon samples successively doped with sulfur and manganese (Si<S,Mn>). For comparison, the EPR spectra of reference Si<S> and Si<Mn> crystals were also studied.

A study of the EPR spectra in reference Si<S> samples showed that they exhibit a single isotropic line with parameters  $g = 2.064 \pm 0.002$  and  $\Delta H_{pp} = 8$  Gs, due to singly positively charged S<sup>+</sup> centers. In reference Si<Mn> samples, the spectra of non-equivalent exchange-coupled Mn<sup>+</sup> - Mn<sup>+</sup> pairs were observed.

In Si<S,Mn> samples, the spectra of the S<sup>+</sup> - center were absent, in addition, in these samples in the weak fields, an EPR spectrum was observed, consisting of several lines, the position and intensity of which varied from sample to sample. In this case, the center of gravity of the lowest field part of the spectrum remained unchanged at 190 G. The results of study of the temperature dependence of the four most intense lines of the spectrum had a maximum at 16 K, in addition, with an increase in temperature  $\sim 80$  K, the lines would shift to the region of stronger fields.

All these facts indicate that the spectrum observed in weak fields differs from the spectra of non-equivalent exchange-coupled Mn<sup>+</sup> - Mn<sup>+</sup> pairs observed in reference Si <Mn> samples. It can be assumed that the observed center is due to exchange-coupled complex based on these atoms, that is, there is an exchange between manganese atoms happens through "sulfur atoms" mechanism.

The absence of a hyperfine structure in the most intense lines and their relatively small width ( $\Delta H = 10-20$  G) indicates that the magnetic electrons are on manganese atoms. At the end, it is indicated that the coupling between the centers of sulfur substitution centers and interstitial centers of manganese is carried out through free d - shell.

## DISCRETE MAGNETIC BREATHERS IN MONOAXIAL CHIRAL HELMAGNET

*Bostrem I.G.<sup>1</sup>, Ovchinnikov A.S.<sup>1</sup>, Sinitsyn V.I.E.<sup>1</sup>, Ekomason E.G.<sup>2</sup>*

<sup>1</sup> Ural Federal University, Yekaterinburg, Russia

<sup>2</sup> Bashkir State University, Ufa, Russia

Irina.Bostrem@urfu.ru

Nonlinear excitations of lattice systems localized in space and periodically varying in time, so-called discrete breathers (DB), are known in atomic chains for a long time. About 20 years ago, the possibility of the existence of discrete breathers was theoretically predicted in Heisenberg spin chains in the phase of forced ferromagnetism [1]. In the present work, DB excitations in a spin chain with the additional Dzyaloshinskii-Moriya (DM) exchange interaction are studied.

The Hamiltonian of the system has the form

$$H = -2J \sum_n S_n S_{n+1} + A \sum_n (S_n^z)^2 + D \sum_n [S_n \times S_{n+1}]_z - H \sum_n S_n^z$$

The first term is the Heisenberg exchange interaction, the second is related to the single-ion magnetic anisotropy, the third term is the antisymmetric Dzyaloshinskii-Moriya interaction. The last term corresponds to the Zeeman interaction of the local magnetic moments with the external magnetic field  $H$  directed along the  $z$  axis. The state of forced ferromagnetism is considered, when the magnetic field magnitude exceeds some critical value.

It is found that discrete breathers of four different types can appear, depending on the value and sign of the exchange integral and single-ion anisotropy [2]. In addition, we show that the DM interaction introduces quantitative and qualitative changes into parameters of the breather solutions [3].

The results of the theoretical analysis were applied to the monoaxial chiral helimagnet  $\text{CrNb}_3\text{S}_6$ . Given the known value of the single-ion anisotropy constant for the compound, the discrete breather excitations of «dark» type can arise with their frequencies lying within the linear spin-wave band close to its bottom edge. The linear stability of these breather modes was verified by means of the Floquet analysis. These results may pave a path to design spintronic resonators on the base of chiral helimagnets [2].

This work was supported by the Ural Federal University Program of Development within the Priority-2030 Program.

[1] S.V. Rakhmanova et al., *Phys. Rev. B.*, **57** (1998) R14012.

[2] I.G. Bostrem et al., *Phys. Rev. B.*, **104** (2021) 214420.

[3] I.G. Bostrem et al., *AIP Advances.*, **11** (2021) 015208.

## DISCRETE BREATHERS IN LINEAR CHAIN OF MAGNETIC NANOPARTICLES

*Kuzmin D.A.<sup>1</sup>, Ekomasov E.G.,<sup>1</sup> Bychkov I.V.<sup>1</sup>, Shavrov V.G.<sup>2</sup>*

<sup>1</sup> Chelyabinsk State University, Chelyabinsk, Russia

<sup>2</sup> Ufa University of Science and Technology, Ufa, Russia

<sup>3</sup> Kotelnikov IRE RAS, Moscow, Russia

bychkov@csu.ru

The work is devoted to the study of the possibility and conditions for the existence of discrete breathers in a chain of magnetic nanoparticles coupled by a dipole-dipole interaction. Each particle is an ellipsoid with  $a$ ,  $b$ , and  $c$  semiaxes. It is assumed that the size of the particles and the temperature regime make it possible to consider the particles as single-domain particles with a uniform distribution of magnetization. The simulation of the dynamics of magnetization in such a chain of nanoparticles was carried out within the framework of the numerical solution of the Landau-Lifshitz equation, considering the dissipative term in the Hilbert form.

In this chain of magnetic nanoparticles, the existence of solitary periodic solutions (discrete breathers) was found, which are especially pronounced in chains of particles with  $a = b \gg c$  (i.e., close in shape to disks). In this case, magnetization oscillations occur in the x-y plane, while the  $z$  component of the magnetization vector remains unchanged. When dissipation is considered, the magnetization vector relaxes to the ground state with  $M_z = 0$ , and the discrete breather has a finite lifetime. For realistic dissipation parameters, the lifetime of a discrete breather substantially exceeds the oscillation period.

Figure 1 shows an example of modeling a discrete breather in chains of 50 Ni nanoparticles with dimensions  $a = b = 100$  nm,  $c = 10$  nm and a distance between particles  $l = 500$  nm in the absence of dissipation. During the simulation, the initial deviation of the 25th particle was  $M_z = 0.85M_0$ , and the magnetizations of all other particles were directed along the x axis.

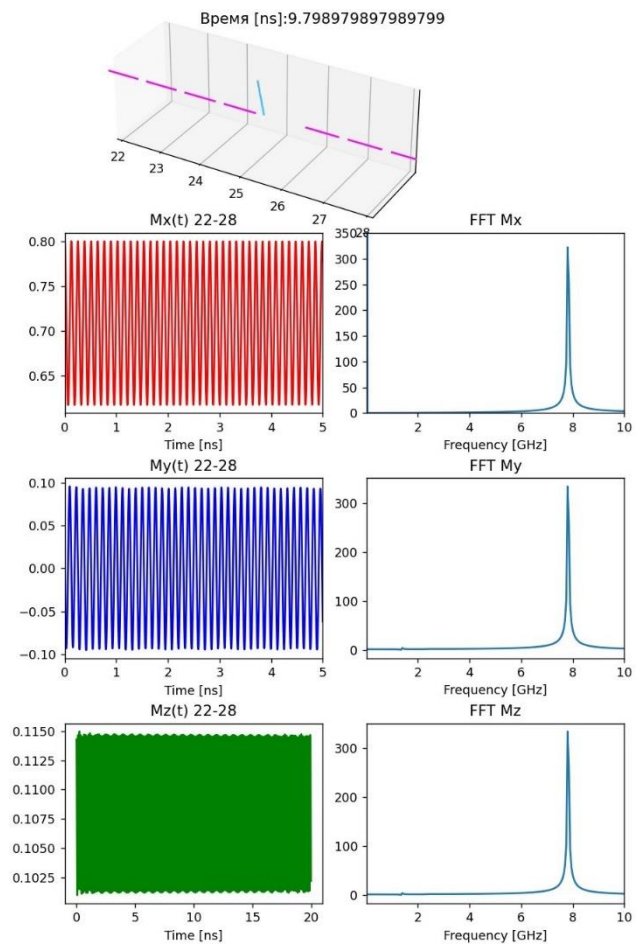


Figure 1. Discrete breather into chains of 50 Ni nanoparticles. The time dependences of the components of the total magnetization of particles with numbers from 22 to 28 and their Fourier transforms are presented.

Support by Russian Science Foundation (22-19-00355) is acknowledged.

2PO-L4-5

**MAGNETISM OF LUDWIGITES  $Mn_{1.17}Co_{1.83}BO_5$  and  $Mn_{1.39}Co_{1.61}BO_5$** *Eremina R.M.<sup>1,2</sup>, Popov D.V.<sup>1</sup>, Batulin R.G.<sup>2</sup>, Cherosov M.A.<sup>2</sup>, Moshkina E.M.*<sup>1</sup> Zavoisky Physical-Technical Institute, Federal Research Center  
“Kazan Scientific Center of RAS”, Kazan, Russia<sup>2</sup> Kazan (Volga Region) Federal University, Kazan, Russia<sup>3</sup> Kirensky Institute of Physics, Federal Research Center KSC SB RAS, Krasnoyarsk, Russia  
REremina@yandex.ru

Oxyborates with ludwigite-type structures (structural formula  $M_2M'BO_5$ , where M and M' being the metallic ions with valence 2+ and 3+ respectively) bears extremely unusual magnetic properties, including, but not limited to random magnetic ions distribution, mixed valence, strong electronic correlations and uncommon charge ordering. These properties are caused by zigzag walls in their crystal structure formed by metal ions of different valence. Another reason is presence of four nonequivalent positions that can be occupied by up to twelve magnetic ions per unit cell. Those positions form two sublattices 3-1-3 and 4-2-4. Former is filled by metallic ions with two valent electrons; latter is filled by metallic ions with three valent electrons. Most of the ludwigites have either orthorhombic crystal structure with Pbam space group or monoclinic structure with P21/c space group. Metallic ions in ludwigite structures are caged in an octahedral structure of six oxygen ions. These structures form the aforementioned zigzag walls [1].

In this work we present the results of the analysis of magnetic properties Mn-Co heterovalent ludwigites  $Mn_{1.17}Co_{1.83}BO_5$  and  $Mn_{1.39}Co_{1.61}BO_5$ .

Ludwigites monocrystals  $Mn_{1.17}Co_{1.83}BO_5$  and  $Mn_{1.39}Co_{1.61}BO_5$  has been grown using flux method. Mn and Co ions ratio in crystals was established via XRF analysis.  $Mn_{1.17}Co_{1.83}BO_5$  has space group Pbam with  $a = 9.25 \text{ \AA}$ ,  $b = 12.41 \text{ \AA}$  and  $c = 3.05 \text{ \AA}$ .  $Mn_{1.39}Co_{1.61}BO_5$  has space group Pbam with  $a = 9.27 \text{ \AA}$ ,  $b = 12.45 \text{ \AA}$  and  $c = 3.05 \text{ \AA}$ . Hysteresis loops were approximated by two ferromagnetic and one paramagnetic contributions in  $Mn_{1.17}Co_{1.83}BO_5$  and  $Mn_{1.39}Co_{1.61}BO_5$ . In  $Mn_{1.17}Co_{1.83}BO_5$  an exchange bias was observed, coercive forces are  $H_{01} = -0.217T$  and  $H_{02} = 0.145T$  at 5K, and are  $H_{01} = 0.256T$  and  $H_{02} = 0.177T$  at 10K, for left and right part of the loop, respectively. Ferromagnetic contribution in hysteresis loop for  $Mn_{1.39}Co_{1.61}BO_5$  almost 100 times higher, than for  $Mn_{1.17}Co_{1.83}BO_5$ , though Co ion concentration has been increased slightly. Magnetic, AC magnetization and specific heat measurements show spin-glass transitions at  $T_{PhT}=42.3K$  for  $Mn_{1.17}Co_{1.83}BO_5$  and ferrimagnetic transition at  $T_{PhT}=60.8K$  for  $Mn_{1.39}Co_{1.61}BO_5$ . The effective magnetic moments per unit cell are  $\mu_{eff}=8.06\mu_B$  for  $Mn_{1.17}Co_{1.83}BO_5$  and  $\mu_{eff} = 9.03\mu_B$  for  $Mn_{1.39}Co_{1.61}BO_5$  obtained through the experiment and agree with theoretical calculations.  $Co^{3+}$  ions taking 0.38 of 3+ position for  $Mn_{1.17}Co_{1.83}BO_5$  and completely fill 3+ position for  $Mn_{1.39}Co_{1.61}BO_5$ . The peaks in specific heat at  $T = 7K$ ,  $12K$  and  $17K$  for both compounds are due to Schottky anomaly or presence of low-dimensional system.

This research was supported by the Russian Science Foundation (Project No. 23-72-00047)

[1] L. Bezmaternykh et al., *Solid State Phenomena*, **233** (2015) 133-136.

2PO-L4-6

## MAGNETIC HYSTERESIS IN PERMALLOY BASED 1D MAGNETOPLASMONIC CRYSTAL

*Gritsenko Ch.A., Mitrofanov T., Kolesnikova. V.G., Murzin D.V., Belyaev V.K., Rodionova V.V.*

Immanuel Kant Baltic Federal University, Kaliningrad. Russia

KByrka@kantiana.ru

To date, one of the current research tasks is to create a digital twin of a magnetoplasmonic crystal based on permalloy thin films. Such systems have found wide application in the production of magnetic field sensors used in such areas as medicine (magnetic cardiographs, magnetic encephalographs, tests of various prostheses and implants [1]), space research (satellite production [2]), and in the field of security (entoscopes and metal detectors [3]).

Implementation of digital twins will make it possible to predict such magnetic characteristics and properties as coercive force, remanent magnetization, and magnetization reversal mechanisms depending on the thickness of the thin film and the geometric parameters of the crystal. This will make it possible to choose optimal parameters for its use in specific applications, bypassing expensive and time-consuming laboratory experiments [4].

In this work, a three-dimensional model of permalloy based 1D magnetoplasmonic crystal with the diffraction lattice of a period of 740 nm and the height of 20 nm was constructed using the COMSOL Multiphysics software. Using the Jiles–Atherton model model, magnetic hysteresis was modeled for various NiFe film thickness in the range of 5-50 nm. Hysteresis properties were studied in details, and were compared with experimental data. The results will be used to further determine the optimal parameters of the magnetic field sensor based on a magnetoplasmonic crystal.

The project was supported by the Ministry of Science and Higher Education of the Russian Federation (agreement no. 075-02-2023-934)

[1] D. Murzin et al., *Sensors*, **20**(6) (2020) 1569.

[2] S. Wei et al., *Sensors*, **21**(4) (2021) 1500.

[3] D. Eleftherakis, *Sensors*, **20**(3) (2020) 737.

[4] S.R. Kalidindi et al., *Frontiers in Materials*, **9** (2022) 48.

## HELMAGNETIC AND CRYSTALLOGRAPHIC GROWTH TEXTURES OF DYSPROSIUM NANOLAYER ON $\beta$ -Ta, Nb AND CoFe BUFFER LAYERS

Naumova L.I.<sup>1,2</sup>, Krinitsina T.P.<sup>1</sup>, Zavornitsyn R.S.<sup>1,2</sup>, Miyaev M.A.<sup>1,2</sup>, Deryaterikov D.I.<sup>1</sup>, Rusalina A.S.<sup>2</sup>, Pavlova A.Y.<sup>1</sup>, Proglyado V.V.<sup>1</sup>, Ustinov V.V.<sup>1,2</sup>

<sup>1</sup> M.N. Mikheev Institute of Metal Physics UB RAS, Yekaterinburg, Russia

<sup>2</sup> Ural Federal University, Yekaterinburg, Russia

krinitsina@imp.uran.ru

Dysprosium nanolayers of various thicknesses are made by magnetron sputtering on  $\text{Al}_2\text{O}_3$  (R) substrates, as well as using buffer layers  $\beta$ -Ta, Nb and  $\text{Co}_{90}\text{Fe}_{10}$ . The correlation between the crystallographic growth texture and the peculiarities of the temperature dependence of the electrical resistance of polycrystalline dysprosium films was investigated. X-ray diffraction measurements show that when Dy is sputtered directly on  $\text{Al}_2\text{O}_3$  (R), a two-component growth texture  $\langle 100 \rangle + \langle 002 \rangle$  is formed in the rare earth metal nanolayer. In  $\langle 100 \rangle$  component, the hexagonal axis  $c$  is parallel to the film plane, and in the  $\langle 002 \rangle$  it is perpendicular to the film plane. The perfection of the two-component texture increases, when Dy is sputtered on the  $\beta$ -Ta buffer layer (Figure 1a). The reason is that microstructures of  $\text{Al}_2\text{O}_3$  and Dy are matched through  $\beta$ -Ta buffer layer. In the antiferromagnetic state, the texture components become phases with different orientation of the magnetic helicoid axis  $c$ . Measurements of electrical resistance on temperature dependencies have shown that the formation of antiferromagnetic ordering occurs at different temperatures  $T_1$  and  $T_2$  (Figure 1b) in the phases  $\langle 100 \rangle$  and  $\langle 002 \rangle$ . The  $T_1$  and  $T_2$  values were evaluated from the position of the local minimums on the  $dR/dT(T)$  [1].

When the Nb buffer layer is used,  $\langle 101 \rangle$ ,  $\langle 100 \rangle$  and  $\langle 002 \rangle$  phases are formed in the dysprosium layer at the initial stage of sputtering. When the layer thickness increases to 40 nm, the  $\langle 002 \rangle$  phase becomes predominant, and the texture is one-component. However, the mean deviation angle of the hexagonal axis  $c$  from the film plane normal is almost twice that of the dysprosium layers sputtered onto the  $\beta$ -Ta buffer layer.

The use of  $\text{Al}_2\text{O}_3$  (R) substrate with  $\beta$ -Ta buffer layers leads to the formation of dysprosium layer, in which, there are crystallites with a magnetic helicoid axis perpendicular to the film plane, even at a small thickness (5-10 nm).

Support by the Russian Science Foundation project 22-22-00220 is acknowledged.

[1] L.I. Naumova et al., *Current Applied Physics*, **19** (2019) 1252–1258.

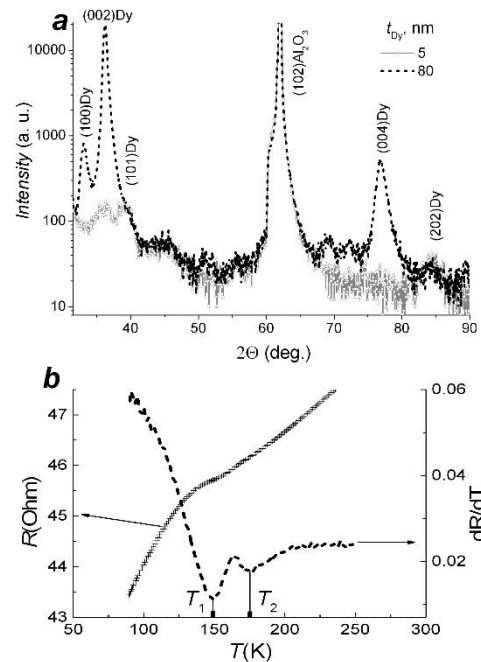


Figure 1. a) XRD patterns for Ta/Dy( $t_{Dy}$ )/Ta; b) resistance and resistance derivative vs temperature for Ta/Dy(80nm)/Ta.

## SPIN GLASS PHASE TRANSITIONS IN $\text{LaSrCo}_{1/2}\text{Fe}_{1/2}\text{O}_4$

*Mazitova D.I.<sup>1</sup>, Batulin R.G.<sup>2</sup>, Yatsyk I.V.<sup>3</sup>, Chupakbina T.I.<sup>4</sup>, Deeva Yu.A.<sup>4</sup>, Levchenko S.V.<sup>1</sup>*

<sup>1</sup> Skolkovo Institute of Science and Technology, Moscow, Russia

<sup>2</sup> Kazan (Volga Region) Federal University, Kazan, Russia

<sup>3</sup> Zavoisky Physical-Technical Institute, Kazan, Russia

<sup>4</sup> Institute of Solid State Chemistry, Yekaterinburg, Russia

Dina.mazitova@skoltech.ru

Ruddlesden-Popper (RP) oxides have shown great potential as catalysts for the oxygen evolution reaction (OER), which is a challenging process in fuel cells and metal-air batteries. These oxides follow a general formula of  $\text{A}_{1+n}\text{B}_n\text{O}_{3n+1}$ , where A represents an alkali or alkali earth element, B represents a transition metal, and n denotes the number of perovskite layers. Due to the delicate balance between the crystal-field-splitting parameter, the on-site Coulomb repulsion, and the energy of charge transfer between transition metal and oxygen, make RP material quite sensitive to temperature, external pressure, or internal pressure through chemical substitution. Perovskite cobaltites, in particular, are of great interest, where  $\text{Co}^{3+}$  ions can exist in three spin states: a nonmagnetic low-spin state (LS), an intermediate spin state (IS), and a high-spin state (HS).

We started our investigation with DFT calculations. We constructed 56- atoms supercells with various distributions of La and Sr and Fe and Co. The most favorable orderings were mostly ferromagnetic except for the case when the layer completely consists of iron. We found out that the spin state of cobalt depends not only on the distribution of transition metals but also on the distribution in A-site. Since no supercell order was observed in X-ray spectroscopy, all these structures are presented in a crystal, and complex magnetic behavior was expected.

We measured the temperature dependences of specific heat, and electronic paramagnetic resonance (EPR), AC and DC magnetic susceptibility, and magnetization in two modes, zero-field cooling, and field cooling. We identified at least two phase transitions: first, broaden, in temperature range 25-200K associated with spin glass ordering and at  $T=10\text{K}$  associated with the transition of spin state of Co. Both transitions are consistent with EPR measurements. According to the imaginary part of AC susceptibility one can identify another broaden phase transition at 200-300K temperature range, but according to the real part the transition starts at 250K.

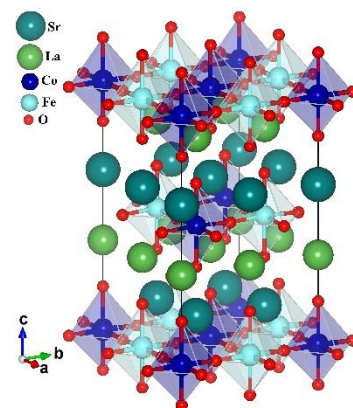


Figure 1. Crystal structure of  $\text{LaSrCo}_{1/2}\text{Fe}_{1/2}\text{O}_4$ . It is believed to be the most energetically favorable one. The number of Fe-O-Co bridges is maximized in this structure.

This work was supported by the Russian Science Foundation under grant no. 21-13-00419.

## COMPARATIVE STUDY OF FeNi/Cu-BASED MAGNETOIMPEDANCE LAYERED ELEMENTS WITH DIFFERENT GEOMETRY OF THE UPPER MULTILAYER

*Melnikov G.Yu.<sup>1</sup>, Svalov A.V.<sup>1</sup>, Buznikov N.A.<sup>2</sup>, Lepalovskij V.N.<sup>1</sup>, Kurlyandskaya G.V.<sup>1</sup>*

<sup>1</sup> Ural Federal University, Yekaterinburg, Russia

<sup>2</sup> Scientific and Research Institute of Natural Gases and Gas Technologies – Gazprom VNIIGAZ, Razvilka, Moscow Region, Russia  
grisha2207@list.ru

Recently, the periodic partly profiled multilayer film elements exhibiting magnetoimpedance (MI) effect have been proposed and theoretically studied [1]. This new type of multilayered film structures may have special advantages for the detection of stray magnetic fields, including evaluation of the magnetic fields of magnetizable labels in magnetic biosensors [2]. In this work, we have designed, prepared and comparatively analyzed the structure, magnetic properties, magnetic domains and MI effect of rectangular [FeNi(100 nm)/Cu(3 nm)]<sub>5</sub>/Cu(500 nm)/ [Cu(3 nm)/FeNi(100 nm)]<sub>5</sub> elements of three types. The bottom layers were non-profiled classic multilayers, and the top layers were the non-profiled (N-P), micro-stripes profiled (M-St) or micro-square profiled (M-Sq) multilayered structures.

The multilayered elements were obtained by magnetron sputtering (the system background pressure was  $1 \times 10^{-7}$  mbar and the working Ar pressure  $3.8 \times 10^{-4}$  mbar) with a shape of stripes having the length of 1 cm and the width of 0.5 mm. An external magnetic field of 250 Oe was applied in plane of the element perpendicular to the long side to create the transverse induced magnetic anisotropy. The patterned structures (M-St and M-Sq) were obtained by sputtering through masks. For M-St structures, the stripe length was equal to the width of the element 0.5 mm, the stripe width was about 0.6 mm and the transition area between the stripes was about 0.1 mm. The square size for M-Sq structures was  $70 \mu\text{m}$  and the distance between squares was  $30 \mu\text{m}$ .

For M-St structure, the magnetization processes along the short and long sides begin in the gaps between micro-stripes, which corresponds to the white (Figure 1a) and black (Figure 1b) areas, respectively. Complicated magnetic domain patterns could be seen in

Figure 1d for M-Sq structure. The magnetization process along the short side begins in the center of the element and delayed at the edges with magnetic domain walls connected to the squares (Figure 1c).

Experimental data on the MI effect are compared with results obtained by electrodynamic model: solution of the linearized Landau–Lifshitz equation and equation for the equilibrium magnetization angles.

Support by Russian Science Foundation (grant № 23-29-00025) is acknowledged.

[1] N.A. Buznikov, G.V. Kurlyandskaya, *Phys. Met. Metallogr.*, **122(8)** (2021) 755–760.

[2] G.Yu. Melnikov et al, *Sensors* **21(11)** (2021) 3621.

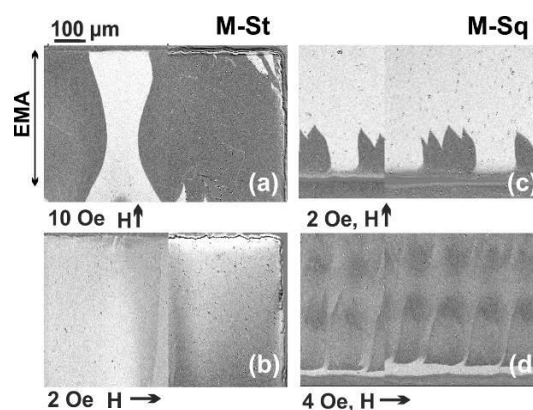


Figure 1. Images of magnetic domains for magnetic field  $H$  applied along the short (a,c) and long (b,d) sides of the element: left column, M-St; right column, M-Sq. EMA is the easy magnetization axis direction.

## CRYSTAL STRUCTURE AND EXCHANGE BIAS IN POLYCRYSTALLINE FILMS WITH ANTIFERROMAGNETIC Cr-Mn

*Moskalev M.E.<sup>1</sup>, Feshchenko A.A.<sup>1</sup>, Kravtsov E.A.<sup>2,3</sup>, Kudyukov E.V.<sup>1</sup>, Lepalonskij V.N.<sup>1</sup>, Vas'kovskij V.O.<sup>1,2</sup>*

<sup>1</sup> Institute of Natural Sciences and Mathematics, UrFU, Yekaterinburg, Russia

<sup>2</sup> M.N. Mikheev Institute of Metal Physics, UB RAS, Yekaterinburg, Russia

<sup>3</sup> Institute of Fundamental Education, UrFU, Yekaterinburg, Russia

mikhail.moskalev@urfu.ru

Due to the growing demand for spintronic devices that actively use the exchange bias effect to pin the magnetization of the ferromagnetic layer, there is a problem of finding and developing new media, characterized by a high temperature stability of the effect, based on antiferromagnetic materials that do not include rare and precious metals [1]. From this point of view, of particular interest are the antiferromagnetic Cr-Mn alloys, in its bulk form capable of exhibiting the antiferromagnetic order up to around 700 K [2].

In this paper we study the formation of the antiferromagnetic Cr-Mn alloys with body-centered cubic crystal structure, and their capability to act as a pinning layer for the exchange bias effect in magnetron-sputtered polycrystalline films. By means of X-ray diffractometry, executed in different geometries, we perform a thorough analysis of Ta/Cr-Mn/Ta films, which results in the construction of a room-temperature phase diagram of Cr-Mn. These results combined with magnetic measurements of films with adjacent antiferromagnetic Cr-Mn and ferromagnetic Fe<sub>20</sub>Ni<sub>80</sub> layers allow us to establish the conditions for the observation of the exchange bias effect, and the composition range in which it is present (Figure 1). We find that the maximum blocking temperature  $T_b$  of samples can be as high as 540 K. Employing a specialized measurement protocol, we establish the median blocking temperatures  $\langle T_b \rangle$  and estimate the effective anisotropy constant  $K_{\text{eff}}$ . The results of our study suggest that Cr-Mn can be considered a viable option in applied film heterostructures with exchange bias.

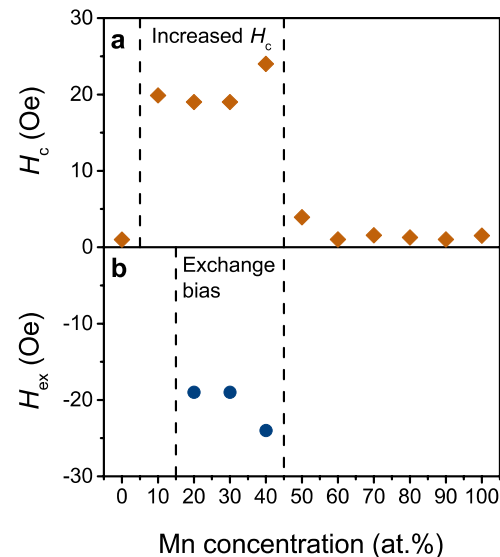


Figure 1. Dependences of the coercivity  $H_c$  and exchange bias field  $H_{\text{ex}}$  on the manganese concentration in the Cr-Mn.

This work was financially supported by the Russian Science Foundation, project No. 22-22-0814.

[1] A. Hirohata et al., *J. Phys. D: Appl. Phys.*, **50** (2017) 443001.

[2] S. Maki, K. Adachi, *J. Phys. Soc. Jap.*, **46** (1979) 1131-1137.

## NONTHERMAL PHOTOINDUCED REDUCTION OF THE COERCIVITY IN THIN EPITAXIAL FILMS OF THE L<sub>1</sub><sub>0</sub>-PHASE FePt AND FePt<sub>0.84</sub>Rh<sub>0.16</sub>

*Petrov A.V.<sup>1</sup>, Nikitin S.I.<sup>1</sup>, Tagirov L.R.<sup>1,2</sup>, Kamzin A.S.<sup>3</sup>, Yusupov R.V.<sup>1</sup>*

<sup>1</sup>Kazan Federal University, Kazan, Russia

<sup>2</sup>Zavoisky Physical-Technical Institute, Kazan, Russia

<sup>3</sup>Ioffe Institute, St.-Petersburg, Russia

flypetrov@yandex.ru

The time-resolved magneto-optical Kerr effect in epitaxial thin films of the FePt compound and the FePt<sub>0.84</sub>Rh<sub>0.16</sub> solid solution with perpendicular magnetic anisotropy on the MgO (001) substrates was studied. The evolution of hysteresis loops on fast (100 fs – 1 ns) and slow (1 – 20 ns) time scales after the excitation with a femtosecond light pulse was studied (Figure 1). The effect of long-lived non-thermal magnetic softening was discovered. The value of the coercive field is restored on a time scale of milliseconds. A hypothesis relating the observed phenomenon to the excitation of high-Q acoustic resonances in the substrate/film system and strong magnetoelastic interaction in FePt and FePt<sub>0.84</sub>Rh<sub>0.16</sub> films is proposed.

Comparison of the hysteresis loops under ultrashort pulse laser excitation with the data of static magnetometry indicates the nonthermal nature of the decrease in coercivity, since the temperature is restored after approximately 2 ns from the pump pulse.

The process of magnetization reversal of a continuous thin film with perpendicular magnetic anisotropy includes two necessary stages, namely, the nucleation of domains with the opposite direction of magnetization and their growth due to the domain wall motion. Since both nucleation and the motion of domain walls are of an activation origin, we suggest that a hypersonic wave induced by a femtosecond laser pulse increases the energy of the magnetic subsystem via inverse magnetostriction. The latter promotes domain nucleation and facilitates the overcoming of potential barriers by domain walls arising from the pinning on defects.

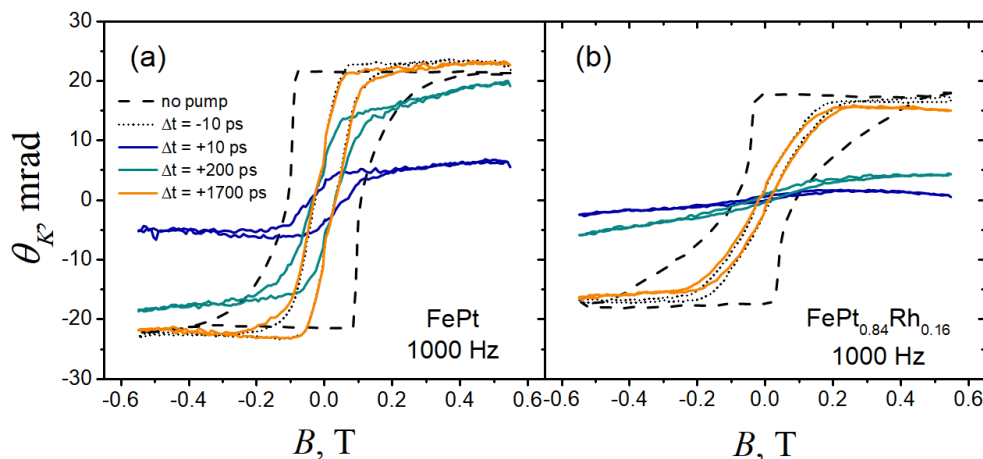


Figure 1. Magnetization reversal curves of thin FePt (a) and FePt<sub>0.84</sub>Rh<sub>0.16</sub> (b) epitaxial films in terms of the Kerr rotation angle at  $T = 300$  K, pump pulse repetition rate 1 kHz, and pump density 6.4 mJ/cm<sup>2</sup>. The colors and line types of the hysteresis curves correspond to different times (see the legend).

Support by the Kazan Federal University Strategic Academic Leadership Program (PRIORITY-2030) is acknowledged.

[1] N.S. Akulov, Z.I. Alizade, K.P. Belov, *Doklady Akademii Nauk SSSR*, **65** (1949) 815.

2PO-L4-12

## MAGNETIZATION, TRANSPORT AND ESR PROPERTIES OF $\text{Sr}_2\text{MnNbO}_6$ DOUBLE PEROVSKITES

*Popov D.V.*<sup>1</sup>, *Batulin R.G.*<sup>2</sup>, *Yatsyuk I.V.*<sup>1</sup>, *Eremina R.M.*<sup>1,2</sup>

<sup>1</sup> Zavoisky Physical-Technical Institute, Federal Research Center  
“Kazan Scientific Center of RAS”, Kazan, Russia

<sup>2</sup> Kazan (Volga Region) Federal University, Kazan, Russia  
kazan-city.dvpopoff@yandex.ru

Perovskites are oxides with formula  $\text{ABO}_3$ , where A is alkaline earth metal ion, B is transition metal ion. Perovskites have octahedral oxygen framework built around B ions. Those frameworks surround A ions in hexagonal (cubic) formation [1]. Double perovskites are the type of perovskites, that consist of two aforementioned formulas at once. Their major difference double perovskites  $\text{A}_2\text{B}'\text{B}''\text{O}_6$  from complex single perovskites is an ordering in the arrangement of B' and B'' ions, B' or B'' ions can be form chains or plane.

The aim of this work is investigation of magnetic, transport and ESR properties of  $\text{Sr}_2\text{MnNbO}_6$  double perovskite. To achieve this, AC and DC magnetization dependences from temperature and external magnetic field were measured, using PPMS-9 device in Kazan Federal University. The  $\text{Sr}_2\text{MnNbO}_6$  compound exhibits four phase transitions: at  $T = 42.5, 38.9, 12.7$  and  $6.7\text{K}$ . In addition, specific heat measurements and isotherm magnetization at  $T = 5, 15, 30, 40$  and  $42\text{K}$  were made on  $\text{Sr}_2\text{MnNbO}_6$ , using the same device. ESR spectra were also measured using a Bruker spectrometer. The measurements were performed at temperature range from 10 to 340K. The four different ESR lines were observed in this material. The unusual behavior for one ESR line was observed for  $\text{Sr}_2\text{MnNbO}_6$  at  $H_{\text{res}} \approx 500$  Oe and temperatures 38-42K (see Figure 1). The behaviors of ESR line were discussed.

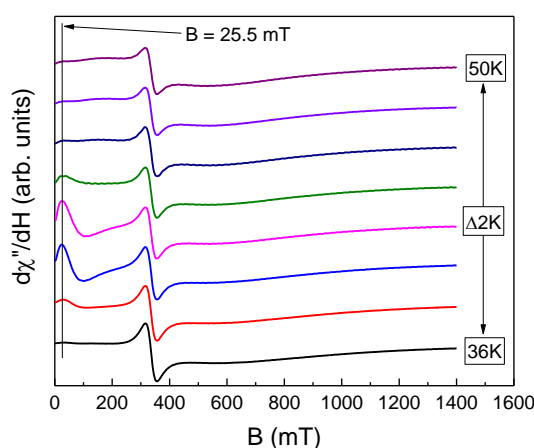


Figure 1. ESR spectra of  $\text{Sr}_2\text{MnNbO}_6$  at temperature range of  $T = 36\text{-}50\text{K}$

This research was supported by the RSF (Project No. 22-42-02014).

[1] A. Bhalla, R. Guo, R. Roy, *Materials Research Innovations*, **4** (2000) 3-26.

## COULOMB TWO-CENTER INTEGRALS AND THEIR COMBINATIONS IN CRYSTAL FIELD THEORY FOR RARE EARTH COMPOUNDS

*Popov D.V.<sup>1</sup>, Eremina R.M.<sup>1,2</sup>, Likerov R.F.<sup>1</sup>, Shafikova A.E.<sup>2</sup>*

<sup>1</sup> Zavoisky Physical-Technical Institute, Federal Research Center  
“Kazan Scientific Center of RAS”, Kazan, Russia

<sup>2</sup> Kazan (Volga Region) Federal University, Kazan, Russia  
REremina@yandex.ru

Oxide crystals doped with rare-earth ions have good prospects to be used as base for various devices, in particular for quantum memory. In order to build such devices, the properties of such materials must be studied. Among all possible properties, the crystal field configuration and magnetic configuration of the impurity centres are important ones.

The problem of the spatial distribution of electrons in the condensed matter theory has been known for very long period of time. There are still no simple analytical equations to calculate the contribution of this distribution to the crystal field. Finding these equations will make it possible to establish the energy level schemes and wave functions of various rare-earth ions in crystals. On the obtained wave functions it will be possible to calculate the crystal field parameters. Both crystal field parameters and experimental data on magnetic properties of the crystals obtained, for example, by electron spin resonance method, will speed up the creation of a microscopic theory of magnetoelectric coupling.

The first work on this topic was done by Kleiner back in 1954 [1]. Using a simplified model of two centres with hydrogen-like wave functions, Kleiner found that the spatial distribution of 2s, 2p electrons of oxygen ions significantly reduces the electrostatic field on the 3d electrons of the chromium ion. In subsequent works, in connection with the emerging possibility of using computer technology, this problem was solved numerically. A successful attempt, which has become quite widely known, to obtain at least partially analytic expressions was made by Garcia and Fouche [2].

The calculations were based on the bipolar expansion of the Coulomb interaction of electrons belonging to different centres. As a result, they got the equations for the spatial distribution contribution to the crystal field parameters. These equations have form of the integrals over space dimensions. A modern version of the analytical equations was presented in the paper by Iglamov [3].

As in Kleiner's paper, the initial point of the calculations is Poisson equation in which the spacial distribution of oxygen ions' electrons written in Gaussian-type orbitals. The radial electron functions of 3d- shell are written in the Gaussian-type orbitals as well. Such simplification allows removing triple two-centered integrals and changing them into single integrals. Corresponding analytical equations for 3d ions are shown in [3].

We obtain analytical equations, which correspond to the effect of spatial distribution of oxygen ion 2s- and 2p- electrons on the crystal field for 4f ions and using for calculation crystal-field parameters in Y<sub>2</sub>SiO<sub>5</sub>:Nd; Sc<sub>2</sub>SiO<sub>5</sub>:Nd.

The work carried out was carried out with the support of the Basis Foundation No 22-1-1-59-1.

[1] W. H. Kleiner, *J. Chem.Phys.*, **20** (1952) 1784.

[2] D. Garcia, M. Faucher, *Phys. Rev. B.*, **30** (1984) 1703.

[3] V.V. Iglamov, M.V. Eremin, *Phys. Solid State*, **49** (2007) 221.

## MAGNETORESISTANCE OF CoFe NANOWIRES AND NANOCOILS

*Rogachev K.A.<sup>1</sup>, Samardak A.Yu.<sup>1</sup>, Sobirov M.I.<sup>1</sup>, Namsaraev Zh.Zh.<sup>1</sup>, Jeon Y.S.<sup>2</sup>, Jeong E.<sup>3</sup>, Samardak A.S.<sup>1</sup>, Ognev A.V.<sup>1</sup>, Kim Y.K.<sup>3</sup>*

<sup>1</sup> Laboratory of thin film technologies, Far Eastern Federal University, Vladivostok, Russia

<sup>2</sup> Institute of Engineering Research, Korea University, Seoul, Republic of Korea

<sup>3</sup> Department of Materials Science and Engineering, Korea University, Seoul, Korea  
samardak.aiu@dvfu.ru

One-dimensional nanostructures such as nanotubes and nanowires are of a high attention for modern material science and for application. With the development of one-dimensional nanostructure synthesis techniques, a facile method was developed to prepare helical-shaped nanostructures (nanocoils). The complex magnetic configuration of nanocoils, caused by their helical shape, is of great interest for investigation of their properties and applications. One area of interest is the use of such nanostructures as elements of spintronics or magnetic field sensors. In our work, we studied the resistance of nanocoils and nanowires in an external magnetic field.

Nanocoils and nanowires were synthesized by electrodeposition in a porous alumina template with a pore diameter of 200 nm for nanocoils [1] and 65 nm for nanowires. For the synthesis of both structures, an electrolyte containing cobalt sulfate ( $\text{CoSO}_4 \cdot 7\text{H}_2\text{O}$ ) and iron sulfate ( $\text{FeSO}_4 \cdot 7\text{H}_2\text{O}$ ) was used. To obtain helical-shaped nanostructures, the electrolyte was modified with vanadium oxide sulfate ( $\text{VOSO}_4 \cdot \text{H}_2\text{O}$ ) and ascorbic acid ( $\text{C}_6\text{H}_8\text{O}_6$ ).

Surface morphology was studied by scanning electron microscopy (SEM, ThermoScientific SCIOS 2). Nanowires and nanocoils were also simulated in MuMax<sup>3</sup> micromagnetic package based on the experimentally measured data.

Investigation of the resistance of a single nanostructure in an external magnetic field was carried out by the four-probe method using a high-precision multimeter (Keithley 2661). For this, nanostructures were etched out of an AAO template and placed on a Si substrate. After that copper contact pads were created using electron beam lithography (EBL) and lift-off lithography. The external magnetic field varied from -5000 Oe to 5000 Oe.

The micromagnetic configuration, simulated in different external magnetic fields oriented along and perpendicular to the long axis was used to calculate dependence on magnetic field.

As a result, we found that nanocoils could have different mechanisms of magnetoresistivity, depending on their compressed or stretched state, while nanowires show classical anisotropic magnetoresistance. The results obtained will be used to study the dependence of the magnetoresistance on the stretching of the nanocoil. In this case, the nanowire is considered to be the maximum stretched nanospring.

This work was supported by the Russian Ministry of Science and Higher Education (State Task No. FZNS-2023-0012).

[1] D. Y. Nam et al., *Nanoscale*, **10** (2018) 20405-20413.

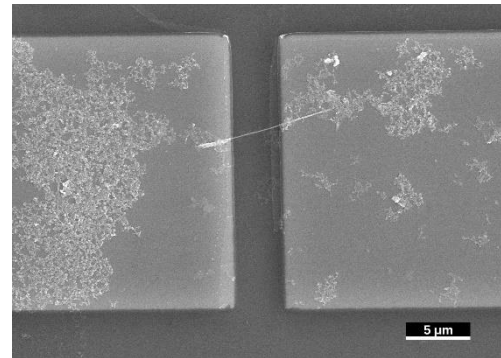


Figure 1. CoFe nanowire in gap between Cu contacts

## THE SYNTHESIS AND MAGNETIC NATURE OF MANGANESE-SUBSTITUTED COBALT FERRITE NANOPARTICLES

*Salnikov V.<sup>1,2</sup>, Omelyanchik A.<sup>1</sup>, Rodionova V.<sup>1</sup>*

<sup>1</sup> Immanuel Kant Baltic Federal University, Kaliningrad, Russia

<sup>2</sup> Dagestan State University, Makhachkala, Russia

russiatvotzach@gmail.com

Nano-sized spinel ferrites have gained significant attention as promising materials due to their unique physical properties and potential applications in various fields such as information storage, magnetic hyperthermia, various biomedical applications [1,2]. The diverse chemical and morphostructural properties offer the opportunity to control the magnetization and coercivity of magnetic nanoparticles (MNPs) [3]. Spinel structure of ferrites determines the properties, in particular, the magnetic properties [4], which are most dependent on the type of metallic cations and the nature of their interaction. The study of such materials also involves investigating size effects, which can lead to changes in their magnetic properties due to differences in the crystalline structure compared to bulk. So, the distribution of cations in the spinel sublattices of MNPs depends on their sizes and synthesis methods, the magnetic properties are influenced by these parameters.

In this study, we investigated the magnetic properties of  $Mn_xCo_{(1-x)}Fe_2O_4$  (where  $x = 0.15, 0.25, 0.35, 0.45$ ) MNPs synthesized via the sol-gel self-combustion method followed by annealing. Vibrating sample magnetometry revealed that the sample with a manganese content of  $x = 0.35$  exhibited the highest saturation magnetization ( $M_s$ ) value of approximately 70 emu/g. Annealing at 500°C led to an increase in coercivity, particle size, for example, for the sample with  $x = 0.25$  from 25 nm to 39 nm, led to a decrease of lattice constant. Annealing at 600°C and higher temperatures resulted in the formation of hematite, which is confirmed by X-ray phase analysis data. Furthermore, we observed a decrease in  $M_s$ , for instance, for a sample with  $x = 0.25$   $M_s$  changed from 72 emu/g at 500°C to 66 and 50 emu/g at 600°C and 700°C, respectively.

Thus, we have developed a strategy for synthesizing of spinel ferrite nanoparticles to increase the saturation magnetization by controlling the structural properties of the MNPs that can be used, for example, as a component of nanocomposite materials.

This work was financially supported by the Russian Science Foundation (grant No. 21-72-30032). We would also like to acknowledge the Center for Gifted Children (Kaliningrad, Russia) for providing the opportunity to conduct X-ray diffraction measurements.

[1] D. Peddis et al., *Frontiers of Nanoscience*, **6** (2014) 129–188.

[2] Z. Li, Y. Zhang, N. Feng, *Expert Opin. Drug Deliv*, **16(3)** (2019) 219–237.

[3] H.L. Andersen et al., *Nanoscale*, **10(31)** (2018) 14902–14914.

[4] M. Sanna Angotzi et al., *J. Phys. Chem. C.*, **125(37)** (2021) 20626–20638.

## SIMULATION OF THE MAGNETIZATION SWITCHING IN Fe/Au BARCODE NANOWIRES

*Samardak A.Yu.<sup>1</sup>, Jeon Y.S.<sup>2</sup>, Kozlov A.G.<sup>1</sup>, Ognev A.V.<sup>1</sup>, Jeong E.<sup>2</sup>, Kim G.W.<sup>3</sup>, Ko M.J.<sup>3</sup>, Samardak A.S.<sup>1</sup>,  
Kim Y.K.<sup>3</sup>*

<sup>1</sup> Laboratory of thin film technologies, Far Eastern Federal University, Vladivostok, Russia

<sup>2</sup> Center for Hydrogen Fuel Cell Research, KIST, Seoul, Korea

<sup>3</sup> Department of Materials Science and Engineering, Korea University, Seoul, Korea  
samardak.aiu@dvfu.ru

One of the most important properties of the memory is the writing speed, which defines the efficiency of future memory device. Magnetic nanowires can achieve speeds of switching up to nanoseconds due to strong shape anisotropy [1] which makes them promising structures for application as memory cells. Barcode nanowires are the further, more cost-efficient development of this idea, but their speed and processes occurred due switching are still not studied. In this work we report of the investigation on switching of Fe/Au barcode nanowire arrays by using a micromagnetic model, precisely tuned by data achieved by the experimental studies.

Fe/Au barcode nanowires arrays with different lengths of segments, were achieved by the single-bath electrodeposition method into the porous alumina template. Their morphology was studied by scanning electron microscopy, magnetic properties were investigated by magnetic force microscopy, vibrating sample magnetometry and FORC-method. In the end, micromagnetic model was built in mumax3 simulation package.

To make sure that micromagnetic model describes the real samples precisely, the array of 12 nanowires with 200-300 nm diameter and 2  $\mu\text{m}$  length were simulated with periodic boundary conditions. For each sample with different lengths of Fe and Au segments, a hysteresis loop was simulated and compared directly to experimentally achieved hysteresis loops. Stray fields were simulated in different external fields and compared to magnetic force microscopy images. In the end, only the segment length was changed from sample to sample, and almost the exact overlay of simulated on experimental data was achieved.

To simulate the process of switching, array of barcode nanowires was saturated along the long axis, and then negative external field with induction of 0.1 T was applied. The simulation revealed, that in the beginning of the switching, in the center of Fe segments skyrmionium-like micromagnetic structure (Figure 1) exists for 0.3-1 ns, then evolves into skyrmion, which exists for another 3-20 ns, and then decay into vortex. In some segments of the samples, skyrmions tend to exist for a much longer time, up to microseconds. Simulation of the array in the room temperature still represents the same structures, yet distorted by thermal fluctuations, which decreases their lifetime. Switching of nanowires takes about 2 ns.

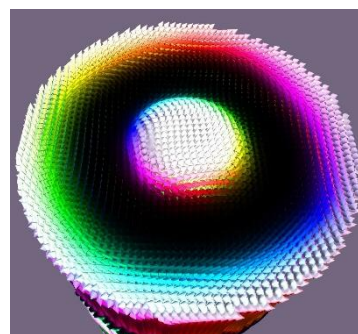


Figure 1. Simulated micromagnetic configuration in the center of Fe(200)Au(200) nanowire after 0.2 ns of application of external magnetic field

This work was supported by the Russian Ministry of Science and Higher Education (State Task No. FZNS-2023-0012).

[1] A.S. Samardak et al., *J. All. Com*, **732** (2018) 683-693.

## UHV TECHNOLOGICAL SYSTEM FOR SYNTHESIS AND IN SITU INVESTIGATION OF NANOSTRUCTURES BY SPECTRAL MAGNETO-OPTICAL ELLIPSOMETRY IN A WIDE TEMPERATURE RANGE

*Shevtsov D.V.<sup>1</sup>, Lyaschenko S.A.<sup>1</sup>, Varnakov S.N.<sup>1</sup>, Ovchinnikov S.G.<sup>1,2</sup>, Maximova O.A.<sup>1,2</sup>*

<sup>1</sup> Kirensky Institute of Physics SB RAS, Krasnoyarsk, Russia

<sup>2</sup> Siberian Federal University, Krasnoyarsk, Russia

sdv@iph.krasn.ru

In recent decades special attention has been paid to the methods of synthesis and investigation of nanoscale structures such as "ferromagnetic metal/semiconductor", where such elements as Ni, Mn, Co, Fe can be used as metal and Si, Ge can be used as semiconductor layer. Non-destructive diagnostics and control of nanosystems directly in the process of their creation offers great opportunities for research; this enables the synthesis of nanomaterials with controllable composition and desired characteristics, structure and properties on the atomic and subatomic level.

Reflectance spectral magnetoellipsometry, a non-destructive in situ method of surface analysis, makes this possible [1,2]. This polarizing optical method makes it possible to obtain quantitative information about the structure and morphology of the surface of the sample under study, to find out its spectral-optical and magneto-optical parameters directly in the process of structure formation, and to perform magneto-optical analysis of thin films by placing a ferromagnetic sample in an external magnetic field. The developed uhv installation in Figure 1 for obtaining thin films and multilayer materials from various elements is described, in which the combined use of in situ magnetoellipsometric method of analysis and systems of specimen temperature setting in a wide range with the application of an external magnetic field of a given value to it is implemented [3,4].

The Fe/SiO<sub>2</sub>/Si(100) structure was used to demonstrate the possibilities of the created uhv complex, i.e. to synthesize ferromagnetic nanostructures on the substrate surface with in situ non-destructive ellipsometric control and to carry out in situ studies of the obtained nanostructure by magneto-ellipsometry in the temperature range 85–1005 K in a single technological cycle.

The study was supported by the Russian Science Foundation No. 21-12-00226, <http://rscf.ru/project/21-12-00226/>.

[1] O.A. Maximova, *JMMM*, **440** (2017) 196–198.

[2] O.A. Maximova, *JMMM*, **440** (2017) 153–156.

[3] D. V. Shevtsov, *Instruments and Experimental Techniques*, **60** (2017) 759–763.

[4] D. V. Shevtsov, *IOP Conference Series: Materials Science And Engineering*, **1** (2016) 155.

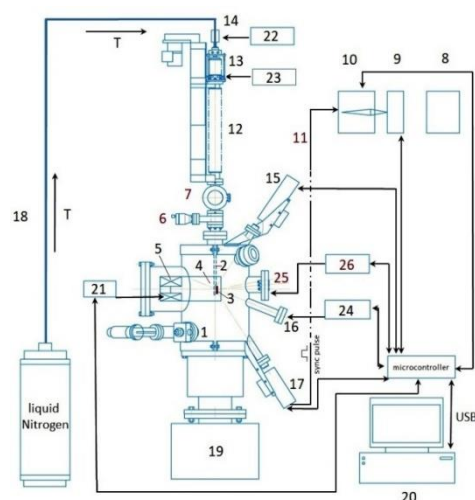


Figure 1. A block diagram of the UHV technological system.

(1) vacuum chamber; (2) rod with the sample holder; (3) sample; (4) electromagnet; (5) magnetic circuit; (6) slide gate; (7) lock chamber; (8) light source; (9) light chopper; (10) monochromator; (11) light guide; (12) linear bellows translator; (13) vacuum bellows three-degree-of-freedom manipulator; (14) flow-type evaporator–heater; (15) analyzer; (16) molecular source; (17) polarizer; (18) nitrogen supply system; (19) magnetic-discharge pump; (20) computer; (21) magnet power-supply; (22) flow-type heater power-supply; (23) sample-heater power-supply; (24) evaporator power-supply; (25) evaporator, (26) evaporator power-supply

## SKYRMIONS AND SKYRMION LATTICES IN EPITAXIAL [Pd/Co/CoO]<sub>n</sub> MULTILAYERS

*Shatilov V.S., Ognev A.V., Samardak A.S., Kozlov A.G.*

Laboratory of Spin-Orbitronics, Institute of High Technologies and Advanced Materials, Far Eastern Federal University, Vladivostok, Russia  
shatilov.vs@dvfu.ru

In this work, we demonstrate the ability to create a skyrmion lattice using magnetic force microscopy methods. The slicing of labyrinthine domains into individual skyrmions, which size depends on the period of the domain structure, is shown. Here we present a mechanism to realize a stable skyrmion lattice at room temperature in epitaxial [Pd/Co/CoO]<sub>n</sub> multilayers. The magnetic structure of the samples provides valuable knowledge for development of a new type of magnetic memory and neuromorphic devices.

Thin magnetic superlattices are very interesting and promising structures that are widely used to create spintronic devices. In particular, multilayer structures with the antisymmetric exchange presented by the interfacial Dzyaloshinskii–Moriya interaction (i-DMI) are very promising for the next generation of magnetic memory and logics. The i-DMI appears in the magnetic systems with broken inversion symmetry and, in combination with perpendicular magnetic anisotropy (PMA), makes it possible to stabilize spin textures such as skyrmions, skyrmion lattices, chiral Néel domain walls, etc. In thin magnetic films at room temperature, skyrmions can be observed in a form of nanosized circular vortices, a kind of magnetic solitons. These spin textures are of interest for spintronics, since they can move under the action of an electric current and, in the future, be used in information storage and processing devices [1]. Magnetic skyrmions can be considered as topologically stable quasiparticles possessing physical characteristics needed to realize the skyrmion racetrack memory. A.V. Ognev et al. [2] have recently showed the cryptographic potential of skyrmion (topological) nanolithography with direct writing (without a mask), where each skyrmion acts as a pixel in the final topological image invisible in optical range.

The inversion symmetry of interfaces can be broken using controlled oxidation. Oxidation can be used as a tool to control the magnetic characteristics of one of the interfaces. The use of epitaxial structures makes it possible to significantly increase of the i-DMI energy. In our study we show that thin magnetic films with an oxidized [Pd/Co/CoO/Pd]<sub>n</sub> multilayers can be a host of skyrmions and skyrmion lattices. Due to the symmetry breaking at the Pd/Co and Co/Pd interfaces, the interfacial Dzyaloshinskii-Moriya interaction appears and contributes to the generation of stable skyrmions in such structures.

The well-known method of slicing the labyrinth domains into individual skyrmions is to use of the stray field of a magnetic force microscopy (MFM) probe. The application of the MFM probe for chiral texture nucleation is described in works [2–4].

Epitaxial [Pd/Co/CoO]<sub>n</sub> superlattices were grown on the single crystal Si(111) substrates by the molecular beam epitaxy technique. The samples were grown in an ultrahigh vacuum chamber (Omicron Nanotechnology) with pressure  $P \approx 10^{-10}$  Torr. Si(111) substrates were prepared by chemical cleaning before loading into the chamber. The samples were degassed by indirect heating for 13 hours and at a temperature of 600°C, and the substrates were annealed by direct current at the temperature of 1200°C by short pulses to clean the surface of silicon oxide and form a 7×7 surface reconstruction. After annealing, a layer of Cu (21 Å thick) was sputtered as the buffer layer. Each ferromagnetic layer (Co) was oxidized for 3 minutes in a dry oxygen atmosphere in the separated chamber which equipped with a gas flow system. The structure of a single film is presented as the Pd(20Å)/Co(10Å)/CoO tiler. The deposition of each following layer was controlled by recording the reflective high-energy electron diffraction pattern. Preservation of the crystalline order with the increasing number of trilayers was observed. The cover layer of Pd (50 Å thick) was sputtered to

prevent subsequent oxidation of the film.

The magnetic parameters of the samples were studied using a vibrating sample magnetometer (LakeShore VSM 7410). The study of the domain structure was carried out using a magneto-optical Kerr microscope (MOKE, Evico Magnetics) and a magnetic force microscope (MFM, Ntegra Aura) allowing the manipulation of the magnetic structure by high coercivity magnetic probes.

The resulting magnetic hysteresis loops demonstrate the presence of perpendicular magnetic anisotropy (Figure 1). The curvature of the loops at values of the applied magnetic field ( $H$ ) close to saturation indicates the manifestation of the dipole-dipole interaction between magnetic layers. This magnetostatic interaction contributes to the formation of the labyrinth ordering of domain walls.

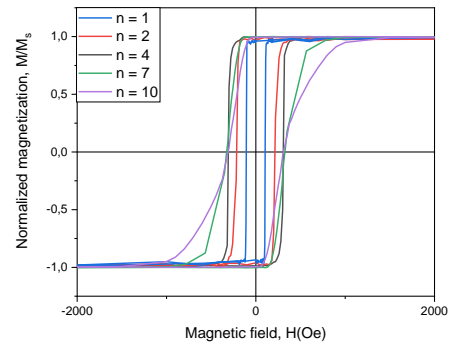


Figure 1. Hysteresis loops measured in the out-of-plane external magnetic field for samples with 7 and 10 repetitions of the [Pd/Co/CoO] trilayer.

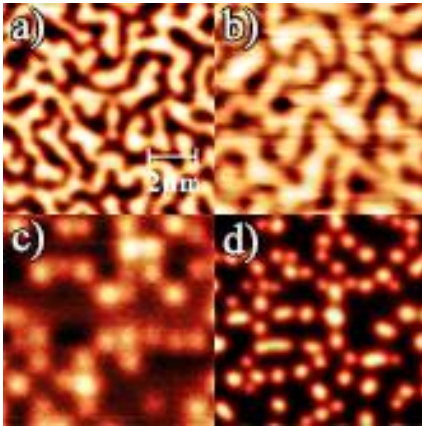


Figure 2. Formation skyrmion lattices (bottom row) from the labyrinth structure (top row) of [Pd/Co/CoO/Pd] $n$  samples, where  $n = 7$  (left column) and  $n = 10$  (right column).

Magnetic force microscopy images were recorded using magnetic probes. To nucleate a skyrmion lattice, a two-pass method was used, when each scan line was passed twice by the MFM probe. On the first pass in the tapping mode, the surface morphology was scanned. Then the probe is lifted to a certain distance, and a second pass was done along the scanned profile keeping some distance from the sample surface. In the end, the MFM tip scanning parameters were set to be able to slice the domain structure into separate segments transforming to skyrmions followed by skyrmion lattice ordering (Figure 2.).

In this work, we showed the ability of the skyrmion lattice nucleation in the epitaxial [Pd/Co/CoO] $n$  superlattices by the MFM probe. The partial oxidation of the Co layer broke the structural inversion symmetry of the system promoting the existence of the interfacial Dzyaloshinskii-Moriya interaction. The competitive contributions of the  $i$ -DMI, PMA and interlayer dipole-dipole interaction create conditions favorable for the origin of chiral domains. We demonstrated that of the two-pass scan by the MFM probe led to the complete formation of the skyrmion lattice. The size and density of skyrmions depended on the periodicity of the labyrinth domain structure and on the distance between two adjacent scanning lines. These results can be used to create a novel type of magnetic memory based on skyrmions, which will allow significantly improve the speed of reading/writing of information.

The authors thank the Russian Ministry of Science and Higher Education for state support of scientific research (State Assignment No. FZNS-2023-0012).

- [1] A. Fert A et al., *Nature Rev. Mater.* **2** (2017) 17031.
- [2] A.V. Ognev et al., *ACS Nano*, **14**(11) (2020) 14960–14970.
- [3] F. Ajejas et al., preprintarXiv:2212.08920, 2022.
- [4] A.G. Temiryazev et al., *Physics of the Solid State*, **60** (2018) 2200–2206.

## NUMERICAL SIMULATION OF THE BREATHERS SOLUTIONS IN LAYERED CHROMIUM DICHALCOGENIDE

*Sinitsyn V.L.<sup>1</sup>, Ovchinnikov A.S.<sup>1</sup>, Bostrem I.G.<sup>1</sup>, Ekomason E.G.<sup>2</sup>*

<sup>1</sup> Ural Federal University, Yekaterinburg, Russia

<sup>2</sup> Bashkir State University, Ufa, Russia

vladimir.sinitsyn@urfu.ru

Nonlinear excitations of lattice systems localized in space and periodically varying in time are called discrete breathers (DBs). Similarly to the ordinary linear excitations in the form of propagating plane waves, DB modes are universal type excitations requiring the nonlinearity and discreteness of the model describing the physical medium for their existence. In most cases, discrete systems admit an adequate description in the continuous medium approximation, and the use of the continuous approximation turns out to be a rather effective tool in searching for and studying the properties of the DB modes. As an alternative approach, the method of the anticontinuous limit suggested by Aubry is widely known [1]. The analysis performed using the continuous approximation and numerical calculations have shown [2] that in the real prototype of our model, the layered chromium dichalcogenide  $\text{Cr}_{0.33}\text{NbS}_2$ , dark-type DB modes arise with a nearly ferromagnetic ordering of local moments. Here, we revisit the problem using the theory of anticontinuous limit for spin systems [3].

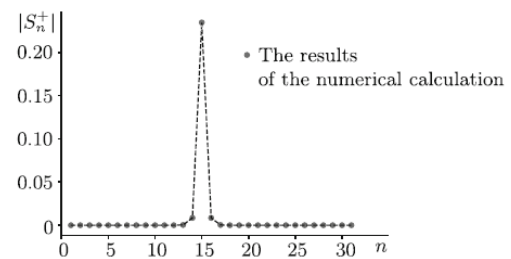


Figure 1. Single-site periodic breather in the chain consisting of  $N = 31$  sites at  $C = 0.001$ . The site 15 is excited. The open boundary conditions are used, and the ratio  $D/2J = 0.16$  is taken

We consider the spin Hamiltonian of the one-dimensional chain used to describe properties of a monoaxial chiral helimagnet,

$$H = -2J \sum_n S_n S_{n+1} + A \sum_n (S_n^z)^2 + D \sum_n [S_n \times S_{n+1}]_z - H \sum_n S_n^z$$

The first term describes the Heisenberg exchange interaction, The second term is related to the single-ion magnetic anisotropy of the “easy plane” type ( $A > 0$ ). The third term corresponds to the Dzyaloshinskii–Moriya antisymmetric exchange interaction with the vector  $\mathbf{D} = D\mathbf{z}$  directed along the  $z$  axis. The last term corresponds to the Zeeman interaction of local moments with the external magnetic field  $H$  directed along the  $z$  axis. To apply the Aubry’s method and get a numerical solution for the whole discrete spin system, the iteration process starts with the single-site breather solution relevant for  $C=0$  ( $C = J/A$ ,  $\beta = H/2AS$ )

$$S_n^+(\tau) = [1 - (\beta - \omega_n)^2]^{1/2} e^{-i\omega_n\tau + i\alpha_n}$$

We show that for the values of  $\beta$  and arbitrary  $\omega_n$  and phase  $\alpha_n$  corresponding this equation the algorithm leads to stable breather solutions up to  $C=0.006$ . Figure 1 shows an example of the breather solution obtained by the Aubry’s method.

This work was supported by the Russian Science Foundation (Grant No. 22-13-00158).

[1] J. L. Mar’ın and S. Aubry, *Nonlinearity*, **9** (1996) 1501–1528.

[2] I. G. Bostrem et al., *Phys. Rev. B*, **104** (2021) 214420.

[3] I. G. Bostrem et al., *Theoretical and Mathematical Physics*, **214(2)** (2023) 250-264.

## SHAPE-DRIVEN MAGNETIC PROPERTIES OF JELLYFISH-LIKE Ni NANOWIRES

*Samardak A.Yu., Sobirov M.L., Ognev N.A., Leiko G.A., Samardak A.S., Ognev A.V.*

Laboratory of thin film technologies, Far Eastern Federal University, Vladivostok, Russia  
samardak.aiu@dvfu.ru

The ability to control the matter on the atomic scale is one of the main goals of nanotechnology. From magnetic point of view manipulation of the shape of one-dimensional ferromagnetic nanostructures is especially important since the geometrical parameters mostly define magnetic behavior of the nanostructure. Differently shaped one-dimensional nanostructures, such as nanosprings [1], barcode [2] and interconnected nanowires [3] were already presented and investigated, showing new unique magnetic effects, resulting in new possible implementations. In this work our group presents new type of one-dimensional nanostructures – so called jellyfish-like nanowires (JFNW) and investigates their magnetic properties experimentally and by micromagnetic simulations.

Bi-layered porous alumina matrices with large difference of diameters of pores in corresponding layers were prepared by anodization of aluminum plate in mild potentiostatic regime. The voltage of the second anodization was varied from sample to sample to achieve different diameters of pores in the top layer of the matrix. After the preparation, bilayered alumina template was used as template in the process of electrodeposition of Ni from Watts solution. In the end, arrays of Ni JFNW were obtained (Figure 1).

Analysis of scanning electron microscopy images showed that the resulting structures had two parts - part with bigger diameter (so-called «head») and part with narrow diameter (so-called «legs»). The diameter of the «head» was set to be the same from sample to sample, while the variation of the voltage due the second anodization allowed to control the diameter and number of the «legs» growing from single «head».

Magnetic properties of the array of JFNWs embedded in alumina template were investigated using vibrating sample magnetometry and showed hysteresis loops with low remanence and coercive force. Easy axis of magnetization was aligned along the long axis of nanowires. Analysis of First Order Reversal Curves diagrams revealed strong magnetostatic interactions in the array. Micromagnetic simulation showed that in remnant state «head» of JFNWs was in the vortex micromagnetic configuration, while «legs» were-in single-domain state.

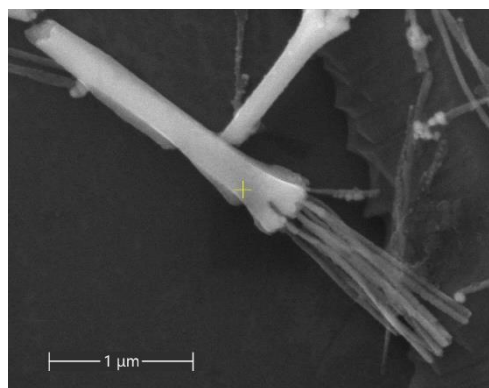


Figure 1. SEM image of single jellyfish-like Ni nanowire, etched out of alumina template.

This work was supported by the Russian Ministry of Science and Higher Education (State Task No. FZNS-2023-0012).

[1] D.Y. Nam et al., *Nanoscale*, **10** (2018) 20405-20413.

[2] A.Y. Samardak et al., *Small*, **18**(47) (2022) 2203555.

[3] J. Martin et al., *Nat. Commun.*, **5** (2014) 5130.

## EXPERIMENTAL AND THEORETICAL STUDY OF THE CATION AND MAGNETIC ORDERING IN $\text{Ni}_x\text{Co}_{3-x}\text{B}_2\text{O}_6$

*Soifronova S., Pavlovskii M., Chernyshov A., Moshkina E., Velikanov D.*

L.V. Kirensky Institute of Physics, Krasnoyarsk Scientific Center, Siberian Branch RAS,  
Krasnoyarsk, Russia  
ssn@iph.krasn.ru

We investigate the electronic structure, structural and magnetic properties of  $\text{Ni}_x\text{Co}_{3-x}\text{B}_2\text{O}_6$  ( $x = 0, 1, 2, 3$ ) using density functional theory calculation including spin-orbit coupling. The distribution of 3d-metal ions on crystallographic positions in  $\text{NiCo}_2\text{B}_2\text{O}_6$  and  $\text{Ni}_2\text{CoB}_2\text{O}_6$  were studied. The spin exchange interactions between the Ni(Co) ions were evaluated.

$\text{Ni}_x\text{Co}_{3-x}\text{B}_2\text{O}_6$  crystals belong to the  $\text{Pnmm}$  ( $D_{2h}^{12}$ ) space group (kotoite structure) [1,2]. The unit cell involves two formula units. Magnetic atoms are Ni (Co) occupying two nonequivalent crystallographic positions 2a and 4f. Thus, there are six magnetic atoms in the unit cell. The  $\text{Ni}_3\text{B}_2\text{O}_6$  and  $\text{Co}_3\text{B}_2\text{O}_6$  crystals are collinear with the easy magnetization axis directed along  $c$  axis for  $\text{Ni}_3\text{B}_2\text{O}_6$  and along  $b$  axis for  $\text{Co}_3\text{B}_2\text{O}_6$ [3]. In  $\text{Co}_3\text{B}_2\text{O}_6$ , in contrast to  $\text{Ni}_3\text{B}_2\text{O}_6$ , there is strong anisotropy of magnetization both above and below the temperature of the magnetic phase transition. The temperature dependences of magnetization of the single-crystal sample for  $\text{NiCo}_2\text{B}_2\text{O}_6$  were measured by applying the magnetic field along  $a, b, c$  axes on the SQUID magnetometer in a field of 50 Oe (Figure 1). The easy magnetization axis is directed along  $b$  axis. The magnetization curves recorded in the zero-field (ZFC) regime have two features.

The calculations of energies of compounds  $\text{Ni}_2\text{CoB}_2\text{O}_6$  in different cation ordered states showed that Ni and Co ions are not randomly distributed. Ni ions prefer to occupy crystallographic position 4f. In agreement with experiment, the anisotropy in  $\text{Ni}_3\text{B}_2\text{O}_6$  is weak with a magnetization easy axis directed along  $c$  axis. The calculated spin exchange interactions are similar for both crystals. There is the competition between the antiferromagnetic and ferromagnetic exchange in both crystals.

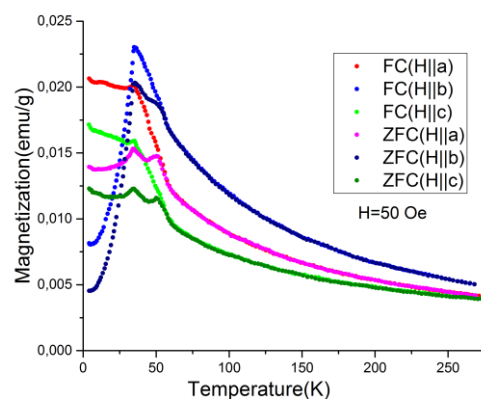


Figure 1. Temperature dependences of magnetization of the single-crystal  $\text{NiCo}_2\text{B}_2\text{O}_6$  when the magnetic field of 50 Oe is applied along  $a, b, c$  axes, recorded in the zero-field (ZFC) and field-cooling (FC) regimes.

The research was funded by Russian Science Foundation and Krasnoyarsk Regional Fund of Science, project № 23-12-20012 (<https://rscf.ru/en/project/23-12-20012/>).

[1] R.E. Newnham et al., *Z. Krist.*, **121** (1965) 418.

[2] R.E. Newnham et al., *Phys. Status.Solidi*, **16** (1966) K17.

[3] L.N. Bezmaternykh et al., *Phys. Status Solidi B*, **249**(8) (2012) 1628-1633.

2PO-L4-22

## PARAMAGNETIC AND FERROMAGNETIC CENTERS OF MANGANESE IN SILICON

*Askarov S.<sup>1</sup>, Sharipov B.<sup>1</sup>, Mavlyanov A.<sup>2</sup>, Saliyeva Sh.<sup>1</sup>, Shukurova D.<sup>1</sup>, Marlonov A.<sup>1</sup>*

<sup>1</sup> Tashkent State Technical University, Tashkent, Republic of Uzbekistan

<sup>2</sup> Semiconductor Physics and Microelectronics Research Institute, Mirzo Ulugbek NUU, Tashkent,  
Uzbekistan  
bashirulla@mail.ru

Paramagnetic centers of a number of transient metals in silicon were investigated by Ludwig and Woodbury, the results of which were reflected in their respective research. In the case of silicon doped with manganese (Si<Mn>), the authors had recorded the EPR spectra corresponding to isolated impurity interstitial centers with various charge states -  $Mn^0(3d^7)$ ,  $Mn^+(3d^6)$ ,  $Mn^{++}(3d^5)$  and  $Mn^-(3d^8)$ , as well as to a number of donor-acceptor pairs of manganese with both shallow and deep acceptor substitution centers.

Unfortunately, as it was revealed later, the concentration of electroactive manganese centers, determined by the silicon compensation method with different concentrations of small acceptor boron impurities, significantly exceeded the total concentrations of deep manganese centers.

To find out in what state the main part of manganese responsible for the compensation of the material happens to be, this work is devoted to a more thorough study of EPR spectra of silicon doped with manganese with various degrees of compensation.

As is shown by the results of studies in overcompensated n - Si<Mn> samples with a resistivity  $\rho \leq 2 \cdot 10^2$  Ohm cm at 3.8 K, a spectrum was observed consisting of six ultrathin lines, due to interaction of d - electrons with their own core  $Mn^{5s}$  ( $I = 5/2$ ). The measured parameters of the spectrum had the values  $g = 2.362 \pm 0.003$ ,  $A = (58.0 \pm 0.2)$  G. The spectrum had a strong temperature dependence and completely disappeared at  $T=8$  K.

The spectrum parameters corresponded to neutral centers of manganese intercalation -  $Mn^0(3d^7)$ . As  $\rho > 5 \cdot 10^2$   $\Omega \cdot cm$  have increased, this center was ionized. It should be noted that the spectra of ionized  $Mn^+(3d^6)$  and  $Mn^{++}(3d^5)$  centers were observed only in newly prepared Si<Mn> samples. In times of long-term storage of these samples at room temperature, the spectra of ionized manganese centers tended to disappear, and instead of them, in high-resistance n-Si<S> samples, as well as in compensated p-Si<S> samples, the spectra were observed that would correspond to donor-acceptor pairs  $Mn^{++} - B^-$ , as well as to clusters of four centers of manganese  $Mn_4$  intercalation.

Moreover, in all overcompensated Si<B,Mn> samples with  $\rho > 5 \cdot 10^2$   $\Omega \cdot cm$  at low temperatures ( $\sim 4$  K) in virtually absent outer magnetic field, the spectrum consisting of a large number of lines, the position and intensity of which changed from sample to sample likely appeared.

We prepared Si<B,Mn> samples, in which the spectrum in zero fields had a well-resolved ultrafine structure. The intensity of the lines and the value of the resonant fields of the spectrum changed strongly with temperature. The spectrum had a maximum intensity at  $T = 4.6$  K, and the center of gravity of the spectrum at a given temperature was practically in zero fields, and part of the spectrum was in the region of negative fields. As the temperature decreased, the intensity of the lines of the spectrum decreased, and the center of gravity shifted towards positive fields, and at  $T = 3.2$  K the spectrum was completely registered at positive fields. At this temperature, in the direction of the magnetic field along the <111> axis, the spectrum consisted of four fine structure lines, each of which consisted of 11 hyperfine structure lines with  $A = 37$  G.

With an increase in temperature from 4.6 K, the intensity of the spectrum lines also decreased, and the center of gravity shifted towards negative fields and already at  $T = 4.9$  K was in the direction of negative fields. This spectrum is associated with the formation of exchange-coupled pairs of  $Mn^+ - Mn^+$  of a ferromagnetic nature. It is this center that is responsible for the compensation of the material.

2PO-L4-23

**MAGNETIZATION CURVES OF 2D IRON NANOWIRES ARRAY***Zagorskiy D.L.<sup>1</sup>, Semenov S.V.<sup>2</sup>, Komogortsev S.V.<sup>2</sup>, Doludenko I.M.<sup>1</sup>, Balaev D.A.<sup>2</sup>, Panina L.V.<sup>3</sup>*<sup>1</sup> FSRC “Crystallography and Photonics” RAS, Moscow, Russia<sup>2</sup> Kirensky Institute of Physics, Federal Research Center KSC SB RAS, Krasnoyarsk, Russia<sup>3</sup> Moscow Steel and Alloys Institute, Moscow, Russia

dzagorskiy@gmail.com

Two-dimensional arrays of ferromagnetic Nanowires (NWs) normally oriented inside non-magnetic film matrix is a promising composite material that combines high magnetization, coercive force, and perpendicular magnetic anisotropy. The properties of such composites are determined both by the individual behavior of single NW and by their collective behavior due to the dipole-dipole interaction. Using the example of iron NWs, ordered in a PETF membrane, we study the magnetization curves of such a two-dimensional array. These data are analyzed on the basis of ideas about magnetization reversal processes in such composites, the effects of misorientation within the ensemble, and interaction effects. Quantitative information to evaluate these effects has been extracted using a range of measurement protocols, from the simplest measurement of major hysteresis loop at different field orientations to Henkel plots, as well as first order magnetization reversal curve (FORC) measurements and analysis.

Ensembles of Fe NWs obtained by electrodeposition into the pores of track etched membranes were studied. A feature of the obtained composites is a fairly perfect orientation of the wires in the ensemble perpendicular to the membrane surface, but the random distribution of the NWs over the area of the membrane. Three types of samples (with NW diameter 100 nm and the length 10  $\mu\text{m}$ ) were studied. The samples differed from each other in the surface density of the NWs and their orientation- strictly perpendicular to the film surface and distributed in small angle interval (+/- 10-15 grad).

The experimental values of the coercive force at applied field deviating from the NWs axis by no more than 45 degrees are in good agreement with the results of micromagnetic simulation for all samples. This means that the interaction in an ensemble of NW does not affect the average magnetization reversal field of an individual NW in the array near its demagnetized state, but is determined solely by the magnetization reversal field of an individual filament. The two main mechanisms of magnetization and remagnetization are rotation and switching processes. An analysis of rotation processes based on the Stoner-Wohlfarth model makes it possible to quantify the effect of misorientation in an ensemble of wires. The interaction was estimated by measuring the average effective demagnetizing field of the array and is in excellent agreement with the calculations within the effective medium model. Random positioning of NW in the ensemble leads to inhomogeneity of the demagnetizing field, information about which is provided by FORC analysis. So, in the experiment it is observed that both the amplitude of the inhomogeneity and the average value of the demagnetizing field correlate with the density of the wires in the ensemble.

This work was supported by RSF Grant 22-22-00983

## SPIN POLARIZED EFFECTS IN SILICON NANOTUBES

*Mukhtarov A.P.*

Institute of Nuclear physics, Tashkent, Uzbekistan  
amukhtarov@gmail.com

Spintronics has gained considerable attention in recent years as an alternative to conventional electronics, as it promises low-power consumption, high-speed operation, and non-volatile memory capabilities. Silicon, being the dominant material in the semiconductor industry, holds particular interest for spintronics research. Silicon nanotubes, with their confined geometries, can exhibit different electronic and magnetic properties compared to bulk silicon. Understanding spin polarization in these nanotubes could open up possibilities for spin-based devices with enhanced functionality and performance. The requestness of this research stems from the ongoing pursuit of new materials and device architectures for spin-based technologies. If silicon nanotubes can be effectively manipulated to achieve and control spin polarization, they may serve as building blocks for future spintronic devices, such as spin transistors or spin-based memory elements.

Theoretical investigations using computational methods, such as density functional theory (DFT), have been conducted to explore the spin-dependent properties of silicon nanotubes. These studies aim to understand the electronic structure, spin polarization, and magnetic properties of different types of silicon nanotubes. We used DFT with GGA functionals, HF and hybrid functionals.

In this report, we will try to answer the question why an (n,0)-type silicon nanotube is a conductor, while an (n,n)-type Si-NT has a semiconductor nature. We found that (n,m)-type silicon nanotubes, which have a chiral structure, conduct electrons in a spiral around the axis of the nanotube, and this type of conduction creates a magnetic field inside the tube, which is easily detected in acid solutions.

Using computer simulations, we found that (n, m)-type silicon nanotubes can be spin-polarized under certain conditions. The dependence of spin polarization on the degree of delocalization of valence electrons on the surface of silicon nanotubes was also studied using the generalized Weiberg-Mayer index [1].

[1] A.P. Mukhtarov, S.K. Mukhtarova, S.A. Usmanova, *J. Phys: Conf.Ser.*, **1** (2022) 012003.

## STRUCTURE AND STABLE STATE OF MAGNETIC VORTEX-LIKE INHOMOGENETIES IN MODULATED ULTRATHIN MAGNETIC FILMS

*Vakhitov R.M., Solonetsky R.V., Akhmetova A.A., Filippov M.A.*

*UUST, Ufa, Russia*

*mikhail.filippov.99@mail.ru*

Magnetic skyrmions are topologically protected vortex-like magnetic inhomogeneities. Skyrmions were first discovered in chiral magnets, in which they are stabilized by the bulk Dzyaloshinskii-Moriya interaction (DMI). Later, skyrmions were observed in multilayer ultrathin films in which interfacial DMI is already present [1].

At the same time, there are methods for obtaining stable single skyrmions even in the absence of DMI in materials. One of such possible options is considered in [2]. It observed the nucleation of a stable skyrmion on a columnar defect of the “potential well” type in a uniaxial ferromagnetic film. With the help of micromagnetic modeling on films with a defect, stable states of Bloch-type skyrmions were obtained [3].

The aim of this work is to find stable states of Neel-type vortex-like inhomogeneities using the OOMMF open access software package [4] with an additional module [5]. A disk of finite size with a columnar defect in the center is considered. It is believed that the material parameters on the disk and the defect are identical, except for the anisotropy constant  $K_u$ :  $K_{u2} < 0$  - on the defect,  $K_{u1} > 0$  - in the rest of the disk. The presence of interfacial DMI (isotropic) in the disk is also taken into account.

Based on the simulation results, it turned out that vortex-like structures in the absence of any external fields are stable with the following material parameters: disk diameter 600 nm, disk thickness 5 nm, defect diameter 60 nm,  $K_{u1} = 3 \times 10^4$  J/m<sup>3</sup> (outside the defect),  $K_{u2} = -0.5 \times 10^4$  J/m<sup>3</sup> (at the defect),  $M_s = 2.0 \times 10^5$  A/m,  $A = 2.5 \times 10^{-11}$  J/m,  $D = 1 \times 10^{-3}$  J/m. With these parameters, a skyrmionium ( $2\pi$ -skyrmion) was found, in which the magnetization reversal occurs by  $360^\circ$  (Figure 1). Yellow shows the direction of magnetization along the z-axis, purple - against the axis.

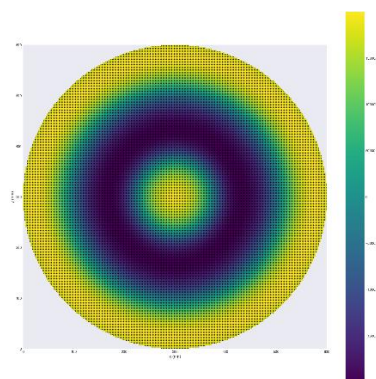


Figure 1. Obtained stable state of skyrmionium.

The authors are thankful for the support of the State assignment of the Russian Federation for the implementation of scientific research by laboratories (Order MN-8/1356 of 09/20/2021).

- [1] K.Everschor-Sitte et al., *J. Appl. Phys.*, **124** (2019) 240901.
- [2] D. Navas et al., *APL Mat*, **7** (2019) 081114.
- [3] R.M. Vakhitov et al., *Symmetry*, **14**(3) (2022) 612.
- [4] M.J Donahue, D.G. Porter, *OOMMF User's Guide, Version 2.0b0* (2022).
- [5] D.A Tatarskiy, *JMMM*, **509** (2022) 166899.

## ELECTRONIC STRUCTURE AND HYPERFINE INTERACTIONS IN $\text{Cr}_x\text{NbSe}_2$ ( $x \leq 0.5$ ) BY DFT AND NMR STUDIES

*Ogloblichev V.V.<sup>1</sup>, Zayats P.A.<sup>1</sup>, Baranov N.V.<sup>1</sup>, Piskunov Yu.V.<sup>1</sup>, Sadykov A.S.<sup>1</sup>, Nosova N.M.<sup>2</sup>, Sherokalova E.M.<sup>2</sup>, Selezneva N.V.<sup>2</sup>*

<sup>1</sup>Mikheev Institute of Metal Physics of Ural Branch of Russian Academy of Sciences,  
Yekaterinburg, Russian Federation

<sup>2</sup>Ural Federal University, Yekaterinburg, Russian Federation  
ogloblichev@imp.uran.ru

The transition metal dichalcogenides  $\text{TX}_2$  (T = transition metal, X = chalcogen) are among the most studied two-dimensional electronic systems due to their intriguing physical and chemical properties and potential applications. The distribution of charge and spin density is the key to understanding the mechanisms responsible for the change in the structural, magnetic, and transport properties of compounds upon intercalation.

In this work, the magnetically ordered phase of polycrystalline chalcogenide samples  $\text{Cr}_x\text{NbSe}_2$  ( $x = 0.33, 0.5$ ) in a zero external magnetic field at a temperature  $T = 4.2$  K is studied by nuclear magnetic resonance (NMR) methods on chromium ( $^{53}\text{Cr}$ ) and niobium ( $^{93}\text{Nb}$ ) nuclei. Ab initio calculations of the electronic structure were carried out to theoretically estimate the parameters of the NMR spectra, the quadrupole interaction, emerging hyperfine fields, and to interpret the NMR data.

The  $^{53}\text{Cr}$  NMR spectra in the composition of  $\text{Cr}_{0.33}\text{NbSe}_2$  can be decomposed into two quadrupole split NMR lines corresponding to two different nonequivalent positions of chromium ions. The first line can be related to the ordering of chromium atoms in the crystal structure with space group  $P6_3/mmc$ , when the ordering of Cr atoms leads to the formation of  $\sqrt{3} \times \sqrt{3}$  superstructures. The second line can be related to the ordering of chromium atoms in the crystal structure with space group  $P6_322$ , where the ordering of Cr atoms leads to the formation of  $2 \times 2$  superstructures. In the composition of  $\text{Cr}_{0.5}\text{NbSe}_2$ , which corresponds to the greater intercalation of chromium atoms, one line is observed, which corresponds only to ions in the structure with space group  $P6_322$ .

The local magnetic field on the nucleus, created by hyperfine interaction with the nearest environment, determines the NMR frequency of chromium and niobium. In our case, the main contribution to the local field on the nuclei will be made by their own unpaired 3d electrons. From the analysis of the local field on the  $^{53}\text{Cr}$  nuclei, the average value of the magnetic moment of chromium was determined ( $\mu_{\text{NMR}} \approx 2.2\mu_{\text{B}}$ ), which is less than the theoretical value for  $\text{Cr}^{3+}$  ( $\mu = 3\mu_{\text{B}}$ ) and closer for  $\text{Cr}^{4+}$  ( $\mu = 2\mu_{\text{B}}$ ) [1]. The presence of a local magnetic field of 160 kOe on Nb nuclei has been experimentally shown. The decrease in the average value of the magnetic moment of chromium and the presence of a local field on the nuclei of niobium can be explained by the high degree of hybridization of the  $a_{1g}$  and  $e_g$  orbitals of the chromium 3d-electrons with the  $4d_{22}$  and  $5s$  orbitals of niobium. The high hybridization of the chromium and niobium orbitals is confirmed by the calculated data from first principles. Such a transfer of electron density from chromium ions to niobium ions most likely also occurs in  $\text{Cr}_{0.33}\text{NbS}_2$  compounds. According to NMR data on  $^{53}\text{Cr}$  nuclei, this compound also exhibits an NMR signal in the range of 48–52 MHz with average values of the local field values of 207.7(2) kOe and a magnetic moment of chromium  $\mu \approx 2.1\mu_{\text{B}}$ .

This work was supported by the Russian Science Foundation (project no. 22-12-00220).

[1] P. Agzamova, V. Ogloblichev, *Appl. Magn. Reason*, **54** (2023) 439.

July 3

9:30 - 11:00

Monday

PLENARY  
LECTURES

3PL-AH-1

**HYDRODYNAMIC SPINTRONICS AND CURRENT VORTEX***Maekawa S.*RIKEN, Saitama, Japan  
sadamichi.maekawa@riken.jp

In metals with disorder, the electron transport is described as diffusive. On the other hand, in those with electron-electron interaction being the dominant source of scattering, the motion of the electrons resembles the flow of classical liquids with shear viscosity, namely, the hydrodynamic fluids. The recent progress of nano-technology has made it possible to extend the study on such hydrodynamic electron fluids in nano-devices and low dimensional materials. In such fluids, the angular momentum of the fluid vorticity, i.e., current vortex, and electron spins couple each other due to the angular momentum conservation, i.e., the spin-vorticity coupling [1]. Combining the Navier-Stokes and the spin diffusion equations in the presence of the spin-vorticity coupling, we examine a variety of spintronic phenomena [2-5]. We present that metals with nano-structure provide unique spintronic devices due to the local hydrodynamic nature. The hydrodynamic phenomena of electron fluids open a door to "Hydrodynamic spintronics".

- [1] M.Matsuo, E.Saitoh and S.Maekawa, *Spin Current* (Oxford University Press, 2017).
- [2] J. Fujimoto et al., *Phys. Rev. B*, **103** (2021) L220404.
- [3] F. Lange et al., *Phys. Rev. Lett.*, **126** (2021) 157202.
- [4] J. Fujimoto et al., *APL Materials*, **9(6)** (2021) 060904-060904.
- [5] G. Okano et al., *Phys. Rev. Lett.*, **122** (2019) 217701.

## TUNEABLE MAGNETIC PHASE TRANSITIONS IN RARE-EARTH INTERMETALLIC COMPOUNDS WITH $\text{ThMn}_2\text{Si}_2$ STRUCTURE

*Mushnikov N.V., Gerasimov E.G.*

M.N. Mikheev Institute of Metal Physics, Yekaterinburg, Russia  
mushnikov@imp.uran.ru

In the  $\text{RMn}_2\text{Si}_2$  compounds ( $R$  is a rare-earth metal) magnetic moments of the Mn atoms form ferromagnetic layers oriented perpendicular to the  $c$ -axis of tetragonal  $\text{ThMn}_2\text{Si}_2$ -type lattice. Relatively weak interlayer exchange interaction can be negative or positive. The compounds demonstrate an unusual variation of the interlayer Mn-Mn ordering from antiferromagnetic (AF) to ferromagnetic (FM) when the distance between Mn ions in the layer increases. Temperature of the AF to FM magnetic phase transition depends on the composition and is strongly influenced by magnetic field and pressure.

We studied magnetic, magnetovolume, thermal and magnetotransport properties of quasi-ternary intermetallic compounds  $\text{La}_{1-x}\text{R}_x\text{Mn}_2\text{Si}_2$ , ( $R = \text{Sm}, \text{Gd}, \text{Tb}, \text{Dy}$ ). In these systems, substitution of different  $R$  atoms allows us to change gradually the interatomic distances, interlayer exchange interactions and contributions of  $R$  and Mn magnetic subsystems to the magnetic anisotropy of the compounds. Using single-crystalline samples, we found that the Mn sublattice is characterized by unusually high magnetic anisotropy. Field-induced magnetic transitions were studied in high pulsed magnetic fields. For  $\text{La}_{1-x}\text{Sm}_x\text{Mn}_2\text{Si}_2$ , large linear and volume magnetostrictions and positive magnetoresistance were observed at the field-induced transition. The values of the adiabatic temperature change and the isothermal magnetic entropy change were determined by direct and indirect methods. It was established that the magnetocaloric effect has a different sign during the AF-FM and ferromagnet-paramagnet transitions.

For the  $\text{La}_{1-x}\text{Gd}_x\text{Mn}_2\text{Si}_2$  and  $\text{La}_{1-x}\text{Tb}_x\text{Mn}_2\text{Si}_2$  compounds in the low-temperature region, negative Mn-Mn interlayer exchange interactions and the easy-axis type magnetocrystalline anisotropy of the manganese sublattice leads to the appearance of an unexpected magnetic structures. For the compounds with Gd, the resulting magnetic moment is oriented perpendicular to the direction of the easy  $c$ -axis of the Mn sublattice. For the Tb-containing compounds, a competition of the negative Tb-Mn and Mn-Mn interlayer exchange interactions and strong uniaxial magnetic anisotropy of both Tb and Mn sublattices lead to formation of a frustrated magnetic state of Tb ions, which prevents magnetic ordering in the Tb sublattice.

The origin of the magnetic phase transition in  $\text{RMn}_2\text{Si}_2$  intermetallics was explored within the ab initio DFT-based approach. The calculated exchange interaction parameters indicate that the antiferromagnetic interlayer ordering is stabilized by a dominant negative interaction via Si-Si dimer, which forms the bonding molecular orbital acting as a mediator in the Mn  $d$  superexchange mechanism.

The obtained results show a significant role of the Mn-Mn and Mn- $R$  exchange interactions and magnetic anisotropy in formation of magnetic structures and realization of magnetic phase transitions in layered intermetallic compounds.

Support by Russian Science Foundation (project No. 23-12-00265) is acknowledged.

**July 3**

Sunday

11:45 - 13:15

ORAL  
SESSIONS I

Section A  
**Magnonics**

**FERRONS VS “FERRONS”***Nikitov S.A.*<sup>1,2,3</sup><sup>1</sup> Kotel'nikov Institute of Radioengineering and Electronics  
RAS, Moscow, Russia<sup>2</sup> Moscow Institute of Physics and Technology, Dolgoprudny, Moscow Region, Russia<sup>3</sup> Chernyshevsky National State University, Saratov, Russia  
nikitov@cplire.ru

A series of papers was recently published concerning new interesting and important effects in ferroelectrics. This research concerns the existence and physical properties of new “quasiparticle” which is called by the authors of [1] as “ferrons”. According to the author’s definitions the “ferrons” are, in fact, polar phonons relating to anharmonic oscillations in the ferroelectric medium. On the other hand, by definition polarons are quasiparticles that are formed in polarizable materials (e.g., ferroelectrics) due to the coupling of excess electrons or holes with acoustic vibrations. In such a way “ferrons” are polar phonons in ferroelectrics. The authors of a recent paper appeared in the Journal of Magnetism and Magnetic Materials even introduced a new term “ferronics”, relating to a new research field. Theoretical and experimental results on physics of these objects in ferroelectrics are quite interesting and exciting.

However, during the decade from 1967 to 1978 the well-known Russian scientist Eduard L. Nagaev published a series of papers devoted to the problem of existence of microregions of self-trapped states of charge carriers in magnetic semiconductors. Essentially, such a region is a bound complex of conduction electrons and a ferromagnetic phase. Later Nagaev considered a number of possible situations: ferromagnetic regions in antiferromagnets and vice versa, influence of magnetoelastic effects on stability of these states, etc. Originally, these states were called magnetic polarons, however, later he called it a new quasiparticle of complex origin or “ferron”. This term was used not only by Prof. Nagaev, but was also widely adopted by scientists who studied magnetic semiconductors and other materials, such as solid helium, spin glasses, singlet magnets, etc. The review of Nagaev’s results on this subject was published in the Journal of Magnetism and Magnetic Materials and his textbook later translated in English [2].

I will discuss the appearance confusion between previously published and recently published results and their formulations concerning ferrons.

This work was supported by the Russian Science Foundation grant No. 19-19-00607-II.

[1] G. E. W. Bauer et al., *Phys. Rev. Lett.*, **126** (2021) 187603.

[2] E.L. Nagaev, *J. Magn. Magn. Mater.*, **10** (1992) 39-60.

# FULL QUANTUM THEORY FOR MAGNON TRANSPORT IN TWO-SUBLATTICE MAGNETIC INSULATORS AND MAGNON JUNCTIONS

Zhang T.<sup>1</sup>, Han X.F.<sup>1,2,3</sup>

<sup>1</sup> Beijing National Laboratory for Condensed Matter Physics, Institute of Physics, University of Chinese Academy of Sciences, Chinese Academy of Sciences, Beijing, China

<sup>2</sup> Center of Materials Science and Optoelectronics Engineering, University of Chinese Academy of Sciences, Beijing, China

<sup>3</sup> Songshan Lake Materials Laboratory, Dongguan, Guangdong, China  
xfhan@iphy.ac.cn

Magnon, as elementary excitation in magnetic systems, is a potential candidate to replace electron as information carrier. Due to the absence of Joule heat during magnon transport, researches on magnon transport have gained considerable interest over the past decade. Here, we propose a Green's function formalism to compute the magnon bulk and interface current in both ferrimagnetic insulators (FIMIs) and antiferromagnetic insulators (AFMIs). We investigated the spatial distribution and temperature dependence of magnon current in FIMIs and AFMIs that resulted from a temperature and spin chemical potential step, and magnon currents in sublattices demonstrate a linear dependence on temperature. Additionally, in AFMIs, magnon currents in the two sublattices cancel each other out. Subsequently, we conducted numerical simulations of the magnon junction effect using the Green's function formalism. This study demonstrates the potential for investigating magnon transport in specific magnonic devices using a full quantum theory.

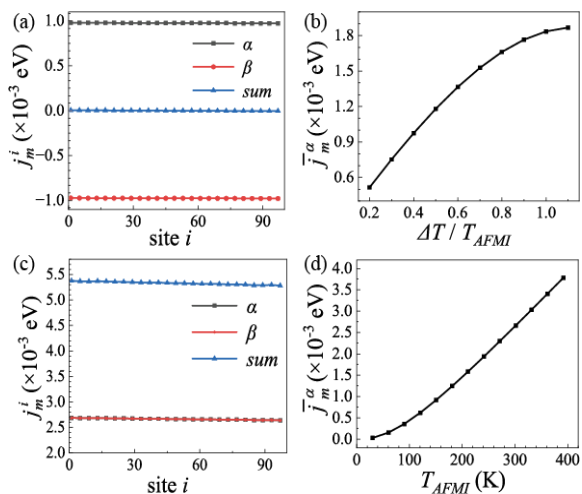


Figure 1. Spatial distribution and temperature dependence of magnon currents excited by SSE (a, b) and SHE (c, d) in AFMI.

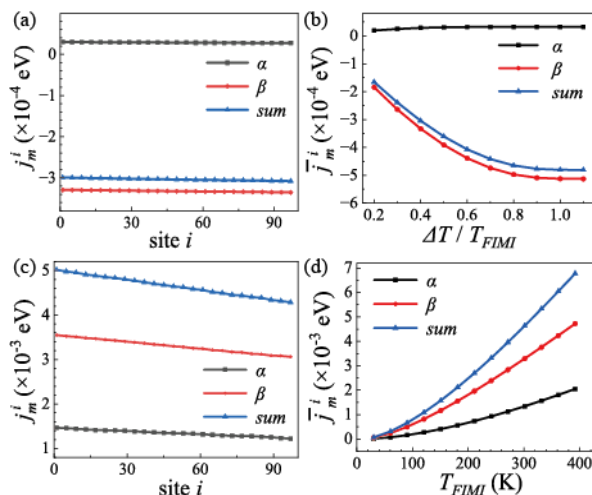


Figure 2. Spatial distribution and temperature dependence of magnon currents excited by SSE (a, b) and SHE (c, d) in FIMI.

3IR-A-3

## DIRECT OBSERVATION OF MAGNON BEC IN YIG FILM BY FARADAY ROTATION

*Bunkov Yu.M.<sup>1</sup>, Belotelov V.I.<sup>1,2</sup>, Knyazev G.A.<sup>1,2</sup>, Kuzmichev A.N.<sup>1</sup>, Petrov P.E.<sup>1,2</sup>  
Savochkin I.V.<sup>1</sup>, Vetoshko P.M.<sup>1,3</sup>*

<sup>1</sup> Russian Quantum Center, Skolkovo, Moscow, Russia

<sup>2</sup> Lomonosov Moscow State University, Moscow, Russia

<sup>3</sup> Kotel'nikov IRE RAS, Moscow, Russia

y.bunkov@rqc.ru

Bose-Einstein condensation occurs at an appropriate density of bosonic particles, depending on their mass and temperature. We were able to experimentally observe the transition from the spin wave regime to the magnon Bose-Einstein condensed state (mBEC) with an increase in the magnon density by microwave pumping. We used an optical setup based on the Faraday rotation effect to record the spatial distribution of the magnon density and phase.

We used the sample of 6  $\mu\text{m}$  YIG film in the form of an ellipse with axes 4.5 by 1.5 mm. A strip line 0.2 mm wide excited magnons near one of the ends of the sample. The external magnetic field was directed out of plan of the film. We have investigated the propagation of magnons outside the region of excitation. At a low amplitude of resonant microwave excitation, we observed the formation of spin waves, the parameters of which are in good agreement with calculations based on the Landau-Lifshitz-Gilbert (LLG) equations for the experimental conditions. At a critical density of excited magnons, its properties changed dramatically. Instead of a pattern of spin waves, a coherent precession was observed even far from the region of excitation. This pattern clearly corresponds to Bose condensation of magnons [1]. We performed a spatial Fourier analysis of the signal outside the excitation region as a function of the excitation energy and found a sharp transition from a wide spectrum in the spin wave mode to a narrow line in the BEC mode. The critical magnon density for the transition corresponds to a  $3^\circ$  deviation of the magnetization, which is in good agreement with the prediction [2].

The Bose condensation of magnons studied by us is formed from magnons with  $k = 0$ . It has the same basic properties as the magnon BEC in antiferromagnetic superfluid  $^3\text{He}$  discovered in 1984 [3-5]. In both cases, it has direct analogies with the atomic Bose condensate. Another type of magnon BEC occurs in in plane magnetized YIG film [6]. In this case, it is formed by traveling magnons with nonzero momentum  $k$ . As a result, this type of magnon BEC can be considered in analogy with photon BEC in media.

This work was supported by the Russian Science Foundation (project no. 22-12-00322).

- [1] P. E. Petrov et al., *Optics Express*, **31** (2023) 8335-8341.
- [2] Yu. M. Bunkov and V. L. Safonov, *J. Magn. Magn. Mat.*, **452** (2018) 30–34.
- [3] A.S.Borovik-Romanov et al., *JETP Letters*, **40** (1984) 1033- 1037.
- [4] Yu. M. Bunkov, *J. Low Temp. Phys.*, **138** (2005) 753-758.
- [5] Yu.M. Bunkov and G.E. Volovik, *Phys. Rev. Lett.*, **98** (2007) 265302.
- [6] A. A. Serga et al., *Nat. Commun.*, **5** (2014) 3452–3458.

## SCATTERING OF SPIN WAVES BY ONE-DIMENSIONAL SOLITONS

*Laliene V.<sup>1</sup>, Campo J.<sup>2</sup>*

<sup>1</sup> Department of Applied Mathematics and IUMA, University of Zaragoza, Zaragoza, Spain

<sup>2</sup> Institute of Nanoscience and Materials of Aragón (CSIC), Zaragoza, Spain

laliene@unizar.es

It is shown, by solving the scattering problem, that spin waves reflected by or transmitted through one dimensional solitons, like domain walls or the chiral solitons of monoaxial helimagnets, suffer a lateral displacement whose origin is similar to the Goos-Hanchen effect that is induced by the reflection at interfaces [1]. The scattering is schematically represented in Figure 1. The displacement is due to the dependence of the phase shift on the wave vector and can be obtained by a stationary phase analysis of the incident and scattered waves. It is a fraction of the wavelength, but for the transmitted wave can be greatly enhanced by using an array of well separated solitons, in a range of frequencies where the reflection coefficient is small enough and the lateral shift large enough.

The scattering of spin waves by a Bloch domain wall in a simple anisotropic ferromagnet will also be discussed. It is known that this domain wall is transparent to spin waves, but this theoretical result is obtained by approximating its effect by an effective anisotropy. We show that the reflection coefficient does not vanish if the dipolar interaction is taken into account properly. We compute the contribution of the dipolar interaction to the scattering parameters (reflection and transmission coefficients and phase shifts) perturbatively, using a distorted wave Born approximation, after splitting the contribution of the dipolar interaction to the spin wave operator into a part that can be treated exactly and another part given by a localized operator suitable for a perturbative analysis [2]. It turns out that the reflection coefficient vanishes *only* at normal incidence, and that the scattered waves suffer a lateral displacement. The displacement of the transmitted wave at normal incidence does not vanish, and has the direction of the magnetization of the domain to which the spin wave is transmitted. Given that the reflection coefficient vanish at normal incidence, this displacement is particularly interesting since it can be greatly enhanced by sending the spin wave through an array of well separated domain walls.

The lateral shift of the scattered waves predicted here might be very useful in magnonics to control and manipulate the spin waves. Contrarily to the Goos-Hänchen effect recently studied in some magnetic systems, which takes place at interfaces between different magnetic systems [3], the effects predicted here takes place at the soliton position, what it is interesting from the point of view of applications, since solitons can be created at different places and moved across the material.

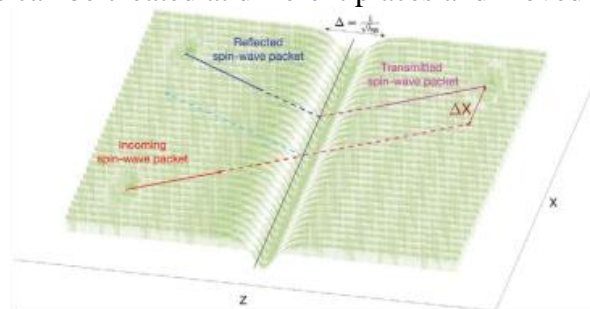


Figure 1. Schematic view of scattering.

[1] V. Laliene, J. Campo, *Adv. Electron. Mater.*, **8(3)** (2021) 2100782.

[2] V. Laliene, A. Athanasopoulos, J. Campo, *Phys. Rev. B*, **105** (2022) 214429.

[3] J. Stigloher *et al.*, *Phys. Rev. Lett.*, **121** (2018) 137201.

**July 3**

Monday

11:45 - 13:15

ORAL  
SESSIONS I

Section B

**Magnetophotonics**

3IT-B-1

## PULSED LASER NANOFABRICATION FOR ULTRAFAST MAGNETO-ACOUSTICS

Temnov V.V.

LSI UMR CNRS 7642, Ecole Polytechnique, IP Paris, France  
vasily.temnov@cnr.fr

Freestanding ferromagnetic membranes and multilayers are basic systems for theoretical and experimental investigations in ultrafast, fs-laser-driven magneto-acoustics [1-4]. In the limit of deeply sub-micrometer thickness, they act as high-Q cavities both for GHz-to-THz frequency eigenmodes of longitudinal acoustic phonons and perpendicular standing spin wave modes (exchange magnon modes). Investigations of resonantly enhanced phonon-magnon interactions in such structures help exploring the ultrahigh frequency limits of non-thermally driven magnetization dynamics.

In the first part of this talk I will discuss the recent progress in theoretical modelling of magnetoacoustic interactions in ferromagnetic thin films on ultrafast timescales. We start with the analysis of the Kim&Bigot experiment [1] discussing the magnetoacoustically driven ferromagnetic resonance (FMR) precession in free-standing 300 nm nickel thin films. The magnetic and acoustic eigenmode decomposition approach [2] highlights the role of symmetries governing resonant phonon-magnon interactions. We show that the symmetry-based selection rules for phonon-magnon interactions allow to discern between the FMR precession and higher-order magnons, even when their frequencies are experimentally indistinguishable [3]. We extend this analysis to the THz frequency scales in ultrathin membranes and discuss the peculiarities of fs-laser excitation of acoustic eigenmodes and the dominant role of acoustic and magnetic Q-factors [4]. In the second part I will introduce the new route to fabricate micrometer-sized ultrathin ferromagnetic membranes and their periodic arrangements (metasurfaces) for ultrafast magneto-acoustics, using single focused ultrashort laser pulses [5]. Some recent results of their microscopic and optical characterization will be presented as well.

Support by the ANR MRSEI “IRON-MAG” is acknowledged.

- [1] J.-W. Kim and J.-Y. Bigot, *Phys. Rev. B*, **95** (2017) 144422.
- [2] U. Vernik et al., *Phys. Rev. B*, **106** (2022) 144420.
- [3] A. Ghita et al., *Phys. Rev. B*, **107** (2023) 134419.
- [4] T. Mocioi et al., (2023, in preparation).
- [5] V.V. Temnov et al., *Nanolett.*, **20** (2020) 7912-2918.

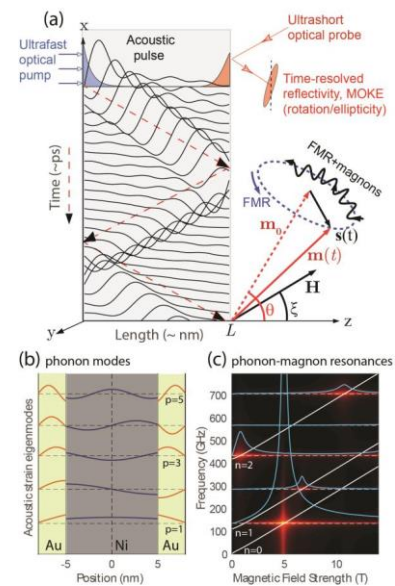


Figure 1. (a) Ultrafast magneto-optical pump-probe experiments allow for (b) excitation of individual modes of coherent acoustic phonons with index  $p=1,2,\dots$ , which resonantly drive (c) the high-frequency FMR ( $n=0$ ) and exchange magnons ( $n=1,2,\dots$ ) in freestanding ferromagnetic gold-nickel multilayers.

## OPTICAL SECOND-HARMONIC GENERATION FOR STUDYING ANTIFERROMAGNETS

*Pavlov V.V.*

Ioffe Institute, St. Petersburg, Russia  
pavlov@mail.ioffe.ru

Among the various optical phenomena associated with frequency conversion, second harmonic generation (SHG) is the simplest nonlinear optical process [1, 2]. This process is described by the second-order nonlinear susceptibility, therefore SHG is sensitive to specific details of the crystallographic or magnetic structures, and to the local symmetry of electric charges and spins. SHG method makes it possible to reveal new complementary information about the mechanisms of interaction between light and matter, which cannot be retrieved using linear optical techniques.

In the electric dipole (ED) approximation, SHG is allowed only in noncentrosymmetric materials. In the magnetic dipole (MD) and quadrupole approximations, SHG is also allowed in centrosymmetric media. This talk is devoted to nonlinear magneto-optical phenomena associated with SHG in several antiferromagnets with different symmetries. Hexagonal manganites with the general formula  $\text{RMnO}_3$  ( $R = \text{Sc, Y, Ho, Er, Tm, Yb, Lu}$ ) are magnetic dielectrics - multiferroics, since they can have both ferroelectric and antiferromagnetic order parameters simultaneously. In these materials, SHG is observed associated with a nonlinear optical polarization of the ED type, which is a bilinear function of two order parameters. In the classical magnetoelectric antiferromagnet  $\text{Cr}_2\text{O}_3$ , the spatial inversion is violated due to the spin order below the Néel temperature  $T_N$ , therefore ED SHG can be observed in the temperature range below  $T_N$  [3]. A new magnetic-field-induced mechanism of SHG is associated with the magnetoelectric effect. SHG is observed in antiferromagnetic centrosymmetric  $\text{EuTe}$ ,  $\text{EuSe}$ ,  $\text{NiO}$  and  $\text{KNiF}_3$  [3-5]. The SHG in these materials is due to the nonlinear optical susceptibility of the MD type. The interference of various SHG contributions is successfully used to visualize antiferromagnetic domains that are invisible in linear optics. SHG is also utilized for monitoring of hidden phase transitions.

Thus, nonlinear optical spectroscopy using the SHG method makes it possible to establish new physical mechanisms of nonlinear optical interaction and obtain unique information about the electronic and spin structures of various classes of antiferromagnets.

Supports by the Russian Foundation for Basic Research (project No. 19-52-12063) and the Deutsche Forschungsgemeinschaft (grant No. TRR160-C8) are acknowledged.

- [1] Y.R. Shen, *The principles of nonlinear optics* (Wiley, New York, 1984).
- [2] R.W. Boyd, *Nonlinear optics* (Academic, London, 1992).
- [3] M. Fiebig, V.V. Pavlov, R.V. Pisarev, *J. Opt. Soc. Am. B*, **22** (2005) 96-118.
- [4] D.R. Yakovlev et al., *Phys. Solid State*, **60** (2018) 1471-1486.
- [5] V.V. Pavlov, *Phys. Solid State*, **62** (2020) 1624-1632.

## LIGHT MODULATION IN HYPERBOLIC MAGNETO-PLASMONIC METASURFACES

*Kuzmin D.A.<sup>1</sup>, Usik M.O.<sup>1</sup>, Bychkov I.V.<sup>1</sup>, Bugaev A.S.<sup>2</sup>, Shavrov V.G.<sup>2</sup>, Temnov V.V.<sup>3</sup>*

<sup>1</sup>Chelyabinsk State University, Chelyabinsk, Russia

<sup>2</sup>Kotelnikov IRE RAS, Moscow, Russia

<sup>3</sup>LSI, Ecole Polytechnique, CEA/DRF/IRAMIS, CNRS, Institut Polytechnique de Paris, Palaiseau, France

kuzminda@csu.ru

Since the active magneto-plasmonics in hybrid metal-ferromagnet structures was proposed, a lot of plasmonically enhanced magneto-optical effects have been demonstrated. Incorporating magneto-active materials in plasmonic structures leads to various magnetoplasmonic effects. One of the effects is the change in the SPP wavenumber, which depends on the magnetization direction, i.e.  $k_{sp}(\pm M) = k_{sp}^0 + \Delta k_{sp}(\pm M)$ , being the strongest for the transversal magnetization configuration with respect to the SPP  $k$ -vector. It was previously shown in hybrid metal-ferromagnet multilayer structures that a small modulation  $|\Delta k_{sp}(M)|/k_0 \sim 10^{-4}$ , accumulated over the long propagation distance, may result in noticeable values of the magneto-plasmonic signal modulation depth  $2|\Delta k_{sp}(M)|d \sim 0.02$  for the SPPs propagation distance  $d = 22 \mu\text{m}$ .

We consider the simplest realization of a hyperbolic plasmonic metasurface (HPM) consisting of densely packed metallic (gold) stripes separated from each other by an air gap. Such a metasurface is deposited on a magnetic dielectric substrate (BIG).

The HPM allow to increase the magnetic SPP modulation. It can reach giant values outperforming uniform plasmonic thin films and hybrid metal-ferromagnet multilayers. The modulation of plasmonic optical properties using the magnetization control in ferromagnetic dielectric substrate suggests a straightforward application of this system as optical switches. Considering experiments with femtosecond light pulses, we believe that the switching speed of our device could eventually reach the terahertz regime in future and allow to realize all-optical magneto-plasmonic switches.

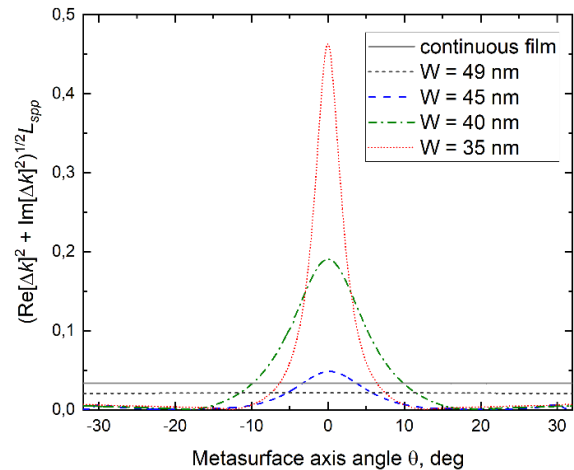


Figure 1. Evolution of the figure of merit  $(\text{Re}[\Delta k]^2 + \text{Im}[\Delta k]^2)^{1/2} \times L_{spp}$  under variation of the SPPs propagation direction with respect to gold stripes orientation shows that maximal modulation may be observed for the SPPs propagating along the stripes.  $\theta$  is an angle between gold stripes and SPPs  $k$ -vector.

Support by Russian Science Foundation (22-19-00355) is acknowledged.

**July 3**

Monday

11:45 - 13:15

ORAL  
SESSIONS I

Section C

**Magnetism and  
Superconductivity**

3IT-C-1

**COHERENT TUNNELING OF MAGNETIC FLUX QUANTA***Ustinov A.*

Institute of Physics, Karlsruhe Institute of Technology, Karlsruhe, Germany  
alexey.ustinov@kit.edu

The existence of magnetic flux quanta in superconductors has a quantum nature. Quantized vortices of supercurrent are accompanied by magnetic flux penetrating the material, and play a key role in determining the properties of superconducting materials and devices. The dynamics of such fluxons are essentially classical, while some earlier studies have hypothesised a collective quantum dynamics. However, the proposition that a magnetic fluxon as a macroscopic entity can exist in a coherent superposition of two or more spatially distinct states has received no experimental evidence till now. We experimentally study the quantum dynamics of magnetic fluxons in long Josephson junctions made of a high kinetic inductance material, in which the effective mass of the fluxon is reduced by orders of magnitude [1]. By probing the fluxon states with a weak microwave signal, we observe a direct evidence for a quantum coherent superposition of spatially distinct magnetic flux configurations. The spectrum of the system has a two-level character, with a coherence time of Rabi oscillations between the states on the order of few microseconds [2]. The observed phenomenon of the quantum superposition between spatially distinct magnetic flux states adds a novel perspective to the well established quantum coherence in lumped circuits made of superconducting qubits.

[1] M. Wildermuth et al., *Appl. Phys. Lett.*, **120** (2022) 112601.

[1] M. Wildermuth et al., *to be published* (2023).

## SUPERCONDUCTING NEURONS AND SYNAPSES FOR ARTIFICIAL NEURAL NETWORK

*Sidorenko A.*<sup>1,2</sup>

<sup>1</sup> Technical University of Moldova, D.Ghitu Institute of Electronic Engineering and Nanotechnologies, Chisinau, Moldova

<sup>2</sup> I.S.Turgenev Orel State University, Russia

Energy efficiency and the radically reduction of the power consumption level becomes a crucial parameter constraining the advance of supercomputers. The most promising solution is design and development of the Brain-like systems with non-von Neumann architectures, first of all – the Artificial Neural Networks (ANN) based on superconducting elements. Superconducting ANN needs elaboration of two main elements – nonlinear switch, analogue of neuron [1] and linear connecting element, synapse [2]. There are presented results of our design and investigation of artificial neurons, based on superconducting spin valves, and superconducting synapse, based on layered hybrid structures superconductor-ferromagnet. Are presented results of the experimental study of the proximity effect in a stack-like superconductor/ferromagnet (S/F) superlattices with Co-ferromagnetic layers of different thicknesses and coercive fields, and Nb-superconducting layers of constant thickness equal to coherence length of niobium.

The superlattices Nb/Co demonstrate change of the superconducting order parameter in thin niobium films due to switching from the parallel to the antiparallel alignment of neighboring ferromagnetic layers. We argue that such superlattices can be used as tunable kinetic inductors for ANN synapses engineering. As the result of design of the ANN using that two elaborated base elements, artificial neurons and artificial synapses, allows construction of the computer with several orders of magnitude lower energy consumption in comparison with the traditional computer designed from semiconducting base elements.

The study was supported by the Grant RSF No. 22-79-10018 “Controlled kinetic inductance based on superconducting hybrid structures with magnetic materials” (theory development, samples measurements, results evaluation), and by the Moldova State Program Project «Functional nanostructures and nanomaterials for industry and agriculture» no. 20.80009.5007.11 (samples fabrication).

[1] N. Klenov et al., *Beilstein J. Nanotechnol.*, **10** (2019) 833–839.

[2] S.Bakurskiy, *Beilstein J. Nanotechnol.*, **11** (2020) 1336–1345.

3IT-C-3

## SPIN PUMPING IN NbRe/Co SUPERCONDUCTOR-FERROMAGNET HETEROSTRUCTURES

*Cirillo C.<sup>1</sup>, Rovirola M.<sup>2,3</sup>, González C.<sup>2,3</sup>, Casals B.<sup>2,3</sup>, Hernández J.M.<sup>2,3</sup>, Macià F.<sup>2,3</sup>, García-Santiago A.<sup>2,3</sup>,  
Attanasio C.<sup>4</sup>*

<sup>1</sup> CNR-SPIN, c/o Università degli Studi di Salerno, I-84084 Fisciano (Sa), Italy

<sup>2</sup> Departament de Física de la Matèria Condensada, Universitat de Barcelona, Barcelona, Spain

<sup>3</sup> Institut de Nanociència i Nanotecnologia (IN2UB), Universitat de Barcelona, Barcelona, Spain

<sup>4</sup> Dipartimento di Fisica "E.R. Caianiello", Università degli Studi di Salerno, Fisciano (Sa), Italy  
cattanasio@unisa.it

Ferromagnetic resonance (FMR) spectroscopy measurements were performed on NbRe/Co/NbRe trilayers in order to probe spin pumping across the superconductor/ferromagnet interface and to detect the possible presence of spin-triplet pairing in the superconducting NbRe layer. FMR spectra were acquired as a function of frequency, magnetic field, and temperature, and reveal that the Gilbert damping parameter associated with spin pumping remains almost constant as temperature goes down through the superconducting transition. Additionally, the dependence of the Gilbert damping parameter on the thickness of the NbRe layer in trilayers is used to determine the values of the spin mixing conductance at the interface ( $18 - 21 \text{ nm}^{-2}$ ) and the spin diffusion length ( $7.1 - 12.5 \text{ nm}$ ) in the NbRe layer. These findings may suggest that spin pumping would still be effective even though NbRe becomes superconducting, which would indicate that the spin-triplet would be the dominant pairing mechanism. Future experiments are proposed in light of these results.

**July 3**

16:00 - 18:00

Sunday

ORAL  
SESSIONS II

Section A

**Spintronics and  
Magnetotransport**

**PLANAR HALL EFFECT IN TWO-LAYER SYSTEMS***Zhuravlev M.<sup>1</sup>, Vedyayev A.<sup>2</sup>, Alexandrov A.<sup>3</sup>*<sup>1</sup> St. Petersburg State University, St. Petersburg, Russia<sup>2</sup> Lomonosov Moscow State University, Moscow, Russia<sup>3</sup> Moscow Institute of Physics and Technology, Dolgoprudny, Russia  
m.zhuravlev@spbu.ru

Spin accumulation, anomalous Hall and spin-Hall effects are the phenomena which take place in magnetic tunnel junctions. Usually, the main current flows perpendicularly to the interfaces in such systems. We demonstrate that similar effects occur in two-layer system when the current flows parallel to the interface. The system consists of a semi-infinite ferroelectric barrier and a thin ferromagnetic layer. We assume that Dresselhaus and Rashba spin-orbit coupling is linear in electron wave number in ferroelectric barrier. Such spin-orbit coupling can be found in ferroelectric materials of C<sub>2v</sub> point group. E.g., HfO<sub>2</sub> is one of such compounds. We demonstrate that planar Hall effect takes place in such two-layer system. There are several kinds of Planar Hall effects. We discuss the origin of the planar Hall effect under consideration and demonstrate that this is a size effect [1]. In particular, we analyze a Hall effect for non-magnetic system.

Also, we describe spin accumulation (a kind of Edelstein effect) and spin-Hall effect in our two-layer system [2]. The charge and spin Hall currents in such system can be manipulated in several ways. In particular, it is shown that spin accumulation and spin current can be reversed by changing the direction of magnetization of the FM layer with respect to the crystallographic axes of the ferroelectric barrier. We estimate the current and magnetization for reasonable parameters.

Besides, we compare the calculation of Hall current based on Berry connection and the calculation based on common expression for the anomalous velocity [3].

[1] A Alexandrov, M. Zhuravlev, *J. Phys. Cond. Matter*, **33** (2021) 415301.

[2] M. Zhuravlev, A. Alexandrov and A. Vedyayev, *J. Phys.: Condens. Matter*, **34** (2022) 145301.

[3] P. Woelfle and K. A. Muttalib, *Ann. Phys.*, **15** (2006) 508.

## EXTRINSIC TUNNEL HALL EFFECT IN MgO-BASED TUNNEL JUNCTIONS

*Sapozhnikov M.V.<sup>1,2</sup>, Pashen'kin I.Yu.<sup>1</sup>, Gusev N.S.<sup>1,2</sup>, Karashtin E.A.<sup>1,2</sup>, Fraerman A.A.<sup>1</sup>*

<sup>1</sup> Institute for Physics of Microstructures RAS, Nizhny Novgorod, Russia

<sup>2</sup> Lobachevsky State University of Nizhny Novgorod, Nizhny Novgorod, Russia  
msap@ipmras.ru

Tunnel (anomalous) Hall effect consists in appearance of the transverse Hall voltage if an electric current flows through a magnetic tunnel junction (MTJ) due to the spin-orbit coupling in an insulating barrier. An external electric field induced by a voltage applied to the barrier can reach values of  $10^9$  V/m, which is close to internal atomic fields. Under these conditions, it becomes possible to observe the effect, when the resulting transverse current (transverse voltage) is caused by the spin-orbit coupling of spin-polarized tunneling electrons with an external electric field applied to the contact. A characteristic feature of this *extrinsic* tunnel Hall effect (eTHE) should be its quadratic dependence on the applied voltage, since in this case  $V_{\text{Hall}} \sim jE \sim E^2$ . Since in this case the effect is proportional to both the flowing ohmic current and the directly applied field, which is determined by the value of spin-orbit coupling. In our work we experimentally study the eTHE in a CoFeB/MgO/NM (NM = Pt, Ta) tunnel junctions shown in Figure 1a). The observed quadratic in  $V_{\text{bias}}$  Hall effect is much stronger than the linear one for a thin (1 nm) Pt (Figure 1b) and is almost independent of the nonmagnetic material (Pt or Ta). This effect decreases as the Pt layer is made thicker which manifests its surface nature. It almost vanishes for a 10 nm Pt layer. We also provide a consequent theory of the effect that takes into account both side-jump and skew scattering mechanisms of tunneling Hall effect. A simple model is used in which a delta-shape barrier possesses a Rashba spin-orbit coupling. We show that the quadratic in the applied voltage  $U_{\text{bias}}$  Hall effect appears in such system.

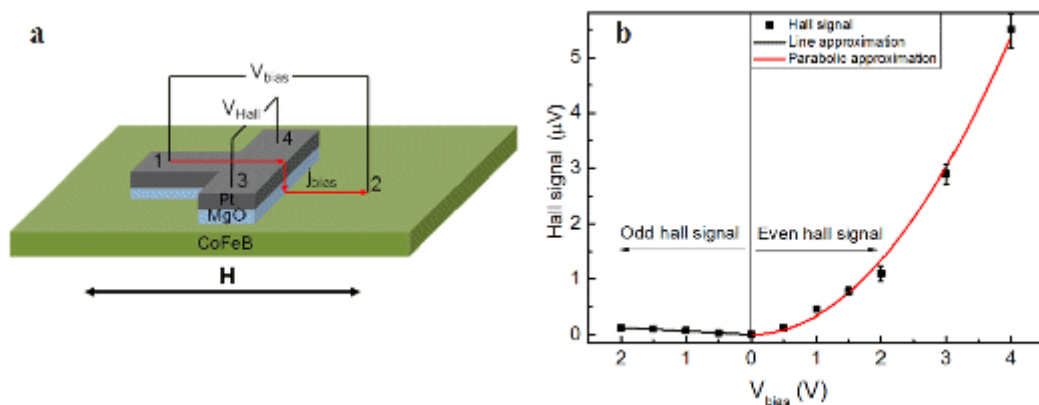


Figure 1. a) Sample and geometry of measurement. b) Even and odd tunneling Hall signal for Pt(1nm).

Support by Russian Science Foundation (Grant No. 21-12-00271) is acknowledged.

## TUNNELING MAGNETORESISTANCE IN $(\text{CoFeB})_x(\text{LiNbO}_3)_{100-x}/\text{Si}$ NANOCOMPOSITE STRUCTURES BELOW PERCOLATION THRESHOLD: MANIFESTATIONS OF CO-TUNNELING AND EXCHANGE EFFECTS

*Nikolaev S.N.<sup>1</sup>, Chernoglazov K.Y.<sup>1</sup>, Yemelyanov A.V.<sup>1</sup>, Sitnikov A.V.<sup>1,2</sup>, Taldenkov A.N.<sup>1</sup>, Patsaev T.D.<sup>1</sup>,  
Vasilev A.L.<sup>1</sup>, Ganshina E.A.<sup>3</sup>, Demin V.A.<sup>1</sup>, Averkiev N.S.<sup>4</sup>, Granovsky A.B.<sup>2,5</sup>, Rylkov V.V.<sup>1,5,6</sup>*

<sup>1</sup> National Research Centre “Kurchatov Institute”, Moscow, Russia

<sup>2</sup> Voronezh State Technical University, Voronezh, Russia

<sup>3</sup> Lomonosov Moscow State University, Moscow, Russia

<sup>4</sup> A.F. Ioffe Physico-Technical Institute RAS, St. Petersburg, Russia

<sup>5</sup> Institute of Applied and Theoretical Electrodynamics RAS, Moscow, Russia

<sup>6</sup> Kotel’nikov Institute of Radio Engineering and Electronics RAS, Fryazino, Moscow Region,  
Russia

vvrylkov@mail.ru; rylkov\_vv@nrcki.ru

The features of magnetoresistance (MR) of  $(\text{CoFeB})_x(\text{LiNbO}_y)_{100-x}$  film nanocomposites (NC) synthesized by ion beam sputtering on Si substrates in the temperature range of 3-250 K in fields up to 14 T at  $x \approx 40-48$  at.% near the percolation threshold on the insulating side are studied in detail. NC films were an ensemble of randomly arranged CoFeB granules about 2.5-4 nm in size in a LiNbO<sub>y</sub> matrix. Under these conditions, at  $x \approx 44-48$  at.%, the conductivity of samples in a wide temperature range is described by the law,  $\sigma \propto \ln T$ , which is changed by the Efros–Shklovskii law "1/2" at  $x < 44$  at.%.

It was found that the value of negative MR significantly depends nonmonotonically on temperature and has a minimum at 40 K. This behavior of MR is explained by the coexistence in NC of superferromagnetic regions with exchange-coupled granules separated by regions of superparamagnetic granules. Under these conditions, the increase in negative MR at  $T \geq 40$  K is due to the destruction of the superferromagnetic ordering [1]. Meanwhile, the sharp increase in MR at  $T \leq 40$  K is caused presumably by virtual processes of elastic co-tunneling of many electrons through chains of "resonant" granules. The latter initiates a sharp increase in spin-dependent MR [2], and under conditions of saturation of magnetization, an additional negative contribution is manifested, probably due to the effects of quantum interference [3].

At  $T \leq 4$  K, a transition to positive MR is observed, presumably associated with the influence of the Zeeman effect on the height of the tunnel barrier [4], which is non-monotonic in nature and is accompanied by the manifestation of two minima in MR.

This work was funded by the Russian Science Foundation, Grant No. 22-19-00171.

[1] I.S. Beloborodov, A. Glatz, and V.M. Vinokur, *Phys. Rev. Lett.* **99** (2007) 066602(4).

[2] S. Mitani et al., *Phys. Rev. Lett.* **81** (1998) 2799-2802.

[3] M.V. Feigel'man, and A.S. Ioselevich, *JETP Lett.* **81** (2005) 277-283.

[4] M.I. Blinov et al., *J. Magn. Magn. Mater.* **469** (2019) 155-160.

## THE ROLE OF SiO<sub>2</sub>/SI INTERFACE IN MAGNETIC FIELD DRIVEN LATERAL PHOTOVOLTAIC EFFECT IN MN/SiO<sub>2</sub>/n-SI AND FE/SiO<sub>2</sub>/p-SI MIS STRUCTURES

*Bondarev I.A.<sup>1</sup>, Rautskii M.V.<sup>1</sup>, Volkov N.V.<sup>1</sup>, Lukyanenko A.V.<sup>1,2</sup>, Yakovlev I.A.<sup>1</sup>, Varnakov S.N.<sup>1</sup>, Tarasov A.S.<sup>1,2</sup>*

<sup>1</sup>Kirensky Institute of Physics, FRC KSC SB RAS, Krasnoyarsk, Russia

<sup>2</sup>Siberian Federal University, Krasnoyarsk, Russia

bia@iph.krasn.ru

Lateral photovoltaic effect (LPE) in metal/insulator/semiconductor (MIS) structures has been actively studied in recent years due to its application prospects in position sensitive detectors and solar cells [1]. Silicon based Mn/SiO<sub>2</sub>/n-Si and Fe/SiO<sub>2</sub>/p-Si are promising for implementation of the LPE, because of compatibility with CMOS and SOI technology and the ability of magnetic control over the electronic transport.

Mn/SiO<sub>2</sub>/n-Si and Fe/SiO<sub>2</sub>/p-Si samples were fabricated on phosphorus and boron doped silicon substrates respectively, with doping densities of 10<sup>15</sup> cm<sup>-3</sup>. 1.5-nm-thick SiO<sub>2</sub> layers were obtained by exposing substrates to an aqueous solution of H<sub>2</sub>O<sub>2</sub> and NH<sub>4</sub>OH (a ratio of 1:1:1) for 30 min at 60°C. 10-nm-thick Fe and 15-nm-thick Mn films were deposited by molecular beam epitaxy.

Spectral dependences of the lateral photovoltage (LPV) in Mn/SiO<sub>2</sub>/n-Si (Figure 1) can be divided into two regions with positive and negative LPV ( $\lambda < 0.9$   $\mu\text{m}$  and  $\lambda > 0.9$   $\mu\text{m}$  respectively). Different LPE mechanisms can be explained by the different absorption depth for photons with high and with low  $\lambda$ . High  $\lambda$  photons are absorbed deep inside the silicon while low  $\lambda$  photons are absorbed closely to the SiO<sub>2</sub>/n-Si interface, therefore, the LPV below  $\lambda = 0.9$   $\mu\text{m}$  is affected by the energy levels of interface states.

The sign change on LPV( $\lambda$ ) curve may indicate the switching of dominant carriers' type contributing to LPV. Magnetic field effect on the LPE is more pronounced in low- $\lambda$  region (near the interface). It is expected due to the shifting of the interface states energy levels in external magnetic field.

The results obtained demonstrate the importance of insulator/semiconductor interfaces for the lateral photovoltaic effect.

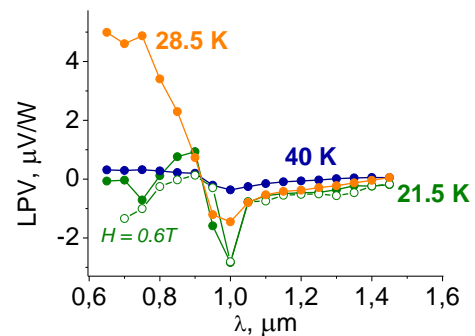


Figure 1. LPV dependences on radiation wavelength at T = 40 K (green); 28.5 K (orange); 21.5 K (green) with H = 0 (closed circles) and H = 0.6 T (open circles) in Mn/SiO<sub>2</sub>/n-Si.

[1] A. Dong, H. Wang., *Ann. Phys.*, **531** (2019) 1800440.

## ULTRAFAST LASER-INDUCED MAGNETIZATION SWITCHING IN CoFeB-BASED NANOSTRUCTURES

*Shelukhin L.A.*<sup>1</sup>, *Gareev R.R.*<sup>2</sup>, *Zbarsky V.*<sup>3</sup>, *Walowski J.*<sup>3</sup>, *Münzenberg M.*<sup>3</sup>, *Scherbakov A.V.*<sup>4</sup>,  
*Kazemwadel D.L.*<sup>5</sup>, *Kirilenko D.A.*<sup>1</sup>, *Hämäläinen S.J.*<sup>6</sup>, *van Dijken S.*<sup>6</sup>, *Pertsev N.A.*<sup>1</sup>, *Kalashnikova A.M.*<sup>1</sup>

<sup>1</sup>Ioffe Institute, St. Petersburg, Russia

<sup>2</sup>Institute of Experimental and Applied Physics, University of Regensburg, Germany

<sup>3</sup>University of Greifswald, Institute of Physics, Germany

<sup>4</sup>Experimental Physics II, Technical University Dortmund, Dortmund, Germany

<sup>5</sup>University of Konstanz, Konstanz, Germany

<sup>6</sup>NanoSpin, Department of Applied Physics, Aalto University School of Science, Aalto, Finland  
shelukhin@mail.ioffe.ru

Femtosecond laser pulses are a powerful tool to switch magnetization in several tens of picoseconds [1, 2]. However, usually it requires specific electronic structure or excitation conditions. In this work we suggest universal approach to magnetization switching using ultrafast laser-induced heating. For this we selected structures promising for spintronic devices based on commercially available alloy, such as synthetic multiferroic CoFeB(50 nm)/BaTiO<sub>3</sub> and magnetic tunnel junction CoFeB(1.2 nm)/MgO(1.2 nm)/CoFeB(1.4 nm) (MTJ).

The main idea is to use magnetic anisotropy dependence on the temperature to manipulate magnetization. In CoFeB/BaTiO<sub>3</sub> the inverse magnetostriction along the transfer of mechanical stress from ferroelectric to ferromagnetic layer results in the imprinting of domain structure from BaTiO<sub>3</sub> to CoFeB where magnetoelastic interactions are the only source of magnetic anisotropy [4]. Main feature of MTJ structure is perpendicular magnetic anisotropy stabilized by the interface anisotropy at the MgO/CoFeB interface which dominates over shape anisotropy if the thickness of the CoFeB layer is below 1.4 nm [5].

Laser-induced dynamics of magnetization was studied using the time-resolved magneto-optical Kerr effect technique [3]. 170 fs laser pulses with the central wavelength of 515 nm and 1030 nm were used as the pump and probe, respectively. Laser-induced changes of magnetization were monitored by measuring the polar Kerr effect of the probe pulses as a function of the pump-probe delay time.

Experimentally, we showed significant reduction of magnetoelastic anisotropy in CoFeB/BaTiO<sub>3</sub> and total quench of perpendicular magnetic anisotropy in MTJ due to ultrafast laser-induced heating. Such anisotropy modification resulted in magnetization precession. Analysis of its parameters allows us to reconstruct the magnetization and anisotropy behavior under impact of femtosecond laser pulses. In the first case, if external magnetic is applied perpendicularly to the easy axis, there are two scenarios of magnetization switching to another equilibrium direction depending on sample parameters relaxation rate to the values of non-excited state. In the CoFeB/MgO/CoFeB interface and shape anisotropy have different response to the ultrafast heating leading to the spin-reorientation transition at certain pump fluence.

Support by RFBR grant 19-52-12065 is acknowledged.

[1] A. Stupakiewicz et al, *Nat Commun*, **10** (2019) 612.

[2] C.D. Stanciu et al, *Phys. Rev. Lett.*, **99** (2007) 047601.

[3] A. Kirilyuk, A. V. Kimel, and Th. Rasing, *Rev. Mod. Phys.*, **82** (2010) 2731.

[4] T. H. E. Lahtinen et al., *Adv.Mater.* **23** (2013) 3187.

[5] R.R. Gareev et al., *Appl. Phys. Lett.*, **106** (2015) 132408.

## DC-BIASED RELOCATION OF THE BROADBAND RECTIFICATION RANGE IN MAGNETIC TUNNEL JUNCTIONS

*Trushin A.S.<sup>1</sup>, Kichin G.A.<sup>1</sup>, Skirdkov P.N.<sup>1,2</sup>, Zvezdin K.A.<sup>1,2</sup>*

<sup>1</sup> New Spintronics Technologies, Russian Quantum Center, Skolkovo, Russia

<sup>2</sup> Prokhorov General Physics Institute of the Russian Academy of Sciences, Moscow, Russia  
a.trushin@nst.tech

Magnetic tunnel junctions have been of great interest for various spintronic applications and fundamental research. Besides the well-known ferromagnetic resonance (FMR) regime, they possess a broadband regime. It was initially theoretically predicted [1] in the case of the out-of-plane bias field. And later observed experimentally [2] in the case of perpendicular magnetic anisotropy of the sample. It opened a new frontier in the development of spintronic energy harvesters and sensors. However, it still lacks thorough research.

Previously, we observed the existence of a new type of broadband mode that appears with an applied in-plane bias field. Here we continue this study with a special accent at ultra-low bias current.

We carried out the spin-torque FMR (ST-FMR) experiment with an external in-plane field and direct bias current. We consider in-plane magnetized Magnetic Tunnel Junctions (MTJs) which were connected to the pulse-modulated RF generator and DC current source via a bias-tee network. Rectified voltage was measured using a lock-in amplifier.

We found a completely new behavior of a broadband regime in the case of ultra-low current injection represented in Figure 1. The region of said regime relocates from a low-frequency range into a high-frequency range with respect to the sign of a bias current. We link this effect to phase shifts between magnetization precession and driving RF current, which is related to different proportions between the exerted torque components. Analytical insight is presented.

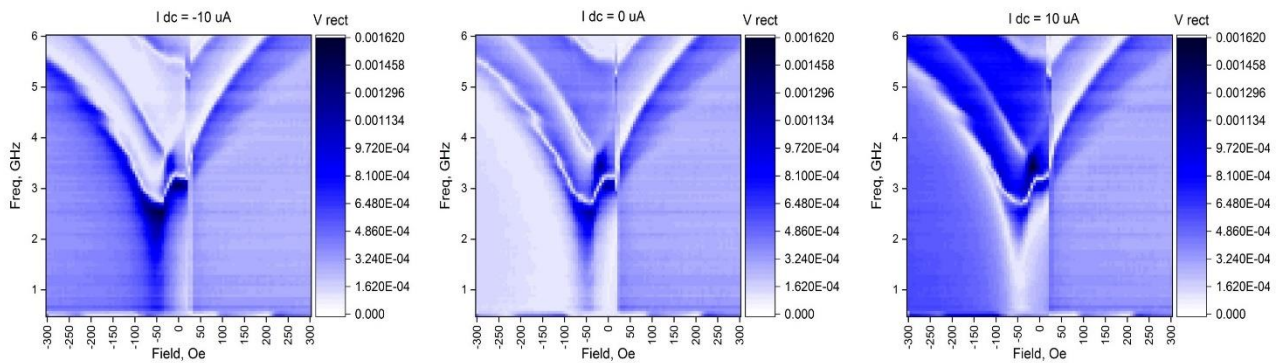


Figure 1. Rectification heat maps with different bias current

The work was supported by the RSF No. 19-12-00432.

[1] O.V. Prokopenko et al., *Journal of Applied Physics*, **111(12)** (2012) 123904.

[2] B.Fang et al., *Physical Review Applied*, **11(1)** (2019) 014022.

**July 3**

Monday

16:00 - 18:00

ORAL  
SESSIONS II

Section B  
**Magnetophotonics**

## NON-COLLINEAR PHASE OF A FERRIMAGNET: ULTRAFAST SPIN DYNAMICS AND QUANTUM PERSPECTIVES

Belotelov V.I.<sup>1,2,3</sup>

<sup>1</sup> Photonic and Quantum Technologies School, Lomonosov Moscow State University, Moscow, Russia

<sup>2</sup> Russian Quantum Center, Skolkovo, Moscow, Russia

<sup>3</sup> Vernadsky Crimean Federal University, Simferopol, Russia  
belotelov@physics.msu.ru

Ferrimagnets containing several partially compensated magnetic sublattices are considered the most promising materials for all-optical data storage and for ultrafast communications based on spin waves. There are two magnetic phases of the ferrimagnets: collinear and non-collinear ones. Up to now spin dynamics in ferrimagnets has been studied mostly in the collinear state without paying much attention to the kind of the magnetic phase. Here we investigate laser induced ultrafast spin dynamics in a rare-earth iron garnet film in the noncollinear phase as well.

We identify an importance of the magnetic phase of a ferrimagnet for its ultrafast spin behavior. A rare-earth iron garnet near magnetization compensation temperature was considered. We demonstrated several crucial peculiarities of spin dynamics in a non-collinear state that contrast sharply with the usually observed spin dynamics of the exchange and ferromagnetic modes in a collinear state far from the compensation point. In particular, when temperature approaches the

compensation point the frequencies of quasi-antiferromagnetic (q-AFM) and quasi-ferromagnetic (q-FM) modes (Figure 1) behave oppositely: the former decreases, while the latter one grows. The situation changes after crossing the compensation point for higher temperatures. We also discovered that the transition from the non-collinear phase

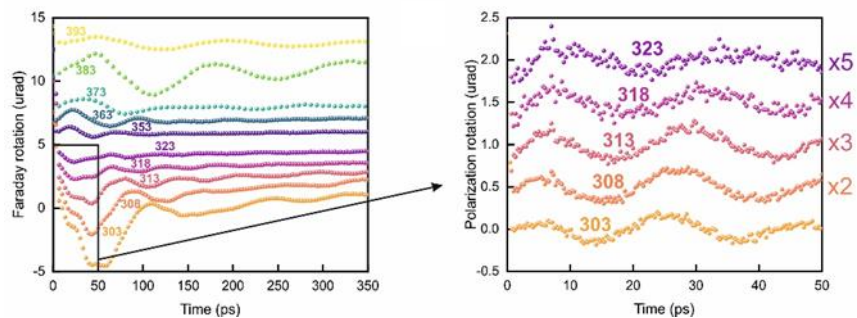


Figure 1. Ultrafast magnetization dynamics represented by the probe Faraday transients for different temperatures from 303 K (below compensation) to 393 K (above compensation).

to the collinear one is accompanied with softening of the q-FM mode which leads to a huge increase of the excitation efficiency and amplitude. The amplitude of the soft mode becomes more than 4 times larger than for the collinear state and up to 10 times higher than for the non-collinear phase. As the deflection angle of the soft mode was found to reach  $\sim 7^\circ$ , it can be interesting for all-optical switching and nonlinear magnonics.

The other crucial property of the non-collinear phase is bistability of the Neel vector. It is described by the double well potential energy. If the number of spins in a sample is small enough ( $\sim 100$ ) then probability of tunneling between two states becomes noticeable and the film will behave in a quantum regime. In this case macroscopic quantum tunneling takes place and one could consider a nanodisk of rare earth iron garnet with compensation point as a kind of magnetic qubit. The latter might be promising for future quantum technologies.

Support by the Russian Science Foundation, project N 23-62-10024 is acknowledged.

[1] D.M. Krichevsky et al., *arXiv:2212.00085v2*.

## BISMUTH-SUBSTITUTED YTTRIUM GARNETS MADE BY METAL-ORGANIC DECOMPOSITION AND CRYSTALLIZED BY LASER ANNEALING, AND GASOGYROCHROMISM IN OXIDIZED PERMALLOY FOR MAGNETO-OPTICAL APPLICATIONS

*Kulikova D.P.<sup>1,2</sup>, Tananaev P.N.<sup>1</sup>, Sgibnev E.M.<sup>1</sup>, Shelaev A.V.<sup>1</sup>, Yankovskii G.M.<sup>1</sup>, Baryshev A.V.<sup>1</sup>*

<sup>1</sup> Dukhov Automatics Research Institute (VNIIA), Moscow, Russia

<sup>2</sup> Lomonosov Moscow State University, Moscow, Russia

baryshev@vniia.ru

Implementation of garnet thin film fabrication technology into the production of miniaturized magneto-optical devices and photonic integrated circuits remains challenging because it requires deposition of garnets on non-garnet elements of the circuit. The first difficulty lies in the lattice mismatch between the garnet and circuit materials. Second, since high-temperature thermal annealing is required for garnet crystallization, a difference in thermal expansion coefficients of the materials can lead to exfoliation of the garnet film and various deteriorations of a circuit. Rapid thermal annealing (RTA) is also critical for magnetophotonic crystals based on Bi:YIG, resulting in worsening of their figure of merit. Since the use of optical isolators/circulators in miniature photonic devices is highly desirable, new technologies for integrating garnets with semiconductors are under development.

In the present talk, bismuth-substituted yttrium iron garnets (Bi:YIG) fabricated by a metal-organic decomposition (MOD) method with subsequent crystallization under *laser* irradiation (LRTA) will be discussed [1, 2]. Structural and optical properties of sub-millimeter- and micron-sized Bi:YIG stripes crystallized in air, oxygen, nitrogen and argon atmospheres are studied together with MOD-made Bi:YIG crystallized under conventional RTA. The demonstrated LRTA can find practical applications for Bi:YIG monolithic integration on non-garnet substrates.

Gasochromism—usually, change in optical properties of metal oxides reacting with a gas—has found application for gas sensing and smart windows. For these applications, a number of researches demonstrate responses of binary systems as, for example, tungsten trioxide/catalyst metal. In the system, the catalyst is responsible for dissociation of reducing (hydrogen) or oxidizing (oxygen) gas molecules and following transfer of atoms into the tungsten trioxide that results in a change of the dielectric constant due to chemical reactions. To the best of our knowledge, magnetic metal oxides (spinel and garnets) have never been considered and applied as a magneto-optical gasochromic sensing material, and no related responses have been studied.

Research on fabrication and applicability of oxidized permalloy nanofilms (NiFeO<sub>x</sub>) to hydrogen sensing [3, 4] will be presented. Structural, magnetic, optical and magneto-optical properties of NiFeO<sub>x</sub> significantly change versus the oxidation temperature. The angle of Faraday rotation ( $\theta_F$ ) rise by an order of magnitude in the near IR wavelength range. For gas-sensing experiments, the as-deposited permalloy and NiFeO<sub>x</sub> nanofilms with the largest  $\theta_F$  response were covered with a Pt catalyst layer. We demonstrate that only the NiFeO<sub>x</sub>/Pt bilayers irreversibly change their magnitude of  $\Delta\theta_F$  in a H<sub>2</sub>-rich atmosphere. Moreover, the bilayers of NiFeO<sub>x</sub>/Pt, which are subjected to hydrogenation, recover sensitivity after heating. The non-reciprocal nature of gasogyrochromic response is confirmed by accumulation of  $\Delta\theta_F$ .

[1] Y.M. Sgibnev et al., *Crystal Growth & Design*, **22** (2022) 1196–1201.

[2] A.V. Shelaev et al., *Optics and Laser Technology*, **155** (2022) 108411.

[3] D.P. Kulikova et al., *Optical Materials*, **107** (2020) 110067.

[4] D.P. Kulikova et al., *Applied Surface Science*, **613** (2023) 155937.

3IR-B-6

## DEVELOPMENT OF SPIN-CONTROLLED LASERS USING VARIOUS MAGNETIC FIELD PULSES

Goto T.

RIEC, Tohoku Univ., Sendai, Japan  
taichi.goto.a6@tohoku.ac.jp

We developed a spin-controlled laser using the magneto-optical (MO) Q-switching effect [1], exhibiting a peak power of one kilowatt and a pulse width of 25 ns [2]. This device comprises a diode-laser pumped solid state laser, magneto-optical garnet film showing magnetic garnet, a tiny electrical magnet, and a pulse generator. The Q-switching effect is generated by a rapid change in the state of the magnetic domain in the magnetic garnet film caused by a pulsed magnetic field generated by a tiny coil. In our previous demonstration of this device, the pulse width of the magnetic field pulse was more than 2  $\mu\text{s}$  because of the design of the coil and the pulse generator. Such a long pulse prohibits increasing the output power and decreasing the pulse width of the spin-controlled laser. To overcome this issue, we fabricated a coil and a pulse generator specialized for applying a short magnetic field pulse to the magneto-optical garnet film, demonstrating a shortening of the output pulse of spin-controlled lasers.

The fabricated diode-pulse solid-state laser comprised a  $3 \times 3 \times 4$  mm dielectric-mirror-coated Nd:GdVO<sub>4</sub> (Nd: 1 at.%) crystal and an output coupler. The input side of the laser crystal so that high transmission at the wavelength of 808 nm and high reflection at the wavelength of 1064 nm. The reflectivity of the output coupler at the wavelength of 1064 nm was 50%. The coil type was solenoid and had five turns. The wire diameter was 0.5 mm because of low resistivity. The electronic circuit was designed by LTspice considering floating inductive components and fabricated using nMOSFET (Infineon, IPD200N15N3G). The obtained shortest pulse width of the generated magnetic field pulse was 158 ns, and the peak field was 200 Oe. The pulse width of the optical output was shortened by 18 ns using this system. Therefore, the shortening of the output pulse of the spin-controlled laser was demonstrated using a fabricated magnetic field pulse generator.

This work was partly supported by Nos. 20H02593, 20K20535, 23H01439 from JSPS, NEDO No. 23200047-0, TI-FRIS fellowship, and Inamori Foundation.

[1] T. Goto et al., *Opt. Express*, **24** 17635 (2016).

[2] R. Morimoto et al., *Sci. Rep.*, **6** 38679 (2016).

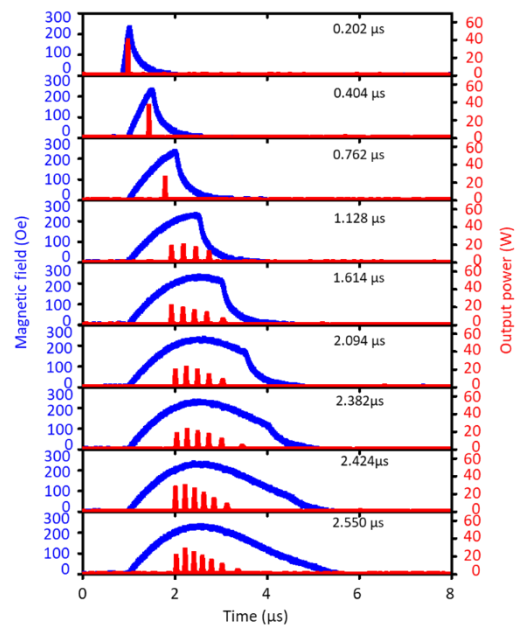


Figure 1. Optical output of the spin-controlled laser with various widths of magnetic field pulses.

## TRANSVERSAL KERR EFFECT ENHANCEMENT IN 2D MAGNETOPLASMONIC CRYSTALS FOR SENSING APPLICATIONS

*Murzjin D.V.<sup>1</sup>, Belyaev V.K.<sup>1</sup>, Gritsenko Ch.A.<sup>1</sup>, Komanicky V.<sup>2</sup>, Rodionova V.V.<sup>1</sup>*

<sup>1</sup> Immanuel Kant Baltic Federal University, Kaliningrad, Russia

<sup>2</sup> Pavol Jozef Šafárik University, Kosice, Slovakia

murzindmitri@gmail.com

Magnetoplasmonic crystals (MPICs) are surfaces based on periodically nanostructured thin films of combined plasmonic and ferromagnetic materials [1]. Such structures possess enhanced magneto-optical effects in comparison to the flat thin films of the same composition due to the excitation of surface plasmonic resonances. This feature allows using MPICs for magnetic field sensing applications [2]. Recently, a new method for magnetic field detection with the use of 1D MPICs was developed, based on the detection of magnetic field-dependent transversal Kerr effect (TKE) [3]. The use of 2D MPICs for magnetic field detection with the proposed method can be used for the simultaneous detection of two orthogonal magnetic field components. Substrates for further MPICs fabrication considered in this work were made by the e-beam lithography with the direct writing doses of 200 - 600  $\mu\text{C}/\text{cm}^2$  with the step of 50  $\mu\text{C}/\text{cm}^2$  to form 9 areas each containing 2D arrays of polymer columns on top of a carbon plate. 2D MPICs were made by covering the substrate with the Ag (50 nm)/Ni<sub>80</sub>Fe<sub>20</sub> (150 nm)/Si<sub>3</sub>N<sub>4</sub> (15 nm) multilayer using a magnetron sputtering method. Fabricated columns were approximately 80 nm in height and had a periodicity of 590 nm. Morphology of the fabricated MPICs was verified with SEM and AFM techniques. Hysteresis loops of fabricated MPICs were measured with the Kerr microscopy method. Reflectivity and TKE spectra in the visible and near-infrared wavelength region were measured with the use of a lock-in detection method. TKE spectra were obtained in the saturation AC modulation magnetic field of 160 Oe. The lock-in detection method was also used to measure the dependence of a magneto-optical response at a resonant wavelength on the magnitude of the applied modulation field. Example of the obtained dependence measured in the modulation field applied along two orthogonal directions is shown in Figure 1. The report demonstrates the results of magnetic, optical, and magneto-optical characterization of the series of 2D MPICs made with different e-beam direct writing doses.

This work was supported by the Russian Science Foundation grant № 22-22-00997. The support of the Slovak Research and Development Agency grant under the contract APVV-20-0324 is acknowledged. Authors appreciate the support of the M.V. Lomonosov Moscow State University Program of Development for the provided Kerr microscopy equipment.

- [1] M.A. Kiryanov, *APL Photonics*, **7** (2022) 026104.  
 [2] G.A. Knyazev, *ACS Photonics*, **5** (2018) 4951–4959.  
 [3] V.K. Belyaev, *Sci Rep*, **10** (2020) 7133.

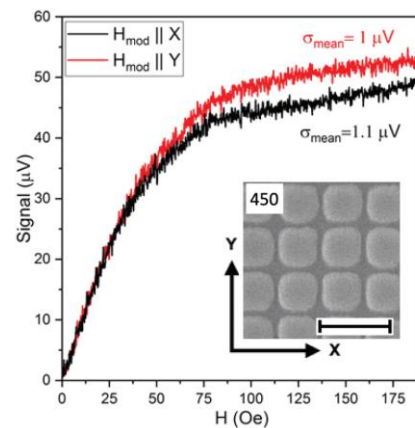


Figure 1. Field dependence of the magneto-optical response measured in the modulation field  $H_{mod}$  applied along  $X$  and  $Y$  axes of the MPIC fabricated with the e-beam dose of 450  $\mu\text{C}/\text{cm}^2$ .  $\sigma$  is the standard deviation of the signal. Inset shows the MPIC SEM image. The scale bar is 1  $\mu\text{m}$ .

## MAGNETIC FIELD TOPOGRAPHY WITH THE USE OF 1D AND 2D MAGNETOPLASMONIC CRYSTALS

Murzin D.V.<sup>1</sup>, Belyaev V.K.<sup>1</sup>, Grunin A.A.<sup>2</sup>, Fedyanin A.A.<sup>2</sup>, Rodionova V.V.<sup>1</sup>

<sup>1</sup> Immanuel Kant Baltic Federal University, Kaliningrad, Russia

<sup>2</sup> Lomonosov Moscow State University, Moscow, Russia

vbelyaev@kantiana.ru

Technological advancements have paved the way for modern fundamental and experimental approaches in the development of magnetic field sensors [1]. The current focus in this field is on achieving a balance between sensitivity and resolution while reducing power consumption and production costs, as well as miniaturizing sensor dimensions. A promising new approach to energy efficient and fast magnetic field sensing involves the use of magnetoplasmonic crystals (MPICs), which are plasmonic crystals composed of noble and ferromagnetic materials [2,3]. The utilization of MPICs can increase magneto-optical response by up to two orders of magnitude, thereby expanding the potential applications of magneto-optical effects [4].

A novel approach to magnetometry involves the utilization of magnetic and magneto-optical properties of one-dimensional (1D) and two-dimensional (2D) MPICs. By exciting surface plasmon-polaritons on the MPICs metal/dielectric interface, the transverse magneto-optical Kerr effect may be enhanced and used for a highly sensitive magnetic field sensing capable of detecting fields as low as  $10^{-7}$  Oe. Furthermore, the optical probe's displacement on a MPIC's surface can be utilized for accurate magnetic field topography.

This work is devoted to the implementation of 1D and 2D MPICs for magnetic field topography of several experimental objects like a wire, a planar coil, and a complex system of permanent magnets. Example of fabricated 2D MPIC, scheme of the experiment and magnetic field map obtained for a planar coil are shown in Figure 1.

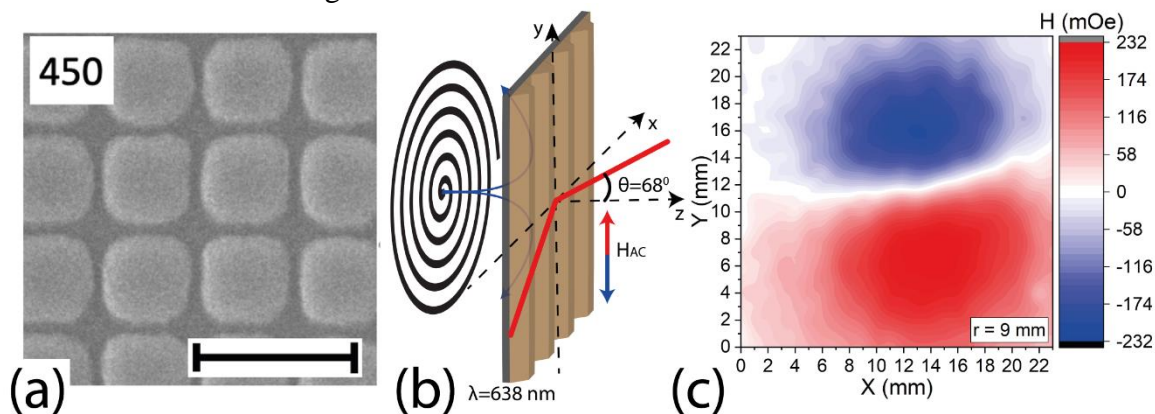


Figure 1. Panel (a) – SEM image of 2D MPIC, fabricated with e-beam dose of 450 in  $\mu\text{C}/\text{cm}^2$ , (b) – Scheme of the experiment, and (c) – example of magnetic field topography, measured for a planar coil at the distance of 9 nm from MPIC surface.

This work was supported by the Russian Science Foundation grant № 22-22-00997.

- [1] M.A. Khan et al., *ERX*, **3(2)** (2021) 022005.
- [2] G.A. Knyazev, *ACS Photonics*, **5** (2018) 4951-4959.
- [3] S. Chandra, *ACS Photonics*, **8** (2021) 1316-1323.
- [4] A.A. Grunin, *J. Magn. Magn. Mater.* **415** (2016) 72-76.
- [5] V.K. Belyaev, *Sci. Rep.*, **10** (2020) 1-6.

## TRIGGERING MAGNETIZATION PRECESSION IN EuO VIA FEMTOSECOND OPTICAL ORIENTATION

Kats V.N.<sup>1</sup>, Shelukhin L.A.<sup>1</sup>, Usachev P.A.<sup>1</sup>, Averyanov D.V.<sup>2</sup>, Karateev I.A.<sup>2</sup>, Parfenov O.E.<sup>2</sup>, Taldenkov A.N.<sup>2</sup>, Tokmachev A.M.<sup>2</sup>, Storchak V.G.<sup>2</sup>, Pavlov V.V.<sup>1</sup>

<sup>1</sup> Ioffe Institute, St. Petersburg, Russia

<sup>2</sup> NRC Kurchatov Institute, Moscow, Russia  
usachev@mail.ioffe.ru

The EuO ferromagnet presents a significant interest due to structural simplicity, exceptional properties, and ability to influence the electronic and magnetic structures of adjacent materials. Here, we provide insight into its magneto-optical properties by carrying out pump-probe measurements of pristine and Gd-doped EuO [1]. An ultrashort laser pulse acts on the ensemble of strongly correlated f-electrons as a magnetic field directed along the wave vector of the photons. The magnetization precession, observed for circularly polarized light excitation, reveals a laser-induced coherent response in the external magnetic field applied parallel to the sample surface. The phase of the magnetization precession depends on the helicity of the pump beam.

We set the experimental data against two potential mechanisms, the inverse Faraday effect and the optical orientation effect. Numerical estimates and comparison between EuO and Eu(Gd)O both point at the optical spin orientation via the electronic transition  $4f^75d^0 \rightarrow 4f^65d^1$  as the mechanism triggering the magnetization precession.

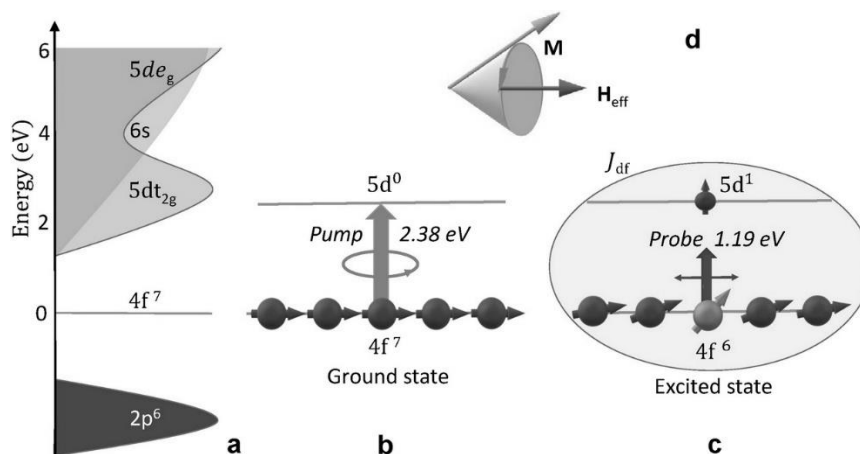


Figure 1. (a) Band structure of EuO; (b) optical excitation of the electronic transition  $4f^75d^0 \rightarrow 4f^65d^1$ ; (c) optical spin orientation; strong exchange interaction between the excited  $5d^1$ -electron and  $4f$ -electrons of  $\text{Eu}^{2+}$  ion pulls the moment of the latter out-of-plane; (d) magnetization precession around the effective magnetic field.

Support by RFBR (19-52-12063, pump-probe studies), NRC “Kurchatov Institute” (infrastructure) and the Russian Science Foundation [22-13-00004 (synthesis), 20-79-10028 (structural characterization), and 19-19-00009 (studies of magnetic and transport properties)] is acknowledged.

[1] V.N. Kats et al., *Nanoscale*, **15** (2023) 2828-2836.

**July 3**

Monday

16:00 - 18:00

ORAL  
SESSIONS II

Section C

**Magnetism and  
Superconductivity**

## INVERSE PROXIMITY EFFECT IN STATICS AND DYNAMICS OF BYLAYERS SUPERCONDUCTOR-FERROMAGNET

*Pugach N.G.<sup>1</sup>, Turkin Ya.V.<sup>1,2</sup>, Seleznev D.V.<sup>1</sup>, Yagovtsev V.O.<sup>1</sup>*

<sup>1</sup> HSE University, Moscow, Russia

<sup>2</sup> V.I. Vernadsky Crimean Federal University, Simferopol  
npugach@hse.ru

In this work we theoretically studied the influence of magnetization orientation and dynamical precession in a ferromagnetic insulating material (FI) on the superconducting condensate properties of the adjacent superconducting layer (S), i.e. the inverse proximity effect (IPE). The static IPE exhibits in the induced magnetization in the superconductor and in its electron density of states, the dynamical IPE also produces a spin current via spin pumping through the FI/S interface.

The goal of the present work is description of the dynamics of the spin of superconducting condensate inside a superconducting film, which is in contact with a ferromagnetic insulating layer under the conditions of the ferromagnetic resonance (FMR). It is calculated spin current and induced magnetization not only at the interface of the S/FI hybrid structure, but also inside the superconducting film. The space distributions and frequency dependencies of these values are presented. The induced magnetization weakly depends on the FMR precession frequency in a contrast with the spin current. It is also shown that increasing of magnetization precession frequency can drastically change the spin polarization distribution of quasiparticles [1].

The static magnetization and spin resolved density of states in a superconductor induced due to the IPE is also studied in bilayers containing a superconductor and a ferromagnetic insulator or a strongly spin-polarized ferromagnetic metal. The study is performed within a quasiclassical Green function framework, wherein Usadel equations are solved with boundary conditions appropriate for strongly spin-polarized ferromagnetic materials. A comparison with recent experimental data is presented. The singlet to triplet conversion of the superconducting correlations because of the proximity effect with a ferromagnet is analyzed. The interesting and unexpected results are the non-monotonous behavior of these values inside the superconducting film and an optimal IPE at a small spin-mixing parameter [2,3].

These results may deepen our knowledge of effects appearing in superconducting spintronics devices and open new perspectives of spin currents and spin density transfer in such devices.

The calculations of IPE at magnetic dynamics were financially supported by the Basic Research Program of the HSE University, calculations of the static IPE were supported via the Mirror Lab collaboration project of the HSE University.

[1] Ya. V. Turkin, N. G. Pugach, *Belstein Journ. Nanotech*, **14** (2023) 233.

[2] V. Yagovtsev, N. Gusev, N. Pugach, M. Eschrig, *Sup. Sci. Tech.*, **34** (2021) 025003.

[3] D. Seleznev et al., *Phys. Met. Met.*, **124** (2023) 196.

3IT-C-5

**RE-ENTRANT FILAMENTARY SUPERCONDUCTIVITY RESULTING  
FROM THE COMPETITION WITH CHARGE ORDER***Venditti G.<sup>1</sup>, Maccari I.<sup>3</sup>, Grilli M.<sup>3</sup>, Lorenzana J.<sup>3</sup>, Caprara S.<sup>3</sup>*<sup>1</sup> SPIN-CNR Institute for Superconducting and other Innovative Materials and Devices, Rome, Italy<sup>2</sup> Department of Physics, Stockholm University, Stockholm, Sweden<sup>3</sup> ISC-CNR and Department of Physics, Sapienza University of Rome, Rome, Italy  
sergio.caprara@roma1.infn.it

High-critical-temperature superconducting cuprates seem to be characterized by a competition between charge order and superconductivity in the underdoped region of their temperature vs. doping phase diagram, the balance being controlled by a non-thermal parameter, like a magnetic field or isovalent doping. To analyze this competition, and shed light on the physical mechanisms underlying it, we derive an effective classical spin model on a square lattice, with nearest neighbor exchange interaction, and study its properties by means of Monte Carlo. The parameters of our model are an exchange anisotropy, apt to tilt the balance between easy-axis (charge) and easy-plane (superconducting) order, a potential barrier that removes the unphysical degeneracy of the  $O(3)$  symmetric point, and a random magnetic field that mimics the coupling of disorder to the charge degrees of freedom. In the absence of disorder, a first-order transition line separates superconductivity and charge order in the temperature vs. exchange anisotropy plane. The slope of this line is positive at low temperature, and the Clausius-Clapeyron equation implies that the superconducting phase has a higher entropy, and manifests as a re-entrant phase. In the presence of disorder, the charge-ordered phase is fragmented into polycrystalline domains, while the stability of the superconducting phase at low temperature is extended in the form of topologically protected parasitic filaments occurring at the boundaries between different charge-ordered domains.

[1] G. Venditti et al., in preparation (2023).

## EXPANDING THE OPERATIONAL TEMPERATURE WINDOW OF A SUPERCONDUCTING SPIN VALVE

*Kamashev A.A.<sup>1</sup>, Garif'yanov N.N.<sup>1</sup>, Validov A.A.<sup>1</sup>, Kataev V.<sup>2</sup>, Fominov Ya.V.<sup>3,4</sup>, Garifullin I.A.<sup>1</sup>*

<sup>1</sup> Zavoisky Physical-Technical Institute, FRC Kazan Scientific Center of RAS, Kazan, Russia

<sup>2</sup> Leibniz Institute for Solid State and Materials Research, Germany

<sup>3</sup> L.D. Landau Institute for Theoretical Physics RAS, Chernogolovka, Russia

<sup>4</sup> Laboratory for Condensed Matter Physics, HSE University, Moscow, Russia  
kamandi@mail.ru

To increase the efficiency of the superconducting spin valve (SSV), special attention should be paid to the choice of ferromagnetic materials for the F1/F2/S SSV multilayer. Here, we report the preparation and the superconducting properties of the SSV heterostructures where Pb is used as the superconducting S layer. In the magnetic part of the structure we use the same starting material, the Heusler alloy  $\text{Co}_2\text{Cr}_{1-x}\text{Fe}_x\text{Al}_y$ , for both F1 and F2 layers. We utilize the tunability of the magnetic properties of this alloy, which depending on the deposition conditions forms either an almost fully spin-polarized half-metallic F1 layer or a weakly ferromagnetic F2 layer. We demonstrate that the combination of the distinct properties of these two layers boosts the generation of the long-range triplet component of the superconducting condensate in the fabricated SSV structures and yields superior values of the triplet spin-valve effect of more than 1K and of the operational temperature window of the SSV up to 0.6 K (see Figure 1).

The achieved values of  $\Delta T_c^{\text{trip}}$  and  $\Delta T_c^{\text{full}}$  set new benchmarks for the design of the superconducting spin valves as the prototype elements for applications in superconducting spintronics. They demonstrate the by far not yet exhausted potential for the optimization of ferromagnetic materials in an F1/F2/S SSV structure together with the simultaneous simplification of its fabrication. The observed boosting of the SSV effect by increasing the strength of the rotating external magnetic field on the background of the overall suppression of  $T_c$  calls for further experimental and theoretical studies for a better understanding of the underlying physics of this phenomenon.

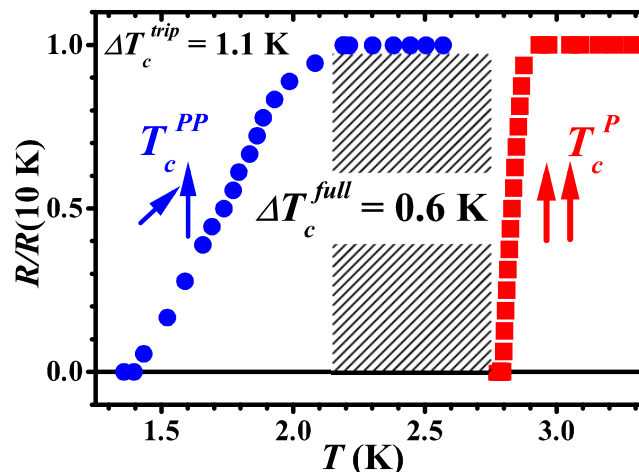


Figure 1. Superconducting transition curves for the P ( $\alpha = 0^\circ$ ) and PP ( $\alpha = 90^\circ$ ) configuration of the cooling field used to fix the direction of the magnetization of the  $\text{HA}^{\text{RT}}$  layer and the applied magnetic field  $H_0 = 4$  kOe that rotates the magnetization of the  $\text{HA}^{\text{hot}}$  layer for the sample  $\text{HA}^{\text{hot}}(20\text{nm})/\text{Al}(4\text{nm})/\text{HA}^{\text{RT}}(5\text{nm})/\text{Al}(1.2\text{nm})/\text{Pb}(60\text{nm})$ . The shaded area marks the operational temperature window of the SSV.

## SUPERCURRENT DIODE EFFECT IN S/F HYBRID STRUCTURES ON TOP OF THE TOPOLOGICAL INSULATOR

*Karabassov T.<sup>1</sup>, Bobkova I.V.<sup>1</sup>, Golubov A.A.<sup>2</sup>, Vasenko A.S.<sup>1,3</sup>*

<sup>1</sup>HSE University, Moscow, Russia

<sup>2</sup>University of Twente, AE Enschede, The Netherlands

<sup>3</sup>P.N. Lebedev Physical Institute RAS, Moscow, Russia  
iminovichtair@gmail.com

Currently the superconducting diode effect (SDE) becomes an active area of research due to its large application potential. Typically, helical superconducting state is responsible for the SDE. Helical state is widely discussed in materials with two-dimensional (2D) superconductivity, spin-orbit coupling and induced in-plane magnetic field [1]. Here we report the presence of the SDE (helical) phase in the diffusive hybrid structures 2D superconductor/ ferromagnet (S/F) on top of the topological insulator surface (TI). In such case nonuniform superconducting state is realized by means of a proximity effect [2]. This proximity induced helical state causes noticeable current nonreciprocity in the system. We provide the calculations for the SDE going beyond linear approximation. Employing the nonlinear quasiclassical approach we investigate the SDE quality factor for a wide range of temperatures and in-plane fields [3]. Moreover, we calculate the upper critical field and demonstrate its dependence on the current direction. Summarizing the results of the calculations we present the phase diagram of the SDE [4]. We also provide comparison between linear and nonlinear approaches.

The work was supported by the Mirror Laboratories Project and the Basic Research Program of the HSE University

- [1] F. Ando et al., *Nature*, **584** (2020) 373.
- [2] T. Karabassov et al., *Physical Review B*, **106** (2022) 224509.
- [3] T. Karabassov et al., *Condensed Matter*. **8(2)** (2023) 36.
- [4] T. Karabassov et al., submitted to SUST.

## FUNDAMENTAL PROBLEMS OF HIGH-SPEED VACUUM MAGNETIC LEVITATION TRANSPORTATION USING HIGH TEMPERATURE SUPERCONDUCTING MATERIALS

*Koledov V., Shavrov V., Terentyev Yu., Kamantsev A., von Gratowski S., Karpukhin D., Babachanakh A.,  
Lryukhin V., Balabanov V.*

Kotelnikov IRE RAS, Moscow, Russia  
victor\_koledov@mail.ru

The creation of vacuum magnetic levitation transport (VMLT), which is expected to provide ultra-high speeds with a sharp decrease in energy consumption and transportation costs, is especially important for our country because of its size and geographical location. The principle of transportation based on magnetic levitation, which was proposed in Russia and began to be studied more than 100 years ago, today, in the world, is practically embodied in passenger ground transportation lines, which are inferior in speed only to air transport. However, high energy costs in the atmosphere have not yet allowed the creation of competitive supersonic commercial airlines. The appearance in recent years of new rare-earth permanent magnets, high-temperature superconductors (HTSC), as well as materials for creating strong magnetic fields, highly efficient cooling, and energy conversion have made the idea of WMLT even more attractive.

This report aims to give an overview of the fundamental problems in the field of magnetism, materials science, various fields of technology that have to be solved before the idea of VMLT is put into practice. Let us note three main problems: the interaction of HTSC and the paths of permanent magnets, including the forces of electromagnetic resistance during levitation at high speed, the creation of self-powered refrigeration systems for highly efficient cooling of superconducting elements without the consumption of liquid gases, for example, based on solid-state magnetic cooling, and the problem of highly efficient overclocking, braking and energy recovery of a vehicle moving at supersonic speed in a vacuum.

This work was supported by the Russian Science Foundation, grant No. 20-19-00745-P.

## LOCALIZED STATES OF CHARGE CARRIERS AND THE POSSIBILITIES OF THE ANDERSON METAL-INSULATOR TRANSITION IN LA-BASED SUPERCONDUCTORS

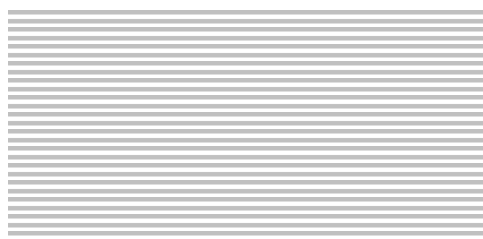
*Dzhumanov S., Kurbanov U.T., Khudayberdiyev Z.S.*

Institute of Nuclear Physics AS RUz, Tashkent, Uzbekistan

zafar-uzb@mail.ru

Theoretical investigation of the mechanisms of carrier (electrons and holes) localization and the metal-insulator transitions (MIT) in doped oxide high-temperature superconductors (HTSC) remains one of the fundamental problems of condensed matter physics [1,2]. Elucidation of the mechanisms of carrier localization and MIT in oxide HTSCs will make it possible to understand the new superconducting (SC) properties of these oxide compounds. In doped oxide HTSCs, such as  $La_{2-x}(Sr,Ba)_xCuO_4$ , the charge carriers are holes in the oxygen valence band and their localization can be associated both with a strong Coulomb correlation between holes, responsible for the Mott transition, and with a strong disorder in the spatial distribution of dopants and impurities responsible for the Anderson transition [3-5]. The present work is devoted to the investigation of the two interrelated phenomena: self-trapping of hole carriers near dopants (or impurities) in doped oxide HTSCs upon strong interaction of holes with dopants (impurities), acoustic and optical lattice vibrations; the possibilities of the Anderson type (i.e., induced by disorder in the distribution of dopants (impurities)) MIT. Theoretical calculations of the energy of localized states of holes (i.e., the depths of their potential wells) in these HTSC compounds were carried out within the framework of the continuum model and the adiabatic approximation using the variational method. We have shown that the localized hole states are formed inside the band gap (i.e., charge transfer energy gap) of oxide HTSCs. As the concentration of dopants (or holes) increases, these localized states form narrow energy bands with band width  $W$  in the band gap, which are close in energy to the oxygen valence band. The formation of such localized zones is considered in the strong coupling model. With a further increase in the density of hole carriers localized near dopants (or impurities) or the width of localized bands, the system approaches an Anderson-type MIT from the dielectric side. We have developed new approaches to the problems of Anderson-type MIT in doped oxide HTSCs and studied the effects of disorder in the distribution of dopants (impurities) and the statistical distribution of the depth of potential wells of localized carriers over a region of width  $V_0$  on the character of Anderson metal-insulator transition. The criteria of the Anderson-type metal-insulator transition, determined by the ratio  $V_0/W$  at different degrees of disorder in the spatial distribution of dopants (or impurities) and the fulfilment of this condition of the Anderson-type MIT in doped oxide HTSCs have been analysed [6]. Using the uncertainty relation, we have obtained specific conditions for the Anderson metal-insulator transition in cuprates. The limits of applicability of these MITs in cuprates are clarified. Our results are in good agreement with existing experiments on lanthanum containing and other doped cuprate compounds.

- [1] P.A. Lee, T.V. Ramakrishnan, *Rev. Mod. Phys.*, **57** (1985) 287.
- [2] D. Belitz, T.R. Kirkpatrick, *Rev. Mod. Phys.*, **66** (1994) 261.
- [3] N.F. Mott, *Metal-Insulator transitions* (London: Taylor and Francis, 1990).
- [4] P. Quemerais, *Mod. Phys. Lett. B*, **9** (1995) 1665.
- [5] M. Imada, A. Fujimori and Y. Tokura, *Rev. Mod. Phys.*, **70** (1998) 1039.
- [6] S. Dzhumanov et al., *Journal of Physics and Chemistry of Solids*, **73** (2012) 484–494.



# July 3

Monday

18:00 - 20:00

POSTER  
SESSIONS

Section L5

**Magnetophotonics**



## THE SPIN WAVES GENERATION IN THE ENGINEERED MAGNETO-PHOTONIC CRYSTAL

*Borovkova O.<sup>1,2</sup>, Kalish A.<sup>1,2</sup>, Belotelov V.<sup>1,2</sup>*

<sup>1</sup> Russian Quantum Center, Moscow, Russia

<sup>2</sup> Lomonosov Moscow State University, Moscow, Russia

o.borovkova@rqc.ru

Magneto-photonic crystal (MPC), photonic crystal containing the magnetic layer, is well-known for its unique transmittance and magneto-optic properties [1, 2]. Due to the defects in the layer alternation its transmittance spectrum as well as the Faraday effect spectrum have a resonant peculiarity in the bandgap related to the excitation of the resonant mode. Light becomes localized inside the defect layer between surrounding Bragg mirrors. The spectral position of such defect mode resonance is defined by the thickness of the additional magnetic layer because the interference conditions can be satisfied at the certain value of the optical path in the defect layer [3]. As soon as the light is localized in the magnetic defect layer the inverse Faraday effect (IFE) causes an excitation of the effective magnetic field in this layer [4].

Here we propose a novel design of the MPC nanostructure with patterned defect magnetic layer. The depth of the magnetic layer should be locally decreased by means of etching, for instance. For the suitable conditions (wavelength or frequency, polarization) the light will experience localization just inside the bounded area of the magnetic layer resulting in the excitation of the effective magnetic field,  $H_{\text{eff}}$ , inside the etching area.

Magnetostatic spin waves can be excited in the films of ferrimagnetic dielectrics by optical means due to the IFE [5]. Similarly, the setting of the MPC with etched magnetic layer one can expect the excitation of the spin waves in the area of the effective magnetic field excitation.

The wavevector of the discussed spin waves is determined by the dimensions of the etched area. In our work we show how it is possible to generate magnons in the spatial areas with 1.6-2.4 $\mu\text{m}$  diameters. The minimum radius (diameter) of the etched disk depends on the illuminating light wavelength. The less is the length and the wavelength in the medium, correspondingly, the smaller radius of the disk one can choose. It was shown that the spin waves excitation area is a bit smaller than the size of the etched disk. For instance, 2-2.4 $\mu\text{m}$  diameter of the disk provides the excitation area of 1.3-1.4 $\mu\text{m}$  in width. Also, it should be noted that the localization of the effective magnetic field occurs when the etching depth exceeds 20nm.

To sum up, there is proposed a design of the MPC nanostructure with the patterned defect magnetic layer. The local decrease of the defect layer results in localization of the light concentration inside such grooves. Due to the IFE the effective magnetic field would be excited just in localized areas of the patterned MPC. Thus, the excitation of the magnetostatic spin waves occurs in the bound area resulting in the certain values of wave vector of such magnons. This approach opens up ample opportunities for the short spin waves generation.

This study was supported by Russian Science Foundation (project no. 23-12-00310).

- [1] M. Inoue et al., *J. Appl. Phys.*, **83** (1998) 6768–6770.
- [2] E. Takeda et al., *J. Appl. Phys.*, **87** (2000) 6782–6784.
- [3] O. Borovkova and V. Belotelov, *Opt. Lett.*, **47** (2022) 5743–5746.
- [4] M.A. Kozhaev et al., *Sci. Rep.*, **8** (2018) 11435.
- [5] A. I. Chernov et al., *Opt. Lett.*, **42** (2017) 279-282.

## NONLINEAR OPTICAL DIAGNOSTICS AND MANIPULATION WITH MAGNETIC DOMAIN WALLS FOR ENERGY-EFFECTIVE NEUROMORPHIC COMPUTING

*Guskov A.A.<sup>1</sup>, Stepanov M.A.<sup>1</sup>, Mitetelo N.V.<sup>1</sup>, Mishina E.D.<sup>1</sup>, Pyatakov A.P.<sup>2</sup>*

<sup>1</sup> MIREA - Russian Technological University, Moscow, Russia

<sup>2</sup> Lomonosov Moscow State University, Moscow, Russia

guskov@mirea.ru

Materials belonging to the class of "multiferroics" and thin magnetic films with domain structures are promising for implementing memory devices and computational devices (including neuromorphic ones) due to the pronounced magnetoelectric effect realized in them. This effect allows controlling local magnetic properties of the material using external influences, thereby implementing a system with logical states, the control of which is energy-efficient and fast. In this scientific field, the areas of domain "boundaries" in films of iron-containing garnets with (210)- and (111)-symmetry are actively researched for controlling the magnetic order parameter. The most known such materials are bismuth ferrite  $\text{BiFeO}_3$  and structures based on it. All of this makes it promising for ultrafast and fully optical neuromorphic computations [1].

For the development of the elemental base for neuromorphic computations, as well as the realization of domain structure transformation using external influences on the domain boundary area it is necessary to thoroughly investigate the magnetization vector distribution in the areas of interest and determine the types of external influences capable of interacting with the localized subwavelength-scale electrical polarization of the medium. In our work, we show the results of research on the micromagnetic structure and non-trivial states of magnetization for the ferrite-garnet film with rare-earth metal composition  $(\text{BiLu})_3(\text{FeGa})_5\text{O}_{12}$  with (210)-symmetry (epitaxially grown on the  $\text{Gd}_3\text{Ga}_5\text{O}_{12}$  substrate).

The orientation parameters of the magnetization vector in the domain boundary area were determined using the method of nonlinear-optical microscopy with polarization resolution and the nonlinear magneto-optical Voigt effect [2]. Registration of the second harmonic nonlinear signal enabled the development of a method for separate registration of the lateral and perpendicular components of magnetization. This method demonstrated localization in the domain boundary area of a non-uniform contribution to magnetization. We also demonstrate three methods of influencing the domain boundary using external factors:

1. attraction-repulsion of domain boundaries with various chirality of magnetization vector distribution using a constant external electric field with a voltage of up to several kV/cm
2. displacement of the boundary under the influence of the dielectric permeability gradient, created by local deformation near the domain wall
3. laser radiation with varying polarization and peak intensity up to  $500 \text{ MW/cm}^2$

The parameters of domain boundary mobility and the requirements for the presence and direction of the external magnetic field were also determined. The characteristics of domain boundary mobility and the dynamics of this area's response to external influences allow for the application of this type of multiferroic medium for the implementation of ultrafast and energy-efficient computational and memory devices.

The work is supported by the Ministry of Science and Education of RF (Project No.075-15-2022-1131).

[1] G.V. Arzamastseva et al., *JETP*, **120** (2015) 687–701.

[2] S. Cherifi-Hertel et al., *Nat. comm.*, **8** (2017) 15768.

## «GRAY» SLIT DIFFRACTION AND THE POSSIBILITY OF ITS USE TO IMPROVE THE SPATIAL RESOLUTION OF MAGNETO-OPTICS

*Shapaeva T.B., Khudaigulova E.F.*

Lomonosov Moscow State University, Moscow, Russia  
 hudaygulovaelya@gmail.com

The double photography method based on the Faraday effect was used to study the antiferromagnetic (AFM) vortices dynamics in a domain wall (DW) of yttrium orthoferrite [1]. It is known that the highest DW velocity and magnetic vortices velocity (20 km/s) was observed in orthoferrites. It was shown on the basis of indirect experiments that AFM vortices cannot exist inside a DW if its velocity is less or equal to the sound velocity (4 km/s) [2]. AFM vortices inside the DW are the DW fine structure. Since a change in the internal DW structure can lead to a change in the apparent width of the wall, the study of the DW dynamics with a high spatial resolution is relevant.

It is known that the use of light diffraction makes it possible to improve the spatial resolution of magneto-optics [3]. In this work, we discuss the possibilities of using light diffraction by a slit, the center and edges of which have different transmittances other than 1 and 0. In contrast to the classical black-and-white slit, we will call such a slit "gray". The intensity of the light incident on the "gray" slit  $I_0$  can be represented as

$$I_0 = I_1 + I_2 + I_3$$

where  $I_1$  and  $I_2$  are the intensities of light passing through a completely transparent and opaque medium, respectively,  $I_3$  is the intensity of light passing through a black-and-white slit. By comparing the first minimum position of the diffraction pattern in statics and in dynamics, it is possible to determine the dependence of the apparent width of the domain wall on the wall velocity with an accuracy of 0.1  $\mu\text{m}$ .

In addition, if the DW dynamics was induced by light, then by comparing the light intensities at the zero maximum and the first minimum, one can determine the change in the optical properties of the medium after excitation. Thus, the combining diffraction and the pump-probe method opens up fundamentally new experimental possibilities.

[1] M.V. Chetkin, Yu.N. Kurbatova, T.B. Shapaeva, *JMMM*, **321** (2009) 800-802.

[2] M.V. Chetkin, Yu.N. Kurbatova, T.B. Shapaeva, *JMMM*, **324** (2012) 3576-3578.

[3] M.V. Gerasimov et al., *Phys. Rev. B*. **94** (2016) 014434.

## SPIN NOISE OF MAGNETICALLY ANISOTROPIC CENTERS

*Kozlov V.O.<sup>1,2</sup>, Ryzhov I.I.<sup>2,1</sup>, Kozlov G.G.<sup>1,3</sup>, Zapasskii V.S.<sup>1</sup>*

<sup>1</sup> Spin Optics Laboratory, St. Petersburg State University, St. Petersburg, Russia

<sup>2</sup> Photonics Department, St. Petersburg State University, St. Petersburg, Russia

<sup>3</sup> Solid State Physics Department, St. Petersburg State University, St. Petersburg, Russia  
vadiim.kozlov@gmail.com

Spin noise spectroscopy (SNS) is an optical method for detecting paramagnetic resonance from magnetization fluctuations [1, 2]. This method is based on the Faraday effect, whereby magnetization noise can be indirectly measured using Faraday rotation noise. When using the SNS method and other magneto-optical methods, the implementation of the Van Vleck theorem [3] is implied: the Faraday rotation is directly proportional to the projection of the magnetization on the wave vector of the probing beam. This fact, together with the fluctuation-dissipation theorem, makes it possible to measure the magnetic susceptibility of a paramagnetic medium, as in the case of using the classical method of electron paramagnetic resonance.

When recording spin noise, two experimental geometries are distinguished [2]: the Faraday geometry, when the external magnetic field is codirectional with the light wave vector, and the Voigt geometry, when they are perpendicular. In isotropic spin systems in the Faraday geometry, as a rule, only fluctuations of the magnetization amplitude are observed, which correspond to a signal near zero frequency. In the Voigt geometry, there are fluctuations in the direction of magnetization, which corresponds to a signal at the Larmor frequency (paramagnetic resonance frequency). However, in systems with anisotropic centers, the Van Vleck theorem ceases to be valid under certain conditions [3]. From a practical point of view, this leads to the fact that the differences between the two geometries disappear, and spin noise at the Larmor frequency is detected for an arbitrary orientation of the external magnetic field. This fact has been experimentally demonstrated for a cubic CaF<sub>2</sub> crystal with anisotropic Nd<sup>3+</sup> centres.

We show that, in the general case, the assumptions underlying the Van Vleck theorem are not necessarily satisfied. In our case, the violation of the Van Vleck theorem was associated with a small detuning of the probing beam from optical resonance. In the case of a large detuning, Van Vleck's theorem is preserved, which was also shown experimentally on another system with magnetically anisotropic particles - on a perovskite halide CH<sub>3</sub>NH<sub>3</sub>PbI<sub>3</sub> single crystal.

The work was financially supported by RSF grant No. 21-72-10021.

[1] M. Römer et al., *Rev. Sci. Instrum.*, **78** (2007) 103903.

[2] V. S. Zapasskii, *Adv. Opt. Photonics*, **5** (2013) 131.

[3] J. H. Van Vleck and M. H. Hebb, *Phys. Rev.*, **46** (1934) 17.

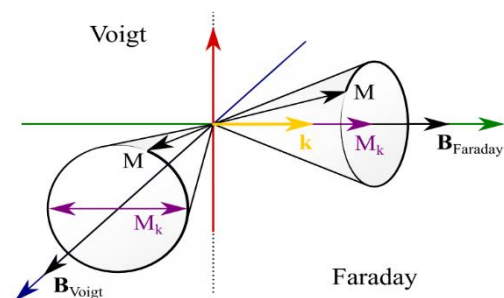


Figure 1. Precession of magnetic moment in the Voigt and Faraday geometry. In the Faraday geometry, magnetization (M) precesses around the direction of light propagation (k).

## ULTRAFAST PHOTO-INDUCED PHASE TRANSITIONS IN MAGNETITE

*Kuzikova A.V.<sup>1</sup>, Shelukhin L.A.<sup>1</sup>, Maximov F.M.<sup>2,3</sup>, Chernov I.E.<sup>2,3</sup>, Pisarev R.V.<sup>1</sup>, Kalashnikova A.M.<sup>1</sup>*

<sup>1</sup> Ioffe Institute, St. Petersburg, Russia

<sup>2</sup> Russian Quantum Center, Skolkovo, Russia

<sup>3</sup> Moscow Institute of Physics and Technology, Dolgoprudny, Russia

anna.kuzikova@mail.ioffe.ru

Laser-induced phase transitions in solids can be used to switch from one phase state to another at picosecond timescales. This raised a question about mechanisms of ultrafast photo-induced transitions (PIPT) and their link to equilibrium ones. The path along which the medium follows during PIPT is especially intriguing in materials, where several transitions occur simultaneously.

In this work we aim at studying ultrafast PIPT in a model ferrimagnet magnetite  $\text{Fe}_3\text{O}_4$ . The magnetic phase transition in magnetite may have a link to electronic and structural ones. The magnetite possesses a first-order Verwey transition from a monoclinic insulating to a cubic metal phase at a temperature of 123 K. Dynamics and mechanism of the laser-driven Verwey transition in  $\text{Fe}_3\text{O}_4$  is the subject of many works [1,2]. At temperature of 130 K,  $\text{Fe}_3\text{O}_4$  demonstrates a spin-reorientation transition (SRT) when the sign of the magnetic cubic anisotropy parameter changes. The relationship between the Verwey transition and the SRT at equilibrium remains open [2]. Our goal was to study how SRT is connected to the Verwey transition during ultrafast laser excitation.

We performed femtosecond time-resolved studies of optical reflectivity and magneto-optical Kerr effect (MOKE) in  $\text{Fe}_3\text{O}_4$  single crystal at various laser pulse fluences and sample temperatures [4]. Based on the characteristic thresholds of the reflectivity change as a function of the pump fluence, we could conclude that a laser pulse induces the ultrafast Verwey transition only when its fluence exceeds certain threshold of  $1.6 \text{ mJ/cm}^2$  as obtained at  $T=80 \text{ K}$ . On the other hand, observation of laser-induced magnetization precession (Figure 1) yielded counterintuitive result, showing that SRT is induced at fluences well below the threshold for a Verwey transition. However, by carefully examining evolution of the precession parameters and equilibrium magnetic hysteresis loops with temperature and laser fluence, we show that laser-induced SRT and Verwey transitions are coupled. However, only by measuring laser-induced precession excited due to SRT it was possible to reveal PIPT occurring at below-threshold fluences.

In conclusion, we have demonstrated that the underlying mechanism laser-induced magnetization precession in magnetite in a wide temperature range 80-200 K is the switching of anisotropy axis due to ultrafast SR transition. Depending on laser fluence, the photo-induced transition occurs either in a whole excited material or in separate domains, signifying its first-order character beyond the thermal equilibrium [3].

Support by Russian Science Foundation (Grant No. 22-72-00039) is acknowledged.

[1] S. de Jong et al., *Nature Mater.*, **12** (2013) 882.

[2] J.E. Lorenzo et al., *Phys. Rev. Lett.*, **101** (2008) 226401.

[3] A.V. Kuzikova et al., *Phys. Rev. B*, **107** (2023) 024413.

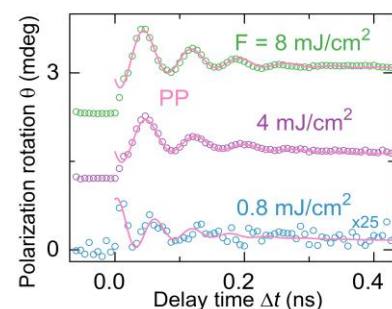


Figure 1. Typical signals in the pump-probe method.

## THE EFFECT OF AN EXTERNAL MAGNETIC FIELD ON SURFACE PLASMON-POLARITONS IN THE VO<sub>2</sub>-SiO<sub>2</sub>-METASURFACE STRUCTURE BASED ON GRAPHENE

*Usik M.O., Kuzmin D.A., Bychkov I.V.*

Chelyabinsk State University (CSU), Chelyabinsk, Russia  
usikmo95@gmail.com

In this paper, the behavior of surface plasmon polaritons (SPPs) in the structure of vanadium dioxide-silicon dioxide-hyperbolic metasurface under the influence of an external magnetic field is studied (Figure 1). Since the effect of phase transitions on the nature of excitation of SPPs is of particular interest, vanadium dioxide was taken as one of the layers, since its phase transition from the dielectric state to the metallic state occurs at temperatures close to room [1].

A lattice of graphene strips was taken as a hyperbolic metasurface [2]. Such a surface is capable of supporting the propagation of both TM and TE-polarized plasmons.

To account for the phase transition of vanadium dioxide, the already known data of its characteristics are taken as a function of temperature. Applying linear approximation and using Drude theory [3], it is possible to obtain a model that is quite simple to describe.

In order to investigate the behavior of surface plasmons, one should solve Maxwell's equations with the corresponding boundary conditions at each interface. For monochromatic wave

$E_{\alpha+}, H_{\alpha+} \sim \exp[-i\omega t + i\mathbf{k}\mathbf{x} \pm \gamma_{\alpha}z]$  [4], where  $\omega$  is an angular frequency,  $\mathbf{k}$  is a propagation constant, and  $\pm\gamma_{\alpha}$  are localization constants ( $\alpha = \text{VO}_2, \text{SiO}_2, \text{a}$  denotes "vanadium dioxide", "silicon dioxide" and "air", consequently). With these notations, Maxwell's equation for the waves in each medium is read:

$$[\mathbf{k}, \mathbf{E}_{\alpha+}] = i\omega \mathbf{B}_{\alpha+}, [\mathbf{k}, \mathbf{H}_{\alpha+}] = -i\omega \mathbf{D}_{\alpha+} \quad (1)$$

$$\mathbf{B}_{\alpha+} = \mu_0 \mathbf{H}_{\alpha+}, \mathbf{D}_{\alpha+} = \varepsilon_0 \hat{\varepsilon}_{\alpha+} \mathbf{E}_{\alpha+}, \alpha = \text{VO}_2, \text{SiO}_2, \text{a.}$$

Boundary conditions should be satisfied for total fields:

$$\begin{aligned} H_{\text{VO}_2, \tau}|_{z=-t_1} &= H_{\text{SiO}_2, \tau}|_{z=-t_1}, E_{\text{VO}_2, \tau}|_{z=-t_1} = E_{\text{SiO}_2, \tau}|_{z=-t_1}, \\ [n, H_{\text{SiO}_2, \tau}|_{z=0} - H_{\text{a}, \tau}|_{z=0}] &= \hat{\sigma} E_{\text{a}, \tau}|_{z=0}, E_{\text{SiO}_2, \tau}|_{z=0} = E_{\text{a}, \tau}|_{z=0}, \end{aligned} \quad (2)$$

where  $\mathbf{n}$  is the unitary vector perpendicular to the interface,  $\hat{\sigma}$  is tensor of graphene conductivity,  $\hat{\varepsilon}_{\alpha}$  is a tensor of permittivity under the influence of an external magnetic field.

As a result of calculations, it is shown how the Isofrequency contour of SPPs changes taking into account the different direction of the external magnetic field. It is also shown how an external magnetic field affects the direction of static magnetization caused by the inverse Faraday effect. This work can offer additional ways to control the behavior of surface plasmons, as well as become the basis for the study of new self-adjusting structures.

Support by RSF (22-19-00355) is acknowledged.

[1] T. Peterseim et al., *Jour. Appl. Phys.*, **120** (2016) 075102.

[2] J.S. Gomez-Diaz, M. Tymchenko, A. Alù, *Physical Review Letters*, **114** (2015) 233901.

[3] M. Tazawa, P. Jin, and S. Tanemura, *Applied optics*, **37(10)** (1998) 1858.

[4] I.V. Bychkov et al., *Optics Letters*, **3(1)** (2018) 26.

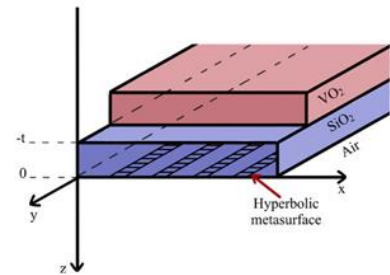


Figure 1. VO<sub>2</sub>-SiO<sub>2</sub>-hyperbolic metasurface structure.

3PO-L5-7

## THE PECULIARITIES OF MAGNETO-OPTICAL SPECTRA OF NiFe-Ta BILAYERS

*Yashin M.M.*<sup>1</sup>, *Pripechenkov I.M.*<sup>2</sup>, *Yurasov A.N.*<sup>1</sup>, *Skidanov V.A.*<sup>3</sup>, *Simdyanova M.A.*<sup>2</sup>, *Gan'shina E.A.*<sup>2</sup>,  
*Gladyshev I.V.*<sup>1</sup>, *Granovsky A.B.*<sup>2</sup>

<sup>1</sup>MIREA — Russian Technological University, Moscow, Russia

<sup>2</sup>Lomonosov Moscow State University, Moscow, Russia

<sup>3</sup>The Institute for Design Problems in Microelectronics, Moscow, Russia  
yashin@mirea.ru

The study of various properties of promising nanostructures is very relevant today. In such structures, it is possible to enhance various effects, for example, such as magnetoresistance, extraordinary Hall effect, large magneto-optical activity, etc. Such systems include layered nanoscale structures. Modeling of optical and magneto-optical observed effects makes it possible to estimate various characteristic parameters of the studied samples in a non-contact way [1].

We present results of magneto-optical investigations of NiFe-Ta bilayers in transverse Kerr effect (TKE) geometry in the spectral range 0.5–4.0 eV and magnetic field up to 3.0 kOe. The samples were fabricated by magnetron sputtering on Si substrates. Recently, by measurements the TKE for the same samples using white light it was revealed the TKE sign inversion and amplitude enhancement even when the thickness of Ta layer exceeds light penetration depth [1]. To understand this surprising behavior we investigated spectral dependences of TKE at room temperature varying thicknesses of both NiFe and Ta, and calculated the TKE spectra for NiFe-Ta/Si structure. Modeling of optical and magneto-optical spectra were performed using Fresnel formulas for multilayer systems [2, 3] using optical and magneto-optical parameters for bulk NiFe and Ta[4].

The obtained TKE spectra exhibit very complicated behavior as a function of NiFe and Ta thickness. We confirm the TKE enhancement for definite light waves and Ta thickness. The calculations show that the TKE signal can be significantly enhanced for rather thick Ta layers.

In the presentation we discuss the possible mechanisms for observed features and reasons for some disagreement between theory and experiment.

The work is supported by Ministry of Science and High Education of RF (State task for the Universities No. FSFZ-2023-0005) and the program "Accelerator MIREA — Russian Technological University".

[1] V.A. Skidanov, *EASTMAG conference*, 2022.

[2] A.N. Yurasov et al., *Bull. Russ. Acad. Sci.: Phys.* **86(5)** (2022) 63.

[3] V.M. Mayevsky, *Physics of Metal and Metallography*, **59** (1985) 213-219.

[4] K.K. Tikuišis et al., *Mater. Des.* **114** (2017) 31-39.

## THEORETICAL AND EXPERIMENTAL STUDY OF EFFECTS IN THE TWO-SUBLATTICE IRON GARNET SYSTEM WITH THE MAGNETIZATION COMPENSATION POINT

*Gusev N.A.<sup>1,2</sup>, Ignatyeva D.O.<sup>1,2,3</sup>, Prisyazhnyuk A.V.<sup>2</sup>, Prilepskii I.V.<sup>2</sup>, Krichevskiy D.M.<sup>1,2,4</sup>, Polulyakh S.N.<sup>2</sup>,  
Zvezdin A.K.<sup>1,5</sup>, Berzhansky V.N.<sup>2</sup>, Belotelov V.I.<sup>1,2,3</sup>*

<sup>1</sup> Russian Quantum Center, Moscow, Russia

<sup>2</sup> Vernadsky Crimean Federal University, Simferopol, Russia

<sup>3</sup> Lomonosov Moscow State University, Moscow, Russia

<sup>4</sup> Moscow Institute of Physics and Technology (MIPT), Dolgoprudny, Russia

<sup>5</sup> Prokhorov General Physics Institute of the Russian Academy of Sciences, Moscow, Russia  
nagusew@gmail.com

Despite the fact that the studies of the temperature dependence of the magnetization of ferrimagnetic films and the corresponding temperature effects have attracted the attention of researchers since the middle of the last century [1], interest in this scientific subject has strongly grown in recent years mainly due to the variety of experimental methods for studying magnetic materials including the optical pump-probe technique [2]. At the same time, the interesting theoretical approach for such problems, named quasi-antiferromagnetic approximation, was proposed by A.K. Zvezdin [3]. The approach consists in reducing the four angular spherical coordinate variables ( $\theta_1, \varphi_1$  and  $\theta_2, \varphi_2$ ) of the magnetization vectors  $\mathbf{M}_1$  and  $\mathbf{M}_2$  of the sublattices of a two-sublattice magnetic system to the two angular spherical coordinate variables ( $\theta$  and  $\varphi$ ) of the antiferromagnetic vector  $\mathbf{L}$ .

This approach makes one possible to obtain the Lagrange function of a two-sublattice system, written in terms of the angles  $\theta$  and  $\varphi$  of the antiferromagnetic vector, to calculate the Lagrange equations and the linearized equations of small oscillations of the angles, which describe the precession of the vector  $\mathbf{L}$  at different temperatures, in magnetic fields of the different magnitudes and the different spatial configurations, taking into account the anisotropy type of "easy axis" or "easy plane". The study of the energy function gives the equilibrium states of a two-sublattice system depending on the temperature, which are divided into two large groups: the  $\mathbf{L}$  vector is parallel to the line along the applied magnetic field  $\mathbf{H}$ , and at an angle to it. The first group of states can be called a collinear phase, and the second - a non-collinear one. The transition between them can be considered as a second-order phase transition, similar to the transition between the paramagnetic and ferrimagnetic states. Next, one can calculate the frequencies and the amplitudes of the precession as a function of temperature and magnetic field, anisotropy constant and interlattice exchange for both phases.

This report focuses on the description the the statics and dynamics of the antiferromagnetic vector of a two-sublattice iron garnet film in the collinear and non-collinear phases by the quasi-antiferromagnetic approximation and comparing this description with the experimental results obtained by the pump-probe technique. Some new effects, such as energy degeneracy in the non-collinear phase and the behavior of the soft quasi-antiferromagnetic mode in the vicinity of the phase transition point are theoretically predicted and searched experimentally.

The work was financially supported by the Ministry of Science and Higher Education of the Russian Federation, Megagrant project No 075-15-2022-1108 and Russian Science Foundation grant No 23-62-10024.

[1] S. Geschwind, L. R. Walker. *J. Appl. Phys.*, **30(4)** (1959) S163-S170.

[2] A. Stupakiewicz, T. Satoh, *J. Phys. Soc. Jap.*, **90(8)** (2021) 081008.

[3] M.D. Davydova et al., *J. Phys.: Cond. Matt.*, **32(1)** (2019) 01LT01.

## OPTICALLY INDUCED LOCALIZED SPIN-WAVE STATES IN ALL-DIELECTRIC NANOPILLARS

*Krichevsky D.*<sup>1,2,3</sup>, *Ignatyeva D.*<sup>2,3,4</sup>, *Kolosvetov A.*<sup>1</sup>, *Chernov A.*<sup>1</sup>, *Shaposhnikov A.*<sup>3</sup>, *Berzhansky V.*<sup>3</sup>, *Belotelov V.*<sup>2,3,4</sup>

<sup>1</sup>Moscow Institute of Physics and Technology, Dolgoprudny, Russia

<sup>2</sup>Russian Quantum Center, Moscow, Russia

<sup>3</sup>Vernadsky Crimean Federal University, Simferopol, Russia

<sup>4</sup>Lomonosov Moscow State University, Moscow, Russia  
krichevskii.dm@phystech.edu

Control of spin waves and their quanta - magnons in ordered magnetic materials is a key for energy efficient devices, such as Boolean logic elements, memory cells, sensors, and elements of quantum computing [1]. Currently, all-dielectric nanophotonics brings a new perspective to low-dissipative light-spin coupling in nanoscale magnetic materials via optical modes excitation [2].

Here we propose an all-dielectric two-dimensional array of bismuth iron garnet (BIG) nanopillars (period 900 nm, height 515 nm and diameter 450 nm) on SiO<sub>2</sub> substrate. The geometric properties of the structure were designed to localize electromagnetic energy inside the nanopillars via specific optical states. It was observed, that such localization induces complex spin-wave behavior excited by the inverse Faraday effect (IFE).

Spin-wave dynamics was studied via magneto-optical pump-probe technique (time-resolved Faraday rotation - TRFR). The system was pumped by 730 nm circularly polarized pulse. This wavelength corresponds to resonant dip in the transmittance spectra of the sample. At the resonance optical energy is highly concentrated inside nanopillar. As a result, IFE effective magnetic field is also highly localized inside the pillar. This IFE field stimulates sophisticated oscillations in TRFR signal (Figure 1). The measured TRFR signal is directly connected with magnetization oscillations and corresponds to spin waves. There are distinct beats in the signal of TRFR (Figure 1) which indicate multiple spin-wave modes excitation.

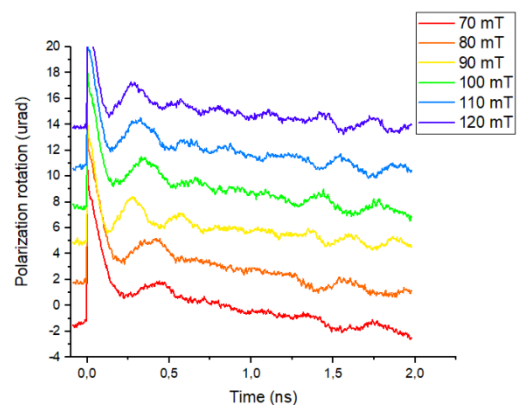


Figure 1. TRFR signals of the sample measured for different values of the external magnetic field.

This work was financially supported by Russian Science Foundation, Grant No. 21-72-10020.

[1] A. Chumak et al., *Nature Physics*, **11** (2015) 453.

[2] A.I Chernov et al., *Nano Lett.*, **20** (2020) 5259.

## ULTRAFAST DYNAMICS OF MAGNETIC ORDER AND SPECTRAL ADDRESSING THE SUBLATTICES IN $\text{FeCr}_2\text{O}_4$ SPINEL

*Yusupov R.V., Petrov A.V., Cherosov M.A., Batulin R.G., Kiiamov A.G., Nasyrova M.I., Nikitin S.I., Eremin M.V.*

Kazan Federal University, Kazan, Russia  
Roman.Yusupov@kpfu.ru

Compounds with the spinel crystal structure have a chemical formula of  $M'M''_2X_4$  ( $M'$  and  $M''$  being metals and  $X$  – oxygen or a chalcogen) and represent a wide class of the materials that may reveal different physical properties. The structure includes the tetrahedrally-coordinated cationic A-sites and B-sites with octahedral surrounding. If either  $M'$  or  $M''$  ions, or both, belong to transition metal group and have unpaired electrons in the  $d$ -shell then different kinds of magnetic ordering develop. On one hand, the high-temperature crystal structure is relatively simple and usually has the cubic symmetry. On the other, the B-site network has the pyrochlore structure and, being occupied with magnetic ions, is the subject to the magnetic frustration. Recently, multiferroicity with a spontaneous or an electric-field induced metastable electric polarization in magnetic spinels has been reported.

In our talk, the results of ultrafast magneto-optical Kerr effect study (in polar geometry) of single-crystal iron chromite  $\text{FeCr}_2\text{O}_4$  (FCO), a representative of multiferroic spinels, will be presented. On cooling from room temperature, FCO experiences a sequence of phase transitions: the structural second-order transition at  $\sim 138$  K from cubic to tetragonal symmetry due to an orbital ordering within the A-site  $\text{Fe}^{2+}$  ion sublattice; at  $T_N \sim 65$  K, a magnetic ordering to a collinear ferromagnetic state takes place, which is accompanied by a crystal structure symmetry lowering to the orthorhombic; at  $T_s \sim 38$  K, magnetic structure rearranges, with presumably a development of the spiral modulation of the magnetic order.

Experiments have been performed in a pump-probe sequence with pumping at 800 nm (1.55 eV) and probing at either 400 nm (3.1 eV) or 2000 nm ( $\sim 0.6$  eV) wavelengths with pulse duration of  $\sim 50$  fs and repetition rate of 1 kHz. A wide temperature range of 4 – 300 K was covered. The chosen probing photon energies of 3.1 eV and 0.6 eV correspond essentially to the on-site  $d-d$  transitions of the  $\text{Cr}^{3+}$  and  $\text{Fe}^{2+}$  ions, respectively.

We find that the extracted ultrafast Kerr rotation angle transients are detected only below  $T_N$ . With the 400-nm probing, the transients can be described with a two-exponent rise with the time scales of 4-6 ps and 50-70 ps followed by a partial recovery on a typical spin-lattice relaxation time of 500-1500 ps. The recovery process reveals a clear critical slowing down on approaching  $T_N$ . The amplitudes of either the rising (demagnetization) or decaying (magnetization recovery) components closely follow the magnetic moment temperature dependence.

Under 2000-nm wavelength probing, in general, the responses can be described as well with three exponents with the same order time scales. However, the fast “rising” component reveals an amplitude sign change at  $\sim T_s$ , intermediate-time component is observed only in a limited temperature range, and the recovery component has a counterintuitive lifetime dependence revealing acceleration on temperature increase.

An observation of strongly different Kerr-angle transients at different probe wavelength allow us to conclude on a possibility of spectral addressing the magnetic dynamics of the  $\text{Fe}^{2+}$  and  $\text{Cr}^{3+}$  ion sublattices. Anomalous temperature evolution of the transient with the 2000-nm probing will be discussed in relation to a pronounced magnetoelectric coupling at the  $\text{Fe}^{2+}$  ion sites [1].

Support by Russian Science Foundation, project No. 19-12-00244 is acknowledged.

[1] K.V. Vasin, M.V. Eremin, *J. Magn. Magn. Mater.*, **537** (2021) 168185.

## MAGNETO-OPTICAL ELLIPSOMETRY OF THIN MAX FILMS WITH OPTICAL UNIAXIAL ANISOTROPY

*Maximova O.A.<sup>1,2</sup>, Lyaschenko S.A.<sup>1</sup>, Yakovlev I.A.<sup>1</sup>, Shentsov D.V.<sup>1</sup>, Andryushchenko T.A.<sup>1</sup>, Varnakov S.N.<sup>1</sup>, Ovchinnikov S.G.<sup>1,2</sup>*

<sup>1</sup> Kirensky Institute of Physics, Federal Research Center KSC SB RAS, Krasnoyarsk, Russia

<sup>2</sup> Siberian Federal University, Krasnoyarsk, Russia

maximo.a@mail.ru

A technique has been developed for magneto-optical ellipsometry characterizing thin-film samples with optical anisotropy, including MAX materials. All magneto-ellipsometric measurements were carried out in the geometry of the magneto-optical transverse Kerr effect, when the magnetization vector lies in the sample plane parallel to the z axis. In contrast to paper [1], where we considered thick MAX films, this time we considered MAX films as an effective thin magnetic medium with optical uniaxial anisotropy characterized by refractive indices  $N_y = N_z$  in the sample plane and  $N_x$  perpendicular to it, on an isotropic substrate.

In order to analyze the reflection of light from the tested sample, instead of the traditional Fresnel coefficients, it was necessary to use reflection coefficients that take into account the optical anisotropy of the sample, which leads to a difference in the diagonal components of the permittivity tensor. In addition, it was necessary to take into account the magneto-optical response, namely, the stimulated anisotropy caused by the application of an external magnetic field to the sample, which led to the presence of nonzero off-diagonal elements of the permittivity tensor. Such expressions were not found in the literature, which led to the need to derive the reflection coefficients ( $r_{01p}$ ,  $r_{10p}$ ) and transmission coefficients ( $t_{01p}$ ,  $t_{10p}$ ) for the interface of these media, already taking into account the magneto-optical response. Accordingly, the appearance of the second term in the reflection and transmission coefficients at the interfaces was shown. The final expressions for the found coefficients for p-polarization are not symmetric due to taking into account both the magneto-optical response and optical anisotropy. In this case, neither one nor the other affects the coefficients for the s-polarization, in view of the fact that the transverse configuration of the magneto-optical Kerr effect is considered and that the s-component of the electric field vector corresponds to an ordinary wave.

As a result, the necessary mathematical expressions were obtained for the analysis of the optical and magneto-optical properties of thin MAX films on a substrate according to spectral magneto-optical ellipsometry data.

Support by the grant from the Russian Science Foundation No. 21-12-00226, <http://rscf.ru/project/21-12-00226/> is acknowledged.

[1] O. A. Maximova et al., *JETP* **133(5)** (2021) 581–590.

## EFFECT OF GRANULE SIZES ON MAGNETO-OPTICAL SPECTRA OF NANOCOMPOSITES

*Simdyanova M.A.<sup>1</sup>, Yurasov A.N.<sup>2</sup>, Yashin M.M.<sup>2</sup>, Gan'shina E.A.<sup>1</sup>, Gladyshev I.V.<sup>2</sup>, Garsbin V.V.<sup>1</sup>,  
Pripechenkov I.M.<sup>1</sup>, Granovsky A.B.<sup>1</sup>*

<sup>1</sup> Lomonosov Moscow State University, Moscow, Russia

<sup>2</sup> MIREA — Russian Technological University, Moscow, Russia

Alexey\_yurasov@mail.ru

Magnetic nanocomposites “ferromagnetic metal-dielectric” are promising materials exhibiting pronounced magnetic, transport and magneto-optical properties. The magneto-optical transverse Kerr effect (TKE) allows non-contact investigation of nanostructures, giving valuable information about the magnetic microstructure of samples [1]. In the presentation, a comprehensive analysis of the effect of the size of granules on the magneto-optical properties of nanocomposites is carried out, focusing on influence of each of the various microscopic parameters such as the mean free path, plasma frequency, relaxation time, the coefficients of the extraordinary Hall effect inside the granule and on its surface, the shape of granules, etc.

Three main mechanisms of the influence of granule sizes on the TKE are considered in the framework of the effective-medium theory. The first mechanism is associated with a quasi-classical dimensional effect when the granular size is less than the mean free path of electrons. Taking into account corresponding to this effect changes in both the diagonal and non-diagonal components of the dielectric permittivity tensor (DPT) [2,3] it is shown that this mechanism is significant only in the IR region of the spectrum. The second mechanism is associated with an increase of the spin-orbit interaction (SOI) on the surface of the granules, affecting the interband transitions. In this case, the non-diagonal component of DPT responsible for the TKE can be written as:

$$\gamma = \gamma_{bulk} \left(1 - \frac{3a}{r}\right) + \gamma_{surf} \frac{3a}{r},$$

where  $a$  is the thickness of the surface layer with reinforced SOI. It can be seen that even minor differences in the SOI on the surface of granules with a thickness of a monolayer will lead to a change in the value of the TKE in the entire optical frequency range. The third mechanism is manifested during annealing of nanocomposites. As a result of annealing, the shape of granules and their size change. It leads to drastic changes of both optical and magneto-optical properties. For example, if magnetic ions dissolved in the matrix during annealing are attached to the granules, then the volume fraction of ferromagnetic component changes, shifting the percolation threshold and DPT. This effect of annealing is strongly pronounced for nanocomposites with the metal volume fraction close to the percolation threshold.

Consideration of all three mechanisms makes it possible to significantly improve the description of recent experimental data.

The work is supported by Ministry of Science and High Education of RF (State task for the Universities No. FSFZ-2023-0005).

[1] E.A. Gan'shina et al., *JETP*, **125** (2004) 1172.

[2] A.B. Granovsky, M.V. Kuzmichev, A.N. Yurasov, *Bull. of the MSU.*, **6** (2000) 67.

[3] A.N. Yurasov et al., *Bulletin RAS, Ser. Phys.*, **86** (2022) 716.

**July 3**

Monday

18:00 - 20:00

POSTER  
SESSIONS

Section L6

**Magnetic**

**Shape Memory Alloys and**

**Magnetocaloric Effect**

## MECHANISMS FOR REGULATING THE FREQUENCY STABILITY OF THE MAGNETOCALORIC EFFECT IN POLYCRYSTALLINE MANGANITES

*Gamzatov A.G., Abdulkadirova N.Z., Kadirbardeev A.T., Aliev A.M.*  
Amirkhanov Institute of Physics, DFRC RAS, Makhachkala, Russia  
nnurizhat@mail.ru

Recent studies [1-4] of materials with giant MCEs have shown that the magnitude of the adiabatic temperature change decreases with increasing frequency of the cyclic magnetic field. In addition, degradation of the effect is observed under long-term exposure to cyclic fields, which directly prevents their practical application. It was shown that the microstructure, domain structure, multiphase nature of the sample, and phase boundaries play an important role in the dynamics of the phase transition and the frequency stability of the MCE.

Manganites are prominent representatives of materials with giant values of the magnetocaloric effect [5]. The study of the influence of grain size on physical properties including the magnetocaloric effect of manganites has been studied in detail. This paper presents the results of a study of the influence of the size of granules (microstructure) on the value and frequency stability of the magnetocaloric effect of  $\text{Pr}_{0.7}\text{Sr}_{0.2}\text{Ca}_{0.1}\text{MnO}_3$  manganite (PSC-1300, 900, 600 -with different microstructure) in a cyclic magnetic field of 1.2 T. These samples were prepared by a combination of the solid-state reaction and the mechanical ball milling methods.

Our results indicate that for all samples, a decrease in the MCE is observed over the entire temperature range with increasing frequency. The decrease in the effect with increasing frequency from 1 to 20 Hz is approximately 47%, 54% and 81%, respectively, for PSC-1300, 900, 600. A decrease in the grain size in  $\text{Pr}_{0.7}\text{Sr}_{0.2}\text{Ca}_{0.1}\text{MnO}_3$  manganite leads both to a decrease in the MCE and to a stronger frequency dependence of  $\Delta T$ . The decrease in the MCE depending on the size of the granules is presumably associated with a decrease in the magnetization, which is associated with a change in the ratio of the core and the near-surface layer of the granule. The strong frequency dependence of the MCE has a more complex origin and may be a combination of several frequency-dependent mechanisms that require more detailed studies.

The study was supported by the Russian Science Foundation grant No. 22-19-00610 (<https://rscf.ru/en/project/22-19-00610/>).

- [1] A. M. Aliev et al., *J. Alloys Compd.*, **676** (2016) 601.
- [2] A. M. Aliev et al., *J. Magn. Magn. Mater.*, **553** (2022) 169300.
- [3] A. G. Gamzatov et al., *J. Appl. Phys.*, **124** (2018) 183902.
- [4] B. Yu et al., *Int. J. of Refrigeration*, **33** (2010) 1029.
- [5] M. H. Phan and S. C. Yu, *JMMM*, **308** (2007) 325.

## PHASE SHIFT AT MAGNETOCALORIC EFFECT MEASUREMENTS IN AC MAGNETIC FIELDS AS A MARKER OF THE MAGNETIC PHASE TRANSITION ORDER

*Aliiev A.M., Alisultanov Z.Z., Gamzatov A.G.*

Amirkhanov Institute of Physics of DFRC RAS, Makhachkala, Russia

lowtemp@mail.ru

When studying the magnetocaloric effect in alternating magnetic fields, the material under study is exposed to an alternating magnetic field  $H = H_0 \sin \omega t$ , where  $H_0$  is the amplitude value of the magnetic field,  $\omega$  is the cyclic frequency of the magnetic field. The temperature response of a material to an alternating magnetic field can be represented as  $\Delta T = \Delta T_0 \sin(\omega t - \varphi)$ , where  $\Delta T_0$  is the amplitude value of the temperature change,  $\varphi$  is the phase shift between the magnetic field and the temperature response of the sample. With the conventional direct measurement of the MCE, we get only the value of the adiabatic temperature change  $\Delta T$ , while measuring in an alternating field, we get two parameters:  $\Delta T$  and phase shift  $\varphi$ . The latter parameter can provide valuable information about the behaviour of a magnetic system in alternating magnetic fields and some peculiarities of magnetic phase transitions.

In the work we present the results of direct measurements of the MCE in alternating magnetic fields of low amplitude (up to 3 kOe) and a frequency of 0.3 Hz in various magnetocaloric materials, including Gd, with a second-order ferromagnetic-paramagnetic phase transition, MnAs compound, with a first-order ferromagnetic-paramagnetic phase transition, Fe<sub>48</sub>Rh<sub>52</sub> alloy, in which a first-order transition from a low-temperature antiferromagnetic phase to a high-temperature ferromagnetic phase is observed, as well as two samples of the Heusler alloys: the first one is Ni<sub>49.3</sub>Mn<sub>40.4</sub>In<sub>10.3</sub>, in which a series of magnetic phase transitions are observed: high-temperature second-order ferromagnetic austenite-paramagnetic austenite transition, the magnetostructural austenite-martensite phase transition and transition to the ferromagnetic state in the martensite state, and the second one is Ni<sub>54</sub>Mn<sub>18</sub>V<sub>3</sub>Ga<sub>21</sub>In<sub>4</sub> with second order ferromagnetic-paramagnetic phase transition.

In the studied compositions, a strong dependence of the phase shift on the magnetic field was found in the region of the first order phase transitions, while at the point of the second order phase transition, the phase shift is almost independent of the magnetic field. The observed results can be explained on the basis of the fluctuation-dissipation theorem. At the second-order phase transition point, fluctuations of the order parameter are strongly developed and they are static, while near a first-order phase transition point, the fluctuations depend on time and rapidly decay. This results in absence a phase shift between the perturbation (magnetic field) and the response, in this case, the signal from the thermocouple at the point of the second-order phase transition. At the same time, due to the short lifetime of fluctuations in the region of first-order phase transitions, the dependence of the phase shift on the perturbing force or its frequency will be observed. It is also shown that phase shift anomalies are well manifested in the region of some magnetic phase transitions, for example, spin-reorientation transitions, which are usually weakly manifested in other physical parameters, such as magnetization, heat capacity, etc. The results obtained show that by studying the phase shift when measuring the MCE in alternating magnetic fields of low amplitude, one can detect some subtle magnetic phase transitions, as well as determine the order of magnetic phase transitions.

This work was supported by the Russian Science Foundation grant no. 22-19-00610.

3PO-L6-3

**PHASE STABILITY OF HEUSLER ALLOYS Ni-Co-Mn-Z (Z = Ga, In, Sn, Sb)***Erager K.R., Sokolovskiy V.V., Buchelnikov V.D.*

Chelyabinsk State University, Chelyabinsk, Russia

eragerk@rambler.ru

Nowadays, Mn-rich  $\text{Ni}_{2-x}\text{Co}_x\text{Mn}_{1+y}\text{Z}_{1-y}$  ( $Z = \text{In, Sn, Sb}$ ) Heusler alloys attract a particular attention due to exhibiting of various multifunctional properties such as the metamagnetic shape memory effect, the giant inverse magnetocaloric effect, the exchange bias effect and etc. It is known that the additional element at the Ni site in Heusler alloys can affect both magnetic and structural phase transitions, which leads to a change in the magnetocaloric properties. For example, doping of Co element at Ni site affects the critical temperatures and exchange interactions of martensite and austenite phases in  $\text{Ni}_{50}\text{Mn}_{30}\text{Ga}_{20}$  alloy [1]. However, the issues of phase stability of that alloys were not considered yet.

This work presents the results of a study of the properties of  $\text{Ni}_{2-x}\text{Co}_x\text{Mn}_{1+y}\text{Z}_{1-y}$  alloys ( $x = 0, 0.25$  and  $0.5$ , and  $y = 0, 0.25, 0.5$  and  $0.75$ ) where  $Z = \text{Ga, In, Sn, Sb}$ . The calculations were performed with the help of VASP software package [2], in the GGA-PBE approximation [3]. The integration of the Brillouin zone was carried out on a  $\Gamma$ -centered grid with a density of  $\sim 5000$  points per site of inverse lattice. Two cases of magnetic moment ordering were considered: ferromagnetic - FM and ferrimagnetic - FIM, as well as the arrangement of magnetic moment as «staggered» and «layered». The stability of the compounds was evaluated using the formula:

$$E_{dec} = E_{tot} - \sum_i E_i,$$

where  $E_{tot}$  is the total energy of the alloy, and  $E_i$  are the energies of the triple, binary compounds and isolated elements, which were calculated using the above-mentioned potentials, taking into account data from the Materials project electronic resource.

It is known [1] that increasing the Co concentration in non-stoichiometric Ni-Co-Mn-Z alloys ( $Z = \text{Ga, In, Sn, Sb}$ ) stabilizes the FM austenitic phase relative to the FIM staggered martensitic phase and results in disappearance the phase transition. However, for tetragonal FIM layered compositions, the opposite dependence is observed as the total energy of the layered martensite increases with increasing Co. In this connection, the main conclusion is that non-stoichiometric Ni-Co-Mn-Z Heusler alloys with a Mn excess of  $\sim 12.5\%$  tend to the ground state with FIM layered ordering. It is also important to note that  $\text{Ni}_{2-x}\text{Co}_x\text{Mn}_{1+y}\text{Z}_{1-y}$  alloys become less stable relative to  $\text{Ni}_2\text{MnZ}$  staggered structure with increasing concentrations Mn and Co because non-stoichiometry is a defect in the structure. At decreasing  $x$  and increasing  $y$  alloy tend to be stable, approaching the  $\text{Ni}_2\text{Mn}_2$  concentration with layered ordering FIM. The authors [4] demonstrated similar results of segregation calculations for ternary Heusler alloys.

This work was supported by the Ministry of Science and Higher Education of the Russian Federation within the framework of the Russian State Assignment under contract No. 075-01493-23-00. K.R. Erager gratefully acknowledges the Young Scientists Support Fund of the Chelyabinsk State University.

[1] F. Albertini et al., *Mater. Sci. Forum.*, **684** (2011) 151.

[2] G. Kresse, J. Furthmüller., *Phys. Rev. B.*, **54** (1996) 11169.

[3] J.P. Perdew, K. Burke, M. Ernzerhof., *Phys. Rev. Lett.*, **77** (1996) 3865.

[4] V.V. Sokolovskiy et al., *Phys. Rev. Materials*, **3(8)** (2019) 084413.

## THERMAL PROPERTIES OF AMORPHOUS FeNiSiC ALLOYS

*Kuvandikov O.K., Subkbankulov I., Khamraev N.S., Razhabov R.M., Imannaazarov D.Kh., Khomitov Sh.A.*

Samarkand State University named after Sharof Rashidov, Samarkand, Uzbekistan

sherxomitov@gmail.com

Amorphous alloys based on transition metals with additions of metalloids belong to the class of promising objects of modern materials science. This is due to the presence of unique properties in these alloys. In this regard, the study of the thermophysical properties of FeNiSiC amorphous alloys at high temperatures makes it possible to build a complete picture of the formation of a nanocrystalline state and reveal the features of the relationship between the crystalline and amorphous states.

To interpret the experimental results, the free volume model [1] was used, within which the concentration dependence of the specific heat capacity would be numerically calculated for these samples, for which the measured specific heat capacity does not change significantly in the temperature range from room temperature to 500°C. At temperatures above 500°C, the specific heat capacity decreases, and its lower value reaches its minimum value at a temperature of 520°C, i.e. the specific heat capacity decreases to a value of the order of 18÷20 J/g•K. Then the curve returns to the original value of the specific heat. After that, starting from a temperature of 655°C, a second decrease in the curve is observed and a decrease in the heat capacity to a temperature of 835°C, and starting from this temperature, it sharply decreases and Cp increases with increasing temperature.

According to the results of calorimetry, the thermal effects occurring in the sample during heating are considered, the desired value is the area under the curve on the graph. It is known that the area under the curve is its antiderivative function, the value of which is found by calculating a definite integral. Having only the results of the experiment on hand, the area on the graph was calculated by numerical integration using the trapezoidal method. The integration segment is divided into several intermediate segments, and the graph of the integrand is approximated by a broken line. The area of the integrand is approximately calculated by the sum of trapezoids. To eliminate the imperfection of the curve, the least squares method is used, which in this case made it possible to accurately calculate the area and, accordingly, the thermal effects occurring in the sample during heating. In this case, the magnitude of the thermal effect (enthalpy change) along the depth is  $\Delta H = -72834$  J/kg. It can be seen that this heat creates crystallization centers in amorphous alloys; one can observe that a first-order phase transition occurs.

Thus, the results of the calorimetric analysis show that no phase changes occur in the sample starting from room temperature to 500 °C, after which an increase in the temperature of the sample causes a significant thermal effect, the first thermal effect being observed at a temperature of 500°C and it continues up to the temperature 525°C. This thermal effect corresponds to the first type of phase transition according to the type of crystallization.

[1] K. Russew, L. Stojanova, *Glassy Metals* (Berlin: Springer, 2016).

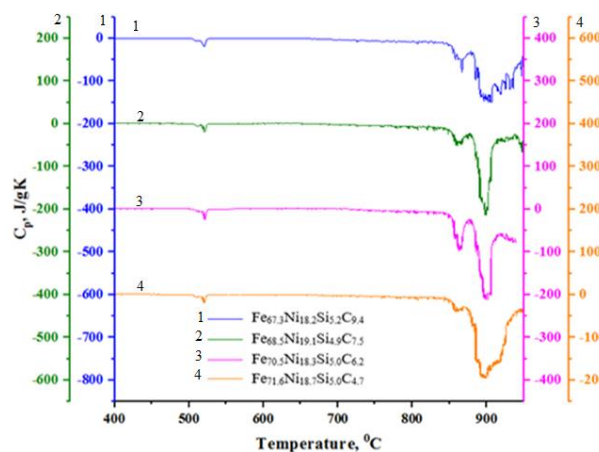


Figure 1. Graph of the dependence of the specific heat capacity of the samples on temperature

3PO-L6-5

## THERMAL CONTACT RESISTANCE AT COPPER-GRAPHENE-COPPER INTERFACE IN STRONG MAGNETIC FIELDS

*Kolesov K.A.<sup>1</sup>, Mashirov A.V.<sup>1</sup>, Kuznetsov A.S.<sup>1</sup>, Chibikov M.V.<sup>2</sup>, Koledov V.V.<sup>1</sup>, Shavrov V.G.<sup>1</sup>*

<sup>1</sup> Kotelnikov IRE RAS, Moscow, Russia

<sup>2</sup> National University of Science and Technology "MISIS", Moscow, Russia

kolesovkka@mail.ru

The implementation of magnetic cooling at cryogenic temperatures is possible using mechanical or gas thermal switches. In turn, the development of mechanical thermal switches requires mechanically resistant thermal interfaces for periodic operation. The aim of this work is to study the possibilities of multilayer graphene as a thermal interface. The paper investigates a detachable contact pair of copper blocks (movable and fixed) and a graphene interface, synthesized on the contact surface of a movable copper block. The contact surfaces of the studied samples were ground and polished, and then the quality of the surface was checked using scanning probe microscopy. Graphene was synthesized in an atmosphere of hydrogen and argon using a PlanarTech GP-CVD-2S setup. The number of graphene layers was determined using Raman spectroscopy based on the ratio of the intensities of G and 2D peaks, which are well studied in the Raman spectrum of graphene [1]. The intensity ratios obtained showed the presence of 3 to 7 graphene layers. For measuring the thermal contact resistance (TRC), a detachable contact pair 1 was placed in a cryostat, the fixed copper sample (position 3) was attached to the rod in the region of the magnetic field, and the movable one (position 4) was attached to the rod of a linear electric motor. Both samples were attached through a PTFE spacer to sample holders made of ABS plastic. The temperature change of the samples was determined using «Cernox» sensors (position 2), and type-T differential thermocouples (position 1). At the opposite end of the copper sample from the contact surface, a heater made of nichrome wire with a resistance of  $4.4 \Omega$  was glued to set the required temperature. To determine the TRC, we used the method for nonstationary heat flow described in [2]. The samples were cooled in helium by cooling the rod using a cryocooler operating on a closed Gifford-McMahon cycle, after which the helium was evacuated and the vacuum evacuation post was turned on, creating a pressure of  $4.5\text{-}5 \cdot 10^{-5}$  mbar. TRC was measured in the temperature range from 15 K to 140 K in magnetic fields of 2, 5, and 10 T. For example, near a temperature of 75K, where the maximum magnetocaloric effect of the GdNi<sub>2</sub> alloy is observed, TRC was about  $2.0 \cdot 10^{-5}$  m<sup>2</sup>K/W, and in a magnetic field of 10 T –  $1.2 \cdot 10^{-5}$  m<sup>2</sup>K/W, that is, a decrease TCR of this thermal interface under the influence of a magnetic field.

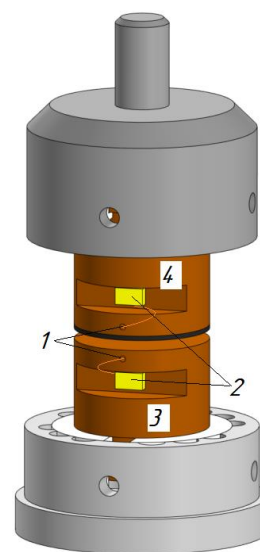


Figure 1. Sample mounting scheme

The study was supported by a grant from the Russian Science Foundation (project no. 20-19-00745, <https://rscf.ru/project/20-19-00745/>).

[1] Y.Hwangbo et al., *Carbon*, **77** (2014) 454–461.

[2] V.M. Popov *Teploobmen v zone kontakta raz'emnuch i ne raz'emnuch soedineni* (Moscow: Energiya, 1971).

## MAGNETORESISTANCE AND MAGNETOCALORIC EFFECT OF $Mn_5Si_3$ COMPOUND UNDER ISOTHERMAL AND ADIABATIC CONDITIONS

*Kuznetsov A.S.<sup>1</sup>, Mashirov A.V.<sup>1</sup>, Musabirov I.I.<sup>2</sup>, Kolesov K.A., Shavrov V.G.<sup>1</sup>*

<sup>1</sup> Kotelnikov IRE RAS, Moscow, Russia

<sup>2</sup> Institute for Metals Superplasticity Problems RAS, Ufa, Russia

kuznetsovalserg@gmail.com

At present, alloys that undergo magnetic and magnetostructural phase transformations (PT) are of considerable interest to researchers due to the combination of their multifunctional properties. The study of such phase transitions makes it possible to establish the mechanisms of the formation of magnetic ordering and the regularities of the behavior of the system in the critical region of the phase transition, as well as to determine the change in magnetothermal parameters: magnetization  $M$ , electrical resistance  $\rho$ , heat capacity  $C_p$ , etc.

One of the most important parameters that determine the influence of external conditions on the state of the system and the change in its parameters is the temperature  $T$  at which the phase transformation occurs. The determination of the characteristic temperature of the phase transformation is possible from the data of measurements of the temperature dependences of the magnetization  $M(T)$  or electrical resistance  $\rho(T)$  of the materials under study, by extrapolating the curves in the region of a significant difference in the parameters of the two phases. In addition, using the curves of isothermal magnetization  $M(H)$  or electrical resistance  $\rho(H)$ , one can determine the magnitude of the magnetic field strength  $H$  at which the phase transition is induced. Mostly, measurements of temperature  $M(T)$ ,  $\rho(T)$  and field  $M(H)$ ,  $\rho(H)$  dependences are carried out in stationary magnetic fields under isothermal conditions [1, 2]. However, if pulsed magnetic fields are used, then the latter can also be obtained under adiabatic conditions [3, 4]. An alternative for measuring  $M$  and  $\rho$  under adiabatic conditions can be the use of the extraction method [4] in stationary magnetic fields. There are differences between the characteristic temperature of the phase transition and the magnetic field strength at which the phase transition is induced, determined under isothermal and adiabatic conditions, which will be considered in the framework of this work.

In this work, the extraction method of measurement [5] is implemented, with the help of which the study of the magnetotransport and magnetocaloric properties of a sample of the  $Mn_5Si_3$  compound under adiabatic and isothermal conditions at cryogenic temperatures in the range from 25 K to 110 K in strong magnetic fields up to 10 T was carried out. The obtained dependences  $\rho(T)$  and  $\rho(H)$  are compared under different thermodynamic conditions. The results of the magnitude of the magnetocaloric effect obtained for a sample of the  $Mn_5Si_3$  compound in the region of the magnetostructural phase transition are discussed.

The study was supported by a grant from the Russian Science Foundation (project no. 20-19-00745, <https://rscf.ru/project/20-19-00745/>).

- [1] C. Surgers et al., *Scientific Reports*, **7** (2017) 42982
- [2] R. F. Luccas et al., *J. Magn. Magn. Mater.*, **489** (2019) 165451
- [3] M. Tokunaga et al., *Phys. Rev. B*, **59** (1999) 11151
- [4] K. Kamishima et al., *Phys. Rev. B*, **63** (2000) 024426
- [5] Yu.S. Koshkid'ko et al., *J. Magn. Magn. Mater.*, **433** (2017) 234.
- [6] A.S. Kuznetsov et al., *Phys. Met. Metallogr.*, **123** (2022) 397–401.

## MAGNETOCALORIC EFFECT IN $R_5Si_4$ ( $R = Tb, Dy, Ho$ ) ALLOYS

*Utarbekova M.V., Orshulevich M.A., Taskaev S.V., Bataev D.S.*

Chelyabinsk State University, Chelyabinsk, Russia

shchichko.marina.csu@gmail.com

Currently, a large number of materials with large magnetocaloric effect (MCE) have been studied at low temperatures, however, interest in a such materials is only growing up. Liquefied natural gases has become one of the strategic energy carriers, thus, a fundamentally new approach to the liquefaction of natural gases based on MCE is being actively developed [1]. Among them the binary systems based on  $4f-3d$  metals are very promising for practical application, especially alloys with the structure of Laves phase -  $AB_2$  [2, 3]. But these compounds have a high content of  $4-f$  element. Therefore, the investigation for alloys in which it is possible to reduce the content of rare-earth component as a expense of transition metals continues. This prompted us to study magnetic and magnetocaloric properties in  $R_5Si_4$  ( $R = Tb, Dy, Ho$ ) compounds in magnetic fields up to 3 T.

The results of measurements of the magnetic hysteresis loops, at  $T = 50$  K, showed that these compounds have a small coercive force and showed tendency to saturation at small external magnetic fields, which agrees with other literature data [4].

The change of magnetic entropy reaches a maximum value of  $\Delta S_m \approx 1,6 \text{ J/kg}^{-1}\text{K}^{-1}$  for  $Tb_5Si_4$ ,  $\Delta S_m \approx 77,6 \text{ J/kg}^{-1}\text{K}^{-1}$  for  $Dy_5Si_4$ , and  $\Delta S_m \approx 1,8 \text{ J/kg}^{-1}\text{K}^{-1}$  for  $Ho_5Si_4$  at the magnetic field change 3 T, and MCE is observed in two broad temperature ranges of 55-160 K and 170-300 K for  $Tb_5Si_4$ , 50-100 K and 105-300 K for  $Dy_5Si_4$ , and 50-60 K and 75-300 K for  $Ho_5Si_4$  due to the rich sequence of magnetic phase transitions in these compounds (see Figure 1).

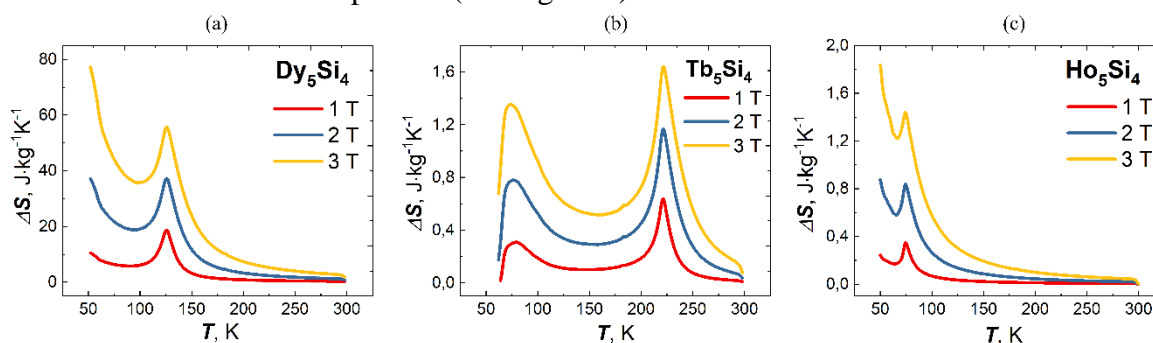


Figure 1. Temperature dependences of magnetic entropy change for  $Dy_5Si_4$  (a),  $Tb_5Si_4$  (b) and  $Ho_5Si_4$  (c).

Authors thanks for the financial support Russian Science Foundation grant No. 22-22-20033.

[1] A. Kitanovski, *Adv. Energy Mater.*, **10** (2020) 1903741.

[2] V. Franco, *Prog. Mater. Sci.*, **93** (2018) 112–232.

[3] W. Liu et al., *Applied Materials Today*, **29** (2022) 101624.

[4] Y. I. Spichkin, V. K. Pecharsky, and K. A. Gschneidner, *J. Appl. Phys.*, **89** (2001) 1738-1745.

## LABORATORY-TYPE MAGNETOCALORIC AND MULTICALORIC PROTOTYPE DEVICES

*Amiron A.A.<sup>1,2</sup>, Yurin I.A.<sup>1</sup>*

<sup>1</sup> National Research Centre “Kurchatov Institute”, Moscow, Russia

<sup>2</sup> Amirkhanov Institute of Physics, DGSC RAS, Makhachkala, Russia

amiroff\_a@mail.ru

In recent years, the multicaloric effect has been actively studied as one of the promising approach for solid-state cooling systems operating on ordinary caloric effects. Systems based on the multi-stimuli with combination of the magnetic field and uniaxial (isotropic) stress were presented and compounds with first-order magnetic phase transition were proposed as working material [1-2]. In our work, two different prototype of cooling systems based on classical magnetocaloric (MCE) and multicaloric effect (multiCE) have been proposed. The main requirements for the prototypes were: price and availability of parts; compliance with existed magnetocaloric prototypes; easy to manufacture and assemble in laboratory.

As known, prototypes of magnetic cooling systems are divided into two types: linear and rotational. In prototypes with a linear type of displacement, a magnetic regenerator or a magnetic field source moves linearly along one axis, and in rotational ones, the principle of operation is based on the analogy of the rotor operation in which a magnetic regenerator or magnet rotates around a central axis. The first versions of linear and rotational prototypes were developed. Technical solutions made it possible to produce prototypes in laboratory conditions, the main structural elements were printed using a 3D printer, and standard CNC-based solutions. To implement the chosen concept, digital version of prototypes were first created using Autodesk Inventor and Solidworks packages, and magnetic field sources were calculated in COMSOL Multiphysics. Based on digital models, the first versions of real prototype models were created.

Magnetic field sources with a Halbach structure were used with 1.45 T– for a linear type and 1 T- for rotational, uniaxial compression was created using a linear actuator with a maximum load of up to 1500 N. The test MCE and multiCE experiments were carried out by direct method through measurements of adiabatic temperature changes  $\Delta T$  under various regimes of applied magnetic field and uniaxial compression (load removal) using a copper-constantane thermocouple glued to a sample.

Test experiments of MCE and multiCE measurements for  $\text{LaFe}_{11.4}\text{Mn}_{0.3}\text{Si}_{1.3}\text{H}_{1.6}$  alloy ( $T_c \sim 295$  K) showed that the absolute values of  $|\Delta T|$  strongly depend on the adiabaticity of the experimental conditions. The absolute values of  $|\Delta T|$  for MCE are in the range of 2.2-2.5 K ( $\Delta\mu_0 H=1.45$  T, linear prototype) and 0.8-1 K ( $\Delta\mu_0 H=1$  T, rotational prototype). The observed values of  $|\Delta T|$  during uniaxial compression (load removal) did not exceed 0.5 K. Further work will be aimed at upgrading prototypes by improving thermal insulation, magnetic system, cycle automation with a combination of magnetic field application and uniaxial compression, etc.).

[1] T. Gottschall et al, *Nat. Mater.*, **17** (2018) 929–934.

[2] A. Czernuszewicz et al, *Energy Convers. Manag.*, **178** (2018) 335–342.

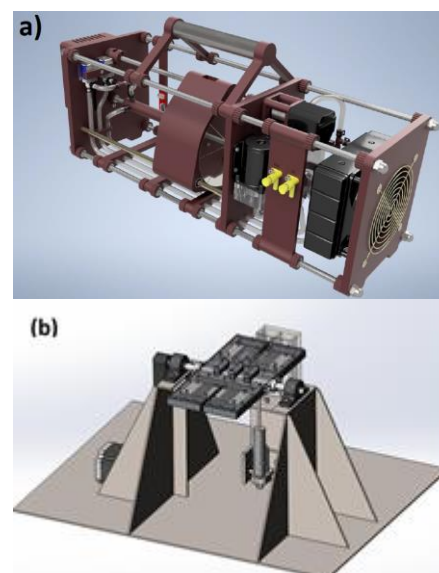


Figure 1. Digital versions of linear (a) and rotational (b) prototype.

## EFFECT OF HYDROGEN ON THE MAGNETIC PROPERTIES OF MULTICOMPONENT COMPOUNDS (Tb,Dy,Ho)(Co,Fe)<sub>2</sub>

*Pankratov N.Yu.<sup>1</sup>, Politova G.A.<sup>2,3</sup>, Aleroev A.-R.A.<sup>4</sup>, Tereshina I.S.<sup>1</sup>*

<sup>1</sup> Lomonosov Moscow State University, Faculty of Physics, Moscow, Russia

<sup>2</sup> Baikov Institute of Metallurgy and Materials Science RAS, Moscow, Russia

<sup>3</sup> Peter the Great St. Petersburg Polytechnic University, St. Petersburg, Russia

<sup>4</sup> Grozny State Oil Technical University, Grozny, Russia

irina\_tereshina@mail.ru

It is known that hydrogen easily penetrates the crystal lattice of rare-earth intermetalides, causing significant changes in their magnetic properties. RT<sub>2</sub> compounds (R – rare-earth metals, T – Fe, Co) with Laves phase C15 structure absorb hydrogen at room temperature and atmospheric pressure. They have not only simple crystal but also magnetic structure. As result, RT<sub>2</sub> compounds are convenient model objects for studies of fundamental physics and applications. Of particular importance is the effect of a dosed content of hydrogen on the magnetic properties of RT<sub>2</sub> compounds.

In our work the structure and magnetic properties of TbCo<sub>2</sub>, Tb<sub>0.3</sub>Dy<sub>0.7</sub>Co<sub>2</sub>, Tb<sub>0.3</sub>Dy<sub>0.7</sub>Fe<sub>2</sub>, Tb<sub>0.15</sub>(Dy<sub>0.5</sub>Ho<sub>0.5</sub>)<sub>0.85</sub>Co<sub>2</sub>, and Tb<sub>x</sub>(Dy<sub>0.5</sub>Ho<sub>0.5</sub>)<sub>1-x</sub>Co<sub>1.75</sub>Fe<sub>0.25</sub> (x = 0.3, 0.4, 0.5) compounds and their hydrides with both low and high hydrogen content were studied. It was established that the unit cell volume increases at hydrogenation and reaches 25% in the maximum hydrogen content equal to 4 H at./f.u. In Fe-free compounds, the Curie temperature (T<sub>C</sub>) exhibits slight increase at low hydrogen content while it sharply decreases at high hydrogen content. This is due to the existence of two types of tetrahedral interstice in the MgCu<sub>2</sub>-type structure, which hydrogen can occupy AB<sub>3</sub> and A<sub>2</sub>B<sub>2</sub> (where A is Tb atoms, B is Fe or Co atoms). Hydrogen atoms predominantly occupy interstice A<sub>2</sub>B<sub>2</sub>, followed by interstice AB<sub>3</sub> [1].

Magnetocaloric and magnetostrictive properties of the obtained compounds were studied. The magnetocaloric effect (MCE) was carried out by both direct and indirect methods. The magnetostriction was studied by the strain gauge techniques. The peculiarities in the field and temperature dependencies of both the magnetostriction and the MCE were obtained both in the moderate magnetic fields (up to 1.8 T) and in high magnetic fields (up to 14 T) in a wide temperature range.

The main regularities of the hydrogen effect on the functional magnetic characteristics of (Tb,Dy,Ho)(Co,Fe)<sub>2</sub> compounds depending on the hydrogen content, as well as on the type of 3d-transition metal (cobalt or iron) were established. It was shown that the Curie temperature shift and the giant force magnetostriction have the same mechanism. Both effects are due to the change in the exchange integral at lattice expansion. Hydrides with a new set of magnetic properties (including the compensated compositions) were obtained. They can be used in hydrogen power engineering. The materials with a joint manifestation of the magnetocaloric effect and volume magnetostriction are useful for robotics.

The research was supported by project no. 22-29-00773 from the Russian Science Foundation, <https://rscf.ru/project/22-29-00773/>.

[1] N. Mushnikov et.al., *Phys. Metals Metallogr.*, **100** (2005) 338.

3PO-L6-10

## MAGNETIC PROPERTIES OF B-DOPED Mn-Ga-C-BASED ALLOYS

*Dubenko I.<sup>1</sup>, Oli A.<sup>1</sup>, Duncan J.<sup>1</sup>, Granovsky A.<sup>2</sup>, Kosbkid'ko Yu.<sup>3</sup>, Stadler S.<sup>4</sup>, Talapatra S.<sup>1</sup>, Ali N.<sup>1</sup>*

<sup>1</sup> School of Physics and Applied Physics, Southern Illinois University, Carbondale, USA

<sup>2</sup> Lomonosov Moscow State University, Moscow, Russia

<sup>3</sup> Institute of Low Temperature and Structural Research, PAS, Wroclaw, Poland

<sup>4</sup> Department of Physics & Astronomy, Louisiana State University, Baton Rouge, USA

igor\_doubenko@yahoo.com

By utilizing a simple ball milling technique, we have synthesized boron doped Mn-Ga-C magnetocaloric materials. In general, we have found that the milling of pristine elements followed by an application of pressure, and subsequent annealing under an ultra-high purity Ar atmosphere of for 24 hours resulted in single-phase compounds of  $\text{Mn}_{60}\text{Ga}_{20}\text{C}_{20}$  with the antiperovskite cubic structure (space group:  $\text{Pm}\bar{3}\text{m}$ ). These compounds are characterized by very distinctive temperature dependencies which are typical for Heusler alloys undergoing a temperature-induced structural transition from an antiferromagnetic martensitic phase to a ferromagnetic austenitic phase with increasing temperature (similar to that observed for Ni-Mn-In based Heusler alloys). However, FM order at low temperature results in an expansion of cell volume. An intermediate magnetic state of the austenitic phase has also been detected.

$\text{Mn}_{60}\text{Ga}_{20}\text{C}_{20}$  shows magnetic and structural instability below room temperature and a rather large magnetocaloric effect (MCE): the adiabatic temperature and magnetic entropy changes of about -3.1 K and  $14 \text{ J}(\text{kgK})^{-1}$  at about 170 K, respectively, have been reported in Ref. [1].

In the present work, we report the results of our studies of the magnetic behavior of the B-doped  $\text{Mn}_{60}\text{Ga}_{20}\text{C}_{20-x}\text{B}_x$  system with  $x=0, 2, 3$  and 5.

According to the XRD diffraction data, all samples can be described as single phase compounds (i.e., with the antiperovskite cubic structure) where impurity phases did not exceed 5 %.

The compounds with  $x < 5$  show similar behavior as the parent  $\text{Mn}_3\text{GaC}$ , which generally can be described by a low temperature transition from low to high magnetization states and a transition at Curie temperature. The relatively higher B concentration was found to completely suppress the antiferromagnetic state (see Figure 1 for  $x=5$ ). The  $(T-x)$  phase diagram for  $H=100 \text{ Oe}$  has been evaluated and will be discussed. The inverse MCE results with magnetic entropy changes of  $-(8-12) \text{ J}(\text{kgK})^{-1}$  for magnetic field changes of 50 kOe at the transition temperatures were observed. It is important to note that the thermal hysteresis of the  $M(T)$  curves were found to depend on the B concentration. The hysteresis of about 40 K for  $x=0$  drastically decreased to 4 K (i.e., by a factor of 10) for  $\text{Mn}_{40}\text{Ga}_{20}\text{C}_{17}\text{B}_3$  (see in Figure 1).

S.Stadler, N. Ali, J. Duncan, I. Dubenko, S. Talapatra, A.Oli, acknowledge support from the U.S. Department of Energy (DE-FG02-13ER46946, DE-FG02-06ER46291).

[1] Ö. Çakır and M. Acet, *Appl. Phys. Lett.*, **100** (2012) 202404.

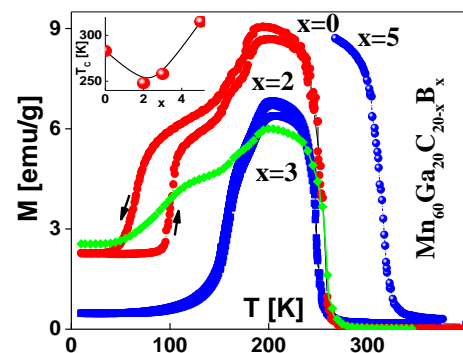


Figure 1.  $M(T)$  curves of  $\text{Mn}_{60}\text{Ga}_{20-x}\text{B}_x$  alloys. Inset:  $(T_C-x)$  phase diagram

**July 3**

Monday

18:00 - 20:00

POSTER  
SESSIONS

Section L7

**Magnetism and  
Superconductivity**

## CRITICAL TEMPERATURE OF SUPERCONDUCTOR/ANTIFERROMAGNET HETEROSTRUCTURES

*Bobkov G.A.<sup>1</sup>, Bobkova I.V.<sup>1</sup>, Bobkov A.M.<sup>1</sup>, Gordeeva V.M.<sup>1</sup>, Golubov A.A.<sup>2</sup>*

<sup>1</sup> Moscow Institute of Physics and Technology, Dolgoprudny, Russia

<sup>2</sup> University of Twente, 7500 AE Enschede, The Netherlands

gabobkov@mail.ru

In this work we study theoretically two different manifestations of the sign-flipping Neel triplet correlations, which are induced in superconductor/antiferromagnet (S/AF) heterostructures by proximity effect [1]. The first one is the oscillating dependence of the superconducting critical temperature of S/AF bilayers on the length of the AF region. It occurs due to the oscillating character of the Neel triplet pair wave function, which in its turn originates from the Umklapp scattering processes at the S/AF interface. This prediction could give a possible explanation for available experimental data [2-4].

The second issue is the interplay of the Neel triplets with Rashba spin-orbit coupling (SOC) in thin-film S/AF structures. A unique effect of anisotropic enhancement of proximity-induced triplet correlations by the SOC is predicted. It manifests itself in the anisotropy of the superconducting critical temperature with respect to orientation of the Neel vector relative to the S/AF interface, which is opposite to the analogous effect in superconductor/ferromagnet structures. The sign of the anisotropy is controlled by the chemical potential of the superconductor and, therefore, can be adjusted in (quasi)2D structures.

The work was supported by RSF project № 22-22-00522

[1] G.A. Bobkov et al., *Phys. Rev. B*, **106** 144512 (2022).

[2] C. Bell et al., *Phys. Rev. B*, **68** (2003) 144517 (2003).

[3] M. Hubener et al., *Journal of Physics: Condensed Matter*, **14** (2002) 8687.

[4] B.L. Wu et al., *APL*, **103** (2013) 152602.

3PO-L7-2

## INVESTIGATION OF THE FEATURES OF A SUPERCONDUCTING SPIN VALVE Fe1/Cu/Fe2/Cu/Pb ON A PIEZOELECTRIC SUBSTRATE PMN-PT

*Kamashev A.A., Garifyanov N.N., Validov A.A., Mamin R.F., Garifullin I.A.*

Zavoisky Physical-Technical Institute, FRC Kazan Scientific Center of RAS, Kazan, Russia  
kamandi@mail.ru

The properties of a superconducting spin valve Fe1/Cu/Fe2/Cu/Pb on a piezoelectric substrate PMN-PT substrate ( $[\text{Pb}(\text{Mg}_{1/3}\text{Nb}_{2/3})\text{O}_3]_{1-x} - [\text{PbTiO}_3]_x$ ) under the influence of an electric and magnetic field have been studied. The magnitude of the shift of the superconducting transition temperature in the magnetic field  $H = 1$  kOe equal to 150 mK was detected, while the full superconducting spin valve effect was demonstrated. Abnormal behavior of superconducting transition temperature was shown, which manifests itself in the maximum values of superconducting transition temperature with orthogonal orientation of the magnetization vectors of ferromagnetic layers, when studying the angular dependence of superconducting transition temperature in an external magnetic field (see Figure 1). This may indirectly indicate the fixation of the magnetization vector of the Fe1-layer on a PMN-PT piezoelectric substrate. It was found that with an increase in the magnitude of the applied electric field to the PMN-PT substrate, the shift in superconducting transition temperature of the Fe1/Cu/Fe2/Cu/Pb heterostructure increases. The maximum shift was 10 mK when an electric field of 1 kV/cm was applied (see Figure 2).

The reported study was funded by Russian Science Foundation according to the research project No. 21-72-10178.

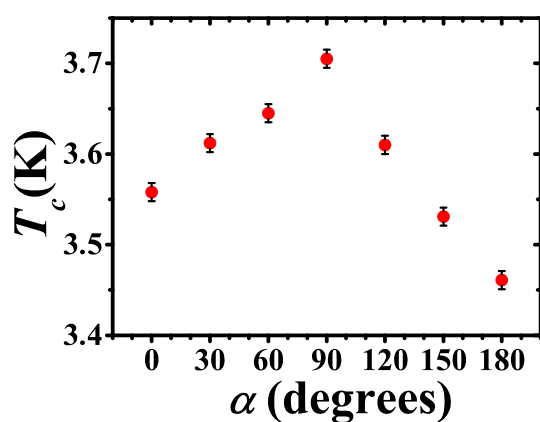


Figure 1. Dependence of  $T_c$  on the angle  $\alpha$  between the direction of the cooling field used to fix the direction of the magnetization of the Fe1 layer and the applied magnetic field  $H = 1$  kOe that rotates the magnetization of the Fe2 layer.

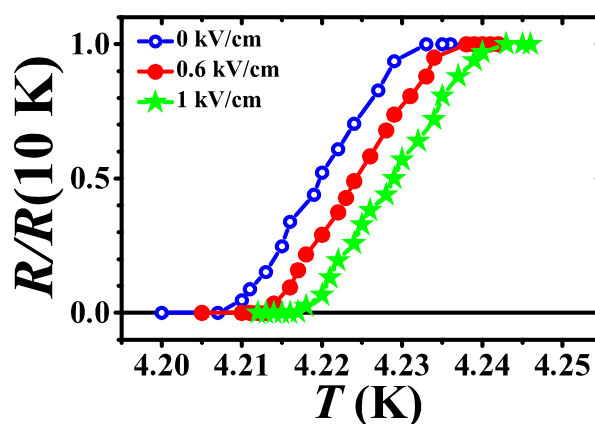


Figure 2. Superconducting transitions curves for the sample PMN-PT/Fe1(3nm)/Cu(4nm)/Fe2(1nm)/Cu(1.2nm)/Pb(60nm)/Si<sub>3</sub>N<sub>4</sub> when applying an electric field to PMN-PT substrate: shift of  $T_c$  is 5 mK when applying an electric field 0.6 kV/cm; shift of  $T_c$  is 10 mK when applying an electric field 1 kV/cm. The error of the experiment corresponds to the size of the characters.

## DESCRIPTION OF UNCONVENTIONAL SUPERCONDUCTIVITY IN THE REGIME OF STRONG FLUCTUATIONS IN THE FRAMEWORK OF THE MODIFIED EFFECTIVE COLEMAN-WEINBERG ACTION

*Siraev F.M., Avdeev M.V., Proshin Yu.N.*

Theoretical Physics Department, Institute of Physics, Kazan Federal University, Kazan, Russia  
yurii.proshin@kpfu.ru

Fluctuations play a crucial role in understanding the transport and critical properties of low-dimensional materials with unconventional superconductivity, significantly affecting the behavior of the material, especially near the critical temperature at which superconductivity occurs [1]. Here one can note the unusual temperature dependence of the superfluid density in ultrathin copper oxide films [2], hysteretic switching between superconducting and normal states with well-defined critical and retrapping currents in two-dimensional superconductors [3] and many other striking phenomena (see review [1]).

We propose and discuss an approach for describing the 2D d-wave superconducting state, that takes into account fluctuations in the superconducting order parameter, where the pair interaction is given by a superexchange potential of the form

$$V(\mathbf{k}_1, \mathbf{k}_2) = -J(e_{\mathbf{k}_1}^s e_{\mathbf{k}_2}^s + e_{\mathbf{k}_1}^d e_{\mathbf{k}_2}^d), \quad e_{\mathbf{k}}^{s,d} = \cos(k_x) \pm \cos(k_y)$$

Using the variational perturbation theory, we derive, similarly to the effective Coleman-Weinberg action [4], for a mixed *s*- and *d*-wave two-component superconducting order parameter  $\Phi = \Phi_s e_{\mathbf{k}}^s + \Phi_d e_{\mathbf{k}}^d$ . The corresponding components  $\Phi_s$  and  $\Phi_d$  are found from minimizing the effective action.

Numerical calculations were performed using the band parameters obtained from experimental data on photoemission for YBCO compounds [5].

Within the framework of this approach, the temperature dependence of the amplitude of the order parameter and the critical temperature of the superconducting transition are calculated. It is shown that the critical temperature renormalized due to fluctuations is much lower than the value obtained in the mean field approximation. The features of the temperature dependence of the order parameter near the superconducting transition are discussed.

Within the framework of this approach, the temperature dependence of the amplitude of the order parameter and the critical temperature of the superconducting transition were calculated. It is shown that the critical temperature renormalized due to fluctuations is much lower than the value obtained in the mean field approximation. The features of the temperature dependence of the order parameter near the superconducting transition are discussed.

This paper has been supported by the Kazan Federal University Strategic Academic Leadership Program.

- [1] T. Uchihashi, *Superconductor Science and Technology*, **30** (2016) 013002.
- [2] I. Hetel, T.R. Lemberger, M. Randeria, *Nature Physics*, **3** (2007) 700-702.
- [3] T. Uchihashi, P. Mishra P., Aono, Nakayama T., *Phys. Rev. Lett.*, **107** (2011) 207001.
- [4] S. Coleman, E. Weinberg, *Phys. Rev. D*, **7** (1973) 1888-1910.
- [5] M.R. Norman, *Phys. Rev. B*, **63** (2001), 092509.

## SUPERCONDUCTING STATES AND PROPERTIES OF DOPED HIGH- $T_c$ CUPRATES

*Dzhumanov S.<sup>1</sup>, Mayinova U.K.<sup>2</sup>*

<sup>1</sup> Institute of Nuclear Physics, Ulugbek, Tashkent, Republik of Uzbekistan

<sup>2</sup> Samarkand State University named after Sharof Rashidov, Samarkand, Uzbekistan

dzhumanov@inp.uz, umayinova@gmail.com

We show that the temperature-dependent superconducting order parameter and related superconducting properties (in particular, the temperature dependences of specific heat, superfluid density and related London penetration depth) of high-  $T_c$  cuprates are fundamentally different from those of conventional superconductors and cannot be understood within the existing theories based on the Bardeen-Cooper-Schrieffer (BCS)-type condensation of weakly-bound Cooper pairs into a superfluid Fermi- liquid and on the usual Bose-Einstein condensation (BEC) of bosonic Cooper pairs. We examine the validity of an alternative approach to the unconventional superconductivity in high-  $T_c$  cuprates and establish that these materials exhibiting a  $\lambda$ -like superconducting transition at the critical temperature  $T_c$  are similar to the superfluid  $^4\text{He}$  and are also superfluid Bose systems. We argue that the doped high- $T_c$  cuprates from underdoped to overdoped regime are unconventional (bosonic) superconductors and the tightly-bound (polaronic) Cooper pairs in these polar materials behave like composite bosons just like  $^4\text{He}$  atoms and condense into a Bose superfluid at  $T_c$ . We identify the superconducting order parameter  $\Delta_{SC}$  in underdoped and optimally doped cuprates as the coherence parameter  $\Delta_B$  of bosonic Cooper pairs, which appears just below  $T_c$  and has a kink-like temperature dependence near the characteristic temperature  $T_c^* < T$ . We find that the  $\lambda$ -like specific heat anomaly in high- $T_c$  cuprates near  $T_c$  predicted by the theory of Bose-liquid superconductivity is similar to that observed both in superfluid  $^4\text{He}$  near  $T_\lambda$  and in Hg-based cuprate superconductor  $\text{HgBa}_2\text{Ca}_2\text{Cu}_3\text{O}_8$  near  $T_c \cong 132\text{K}$ . We demonstrate that in high- $T_c$  superconductor  $\text{YBa}_2\text{Cu}_3\text{O}_{6.97}$  the superfluid density  $\rho_c$  exhibits distinctly different temperature dependences in the temperature ranges  $0 \leq T \leq T_c^*$  and  $T_c^* < T < T_c$ . In this superconductor, a pronounced anomaly in  $\rho_c(T)$  exists near  $T_c^* \cong 0.4T_c$  and the temperature dependence of  $\lambda_L^2(0)/\lambda_L^2(T)$  below  $T^*$  deviates downwards from the high-temperature behavior (see Figure 1.).

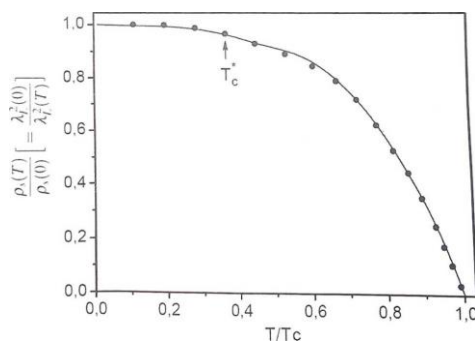


Figure 1. The temperature dependence of  $\Delta_{SC}(T)$  in YBCO calculated using the parameters  $\rho_B = 1.41 \times 10^{19} \text{cm}^{-3}$ ,  $m_B = 5.0m_e$  and  $\xi_{BA} = 0.08\text{eV}$  and a pronounced kink-like feature in  $\Delta_{SC}(T)$  near  $T_c^*$ .

Our results for the normalized superfluid density  $\rho_s(T)/\rho_s(0) = \lambda_L^2(0)/\lambda_L^2(T)$  are in good agreement with the experimental data on the temperature dependence of  $\lambda_L^2(0)/\lambda_L^2(T)$  in  $\text{YBa}_2\text{Cu}_3\text{O}_{6.97}$ . The anomalous temperature dependences of specific heat and superfluid density observed in Hg- and Y-based high- $T_c$  superconductors are clear signatures of Bose-liquid superconductivity.

## INFLUENCE OF MAGNONS ON THE SUPERCONDUCTING STATE IN SUPERCONDUCTOR-MAGNET HETEROSTRUCTURES

*Ianovskaia A.S., Bobkov A.M., Bobkova I.V.*

Moscow Institute of Physics and Technology, Moscow, Russia  
sveti24h@mail.ru

It is well known that the proximity effect in thin-film hybrid superconductor/ferromagnetic insulator structures provides the suppression of the superconductivity [1] and Zeeman splitting of the density of states in the superconductors [2]. In this work we investigate the influence of ferromagnetic magnons on this effect. The density of states in the superconductor (DOS) and the quasiparticle spectra are calculated in the framework of Gor'kov Green's function approach (Figure 1). It is obtained that the interaction of superconducting electrons with magnons can result in a decrease of the Zeeman splitting of the DOS coherence peaks. It also inverts the ratio between the internal and external coherence peaks and smears the external peaks. The temperature dependence of the observed DOS characteristic features is investigated. It is demonstrated that quasiparticle spectra are also strongly modified by the electron-magnon interaction revealing characteristic kinks (Figure 2). The sensitivity of the results to the choice of materials and relevance to experiments are discussed.

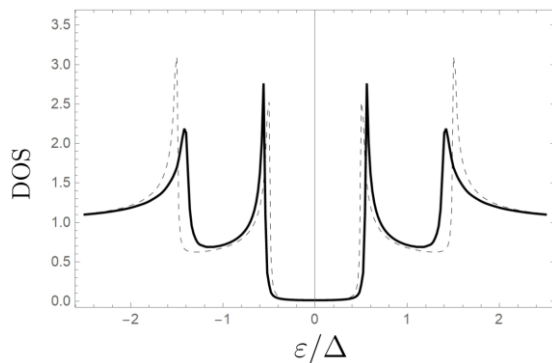


Figure 1. DOS. Dashed line is for the standard DOS of a superconductor; solid line is for the DOS, which is modified by the electron-magnon interaction.

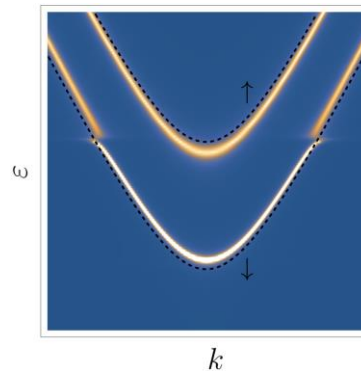


Figure 2. Quasiparticle spectra. Dashed lines are the branches of the standard spectra of the superconductor; solid lines are for the branches of the spectra, which are modified by the magnon influence.

The support by RSF project No. 22-42-04408 is acknowledged.

[1] G. Sarma, *J. of Phys. and Chem. of Solids*, **24** (1963) 1029.

[2] E. Strambini et al., *Phys. Rev. Materials*, **1** (2017) 054402.

July 3

18:00 - 20:00

Monday

POSTER  
SESSIONS

Section L8  
**Multiferroics**

## MAGNETOELECTRIC EFFECT IN LAYERED HETEROSTRUCTURE ANTIFERROMAGNET - PIEZOELECTRIC

Burdin D.<sup>1</sup>, Fetisov L.<sup>1</sup>, Chashin D.<sup>1</sup>, Ekonomov N.<sup>1</sup>, Preobrazhensky V.<sup>2</sup>, Fetisov Y.<sup>1</sup>

<sup>1</sup>MIREA - Russian Technological University, Moscow, Russia

<sup>2</sup>Prokhorov General Physics Institute RAS, Moscow, Russia

fetisovl@yandex.ru

The magnetoelectric (ME) effect in planar ferromagnet-piezoelectric (FM-PE) heterostructures arises due to combination of magnetostriction of the FM layer and piezoelectricity in the PE layer and manifests itself in the generation of an electric voltage when an ac excitation magnetic field is applied to the structure [1].

In this work, for the first time, we observed and investigated the resonant ME effect in antiferromagnet-piezoelectric (AFM-PE) structure. The structure contained an AFM plate of “easy-plane” anisotropy  $\alpha$ -Fe<sub>2</sub>O<sub>3</sub> (hematite) with dimensions of 17 x 5 x 0.35 mm<sup>3</sup> and a layer of piezoelectric polymer PVDF with dimensions of 2 x 10 x 0.05 mm<sup>3</sup>, connected by adhesive. The structure was placed in dc magnetic field  $H=0-600$  Oe, created by Helmholtz coils, and excited by a field  $h\cos(2\pi ft)$  with amplitude of  $h=0-3$  Oe and frequency  $f=0-400$  kHz, as shown in Figure 1.

Figure 2 shows the dependence of the voltage  $u$  generated by the PVDF layer on the field frequency  $f$  for different  $H$ . The voltage peak corresponds to the excitation of the main mode of acoustic oscillations along the length of the structure. The resonant frequency was tuned (in contrast to structures with FM layers) by  $\sim 24\%$  due to strong coupling of magnetic and acoustic subsystems of the hematite [2]. The ME coefficient for the hematite-PVDF structure reached  $\alpha_E \approx 58$  mV/(Oe·cm). Similar measurements were carried out for the hematite-piezoceramic PZT structure. Resonance frequency in such a structure was tuned on 4.4% with magnetic field  $H$ . At a resonant frequency of 140 kHz, the ME coefficient reached maximum value of  $\alpha_E \approx 4.8$  mV/(Oe·cm) at  $H=0$  and decreased gradually with increasing field.

The ME effects observed in AFM-PE structures can be used to elaborate high-sensitivity magnetic field sensors with extended functionality.

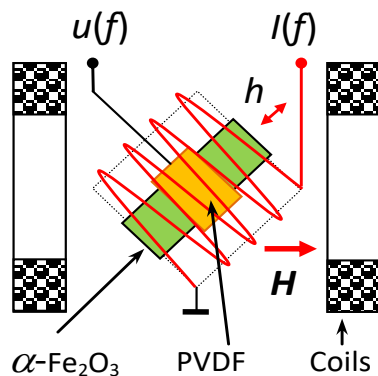


Figure 1 Experimental set up.

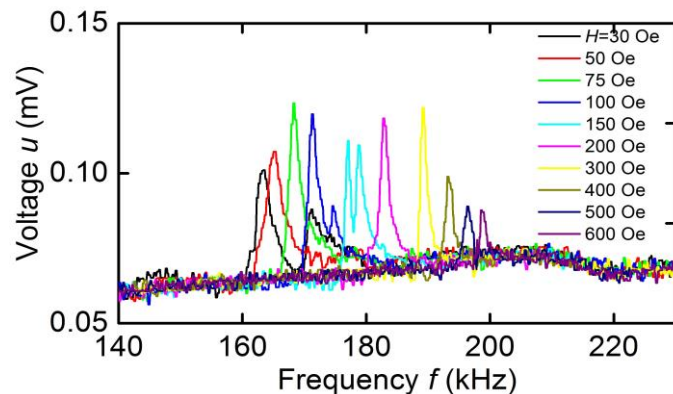


Figure 2 Frequency response of hematite-PVDF structure.

The research was supported by the Russian Science Foundation, project No 22-29-01093.

[1] C.W. Nan et al, *J. Appl. Phys.*, **103** (2008) 31101.

[2] V.I. Ozhogin, V.L. Preobrazhenskii, *Sov. Phys. Usp.*, **31** (1988) 713-729.

## NONLINEAR MAGNETOELECTRIC EFFECTS IN FERROMAGNETIC – PIEZOELECTRIC RING STRUCTURE

*Fetisov L., Savelev D., Chashin D., Musatov V., Fedulov F., Fetisov Y.*  
MIREA - Russian Technological University, Moscow, Russia  
fetisovl@yandex.ru

The magnetoelectric (ME) effects in ferromagnet-piezoelectric (FM-PE) heterostructures manifest themselves as voltage generation under the action of an alternating magnetic field. The effects arise due to combination of magnetostriction of the FM layer and piezoelectricity in the PE layer [1].

In this work, for the first time, we observed and investigated a nonlinear ME effect of harmonics generation in a layered Metglas-PZT ring-type heterostructure under circumferential magnetization with an ac magnetic field. Permanent magnetic field was directed circumferentially, and parallel or perpendicular to the axis of the structure. The structure was a two-layer ring with a PE outer layer and a FM inner layer. The piezoceramics  $\text{Pb}(\text{Zr}_x\text{Ti}_{1-x})\text{O}_3$  (PZT) ring had an inner diameter of 16mm, a thickness of  $a_p=1$  mm, and a height of 5 mm. The FM layer of the structure was made of an amorphous alloy ribbon FeBSiC (Metglas 2605SA1), 50.2 mm long, 5 mm wide and 27  $\mu\text{m}$  thick. Two coils of 0.2mm copper wire, 90 turns each, were wound on the ring structure in order to generate ac field  $h\cos(2\pi ft)$  with amplitude of  $h=0-3.6$  Oe and frequency  $f=0-100$  kHz and dc magnetic field  $H=0-40$  Oe directed circumferentially. Helmholtz coils created magnetic field of other orientations.

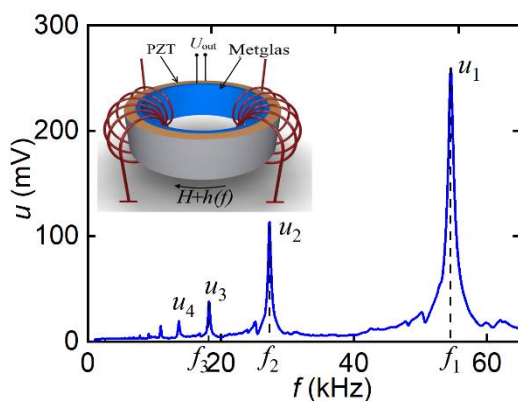


Figure 1 Dependence of the ME voltage  $u$  on the frequency  $f$  of the ac field at field amplitude  $h=1.5$  and  $H=0.4$  Oe.

Figure 1 shows dependence of the ME voltage  $u$  on the excitation field frequency  $f$ , measured while tuning the frequency at field amplitude  $h=1.5$  and  $H=0.4$  Oe. Both dc and ac magnetic fields were directed circumferentially. In addition to the main peak  $u_1$  at frequency  $f_1$ , new peaks appeared at frequencies  $f_n = f_1/n$  (where  $n=2, 3, 4, \dots$ ) with amplitudes  $u_2$ ,  $u_3$ , and  $u_4$ , respectively. The frequency of the generated ME voltage  $u$  for all peaks corresponded to the main resonant frequency  $f_1 \approx 54.2$  kHz. ME coefficients for the first three harmonics were  $\alpha_{E1} = 2.9$  V/(Oe·cm),  $\alpha_{E2} = 0.95$  V/(Oe<sup>2</sup>·cm), and  $\alpha_{E3} = 0.21$  V/(Oe<sup>3</sup>·cm). Similar ME coefficients were obtained for two other orientations of a

permanent magnetic field. These coefficients are comparable in magnitude with the coefficients for the ME effect in planar Metglas-PZT structures [2].

The research was supported by the Russian Science Foundation, project No 19-79-10128-P.

[1] C.W. Nan et al, *J. Appl. Phys.*, **103** (2008) 31101.

[2] L.Y. Fetisov et al, *J. Phys. D: Appl. Phys.*, **51(5)** (2018) 154003.

3PO-L8-3

## STRUCTURE AND PROPERTIES OF MULTIFERROIC FERROBORATES OF MIXED COMPOSITION $\text{SmFe}_{3-x}\text{Al}_x(\text{BO}_3)_4$ AND $\text{Eu}_{1-y}\text{La}_y\text{Fe}_3(\text{BO}_3)_4$

*Erolov K.V.*<sup>1</sup>, *Smirnova E.S.*<sup>1</sup>, *Sidorova E.V.*<sup>1</sup>, *Alekseeva O.A.*<sup>1</sup>, *Sorokin T.A.*<sup>1</sup>, *Artemov V.V.*<sup>1</sup>,  
*Chmelenin D.N.*<sup>1</sup>, *Gudim I.A.*<sup>2</sup>

<sup>1</sup> Shubnikov Institute of Crystallography FSRC “Crystallography and Photonics” RAS, Moscow,  
Russian Federation

<sup>2</sup> Kirensky Institute of Physics, FRC KSC SB RAS, Krasnoyarsk, Russian Federation  
green@crys.ras.ru

Oxoborates of rare earth elements  $RM_3(\text{BO}_3)_4$  ( $R = \text{Y, La-Lu}$ ,  $M = \text{Al, Fe, Ga, Cr, Sc}$ ) with the huntite structure ( $\text{CaMg}_3(\text{CO}_3)_4$ , sp. gr. R32) have been actively studied during the last 20 years because they exhibit a wide variety of physical properties and phase transitions. In particular,  $R\text{Al}_3(\text{BO}_3)_4$  aluminoborates are of interest primarily for their optical properties [1], while  $R\text{Fe}_3(\text{BO}_3)_4$  ferroborates are multiferroics in the presence of two magnetic subsystems of  $R$  and Fe ions [2, 3].

Of particular interest to researchers are oxoborates with a mixed composition, in which ions of one rare earth element  $R1$  or metal  $M1$  are partially replaced by ions of another rare earth element  $R2$  or metal  $M2$ , respectively. Such substitutions are considered as one of the possible ways to change the known physical properties (optical or multiferroic) or to form new ones (for example, magneto-optical). In particular, it was previously shown that the  $\text{GdAl}_3(\text{BO}_3)_4$  compound, when doped with Sm ions, becomes a warm orange-red phosphor upon excitation with vacuum ultraviolet [4]. In the  $\text{Eu}_{0.88}\text{La}_{0.12}\text{Fe}_3(\text{BO}_3)_4$  compound, it was established [5] that below the Neel temperature of the magnetic phase transition  $T_N = 32$  K of the subsystem of Fe ions, a structural phase transition to the magnetically ordered state occurs, and a further slight increase in the content of La ions to  $y = 0.15$  leads to complete suppression of the structural phase transition [6].

In our work, we present the results of studies of the composition, crystal structure, and phase transitions of single crystals of mixed compounds  $\text{SmFe}_{3-x}\text{Al}_x(\text{BO}_3)_4$  and  $\text{Eu}_{1-y}\text{La}_y\text{Fe}_3(\text{BO}_3)_4$  by precision X-ray diffraction analysis in a wide temperature range from 25 K to 500 K, and by the methods of X-ray fluorescence and energy-dispersive elemental analysis.

Support by Russian Scientific Foundation (project # 23-22-00286) is acknowledged.

[1] G.M. Kuz'micheva et al., *Crystals*, **9** (2019) 100.

[2] A.M. Kadomtseva et al., *Low Temp. Phys.*, **36** (2010) 511-521.

[3] O.A. Alekseeva et al., *Crystals*, **12** (2022) 1203.

[4] J. He et al., *Opt. Mat.*, **39** (2015) 81-85.

[5] K.N. Boldyrev et al., *Phys. Rev. Mat.*, **5** (2021) 094414.

[6] M.N. Popova et al., *Phys. Rev. B*, **94** (2016) 184418.

## NON-MAGNETIC & MAGNETIC FERROELECTRIC TUNNEL JUNCTION MODELLING

*Jagga D., Useinov A.*

International College of Semiconductor Technology,  
National Yang-Ming Chiao-Tung University, Hsinchu, Taiwan ROC  
artu@nctu.edu.tw

Theoretical model is developed for the current density ( $J$ ) and tunnel electro-resistance (TER) vs applied voltage ( $V$ ) in the tunnel junctions with ferroelectric (FE) barriers. NM/FE(3 nm)/MM (shown in Figure 1), NM/DE/FE(5 nm)/DE/MM and NM/FE(1 nm)/HM systems are considered, where the magnetic metal (MM)/dielectric (DE), MM/FE, non-magnetic metal/FE (NM/FE) and half-metal/FE (HM/FE) interfaces are simulated with approaches of the linearized Thomas Fermi screening, FE hysteresis and presence of the oxygen vacancies  $V_O$ . In addition, it is found that theoretical model modification, where screening lengths grow up with  $V$ , allows to reproduce exp. data [1] with a better precision at  $V < 0.5$  V than the previous approach with the constant screening lengths [2]. For example, the potential barrier and related  $J$ - $V$  are shown in Figure 1 for NM/FE(3 nm)/MM system.  $J$ - $V$  deviation at  $V > 0.5$  V is related with electrostriction effect when lattice constant in FE is modified under  $V$ , enhancing the barrier width.

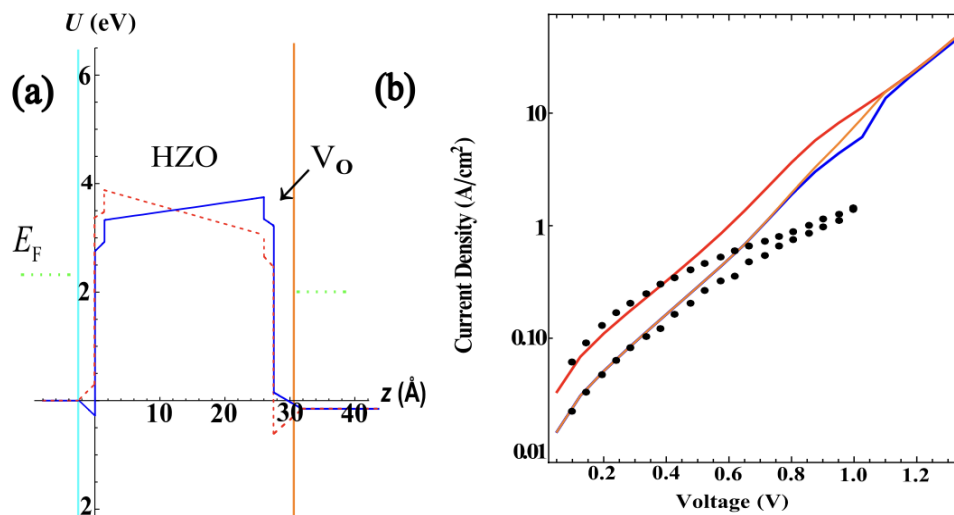


Figure 1. (a) Potential energy profile with positive and negative saturated FE polarizations ( $P_s$ ) - red dashed and blue solid curves, respectively. Total barrier thickness is accounted between cyan and orange vertical lines together with screening regions. (b)  $J$ - $V$  behavior, where red and blue curves are theoretical data of the model for  $P_s = \pm 6 \mu\text{C}/\text{cm}^2$ , respectively. Orange curve is derived, accounting hysteresis. Black dots are exp. data [1] for TiN/ HZO (2.8 nm)/ Ni, where HZO denotes  $\text{Hf}_{0.5}\text{Zr}_{0.5}\text{O}_2$  material.

NSTC 111-2221-E-A49-120- is acknowledged.

[1] Y.-H. Chu et al., *Int. Symp. on VLSI Tech., Sys. and App. (VLSI-TSA)*, IEEE (2021) 1–2.

[2] A. Useinov et al., *ACS Appl. Electron. Mater.* **4**(5) (2022) 2238-2245.

3PO-L8-5

## CRYSTAL FIELD PARAMETERS AND MAGNETIC PROPERTIES CORRELATIONS IN RARE-EARTH ORTHOFERRITES

*Usmanov O.V., Zobkalo I.A., Ovsianikov A.K.*

B.P. Konstantinov Petersburg Nuclear Physics Institute of NRC Kurchatov Institute, Gatchina,  
Russia

usmanov\_ov@npfi.nrcki.ru

The crystal structure and magnetic properties investigations of holmium, terbium and thulium orthoferrites were performed in temperature range 4 – 300 K. Obtained XRD data confirm that all compounds retain the orthorhombic perovskite structure of  $Pbnm$  space group [1]. The crystal electric field (CEF) parameters of  $R^{3+}$  ( $R = Ho, Tb, Tm$ ) ion subsystem have been revealed numerically on the base of point charge model in the same temperature range [2-4]. By the sets of CEF parameters the splitting of considered  $R^{3+}$  energy levels were calculated and their temperature evolution was obtained. Modelling of isothermal magnetization  $M(H)$  with obtained sets of parameters was carried out. Single ion anisotropy due to CEF effects is considered. Bulk magnetization evaluated from CEF was compared to experimental data [5, 6].

- [1] M. Marezio et al., *Acta Cryst. B*, **26** (1970) 2008.
- [2] K. W. H. Stevens, *Proc. Phys. Soc. A*, **65** (1952) 209.
- [3] M. T. Hutchings, *Solid State Physics*, **16** (1964) 227-273.
- [4] M. Rotter, *J. Magn. Magn. Mater.*, **E481** (2004) 272-276.
- [5] M. Shao et al., *Solid State Commun.*, **152** (2012) 947.
- [6] A. Ovsianikov et al., *J. Magn. Magn. Mater.*, **557** (2022) 169431.

## FEATURES OF THE ORIGIN OF $0^\circ$ DOMAIN WALLS IN UNIAXIAL FILMS WITH FLEXOMAGNETOELECTRIC EFFECT IN A MAGNETIC FIELD

*Vakhitov R.M., Nizyamova A.R., Solonetsky R.V.*

Ufa University of Science and Technology, Ufa, Russia  
vakhitovrm@yahoo.com

Currently one of the promising directions in the development of magnetism closely related to the development of various spintronics devices is the study of magnetoelectric materials [1,2]. They are characterized by two or more order parameters and possess a number of interesting and extraordinary properties. In particular, the phenomenon of displacement of domain walls (DW) under the action of an inhomogeneous electric field found in ferrite-garnet films at room temperatures also applies to them [2]. It was suggested that this phenomenon is due to the presence of inhomogeneous magnetoelectric interaction in the films (flexomagnetolectric effect [1]), which was confirmed in further studies [3]. In particular, in [4], a theoretical analysis of micromagnetic structures possible in thin films with flexomagnetolectric (FME) interaction was carried out and it was shown that in them, along with  $180^\circ$  DW, two more types of DW can exist as stable formations:  $0^\circ$  DW with a quasi-Bloch structure and  $0^\circ$  DW of the Neel type. They are characterized by nontrivial properties, but have not been studied enough yet, and have not been experimentally detected [2]. In particular, the first type  $0^\circ$  DW can originate only at large values of the electric field, significantly exceeding their characteristic values, and in the second type, the structure of the DW is such that the charges formed in the region of the DW shield each other (the integral polarization value is zero). Therefore, it is of interest to study the influence of the magnetic field on the conditions of nucleation, structure and polarity  $0^\circ$  DW in the film under consideration (as an external factor with the potential to change their properties).

Numerical analysis of the Euler-Lagrange equations showed that the presence of a magnetic field significantly changes the structure and properties of  $0^\circ$  DW of both types. At the same time, for each type of  $0^\circ$  DW, there is always a direction of the magnetic field at which the value of the integral polarization increases. In particular, in the case of  $0^\circ$  DW of the quasi-Bloch type, the effect of increasing the integral polarization (i.e., strengthening the FME effect) can be achieved in weak magnetic fields with  $\mathbf{H} \parallel \text{Oz}$ . However, the electric field should not be small. In addition, by the action of the magnetic on the quasi-Bloch  $0^\circ$  DW, it is possible to change the critical field of nucleation in one direction or another and even achieve that there is no threshold of nucleation.

In the second case, if the external magnetic field  $\mathbf{H}$  is directed along the Ox axis, then (and only in this case) an FME effect may occur, sufficient for its observation under experimental conditions.

The work was carried out with the financial support of the State Task for the performance of scientific research by laboratories (Order MN- 8/1356 of 09/20/2021)

[1] A.P. Pyatakov, A.K. Zvezdin, *Phys. Usp.*, **55** (2012) 557-581.

[2] A.S. Logginov et al., *JETP Letters*, **86** (2007) 115-118.

[3] I.S. Veshchunov et al., *Phys.Rev.Lett.*, **115** (2015) 027601.

[4]. F.A. Maksutova et al., *EPL.*, **129** (2020) 27004.

## FEATURES OF THE MANIFESTATION OF THE FLEXOMAGNETOELECTRIC EFFECT IN (111)-ORIENTED FERRITE-GARNET FILMS

*Vakhitov R.M., Gridneva G.T., Yumaguzin A.R.*

Ufa University of Science and Technology, Ufa, Russia  
azyum@rambler.ru

It is known that ferrite-garnet films are multifunctional materials [1], which also demonstrate magnetoelectric properties. This causes increased interest in them due to the possibility of their use in various spintronic devices. Thus, a new phenomenon was discovered in ferrite-garnet films, which consists in the fact that with the help of an electric field it is possible to control the displacement of domain walls (DWs) in these films [2]. Further study of the discovered phenomenon (the flexomagnetolectric effect [2]) revealed a number of features, among which we can single out its significant dependence on the orientation of the developed film surface relative to the crystallographic axes; Thus, in the (210)-oriented film, the effect manifests itself most strongly, in the (011)-film, it is weaker, and in the (111)-film, it was not observed at all [2, 3]. Obviously, to explain such a dependence, it is necessary to study the possible types of micromagnetic structures that appear in each of the films under consideration and to reveal their topological differences. Therefore, a detailed study of the distribution of the magnetization and the polarization induced in the region of the domain wall as a function of the applied electric field in the (111)-oriented iron garnet film is important and necessary for understanding the essence of the phenomenon under study.

Numerical studies show that the structure and properties of the DW in the film under study are significantly affected by factors such as the presence of uniaxial anisotropy, cubic anisotropy, and inhomogeneous magnetoelectric interaction. It follows from the calculations that changes in the DW structure are most pronounced in the dependence  $\varphi=\varphi(y)$ , which represents the angle of exit of the magnetization vector  $M$  from the wall plane ( $y$ -coordinate along which the magnet is inhomogeneous). In this case, the first and third factors lead to the fact that  $\varphi(y)$  is an even function, and the second factor is an odd function. Accordingly, the resulting dependence  $\varphi(y)$  is a rather complex function. This leads to the fact that the integral polarization (total wall charge) is achieved at high values of the electric field. Hence it follows that the cubic anisotropy in the (111) film significantly weakens the manifestation of the flexomagnetolectric effect in it.

[1] V.V.Randoshkin, A.Ya.Chervonenkis, *Applied magneto-optics* (Moscow: Energoizdat, 1990).

[2] A.S. Logginov et al, *Appl.Phys.Lett.*, **93** (2008) 182510.

[3] A.P. Pyatakov et al, *Physics-Uspekhi*, **58** (2015) 981-992.

3PO-L8-8

## MAGNETIC PROPERTIES OF $\text{TbCr}_3(\text{BO}_3)_4$ GROWN FROM MELT-SOLUTIONS BASED ON $\text{Bi}_2\text{Mo}_3\text{O}_{12}$ AND BASED ON $\text{Li}_2\text{WO}_4$

*Gudim I.A., Eremin E.V., Titova V.R., Mikhashenok N.V.*

<sup>1</sup> Kirensky Institute of Physics, Federal Research Center KSC SB RAS, Krasnoyarsk, Russia  
irinagudim@mail.ru

Single crystals of trigonal oxyborates ( $\text{RM}_3(\text{BO}_3)_4$  (R - rare-earth element, M = Al, Ga, Sc, Fe) with the huntite structure are multiferroics.

For the  $\text{TbCr}_3(\text{BO}_3)_4$  terbium chromborate with the huntite structure, there is no technology for reproducible synthesis of high-quality crystals suitable for a comprehensive study of their properties. For the first time, these crystals were grown from a melt solution based on potassium trimolybdate [1], however, the authors recognize the presence of up to 10% of the monoclinic phase in their crystals, which clearly affects the properties of the grown crystals.

We have attempted to grow crystals of terbium chromium borate from a melt solution based on bismuth trimolybdate. 88% wt.  $\{\text{Bi}_2\text{Mo}_3\text{O}_{12} + 2\text{B}_2\text{O}_3 + 0,3\text{Tb}_2\text{O}_3\}$  + 12% wt.  $\text{TbCr}_3(\text{BO}_3)_4$  (1) However, it was possible to obtain only crystals of the C2/c monoclinic phase in the entire temperature range. And only with the use of a melt solution based on lithium tungstate, it was possible to obtain both modifications of terbium chromoborate in pure form. 92% wt.  $\{\text{Li}_2\text{WO}_4 + 3\text{B}_2\text{O}_3 + 0,3 \text{Tb}_2\text{O}_3\}$  + 8% wt.  $\text{TbCr}_3(\text{BO}_3)_4$  (2). Moreover, the trigonal phase is high-temperature and exists only above 1100 oC, below this temperature only the monoclinic phase crystallizes.

Samples for measuring magnetic properties were made from grown trigonal crystals. The magnetic characteristics are measured.

Two anomalies appeared on the temperature dependence of magnetization at 5.6 K and 9.5 K. They are determined by the ordering of  $\text{Tb}^{3+}$ , which then magnetizes  $\text{Cr}^{3+}$ .

The field dependence of the magnetization measured at  $T = 2$  K and  $H \parallel c$  shows two anomalies. A sharp jump of the magnetization occurring at  $H_{C1} \approx 3$  kOe is most likely due to a metamagnetic transition in the antiferromagnetically ordered Tb subsystem. This jump ends with the saturation of the magnetization, which level is close to the saturation magnetization  $M_s = 8.3 \mu\text{B}/\text{F.u.}$  of the Tb subsystem in the crystal of the isomorphic diamagnetic analogue  $\text{TbAl}_3(\text{BO}_3)_4$ . The weak hysteresis observed upon this reorientation suggests that this is a first-order transition.

Another anomaly observed at  $H_{C2} = 7.5$  kOe is most likely due to the spin-flop transition occurring in the Cr subsystem. Both anomalies exist only in the easy-axis state and disappear at temperatures above 5.5 K.

Support by RSF and KRFS are acknowledged.

[1] N. N. Kuzmina, V. V. Maltsev, E. A. Volkova, *Neorgan, Materialy*, **56(8)** (2020) 873–881.

**July 3**

Monday

18:00 - 20:00

POSTER  
SESSIONS

Section L9

**Diluted Magnetic  
Semiconductors and Oxides**

3PO-L9-1

## PARAMAGNETIC PROPERTIES OF PYRRHOTINE AND PENTLANDITE MOUNTAIN MINERALS AT HIGH TEMPERATURES.

*Kuvandikov O.K., Shodiev Z.M., Khasanov H.B., Akhtamov J.Sh.*

Samarkand State University named after Sharof Rashidov, Samarkand, Uzbekistan  
quvandikov@rambler.ru.

The greatest number of sulfide compounds form transition metals, especially iron. These compounds include the natural minerals pyrrhotite ( $Fe_7S_8$ ) and pentlandite ( $Ni_9S_8$ ). Iron sulfides are of particular interest in terms of their magnetic properties. The study of the structural, electronic and physical, including the magnetic properties of iron sulfides makes it possible to discover new promising areas of application of magnetic materials.

In the present time, to the study of the magnetic properties of minerals; containing elements of the iron group - pyrrhotite and pentlandite at high temperatures has received insufficient attention.

The purpose of this work is to study the paramagnetic properties of minerals - pyrrhotite and pentlandite in their paramagnetic state, i.e. at high temperatures. For achieve this goal, the temperature dependences of the magnetic susceptibility [ $\chi(T)$ ] of the mineral were measured, respectively, in the temperature ranges of 250-900 °C and 480-900°C.

By processing the experimental dependences  $\chi^{-1}(T)$  of the studied minerals, the paramagnetic Curie temperature ( $\theta_p$ ), the Curie-Weiss constant ( $C$ ), the magnetic moment per chemical formula of the mineral ( $\mu_{for}$ ) and the effective magnetic moment per magnetically active atom are found (Fe and Ni) ( $\mu_{eff}$ ) minerals.

The calculation results are shown in Table 1.

Table 1. Calculation results

Minerals	Interval temperature, °C	$\theta_p$ , K	$C$ , $10^4 K \cdot cm^3 / \varepsilon$	$\mu_{for}, \mu_B$	$\mu_{eff}, \mu_B$
Pyrrhotite- $Fe_7S_8$	650-900	583	76,6	6,3	2,37
Pentlandite- $Ni_9S_8$ .	650-900	853	19,15	3,47	1,16

Table 1 shows that the value of  $\theta_p$ ,  $C$ ,  $\mu_{for}$  and  $\mu_{eff}$  does not show general pattern. It should be noted that our results on the value of  $\theta_p$  for pyrrhotite (583K) are in satisfactory agreement with the result of work ( $\theta_p = 538K$ ) [1], where it was found that at this temperature the magnetic phase transition ferrimagnetism-paramagnetism occurs. In addition, our result on the value of the magnetic moment  $\mu_{for}$  of pyrrhotite also satisfactorily agrees with the result of this work. Taking into account these correspondences, it can be assumed that the magnetic moments in the sublattice of magnetically active ions of minerals (iron or nickel), their magnetic moments are ordered ferromagnetically inside the atomic layers, and antiferromagnetically between the layers, however, due to the presence of vacancies, the magnetic moments are not completely compensated, which leads to ferrimagnetism .

[1] E.N. Selivanov, R.I. Gulyaeva, A.D. Vershinin, *Inorganic Materials*, **44** (2008) 438-442.

## COMPARATIVE STUDY OF THE STRUCTURE AND ELECTROMAGNETIC CHARACTERISTICS OF MANGANITES DOPED WITH CATION PAIRS (Fe, Zn), (Fe, Co), (Fe, Mg)

*Badelin A.G.<sup>1</sup>, Karpasyuk V.K.<sup>1</sup>, Estemirova S.Kh.<sup>1,2</sup>*

<sup>1</sup> Astrakhan State University named after V.N. Tatishchev, Astrakhan, Russia

<sup>2</sup> Institute of Metallurgy, Ural Branch, Russian Academy of Sciences, Yekaterinburg, Russia  
alexey\_badelin@mail.ru

The aim of this work is to establish the influence of electronic configuration of  $\text{Me}^{2+}$  ions on crystal lattice parameters, magnetization, Curie point, “semiconductor-metal” transition and magnetoresistance in pared substituted manganites  $\text{La}_{0.7}\text{Sr}_{0.3}\text{Mn}_{0.9}\text{Fe}_{0.05}\text{Me}_{0.05}\text{O}_3$  ( $\text{Me} = \text{Zn}, \text{Co}, \text{Mg}$ ). In this system, manganese is replaced by combinations of iron ion  $\text{Fe}^{3+}(3d^5)$  with ions having different configurations:  $\text{Zn}^{2+}(3d^{10})$ ,  $\text{Co}^{2+}(3d^7)$ ,  $\text{Mg}^{2+}(2p^6)$ . The radii of  $\text{Fe}^{3+}$  (0.645 Å) and  $\text{Mn}^{3+}$  (0.645 Å) ions coincide. Zinc, cobalt and magnesium ions have very similar values of ionic radii: 0.74 Å, 0.745 Å and 0.72 Å, respectively [1]. This makes it possible to study the role of electronic configuration of these ions in its purest form, since under the specified conditions lattice effects are practically absent.

Ceramic samples were sintered in air at 1473 K for 10 h, and then the samples were cooled together with the furnace. All synthesized manganites have rhombohedral structure. The impurity content is less than one percent.

Crystal lattice parameters and electromagnetic characteristics are given in the Table 1.

Magnesium-containing manganite has the lowest values of magnetization, Curie point and “semiconductor-metal” transition temperature. At the same time, the maximum absolute magnitude of the magnetoresistance reaches 33% at 110 K in Mg-containing manganite.

It is interesting to note that magnetization of Co-substituted manganite is almost 1.7 times higher than magnetization of zinc-containing one, and unit cell volume is smaller. These facts indicate the presence of trivalent cobalt ions  $\text{Co}^{3+}(3d^6)$ .

Table 1. Lattice parameters (a, c), unite cell volume (V), specific magnetization ( $\sigma$ ) at 80 K, Curie point ( $T_c$ ) and “semiconductor-metal” transition temperature ( $T_{ms}$ )

Compositions	a (Å)	c (Å)	c/a	V (Å <sup>3</sup> )	$\sigma$ (emu/g)	$T_c$ (K)	$T_{ms}$ (K)
$\text{La}_{0.7}\text{Sr}_{0.3}\text{Mn}_{0.9}\text{Fe}_{0.05}\text{Zn}_{0.05}\text{O}_3$	5.5068	13.3522	2.425	350.659	80	267	283
$\text{La}_{0.7}\text{Sr}_{0.3}\text{Mn}_{0.9}\text{Fe}_{0.05}\text{Co}_{0.05}\text{O}_3$	5.5044	13.3459	2.425	350.196	133	265	256
$\text{La}_{0.7}\text{Sr}_{0.3}\text{Mn}_{0.9}\text{Fe}_{0.05}\text{Mg}_{0.05}\text{O}_3$	5.5023	13.3467	2.426	349.941	46	248	150

Interpretation of experimental results is given taking into account the ratio of various types of interactions responsible for magnetic and transport properties of manganites [2] (double and indirect exchange, electrostatic interaction), in connection with the processes of charge compensation when introducing inovalent impurities with different configurations of electron shells.

The study was carried out at the expense of a grant from the Russian Science Foundation No. 23-22-10005.

[1] R.D. Shannon, *Acta Crystallogr.*, **A32** (1976) 751-767.

[2] N.G. Bebenin, R.I. Zainullina, V.V. Ustinov, *Physics-Uspekhi*, **61** (2018) 719-738.

## LIGHT ENVELOPE SOLITONS IN A TRANSVERSELY MAGNETIZED FERROMAGNETIC SEMICONDUCTOR FILM WITH THE PROPERTIES OF THE "LEFT-HANDED" MEDIA

*Bogomolova A.V., Romanenko D.V., Grishin S.V.*  
Saratov State University (SSU), Saratov, Russia  
aleksis\_bogomolova@mail.ru

To date, magnetic semiconductors (SC) are of considerable interest for modern electronics and spintronics, as they allow to manipulate variable magnetization using magnetized solid-state plasma [1]. Theoretically, it was found that magnetic SC have the properties of the left-handed media and support the propagation of backward electromagnetic waves (BEMW) [2]. This paper presents the results of numerical simulation of light envelope solitons in the left-handed media based on ferromagnetic (FM) SC. It is shown that the light envelope solitons are formed on a BEMW existing in a transversely magnetized thin film of FMSC (see Figure 1). It is established that the wave number  $k$  of the BEMW, on which such a soliton is formed, decreases with a decrease in the concentration of electrons in the plasma  $N$  and reaches the value  $k = 2690 \text{ cm}^{-1}$  at  $N = 1017 \text{ cm}^3$ . In this case, the length at which the light soliton is formed does not exceed 9,5 mm. The paper also evaluate the dependence of the length of the formation of the light envelope soliton on the thickness of the FM SC film. It is established that in super-thin films of FM SC, the formation of a light envelope soliton is observed at significantly bigger values of the wave number  $k$ . The results obtained in this work are of interest for the development of nonlinear magnon spintronics devices.

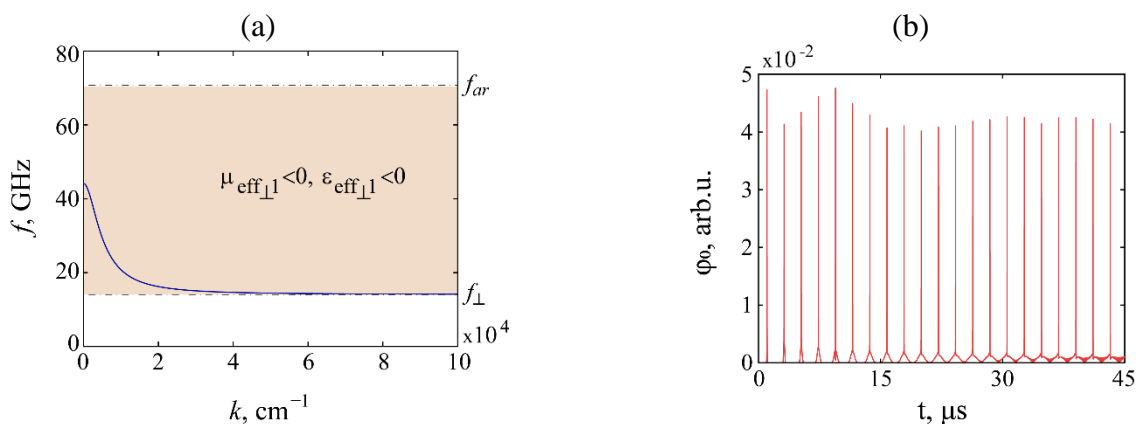


Figure 1. (a) The dispersion characteristic of the backward EMW and (b) the temporal realization of a periodic sequence of light envelope solitons in a transversely magnetized FM SC film with a thickness of 10 mkm, with a magnetization of 24300 Gs, a concentration of  $N=1017 \text{ cm}^3$  magnetic field strength of 103 Oe.

The work was supported by the Russian Science Foundation grant No. 19-79-20121, <https://rscf.ru/en/project/19-79-20121/>.

[1] A.S. Boruhovich et al., *Semiconductor and ferromagnet europium monoxide in spintronics*. (SPb: Lan', 2017).

[2] S.V. Grishin, A.V. Bogomolova, S.A Nikitov, *JETP Letters*, **48(5)** (2022) 39-42.

## STUDY OF CHANGES IN THE COMPOSITION OF THE CdTe SURFACE UPON IMPLANTATION OF O<sup>2+</sup> IONS AND SUBSEQUENT ANNEALING

*Abdumaitov A.A., Boltaev Kh.Kh., Umirzakov B.E., Tashmukhamedova D.A.*

Tashkent State Technical University, Tashkent, Uzbekistan  
khurshid.boltaev@gmail.com

It is known that thin films of A<sup>II</sup>B<sup>VI</sup> semiconductors are widely used in the production of multilayer heterostructures used in various optical and electronic devices, solar cells and photosensitive devices. Thin films of CdTe oxide can have several practical applications; for example, in the production of highly efficient solar cells [1, 2]. Therefore, a large number of works have been devoted to obtaining and studying the properties of two and three component films based on A<sup>II</sup>B<sup>VI</sup> (for example, CdTe, CdS, Me–CdTe–CdS, Cd<sub>x</sub>Hg<sub>1-x</sub>Te, Cd<sub>1-x</sub>Zn<sub>x</sub>Te). The results of experimental work have shown that the perfection and properties of films largely depend on the method of synthesis, their thickness, and surface morphology [3].

CdTe films were obtained on the surface of Mo(111) single crystals by vapor phase condensation. The studies were carried out using a set of methods: Auger electron spectroscopy (AES) and high-speed electron diffraction (HEED). The Auger spectra were recorded using an electrostatic analyzer of the Yuz–Rozhansky type with a resolution of 0.2% and small-angle detection of scattered ions and electrons. The depth distribution profiles of atoms were determined by AES in combination with layer by layer etching with argon ions with E<sub>0</sub> = 2 keV at an angle of 5–10° relative to the sample surface.

The X-ray diffraction pattern shows that tellurium cadmium films have a cubic lattice of the zinc mixture type with the dominant atomic peak of the growth direction in [110]. Note that an increase in temperature to 800 K leads to an increase in the intensity of the peaks. The Auger spectrum of CdTe shows that the spectrum of pure CdTe mainly contains intense peaks, Cd, Te and low-intensity oxygen peaks. The concentration of C<sub>x</sub> atoms that make up the film and substrate was determined from the relative change in the intensity of the Auger peaks. The method of coefficients (factors) of elemental Auger sensitivity with matrix corrections was used in the calculations:

$$C_x = \frac{I_x/S_x}{\sum I_i/S_i} \alpha$$

where I<sub>x</sub> and S<sub>x</sub> are the height of the Auger peak and the elemental Auger sensitivity factor of the x<sup>th</sup> element, respectively;  $\sum I_i/S_i$  is the sum of the I/S ratios of all elements present in the sample; α is the matrix correction. The measurement error of the atomic concentration was ~5 at.%. The calculation showed that on the surface of the CdTe film there are ~50 at.% Cd, ~48 at.% Te, and O, C atoms, the total concentration of which is ~1.5–2.0 at.%. After ion bombardment with a high dose (D = 6 · 10<sup>16</sup> cm<sup>-2</sup>), almost all the Auger peaks of impurity atoms disappear, the intensity of the Te and Cd Auger peaks sharply decreases, and intense oxygen Auger peaks appear. After heating at T=800K CdTe implanted with O<sup>2+</sup> ions with E<sub>0</sub> = 1 keV at a dose D = 6 · 10<sup>16</sup> cm<sup>-2</sup>, a compound of the CdTeO<sub>3</sub> type was formed.

[1] R.H. Bube, *Proc. of the Symp. on Mat. and New Proc. Tech. for Photovoltaics*, **83-11** (1983) 359.

[2] C.H. Lee et al., *J. Electron. Mater.*, **27(6)** (1998) 668.

[3] V.V. Vasylyev et al., *Phys. Tech. Semicond.*, **35(2)** (2001) 203–207.

## REGULARITIES AND MECHANISMS OF COMPOSITION INFLUENCE ON MAGNETIC AND NONLINEAR ELECTRICAL CHARACTERISTICS OF La-Sr MANGANITES WITH COMBINED SUBSTITUTION FOR MANGANESE

*Karpasyuk V.K.<sup>1</sup>, Badelin A.G.<sup>1</sup>, Derzhavin I.M.<sup>1</sup>, Estemirova S.Kb.<sup>1,2</sup>, Merkulov D.I.<sup>1</sup>*

<sup>1</sup> Astrakhan State University named after V.N. Tatishchev, Astrakhan, Russia

<sup>2</sup> Institute of Metallurgy, Ural Branch, Russian Academy of Sciences, Yekaterinburg, Russia  
derzh\_igor@mail.ru

In the present work comprehensive experimental data are shown for magnetic properties and current-voltage ( $I$ - $V$ ) characteristics at different temperatures of manganites with partial substitution of  $(\text{Fe}^{3+}_{0.5}\text{Sc}^{3+}_{0.5})$ ,  $(\text{Ni}^{2+}_{0.5}\text{Ge}^{4+}_{0.5})$ ,  $(\text{Zn}^{2+}_{0.5}\text{Ge}^{4+}_{0.5})$ ,  $(\text{Mg}^{2+}_{0.5}\text{Ge}^{4+}_{0.5})$  pairs for manganese in  $\text{La}_{1-c}\text{Sr}_c\text{Mn}_{1-x}(\text{Me}^{\text{I}}_{0.5}\text{Me}^{\text{II}}_{0.5})_x\text{O}_3$  basic system ( $c = 0.3, 0.35$ ;  $x = 0.1, 0.15$ ). Polycrystalline samples were prepared by solid state reactions in air with final sintering step performed at 1473 K for 10 h.  $I$ - $V$  characteristics in the 120-280 K temperature range were measured using sputter-deposited electrodes made of Ag.

All synthesized manganites have rhombohedral structure. Samples containing (Fe,Sc), (Ni,Ge) and (ZnGe) have slightly different values of magnetization at 80 K and Curie temperature, while the values of these parameters are significantly lower for (Mg,Ge)-substituted manganites.

(Fe,Sc)- and (Ni,Ge)-containing manganites exhibit “metal-semiconductor” transition, and with an increase in the electric field strength the transition temperature decreases. In the studied temperature range, (Zn,Ge)-substituted manganite has a metallic type of conduction, while (Mg,Ge)-containing sample exhibits semiconductor properties.

Figure 1 shows the most interesting current-voltage characteristics obtained, containing S-shaped sections of negative differential resistance in samples 1, 2, 3, and  $I$ - $V$  characteristic of (Mg,Ge)-substituted manganite with a sharp increase in current at almost constant voltage. The latter manganite has the smallest grain diameter and the highest porosity compared to other samples.

Experimental data obtained are discussed taking into account electronic configuration and radii of  $\text{Fe}^{3+}(3d^5)$ ,  $\text{Sc}^{3+}(3p^6)$ ,  $\text{Ni}^{2+}(3d^8)$ ,  $\text{Zn}^{2+}(3d^{10})$ ,  $\text{Mg}^{2+}(2p^6)$ ,  $\text{Ge}^{4+}(3d^{10})$  ions, insulator-metal transition in phase separation model, intrinsic inhomogeneities, self-heating effect, jumps of oxygen ions [1-4].

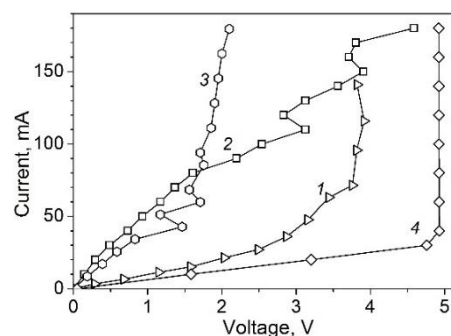


Figure 1. Current-voltage characteristics of manganites with various substituents: 1 –  $(\text{Fe}_{0.5}\text{Sc}_{0.5})$ ,  $x = 0.10$ ,  $c = 0.30$ , at 180 K; 2 –  $(\text{Ni}_{0.5}\text{Ge}_{0.5})$ ,  $x = 0.15$ ,  $c = 0.35$ , at 260 K; 3 –  $(\text{Zn}_{0.5}\text{Ge}_{0.5})$ ,  $x = 0.15$ ,  $c = 0.35$ , at 260 K; 4 –  $(\text{Mg}_{0.5}\text{Ge}_{0.5})$ ,  $x = 0.15$ ,  $c = 0.35$ , at 200 K

The study was carried out at the expense of a grant from the Russian Science Foundation No. 23-22-10005.

- [1] N.A. Tulina et al., *Phys. C*, **444** (2006) 19-22.
- [2] X.D. Wu et al., *IEEE Trans. Magn.*, **46** (2010) 1705-1707.
- [3] O.I. D'yachenko et al., *Metallophysics and Adv. Tech.*, **40** (2018) 291-299.
- [4] K.A. Shaykhutdinov et al., *Phys. B*, **405** (2010) 4961-4965.

## CONTRIBUTION OF RARE EARTH ELEMENTS TO THERMAL CONDUCTIVITY OF YTTRIUM ALUMINUM GARNET CRYSTALS

*Djabbarov I., Salakhitdinova M.K., Kulmatova G.*

Samarkand State University named after Sharof Rashidov, Samarkand, Uzbekistan  
smaysara@yandex.ru

Recently, as a result of large-scale studies of outer space, to solve many physicochemical and astrophysical problems, stable operation of quantum electronics devices using crystals and glasses as working elements, much attention is paid to their thermophysical properties [1,2].

This work presents the results of studies of the thermal conductivity of crystals of yttrium aluminum garnet (YAG) unactivated and activated by rare earth ions ( $Y_3Al_5O_{12}-TR^{3+}$ ). When rare-earth ions are introduced into crystals, their inhomogeneous distribution can be observed, which, as rule, leads to the appearance of microdefects in the sample matrix. Temperature fluctuations during the treatment and crystallization process usually lead to an uneven entry of impurities, which can also lead to shift in energy levels. These fluctuations cause density fluctuation. Displacement waves carrying the energy of thermal motion will dissipate. These scatterings are the stronger, the greater the maximum displacement of atoms from their average positions in the lattice, i.e. the higher the temperature. This explains the fact that the thermal conductivity of solid dielectrics decreases at sufficiently high temperatures:  $\alpha_p \sim 1/T$ . The thermal conductivity of the crystal lattice ( $\alpha_p$ ) can give a lot of information about various processes of phonon scattering in crystals.

From the point of view of the quantum theory of solid state, thermal lattice vibrations can be represented as set of finite number of normal vibrations, the interference of which gives rise to phonons. The most important processes for thermal conductivity are the energy exchange between three phonons: one phonon is annihilated and two others are born, or two phonons disappear and a third is born. At temperatures below the Debye  $\theta_D$ , collisions of long-wavelength phonons do not lead to Umklapp processes. Therefore, the phonon energy dissipation stops and their mean free path  $\lambda$  increases exponentially with decreasing temperature;  $\lambda \sim \exp\left(\frac{\theta_D}{bT}\right)$ , where  $b \approx 2$ . According to Debye's law, the heat capacity  $C \sim \left(\frac{T}{\theta_D}\right)^3$ , therefore, the thermal conductivity coefficient  $\alpha$  must increase both  $\left(\frac{T}{\theta_D}\right)$  and  $\left(\frac{\theta_D}{bT}\right)$ . At  $T < \left(\frac{1}{20}\right)\theta_D$  the value  $\lambda$  becomes comparable.

Thus, at  $T \rightarrow 0$ , the thermal conductivity coefficient  $\alpha$  must decrease with increasing temperature as  $T^3$ . Our experimental studies have shown that with a decrease in the ionic radius and an increase in the atomic mass, the thermal conductivity of YAG- $TR^{3+}$  crystals decreases significantly. The decrease in the ionic radius ( $TR^{3+}$ ) is associated with lanthanide contraction.

[1] F. Doniels, Ch. Boyd, D.Saunders, *Uspekhi fizicheskikh nauk*, **51(2)** (1953) 271-286.

[2] I. Djabbarov *Thermal conductivity of single crystals of yttrium aluminum garnet with impurities* (LAP Lambert, 2021).

## STRUCTURAL DISORDER, HEAT CAPACITY, AND MAGNETIC TRANSITIONS IN $\text{Cu}_2\text{FeBO}_5$

*Kazak N.V.<sup>1</sup>, Gokhfeld Yu.S.<sup>1</sup>, Belskaya N.A.<sup>2</sup>, Molokeev M.S.<sup>1</sup>, Gudim I.A.<sup>1</sup>, Eremin E.V.<sup>1</sup>, Knyazev Yu.V.<sup>1</sup>, Velikanov D.A.<sup>1</sup>, Ovchinnikov S.G.<sup>1</sup>*

<sup>1</sup>Kirensky Institute of Physics, Krasnoyarsk, Russia

<sup>2</sup>Ioffe Institute, St. Petersburg, Russia  
nat@iph.krasn.ru

The crystal structure of the  $\text{Cu}_2\text{FeBO}_5$  ludwigite was first solved in Ref. [1]. The cationic disorder and anomalously high equivalent atomic displacement parameter  $U_{\text{eq}}(\text{O4}) = 0.034(1) \text{ \AA}^2$  were reported. The compound was found to undergo three magnetic transitions at  $T^{\text{Fe}} = 63 \text{ K}$ ,  $T^{\text{Cu}} = 38 \text{ K}$ , and  $T_{\text{SG}} = 20 \text{ K}$  [2], which were assigned to the orderings of the iron and copper sublattices and freezing of spins in the 3D spin-glass state, respectively. An antiferromagnetic transition at  $T_{\text{N}} = 32 \text{ K}$  was reported in Ref. [3].

Here, we focus on the crystal and magnetic properties of the  $\text{Cu}_2\text{FeBO}_5$  single crystal. The sample has been grown using the flux and characterised by means of X-ray diffraction, magnetic, and heat capacity measurements. The compound is crystallised in a monoclinic structure (sp.gr.  $P2_1/c$ ). There are four non-equivalent symmetry positions for the metal ions: M1 ( $2b$ ), M2 ( $2c$ ), M3 ( $4e$ ), M4 ( $4e$ ), five for the oxygen, and one for the boron. The metal ions are disordered over M2 and M4 positions with the occupation factors of Cu:Fe = 0.496:0.504 and 0.328:0.672, respectively. We show that the cationic disorder results from the structural disordering of the O4 oxygen position, which splits into two ones. As a result, an unit cell contains two types of triads: Fe(4A)-Fe(2A)-Cu(4A) and Fe(4B)-Cu(2B)-Fe(4B), which are random distributed.

Mössbauer spectra in the temperature range of  $T = 40 - 300 \text{ K}$  present the sum of several symmetric quadruple doublets with the hyperfine parameters typical for high-spin  $\text{Fe}^{3+}$  ions in the octahedral coordination. The  $dc$  magnetization measurements have shown two magnetic transitions at  $T_1 = 35 \text{ K}$  and  $T_2 = 20 \text{ K}$  and divergence of the FC and ZFC curves below  $T_1$ , implying spin-glass behaviour. The heat capacity measurements of  $\text{Cu}_2\text{FeBO}_5$  have been done in the range of  $4.2 - 300 \text{ K}$  in zero and 90 kOe magnetic fields, which did not reveal any anomalies confirming the assumption of the spin-glass state (Figure 1). The magnetic entropy is saturated at about 100 K and amounts to  $\Delta S = 7.0 \text{ J/mol K}$ , that is 3.5 times smaller than the expected one in the mean-field model. The present results show that the magnetic state of the ludwigites in general and  $\text{Cu}_2\text{FeBO}_5$  in particular, strongly depends on the cation distribution, which, in turn, is extremely sensitive to the synthesis conditions.

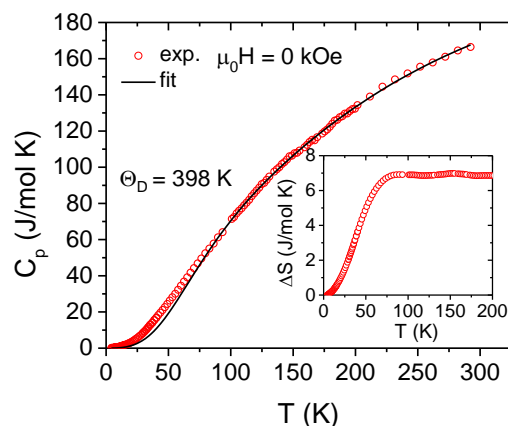


Figure 1 The temperature dependence of the heat capacity of  $\text{Cu}_2\text{FeBO}_5$  single crystal.

Support by Russian Foundation for Basic Research (project no. 21-52-12033) is acknowledged.

[1] J. Schaefer, K. Bluhm, *Z. Anorg. Allg. Chem.*, **621** (1995) 571.

[2] M.A. Continentino et al., *Eur. Phys. J. B*, **9** (1999) 613.

[3] G.A. Petrakovskii et al., *Phys. Solid State*, **51** (2009) 2077.

## INVESTIGATION OF FERRIMAGNETIC PROPERTIES OF IMPURITY ATOMS OF MANGANESE DIFFUSIONLY DOPED IN SILICON

Zikrillaev N.F., Isamov S.B., Kushiev G.A., Abduganiev Y.A., Urakova F.E.

Tashkent State Technical University, Uzbekistan  
zikrillaev.n@gmail.com

Nowadays, much attention in the world is paid to creation of nanoclusters with magnetic properties in alloys and heterostructures by ion implantation or epitaxial growth. The development of technology for producing magnetically nanostructured silicon in a crystal lattice, through the formation of magnetic nanoclusters of manganese atoms and the study of the possibility of controlling magnetic properties in a wide temperature range is an urgent problem [1-2]. The influence of magnetic fields on electrophysical parameters of silicon samples doped with impurity manganese atoms was investigated and the possibility of using these materials for magnetic sensors in spinoelectronics was shown.

The ferromagnetic properties of silicon doped with manganese atoms were first discovered at relatively low temperatures ( $T_1=30$  K). Studies of the ferromagnetic states of silicon diffusion-doped with impurity manganese atoms at a temperature of  $T=300$  K showed that these samples have ferromagnetic properties that have not been discovered to date.

Diffusion of germanium atoms in silicon requires a rather long time due to the small diffusion coefficient. Therefore, it is practically impossible to obtain volumetrically doped silicon with impurity germanium atoms. In this regard, the source material was chosen, pre-doped with germanium atoms during silicon growth by the Czochralski method with a concentration of  $N_{Ge}=9 \cdot 10^{19} \text{ cm}^{-3}$ . Initial samples with the same dimensions were cut from Si<Ge> wafers. Then, in these Si<Ge> samples, the diffusion of manganese atoms was carried out in a two-stage mode. Conducted studies of the obtained samples of Si<GeMn> in a magnetic force microscope brand FM-Nanoview 1000 at the submicron level, we present an analysis of the obtained "magnetic" images of the relief (Figure 1) on samples of Si<GeMn>. After diffusion, the samples were subjected to appropriate mechanical and chemical treatment to remove the layer of manganese silicides from the surface [3].

We have analyzed the obtained "magnetic" images of the relief (Figure 1) on Si<GeMn> samples studied in a magnetic force microscope of the FM-Nanoview 1000 brand at the submicron level.

An analysis of the results of the study showed that silicon samples doped with impurity manganese atoms have ferromagnetic properties not only at low temperatures ( $T_1=30$  K), but also at relatively high temperatures. Studies of the magnetic properties of Si<GeMn> samples have shown that manganese atoms in silicon have a high magnetic sensitivity, which makes it possible to create magnetic sensors and magnetic switches in the field of spin electronics.

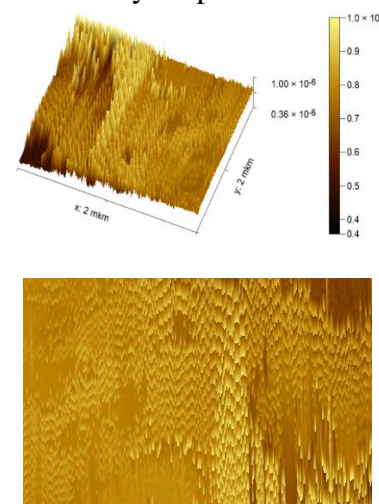


Figure 1. 3D-representation of the topography of magnetic domains and images of the magnetic relief in Si<GeMn> samples.

- [1]. S, Zhou, H. Schmidt, *Materials*, **3** (2010) 5054-5082.
- [2]. Thi Giang Le, IntechOpen (10.5772/ intechopen. 92709) (2020).
- [3]. N.F. Zikrillaev et al., *J. JNEP.*, **15** (2023) 01021.

## ISOTHERMAL-MAGNETOSTATIC MODULI OF THE JAHN-TELLER SUBSYSTEM IN ZINC SELENIDE CRYSTAL DOPED WITH CHROMIUM

*Sarychev M.N.<sup>1</sup>, Zhenstovskikh I.V.<sup>1,2</sup>, Ofitserova N.Yu.<sup>1</sup>, Averkiev N.S.<sup>3</sup>, Gudkov V.V.<sup>1</sup>*

<sup>1</sup> Ural Federal University, Yekaterinburg, Russia

<sup>2</sup> M.N. Mikheev Institute of Metal Physics UB RAS, Yekaterinburg, Russia

<sup>3</sup> Ioffe Institute, RAS, St. Petersburg, Russia

n.ofitserova@mail.ru

Physical acoustics techniques proved to be a very informative one for study the properties of the Jahn-Teller (JT) complexes in doped crystals. They provide information about the symmetry properties of the global minima and saddle points (the energy barriers) of adiabatic potential energy surface (APES) and about the dynamic properties of the JT sub-system (i.e., relaxation time and the mechanisms which define its temperature dependence). Recently, we reported the results of magneto-acoustic investigation of the JT effect (JTE) in  $A^{II}B^{IV}$  crystals doped with  $Cr^{2+}$  ions [1], namely, in cubic  $ZnSe:Cr^{2+}$  and hexagonal  $CdSe:Cr^{2+}$ . The  $Cr^{2+}$  ion substitutes cation in tetrahedral coordination of selenium ions. It has  ${}^5T_2(e^2t^2)$  high-spin ground state and subject to the  $T \otimes (e + t_2)$  JTE problem.

The experiments revealed the tetragonal symmetry of the APES global minima meaning the complex can be described with the vibronic Hamiltonian in linear approximation with respect to symmetrized (tetragonal) deformations. While investigating  $Al_2O_3:Ni^{3+}$  crystal, Sturge et al. [2] interpreted temperature dependence of ultrasonic attenuation caused by the JT subsystem in terms of the relaxed elastic moduli  $c^R$  and the factor of temporal dispersion  $\omega\tau$ , where  $\omega$  is the cyclic frequency of a wave and  $\tau$  is relaxation time. The relaxed moduli describe static properties of the JT subsystem and the factor  $\omega\tau/[1+(\omega\tau)^2]$  describes its dynamics. In zero magnetic field, the relaxed moduli are the isothermal moduli of the subsystem  $c^R=c^T$ . In ref. [1], the magnetic field dependences of attenuation  $\alpha(B)$  were discussed. Therefore, the relaxed moduli were represented by the moduli defined at constant temperature and magnetic induction ( $\mathbf{B}$ )  $c^R=c^{T,\mathbf{B}}$  (i.e., isothermal-magnetostatic moduli). Simulation of such moduli was done with the use of the magnetic field dependences of the ground state energies with account of the lowest levels described by the spin Hamiltonian [3,4]. Such approach made it possible to interpret the high field ( $B \geq 2$  T) behavior of the magnetic induction dependence of attenuation  $\alpha_E(B)$  of the ultrasonic mode associated with the tetragonal modulus  $c_E=(c_{11}-c_{12})/2$ . Two the cases were studied:  $\mathbf{B}||[100]$  and  $\mathbf{B}||[110]$ . At low fields, tunneling mechanism of relaxation defines the mentioned dependence and a more accurate description of the relaxed moduli is a must. In our report, we present the results of calculation of the isothermal-magnetostatic moduli for  $ZnSe:Cr^{2+}$  crystal with account of two energy levels: the lowest and the first higher one which are degenerate at  $B=0$ . Such approach showed appreciable differences with respect to the former one at low fields. It should be used for simulation of ultrasonic attenuation and further comparison with the experimental results.

Support by the Russian Science Foundation (project № 22-22-00735) is acknowledged.

[1] M.N. Sarychev et al., *JETP*, **136** (2023) 80-88.

[2] M.D. Sturge et al., *Phys. Rev.*, **155** (1967) 218-224.

[3] J.T. Vallin et al, *Phys. Rev. B*, **2** (1970) 4313-4333.

[4] J.T. Vallin, G.D. Watkins, *Phys. Rev. B*, **9** (1974) 2051-2072.

## DISTRIBUTION OF $\text{Co}^{2+}$ IONS IN SINGLE CRYSTALS OF $\text{Li}_{0.5}\text{Ga}_{2.5}\text{O}_4$

*Shapovalov V.A.<sup>1</sup>, Shapovalov V.V.<sup>2</sup>, Drokina T.V.<sup>3</sup>, Vorotynov A.M.<sup>3</sup>, Valkov V.I.<sup>1</sup>*

<sup>1</sup> A. Galkin Donetsk Institute for Physics and Engineering, Donetsk, Russia

<sup>2</sup> Organization "Mathematics for America", New York, USA

<sup>3</sup> Institute of Physics n.a. L.V. Kirensky RAS, Krasnoyarsk, Russia

vashapovalov1@mail.ru

The active study of spinels is due to their wide scientific and technological applications [1]. The distribution of cobalt  $\text{Co}^{2+}$  ions in single crystals of ordered reversed lithium–gallium spinel  $\text{Li}_{0.5}\text{Ga}_{2.5}\text{O}_4$  has been studied by Electron Spin Resonance (ESR). The distribution of cobalt  $\text{Co}^{2+}$  ions depends on the structural and magnetic nonequivalence of ions in the elementary cells of single crystals. When an admixture of cobalt  $\text{Co}^{2+}$  is introduced into the matrix of an ordered lithium–gallium spinel, the latter replaces  $\text{Ga}^{3+}$  ions in tetra-positions (upper row – tetrahedra) and in octahedra (lower row - octahedra), and  $\text{Li}^+$  ions located in octahedrons (Figure 1).

The study of the angular dependence of the position of the lines of the ESR spectrum of "tetrahedral  $\text{Co}^{2+}$ " showed the presence of four magnetically nonequivalent positions of ions in the unit cell. The Hamiltonian constants at  $T=4.2\text{K}$  are  $g_{\parallel} = 2.203 \pm 0.002$ ,  $A = (30 \pm 1) \cdot 10^{-4} \text{ cm}^{-1}$ ,  $g_{\perp} = 4.621 \pm 0.005$ ,  $B=0$ . The analysis of the angular dependence of the spectrum of "octahedral  $\text{Co}^{2+}$ " indicates the presence of four magnetically nonequivalent positions of  $\text{Co}^{2+}$  ions in the unit cell. The nearest cationic environment of the ion under study creates only axial distortions along the axes  $\langle 111 \rangle$ . Experimental values of spin-Hamiltonian constants are  $g_{\parallel} = 7.295 \pm 0.005$ ,  $A = (283 \pm 2) \cdot 10^{-4} \text{ cm}^{-1}$ ,  $g_{\perp} = 2.311 \pm 0.002$ ,  $B=0$ .

The study of the angular dependence of the spectrum of "octahedral  $\text{Co}^{2+}$ " located in a crystal field of low symmetry showed the presence of twelve magnetically nonequivalent positions of rhombic  $\text{Co}^{2+}$  in the unit cell. Experimental values of spin-Hamiltonian constants in three main orientations are  $g_z = 6.927 \pm 0.005$ ,  $A = (229.6 \pm 3) \cdot 10^{-4} \text{ cm}^{-1}$ ,  $g_x = 1.972 \pm 0.002$ ,  $B = (30.4 \pm 1) \cdot 10^{-4} \text{ cm}^{-1}$ ,  $g_y = 2.855 \pm 0.005$ ,  $C=0$ .

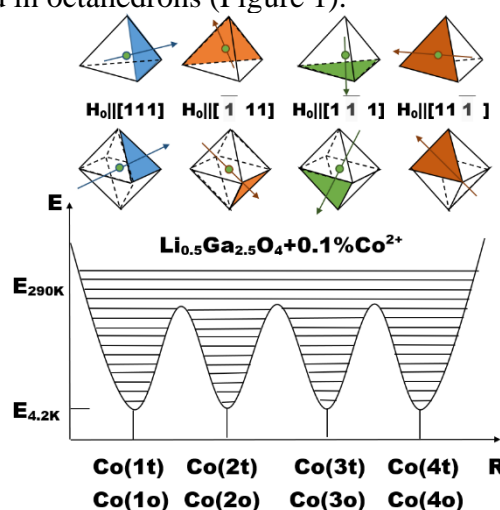


Figure 1. The dependence of the potential of the crystal field  $E$  on the distance  $R$ . The minima are located along the axes of type  $[111]$ . Tetrahedral (t) and octahedral (o) magnetically unequal positions of  $\text{Co}^{2+}$  ions in the unit cell are shown.

[1] V. Tsurkan et al., *Physics Reports*, **926** (2021) 1–86.

## FERRIMAGNETIC PROPERTIES OF THE MINERALS CHROMITE - $\text{FeCr}_2\text{O}_4$ AND TITANOMAGNETITE - $\text{TiFe}_2\text{O}_4$ AT HIGH TEMPERATURES

*Kuvandikov O.K., Shodiev Z.M., Khasanov Kh.B., Khairullaev B.A., Akhtamov Zh.Sh.*

Samarkand State University named after Sharof Rashidov, Samarkand, Uzbekistan  
quvandikov@rambler.ru.

Investigation of the magnetic properties of minerals in rocks from the point of view of mineralogist is topical. In the present time, the magnetic properties of these minerals have been studied mainly in their magnetically ordered state, while their paramagnetic state has hardly been studied [1].

The purpose of this work is to determine the main magnetic characteristics of the iron-bearing minerals chromite and titanomagnetite included in the composition of rocks, by measuring the temperature dependence of their magnetic susceptibility [ $\chi(T)$ ] in the high temperature range of 20-1000°C. The magnetic susceptibility was measured by the Faraday method using high-temperature pendulum balance with relative error of 3%. It can be seen (Figure .) that the dependences  $\chi^{-1}(T)$  of minerals in the temperature range under study are non-linear: the slope of the dependence  $\chi^{-1}(T)$  for chromite increases sharply at the temperature of approximately 550°C, and decreases at 630°C, for titanomagnetite at 780°C it sharply increases, and at 900°C it decreases.

The linear nature of the dependence in the higher indicated temperature range indicates that these dependences obey the Curie-Weiss law.

Changes in dependence  $\chi^{-1}(T)$  in the studied minerals can only be explained by structural (polymorphic) transitions occurring at higher indicated temperatures in the iron sublattices of these minerals. The experimental dependences

$\chi^{-1}(T)$  of the studied samples were calculated for their main paramagnetic characteristics:  $C$ ,  $\theta_p$  and  $\mu_{form}$ .

Table 1. Paramagnetic characteristics of the samples.

Minerals	Temperature range t, C	$\theta_p, K$	$C, 10^4 \text{ cm}^3 \cdot \text{g}^{-1} \cdot K$	$\mu_{form}, \mu_B$
Chromite - $\text{FeCr}_2\text{O}_4$	20-450	63	1343	15,51
	660-900	523	72.05	3,59
Titanomagnetite - $\text{TiFe}_2\text{O}_4$	650-770	853	250	7,48
	910-1000	913	55,56	3,5

An analysis of the table shows that during the structural transition of minerals, their values  $\theta_p$  increase and their  $C$  and  $\mu_{form}$  values decrease. This is explained by the fact that if  $\text{Fe}^{3+}$  ions are partially or completely replaced by  $\text{Cr}^{3+}$  ions in the crystal lattice of minerals, which in both structures show strong tendency to occupy octahedral positions, this will lead to the significant decrease in the Curie temperature.

[1] G.P. Kudryavtseva, *Ferrimagnetism of natural oxides* (Moscow.: Nedra, 1988).

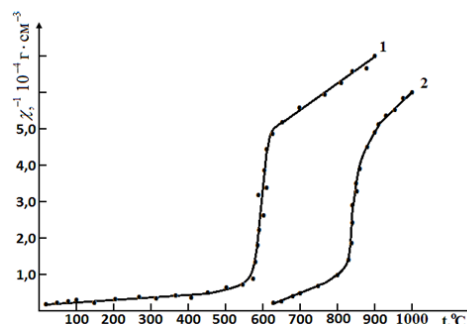


Figure 1. Dependences  $\chi^{-1}(T)$  of the studied samples of chromite (1) and titanomagnetite

## ORIGIN OF WEAK FERROMAGNETISM IN $Zn_{1-x}Co_xO$

*Arslanov A.<sup>1</sup>, Xudoyqulov J.<sup>1</sup>, Nebesniy A.<sup>1</sup>, Nasirov A.<sup>1</sup>, Yuldashev Sh.U.<sup>1,2</sup>*

<sup>1</sup> Physics Department of NUUz, Tashkent, Uzbekistan

<sup>2</sup> Center of Nanotechnology Development, NUUz, Taskent, Uzbekistan  
shavkaty@yahoo.com

ZnO-based diluted magnetic semiconductor (DMS) is a promising candidate for realizing a ferromagnetic semiconductor with high Curie temperature [1]. However, the magnetic properties of  $Zn_{1-x}Co_xO$  reported so far by different research groups are quite contradict. Some reports found that  $Zn_{1-x}Co_xO$  is ferromagnetic at room temperature [2]. While, there are also papers that report on the absence of ferromagnetism in  $Zn_{1-x}Co_xO$  materials [3,4].

This work presents the results of study on the origin of weak ferromagnetism in  $Zn_{0.97}Co_{0.03}O$  thin films grown by using ultrasonic spray pyrolysis. The temperature dependencies of the magnetization and the thermal diffusivity have been conducted. The thermal diffusivity method is very useful for a study of the critical behavior near the phase transition. Taking into account the relationship between the specific heat  $C$  and the thermal diffusivity  $D$  through the equation  $C = K/\rho D$  (where  $\rho$  is the density and  $K$  is the thermal conductivity), the inverse of the thermal diffusivity has the same critical behavior as the specific heat.

$Zn_{1-x}Co_xO$  ( $x = 0.03$ ) thin films were deposited on Si (100) substrates by using ultrasonic spray pyrolysis. Aqueous solutions of zinc acetate (0.5 mol/l) and cobalt acetate (0.5 mol/l) were used as sources of Zn and Co, respectively. These solutions were mixed in the appropriate proportions in order to obtain the desired Co concentration. The substrate temperature was set at 400 °C, and the thickness of  $Zn_{0.97}Co_{0.03}O$  films was about 200 nm.

Figure 1 shows the temperature dependence of the magnetic specific heat of the  $Zn_{0.97}Co_{0.03}O$ , which was obtained by using the equation given above.

The useful quantity which can be extracted from the magnetic specific heat is the magnetic entropy, associated with the ordering of the local magnetic moments. The magnetic entropy calculated from the magnetic specific heat of the  $Zn_{0.97}Co_{0.03}O$  is shown in the inset of Figure 1, and its value is about 0.12 J mol<sup>-1</sup>K<sup>-1</sup>, which is approximately three times lower than the expected 0.35 J mol<sup>-1</sup>K<sup>-1</sup> or  $0.03R\ln(2S+1)$  value for the  $Zn_{0.97}Co_{0.035}O$  with the  $S = 3/2$  spin of Co<sup>2+</sup> ions. These results show that only a small part of Co ions in the  $Zn_{0.97}Co_{0.03}O$  is involved in the ferromagnetic ordering. The uncompensated magnetic moment at the surface of CoO nanoclusters causes the weak ferromagnetism in the  $Zn_{0.97}Co_{0.03}O$ .

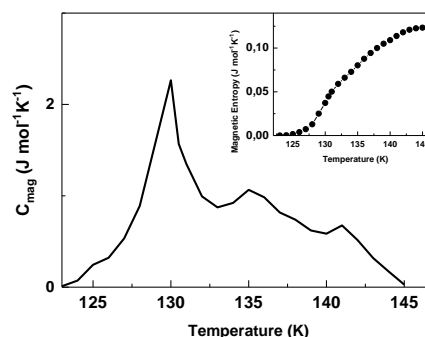


Figure 1. The magnetic specific heat as a function of temperature for the  $Zn_{0.97}Co_{0.03}O$ . The insert shows the magnetic entropy of the phase transtion.

Support by IEEE, ARC, and ARCNN is acknowledged.

- [1] T. Dietl et al., *Science*, **287** (2000) 1019-1022.
- [2] K. Ueda, H. Tabata, T. Kawai, *Appl. Phys. Lett.*, **79** (2001) 988-990.
- [3] M. Bouloudenine et al., *Appl. Phys. Lett.*, **87** (2005) 052501.
- [4] S. Deka, R. Pasricha, P.A. Joy, *Phys. Rev. B*, **74** (2006) 033201.

## OPERANDO SYNCHROTRON STUDIES OF MAGNETOELECTRIC COUPLING AT THE FM/FE-HfO<sub>2</sub> INTERFACE (FM= Co-Ni, Pt-Fe, EuS)

Zenkevich A.

Moscow Institute of Physics and Technology, Dolgoprudny, Moscow region, Russia  
zenkevich.av@mipt.ru

Composite multiferroic materials with coexisting ferroelectric and ferromagnetic orders open alternative prospects for development of multifunctional electronic devices. However, the application of multiferroic materials is limited by poor compatibility of ferroic materials with the modern Si-based technology. This limitation can be overcome by the use of ferroelectric (FE) doped HfO<sub>2</sub> or alloyed Hf<sub>0.5</sub>Zr<sub>0.5</sub>O<sub>2</sub> (HZO) films. In this regard, exploring the possible magnetoelectric (ME) effect at the FE/FM interface in the heterostructures comprising FE-HfO<sub>2</sub> is crucial for development of Si-compatible composite multiferroics. By using the prototypes of FE-HfO<sub>2</sub> based memory capacitors on the chip with wiring to external source-meter unit, which enables *in situ* electrical polarization switching/measurement, we perform *operando* synchrotron experiments to establish the ME coupling effects at FM/FE-HfO<sub>2</sub> interface.

In particular, X-ray magnetic circular dichroism (XMCD) and magnetic circular dichroism in angular distribution of photoelectrons (MCDAD) have been employed to probe element-selectively the local magnetic properties at Ni/FE-HZO interface and to demonstrate the effect of FE polarization switching on the magnitude and/or orientation of the magnetic moment of a nm thick marker Ni layer at the interface (Figure 1) [1].

Alternatively, using synchrotron based <sup>57</sup>Fe Mössbauer spectroscopy technique *in operando*, the local magnetic properties of a nanometer-thick enriched <sup>57</sup>Fe marker layer in functional Pt/<sup>57</sup>Fe/HZO/TiN capacitors are probed element-selectively and the evidence of the FE polarization effect on the  $\alpha$ -Fe FM response is demonstrated [2].

Furthermore, low T FM semiconductor EuS integrated with FE-HZO in a bilayered structure is promoted as a prospective composite multiferroic. The comprehensive information on the structural, chemical, and electronic properties of EuS/HZO interface endorses it as a promising medium for magnetoelectric coupling phenomena, particularly, the effect of polarization reversal in FE-HZO on the magnetic and transport properties in EuS [3].

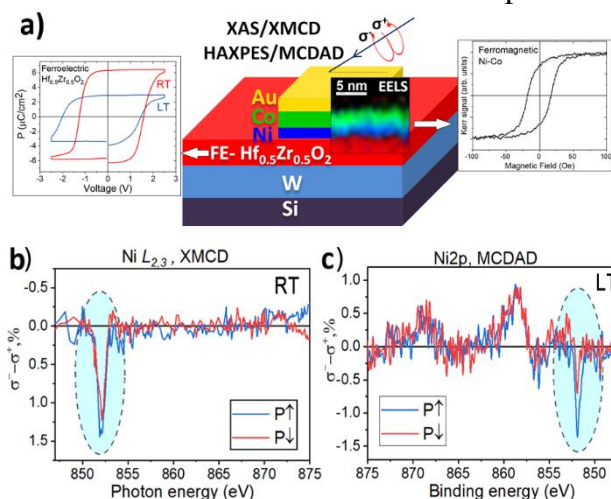


Figure 1. a) capacitor device structure used in the experiments; b) Ni 2*p* line taken at LT for  $\sigma^+$  and  $\sigma^-$  circular polarization of X-rays demonstrating MCD effect; c) the effect of ferroelectric polarization switching on MCDAD signal for Ni 2*p* core level line.

The support from Grant No. 075-11-2021-086 (Minobranauki) is acknowledged.

[1] A. Dmitriyeva et al., *ACS Nano* **15** (2021) 14891-14902.

[2] V. Mikheev et al., *Adv. Mat. Interfaces*, **9** (2022) 2201341.

[3] A. Khanas et al., *Adv. Mat. Interfaces*, **7** (2020) 2000411.

**July 3**

Monday

18:00 - 20:00

POSTER  
SESSIONS

Section L10

**Magnetic materials.**

**High Frequency Properties**

## PHOTOELASTIC PROPERTIES OF LEAD MOLYBDATE CRYSTALS WITH PARAMAGNETIC IMPURITIES OF SODIUM AND NEODYMIUM

*Akhmedzhanov F.H., Elboeva M.I., Mirzaev S.Z.*

<sup>1</sup> Institute of Ion-plasma and Laser Technologies, Tashkent, Uzbekistan  
akhmedzhanov.f@gmail.com

In this work, the photoelastic properties of  $\text{PbMoO}_4$  crystals, which are widely used as an active medium in acousto-optic devices [1] have been studied. In particular, the influence of paramagnetic impurities of sodium and neodymium on the effective photoelastic constant  $p_{\text{eff}}$ , which is the convolution of the values of the components of the photoelastic tensor  $p_{ijkl}$  of the crystal over the normalized polarization vectors of the diffracted and incident light  $\alpha$  and  $\beta$ , respectively, and the direction and polarization of the acoustic wave  $\kappa$  and  $\gamma$  [1]:

$$p_{\text{eff}} = p_{ijkl} \alpha_i \beta_j \gamma_k \kappa_l, \quad (1)$$

The experiments were carried out on pure and doped with sodium or neodymium impurities  $\text{PbMoO}_4$  samples. The concentration of Na and Nd impurities was about 0.3 mol.%. The samples were oriented along the [100] and [001] axes. The measurements were performed using the Bragg light diffraction method on acoustic waves, which were excited by X-cut quartz piezoelectric transducers in the range of 400–1600 MHz. The light source was a helium-neon laser ( $\lambda_0=632.8$  nm). The modified Dixon-Cohen method was used to determine the effective photoelastic constants [1]. The accuracy of determining the value of  $p_{\text{eff}}$  with respect to the standard (fused quartz) was about 20%.

Studies have shown that in doped  $\text{PbMoO}_4$  crystals, the velocity of acoustic waves along the crystallographic axes remains practically unchanged, however, a strong dependence of the effective photoelastic constant on the direction of propagation of the acoustic wave and the polarization of the incident light is observed. This effect is most pronounced in crystals of lead molybdate with an admixture of neodymium.

Figure 1 shows the dependence of the effective photoelastic constant on the direction of polarization of light incident on a  $\text{PbMoO}_4:\text{Nd}$  sample, along the crystallographic axis [010]. It can be seen that the experimental values are in good agreement with the theoretical curve calculated from the expression:

$$p_{\phi\psi}^2 = p_{11}^2 \cos^2 \psi + p_{31}^2 \sin^2 \psi \quad (2)$$

where  $\psi$  is the angle between the light polarization vector and the [100] axis in the (010) plane.

It can be seen that, by changing the direction of polarization of the incident light, one can control the value of the effective photoelastic constant and, accordingly, the efficiency of the Bragg light diffraction.

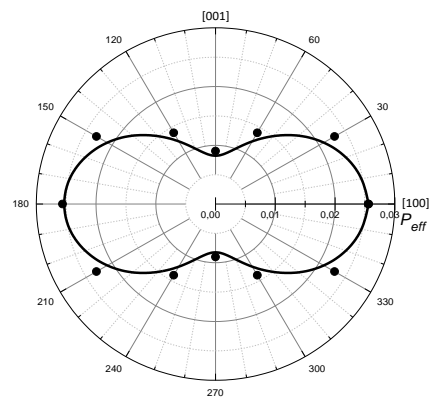


Figure 1. Dependence of the effective photoelastic constant on the direction of polarization of light in  $\text{PbMoO}_4:\text{Nd}$  crystals. Curve line is calculation, points are experiment

[1] R.W. Dixon, *IEEE Trans*, **17**(1) (1980) 229-235.

## ATTENUATION OF ACOUSTIC WAVES IN CUBIC CRYSTALS AT HIGH FREQUENCIES

*Akhmedzhanov F.H., Kurbanov J.O., Makharov N.M.*

Institute of Ion-plasma and Laser Technologies, Tashkent, Uzbekistan  
akhmedzhanov.f@gmail.com

In contrast to the propagation velocity the anisotropy of attenuation of high-frequency acoustic waves in cubic crystals is investigated insufficiently. In this work the attenuation of acoustic waves in NaCl, NaBr, Bi<sub>12</sub>SiO<sub>20</sub> and MgO cubic crystals has been investigated on the basis of experimental data on the attenuation of acoustic waves at high frequencies propagating along the main crystallographic directions. Measurements were carried out using Bragg diffraction of light by acoustic waves at room temperature in the frequency range from 0.4 to 1.8 GHz.

According to the known perturbation theory, the attenuation coefficient can be defined in terms of the effective viscosity. Since the viscosity tensor has the same symmetry as the elastic stiffness tensor, three independent constants must be determined for the crystal class 23, to which belong the investigated crystals. All the viscosity components were determined by substituting effective viscosity values obtained from measured attenuation data into the mode viscosity equations

The obtained viscosity components were used for calculation of the anisotropy of attenuation of three wave modes propagating along any selected direction using equation:

$$\alpha = \omega \cdot \eta_{\text{eff}} / 2\rho \cdot V_3 \quad (1)$$

where  $\omega$  is the circular frequency,  $\eta_{\text{eff}}$  is the effective viscosity for selected direction,  $\rho$  is the density and  $V$  is the propagation velocity of acoustic wave.

Calculations have been carried out for acoustic waves propagating in (001) and (110) crystallographic planes. At the same time the contribution of dielectric loss in the total attenuation coefficient of piezoactive waves was assessed for piezoelectric crystals [1]. It is shown that the dielectric loss can produce a significant influence on the magnitude and anisotropy of the attenuation coefficient for piezoactive longitudinal and transverse waves in Bi<sub>12</sub>SiO<sub>20</sub> crystals.

The cross-section of the attenuation surfaces of (1) quasi-longitudinal, (2) quasi-transverse, and (3) purely transverse acoustic waves by the (110) plane in MgO crystals is shown at Figure 1. It can be seen that the strongest attenuation anisotropy in this plane is observed for quasi-transverse waves whose polarization vector lies in the same plane. The obtained results can be due to the spatial dispersion of the effective Grüneisen constant [2, 3].

[1] I.G. Shaposhnikov, *JETP*, **11** (1941) 332-339.

[2] Yu.A. Logachev, B.Ya Mozhes. *Solid State Physics*, **16(8)** (1974) 2219-2223.

[3] R. Nava et al., *Phys. Rev. B*, **14(2)** (1975) 800-807.

## SPIN CURRENT FOR TUNING THE BAND GAPS OF SPIN WAVES

*Morozova M.M., Lobanov N.D., Matveev O.V.*

Saratov State University, Saratov, Russia

mamorozovama@yandex.ru

Layered structures of magnetic dielectrics (for example, yttrium iron garnet, YIG) and conductors with strong spin-orbit coupling and large Hall angle (for example, Pt) are considered as one of the basic elements for the development of purely spin information and communication technologies, in which moving charges are replaced by spin waves or magnons [1,2]. The electric current in Pt, due to the inverse spin Hall effect, generates a spin current, in turn, due to the transfer of spin transfer torque at the YIG/Pt interface, it leads to an increase or decrease in the spin waves in YIG [3]. Accordingly, in layered structures consisting of two YIG layers separated by a Pt layer, spin current leads to an increase in spin waves power in one YIG layer and a decrease in the other [4]. The use of magnonic crystals (MC) - ferromagnetic films with periodic modulation of parameters creates conditions for the formation of band gaps - non-transmission bands in the spin waves spectrum [5].

The aim of this research is to study the possibility of band gaps tuning using spin current in a layered structure consisting of two MCs with a system of grooves on the surface separated by a Pt layer. The wave model has been constructed to describe the spin-wave evolution, and a dispersion relation for spin waves under the action of spin current has been obtained.

It is shown that the formation of two band gaps in the first Brillouin zone is possible in the structure under study. The mechanism of the formation of band gaps is related to the interaction at phase-matching frequencies of symmetric and antisymmetric direct and reflected normal waves of the coupled structure. Band gaps are formed at Bragg wave numbers and frequencies different from the Bragg frequencies for each of the MC in the absence of coupling between them through the Pt layer.

The spin current in Pt leads to a change in the effective magnetic field for each of the noted types, which makes it possible to control the frequency position of the band gaps, the width of the band gaps, the frequency interval between the bands, and the band gap depth. In particular, in a structure based on a single MC and Pt layer, depending on the direction of the spin current, the same amplification (or attenuation) of the spin wave takes place in the frequency range both outside and in the band gap. In two MCs separated by Pt layer, the introduction of spin current leads to an increase in the spin waves attenuation in the frequency range of band gaps and to increase in the depth of the band gaps. In addition, the high-frequency band gap is shifted down in frequency, and the low-frequency band gap is shifted up in frequency, i.e. the frequency interval between the band gaps decreases.

The practical importance of the result lies in the fact that the control of band gaps of spin waves using a spin current makes it possible to use such a structure as a basic functional element of frequency-selective microwave devices with a double (electric and magnetic) based on the principles of spintronics.

Support by Russian Science Foundation (grant № 23-29-00759).

[1] A. Barman et al., *J. Phys. Condens. Matter*, **33** (2021) 413001.

[2] P.G. Baranov et al., *Phys.-Usp.*, **62** (2019) 795.

[3] Y. Zhou et al., *Phys. Rev. B.*, **88** (2013) 184403.

[4] Xg. Wang, Gh. Guo, J. Berakdar., *Nat Commun.*, **11** (2020) 5663.

[5] A.V. Chumak et al., *J. Phys. D: Appl. Phys.*, **50** (2017) 244001.

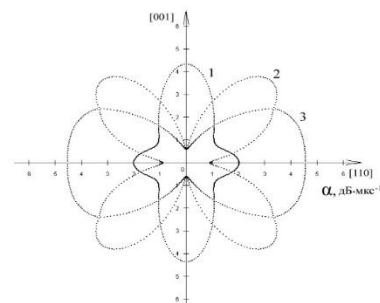


Figure 1. Cross-section of attenuation surfaces of quasi-longitudinal (1), quasi-transverse (2), and pure transverse (3) acoustic waves by the (110) plane in MgO crystals.

## SPIN WAVES BRAGG IN RESONANCES IN MULTIFERROIC SANDWICH YIG/HZO

*Morozova M.M.<sup>1</sup>, Matveev O.V.<sup>2</sup>, Markeev A.M.<sup>1,2</sup>, Nikitov S.A.<sup>1,2</sup>*

<sup>1</sup> Saratov State University, Saratov, Russia

<sup>2</sup> Moscow Institute of Physics and Technology, Dolgoprudny, Russia

<sup>3</sup> Kotel'nikov Institute of Radioengineering and Electronics RAS, Moscow, Russia

mamorozovama@yandex.ru

We have demonstrated the hysteresis and frequency tuning (electrical and magnetic) of the Bragg resonance in the spectrum of spin waves in a sandwich structure YIG/TiN/HZO/TiN (yttrium iron garnet/ titanium nitride/ hafnium-zirconium oxide/ titanium nitride, 100 nm/20 nm/10 nm/20 nm) with periodic modulation of the parameters.

The originality of the structure lies, firstly, in the technology of creation using liquid-phase epitaxy of YIG film and atomic layer deposition of TiN and HZO films, which makes it possible to effectively combine the layers and allows to keep the ferromagnetic and ferroelectric properties of each layer. Secondly, such structure is the monolithic multiferroic structure with layer thicknesses on the order of tens of nanometers, which demonstrates the interaction of the magnetic and ferroelectric subsystems. Thirdly, the developed technology for creating grooves on the surface makes such a structure a Bragg reflecting grating.

In particular, it is shown that the HZO layer in the composition of the sandwich structure demonstrates the hysteresis property (saturation voltage up to 3 V, remanent polarization up to 9.2  $\mu\text{C}/\text{cm}^2$ ), a two-level state, and the wake-up effect. In the YIG layer, the propagation of spin waves at frequencies of 1–4 GHz with a change in the magnetic field of 120–800 Oe was discovered. A Bragg band gap is observed in the spin waves excitation band. The position of the band gap depends on the voltage (HZO polarization); when the voltage changes to 3 V, the frequency tuning is up to 1.3 MHz; the direction of the BG shift on the electric field changed at a coercive voltage of 1.1 V. The alteration characteristic is of the “butterfly” type.

The theoretical model is developed and it is shown that the main mechanism for the formation of a band gap is the interaction of direct and reflected from periodic inhomogeneities spin waves. When a voltage is applied to the ferroelectric layer and its polarization changes, a magnetoelectric effect takes place, which affects the mechanism of interaction between direct and reflected waves. As a result, the position of the band gap in the spectrum of spin waves is determined by the remanent polarization of the ferroelectric layer and also has the property of hysteresis.

The practical importance of the result lies in the fact that the hysteresis dependence of the Bragg resonance of spin waves on the ferroelectric polarization, which was revealed in a nanoscale monolithic multiferroic structure, makes it possible to use such structure as a memory cell. This memory cell will allow combining the advantages of ferroelectricity and magnonics in one structure and can be integrated into modern CMOS electronics.

Support by Russian Science Foundation (grant № 19-79-20121).

[1] A. Barman et al., *J. Phys. Condens. Matter*, **33** (2021) 413001.

[2] Y. K. Fetisov and G. Srinivasan, *Appl. Phys. Lett.*, **93** (2008) 033508.

[3] *Ferroelectricity in Doped Hafnium Oxide: Materials, Properties and Devices* (Elsevier, 2019).

## EFFECTS OF THE COMPOSITION OF A 2D-SEMICONDUCTOR LAYER ON THE EFFICIENCY OF SPINTRONIC THZ EMITTER

*Lebedeva E.D.<sup>1</sup>, Buryakov A.M.<sup>1</sup>, Andeev P.Yu.<sup>1</sup>, Gorbatova A.V.<sup>1</sup>, Sapozhnikov M.V.<sup>2,3</sup>, Pashenkin I.Y.<sup>2,3</sup>, Mishina E.D.<sup>1</sup>*

<sup>1</sup> MIREA - Russian Technological University, Moscow, Russia

<sup>2</sup> Institute for Physics of Microstructures RAS, Nizhny Novgorod, Russia

<sup>3</sup> Lobachevsky State University, Nizhny Novgorod, Russia  
caterina-lebedewa2015@yandex.ru

THz radiation has shown great potential for medical, security, and communications applications in recent years, which explains the demand for compact, controllable, highly efficient, and wideband THz emitters. In 2013, Kampfrath et al. [1] demonstrated the generation of THz radiation by irradiation with femtosecond laser pulses of ferromagnetic/non-magnetic heterostructures, due to spin-charge conversion. Such spintronic THz emitters are not inferior to traditional THz emitters (nonlinear optical crystals, photoconductive antennas, etc. [2,3]), and surpass them in their architecture, cost and polarization control possibility [4]. But it is worth noting that the combination of a ferromagnet and a semiconductor with a high spin-orbit interaction leads to an increase in the efficiency of THz radiation generation [5]. Monolayer transition metal dichalcogenides (TMDs) can be used as such semiconductors, whose electrical and optical properties depend on their thickness and composition [6].

The object of this work is to evaluate the effect of the monolayer TMD on the magnetic properties of the THz spintronic emitter. A series of samples were made: IrMn/Co/Sapphire, IrMn/Co/WSe<sub>2</sub>/Sapphire, and IrMn/Co/MoSe<sub>2</sub>/Sapphire. The antiferromagnetic layer (IrMn) was used to create uniaxial magnetic anisotropy.

THz time-domain spectroscopy was used to obtain THz-H hysteresis depending on the laser radiation energy density for a series of investigated samples. The value of the coercive field increases with increasing laser energy. When reaching 1 mJ/cm<sup>2</sup> the coercive field reaches saturation. It is shown that at an optical power of 0.35 mJ/cm<sup>2</sup>, the coercive field values for the spintronic generator with WSe<sub>2</sub> and MoSe<sub>2</sub> layer are 0.2 kOe and 0.39 kOe, respectively.

Despite the decrease in the coercive field, the amplitude of the THz signal increases as the power density increases. This indicates that only the cobalt layer is the source of the spin current. And the change in the coercive field is due to the antiferromagnetic manganese iridium layer.

The study was supported by the Russian Science Foundation grant No. 23-19-00849.

[1] T. Kampfrath et al., *Nature nanotechnology*, **8(4)** (2013) 256-260.

[2] A. Rice et al., *Applied physics letters*, **64(11)** (1994) 1324-1326.

[3] D.H. Auston, K.P. Cheung, P.R. Smith. *Applied physics letters* **45(3)** (1984) 284-286.

[4] T. Seifert et al., *Nature photonics*, **10(7)** (2016) 483-488.

[5] D. Khusyainov et al., *Materials*, **14(21)** (2021) 6479.

[6] G.-H. Jung, Y. SeokJae, Q.-H. Park., *Nanophotonics*, **8(2)** (2018) 263-270.

## THz GENERATION BY A MAGNETIC SPINTRON EMITTER BASED ON Co/IrMn<sub>3</sub>

*Avdeev P.Yu.<sup>1</sup>, Gorbatova A.V.<sup>1</sup>, Buryakov A.M.<sup>1</sup>, Lebedeva E.D.<sup>1</sup>, Pashenkin I.Y.<sup>2,3</sup>, Sapozhnikov M.V.<sup>2,3</sup>, Mishina E.D.<sup>1</sup>*

<sup>1</sup> MIREA - Russian Technological University, Moscow, Russia

<sup>2</sup> Institute for Physics of Microstructures RAS, Nizhny Novgorod, Russia

<sup>3</sup> Lobachevsky State University, Nizhny Novgorod, Russia  
pasha.avdeev.2000@mail.ru

The conversion of spin polarization into a charge current under the action of femtosecond laser pulses is one of the main mechanisms for the generation of terahertz (THz) radiation in spintronics emitters based on metal bilayers of nanometer thickness of ferromagnetic/nonmagnetic metal (FM/NM) type [1–2]. The effect of converting the spin current into the charge current was also demonstrated for the ferromagnet/antiferromagnet (FM/AFM) structure in [3]. The use of an AFM layer in spintronic emitters can expand their potential, since AFM provides resistance to external magnetic fields, faster magnetic order manipulation, amplification of terahertz radiation, and many other advantages [4–5].

Our work was focused on the Co(3 nm)/IrMn<sub>3</sub>(5 nm) structure as a source of THz radiation. Our study was focused on the magnetization properties of the sample and the polarization of the terahertz signal generated by it.

The experiment was carried out by the THz-TDS method in the transmission geometry described in detail in [6]. The magnetic interaction of IrMn<sub>3</sub> with Co enhances the uniaxial magnetic anisotropy of the sample. This confirms the dependence of the amplitude of the THz signal peak on the magnitude of the magnetic field applied to the sample (THz hysteresis), shown in Figure 1. An increase in the energy density of the pump pulse from 0.35 to 3.85 mJ/cm<sup>2</sup> led to a decrease in the coercive force of the sample from 270 to 40 Oe. This is due to an increase in the demagnetization of the sample with increasing laser heating.

The distortion of the THz hysteresis loops (yellow regions in Figure 1) obtained by applying a magnetic field along the easy magnetization axis of the sample indicates the presence of intermediate states of magnetization. This phenomenon can provide an additional degree of freedom to control the device's terahertz polarization. However, the terahertz polarization profile obtained by rotating the terahertz polarizer along the path of the terahertz signal is unstable. In other words, the magnetization in this state tends to saturation.

The study was supported by the Russian Science Foundation grant No. 23-19-00849.

[1] E.T. Papaioannou, R. Beigang, *Nanophotonics*, **10(4)** (2021) 1243–1257.

[2] W. Wu et al., *JAP*, **130(9)** (2021) 091101.

[3] O. Gueckstock et al., *Applied Physics Letters*, **120(6)** (2022) 062408.

[4] E.V. Gomonay, V.M. Loktev, *Low Temperature Physics*, **40(1)** (2014) 17-35.

[5] Y.Y. Wang et al., *Progress in Nat. Science: Materials International*, **27(2)** (2017) 208-216.

[6] D. Khusyainov et al., *Scientific reports*, **11(1)** (2021) 1-8.

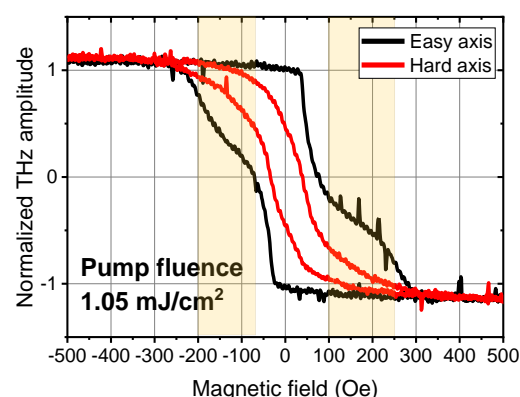


Figure 1. THz hysteresis loops.

## VALIDITY OF THE QUASI-TEM APPROXIMATION FOR PERMITTIVITY AND PERMEABILITY MEASUREMENTS IN ONE-PORT AND TWO-PORT STRIPLINES

*Ivanov P.A., Petrov D.A., Rozanov K.N.*

Institute of Applied and Theoretical Electrodynamics RAS, Moscow, Russia  
p.ivanov.a@mail.ru

Currently, coaxial and quasi-optic techniques are the most conventional for wideband measurement of frequency-dependent dielectric and magnetic performance of materials. However, these measurement methods are not universal. A significant limitation of the coaxial technique is that the sample under test must have a special shape, with very high sensitivity to the air gaps between the sample and the measuring cell. The quasi-optic method requires samples of large size, which is frequently not feasible, especially for low-frequency measurements.

These limitations can be circumvented by the use of strip transmission lines, where a small sample fills a part of the cross section of the stripline measuring cell. The standard approach of processing the measurement data in this method employs the quasi-TEM approximation that has been proven to be valid for the case when the measured sample is a film of small thickness [1]. However, if the sample under test is either a composite material or metamaterial, its thickness may be high that can result in large measurement error [2].

This work is aimed at studying the validity range of the quasi-TEM approximation in extracting the permittivity and permeability of a sample under test from the measured data collected with one-port and two-port stripline measuring cells in case when the sample has a thickness comparable with the height of the stripline cell.

With the use of numerical and experimental methods, the validity limits of the quasi-TEM approximation have been shown to be determined by the magnitude of the longitudinal wave components exciting at the sample. The study covers the dependence of these limits on the size of the measuring stripline cell, on the material parameters and the size of the sample, and on the position of the sample in the measuring cell.

This study was financially supported by the Russian Science Foundation (RSF) under project no. 21-19-00138 (<https://rscf.ru/en/project/21-19-00138/>).

[1] T. Sebastian et al., *J. Appl. Phys.*, **113** (2013) 033906.

[2] P.A. Ivanov et al., *Bull. Russian Acad. Sci.: Physics*, **86** (2022) 574-578.

## NUMERICAL SIMULATION OF LEFT-HANDED BEHAVIOR IN THE FERROMAGNETIC METAMATERIAL WITH AN ARRAY OF HIGH PERMITTIVITY DIELECTRIC RODS

*Amelchenko M.D.<sup>1</sup>, Ogrin F.Yu.<sup>2,3</sup>, Grishin S.V.<sup>1</sup>*

<sup>1</sup> Saratov State University, Saratov, Russia

<sup>2</sup> The University of Exeter, Exeter, England

<sup>3</sup> MaxLLG Ltd., England

amelchenko.mar@gmail.com

It is well known that metamaterials are artificial structures possessing electromagnetic properties that natural materials do not have [1]. There is a class of metamaterials called as left-handed metamaterials (LH) with both negative permittivity  $\epsilon$  and permeability  $\mu$ . To produce LH metamaterials for microwave range the thin conductive wire array and the array of split ring resonators (SRR) structured on the subwavelength scale are usually used [2]. These structures have effective permittivity and permeability ( $\epsilon_{eff}$  и  $\mu_{eff}$ ) respectively. The paper [3] demonstrates the results of electromagnetic simulation conducted via MaxLLG software [4] of the LH media composed of the superconductive wire array and ferromagnetic (FM) matrix. Here, we consider the model, in which metallic wires are replaced by dielectric rods with the high relative permittivity  $\epsilon_1$  [5] (Figure 1a). We analyze a metallized layer of the FM metamaterial with an external constant magnetic field parallel to rods and normal to electromagnetic wave (EMW) propagation. The dispersion characteristics for slow EMWs propagating in the structure are shown in Figure 1b. There are two backward waves with similar bands can be seen, whereas there is a single corresponding wave in case of metallic wires.

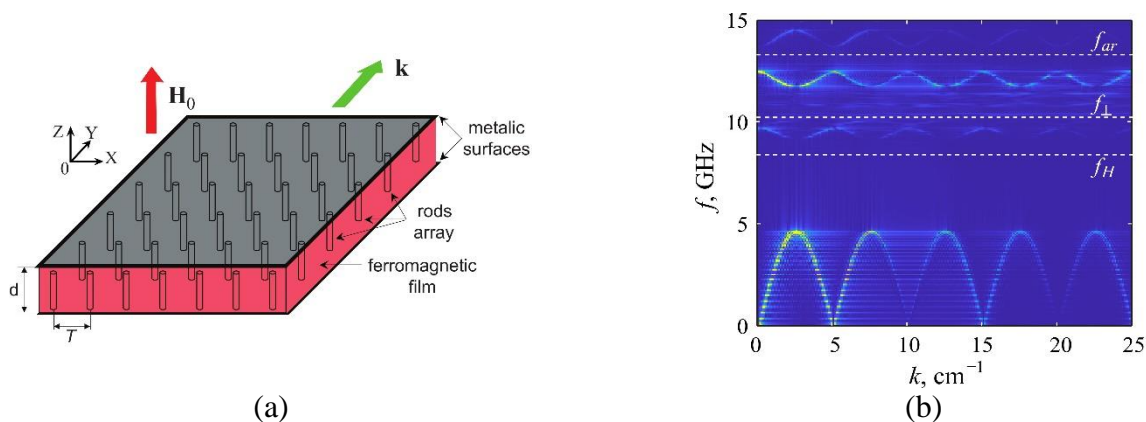


Figure 1. (a) Two-dimensional magnetic metamaterial. (b) Dispersion characteristics for slow EMWs in the FM metamaterial with covered dielectric rods,  $H_0 = 3$  kOe,  $M_0 = 139.3$  G,  $T = 2$  mm,  $r_1 = 0.3$  mm,  $r_2 = 0.4$  mm,  $d = 0.5$  mm  $\epsilon_1 = 600$  and  $\epsilon_r = 16$ .

The work was supported by the Russian Science Foundation grant No. 23-79-30027, <https://rscf.ru/en/project/23-79-30027/>.

[1] Metamaterials. Devices and Applications, Ed. by A.L. Borja. Intech Open. (2017).

[2] D.R. Smith et al., *Phys. Rev. Lett.*, **84**(18) (2000) 4184–4187.

[3] M.D. Amelchenko et al., *Izv. VUZ. AND*, **30**(5) (2022) 563-591.

[4] High Frequency Magnetics Software [Electronic resource]. Available from: <https://www.maxllg.com>.

[5] L. Peng et al., *Phys. Rev. Lett.*, **98**(15) (2007) 157403.

## INFLUENCE OF MAGNETIC FIELDS ON THE REFLECTION OF MICROWAVE WAVES FROM THE STRUCTURES $\text{Fe}_3\text{O}_4/\text{CoO}$ AND $\text{Fe}_2\text{O}_3$

*Antonets I.V., Koton L.N.*

Syktyvkar State University named Pitirim Sorokin, Syktyvkar, Russia  
aiv@mail.ru

In this paper, the results of studies of the effect of weak magnetic fields (up to 0.30 T) on the reflection coefficient of microwave radiation of magnetic structures with the compositions  $\text{Fe}_2\text{O}_3$  (Fe~38.44 at. %, O~61.56 at. %) and  $\text{Fe}_3\text{O}_4/\text{CoO}$  (Co~7.85 at. %, Fe~25.98 at. %, O~66.17 at. %) were presented.

Magnetic structures were obtained by ion-beam sputtering on a polymer substrate. The thickness of the samples was 65.60  $\mu\text{m}$  for  $\text{Fe}_2\text{O}_3$  structures and 64.92  $\mu\text{m}$  for  $\text{Fe}_3\text{O}_4/\text{CoO}$  structures. The thickness of the magnetic layer was estimated at 0.80  $\mu\text{m}$  and 0.75  $\mu\text{m}$ , respectively.

The reflection coefficient of microwave waves from structures was measured in the frequency range 8–12 GHz. The method for determining the structural and reflective characteristics is described in [1,2]. A piece of the waveguide with a film was placed in the gap of an electromagnet, in which the magnetic field induction varied from 0 to 0.30 T.

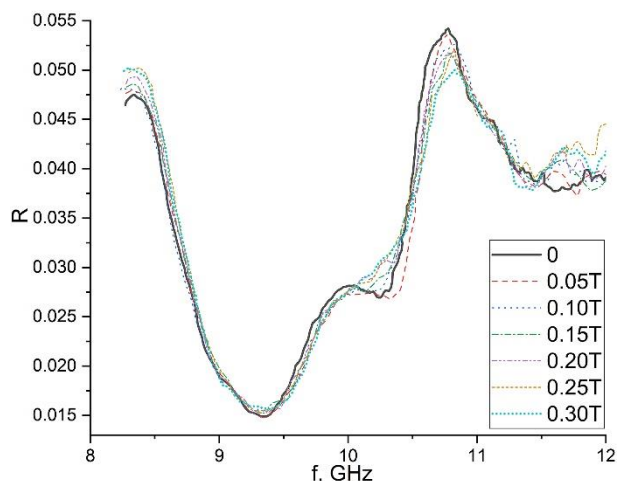


Figure 1. Frequency dependences of the microwave reflection coefficient for  $\text{Fe}_3\text{O}_4/\text{CoO}$  structures.

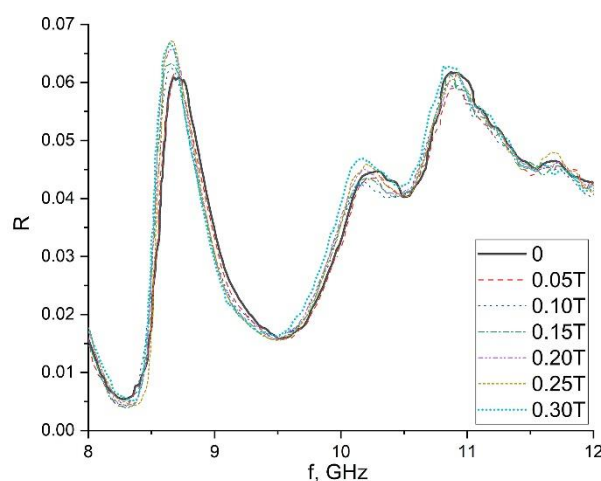


Figure 2. Frequency dependences of the microwave reflection coefficient for  $\text{Fe}_2\text{O}_3$  structures.

As follows from Figure 1, 2, magnetic field induction affects the microwave reflection coefficient of  $\text{Fe}_2\text{O}_3$  and  $\text{Fe}_3\text{O}_4/\text{CoO}$  structures. For  $\text{Fe}_3\text{O}_4/\text{CoO}$  structures (Figure 1), the effect of a magnetic field at various frequencies allows both increasing the maximum value of the reflection coefficient and decreasing it. For  $\text{Fe}_2\text{O}_3$  structures (Figure 2), exposure to a magnetic field mainly leads to an increase in the microwave reflection coefficient. The frequency shift of the extremes of the reflection coefficient is primarily determined by the dependence of the magnitude of the real component of the magnetic susceptibility of the sample on the induction of the magnetic field, and the change in the absolute value of the reflection coefficient in the extremes is determined by the dependence of the magnitude of the imaginary component of the magnetic susceptibility of the sample on the magnetic field.

The reported study was funded by RSF according to the research project № 21-72-20048.

[1] I.V. Antonets et al., *Mater. Chem. and Phys.*, **240** (2020) 122097.

[2] I.V. Antonets et al., *Current Appl. Phys.*, **29** (2021) 97.

**July 3**

Monday

18:00 - 20:00

POSTER  
SESSIONS

Section L11  
**Miscellaneous**

## MAGNETIC CHARGE AND PROBLEMS OF MAGNETISM

*Kuvandikov O., Amonov B.*

Samarkand State University named after Sharof Rashidov, Samarkand, Uzbekistan  
quvandikov@rambler.ru

Physicists - researchers have been looking for magnetic monopole for more than hundred years, but they finally found it in nature and wrote about this discovery in the pages of the journal Science in January 2010. According to the concepts of modern physical theory, the magnetic field can be generated both by an electric current, i.e. moving electric charges, and the hypothetical pole of magnetism - magnetic monopole or magnetic charge.

The first source of the magnetic field is the moving electric charge, determined by experience. For the first time, the magnetic field of an electric current was observed by H. Oersted in 1820. The process of formation of magnetic field around conductor with current was described by the Maxwell equation.  $\frac{4\pi}{c} \vec{j} = \text{rot} \vec{H}$ , where  $\vec{j}$  - electric current density vector,  $\vec{H}$  - magnetic field strength vector,  $c$  - speed of light.

The second source of the magnetic field - the magnetic charge (magnetic pole, monopole) has so far remained hypothetical particle. It is important to note here that in the literature there are reports of more than forty experimental works carried out from 1910 to 1945. F. Ehrenhart with collaborators dedicated to the detection of magnetic charge [1-3].

The experimental and theoretical state of the problem of magnetic particles dates back to the mid-seventies. Work on the problem of magnetic charge was carried out in the mode of a scientific "hobby" and continued intermittently until the mid-1990s.

The proposed magnetic particles are magnetic analogs of electrons, i.e. have the same charges and masses with it, and also belong to the class of fermions. Therefore, the magnetic poles in matter turned out to be "disguised" by nature as electrons, and in theory they are sometimes presented as anomalous "electrons". An example of such representation is uncompensated 3d and 4f electrons, which are called magnetic in theory. The question is quite appropriate: what would the discovery of monopole bring to science? Before answering it, it is expedient once again to draw the attention of researchers to this problem in modern physics. The electron was the first elementary particle known to physicists. The question is quite appropriate: what would the discovery of monopole bring to science? Before answering it, it is expedient once again to draw the attention of researchers to this problem in modern physics. The electron was the first elementary particle known to physicists. It was directly involved in the discovery of the quantum of light (photon) and the first antiparticle (positron). The development of the theory of the electron contributed to the creation of the theory of relativity, the crowning achievement of classical physics. Physics of the 20th century grew out of the theory of the electron - the quantum theory of electron interactions serves as powerful tool for comprehending the structure of hadrons.

And what can you expect from the monopole? First, the possibility of creating completely new super-powerful accelerators, since the monopole acquires enormous energy at relatively short distances under the influence of strong magnetic packets. For example, the 90 m long accelerator would have more energy than the accelerator in Botavia, the length of the ring, which is 3 km; Secondly, one can hope to find new sources of energy, the creation of "microscopic" generators and engines, as well as large-scale applications in biology and medicine; Thirdly, fundamental change in the theory of magnetism and an explanation of number of magnetic phenomena and processes.

[1] F. Ehrenhaft, *Kais. Akad. Wiss. Wien*, **119(110)** (1910) 815–867.

[2] F. Ehrenhaft, *Journal of the Franklin Institute* 233, (1942) 235-255.

[3] F. Ehrenhaft, *Acta. Phys. Ausrtiaca*, **5** (1951) 12.

## PHOTOELECTRIC CHARACTERISTICS OF SI PHOTODETECTORS

Gaibov A.G., Eshqulov A.A., Vahabov Q.I.

Tashkent State Technical University named after Islam Karimov. Tashkent. Uzbekistan  
abdigani4@rambler.ru

A characteristic feature of the studies of acoustically stimulated effects in silicon detectors carried out at the time of the present studies is that they were carried out exclusively for silicon detectors compensated by lithium (Li), the so-called silicon-lithium detectors - drift Si (Li) - detectors. Intensive scientific research led to the discovery of the decay of some local inhomogeneities in ultrasonic fields [1, 2].

The purpose of this work is to analyze in detail the behavior of the photoelectric characteristics of Si-n-p optical receivers before and after ultrasonic treatment. Silicon photodetectors belong to the class of radiation detectors and the results of their research will provide valuable information that can be used to improve the functional characteristics of semiconductor photoelectronic devices (photodiodes, photoresistors, etc.).

The presented spectral dependence of the photoresponse after sonication (Figure 1, curve 2) in the region  $\lambda_0 = 0,6 \mu\text{m} \div 0,8 \mu\text{m}$  shows its increase compared to the original curve. This indicates that the surface recombination has a low rate and it is suppressed by ultrasound in the surface layers of the np junction of the Si photodetector. In the wavelength range  $\lambda_0 = 0,7 \mu\text{m} \div 0,8 \mu\text{m}$ , an increase in photosensitivity by approximately 15÷20% is observed. The increase in the photoresponse is also clearly manifested in the longer wavelength region of the spectrum  $\lambda_0 \geq 0,8 \mu\text{m} \div 1,2 \mu\text{m}$ , that is, the collection of nonequilibrium charge carriers, which are formed during the absorption of photons of lower energies, is facilitated due to the acoustically stimulated increase in the diffusion length of carriers in silicon.

It has been established that ultrasonic irradiation of receivers by the radiation of the "input" window leads to a change in the concentration of electrically active centers in the sensitive region of the receiver, which smooth the impurity relief by the mechanism of acoustically stimulated diffusion. In this case, there is an increase in the lifetime, diffusion length of carriers and, as a consequence, an increase in the efficiency of carrier collection at the electrical contacts of Si-n-p receivers. As a result of these processes, an increase in the short circuit current is observed, which causes an increase in the open circuit voltage and the efficiency of such a diffusion Si-n-p structure operating in the photoconversion mode.

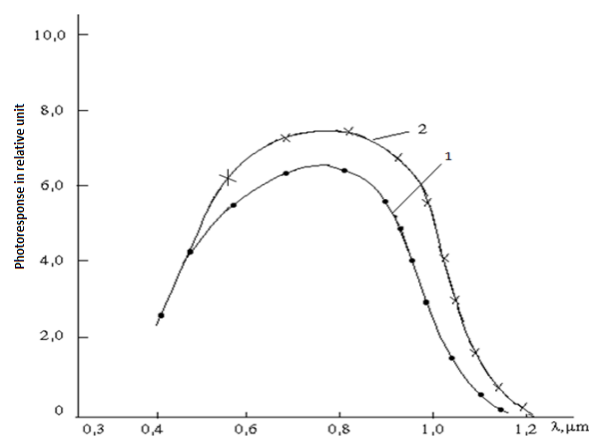


Figure 1. Spectral dependence of the photoresponse of a Si-n-p photodetector before (curve 1) and after (curve 2) the action of ultrasound with  $I^* = 0.25 \text{ W/cm}^2$  and frequency  $f = 25 \text{ MHz}$  for  $t = 40 \text{ min}$  at  $T = 300\text{K}$

[1] A.G. Gaibov et al., *Letters to JETP*, **10(10)** (1984) 616-620.

[2] N.N. Zaveryukhina, K.I. Vakhobov, A.G. Gaibov, *Reports by AS of RUz*, **6** (2005) 20-23.

## DETERMINATION OF THE ELEMENTAL COMPOSITION OF ENVIRONMENTAL OBJECTS USING INSTRUMENTAL NEUTRON ACTIVATION ANALYSIS

*Kurbanov B.I., Khaydarov A.A., Danilova E.A., Osinskaya N.S.*

<sup>1</sup> Institute of Nuclear Physics of the Academy of Sciences of the Republic of Uzbekistan, Tashkent, Republic of Uzbekistan

<sup>2</sup> Tashken State Technical University named after I. Karimov, Tashkent, Republic of Uzbekistan  
abduaziz.81@mail.ru

Currently, due to the intensive development of the country's industrial enterprises, environmentally unfavorable territories are increasingly observed, which in turn greatly affects the health of the population. In order to assess the situation in advance and take preventive measures, highly sensitive analytical methods for analyzing macro- and microelement composition in objects of the human environment play an important role. Studies of the ecological situation of the environment around us (in samples of soil, water, plants, etc.) in terms of macro- and microelement composition are becoming increasingly important, which is associated with many factors. Due to the ability to deposit chemical elements in its structure, hair can act as an indicator of changes in the environment, living conditions, nutrition and labor activity of a person over the past 1-2 years [1-4]. In addition, hair is a convenient, affordable and easy material for sampling and analysis.

The prevalence of macro- and microelements in soil, water, plant and food samples, especially in agricultural products, makes it possible to assess the impact of technogenic impacts of industrial facilities, incl. used toxic elements.

The elemental composition of human hair can be affected by emissions of heavy and toxic elements from vehicles, industrial enterprises, thermal power plants, agricultural fertilizers, etc. The study of the microelement composition of biological tissues of the population living at different distances from pollution sources makes it possible to estimate the distribution range of emissions and to identify their specificity [2].

The relationship between indicators of public health and the state of the human environment has been studied by many authors [1-4]. The stability of the distribution of chemical elements in the body is one of the most important and indispensable conditions for its normal functioning. Accordingly, deviations in the content of chemical elements caused by environmental and geographical factors can lead to a wide range of disorders in human health [1-3]. The data on the elemental composition of hair make it possible to assess the elemental status of the body and identify risk groups [3].

The purpose of the study is to use instrumental neutron activation analysis to assess the prevalence of macro- and microelements in environmental objects (soil, water, plants, food) and hair of residents of various regions of Uzbekistan and to study the distribution of microelements in our environment and in the body of people in the study areas.

[1] A.P. Avcyn, A.A. Zhavoronkov, *Mikrojelementozy cheloveka: jetiologija, klassifikacija, organopatologija* (Moscow: Medicina, 1991).

[2] N.A. Agadzhanjan, A.V. Skal'nyj, *Himicheskie jelementy v srede obitanija i jekologicheskij portret cheloveka* (Moscow: KMK, 2001).

[3] Ju.F. Babikova et al., *Mikrojelementnyj sostav volos naselenija kak indikator zagryaznenija prirodoj i proizvodstvennoj sred in Aktivacionnyj analiz: Metodologija i primenenie*. (Tashkent: Fan, 1990).

[4] L.I. Zhuk, A.A. Kist, *Kartirovanie jelementnogo sostava volos. in Aktivacionnyj analiz. Metodologija i primenenie*. (Tashkent: Fan, 1990).

3PO-L11-4

## MONITORING OF ATMOSPHERIC OZONE BY THERMAL RADIATION SPECTRA

*Kurbaniyazov S.Kh., Kurbaniyazov A.S., Turniyazov R.K.*

<sup>1</sup> Samarkand State University named after Sharof Rashidov, Samarkand, Uzbekistan

<sup>2</sup> Samarkand branch of Tashkent University of Information Technology, Samarkand, Uzbekistan  
safarjan@mail.ru

One of the serious problems of the coming century is the study of the ozone layer of the atmosphere, which protects life on Earth from UV radiation from the Sun and affects the thermal regime of the atmosphere and climate. The depletion of the ozone layer in the polar and middle latitudes and the appearance of "ozone holes" and "mini-holes" over Antarctica and the Northern Hemisphere give a particular urgency to this problem. To obtain prompt and accurate information about the state of the ozone layer and predict changes in it, reliable methods for measuring the ozone content at various altitudes are needed. This problem can be solved by studying atmospheric ozone from the spectra of thermal radiation. A strong emission band of the main ozone oscillation  $\nu_3=1042\text{ cm}^{-1}$ , which opens up the possibility of round-the-clock ground-based registration of ozone radiation using a standard two-beam infrared spectrophotometer. To do this, atmospheric radiation is directed into the channel of the spectrometer sample, and radiation from cold standard with temperature much lower than  $-50^{\circ}\text{C}$  is directed into the comparison channel. The tracking system is a photometric wedge-diaphragm, which, moving in the comparison channel, maintains the equality of both streams at the receiver.

To implement the proposed method, it is necessary to change the phase of the signal that controls the movement of the wedge by  $180^{\circ}$ . Otherwise, the wedge of a typical spectrometer will completely move out of the comparison channel and "go off scale" when the comparison flow becomes much weaker than the sample flow.

Thus, the experimental results obtained by us and the calculated value of the integral radiation coincide with the quantitative and temperature parameters of ozone. To find the parameters, it suffices to know two values of the area of the emission band. For example, measuring at different angles to the horizon. (Such solution is possible because the integral absorption is not directly proportional to the optical path in the ozone layer).

[1] A.P. Kapitsa, A.A. Gavrilov, *DAN-1999*, **366(4)** 543-546.

[2] S.P. Perov, A.Kh. Khrchianu, *Modern problems of atmospheric ozone* (1980).

[3] V.B. Kashkin, T.V. Rubleva, *Bull. of the Tomsk Polytech. Uni.*, **311(5)** (2007) 116-119.

## INVESTIGATION OF HYDROGEN-BONDED COMPLEXES OF THE FORMAMIDE IN THE PROTON-ACCEPTOR SOLUTIONS BY POLARIZED RAMAN SPECTROSCOPY AND DFT CALCULATIONS

*Jumabaev A., Husbvaktoev H., Absanov A., Holikulov U., Norkulov A.*

Samarkand State University named after Sharof Rashidov, Samarkand, Uzbekistan

jumabaev2@rambler.ru

In condensed phase molecular systems, intermolecular and intramolecular interactions give rise to different spectral features. Hydrogen bonding plays a central role in the structure and function of biological systems [1]. Spectroscopic analysis of the structure and dynamics of weakly interacting molecular complexes is the starting point for a detailed understanding of various macroscopic properties. Polarized Raman spectroscopy is well suited to study these interactions in liquid phases [2]. Also, density functional theory (DFT) can be used to determine molecular-level parameters in addition to experimental results.

Experimental studies of hydrogen-bonded binary solutions using Raman spectroscopy increase our understanding of intermolecular interactions. The analysis of line profiles and wavenumber shifts of selected vibrational Raman bands allows studying intermolecular and molecular interactions as well as molecular reorientations. In this study, we focused on studying the intermolecular interactions and formation mechanisms of molecular complexes of formamide in proton acceptor solvents such as acetonitrile and dimethylsulfoxide (DMSO).

Raman spectra of pure and 0.1–0.9 mol fraction concentration solutions of formamide were recorded at room temperature using a Renishaw inVia Raman spectrometer. The geometric structures of molecular complexes in solutions were optimized based on the set of DFT:B3LYP/6-311++G(d,p) functions in the Gaussian 09W program [3].

It can be seen from the total Raman spectrum of pure formamide that there are spectral lines of high intensity in the region of 1200–1500 cm<sup>-1</sup>. The spectral line at 1312 cm<sup>-1</sup> has a wide half-width and shifts to a lower frequency as the percentage of solvents increases. A change in the concentration of the solution does not cause a shift of the high-intensity spectral line at 1392 cm<sup>-1</sup>. Two spectral peaks are also observed in the 1500–1800 cm<sup>-1</sup> region: the peak at 1593 cm<sup>-1</sup> belongs to NH<sub>2</sub> symmetric bending vibrations, and the peak at 1668 cm<sup>-1</sup> belongs to C=O stretching vibrations. The 1668 cm<sup>-1</sup> spectral line has asymmetry on the high-frequency side. As the amount of solvents in the solutions increases, it is observed that the spectral lines related to C=O stretching and NH<sub>2</sub> bending vibrations shift to a lower frequency by 15–20 cm<sup>-1</sup> and show a significant increase in asymmetry.

AIM analysis based on Bader's theory [4] confirmed the presence of N-H...O and N-H...N hydrogen bonds in the complexes formed by formamide molecules with acetonitrile and DMSO molecules.

[1] A. Jumabaev et al., *J. of Mol. Liq.*, **377** (2023) 121552.

[2] F. Tukhvatullin et al., *J. of Mol. Liq.*, **160(2)** (2011) 88–93.

[3] M. J. Frisch et al., Gaussian 09, Gaussian, Inc., Wallingford CT, 2009.

[4] R. F. W. Bader., *Chem. Rev.* **91(5)** (1991) 893–928.

## STUDY OF STRUCTURAL PHENOMENA IN AQUEOUS SOLUTIONS OF NON-ELECTROLYTE BY THE METHOD OF DYNAMIC LIGHT SCATTERING

*Sabirov L.M.<sup>1</sup>, Khaidarov X.S.<sup>1</sup>, Jurayev Y.T.<sup>1</sup>, Karshiboyev Sh.E.<sup>1,3</sup>, Kadirov Sh.A.<sup>2</sup>, Khasanov M.A.<sup>1</sup>, Norjigitov A.<sup>1</sup>*

<sup>1</sup> Samarkand State University named after Sharof Rashidov, Samarkand, Uzbekistan

<sup>2</sup> Urgench state university, Urgench, Uzbekistan

<sup>3</sup> Uzbek-Finnish Pedagogical Institute of SSU, Samarkand, Uzbekistan

leonard.sabirov@gmail.com

A whole class of aqueous solutions of organic substances at a certain temperature and concentration has an unusual thermodynamic properties. The diagram of the phase states of such solutions is observed with a significant deviation of thermodynamic parameters [1]. Physical processes leading to these anomalies can be manifested in the molecular scattering of light. Since scattering is due to fluctuations of thermodynamic parameters, the scattering intensity will depend on these fluctuations. We have completed the study of the indicator's indicators of the light in the aqueous solutions of non-electrolytes. The experiment technique is described in [2]. The figure shows the graphical behavior of the relative intensity of the molding, depending on the scattering angle: for clean water and for a solution of  $\gamma$ -pycolin with different concentrations at a temperature  $T = 350$  C at a scattering angle from 300 to 900. As can be seen from the figure, the relative intensity of the molding of the mold light is strongly dependent on the concentration of  $\gamma$ -pycolin in the water. And this change is different for different scattering angles. On angular dependence, a straight line depends to be different for different concentrations. A small amount of  $\gamma$ -pycoline molecules significantly affects the intensity of MDS for all scattering angles. Thus, we can conclude that the presence of alien molecules of a continuous mesh of hydrogen water lines lead a noticeable change in the structure of a three-dimensional solid mesh in the scattering volume of aqueous solution. Thus, the studies of the MDS, depending on the concentration at various scattering angles, can be used to diagnose the solution structure [2].

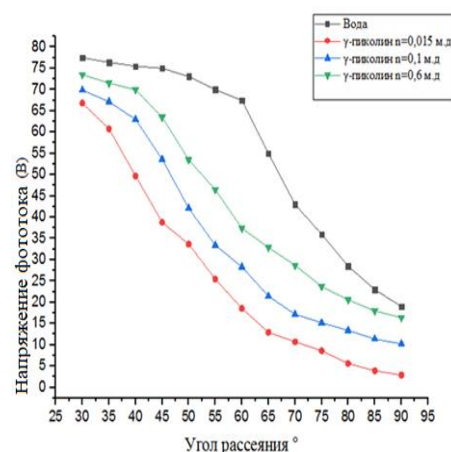


Figure 1. Relative intensity of the molding, depending on the scattering angle.

[1] D. Subramanian, *Journal of Sankt-peterburg SU*, **4** (2013) 139-153.

[2] B.E. Eskin, *Scattering of light by solutions of polymers* (Spb: Nauka, 1986).

## STUDY THE DEPENDENCE OF HOLE MOBILITY AND ELECTRICAL CONDUCTIVITY ON THE THICKNESS OF THE SILICIDE LAYER

*Isaev M.Sh.<sup>1</sup>, Eshkulov A.A.<sup>2</sup>*

<sup>1</sup> National University of Uzbekistan named after M.Ulugbek. Tashkent, Uzbekistan

<sup>2</sup> Tashkent State Technical University, Tashkent, Uzbekistan

abdugani4@rambler.ru

One of the urgent problems of today is the study of physical processes occurring in the surface and near-surface regions of single-crystal silicon, diffusively doped with impurities that create deep levels. In diffusion-doped silicon crystals, a surface layer with a thickness of 30-40 microns is formed with a concentration of impurity carriers exceeding their solubility by 2-4 orders of magnitude and with other electrophysical parameters, namely, with high specific conductivity and low mobility relative to the parameters of the bulk part.

The attention of most researchers focused on the bulk part of the crystal obtained by removing the near-surface region, so the near-surface layer was considered to be disturbed and not of practical interest.

However, for a deep study of the process of diffusion doping of silicon with metals and rare-earth atoms, it is necessary to consider such important issues as the physics of the formation of a strongly doped near-surface region, the nature of the formation of metal silicides, which are very different from metal and semiconductor, as well as physical and chemical processes occurring in the near-surface region (mutual diffusion, solid-phase reactions, etc.)

Currently, transition metal silicides are becoming the basic materials for new promising technological schemes of future generations due to their resistance to aggressive environments and high-temperature treatments. Therefore, a comprehensive study of the mechanism of impurity entry into the crystal volume and their interaction with both matrix atoms of the crystal and technological impurities is relevant.

From this point of view, the study of the formation of silicides in the surface region of silicon during diffusion doping and the development of new semiconductor devices based on them is of particular scientific importance in the context of creating new materials for micro - and nanoelectronics.

In this paper, we study the galvanomagnetic properties of the silicide layer formed during the diffusion of single-crystal silicon by chromium, cobalt, and manganese atoms, which play an important role when used as a material for GIS, SGIS, photoelectric, thermoelectric, and other semiconductor devices.

Based on studies of the temperature dependences of the electrical conductivity of the near-surface region of silicon doped with manganese and cobalt, it is established that the electrical conductivity monotonically increases with decreasing temperature. The same dependence for Si<Cr> is expressed by a curve with a minimum at 450-470K. It is shown that the conductivity of the near-surface region in the studied temperature ranges for Si<Mn>, and Si<Co> crystals (Si<Cr> at T<450K) is metallic. In crystals of chromium-doped silicon at high temperatures (T>450 K), a semiconductor character of conductivity is observed. The temperature course of conductivity is explained by the scattering of current carriers on phonons and impurity ions.

It is established that the removal of layers from the surface of Si<Cr>, Si<Mn>, and Si<Co> samples results in a decrease in the conductivity and an increase in the mobility of current carriers. An increase in the surface resistivity from 10-25  $\Omega/\square$  to 120-130  $\Omega/\square$  deep into the crystal is shown in all doped samples.

[1] M.Sh. Isaev et al., *Electronic processing of materials*, **5** (2006) 80-83.

[2] M.Sh. Isaev, *Bulletin of TSTU*, **1** (2002) 10-14.

## ON THE APPLICATION OF THE METHOD OF DIAMAGNETIC ANISOTROPY TO STUDY THE ORIENTATION OF MOLECULAR CHAINS NATURAL FIBERS

*Islamov B.Kh.<sup>1</sup>, Vakbobotov K.I.<sup>2</sup>*

<sup>1</sup> Tashkent Institute of Textile and Light Industry. Tashkent, Republic  
Uzbekistan

<sup>2</sup> Tashkent State Technical University. Tashkent, Republic of Uzbekistan  
b.islamov.mkb@mail.ru.

Taking into account that all fibers have a diamagnetic anisotropy, which is very sensitive to the molecular orientation of the polymer and the close packing factor of pressure macromolecules, it seems appropriate, based on measurements of this structural parameter, to try to estimate the contribution to the deformation-strength properties of natural silk of its protein components - fibroin and sericin [1].

The studies of the specific diamagnetic anisotropy from the drawing temperature to the multiplicity  $\lambda=1.2$  for the original silk fiber and the fiber processed in boiling water for different times showed that in the processed silk the degree of molecular orientation of the fibers decreases in proportion to the time of thermal-moist treatment. Moreover, due to thermal stretching,  $\Delta\chi'$  of the processed silk increases less than that of the original silk. The increase in  $\Delta\chi'$  up to  $T=140^\circ\text{C}$  during silk thermal drawing with  $\lambda=1.2$  is due to the achievement of a higher degree of orientation of macromolecules in the thread, due to the implementation of a higher level of molecular mobility in it. The decrease in  $\Delta\chi'$  after the drawing temperature  $T=140^\circ\text{C}$  is associated with the occurrence of a flow in the polymer due to the sliding of macromolecules relative to each other.

The performed studies, the dependence of fibroin  $\Delta\chi'$  on the stretching ratio at different temperatures, showed that in this case, with an increase in the stretching,  $\Delta\chi'$  of the fiber quickly increases, reaching values comparable with  $\Delta\chi'$  of the original silk. It should be noted that the extraction of the original silk (from the cocoon) up to a factor of  $\lambda=1.25$  and at temperatures below  $120^\circ\text{C}$  is already accompanied by a rupture of individual fibers.

It is known that sericin has ordered regions consisting of  $\beta$ -structural pressure sites. But the results obtained on diamagnetic anisotropy cannot be explained only by the washing out of part of the sericin during the processing of silk in boiling water. First of all, the decrease in  $\Delta\chi'$ , processed silk is caused some times by the orientation of molecular chains in fibroin and sericin. This is also confirmed by a decrease in the breaking load of the pre-treated silk fiber (table).

The fact that fibers shrink by 4-5% in boiling water, as well as an increase in stability in double bends, testifies in favor of the mechanism of disordering the structure in processed silk. This stability is extreme in nature and depends on the time of thermal and moist treatment, which is explained by the presence of two competing processes - the misorientation of fibroin macromolecules, leading to an increase in resistance to double bending, and the leaching of sericin and fat-wax parts, causing the opposite effect.

Thus, during the thermal-moist treatment of natural silk, in addition to the washing out of sericin, the fibroin macromolecules pass into a less oriented (compared to the initial) state. Processing temperature and time during which one or another part of sericin is extracted and one or another degree of fibroin molecular orientation ( $\Delta\chi'$ ) is achieved, which characterizes the deformation-proportional properties of natural silk.

[1] B.Kh. Islamov, *The American Journal of Engineering and Technology*, **5** (2023) 01-06.

**STUDY BY ELECTRONIC PARAMAGNETIC RESONANCE  
SPECTROSCOPY OF THE FEATURES OF RADICAL FORMATION IN  
THE PROCESS OF NATURAL FIBERS PROCESSING**

*Islamov B.Kb.<sup>1</sup>, Vakobov K.I.<sup>2</sup>, Mirkamilova M.S.<sup>2</sup>*

<sup>1</sup>Tashkent Institute of Textile and Light Industry. Tashkent, Uzbekistan

<sup>2</sup>Tashkent State Technical University. Tashkent, Uzbekistan

b.islamov.mkb@mail.ru

Under the influence of mechanical loads on the polymer, it is deformed, and in this case, the individual macromolecules are in a stressed state. The value of the accumulated internal energy depends mainly on the degree of deformation and on the structure of a particular molecule. Intertwined chains can slip, stretch, or break depending on the rate of relaxation.

In the process of studying the bond breaking mechanism, it was suggested that under the action of stress, the development of any of the three principal types of reactions becomes possible: radical, ionic, or ion-radical.

Grinding is one of the oldest methods used to effect the degradation of polymers. This process is especially convenient for studying the number and type of primary radicals formed by mechanical action, since it proceeds at very low temperatures and a high ratio to surface area and volume.

Crushing under compression is analogous to the structural changes that occur during the operation or degradation of polymers. The grinding of polymers includes the following stages: changing the size and shape of particles, destruction of the supramolecular structure, weakening and disintegration of molecular aggregates during the destruction of intra- and intermolecular bonds, a decrease in crystallinity, a drop in molecular weight; formation of macroradicals on new surfaces; change in the properties of polymers.

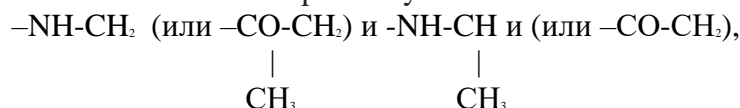
Mechanical destruction of polymers occurs by breaking chemical bonds in macromolecules. The formation of free radicals due to the breaking of intramolecular bonds has been studied by the EPR method in a number of works. In polymers destroyed by crushing at low temperatures, primary "mechanical" radicals resulting from bond breaking were found and identified.

Free radicals found in stressed polymers at moderate temperatures turned out to be secondary, relatively stable radicals, formed mainly as a result of the abstraction of hydrogen atoms. Such radicals were considered as products of radical reactions initiated by the cleavage of macromolecules.

This work is devoted to a structural study of natural silk and polyethylene occurring during the grinding process, as well as to the study of free radical stages of mechanical destruction of natural silk and polyethylene by the EPR method.

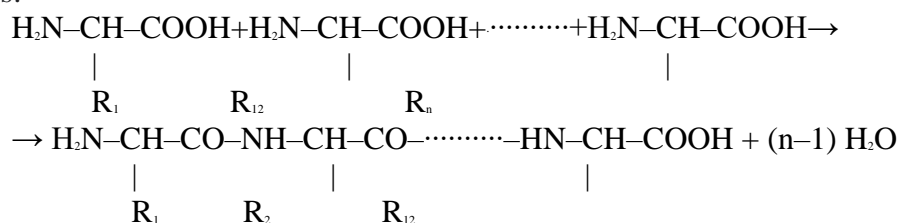
The destruction (grinding) of polymers was carried out in a vibrating mill cooled with liquid nitrogen. To ensure effective cooling of the destructible (ground) polymers, the mill flask was filled with gaseous helium. This made it possible to record the EPR spectra of the primary radicals of the studied polymers. The spectra were recorded on an EPR-3 setup.

The performed studies have shown that the resulting spectrum can be considered as the position of a triplet  $c$  in the region  $\Delta H \sim 20$  e and a quintuplet with approximately the same splitting into a doublet. As the temperature rises, the fraction of the doublet spectrum increases, and as the temperature drops to room temperature, an almost pure doublet is recorded with splitting in the region of  $\Delta H \sim 18$  e. A symmetrical doublet with such splitting belongs to the  $-\text{NH}-\text{CH}-\text{CO}-$  radicals. Triplet and quintuplet, naturally associated with radicals respectively

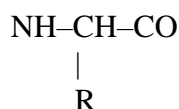


the formation of which most likely occurs during the development of a protein molecule. The main amino acids from which the natural silk protein is built are glycine and alanine, therefore, the peptide groups in the molecule most often include  $-\text{CH}_2-$  and  $-\text{CH}(\text{CH}_3)-$  groups. Since the peptide bond in a protein molecule is the strongest, chain breakage should predominantly occur along the bonds between the peptide and the above groups.

Therefore [1-3], the structure of fibroin molecules is explained on the basis of the polypeptide theory, according to which the polypeptide formation reaction can be schematically represented as follows:



The polypeptide chain is built according to the type of  $\beta$ -helix and is formed by the repetition of groups



and, if fully extended, its frame is zigzag. The length of the chain can be different (up to  $15 \cdot 10^{-8}$  m). and the thickness of the core is  $45 \cdot 10^{-11}$  m. Fibroin is a relatively highly oriented substance, oriented areas make up 40-60% of the fiber mass. The side chains consist of radicals R, which are characteristic of individual amino acids, and make up 19% of the mass of the molecule.

With an increase in temperature during the destruction of silk, the absolute number of radicals  $-\text{NH}-\text{CH}-\text{CO}-$  increases. This appears as a result of a reaction involving the radicals  $-\text{CH}_2$  and  $-\text{CH}(\text{CH}_3)$ . In all likelihood, these reactions occur even in the process of crushing silk at low temperatures.

[1] E.S. Sashina et al., *J. of App. Chem.*, **79(6)** (2006) 881-888.

[2] E.S. Sashina et al., *J. of Therm. An. and Calor.* 89(3) (2007) P 887 -891.

[3] B.Kh. Islamov, *The American Journal of Engineering and Technology*, **5** (2023) 01-06.

July 4

9:00 - 10:30

Tuesday

PLENARY  
LECTURES

## TOWARD HELIMAGNET BASED SPINTRONICS

*Ustinov V.V., Yasyulevich I.A.*

M.N. Mikheev Institute of Metal Physics UB RAS, Yekaterinburg, Russia

ustinov@imp.uran.ru

In the present plenary talk, we review the state of the art in the theoretical description of spin transport in conductive helimagnets (HM). We demonstrate that the most significant features of the conduction electrons spin transport in HM are formed under the action of two main factors. The first factor is the action on the conduction electrons of the spin-motive force (SMF) generated by the spatially inhomogeneous exchange field, which is created by localized magnetic moments ordered into a spin helix. The second one is the effect of spin torque transfer (STT) from the system of itinerant electrons to the system of localized magnetic moments. Both the SMF and the STT in HM depend most significantly on the chirality of the spin helix formed by the localized magnetic moments.

We have demonstrated [1] that two physical effects – the electrical magnetochiral effect (EMChE) and the kinetic magnetoelectric effect (KMEE) – can be explained through the interaction of the spins of itinerant electrons in HM with spatially inhomogeneous effective magnetic field of exchange origin. All the parameters of EMChE and KMEE are presented in terms of the characteristic frequencies of spin relaxation of conduction electrons in a HM and the frequencies of their Larmor precession in exchange field.

The frequency regions of spin relaxation and spin precession are determined to observe a giant electrical magnetochiral effect and resonant behavior of the chiral magnetoresistance. We have called the appropriate effect as “magnetochiral kinetic resonance” (MChKR). The physical nature of MChKR is elucidated. The latter arises due to the coincidence of the Larmor precession frequency of an electron in the effective field and the phase change frequency of the helicoidal exchange field acting on the electron moving along the helicoid’s axis with a speed equal to that of the electron flow. We have demonstrated how the experimental studies of the KMEE can be used to directly determine the chirality of HM.

We have built a consistent theory of the STT-effect in conductive chiral HM [2]. It is shown that the STT leads to the rotation of the HM magnetization spiral around its axis. The frequency of such rotation of the HM magnetization is found. We have showcased that both the direction of rotation of the HM magnetization and the changes in the shape of the magnetic spiral are determined by the electron flow direction and the chirality of the HM.

Pure spin current injection into the HM has been described in [3,4]. In HM the characteristic length of decay for nonequilibrium electron magnetization appears to be always less than the spin diffusion length, the decrease being determined by the ratio of the HM spiral period to the spin diffusion length. We predict the existence of the “effect of the chiral polarization of a pure spin current,” i.e., the emergence of the spin current with longitudinal (transverse) polarization, which depends on the spiral chirality, upon the injection of a pure spin current with the transverse (longitudinal) polarization relative to the spiral axis.

Support by the Russian Science Foundation grant No. 22-22-00220 is acknowledged.

[1] V.V. Ustinov, I.A. Yasyulevich, *Phys. Rev. B*, **102** (2020) 134431.

[2] V.V. Ustinov, I.A. Yasyulevich, *Phys. Rev. B*, **106** (2022) 064417.

[3] V.V. Ustinov, I.A. Yasyulevich, N.G. Bebenin, *Phys. Met. Metallogr.*, **124** (2023) 195-204.

[4] I.A. Yasyulevich, N. G. Bebenin, V.V. Ustinov, *J. Exp. Theor. Phys.*, **136** (2023) 509-518.

## MAGNON QUANTUM EFFECTS BASED ON NANOLAYERED VERTICAL MAGNON HETEROJUNCTIONS

Han X.F.

Institute of Physics, Chinese Academy of Sciences, Beijing, China  
xfhan@iphy.ac.cn

Magnonics uses magnons (spin waves) excitation, propagation, manipulation, and detection to process the information, aim to reduce the energy consumption by using low-Gilbert damping materials without Joule heating [1-3]. Many works have been focused on this exciting area, such as magnonic crystals, magnon valve, magnon junction, magnonics logic and memory, magnonic circuits, THz magnonics, cavity magnonics, and so on [4]. In this presentation, the interesting magnon quantum effects observed in some nanolayered vertical magnon heterojunctions micro-fabricated by our group are mainly introduced for inspiring more possibilities in this area.

The vertical magnon heterojunction devices, consisted of Ferromagnetic insulator/Spacer/Ferromagnetic insulator [FMI/Spacer/FMI] core structures, can be expected by manipulation of magnon current and magnon transfer torque (MTT), which are similar to the classical spin valve (SV) and magnetic tunnel junction (MTJ) switching by spin transfer torque (STT). In our group, we demonstrated a magnon valve (MV, such as YIG/Au/YIG and YIG/Pt/YIG) [5] and magnon junction (MJ, such as YIG/NiO/YIG) [6,7] which consists of two magnetic insulators (FMI=YIG) and a nonmagnetic or antiferromagnetic spacer (S=Au, Pt or NiO, CoO, Cr<sub>2</sub>O<sub>3</sub> etc.). Such magnon valve, magnon junction and magnon heterojunctions can manipulate flow of magnon current well.

We used the temperature gradient or electric manipulation to excite the magnon current in FMI, and inverse spin Hall effect (ISHE) to detect the magnon current across the magnon valve or magnon junction by the electrical method. Our results show that the magnon current transmission between two magnetic insulating layers (YIG) mediated by the space layer (Au, Pt or NiO, CoO) has high efficiency, and the transmission of the magnon current in a magnon valve and magnon junction becomes high (low) as magnetizations of the two magnetic insulators are parallelly (anti-parallelly) configured. The distinct magnon valve effect (MVE) and magnon junction effect (MJE) by the angular momentum conversion and propagation between magnons in two YIG layers via the space layer were observed. A large switching on-off ratio can be expected to  $\pm 100\%$  in the MJ and MV. Furthermore, novel magnon blocking effect (MBE) in an antiferromagnet spaced MJ [8] and magnonic skin effect (MSE) in an antiferromagnetically coupled heterojunction [9] were interpreted respectively, and a magnon nonlocal spin Hall magnetoresistance (MNSMR) effect in a platinum layer deposited on an MJ was observed [10]. These works conceptually proves the possibility of using MVs and MJs to manipulate the magnon transfer torque (MTT), in magnon heterojunctions [11,12], which has potential applications on magnon resonant tunneling (MRT) and Magnon resonant transmission (MRT) in magnonic crystals, magnonic devices and circuit in future [13-18].

- [1] V. V. Kruglyak, S. O. Demokritov and D. Grundler, *J. Phys. D: Appl. Phys.*, **43** (2010) 264001.
- [2] A. A. Serga, A. V. Chumak and B. Hillebrands, *J. Phys. D: Appl. Phys.*, **43** (2010) 264002.
- [3] A. V. Chumak, V. I. Vasyuchka, A. A. Serga and B. Hillebrands, *Nat. Phys.*, **11** (2015) 453-461.
- [4] A. Barman et al., *J. Phys.: Condens. Matter*, **33** (2021) 413001.
- [5] H. Wu and X. F. Han et al., *Phys. Rev. Lett.*, **120** (2018) 097205.
- [6] C. Y. Guo et al., *Phys. Rev. B*, **98** (2018) 134426.
- [7] W. Q. He, H. Wu, and X. F. Han et al., *Appl. Phys. Lett.*, **119** (2021) 212410.
- [8] Z. R. Yan, C. H. Wan and X. F. Han, *Phys. Rev. Applied*, **13** (2020) 044053.
- [9] Z. R. Yan, Y. W. Xing and X. F. Han, *Phys. Rev. B*, **104** (2021) L020413.
- [10] C. Y. Guo et al., *Nature Electronics*, **3** (2020) 304.

- [11] C. Y. Guo et al., *Appl. Phys. Lett.*, **114** (2019) 192409.
- [12] C. Y. Guo et al., *Phys. Rev. B.*, **104** (2021) 094412.
- [13] P. Tang, X. F. Han., *Phys. Rev. B.*, **99** (2019) 054401.
- [14] Y. W. Xing, Z. R. Yan, X. F. Han, *Phys. Rev. B.*, **103** (2021) 054425.
- [15] Y. W. Xing, Z. R. Yan, X. F. Han, *Phys. Rev. B.*, **105** (2022) 064427.
- [16] Z. R. Yan, Y. W. Xing, X. F. Han, *J. Magn. Magn. Mater.*, **563** (2022) 169976.
- [17] Y. Z. Wang et al., 2023, arXiv 2301.05592.
- [18] X. F. Han *et al.*, *Chinese Phys., B*, **31**(2022) 117504.

**July 4**

Tuesday

11:00 - 13:00

ORAL  
SESSIONS I

Section A

**Spintronics and  
Magnetotransport**

4IT-A-1

## SKYRMIONS AND BIMERONS IN FERROMAGNETIC TOPOLOGICAL MATERIALS AND ELECTRICALLY GENERATED ANTIFERROMAGNETIC HALF-SKYRMIONS

*Tretiakov O.A.*

School of Physics, The University of New South Wales, Sydney, Australia  
o.tretiakov@unsw.edu.au

I will discuss topologically protected magnetic textures, such as skyrmions, half-skyrmions (merons), bimerons and their antiparticles, which constitute tiny whirls in the magnetic order. They are promising candidates for information carriers in next-generation memory devices, as they can be efficiently propelled at very high velocities using current-induced spin torques [1]. First, I will talk about skyrmions [2] and bimerons [3] in ferromagnetic systems coupled to heavy metals or topological materials. Then I will show that antiferromagnets can also host versions of these textures, which have gained significant attention because of their potential for terahertz dynamics, deflection free motion [4], and improved size scaling due to the absence of stray field. Finally, I will demonstrate that topological spin textures, merons and antimerons, can be generated at room temperature and reversibly moved using electrical pulses in thin film CuMnAs, a semimetallic antiferromagnet that is a test-bed system for spintronic applications [5]. The electrical generation and manipulation of antiferromagnetic merons is a crucial step towards realizing the full potential of antiferromagnetic thin films as active components in high density, high speed magnetic memory devices.

- [1] B. Göbel, I. Mertig, and O. A. Tretiakov, *Physics Reports*, **895** (2021) 1.
- [2] D. Kurebayashi and O. A. Tretiakov, *Physical Review Research*, **4** (2022) 043105.
- [3] B. Göbel, A. Mook, I. Mertig, and O. A. Tretiakov, *Physical Review B*, **99** (2019) 060407(R).
- [4] J. Barker and O. A. Tretiakov, *Physical Review Letters*, **116** (2016) 147203.
- [5] O. J. Amin et al., *Nature Nanotechnology*, <https://doi.org/10.1038/s41565-023-01386-3> (2023).

## SPIN-ORBIT SPLITTING IN QUANTUM WELLS: MICROSCOPIC MECHANISMS AND ROLE IN SPIN TRANSPORT

*Tarasenko S.A.*

Ioffe Institute, St. Petersburg, Russia  
tarasenko@coherent.ioffe.ru

Spin-orbit interaction in semiconductor structures lacking the center of space inversion leads to spin splitting of electron and hole subbands even at zero magnetic field. The well known contributions to such a splitting are the Rashba and Dresselhaus terms originating, respectively, from structure and bulk inversion asymmetry [1,2]. The spin-orbit splitting plays an important role and is responsible for a bunch of optical and transport phenomena, including the spin-galvanic effect, spin orientation of current, emergence of persistent spin helices, etc.

In the talk, we discuss the physics of the  $k$ -linear spin-orbit splitting of electron and hole states in two-dimensional systems based on semiconductor quantum wells and the related spin phenomena. Combining the theory of group representations and the  $k$ - $p$  method, we construct the effective Hamiltonian of  $k$ -linear splitting and calculate the splitting parameters. It is found that, in quantum wells grown along low-symmetry crystallographic directions, such as [013], there is an additional (beyond the Rashba and Dresselhaus terms) contribution to the spin-orbit splitting Hamiltonian [3]. Moreover, in a wide range of parameters, this contribution dominates the  $k$ -linear spin-orbit splitting of heavy-hole subbands in III-V quantum wells.

We also discuss the fine structure of two-dimensional Dirac states in HgTe/CdHgTe quantum wells near the «topological insulator - trivial insulator» transition. It is shown that bulk, interface, and structure inversion asymmetries lead to anti-crossing of energy levels even at  $k = 0$  and remove the degeneracy of Dirac states [4]. In quantum wells of critical thickness, the doubly degenerate Dirac cone splits into non-degenerate Weyl cones. The position of the Weyl points in the two-dimensional Brillouin zone depends on the quantum well crystallographic orientation.

Finally, we discuss the transport of spin polarized electrons in two-dimensional structures with  $k$ -linear splitting with the focus on recent experimental and theoretical results on the dynamical formation of persistent spin helices [5]. In (001)-grown quantum wells, this regime occurs at the balanced Rashba and Dresselhaus terms and leads to the emergence of unidirectional spin grating with enhanced lifetime at the optical orientation with focused pulsed or circularly polarized light.

Support by the Russian Science Foundation (grant № 22-12-00211) is acknowledged.

- [1] E.L. Ivchenko G.E. Pikus, *Superlattices and Other Heterostructures. Symmetry and Optical Phenomena* (Berlin: Springer-Verlag, 1997).
- [2] R. Winkler, *Spin-Orbit Coupling Effects in Two-Dimensional Electron and Hole Systems* (Berlin: Springer-Verlag, 2003).
- [3] G.V. Budkin and S.A. Tarasenko, *Phys. Rev. B*, **105** (2022) L161301.
- [4] M.V. Durnev, G.V. Budkin, S.A. Tarasenko, *JETP*, **135** (2022) 540.
- [5] F. Passmann et al., *Semicond. Sci. Technol.*, **34** (2019) 093002.

4IR-A-3

## PHENOMENOLOGICAL DESCRIPTION OF SURFACE ACOUSTIC WAVES HYBRIDISED WITH SPIN WAVES

*Yamamoto K.*

Advanced Science Research Center, Japan Atomic Energy Agency, Tokai, Ibaraki, Japan  
yamamoto.kei@jaea.go.jp

Hybridisation between surface acoustic waves and spin waves has proven to be a powerful tool in studying properties of magnetic thin films. It provides us with a means to drive spin wave resonance at a nonzero wavenumber [1], which enables precision measurement of certain magnetic parameters such as magneto-elastic coupling and Dzyaloshinskii-Moriya interaction [2]. More recently, the method has been applied to synthetic and elemental antiferromagnetic materials, offering abundant information on the complicated magnetic structures [3,4]. A general and optimal theoretical formalism is required to extract material properties out of the microwave signals. In this talk, I describe a phenomenological model of surface acoustic wave modes interacting with spin waves in a thin magnetic film attached onto the surface [5]. I demonstrate how the formalism can be applied to various experimental setups.

- [1] M. Weiler et al., *Phys. Rev. Lett.*, **106** (2011) 117601.
- [2] M. Xu et al., *Science Advances*, **6** (2020) eabb1724.
- [3] H. Matsumoto et al., *Appl. Phys. Exp.*, **15** (2022) 063003.
- [4] T. Lyons et al., arXiv:2023.08305 (2023).
- [5] K. Yamamoto et al., *J. Magn. Magn. Mater.*, **545** (2022) 168672.

## GEOMETRIC ASYMMETRY INDUCED NONRECIPROCITY OF MAGNETOSTATIC SPIN WAVES IN DIPOLAR COUPLED FERROMAGNETIC LAYERS

*Gerevenkov P.I.<sup>1</sup>, Bessonov V.D.<sup>2</sup>, Teplov V.S.<sup>2</sup>, Telegin A.V.<sup>2</sup>, Kalashnikova A.M.<sup>1</sup>, Khokhlov N.E.<sup>1</sup>*

<sup>1</sup> Ioffe Institute, St. Petersburg, Russia

<sup>2</sup> M.N. Mikheev Institute of Metal Physics UB of RAS, Yekaterinburg, Russia  
petr.gerevenkov@mail.ioffe.ru

Creation of magnonic elements for data transfer and processing is an actively developing area of modern magnetism. Numerous recent works have demonstrated an adder [1] and a diode [2] for magnetostatic spin waves (MSWs) in coupled waveguide systems. The most important characteristic of these structures for the design of spin-wave logic is the dispersion of MSWs, which dictates waves propagation features, including non-reciprocity. In presented work [3], we study MSWs experimentally and theoretically in a structure of two dipolarly coupled ferromagnetic films with different thicknesses to reveal the effect of such a geometrical asymmetry on MSW dispersion.

We use multilayered structure of two layers of ferromagnetic metallic alloy galfenol (Fe<sub>81</sub>Ga<sub>19</sub>) separated by nonmagnetic copper layer, FeGa(7 nm)/Cu(5 nm)/FeGa(4 nm), on (100)-GaAs substrate. We choose the galfenol as this alloy exhibits large values of the magnetization precession lifetime [4] and the MSW propagation length [5] which promotes the galfenol as suitable material for magnonic applications. The experimental dispersion of two spin wave branches, corresponding to collective acoustic and optical modes, was obtained by the Brillouin light scattering method in the backscattering geometry. As a theoretical approach, we used a method developed in [6] designed specifically for multilayered structures.

Experimental reconstruction and theoretical modeling of the dispersion of acoustic and optical collective MSW modes reveal that both possess a frequency nonreciprocity reaching several percents at the wavenumber of  $22 \cdot 10^4$  rad/cm. The analysis demonstrates that the reason for the nonreciprocity is the shift of the partial amplitudes of counter-propagating coupled modes towards the thicker or the thinner layer. It is shown that this behavior occurs due to the pronounced dependence of spin wave frequency on the layer thickness for sufficiently thin layers (less than 10 nm for the films under study). The proposed approach paves the way for the design of three-dimensional magnonic gates based on the predicted dispersion and frequency nonreciprocity of the MSW [7].

The work was supported by RSF grant No. 21-72-20160.

- [1] Q. Wang et al., *Nature Electronics.*, **3** (2020) 765.
- [2] K. Szulc et al., *Phys. Rev. Applied*, **14** (2020) 034063.
- [3] P. I. Gerevenkov et al., *Nanoscale*, **15** (2023) 6785.
- [4] A. V. Scherbakov et al., *Phys. Rev. Applied*, **11** (2019) 031003.
- [5] N. E. Khokhlov et al., *Phys. Rev. Applied*, **12** (2019) 044044.
- [6] G. Carlotti et al., *La Rivista del Nuovo Cimento*, **22** (1999) 1.
- [7] A. Mahmoud et al., *J. Appl. Phys.*, **128** (2020) 161101.

## REGULATING VALLEY-POLARIZED TRANSPORT IN GRAPHENE WITH STRAIN AND LINE DEFECT

Du L.<sup>1</sup>, Tian H.<sup>1</sup>, Wang S.<sup>2</sup>

<sup>1</sup> Linyi University, Linyi, China

<sup>2</sup> Jinling Institute of Technology, Nanjing, China

IsaacWang@jlit.edu.cn

We theoretically investigate the manipulation of valley-polarized currents and the optical-like behaviours of Dirac fermions in graphene with single line defect and/or smoothed strain barrier by employing the wave-function matching and the non-equilibrium Green's function technique.

1) For single line defect and local uniaxial strain [1], the valley transmission probability increases and the transmission plateau emerges in a large angle range. Such phenomenon originates from resonant tunnelling, and the strain act as an antireflective coating for the valley states, analogous to the antireflective coating in an optical device. This indicates that perfect valley polarization can occur in a larger incident angle range compared with solely line defect. Interestingly, in the presence of Anderson disorder, even though the transmission decreases, the valley polarization is still robust.

2) For the smoothed strain barrier [2], we explore the influence of strain on the valley-polarized transmission of graphene. When the transmission is along the armchair direction, we show that the valley polarization and transmission can be improved by increasing the width of the strained region and increasing (decreasing) the extensional strain in the armchair (zigzag) direction. It is noted that the shear strain does not affect transmission and valley polarization. Furthermore, when we consider the smooth strain barrier, the valley-polarized transmission can be enhanced by increasing the smoothness of the strain barrier, as shown in Figure 1.

We hope that our finding can shed new light on constructing graphene-based valleytronic and quantum computing devices by solely employing strain.

Support by National Natural Science Foundation of China, the China Scholarship Council, Research Foundation-Flanders (FWO), the Natural Science Foundation of Jiangsu and Shandong Province, as well as the Qinglan Project of Jiangsu Province of China and Suqian Key Laboratory is acknowledged.

[1] L. Du et al., *Phys. Scr.*, **97** (2022) 125825.

[2] S. Wang, H. Tian, M. Sun, *J. Phys.: Condens. Matter*, **35** (2023) 304002.

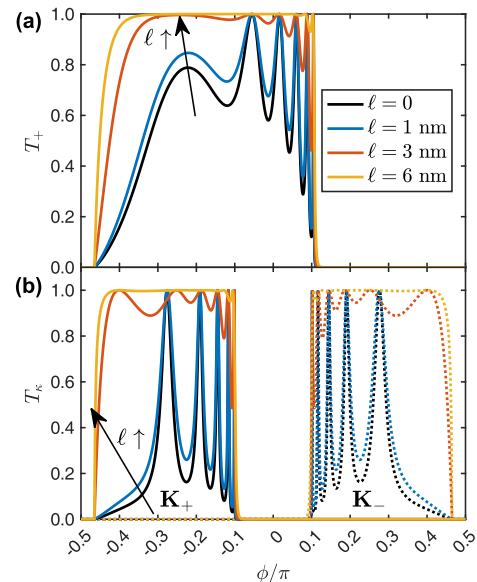


Figure 2. The valley-polarized transmission  $T_k$  can be enhanced by increasing the smoothness of the strain barrier  $l$ .

**July 4**

Tuesday

11:00 - 13:00

ORAL  
SESSIONS I

Section B

**Magnetic Nanostructures and  
Low Dimensional Magnetism**

## FERMI SURFACE CHIRALITY IN A LOW SYMMETRY TaSe<sub>2</sub> MONOSHEET GROWN BY Ta/Bi<sub>2</sub>Se<sub>3</sub>(0001) INTERFACE REACTION

*Meyerheim H.L.*<sup>1</sup>, *Polyakov A.*<sup>1</sup>, *Mohseni K.*<sup>1</sup>, *Felici R.*<sup>2</sup>, *Tusche C.*<sup>3,4</sup>, *Chen Y.-J.*<sup>3,4</sup>,  
*Feyer V.*<sup>3,4</sup>, *Geck J.*<sup>5</sup>, *Ritschel T.*<sup>5</sup>, *Ernst A.*<sup>6</sup>, *Rubio-Zuazo J.*<sup>7</sup>, *Castro G.*<sup>7</sup>,  
*Parkin S.S.P.*<sup>1</sup>

<sup>1</sup> Max-Planck-Institut für Mikrostrukturphysik, Halle, Germany

<sup>2</sup> Consiglio Nazionale delle Ricerche –SPIN, Roma, Italy

<sup>3</sup> FZ Jülich, Peter Grünberg Institut (PGI-6), Jülich, Germany

<sup>4</sup> Fakultät f. Physik, Univ. Duisburg-Essen, Duisburg, Germany

<sup>5</sup> Institut f. Festkörper und Materialphysik, TU Dresden, Dresden, Germany

<sup>6</sup> Institut f. Theoretische Physik, Johannes-Kepler Universität, Linz, Austria

<sup>7</sup> SpLine CRG BM25 at the ESRF, Grenoble, France

holger.meyerheim@mpi-halle.mpg.de

Two-dimensional transition metal dichalcogenides (TMDCs) containing heavy metals (Mo, W, Pt) are characterized by a non-trivial electronic structure and have found increasing interest as spin source materials. By contrast, bulk 2H-TaSe<sub>2</sub> has a trivial electronic structure and crystallizes in space group P6<sub>3</sub>/mmc. In the ultra-thin film limit, TMDC films have been generally assumed to be rigid units with bulk-like symmetry. Here we show that this assumption is not justified which also leads to significant modifications of the electronic structure [1]. The TaSe<sub>2</sub> monosheet (MS) was prepared by deposition of a sub-monolayer amount of Ta on a Bi<sub>2</sub>Se<sub>3</sub> (0001) single crystal followed by annealing at 480°C. Figure 1a shows the structural model derived by surface-x-ray diffraction. Like in the bulk, the TaSe<sub>2</sub> MS crystallizes in the hexagonal form but the central Ta atom relaxes downward from  $z=0.5$  lattice units (l.u.) to  $z=0.42$  l.u., thereby leading to a reduction of the point group symmetry from D<sub>3h</sub> to C<sub>3v</sub>. As a result of the symmetry lowering the electronic states at the Fermi surface (FS) acquire a chirality which is antiparallel to that of the TSS of the Bi<sub>2</sub>Se<sub>3</sub> substrate near the point. This indicates spin momentum locking across the van der Waals gap at the TaSe<sub>2</sub>/Bi<sub>2</sub>Se<sub>3</sub> interface. Our approach provides a novel route to realize chiral 2D electron systems via interface engineering in van der Waals epitaxy that do not exist in the corresponding bulk materials.

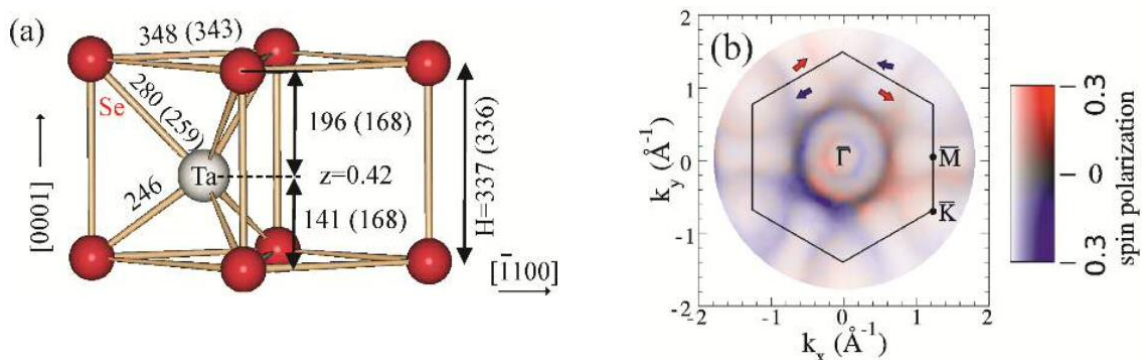


Figure 1. (a) Structural model for TaSe<sub>2</sub> monosheet. Numbers indicate distances in picometers, (bulk values in brackets). The Ta atom is displaced to  $z=0.42$ . (b) Experimental spin-resolved photoemission momentum map of the H-TaSe<sub>2</sub> monosheet on Bi<sub>2</sub>Se<sub>3</sub> at the Fermi surface.

[1] A. Polyakov et al., *Nat. Commun.*, **13** (2022) 2472 (2022)

4IT-B-2

**SOME EXPERIMENTS AND APPLICATIONS USING MAGNETIC  
NANOPARTICLES AND THE CASE OF FRICTIONLESS, SPHERICALLY  
SYMMETRICAL NANOMAGNETIC HORSES**

*Socolovsky L.M.*

UTN FRSC – CONICET, Argentina

leandro.socolovsky@frsc.utn.edu.ar

For years, the preparation, the properties and the applications of magnetic nanoparticles have been the focus for researchers. Despite the enormous volume of work in this subject, there is still room for new discoveries and possible new applications. In our talk, we will present results from experiments using silica-covered magnetic nanoparticles alone and in nanoheterostructures. We will comment about magnetic measurement analysis, and the structural studies techniques we have used. Also, we are presenting technological applications that use some magnetic nanoparticles we are working on.

## FLEXOMAGNETIC EFFECT IN A CrI<sub>3</sub> BILAYER

*Pyatakov A.P., Kaminskiy A.S.*

Lomonosov Moscow State University, Moscow, Russia

Pyatakov@physics.msu.ru

Recently the flexomagnetic effect, i.e. a magnetization caused by flexural deformation (bending) was theoretically proposed [1,2] and experimentally confirmed [3,4]. In contrast to flexoelectric effect it is not straightforward consequence of strain gradient-induced polar direction in crystal, and requires special antisymmetric magnetic ordering. In 2D magnetic materials that are natural candidates for enhance flexo-phenomena due to their ultra-flexibility, the flexomagnetolectric coupling in MoS<sub>2</sub> [5] and curvature-induced spin cycloid ordering in CrI<sub>3</sub> [6] were predicted by ab initio calculations, and the flexomagnetic phase transition from antiferromagnetic to ferromagnetic order in rippled Heusler membranes was observed [7].

In this report the flexomagnetic effect in a bilayer of CrI<sub>3</sub> is proposed. By first principle DFT simulation accompanied by analytical consideration of decompensation of two antiferromagnetic layer magnetization induced by strain gradient, the magnetization was calculated for two boundary problems (Figure 1):

A) Problem A: the positions of ions along the normal direction to the film is parabolic dependence of in-plane and out of plane coordinate.

B) Problem B: the positions of ions along the in-plane direction is parabolic dependence of in-plane and out of plane coordinate.

It is shown that along the magnetization along the normal to the film (Problem A) is nonzero and it is linearly proportional to the strain gradient, i.e the flexoelectric effect is present.

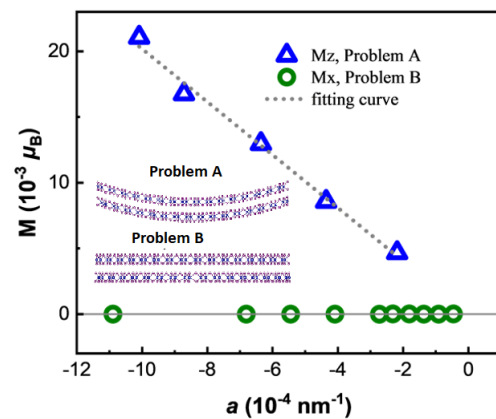


Figure 1. The calculated magnetization per Cr ion in a bilayer for two boundary problems.

The support by Russian Science Foundation grant #23-22-00162 is acknowledged.

- [1] E.A. Eliseev et al., *Phys. Rev. B*, **79** (2009) 165433.
- [2] P. Lukashev and R. F. Sabirianov, *Phys. Rev. B*, **82** (2010) 94417.
- [3] B.A. Belyaev et al., *Phys. Status Solidi RRL*, **2019** (2019) 1900467.
- [4] P. Makushko et al, *Nat. Commun.*, **13** (2022) 6745.
- [5] Y.H. Shen et al, *Adv. Theory Simulations*, **2018** 1800048 (2018).
- [6] A. Edström et al., *Phys. Rev. Lett.*, **128** (2022) 177202.
- [7] D. Du et al., *Nat. Commun.*, **12** (2021) 2494.

4OT-B-4

## AB INITIO INVESTIGATION OF RASHBA SPLITTING ON POLAR/NON-POLAR HETEROSTRUCTURES

*Enseev A.A., Pijanžina I.I., Nedopekin O.V., Tayurskii D.A.*  
 Institute of Physics, Kazan Federal University, Kazan, Russia  
 Dmitry.Tayurskii@kpfu.ru

The Rashba effect is a spin-orbit splitting caused by inversion symmetry breaking on surfaces/interfaces [1]. It is desirable that the materials used in spintronics devices, for detecting Majorana fermions in solids and other applications to have a large and ideal spin-orbit (SO) splitting of the Rashba type.

A few approaches exist to create a material with large splitting parameters:

- 1) Enhancing the strength of SO coupling by introducing heavy elements, for example Bi/Ag(111) ( $E_R=200$  meV  $k_R=0.13$  Å<sup>-1</sup>) [2].
- 2) Using semiconductor substrates to avoid the mixing of the Rashba states and the spin-degenerate substrate states, in order to create so-called ideal Rashba states [3].
- 3) Using polar semiconductors enhance giant SO splitting, i.e. BiTeX (X=Cl, Br, I) [4].
- 4) Enhancing and controlling the SO splitting by ferroelectric polarization [5].

However, natural materials exhibiting both giant and ideal Rashba states are rare. That is why the superlattice approach is a key approach here.

In this work, we studied film heterostructures based on simple metal Cu (CuO/Cu and Cu<sub>3</sub>N/Cu), as well as heterostructures based on ferroelectrics (Bi/BaTiO<sub>3</sub>, and Bi/PbTiO<sub>3</sub>). In these heterostructures, due to the electron density gradient at the interfaces, a current vortex arises associated with the electron spins. The structural and electronic properties of these systems were studied using DFT+*U* approach. All calculations were carried out using the VASP 6 program [6] built into the MedeA computational software [7].

For CuO/Cu Cu<sub>3</sub>N/Cu heterostructures the relatively big values of Rashba splitting were found depending on structure configuration as well as computational parameters used (Coulomb repulsion parameter in particular).

For heterostructures with ferroelectrics the effect of polarization direction onto the Rashba parameters was checked. We have demonstrated that the replacement of BaTiO<sub>3</sub> by PbTiO<sub>3</sub> in the film heterostructure leads to a larger spin-orbit splitting (an increase in the value of the Rashba parameter), that the polarization direction along z-axis of the heterostructure does not change the Rashba parameters significantly.

Calculations were supported by the Kazan Federal University Strategic Academic Leadership Program (Priority-2030) within the Laboratory of Computer design of new materials and machine learning.

- [1] E.I. Rashba and V.I. Sheka, *Fiz. Tverd. Tela – Collected Papers (Leningrad)*, **II** (1959) 162-176.  
 [2] C.R. Ast et al., *Phys. Rev. Lett.*, **98** (2007) 186807.  
 [3] S. Singh and A.H.Romero, *Phys.Rev. B.*, **95** (2017) 165444.  
 [4] S.V. Eremeev et al., *Phys. Rev. Lett.*, **108** (2012) 246802.  
 [5] P. Lutz et al., *Phys. Rev. Appl.*, **7** (2017) 044011.  
 [6] G. Kresse and J. Furthmüller, *Comput. Mater. Sci.*, **6** (1996) 11169–11186.  
 [7] MedeA version 3.7; MedeA is a registered trademark of Materials Design, Inc., San Diego, USA.

**July 4**

Tuesday

11:00 – 13:00

ORAL  
SESSIONS I

Section C

**Magnetism in Biology and  
Medicine**

4IT-C-1

## GOLD/COBALT FERRITE NANOCOMPOSITE AS AN INSTRUMENT FOR PHOTOTHERMAL THERAPY

*Pshenichnikov S.E.<sup>1</sup>, Motorzhina A.V.<sup>1</sup>, Anikin A.A.<sup>1</sup>, Belyaev V.K.<sup>1</sup>, Litvinova L.S.<sup>2</sup>, Jovanović S.<sup>3,4</sup>, Panina L.V.<sup>1,5</sup>, Rodionova V.V.<sup>1</sup>, Levada K.V.<sup>1</sup>*

<sup>1</sup> REC SMBA, Immanuel Kant Baltic Federal University, Kaliningrad, Russia

<sup>2</sup> Center for Immunology and Cellular Biotechnology, Immanuel Kant Baltic Federal University, Kaliningrad, Russia

<sup>3</sup> Department of Physics, Vinča Institute of Nuclear Sciences – National Institute of the Republic of Serbia, University of Belgrade, Belgrade, Serbia

<sup>4</sup> Advanced Materials Department, Jožef Stefan Institute, Ljubljana, Slovenia

<sup>5</sup> National University of Science and Technology “MISIS”, Moscow, Russia

kateryna.levada@gmail.com

Nanocomposites are multicomponent materials, which can possess wide range of structural and physical characteristics. Combinations of different characteristics performs opportunities to produce novel nanomaterials for biomedical applications. In current research we propose the nanocomposite (CNP, Figure 1S) consisting of gold nanoparticles surrounded by cobalt ferrite (CFO) nanoparticles, as the instrument for the photothermal therapy (PTT). CFO nanoparticles are covered with DHCA. Additionally, CNP are covered with arginine. CNP synthesis technique described in previous publications [1,2]. For PTT efficacy measurements CNP 100 µg/ml solutions in nutrient medium (DMEM) were affected by 815 nm laser irradiation at 0.6 W output optical power (ThorLabs L808P500MM laser diode, data not shown). On the next step experiment was performed on human hepatocarcinoma (Huh7) cells. Huh7 cells were cultured according to common methods and manufacturer's protocols. During the experiments Huh7 cells were cultured in 96-well plates in cultural medium (DMEM) supplemented with CNP at a concentration  $1 \times 10^4$  cells/ml. After 24 h cells were trypsinized and placed to PTT chamber. On the next step suspension of the cells were affected by laser irradiation for 15 minutes. After treatment cell viability was measured using WST-1 test (Thermo Scientific, Germany). CNP resuspended in the medium significantly increased under laser irradiation (Figure 1A). Data show that PTT decreased the survivability of hepatocarcinoma cells (Figure 1B).

This research was funded by RSF, grant number 21-72-20158.

[1] A. Motorzhina et al., *Processes*, **9** (2021) 1.

[2] A.V. Motorzhina et al., *Nanobiotechnology Reports*, **17** (2022) 436.

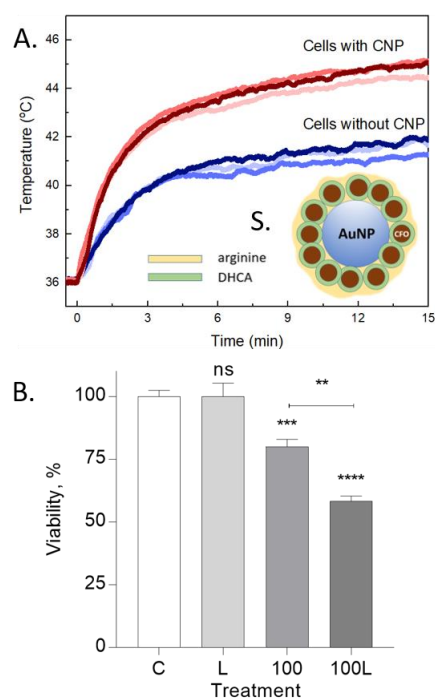


Figure 1. Photothermal therapy induced Huh7 cell death. A – heating of experimental solutions during the therapy, B – viability testing of cells after application of infrared irradiation (L), CNP treatment (100) and photothermal therapy (100L). C – control cells, S – CNP structure.

## MULTI-PARAMETRIC MAGNETIC PARTICLE IMAGING

*Zhong J., Zhang R., Sun Sh., Sun Sh., Xu L.*

School of Instrumentation and Optoelectronic Engineering, Beihang University, Beijing, China  
zhongjing@buaa.edu.cn

Magnetic particle imaging (MPI) is a new imaging modality, which directly measures the magnetic response of magnetic nanoparticles (MNPs) to visualize the spatial distribution of the MNPs with a temporal resolution of up to 46 frames per second, a spatial resolution of about 0.5 mm, and high sensitivity of about 5 ng iron [1]. It has shown great promise in biomedical applications, such as cancer theranostics [2], and intracranial cerebral hemorrhage [3]. In addition, the magnetic response of the MNPs – magnetic particle spectroscopy (MPS) signal – is sensitive to the local environmental parameters, including temperature, and viscosity. Therefore, by measuring the magnetic response of the MNPs, including the dynamic spectra, MPI allows the visualization of the MNP concentration, the local environmental temperature and viscosity, realizing multi-parametric MPI.

The MNP concentration is a linear parameter that affects the magnetic response of the MNPs whereas temperature, and viscosity are nonlinear parameters. Furthermore, temperature and viscosity are coupled parameters. Note that viscosity only affects the Brownian relaxation of the MNPs whereas temperature affects both the Brownian and Neel relaxation, as well as the Langevin parameter. The decoupling of the multi-parameters from the measurement of the MNP magnetization, e.g. magnetic particle spectroscopy (MPS) signal is of great importance. In this study, we represent the principles of MPI and the scanner design, allowing for the MNP concentration imaging. Afterwards, a phenomenological model is proposed to decouple the MNP concentration, temperature and viscosity from the numerical solutions of Fokker-Planck equation with Brownian relaxation. Finally, multi-parametric MPI is realized for the MNP concentration, temperature and viscosity imaging.

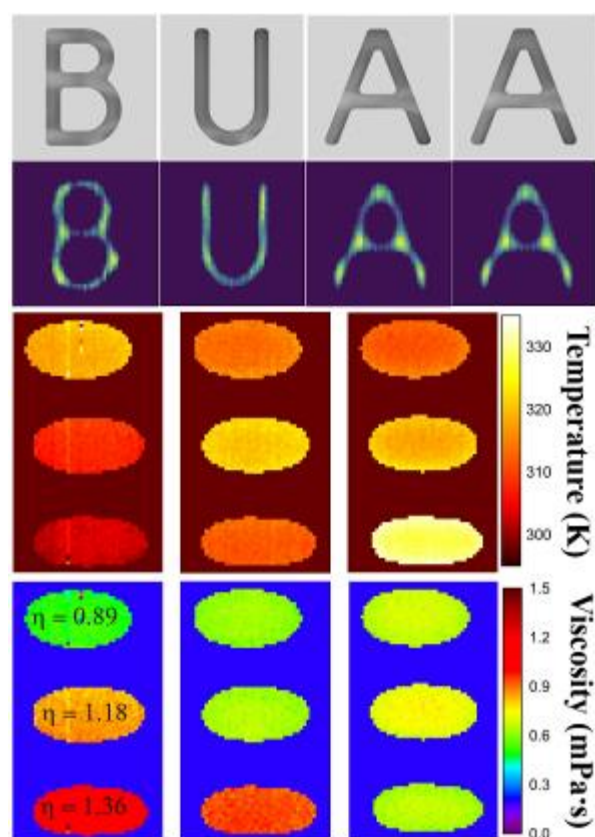


Figure 1. Multi-parametric magnetic particle imaging for MNP concentration, temperature and viscosity.

Final support from National Natural Science Foundation of China (62271025) is gratefully acknowledged.

- [1] B. Gleich, J. Weizenecker, *Nature*, **435** (2005) 1214–1217.
- [2] E.Y. Yu et al., *Nano Lett.*, **17** (2017) 1648–1654.
- [3] P. Szwargulski et al., *ACS Nano*, **14** (2020) 13913–13923.
- [4] J. Zhong et al., *Meas. Sci. Technol.*, **33** (2022) 095405.
- [5] J. Zhong et al., *Phys. Rev. Appl.*, **16** (2021) 054005.

4IR-C-3

## DRUG COMPOUNDS OF MAGNETIC PARTICLES WITH MOLECULES OF PHARMACOLOGICAL INTEREST: STRUCTURAL PROPERTIES

*Bălăsoiu M.*<sup>1,2,3</sup>, *Chilom C.G.*<sup>4</sup>, *Stolyar S.*<sup>5,6</sup>, *Creanga D.*<sup>7</sup>, *Ficai D.*<sup>8</sup>, *Rogachev A.*<sup>1,9</sup>, *Ivanikov A.*<sup>1</sup>, *Orelovich O.*<sup>1</sup>, *Turchenko V.*<sup>1</sup>, *Kuklin A.*<sup>1,9</sup>

<sup>1</sup> Joint Institute of Nuclear Research, Dubna, Moscow Region, Russia

<sup>2</sup> West University of Timisoara, Timisoara, Romania

<sup>3</sup> IFIN-HH, Magurele, Romania

<sup>4</sup> University of Bucharest, Faculty of Physics, Măgurele, Ilfov, Romania

<sup>5</sup> Federal Research Center KSC, Siberian Branch, RAS, Krasnoyarsk, Russia

<sup>6</sup> Siberian Federal University, Krasnoyarsk, Russia

<sup>7</sup> “Alexandru Ioan Cuza” University, Iasi, Romania

<sup>8</sup> University “Politehnica” of Bucharest, Romania

<sup>9</sup> Moscow Institute of Physics and Technology, Dolgoprudniy, Russia

masha.balasoiu@gmail.com

The use of various magnetic iron oxide nanoparticles (IOMNPs) in biomedical and pharmaceutical fields has increased in recent decades. Very different aspects of the properties and applications of drug compounds with magnetic particles are currently being intensively investigated [1-7].

The present paper reviews some of our work on the properties of such systems, with an emphasis on structural aspects. Small-angle neutron and X-ray scattering (SANS and SAXS) are powerful techniques for obtaining valuable information related to the structure and morphology of nanoparticles and their composites of biomedical interest.

[1] N. Cazacu et al., *Nanomaterials*, **12**(2) (2022) 1-18.

[2] M. Racuciu et al., *Antioxidants*, **11**(6) (2022) 1193.

[3] M. Racuciu et al., *Nanomaterials*, **12**(7) (2022) 1151.

[4] C.G. Chilom et al., *International Journal of Molecular Sciences*, **22**(13) (2021) 7034.

[5] C. G. Chilom et al., *International Journal of Molecular Sciences*, **21**(24) (2020) 9734.

[6] C.G. Chilom et al., *International Journal of Biological Macromolecules*, **164** (2020) 3559.

[7] C.G. Chilom et al., *Romanian Journal of Physics*, **62** (2017) 701(13).

## ON THE ISSUE OF MAGNETICALLY INDUCED FLOWS IN THROMBOSED CHANNELS

*Musikbin A.Y., Zubarev A.Y.*

Ural Federal University, Yekaterinburg, Russia  
Antoniusmagna@yandex.ru

A theoretical model and a method for its approximate analysis are proposed for flows induced by an inhomogeneous magnetic field in a channel filled with a nonmagnetic fluid and a drop of ferrofluid immersed in it. The study was carried out as part of the development of a scientific foundation for magnetically induced intensification of drug transport in thrombosed vessels.

To simplify the mathematical problem as much as possible, as a model of a blood vessel, we will consider not a cylindrical channel, but a semi-infinite flat slot filled with a non-magnetic Newtonian fluid. The presented model system is shown in Figure 1. The right end of the gap is closed by a liquid-impermeable wall simulating a thrombus; in the slot not far from the wall there is a cloud of soluble ferrofluid.

The equations for the flow velocity  $\mathbf{v}$  of a magnetizable fluid in an inhomogeneous magnetic field at low Reynolds numbers can be represented as [1]:

$$\begin{aligned} \rho \frac{\partial v_x}{\partial t} &= -\frac{\partial p}{\partial x} + \eta \Delta v_x + \frac{1}{2} \frac{\partial}{\partial z} (\Phi \Gamma), \\ \rho \frac{\partial v_z}{\partial t} &= -\frac{\partial p}{\partial z} + \eta \Delta v_z - \frac{1}{2} \frac{\partial}{\partial x} (\Phi \Gamma), \\ \frac{\partial}{\partial x} v_x + \frac{\partial}{\partial z} v_z &= 0 \end{aligned} \quad (1)$$

This model makes it possible to calculate the magnetic field inside the channel created by the solenoids according to the Biot-Savart law. Using our method for solving the equations of ferrohydrodynamics [1], we plan to calculate the flow rate of ferrofluid depending on the external magnetic field.

Preliminary calculations show that, with quite realistic system parameters, frequency, and magnetic field strength, flows can be generated in the channel at a speed with an amplitude of about 1 mm/s. These flows can significantly intensify the transport of a neutral molecular impurity (drug) in the carrier liquid, which confirms the idea expressed in [2] about the prospects of the method of generating magnetically induced flows in thrombosed blood vessels to intensify the transport of thrombolytics in them.

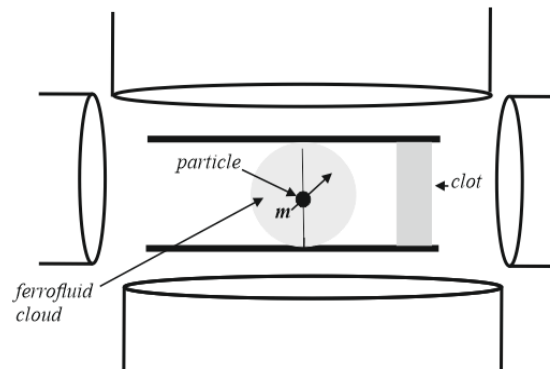


Figure 1. Illustration of the simulated system.

[1] R. E. Rosensweig, *Ferrohydrodynamics* (Cambridge University Press, 1985).

[2] M.J. Clements, *A mathematical model for magnetically-assisted delivery of thrombolytics in occluded blood vessels for ischemic stroke treatment*: Doctoral dissertation (Texas University, 2016).

**July 4**

Tuesday

16:00 - 18:15

ORAL  
SESSIONS II

Section A

**Magnetic Soft Matter**

(magnetic polymers,  
complex magnetic fluids  
and suspensions)

**TEXTURING OF THE MAGNETIC NANOPARTICLE EASY AXES  
DURING FREEZING OF A MAGNETIC SUSPENSION UNDER THE  
PRESENCE OF AN EXTERNAL FIELD**

*Ivanov A.O., Solovyova A.Yu., Elfimova E.A., Musikhin A.Yu., Subbotin I.M.*

Ural Federal University, Yekaterinburg, Russian Federation

Alexey.Ivanov@urfu.ru

Solidification of a ferroparticle suspension under the action of permanent magnetic field allows to obtain a ferrocomposite, characterized by some orientational texture of the nanoparticle easy magnetization axes [1]. We consider here that the textured ferrocomposite is obtained after fast solidification (or polymerization) of the ferrofluid liquid matrix under the condition when during this solidification some equilibrium distribution of the ferroparticle easy axes is established as a result of the balance between the Zeeman magnetic moment–magnetic field interaction energy, the magneto crystalline anisotropy energy, the interparticle dipole-dipole interaction of the ferroparticle magnetic moments and the thermal energy (thermal fluctuations). We suppose that the positions of ferroparticles and the orientations of their easy magnetization axes become fixed after solidification of the matrix, but the ferroparticle magnetic moments are still able to rotate inside the ferroparticle bodies due to superparamagnetic fluctuations. So, the texturing of the composite means that there is a highlighted line, along which the ferroparticle easy axes are mainly directed. Since the ferroparticles lose the rotational degrees of freedom as structural units, the application of a static magnetic field results in a different magnetic response of the ferrocomposite in comparison with the initial ferrofluid.

We calculated the orientation probability density of the ferroparticle easy magnetization axes in the initial ferrofluid at some polymerization temperature and some polymerization field strength. This orientational distribution is defined as the Boltzmann probability density for the randomly chosen ferroparticle, averaged over the magnetic moment rotational degrees of freedom; the interparticle magnetic interaction is taken into account here within the framework of the approach known as the “modified mean-field model of the 1-st order” [2].

The magnetic response of interacting ferroparticles, both static and dynamic, is stronger than for noninteracting ones. This means that the effect of enhancing the magnetic response, due to the formation of texture, will be even more pronounced in the textured composite of interacting ferroparticles. To support the obtained theoretical results and to validate the analytical expressions we performed Monte Carlo simulations, averaging the data over several microstructural configurations of ferroparticle positions and easy axis orientations, equilibrated in the presence of a polymerization field. We get very accurate quantitative agreement between theory and simulations for the case of weakly interacting ferroparticles.

Support by Russian Science Foundation (Project No. 23-12-00039) is acknowledged.

[1] A.Yu. Solovyovs, E.A. Elfimova, A.O. Ivanov, *Phys. Rev. E*, **104** (2021) 064616.

[2] E.A. Elfimova, A.O. Ivanov, P.J. Camp, *Nanoscale*, **11** (2019) 21834-21846.

4IT-A-7

## DESIGN OF POLYMER MATRICES FOR MAGNETOACTIVE ELASTOMERS

*Kramarenko E.Yu.*

Lomonosov Moscow State University, Moscow, Russia  
kram@poly.phys.msu.ru

Magnetoactive elastomers (MAEs) comprising soft elastomer matrices filled with the  $\mu\text{m}$ -sized magnetic particles belong to a class of smart materials due to their ability to change a number of physical properties when an external magnetic field is applied. They are receiving a lot of attention nowadays demonstrating a high potential in various industrial and medical applications [1,2].

The properties of MAEs, in particular, their magnetic response depends strongly on the properties of their main components, namely, polymer matrix and magnetic particles. Softer polymer matrix allows a higher degree of magnetic particles restructuring in a magnetic field, thus resulting in a larger magnetic response. The MAEs properties are also defined by the shape of magnetic particles and their arrangement within the polymer matrix. Anisotropic distribution of particle can be achieved via synthesis of the composites in an external magnetic field [1].

The report presents an analysis of modern achievements in the field of creating magnetically active elastomers, experimental study of their properties, and also demonstrates new ways of its practical application. The main attention is paid to the results of the development of new supersoft, biomimetic MAEs based on molecular bottlebrushes [3], and magnetically active thermoplastic materials, the properties and magnetic response of which can be programmed and controlled *in situ* in the integral coordinates "temperature-magnetic field".

Financial support by the Russian Science Foundation (grant no. 19-13-00340-II) is gratefully acknowledged.

[1] M. Shamonin, E.Y. Kramarenko, *In: Novel Magnetic Nanostructures* (Elsevier, 2018).

[2] Iu. Alekhina, E. Kramarenko, L. Makarova, N. Perov. *In: Magnetic Materials and Technologies for Medical Applications* (Elsevier Ltd., 2022).

[3] S.A. Kostrov et al., *ACS Appl. Mater. Interfaces*, **13** (2021) 38783–38791.

## EXTENDED TREATMENT OF PARTICLE MAGNETISATION IN MOLECULAR DYNAMICS SIMULATIONS

*Kantorovich S.S., Kuznetsov A., Mostarac D., Rosenberg M., Helbig S., Suess D.*

University of Vienna, Vienna, Austria  
sofia.kantorovich@univie.ac.at

Following experimental advances in the early 2000s, anisotropic and anisometric magnetic nanoparticles have become a veritable subfield of magnetic soft matter [1,2]. It has been shown that even small alternations in particle shape strongly affect the overall microscopic properties of such particle suspensions [3], which is what makes them appealing candidates for applications with tailored requirements [4]. What is not yet clear, albeit being of primary interest, it is how the dynamics of the systems of anisotropic and anisometric particles is affected by their intrinsic features.

Here, we present an extensive study on how to correctly merge intrinsic magnetisation processes of nanoparticles with their spatial motion and structural transitions in molecular dynamics simulations. We put forward three different approaches based on egg-model [5], hot Stoner-Wolfarth paradigm [6] and extended dipoles [7] to allow for particle magnetic nature. We apply those models to investigate static and dynamic susceptibilities of the systems as well as the cluster formation dynamics.

[1] S. Sacanna, D. J. Pine, *Current Opinion in Colloid and Interface Science*, **16** (2011) 96–105.

[2] L. Rossi et al., *Soft Matter*, **7** (2011) 4139–4142.

[3] J. G. Donaldson, E. S. Pyanzina and S. S. Kantorovich, *ACS Nano*, **11** (2017) 8153–8166.

[4] P. Tierno, *Phys. Chem. Chem. Phys.*, **16** (2014) 23515–23528.

[5] V. I. Stepanov, M. I. Shliomis, *Bull. of the Russ. Acad. of Sci.: Physics*, **55** (1991) 1-8.

[6] M.A. Chuev, J. Hesse, *J. Phys.: Condens. Matter*, **19** (2007) 506201.

[7] G. Steinbach et al., *Soft Matter*, **12** (2016) 2737-2743.

## MAGNETOACTIVE ELASTOMER AS A COMPONENT FOR MAGNETOELECTRIC COMPOSITES

*Makarova L.A.*<sup>1,2</sup>, *Alekhina Iu.A.*<sup>1,2</sup>, *Makarin R.A.*<sup>1</sup>, *Isaev D.A.*<sup>1</sup>,  
*Kolesnikova V.G.*<sup>1,2</sup>, *Rodionova V.V.*<sup>2</sup>, *Perov N.S.*<sup>1,2</sup>

<sup>1</sup> Lomonosov Moscow State University, Moscow, Russia

<sup>2</sup> REC SMBA, Immanuel Kant BFU, Kaliningrad, Russia  
la.loginova@physics.msu.ru

Magnetoactive elastomers (MAE), which consist of a polymer matrix filled with ferromagnetic micro- or nanoparticles, attract the great interest due to their giant magnetomechanical effects and interesting magnetoelectrical properties [1]. Recent studies have focused on the intrinsic properties of the interparticle and polymer-particle interactions. The particles' displacements at the applied external magnetic field generate the internal elastic stresses, which can affect the properties of the particles and the macro-properties of the composites.

The study of the influence of elastic stresses on the properties of MAE was continued with the development of three-component composite based on soft polymer and ferromagnetic and ferroelectric properties [2]. The elastic coupling between two types of particles leads to multiferroic properties in such a composite. Moreover, the multiferroic coupling is mediated by an electromagnetically neutral matrix, namely: the magnetic field acts on the ferromagnetic particles, which generate the internal elastic stresses that affect the electrical interaction between the ferroelectric particles, and vice versa. The magnetization causes an electrical response and the electrical polarization causes a change in the magnetic response. It is worth noting, that the particles' displacements in a uniform field only occur due to dipolar interactions between particles, where one particle is influenced by the effective field of the neighbouring particles.

Furthermore, the interaction between particles can be divided into several sub-phase interactions. The changes in the solid component (namely, the total concentration of ferromagnetic and ferroelectric particles) concentration at the same content of ferromagnetic particles lead to the interaction changes of the sub-phases. The internal interactions in MAE can be studied by FORC analysis, which indicates the competition of elastic and magnetic dipole-dipole interactions between ferromagnetic particles. The knowledge of the internal interactions provides a new possibility to predict and tune the magnetic properties of both MAE and MAE with the mixture of particles, and it allows to adjust the magnetoelectric properties for further applications.

The deformability of MAE makes it one of the promising elements for the development of soft electronic devices, such as soft energy harvesting devices. The flexible layered structures consisting of soft components can reveal lower values of the resonant frequency for the dynamic magnetoelectric effect appearing in the bending deformation mode. The double-layered structure based on the piezoelectric polymer and MAE bends in the AC gradient magnetic field and shows the magnetoelectric conversion. The resonant enhancements were observed for the structure, several resonance-like peaks were observed at sub-multiple frequencies. The uniform DC bias magnetic field increases the induced voltage and shifts the resonant frequency.

The study of MAE can extend the application range of energy harvesting devices, sensors for vibration control, elements for real external conditions with scattered inhomogeneous magnetic fields. Support by RSF, grant number 22-72-10137 is acknowledged.

[1] E.Yu. Kramarenko et al., *Smart Mat. Struct.*, **24** (2015) 035002.

[2] L.A. Makarova et al., *Polymers*, **14** (2022) 1-11.

## MAGNETOACTIVE ELASTOMER WITH ANISOTROPIC STRUCTURE AS MAGNETIC FIELD AND PRESSURE SENSORS

*Stepanov G.V., Lobanov D.A., Bakhtiarov A.V., Storozhenko P.A.*

State Scientific Research Institute for Chemical Technologies of Organoelement Compounds  
(GNIChTEOS), Moscow, Russia  
gstepanov@mail.ru

Investigated for the last decade, magnetoactive elastomers (MAE) are a logical prolongation of magnetorheological elastomeric composites. Based on an elastic polymer matrix filled with magnetic particles possessing various properties, they give the possibility to obtain materials with extensive sets of features by varying the parameters of the polymer, type of magnetic filler, and interior structure of the composite, namely the preferred orientation of the particles it contains. Within the frames of this work, we focused our attention on the electroconductive capability of MAE and its relationship with exterior magnetic fields and hydrostatical pressure.

The samples we used in this research were prepared by the impregnation of elastic silicone with particles of a permalloy ( $\text{Fe}_{75}\text{Ni}_{25}$ ) synthesized in a mechanochemical way by grinding the appropriate amounts of carbonyl iron and nickel powders in a planetary mill. Among the distinctive features of this product are pronounced magnetism and high electroconductivity.

Polymerization of some MAE specimens was carried out under the influence of an exterior magnetic field, which made it possible to create anisotropic structure in them. The obtained composites were studied for the capability to conduct direct current as a function of external field and pressure. As was unveiled by the investigations, the volt-ampere characteristic exhibited by the material is exponential (Figure 1), which suggests that the current conduction occurs according to a tunneling mechanism. In addition, voltage magnification causes resistance reduction in the sample (Figure 2).

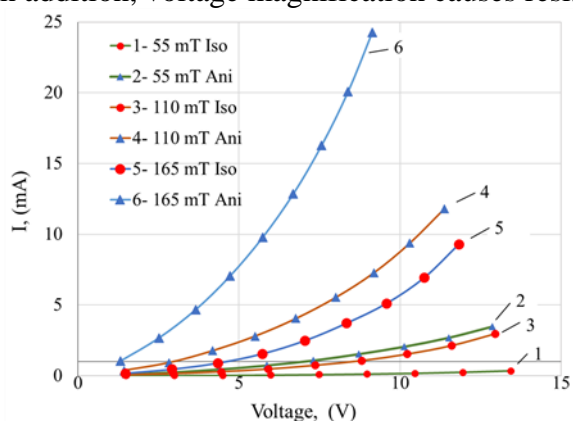


Figure 1. VA-characteristic of isotropic (Iso) and anisotropic (Ani) MAE in different magnetic fields.

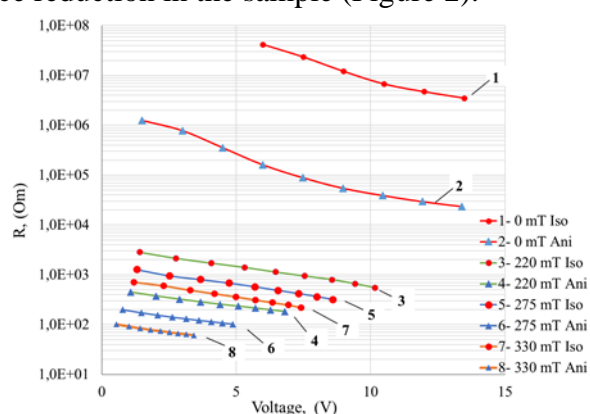


Figure 2. MAE resistance in different magnetic fields as a function of voltage in logarithmic coordinates.

Also, a significant relationship between the anisotropy and electroconductivity of the material is observed. All in all, samples with preferred orientation demonstrate a capability to conduct electric current higher by 1-3 orders of magnitude as compared to isotropic counterparts. The hydrostatical pressure applied to the sample along with the anisotropy and current flow direction also promotes an increase in conductivity. These facts give ground to view MAE, especially prepared in anisotropic form, as a prospective material to be utilized in pressure and magnetic field sensors.

Support by RFBR 19-53-12039 is acknowledged.

## EFFECT OF A MAGNETIC FIELD ON THE TRANSMISSION SPECTRA OF MAGNETIC FLUIDS WITH DIFFERENT SIZES OF NANOPARTICLES

*Yerin C.V., Vivchar V.I.*

Department of Experimental Physics, North Caucasus Federal University, Stavropol, Russia  
exiton@inbox.ru

When exposed to a magnetic field, several optical effects are observed in magnetic fluids: birefringence, dichroism, changes in optical transparency and light scattering intensity. The magnitude of the effects is determined by various factors, such as the particle size and concentration, the complex refractive index of the particle material, the presence of particle aggregates in the magnetic fluid, the strength of the external field, etc. [1,2]. In this paper, we present the results of a study of the influence of a magnetic field on the transmission spectra of colloids of magnetite in kerosene with different particle sizes.

Kerosene-based magnetic fluids with magnetite nanoparticles with an average particle size of 6.6 nm and 13.9 nm were studied. The volume concentration of magnetite in the both samples was 0.1%. Transmission spectra were studied using an Ellipse-1891 spectral ellipsometer in transmitted light in cuvettes with a thickness of 2 mm.

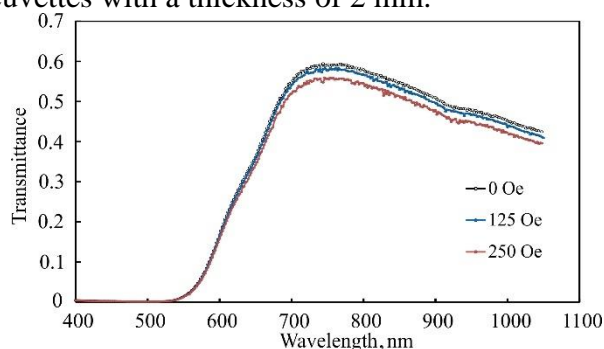


Figure 1. Transmission spectra in a magnetic field for a ferrofluid sample with an average particle size of 6.6 nm.

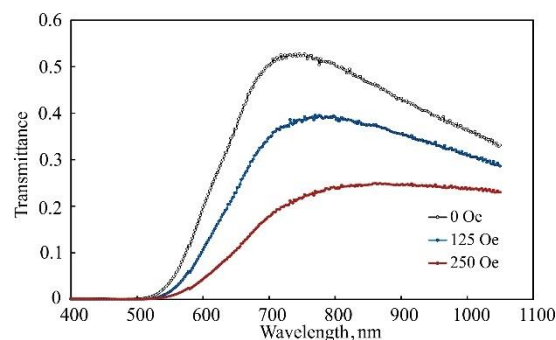


Figure 2. Transmission spectra in a magnetic field for a ferrofluid sample with an average particle size of 13.9 nm.

The transmission spectra of magnetic fluids with the same concentration but different particle sizes are shown in Figure 1 and Figure 2. In the short-wavelength part of the visible region of the spectrum 350-500 nm, the transparency of magnetite colloids is very low and increases with increasing wavelength. Spectra feature is the presence of a transmission maximum in the region of 740-750 nm. When exposed to a magnetic field with a strength of up to 400 Oe, the transmission spectra of a magnetic fluid with a smaller particle size, the transparency decreases slightly. In a ferrofluid with larger particles, the effect of a magnetic field on light transmission is much stronger. Transparency decreases by more than 2 times, and the intensity of the maximum in the region of 740–750 nm decreases. Differences in the influence of the magnetic field on the transmission spectra can be explained by the tendency to form aggregates in the magnetic fluid with larger particles.

Support by the Ministry of Science and Higher Education of Russia (project FSRN-2023-0006) is acknowledged.

[1] J. Philip and J.M. Laskar, *J. Nanofluids*, **1(1)** (2012) 3-20.

[2] C.V. Yerin, V.I. Vivchar, S.S. Belykh, *Eurasian Phys. Tech. J.*, **19(2)** (2022) 86–92.

**July 4**

Tuesday

16:00 - 18:00

ORAL  
SESSIONS II

Section B

**Magnetic Nanostructures and  
Low Dimensional Magnetism**

## EXPLORING MAGNETIC DISORDER AT THE NANOSCALE

*Peddis D.<sup>1,2</sup>*

<sup>1</sup> Istituto di Struttura della Materia-CNR, Monterotondo Scalo (RM), Italy

<sup>2</sup> DCCI, Università di Genova, Genova, Italy

Nanoscience became in the last two decades one of the most important research areas in modern science generating new knowledge frontiers. In particular, magnetic nanoparticles (MNPs) show many interesting phenomena due to their unusual physical properties strongly correlated with their size and morphology. Among the relevant features of the size reduction of MNPs, the occurrence of surface magnetic disorder deserves a special attention as it strongly modifies the magnetic properties of the materials. In the case of magnetic nanoparticles with surface to volume ratio ( $S/V$ ) higher than 1 (i.e. for spherical nanoparticle with diameter below 5 nm) the fraction of spins lying at/or near the surface produces a great enhancement of surface anisotropy and magnetic frustration due to the spin disorder. In this frame, this communication will present two kinds of nanoparticle systems with very high  $S/V$  ratio, highlighting the effect molecular coating and peculiar magnetic structure in hollow nanoparticles with  $R > 1$ . Surface molecular coating can produce strong changes on the surface magnetism and then it provides a further tool to tailor the magnetic properties of nanoparticles. We investigated the effect of coating 5 nm  $\text{CoFe}_2\text{O}_4$  particles by diethylene glycol (DEG) and oleic acid (OA). The results of DC susceptibility and Mössbauer spectroscopy measurements together with theoretical modelling, based on electronic structure calculations and Monte Carlo simulations, reveal the effect of different ionic distributions on the particle surface, due to the different surfactant layers, on the magnetic properties. An unexpected increase of the saturation magnetisation and the blocking temperature, and a decrease of the coercive field was observed DEG coated  $\text{CoFe}_2\text{O}_4$  nanoparticles with respect to nanoparticles coated by OA, This can be attributed to the larger atomic magnetic moments and to the lower magnetocrystalline anisotropy of the DEG sample as was demonstrated by DFT calculations[1]. Starting from these results and having in mind the exploration of “the no man’s land” [2] of system with very high value of  $R > 1$  hollow iron oxide nanoparticles with external diameter  $\sim 9.4$  nm has been investigated. High-resolution transmission electron microscopy images confirmed the crystalline structure and the presence of an ultrathin shell thickness of  $\sim 1.4$  nm, implying, to the best of our knowledge, the highest value of  $R$  observed in the literature ( $R \approx 1.5$ ). These hollow nanoparticles have been investigated by AC/DC magnetization measurements and using zero-field/in-field  $^{57}\text{Fe}$  Mössbauer spectrometry. The zero-field hyperfine structure suggests some topological disorder, whereas the in-field one shows the presence of a complex magnetic structure that can be fairly described as due to two opposite pseudo speromagnetic sublattices attributed to octahedral and tetrahedral iron sites. Such an unusual feature, observed for the first time in crystalline materials, is consistent with the presence of non-collinear spin structure originated from the increased surface role due to the hollow morphology. Such a complex local spin structure evidenced from Mössbauer experiments was correlated with the exchange bias effect observed at low temperature by magnetization measurements. Monte Carlo simulations on a ferrimagnetic hollow nanoparticles unambiguously corroborate the critical role of the surface anisotropy on the non-collinearity of spin structure in our samples. Tuning of the magnetic properties through the control of the degree of the surface disorder represents an interesting perspective in developing magnetic nanoparticles based materials [3].

This work was partially supported by romtheHorizon Europe EIC Pathfinder Open Program: under g.a. No.101046909 (REMAP)

[1] M. Vasilakaki et al., *Nanoscale*, **10** (2018) 21244–21253.

[2] D. Gattesanoscalechi et al., *Angew. Chemie Int. Ed.*, **51** (2012) 2–11.

[3] F. Sayed et al., *J. Phys. Chem. C.*, **122** (2018) 7516–7524.

4IT-B-6

## PHASE TRANSITIONS IN $\text{Sr}_2\text{MeNbO}_6$ (Me=Mn, Cr, Fe) DOUBLE PEROVSKITES

*Eremina R.M.<sup>1,2</sup>, Popov D.V.<sup>1</sup>, Batulin R.G.<sup>2</sup>, Yatsyk I.V.<sup>1</sup>,  
Cherosov M.A.<sup>2</sup>, Chupakhina T.I.<sup>3</sup>, Deeva Yu.A.<sup>3</sup>, Maiti T.<sup>4</sup>*

<sup>1</sup> Zavoisky Physical-Technical Institute, Federal Research Center  
“Kazan Scientific Center of RAS”, Kazan, Russia

<sup>2</sup> Kazan (Volga Region) Federal University, Kazan, Russia

<sup>3</sup> Institute of Solid State Chemistry of the Russian Academy of Sciences (UB),  
Yekaterinburg, Russia

<sup>4</sup> Department of Materials Science and Engineering Indian Institute of Technology Kanpur,  
Kanpur, India

REremina@yandex.ru

Perovskites are oxides with formula  $\text{ABO}_3$ , where A is alkaline earth metal ion, B is transition metal ion. Perovskites have octahedral oxygen framework built around B ions. Those frameworks surround A ions in hexagonal (cubic) formation [1]. Double perovskites are a type of perovskites that simultaneously consist of two of the above formulas. The ions in double perovskites usually have a mixed valence. The magnetic properties of perovskites strongly depend on their composition. Their major difference double perovskites  $\text{A}_2\text{B}'\text{B}''\text{O}_6$  from complex single perovskites is an ordering in the arrangement of B' and B'' ions, B' or B'' ions can be form chains or plane.

The aim of this work is investigation of magnetic, transport and ESR properties of  $\text{Sr}_2\text{MeNbO}_6$  (Me=Mn, Cr, Fe) double perovskite. Polycrystalline powders of perovskite were synthesized via the solution combustion precursor method. X-ray phase analysis showed that the sample is single-phase and does not contain impurities.  $\text{SrNbO}_3$  has the same perovskite-type structure but with a heavier transition metal Nb and an  $4d^1$  electronic configuration for niobium, thus exhibiting metallic behavior. Bulk  $\text{SrNbO}_3$  is not stable under ambient conditions [2]. Temperature dependencies of magnetization were measured for the  $\text{Sr}_2\text{MeNbO}_6$  (Me=Mn, Cr, Fe) ceramic in the temperature range of 5-300K at magnetic fields of 10 Oe, 500 Oe, 1000 Oe, and 10000 Oe in zero field cooling and field cooling regimes. The magnetization data of  $\text{Sr}_2\text{MnNbO}_6$  revealed several phase transitions: at  $T_N = 42,5$  K, then to the incommensurate phase at  $T_1 = 38.9$  K, to the ferrimagnetic phase ordering phase at  $T_1 = 12.7$  K, and, finally, to the two-dimensional ordering phase at  $T_3 = 6.7$  K. The presence of phase transitions at these temperatures is confirmed by the temperature dependencies of the ESR linewidth, the magnetic contribution to the specific heat, and AC magnetization. The unusual behavior for one ESR line was observed for  $\text{Sr}_2\text{MnNbO}_6$  at  $H_{\text{res}} \approx 500$  Oe and temperatures 38-42K. The behaviors of ESR line were discussed.

According to magnetization data the perovskite  $\text{Sr}_2\text{CrNbO}_6$  demonstrated two phase transitions to an antiferromagnetic phase at  $T_N = 5$  K, and into a three-dimensional antiferromagnetic ordering phase at  $T_3 = 2$  K and for  $\text{Sr}_2\text{FeNbO}_6$  at  $T_N = 25$  K, and into a three-dimensional antiferromagnetic ordering phase at  $T_3 = 12$  K.

This research was supported by the RSF (Project No. 22-42-02014).

[1] A. Bhalla, R. Guo, R. Roy, *Materials Research Innovations*, **4** (2000) 3-26.

[2] H. Okuma, Y. Katayama, K. Ueno, *arXiv preprint arXiv*, 2209 (2022) 09730.

4OT-B-7

**FRACTIONAL METAL PHASES IN DOPED AB BILAYER GRAPHENE***Sboychakov A.O., Rozhkov A.V., Rakhmanov A.L.*

Institute of Applied and Theoretical Electrodynamics RAS, Moscow, Russia

sboycha@mail.ru

We theoretically argue that, in doped AB bilayer graphene [1], the electron-electron coupling can give rise to the spontaneous formation of fractional metal phases [2]. These states, being generalizations of a more common half-metal, have a Fermi surface that is perfectly polarized not only in terms of a spin-related quantum number, but also in terms of the valley index. The proposed mechanism assumes that the ground state of undoped bilayer graphene is a spin density wave insulator, with a finite gap in the single-electron spectrum. Upon doping, the insulator is destroyed, and replaced by a fractional metal phase. As doping increases, transitions between various types of fractional metal (half-metal, quarter-metal, etc.) are triggered. Our findings are consistent with recent experiments on doped AB bilayer graphene, in which a cascade of phase transitions between different isospin states was observed.

This work is supported by RSF grant № 22-22-00464, <https://rscf.ru/en/project/22-22-00464/>.

[1] A.V. Rozhkov et al., *Phys. Rep.*, **648** (2016) 1.

[2] A.L. Rakhmanov et al., *Phys. Rev. B*, **107** (2023) 155112.

4OT-B-8

### CLIMBING THE SPIN LADDERS IN MoOBr<sub>3</sub>

Vorobyeva A.<sup>1,2</sup>, Komleva E.<sup>3,4</sup>, Morozov I.<sup>1,2</sup>, Geidorf M.<sup>1,2</sup>, Zakharov K.<sup>1</sup>, Zaikina A.<sup>3</sup>, Vasilchikova T.<sup>1,2</sup>,  
Ovchenkov E.<sup>1,2</sup>, Shvanskaya L.<sup>1,2</sup>, Streltsov S.<sup>3,4</sup>, Vasiliev A.<sup>1,2</sup>, Volkova O.<sup>1,2</sup>

<sup>1</sup> Lomonosov Moscow State University, Moscow, Russia

<sup>2</sup> National University of Science and Technology "MISIS", Moscow, Russia

<sup>3</sup> Ural Federal University, Yekaterinburg, Russia

<sup>4</sup> M.N. Mikheev Institute of Metal Physics UB RAS, Yekaterinburg, Russia

komleva.evg95@gmail.com

The crystal structure of the MoOBr<sub>3</sub> can be represented as a set of infinite ladders of Mo atoms. The ladders are orthogonal to each other (Figure 1) [1]. Each Mo ion is in an octahedral surrounding made of four bromine and two oxygen atoms. With the help of first-principles calculations based on the electron density functional theory, additional (relative to the previously available structural data) distortions were found: codirectional displacements of Mo atoms from the plane of bromine atoms in the ladder (neighboring ladders have opposite displacements of Mo).

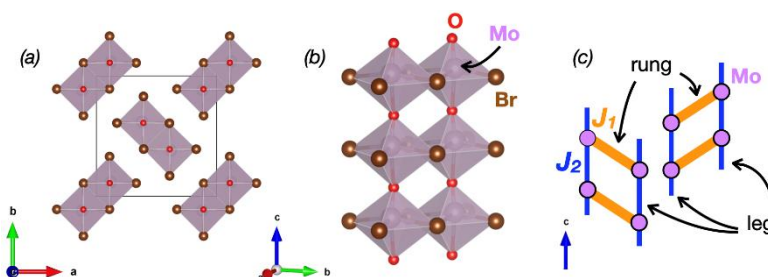


Figure 1. Crystal structure of MoOBr<sub>3</sub>.

The temperature dependence of the inverse magnetic susceptibility exhibits a behavior corresponding to the dominant ferromagnetic exchange interaction ( $\theta \sim 25$  K). The magnetic ordering temperature is  $T_N = 33$  K. *Ab initio* calculations give a ferromagnetic exchange interaction between Mo atoms in one ladder ( $J_1 = -10$  meV for the "step" of the ladder in the case of  $(\text{MoO}_2\text{Br}_4)^{3+}$  octahedra with a common edge Br-Br and  $J_2 = -1$  meV for the "legs" of the ladder -  $(\text{MoO}_2\text{Br}_4)^{3+}$  octahedra with a common corner O). This is due to the superexchange interaction *via* p-orbitals of Br atoms. The magnetic moments of Mo atoms from neighboring ladders are ordered antiferromagnetically with  $J_{inter} = 0.2$  meV.

The authors are grateful to the Russian Science Foundation for supporting the research (projects RSF 23-12-00159 and RSF 23-42-00069).

[1] M.G.B. Drew, I.B. Tomkins, *Acta Cryst. B*, **26** (1970) 1161.

## UNBIASED IDENTIFICATION OF THE GRIFFITHS PHASE IN INTERCALATED TRANSITION METAL DICHALCOGENIDES BY USING LEE-YANG ZEROS

*Ovchinnikov A.S.<sup>1,2</sup>, Nosova N.M.<sup>1</sup>, Sherokalova E.M.<sup>1</sup>, Selezneva N.V.<sup>1</sup>, Baranov N.V.<sup>1,2</sup>*

<sup>1</sup> Ural Federal University, Yekaterinburg, Russia

<sup>2</sup> M.N. Miheev Institute of Metal Physics UB of RAS, Yekaterinburg, Russia  
alexander.ovchinnikov@urfu.ru

Due to their unique layered structure, transition metal (T) dichalcogenides TCh<sub>2</sub> (Ch = chalcogen) are known as an effective platform for obtaining new objects for research and new materials with a potential for practical applications [1]. An intriguing magnetic behavior of intercalated M<sub>x</sub>TCh<sub>2</sub> compounds was observed not only in the magnetically ordered region but also in the nominally paramagnetic state. It has recently been revealed that the inverse magnetic susceptibility measured above the magnetic ordering temperature of some Cr<sub>x</sub>NbS<sub>2</sub> and Fe<sub>x</sub>TiS<sub>2</sub> compounds significantly deviates upon cooling from the high-temperature straight line corresponding to the Curie-Weiss (CW) law [2]. Such a behavior was suggested to result from the presence of short-range magnetic correlations and the so-called Griffiths phase [3] in a wide temperature range above the magnetic critical temperature. However, the problem of how to answer the question of whether a given material contains the Griffiths phase or whether the anomalous behavior of the magnetic susceptibility above T<sub>c</sub> is due to the ordinary short-range magnetic order has not yet been resolved.

The aim of our work [4] is to elaborate such a practical criterion and probe it analyzing the magnetic susceptibility data for the Cr<sub>x</sub>NbS<sub>2</sub> and Fe<sub>x</sub>TiS<sub>2</sub> intercalated systems. An analysis of the magnetization behavior above T<sub>c</sub> performed for Cr<sub>x</sub>NbSe<sub>2</sub> and Fe<sub>x</sub>TiS<sub>2</sub> by using the scaling law derived from the theory of Lee-Yang zeros distribution [5] allowed us to determine the concentrations of intercalated atoms at which the Griffiths phase consisting of magnetic clusters with high susceptibilities is realized (Figure 1). As a result, in the Cr<sub>x</sub>NbSe<sub>2</sub> system the Griffiths phase is found to exist in an extended concentration range (0.33 < x < 0.5), while in Fe<sub>x</sub>TiS<sub>2</sub>, it appears only at x = 0.25.

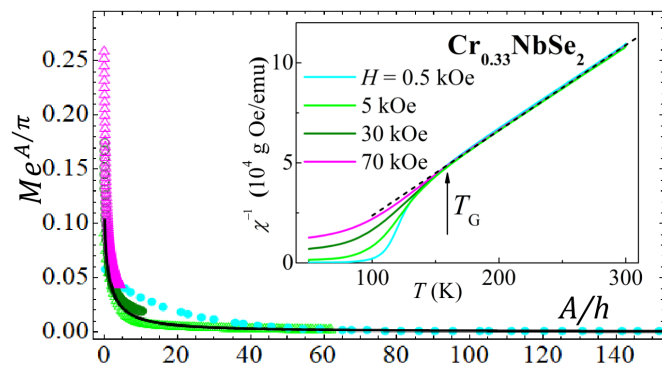


Figure 1. Verification of the magnetization scaling behavior (black solid line) for Cr<sub>0.33</sub>NbSe<sub>2</sub>. The inset shows the data of the inverse susceptibility vs T, where the dotted straight line marks the CW law behavior.

This work was supported by the Russian Science Foundation (Grant No. 22-13-00158).

- [1] S. Manzeli et al., *Nat. Rev. Mater.*, **2** (2017) 17033.
- [2] N. V. Selezneva et al., *Phys. Rev. B*, **104** (2021) 064411.
- [3] R.B. Griffiths, *Phys. Rev. Lett.*, **23** (1969) 17.
- [4] A.S. Ovchinnikov et al., *Phys. Rev. B*, **106** (2022) L020401.
- [5] P.Y. Chan et al., *Phys. Rev. Lett.*, **97** (2006) 137201.

## TUNABLE SINGLE-ATOMIC CHARGES ON A CLEAVED INTERCALATED TRANSITION METAL DICHALCOGENIDE $\text{Co}_{1/3}\text{NbS}_2$

*Lim S.<sup>1</sup>, Pan Sh.<sup>1,2</sup>, Wang K.<sup>1</sup>, Ushakov A.V.<sup>3</sup>, Sukhanova E.V.<sup>4</sup>, Popov Z.I.<sup>4,5</sup>, Kvashnin D.G.<sup>4,6</sup>, Streltsov S.V.<sup>3,7</sup>, Cheong S.-W.<sup>1</sup>*

<sup>1</sup> Rutgers University, Piscataway, USA

<sup>2</sup> Ningbo University, Ningbo, China

<sup>3</sup> M.V. Mikheev Institute of Metal Physics, Yekaterinburg, Russia

<sup>4</sup> Emanuel Institute of Biochemical Physics, Moscow, Russia

<sup>5</sup> Plekhanov Russian University of Economics, Moscow, Russia

<sup>6</sup> Moscow Institute of Physics and Technology, Dolgoprudny, Russia

<sup>7</sup> Ural Federal University, Yekaterinburg, Russia

alexushv@mail.ru

Control of a single ionic charge state by altering the number of bond electrons using scanning probe microscopy has been considered as an ultimate tested for atomic charge-induced interactions and manipulations, and such subject has been studied in artificially deposited objects on thin insulating layers. We demonstrate that a whole layer of controllable atomic charges can be obtained by cleaving metallic  $\text{Co}_{1/3}\text{NbS}_2$ , an intercalated transition metal dichalcogenide. We identified metastable charged states of Co with different valences and manipulated atomic charges to form a linear chain of the metastable charged state. Density functional theory investigation reveals that the charged state is stable due to modified crystal field at the surface in spite of the coupling between NbS<sub>2</sub> and Co occur via *d* orbitals. The idea can be generalized to other combinations of intercalants and base matrixes, suggesting that they can be a new platform to explore single-atomic-operational 2D electronics/spintronics. This work was supported by the Russian Science Foundation via RSF 23-12-00159.

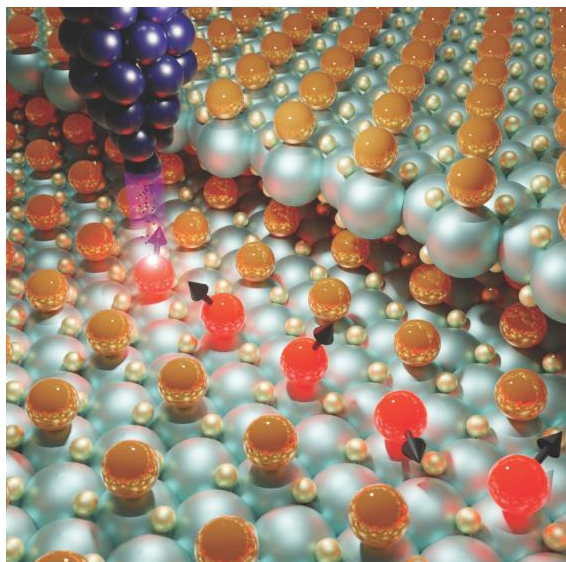
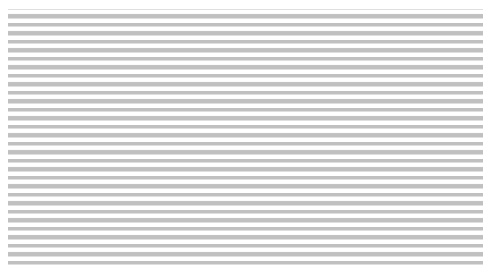


Figure 1. Illustration of possibility to form the metastable spin state charges on Co surface in  $\text{Co}_{1/3}\text{NbS}_2$  using STM tip.



**July 4**

Tuesday

16:00 – 18:00

ORAL  
SESSIONS II

Section C

**Magnetic Materials.**

**High Frequency Properties**

## EFFECTS OF MAGNETIZATION INERTIA IN SPIN DYNAMICS

*Semisalova A.S.<sup>1</sup>, Cherkasskii M.<sup>2</sup>, Mondal R.<sup>3</sup>, Barsukov I.<sup>4</sup>, Farle M.<sup>1</sup>*

<sup>1</sup> University of Duisburg-Essen, Faculty of Physics & CENIDE, Duisburg, Germany

<sup>2</sup> Institute for Theoretical Condensed Matter, RWTH Aachen, Germany

<sup>3</sup> Department of Physics, Indian Institute of Technology (ISM) Dhanbad, India

<sup>4</sup> Department of Physics and Astronomy, University of California, Riverside, California, USA  
anna.semisalova@uni-due.de

Recently, a game-changer concept was suggested to exploit so far unexplored functionalities of magnetic materials, namely the *inertial* regime of magnetization [1-3]. One of the most remarkable effects arising due to inertia in ferromagnets is a *nutaton*, an additional THz-frequency motion of magnetization superimposed on the regular GHz-frequency precession [3-6]. The manipulation of spin on these timescales paves the way to new ultrafast spintronic applications of ferromagnetic materials opening a prominent field of research.

Here we will discuss the recent findings and possible consequences of magnetization inertia on spin dynamics. We present a revisited framework based on extended Smit-Beljers formalism to resolve an effect of inertia on high-frequency magnetization dynamics and ferromagnetic resonance in anisotropic ferromagnets [7]. We show that the inertia in general leads to the reduction of the ferromagnetic resonance frequency for both aligned and non-aligned modes, and illustrate it with examples of single-crystalline thin films with cubic and uniaxial anisotropy. For an out-of-plane applied magnetic field the frequency dependence of resonance field becomes non-linear, in contrast to conventionally used Kittel formula. We also find that the nutational resonance frequency increases with the magnetic anisotropy and field. We conclude that inertia needs to be taken into account for an accurate evaluation of magnetic parameters such as magnetic anisotropy and g-factor, and for an interpretation of spin dynamics experiments, especially at high magnetic fields (> few T). Our findings might contribute to a new concept of high-speed information processing with THz frequencies which has recently moved into the focus of spintronics.

Authors acknowledge funding by Deutsche Forschungsgemeinschaft (DFG, German Research Foundation), Project No. 392402498 (SE 2853/1-1) and Project No. 405553726 (CRC/TRR 270).

- [1] M.-C. Ciornei, J.M. Rubi, J.-E. Wegrowe, *Phys. Rev. B*, **83** (2011) 020410.
- [2] R. Bastardis, F. Vernay, H. Kachkachi, *Phys. Rev. B*, **98** (2018) 165444.
- [3] K. Neeraj, ... A. Semisalova et al., *Nat. Phys.*, **17** (2021) 245-250.
- [4] E. Olive et al., *J. Appl. Phys.*, **117** (2015) 213904.
- [5] V. Unikandanunni et al., *Phys. Rev. Lett.*, **129** (2022) 237201.
- [6] M. Cherkasski, ... A. Semisalova, *Phys. Rev. B*, **102** (2020) 184432.
- [7] M. Cherkasski, ... A. Semisalova, *Phys. Rev. B*, **106** (2022) 054428.

## TAILORING MAGNETIC PROPERTIES OF MXENE NANOCOMPOSITES THROUGH CO-PRECIPITATION SYNTHESIS AT REDUCED SCALE

*Omelyanchik A.S.<sup>1</sup>, Sobolev K.V.<sup>1</sup>, Shilov N.R.<sup>1</sup>,*

*Andreev N.V.<sup>1,2</sup>, Gorshenkov M.V.<sup>2</sup>, Rodionova V.V.<sup>1</sup>*

<sup>1</sup> REC SMBA, Immanuel Kant Baltic Federal University, Kaliningrad, Russia

<sup>2</sup> National University of Science and Technology “MISIS”, Moscow, Russia  
ASOmelyanchik@kantiana.ru

MXenes are graphene-like two-dimensional materials consisting of carbon and transition metals [1-43]. Due to their large specific surface area, chemical variability, and optical and transport properties, MXenes are promising materials for use in microelectronics, energy carriers, catalysts, biomedical materials and for water remediation. The  $Ti_3C_2T_x$  MXenes are one of the most promising materials in this area due to their large specific surface area rich in adsorption centers. In addition, the composition of this material can be selected optimally to ensure maximum adsorption efficiency, including by controlling the surface functionalization.

An important task of current research is to obtain MXenes with magnetic properties that will make their use more efficient or expand their range of applications. For example, a magnetic material with a large specific surface area can be used as a nanosorbent that can be removed from the solvent using a magnetic field. For this purpose, magnetic nanocomposites, comprising magnetic nanoparticles (MNPs) and MXenes, can be used. These nanoadsorbents possess a high sorption capacity for heavy metal ions, cationic dyes, and other contaminants [5]. Controlling the magnetic properties of magnetic nanocomposites is crucial for optimizing their performance in water remediation applications.

In this study, we employed a modified co-precipitation technique to fabricate magnetic MNPs/MXene nanocomposites. Our results indicate that the use of ultrasonic stirring enables the production of iron oxide MNPs with high saturation magnetization values (Figure 1). These values, which reach up to  $79 \pm 4$  Am<sup>2</sup>/kg at room temperature, are comparable to those obtained through other methods that require the use of toxic solvents and high temperatures. Furthermore, we investigated the effect of the concentration of iron cations in the initial solution on the structural and magnetic properties of the produced MNPs and nanocomposites.

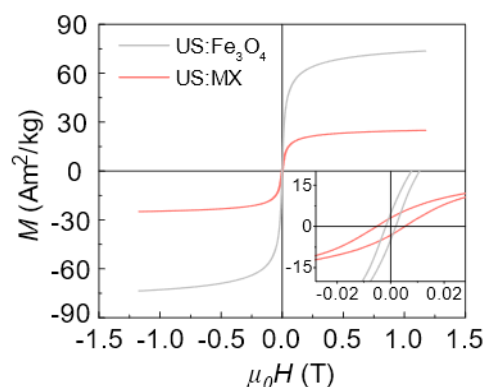


Figure 1. Magnetic hysteresis of iron oxide magnetic nanoparticles (US:Fe<sub>3</sub>O<sub>4</sub>) and MXene-based nanocomposite measured at 300 K.

This work was supported by the Russian Science Foundation under grant no 22-12-20036.

- [1] Y. Gogotsi et al., *ACS Nano*, **13**(8) (2019) 8491–8494.
- [2] X. Qin et al., *J. Solid State Chem.*, **306** (2022) 122750.
- [3] Y. Peng Y et al., *JMMM*, **541** (2021) 168544.
- [4] F. Qiu et al., *Ceram. Int.* **47**(1) (2021) 24713–24720.
- [5] M. Rethinasabapathy et al., *Chemosphere*, **286** (2022) 131679.

## DEVELOPMENT OF A GENERALIZED MODEL OF THE METAMAGNETIC PHASE TRANSITION IN $\text{La}(\text{Fe},\text{Si})_{13}$ ALLOYS WITHIN LANDAU APPROXIMATION

Makarin R.A.<sup>1</sup>, Karpenkov D.Yu.<sup>1,2</sup>, Zhelezniy M.V.<sup>2</sup>, Komlev A.S.<sup>1</sup>

<sup>1</sup> Lomonosov Moscow State University, Moscow, Russia

<sup>2</sup> National University of Science and Technology “MISIS”, Moscow, Russia

makarin.ra16@physics.msu.ru

The commercial implementation of solid-state magnetic cooling technology encounters significant challenges, including limited adiabatic temperature change values within a restricted magnetic field range (up to 1T), a narrow operating temperature range for materials exhibiting first-order phase transitions, and accompanying temperature and field hysteresis phenomena that further reduce the cooling capacity of magnetic refrigerators. Various approaches have been explored to overcome these challenges. Firstly, one approach involves utilizing active magnetic regenerators, which can expand the temperature range but require a set of working bodies. Moreover, the cooling capacity achieved with such regenerators remains considerably lower compared to classical refrigeration cycles. Secondly, the manipulation of materials' hysteresis characteristics through microstructural and compositional adjustments has reached a critical point. Here, the material exhibits sufficiently high magnetic entropy change ( $\Delta S_M$ ) values, while the hysteresis behavior vanishes. The most auspicious way lies in employing multi-stimulus materials and constructing novel cooling cycles based on them. This approach implies the simultaneous application of several generalized forces, including temperature, external magnetic field, and pressure, upon the material in proximity to the phase transition between two magnetic states. The realization of magnetic cooling cycles employing multi-stimulus materials holds the promise of not only expanding the operating temperature range by shifting the Curie point through field and pressure influences. It can also enhance the cooling capacity of magnetic refrigerators by effectively utilizing the interpolar volume of the magnetic system. Moreover, the application of external pressure serves to amplify the adiabatic temperature change in these materials by intensifying the sharpness of the transition. Several approximate models [1, 2] have been developed to predict the behavior of magnetocaloric materials near phase transitions under the simultaneous influence of temperature, an external magnetic field, and pressure. However, the existing phenomenological models have limitations as they do not fully consider the impact of the crystal lattice on free energy, leading to insufficient accuracy in describing and predicting the material's behavior under pressure. Therefore, the objective of this study was to incorporate the Debye entropy of the crystal lattice into the Helmholtz free energy within the framework of the L.D. Landau approximation. This work includes estimates of the internal hysteresis for the  $\text{La}(\text{Fe},\text{Si})_{13}$  alloy and the prediction of the optimal combination of external magnetic field and pressure values to achieve maximum efficiency of the multi-stimulus cycle and of the dynamic effects during the first-order magnetic phase transition.

The authors acknowledge support from the Russian Science Foundation grant No. 21-72-10147.

[1] D. Yu. Karpenkov et al., *Phys. Rev. Appl.*, **3(13)** (2020) 034014.

[2] H. Yamada, K. Fukamichi, T. Goto, *Phys. Rev. B.*, **2(65)** (2001) 024413.

## MAGNETIZATION REVERSAL PROCESSES OF NANOSTRUCTURED Pr-Fe-B ALLOYS

*Maltseva V.E.<sup>1</sup>, Andreev S.V.<sup>1</sup>, Selezneva N.V.<sup>1</sup>, Golovnia O.A.<sup>1,2</sup>, Volegov A.S.<sup>1</sup>*

<sup>1</sup> UrFU named after the First President of Russia B. N. Yeltsin, Yekaterinbug, Russia

<sup>2</sup> M.N. Mikheev Institute of Metal Physics, UB of RAS, Yekaterinburg, Russia

Alexey.Volegov@urfu.ru

Hard magnetic materials and permanent magnets made from them are mainly used in electrical machines, which operate in alternating magnetic fields. As a result of eddy currents, the magnets are heated to temperatures up to 200 °C. The coercivity of the magnet decreases by a factor of 2 to 4 compared to that at room temperature. Current methods of intergranular boundary modification allow the coercivity of permanent magnets to be increased from 10 kOe to 25 kOe. However, the mechanism for such a significant increase in coercivity is not fully understood.

The work considers the high-coercivity state of the rapidly quenched PrFeB alloys with different phase composition: overstoichiometric (the main Pr<sub>2</sub>Fe<sub>14</sub>B phase grains separated by the paramagnetic layers), stoichiometric (Pr<sub>2</sub>Fe<sub>14</sub>B grains only), and prestoichiometric (combination of Pr<sub>2</sub>Fe<sub>14</sub>B and  $\alpha$ -Fe phase grains). The phase composition and microstructure of the alloys, as well as their magnetic properties in the temperature range of 2 - 300 K will be presented. To establish the prevailing mechanism of the high-coercivity state, magnetometric techniques were used, including the study of the reversible magnetic susceptibility, and simulations by the finite difference method. The simulations of the magnetization reversal of these alloys demonstrate the complexity of this processes, which go beyond simple nucleation or pinning, and cannot be described in the framework of the Kneller-Hawig model. Models of magnetization reversal of the alloys under study are proposed. The presence and composition of the intergranular layer has a significant effect on the mechanism of the high-coercivity state. The main reason for the increase in coercivity in the presence of an intergranular layer is the local increase in magnetocrystalline anisotropy near the grain surface.

This work was supported by Russian Science Foundation (Grant Number 21-72-10104). The simulation was performed using the «Uran» supercomputer of Institute of Mathematics and Mechanics UB RAS under state assignment Magnet 122021000034-9.

## RETRIEVING THE INTRINSIC MICROWAVE PERMITTIVITY AND PERMEABILITY OF Ni-Zn FERRITES

*Shiryayev A.O.<sup>1</sup>, Rozanov K.N.<sup>1</sup>, Kostishin V.G.<sup>2</sup>, Petrov D.A.<sup>1</sup>, Dolmatov A.V.<sup>1</sup>, Maklakov S.S.<sup>1</sup>*

<sup>1</sup> Institute for theoretical and applied electromagnetics, Moscow, Russia

<sup>2</sup> National University of Science and Technology "MISIS", Moscow, Russia

artemshiryayev@mail.ru

Bulk ferrites and composite materials filled with ferrite powders are often used for developing novel materials and coatings for microwave applications. Evaluation of their microwave dielectric and magnetic properties is important for assessing the potential for practical use. An important problem is the description of the effective properties of composite as a function of the properties of inclusions and matrix. Mixing rules are often used to solve this problem. Microwave properties of bulk ferrites, in contrast to the bulk ferromagnets may be measured by standard techniques due to the smallness of the skin effect. This makes it possible to compare the measured permeability with the one found by the mixing rules.

The work is devoted to the study of microwave magnetic and dielectric properties of Ni-Zn ferrites and analysis of the possibility of retrieving the intrinsic permeability of inclusions. The frequency dependences of permittivity and permeability of both bulk ferrites and composite materials filled with ferrite powder were measured by vector network analyzer. To study the applicability of various mixing rules, the method proposed in [1] was used. The method is based on the analysis of the normalized inverse susceptibility  $\eta$  of composite material:

$$\eta = \frac{p}{\varepsilon_{eff}/\varepsilon_m - 1} \text{ and } \eta = \frac{p}{\mu_{eff} - 1},$$

where  $p$  is the volume concentration of inclusions,  $\mu_{eff}$  and  $\varepsilon_{eff}$  are the effective permeability and permittivity of the composite material,  $\varepsilon_m$  is the permittivity of the matrix. The behavior of the inverse susceptibility at different frequencies was studied.

The dependences of the real and imaginary parts of normalized inverse magnetic susceptibility  $\eta$  on the volume concentration  $p$  of ferrite inclusions in composite material are presented in Figure 1. It is shown that both permittivity and permeability of composite materials are described by the Maxwell Garnett mixing rule up to a concentration of 60 vol.% with high accuracy. A strong discrepancy between the measured permeability of bulk ferrite and permeability retrieved by mixing rules from composite was found. The possible reasons for the discrepancy (different magnetic structure, change in the material during annealing, inapplicability of mixing rules) were investigated.

This study was financially supported by the Russian Science Foundation (RSF) under project No. 21-19-00138 (<https://rscf.ru/en/project/21-19-00138/>).

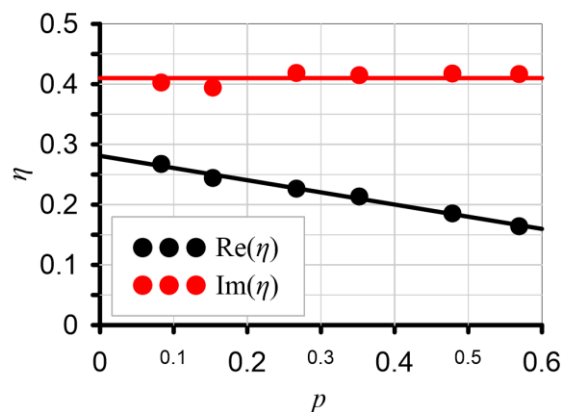


Figure 1. The dependence of inverse susceptibility  $\eta$  on the volume concentration  $p$  of inclusions at frequency of 3 GHz.

[1] K.N. Rozanov et.al., *Procedia Engineering*, **216** (2017) 85–92.

## **ELOW CARBON STEEL FOR ELECTRIC VEHICLE MAGNETIC SHIELDING**

*Damatopoulou T.<sup>1</sup>, Angelopoulos S.<sup>1</sup>, Svec P.<sup>2</sup>, Hristoforou E.<sup>1</sup>*

<sup>1</sup>Laboratory of Electronic Sensors, National TU of Athens, Athens, Greece

<sup>2</sup>Institute of Physics, SAS, Bratislava, Slovak Republic

damatat5@central.ntua.gr

In this paper, results on the use of the low carbon steel (LCS), being the structural material of the cabin of several electric vehicles, as the magnetic shielding material after thermal and magnetic annealing are presented, illustrating acceptable shielding levels without any significant loss of mechanical properties in terms of hardness and microhardness. Furthermore, other materials, such as permalloy films or amorphous ribbons have also been investigated and reported to be either added on top of the LCS to enhance shielding, or to decorate other structural cabin material, such as aluminum or composite, with acceptable shielding characteristics. The main magnetic property, determining magnetic shielding ability is the differential magnetic permeability, that has been determined and studied in terms of structure – properties correlation. The proper instrumentation for the determination of permeability, namely the reference single sheet tester together with the corresponding transfer standard, the electromagnetic yoke, are also discussed in the paper.

July 5

9:00 - 10:30

Wednesday

PLENARY  
LECTURES

## CYLINDRICAL MICRO- AND NANOWIRES: FROM CURVATURE EFFECTS ON MAGNETIZATION TO SENSING APPLICATIONS

*Vázquez M.*

Institute of Materials Science of Madrid, Consejo Superior de Investigaciones Científicas, Spain  
mvazquez@icmm.csic.es

Research on curvature effects in magnetic nanostructures is attracting much interest as they offer novel alternatives to planar systems. In particular, the cylindrical geometry introduces significant singularities in the magnetic response of ferromagnetic wires just from their curvature, which primarily depends on their diameter, length, and aspect ratio. The main magnetic configurations include axial, transverse, and vortex (circular with a singularity at the axis). Microwires, 1 to 180 micrometer, are fabricated by in-rotating-water and by quenching and drawing ultrarapid solidification techniques. Micrometric-diameter amorphous wires with high magnetostriction remagnetize through an ideal millimeter-long single domain wall propagating at kilometer-per-second speeds that results in a square hysteresis loop. Such bistable behavior and their magnetoelastic properties are the basis for various devices (e.g., field, stress and temperature sensors, electromagnetic shielding). On the other hand, ultrasoft non-magnetostrictive microwires are employed in very sensitive field sensors based on their Giant MagnetoImpedance, GMI, effect or in flux-gate magnetometers. Nanowires (20 nm to 400 nm in diameter) present an outstanding behavior where the crystalline structure plays a major role in competition with shape anisotropy. Cylindrical nanowires are considered as scaffolds for advanced three-dimensional nanoarchitectures exploiting intrinsic curvature that introduces significant differences from planar-based nanotechnologies. They are proposed for novel sensor devices and magnets, and their interconnecting arrays are considered for energy devices or brain-inspired computing. An ultimate goal is currently the investigation of the magnetization reversal modes in individual nanowires by advanced techniques, e.g., X-ray magnetic circular dichroism (XMCD) coupled to photoemission electron microscopy (PEEM), magnetic force microscopy (MFM), magneto-optical Kerr effect (MOKE), electron holography, and micromagnetic simulations. They show axial, transverse, vortex, and more complex, exotic magnetic configurations and effects (e.g., magnetization ratchets, skyrmion tubes, helical vortices). The reversal nucleates at the nanowire ends involving singularities (e.g., Blochpoint walls) and at local transition regions (e.g., modulations in diameter and composition between segments of differently designed magnetic properties). Individual nanowires are currently used or proposed for biomedical applications, such as cancer treatment, magnetic resonance imaging (MRI) contrast agents, or in composites for their antimicrobial activity.

5PL-A-2

## TUNING THE PROPERTIES OF SPINEL FERRITE NANOPARTICLES BY COLLOIDAL CHEMISTRY

*Sangregorio C.*

ICCOM – CNR, Sesto F.no, Italy  
csangregorio@iccom.cnr.it

Thanks to the large variety of unique physical properties (high magnetic permeability, high magnetic anisotropy or high electrical resistance), spinel ferrite-based nanostructures, either as single phase or enclosed in complex architectures, have been extensively investigated in the recent past. In particular, the demanding requirements of technological applications where they could be exploited has fueled the search for suitable strategies to improve the physical properties by fine controlling their chemical and morpho-structural features.

In this contribution we will present some examples aimed at showing how wet-chemistry syntheses can represent an effective tool to reach this goal. Among the others, we will discuss the effect of size, relative amount and composition on the magnetic properties of core@shell antiferromagnetic@ferrimagnetic ( $M_{1-x}Fe_xO@MFe_2O_4$ ,  $M=Fe, Co, Ni$ ) nanoparticles prepared by thermal decomposition of metal oleates in high boiling solvent.[1,2] Moreover, since lattice defects such as vacancies, dislocations, stacking faults and antiphase boundaries, have been recently recognized as an additional tool for modifying the intrinsic magnetic properties (e.g. high coercive field and/or exchange bias) of spinel ferrites nanoparticles, we will show that the controlled oxidation of core@shell antiferromagnetic@ferrimagnetic nanoparticles is an efficient strategy to introduce defects into the ferrite spinel lattice producing defected cobalt-nickel ferrite with very large exchange bias. On the other hand, a low temperature solvent-mediated thermal treatment can be also exploited to reduce the local internal stress in chemically synthesized cobalt ferrite nanoparticles, leading to an unprecedented increase of the total magnetic anisotropy without affecting any other structural or magnetic parameter [3].

Research funded under the National Recovery and Resilience Plan (NRRP), Mission 4 Component 2 Investment 1.3 - Call for tender No. 1561 of 11.10.2022 of Ministero dell'Università e della Ricerca (MUR); funded by the European Union – NextGenerationEU. Project code PE0000021, CUP B53C22004060006, Title “NEST - Network 4 Energy Sustainable Transition”.

[1] A. López-Ortega et al., *Chem. Mater.*, **29** (2017) 1279.

[2] B. Muzzi et al., *Small*, **18(16)** (2022) 2107426.

[3] B. Muzzi, C. Sangregorio et al., *ACS App. Nano Mater.*, **5(10)** (2022) 14871-14881.

**July 5**

Wednesday

11:00 - 13:00

ORAL  
SESSIONS I

Section A

**Magnetic Nanostructures and  
Low Dimensional Magnetism**

## MAGNETIC FRUSTRATION AND MAGNETOCALORIC EFFECT IN A DIPOLAR-HEISENBERG MAGNET $\text{LiGdF}_4$

*Glazkov V.N.<sup>1,2</sup>, Sosin S.S.<sup>1,2</sup>, Iafarova A.F.<sup>1,2</sup>, Andreev G.Yu.<sup>3</sup>, Batulin R.G.<sup>3</sup>, Korableva S.L.<sup>3</sup>, Morozov O.A.<sup>3</sup>, Romanova I.V.<sup>3</sup>*

<sup>1</sup> P.Kapitza Institute for Physical Problems RAS, Moscow, Russia

<sup>2</sup> Faculty of Physics, HSE University, Moscow, Russia

<sup>3</sup> Kazan Federal University, Kazan, Russia  
glazkov@kapitza.ras.ru

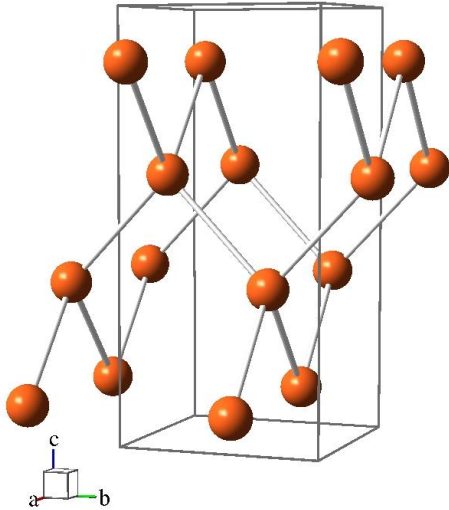


Figure 1. Position of magnetic rare-earth ions in tetragonal  $\text{Li(Re)F}_4$  crystal. Positions of Li and F ions are not shown.

Rare earth tetrafluorides  $\text{Li(Re)F}_4$ , are known for a long time as an optical media for lasers [1]. From the viewpoint of magnetism, these compounds provide an example of unusual kind of magnetic frustration: while the network of nearest-neighbor exchange bonds is not frustrated by itself (see Figure 1) various interactions have similar strength and final choice of the ordered phase and ordering temperature depends on a minute balance of these interactions. E.g.,  $\text{LiHoF}_4$  is an example of a dipolar Ising ferromagnet with Curie temperature  $T_C=1.53\text{K}$ , while  $\text{LiErF}_4$  is an XY-antiferromagnet with Neel temperature  $T_N=0.38\text{K}$  [2]. We focus our study on a most isotropic member of this family,  $\text{LiGdF}_4$ , which is close to Heisenberg model, since  $\text{Gd}^{3+}$  is an S-state ion.

Electron spin resonance on a diluted isostructural nonmagnetic compound  $\text{LiY}_{1-x}\text{Gd}_x\text{F}_4$  with  $x=0.005$  revealed characteristic fine structure of ESR absorption spectrum, which allowed to determine single-ion anisotropy parameters. Single-ion anisotropy for  $S=7/2$   $\text{Gd}^{3+}$  ions turns out to be of easy-axis type with the splitting between two lowest-energy doublets equal to  $0.82\text{K}$ . This value is comparable with the

characteristic dipolar energy for  $\text{LiGdF}_4$ , which is  $0.56\text{K}$ .

Besides of the fine structure due to the isolated  $\text{Gd}^{3+}$  ions, electron spin resonance spectra in a  $\text{LiY}_{1-x}\text{Gd}_x\text{F}_4$  samples with higher concentration of magnetic ions  $x=0.05$  features series of a much weaker absorption components, the later can be interpreted as an ESR absorption from the exchange coupled pairs. Positions of these weak absorption components were determined at different microwave frequencies (25–40 GHz) and field orientations, experimental values are in agreement with the model assuming nearest neighbors antiferromagnetic coupling with exchange integral  $J_{\text{NN}}=0.067\text{K}$ . This yields characteristic exchange energy  $J_{\text{NN}}S^2=0.82\text{K}$ , the value close to both dipolar energy and single-ion anisotropy energy scale.

Competing interaction results in unusual magnetic properties of the bulk  $\text{LiGdF}_4$ .  $M(T)$  measurements yields strongly anisotropic Curie-Weiss temperature: for the field applied along tetragonal axis  $\Theta_c=0$ , while for the field applied in orthogonal direction  $\Theta_a=1.37\text{K}$ . These values of Curie-Weiss temperature are in a perfect agreement with the parameters of spin-Hamiltonian determined from ESR measurements [3].

This means, that for  $H||c$  effects of dipolar interaction, exchange couplings and single-ion anisotropy practically cancels each other and *concentrated*  $\text{LiGdF}_4$  (with Gd-Gd distance of  $3.8\text{\AA}$ ) behaves like an ideal paramagnet. Such a behavior is of interest for magnetic refrigeration applications. To check this possibility we have measured  $M(H)$  curves at different temperatures, which allowed to calculate  $(\partial M/\partial T)_H=(\partial S/\partial H)_T$  and to estimate entropy absorbed by magnetic system on isothermic demagnetization process. We have found that, indeed, magnetocaloric effect in  $\text{LiGdF}_4$

is anisotropic, the magnitude of this effect at  $T > 2\text{K}$  for  $H \parallel c$  is practically the same as for the ideal  $S=7/2$  paramagnet.

The work was supported by the Russian Science Foundation Grant 22-12-00259 (sample growth and ESR measurements) and by the PRIORITY-2030 program of Kazan Federal University (magnetization measurements).

- [1] R.Burkhalter, *Prog. Cryst. Growth*, **42** 1 (2001).
- [2] P. Beauvillain et al., *Phys Rev B*, **18** 3360 (1978).
- [3] C. Kraemer et al., *Science*, **336** 1416 (2012).
- [4] S.S.Sosin et al, *JETP Letters*, **116** 771 (2022).

## MAGNETIC ORDERING IN A DIPOLAR MAGNET $\text{LiGdF}_4$

*Sosin S.S.<sup>1,2</sup>, Smirnov A.I.<sup>1</sup>, Soldatov T.A.<sup>1</sup>, Iafarova A.F.<sup>1,2</sup>, Edel'man V.S.<sup>1</sup>, Korableva S.L.<sup>3</sup>, Morozov O.A.<sup>3</sup>, Romanova I.V.<sup>3</sup>*

<sup>1</sup> P. Kapitza Institute for physical problems RAS, Moscow, Russia

<sup>2</sup> HSE University, Moscow, Russia

<sup>3</sup> Kazan Federal University, Kazan, Russia

sosin@kapitza.ras.ru

Rare-earth tetrafluorides  $\text{LiREF}_4$  are considered as magnetic systems with dominant dipolar interaction. However, the magnetic ordering in different members of this family is strongly influenced by anisotropy of magnetic ions, varying from a dipolar Ising ferromagnet ( $T_C=1.53$  K) for holmium system to a planar antiferromagnet ( $T_N=0.38$  K) for erbium compound. Lack of magnetic ordering in the most isotropic  $\text{LiGdF}_4$  down to at least 400 mK [1] results from a recently established fine balance of various competing magnetic interactions which can be treated as a new type of “hidden” magnetic frustration [2]. This opens a wide space for experimental studies both of fundamental and practical importance. The former implies the search for novel exotic low-temperature types of magnetic ordering while the latter promises achievements in the sphere of magnetic refrigeration applications.

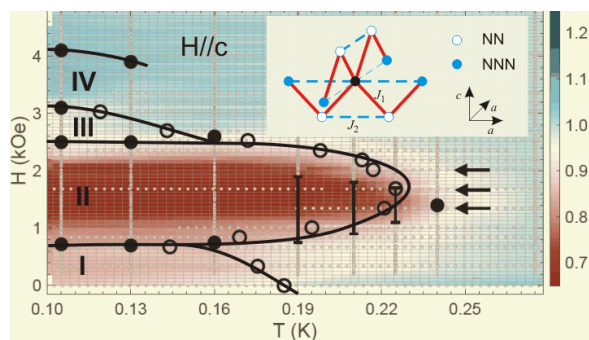


Figure 1. Phase diagram of  $\text{LiGdF}_4$  measured in magnetic field along the tetragonal axis. Color map corresponds to the intensity of the microwave absorption at a frequency  $\nu=35.35$  GHz, points mark clear non-resonant features on the absorption curves, lines are guide-to-eye to separate different ordered phases, arrows indicate positions of magnetic resonance modes in the ordered state. Inset shows the magnetic surrounding of each magnetic ion.

A detailed study of the phase diagram and magnetic resonance spectra was performed at temperatures below 400 mK using a home-made microwave spectrometer built into the dilution fridge cryostat. Phase boundaries were determined by non-resonant features on absorption curves recorded at sweeping temperature or field at a given microwave frequency. At  $H=0$  the system undergoes the transition into a magnetically ordered phase below  $T_N=0.19(1)$  K. In magnetic field applied along the tetragonal easy-axis we observed a cascade of transitions with the following critical fields at minimum  $T=100$  mK:  $H_{c1}=0.70(5)$ ,  $H_{c2}=2.5(1)$ ,  $H_{c3}=3.1(1)$  and  $H_{c4}=4.10(5)$  kOe (see Figure 1), the last critical point being the saturation field. The transition at  $H_{c1}$  is probably first order and accompanied by abrupt appearance of intense resonance modes in the absorption spectrum. The trivial phase diagram in the transverse magnetic field consists of the only ordered phase saturated above  $H_{\text{sat}}=7.0(5)$  kOe. The magnetic resonance of a ferromagnetic type is developed above  $H_{\text{sat}}$  in both field directions.

The origin of the peculiar phase diagram (Figure 1) remains unclear, however the first step to interpret it can be made by taking into account that magnetic ions in  $\text{LiGdF}_4$  are arranged into a network of orthogonal chains of edge-sharing triangles with two nearest- and one next-nearest-neighbour bonds (see Inset to Figure 1). The effective  $J_1$ ,  $J_2$  couplings of exchange and/or dipolar origin introduce initial frustration which can be overwhelmed by magnetic field and anisotropy.

The work is supported by RSCF, grant #22-12-00259.

[1] T. Numazawa et al., *AIP Conf. Proc.*, **850** 1579 (2006).

[2] S.S. Sosin et al., *JETP Lett.*, **116** 771 (2022).

## MAGNETIC PROPERTIES OF MICRO- AND NANOSIZED POWDERS AND SINGLE CRYSTALS OF $\text{LiREF}_4$ (RE = Tb, Dy, Yb)

*Romanova I.V.*<sup>1</sup>, *Abe S.*<sup>2</sup>, *Andreev G.I.*<sup>1</sup>, *Cherosov M.A.*<sup>1</sup>, *Gilmutdinov I.F.*<sup>1</sup>, *Kiiamov A.G.*<sup>1</sup>, *Korableva S.L.*<sup>1</sup>,  
*Matsumoto K.*<sup>2</sup>, *Nuzhina D.S.*<sup>1</sup>, *Morozov O.A.*<sup>1,3</sup>, *Semakin A.S.*<sup>1</sup>, *Ubukata K.*<sup>2</sup>, *Tagirov M.S.*<sup>1</sup>

<sup>1</sup> Institute of Physics, Kazan Federal University, Kazan, Russia

<sup>2</sup> Graduate School of Natural Science and Technology, Kanazawa University,  
Kakuma-machi, Kanazawa, Japan

<sup>3</sup>Zavoisky Physical-Technical Institute, FRC Kazan Scientific Center of RAS, Kazan, Russia  
romanova.irina.vladimirovna@gmail.com

Double fluorides  $\text{LiREF}_4$  (RE = Gd-Yb) have gained attention as model objects in physics of dipolar magnetism. These fluorides share scheelite type,  $I4_1/a$  crystal symmetry; unit cell contains two magnetically equivalent rare-earth  $\text{Re}^{3+}$  ions at sites with the  $S_4$  point symmetry that compose two sublattices.  $\text{LiTbF}_4$  is dipolar Ising ferromagnet, magnetic moments order along [001] axis,  $T_C = 2.89$  K.  $\text{LiDyF}_4$  and  $\text{LiYbF}_4$  are dipolar XY-antiferromagnets, magnetic moments order in (001) plane, the  $T_N = 0.62$  and 0.13 K, respectively [1, 2].

Microsized powders of  $\text{LiREF}_4$  (RE = Tb, Dy, Yb) are synthesized by sintering powders of fluorides taken in proportions according to the phase diagrams [3]. Nanosized powders are synthesized using hydrothermal method [4], single crystals were grown by the Bridgman-Stockbarger method. Magnetization of the samples is measured by vibration sample magnetometer VSM at PPMS system at the temperature range 2-300 K and applied magnetic field range 0-9 T, magnetostriction was measured in strong magnetic fields on a capacitive dilatometer [5] in static magnetic fields in the range of 0-8 T at different temperatures. Theoretical analysis is performed within exchange charge model taking into account dipole-dipole and electron-deformation interactions, using Hamiltonian of rare earth ion diagonalized in the full space of the free ion energy states [6].

Qualitative agreement of calculations and experimental data is achieved for all samples of all compounds. Also, our theoretical approach presents quantitative agreement with low-temperature magnetization and magnetostriction measurements of the single crystal  $\text{LiYbF}_4$  samples and  $\text{LiYbF}_4$  single crystal inverse susceptibility experimental data from [2]. Magnetization measurements at  $B = 10$  mT show transition of  $\text{LiTbF}_4$  samples in ferromagnetic state; Curie temperature of nanosized powder decreases at 0.1 K in comparison with single crystal and microsized powder sample.  $\text{LiDyF}_4$  microsized powder sample reveals anomalous magnetic properties: magnetic hysteresis in paramagnetic state (butterfly hysteresis) and slow magnetic relaxation, at  $T < 7$  K.  $\text{LiDyF}_4$  single crystal magnetization measurements prove existence of these phenomena, while diluted single crystal  $\text{LiYF}_4\text{:Dy 1\%}$  experiments do not display any magnetic hysteresis and slow magnetic relaxation in the temperature range of 2-10 K [6].

Support by Russian Science Foundation (project No22-22-00257) is acknowledged. The authors are grateful to Prof. B. Z. Malkin for helpful discussions and to Prof. R. V. Yusupov for kind permission to use laboratory computer for calculations.

- [1] I. V. Romanova and M. S. Tagirov, *Magn. Res. Solids*, **21** (2019) 19412.
- [2] P. Babkevich et al., *Phys. Rev. B*, **92** (2015) 144422.
- [3] P. P. Fedorov, V. V. Semashko, S. L. Korableva, *Inorg. Mater.*, **58** (2022) 233–245.
- [4] Q. Zhang, B. Yan, *Inorg. Chem.*, **49** (2010) 6834–6839.
- [5] S. Abe et al., *Cryogenics*, **52** (2012) 452–456.
- [6] G. Iu. Andreev et al., *Mat. Res. Bulletin*, **156** (2022) 112002.

## DOMAIN STRUCTURE IN $\text{La}_{0.7}\text{Sr}_{0.3}\text{MnO}_3$ THIN FILMS DEPOSITED ON AN $\text{NdGaO}_3$ SUBSTRATE

*Shaikhulov T.A.*<sup>1</sup>, *Temiryazeva M.P.*<sup>2</sup>, *Luzanov V.A.*<sup>2</sup>, *Markelova M.N.*<sup>3</sup>, *Amelichev V.A.*<sup>4</sup>, *Safin A.R.*<sup>1,5</sup>,  
*Kaul A.R.*<sup>3</sup>, *Kalyabin D.V.*<sup>1</sup>, *Nikitov S.A.*<sup>1,6</sup>

<sup>1</sup> Kotel'nikov IRE RAS, Moscow, Russia

<sup>2</sup> Kotel'nikov IRE RAS, Fryazino Branch, Fryazino, Russia

<sup>3</sup> Department of Chemistry, Moscow State University, Moscow, Russia

<sup>4</sup> S-Innovations, Moscow, Russia

<sup>5</sup> National Research University "MPEI", Moscow, Russia

<sup>6</sup> Moscow Institute of Physics and Technology, Dolgoprudny, Moscow Region, Russia  
shcaihulov@hitech.cplire.ru

The observed bright and dark contrast images represent domains with different magnetic orientations along the out-of-plane direction since the magnetic force microscopy (MFM) data correspond to the out-of-plane magnetization component only. The MFM images shown in Figure 1. reveal the thickness dependent evolution of magnetic stripe domains in  $\text{La}_{0.7}\text{Sr}_{0.3}\text{MnO}_3$  (LSMO) films. Samples thinner than 30 nm (Figure 1f) do not provide any MFM contrast. A similar situation was observed in [1]. As the thickness increases to 75 nm, the MFM contrast increases and stripe domains appear locally (Figure 1(e)). Such stripe domains indicate a film with an out-of-plane magnetization, and thus it suggests the presence of a perpendicular anisotropy in thicker films than 75 nm [2]. At a thickness 147 nm, the shape of the domains changes, and they become labyrinthine [1]. We obtain two LSMO thickness critical points at 75 nm and 150 nm.

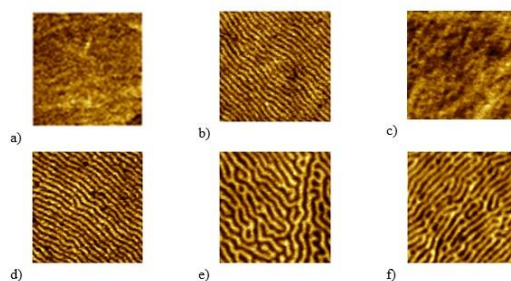


Figure 1. MFM images of thin LSMO films of various thicknesses deposited on  $\text{NGO}(110)$  substrates without an external field. a) 200 nm, b) 75 nm, c) 75 nm, d) 104 nm, e) 147 nm, f) 200 nm.

Work was supported by the Russian Science Foundation grant No. 19-19-00607-P.

[1] S. R. Bakaul, W. Lin, and T. Wu, *APL*, **99** (2011) 042503.

[2] J. Dho, N.H. Hur, *Journal of Magnetism and Magnetic Materials*, **318** (2007) 23.

5OT-A-5

## MAGNETIC HYSTERESIS, MAGNETORESISTANCE AND STRUCTURE OF $\text{Co}_n(\text{CoO})_{100-n}$ THIN-FILM COMPOSITES

*Sitnikov A.V.<sup>1</sup>, Makagonov V.A.<sup>1</sup>, Kalinin Yu.E.<sup>1</sup>, Kushchev S.B.<sup>1</sup>, Foshin V.A.<sup>1</sup>, Granovsky A.B.<sup>2</sup>, Gan'shina E.A.<sup>2</sup>, Perova N.N.<sup>2</sup>*

<sup>1</sup> Voronezh State Technical University, Voronezh, Russia

<sup>2</sup> Lomonosov Moscow State University, Moscow, Russia  
perova.n@physics.msu.ru

Magnetic, structural and magnetoresistive properties of  $\text{Co}_n(\text{CoO})_{100-n}$  composite films, synthesized by the method of ion-beam sputtering of composite target in argon atmosphere and mixed atmosphere (argon + oxygen), have been studied. Composite water-cooled target, consisting of a cobalt plate with unevenly installed on its surface CoO strips, which made it possible to obtain samples with different Co content in CoO matrix at one technological cycle. As substrates, ceramic plates of glass-ceramic ST 50, glass and silicon have been used. Thickness of the obtained films was measured on an MII-4 optical interferometer and was  $\sim 2 \mu\text{m}$ . The content of Co was determined using X-ray phase analysis and varied from 2 to 24 at. %.

The structure of the obtained  $\text{Co}_n(\text{CoO})_{100-n}$  thin films, where  $n$  – content of metallic Co in at. % has been investigated by X-ray diffraction method on a Bruker D2 Phaser diffractometer ( $\lambda_{\text{CuK}\alpha 1} = 1,54 \text{ \AA}$ ) and an electron microscopy analysis. Both phases (Co and CoO) of the heterogeneous system are crystalline, where Co particles have a face-centered cubic structure. Estimates of the average size of coherent scattering regions (CSRs), carried out according to the Scherrer formula showed, that with an increase in content of the metallic cobalt phase, the size of CoO grains decreases from 45 nm to 15 nm, and Co – increases from 4 nm to 21 nm. In this case, the addition of oxygen during deposition leads to the decrease in the grain size Co from 3.5 nm to 5.1 nm and the grain growth CoO from 25 to 80 nm.

For the  $\text{Co}_n(\text{CoO})_{100-n}$  films, experimentally determined percolation threshold turned out to be significantly lower, than observed for most previously studied nanocomposites:  $\sim 12$  at. % Co and  $\sim 8,7$  at. % Co for the films, deposited in an inert atmosphere and with the addition of oxygen, respectively. This is due to the peculiarity of the film morphology, which lies in the fact that the structure consists of small metal Co nanoparticles located on the surface of larger CoO particles. For compositions with Co content near the percolation threshold, a negative tunnel-type magnetoresistance was found. Measured at room temperature values of magnetoresistance reaches 4 % in a field of 10 kOe, are proportional to the square of the magnetization and characterized by hysteresis which well correlation with magnetic hysteresis.

Magnetic hysteresis with coercive force of about 700 Oe is observed for dielectric-like compositions with up to 4 at. % Co, that is paradoxical for an ensemble of diluted Co nanoparticles with a cubic structure and size of 4–5 nm. The correlation between magnetoresistance and magnetic hysteresis proves that this hysteresis is not associated with the formation of large Co clusters. A possible reason for this behavior, along with a special morphology, is appearance of thin layers of antiferromagnetic oxide at the interface between Co nanoparticles and CoO paramagnetic at room temperature particles,  $\text{Co}_2\text{O}_3$  as for example, causing a significant increase in magnetocrystalline anisotropy.

The work was supported by the Ministry of Science and Higher Education of the Russian Federation (project FZGM-2023-0006).

## ANTIFERROMAGNETISM OF IRON OXIDE NANOPARTICLES IN THE MATRIX OF POTASSIUM ALUMINOBORATE GLASSES AT THE THERMORADIATION TREATMENT.

*Salakhitdinova M.K.<sup>1</sup>, Ibragimova E.M.<sup>2</sup>, Kuvandikov O.K.<sup>1</sup>*

<sup>1</sup> Samarkand State University named after Sharof Rashidov, Samarkand, Uzbekistan

<sup>2</sup> Institute of Nuclear Physics Academy of Science of Uzbekistan, Tashkent, Uzbekistan  
smaysara@yandex.ru

The optical and paramagnetic properties of potassium aluminoborate (KAB) glasses, both pure and with additions of  $\text{Fe}^{3+}$  ions, depend significantly on the melting and heat treatment conditions (outside and in the  $\gamma$ -field), the content of additives, and the power of  $^{60}\text{Co}$   $\gamma$ -irradiation. The dependence of the properties of KAB glasses on the dose rate of the radiation field during high-temperature irradiation (thermoradiation treatment) or melting in  $\gamma$ -field (thermoradiation melting) is one of the determining factors in the occurrence of thermoradiation phenomena in the investigated glasses. Simultaneous heating and irradiation of sample in powerful radiation field ( $\geq 10$  Gy/s) by a qualitatively timely method of influencing materials, in which number of physical and chemical parameters change. However, the discovered phenomena and processes are still insufficiently studied, and their use for nanotechnology of glass and glass-forming systems can lead to an improvement in their properties in such important technological parameters as controlling the size of the formed nanostructures, reducing radiation and chemical resistance, etc.

We present the results of studying magnetic properties of the  $\text{K}_2\text{O}\cdot\text{Al}_2\text{O}_3\cdot\text{B}_2\text{O}_3$  (KAB) glasses with the addition of  $\text{Fe}_2\text{O}_3$  2.0 and 3.0 wt.%, subjected to radiation treatment in  $^{60}\text{Co}$  gamma-field at the dose rate of 236 R/s within 2 hours at room temperature and when the samples are heated to 423 K are presented. Under both radiation and thermoradiation exposure, the magnetic susceptibility of glasses follows the Curie–Weiss law at 4.2–200 K and slightly deviates from this dependence at 200–340 K (Figure 1). The weakly pronounced magnetic hysteresis with low coercive force was found at low temperatures against the background of magnetization that depends almost linearly on the field. An analysis of data on the temperature and field dependences of magnetization in weak and strong fields, combined with data on structural and optical properties, indicates that mainly  $\text{Fe}_2\text{O}_3$  nanoparticles in the uncompensated antiferromagnetic state are formed in glasses, as well as an insignificant amount of dissociated Fe and  $\text{Fe}_3\text{O}_4$  ions.

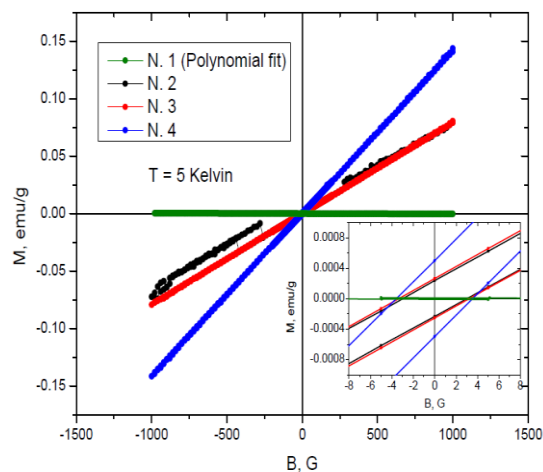


Figure 1. Field dependences of the magnetization of KAB glasses at 5 K.

[1] E.M. Ibragimova et al, *Journ. Magn. Magn. Mater.*, **459** (2018) 12-15.

## STRUCTURAL AND MAGNETIC PROPERTIES OF THIN Co/Pt FILMS

*Tatarskiy D.A.<sup>1,2</sup>, Gusev N.S.<sup>1</sup>, Ermolaeva O.L.<sup>1</sup>, Orlova A.N.<sup>1</sup>, Mironov V.L.<sup>1</sup>, Gusev S.A.<sup>1</sup>*

<sup>1</sup> Institute for physics of microstructures RAS, Nizhny Novgorod, Russia

<sup>2</sup> Lobachevsky university, Nizhny Novgorod, Russia

tatarsky@ipmras.ru

The results of systematic experimental studies of the magnetic state and crystal structure of multilayer films based on a ferromagnet/heavy metal pair (Co/Pt) by optical magnetometry, magnetic force microscopy, Lorentz and analytical transmission electron microscopy are presented. It is shown that with an increase in the number of Co/Pt periods in the films, an increase in the average size of crystal grains is observed, which leads to an increase in the dispersion of perpendicular anisotropy and, as a consequence, to a decrease in the size of magnetic domains and magnetization reversal fields. In addition, in films with  $n \geq 6$  periods, the domain wall becomes hybrid; has an intermediate structure between the walls of the Neel and Bloch types.

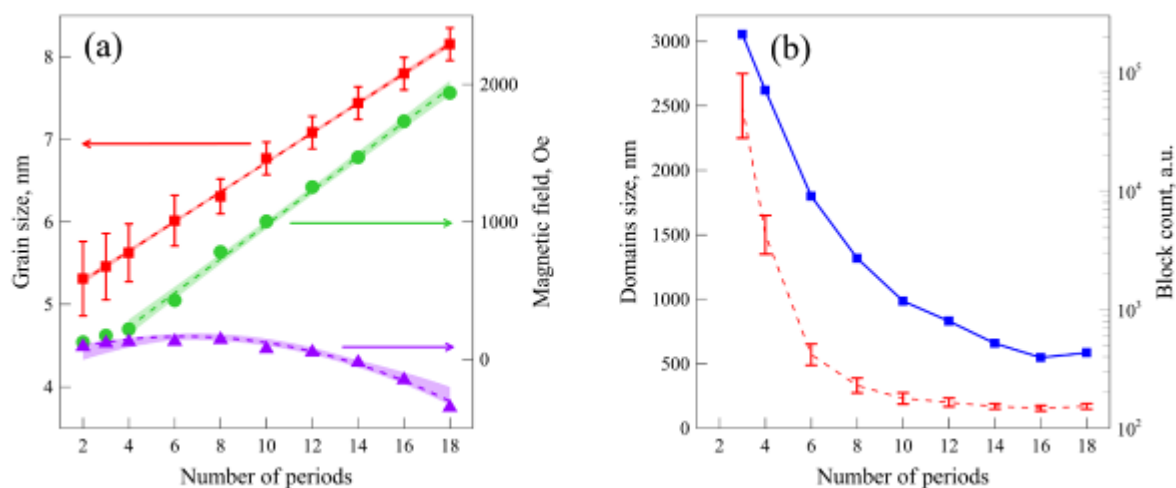


Figure 1. (a) Dependences of the saturation field (green curve, circles) and magnetization reversal field (violet curve, triangles), as well as the average size of crystal grains (red curve, squares) on the number of periods  $n$  in the [Co/Pt]\* $n$  structure. (b) Dependences of the average lateral size of magnetic domains (red dotted line) and the average number of crystalline blocks in one domain in the demagnetized state (blue line, squares) on the number of periods  $n$  in the [Co/Pt]\* $n$  structure.

This study is supported by the Russian Science Foundation (Project no.21-72-10176). The facilities of Center “Physics and technology of micro- and nanostructures” at IPM RAS were used for the analysis of the samples.

**July 5**

11:00 - 13:15

Wednesday

ORAL  
SESSIONS I

Section B

**Magnetism and  
Superconductivity**

5IT-B-1

## QUANTUM SIZE PHENOMENA IN THIN SUPERCONDUCTING FILMS

*Arutyunov K. Yu.<sup>1,2</sup>, Sedov E. A.<sup>1,3</sup>, Bezymiannykh D. G.<sup>1</sup>, Pugach N. G.<sup>1</sup>*

<sup>1</sup> HSE University, Moscow, Russia

<sup>2</sup> Kapitza Institute RAS, Moscow, Russia

<sup>3</sup> Lebedev Physical Institute RAS, Moscow, Russia

karutyunov@hse.ru

It has been known for decades that critical temperature  $T_c$  of a superconducting thin film or nanowire might significantly differ from the one of the corresponding bulk sample. For some materials (e.g. *Nb*) it decreases, for some (e.g. *Al*) the  $T_c$  increases with decrease of the characteristic dimension. Though numerous models have been developed to describe the phenomenon, so far there is no universally accepted consensus on its origin. One of common opinions among theorists is that low-dimensional superconducting objects, studied in real experiments, noticeably vary (e.g. by grain size and/or morphology), and there is plenty of competing mechanisms making it difficult to figure out the dominating one.

Here aluminum has been selected as the material where the size dependence of  $T_c$  is very pronounced. The films with thickness from 5 nm to 100 nm were deposited on *GaAs* and sapphire  $Al_2O_3$  substrates both by the traditional electron beam sputtering at  $\sim 10^{-9}$  mbar at room temperature, and by molecular beam epitaxy at a lower residual vapor pressure  $\sim 10^{-12}$  mbar. An analysis of the samples by high resolution transmission electron microscopy revealed that the mean grain size and the metal – substrate interface drastically depend on the method used for film formation. However, irrespectively of all these differences, the same tendency is clearly observed: the thinner the film, the higher the  $T_c$  (Figure 1).

We account the observation to quantum size effect (QSE) [1,2], which leads to variation of the important electronic parameters (e.g. DOS) with periodicity of about one interatomic distance. Hence, these oscillations should be somehow washed out due to inevitable fluctuations of the film thickness in realistic polycrystalline samples studied in our and many other experiments. However, our recent studies based on microscopic Green function approach, nicely describe the experiment (Figure 1). We demonstrate that consideration of electron scattering at crystal lattice defects like grain boundaries does not null the impact of the QSE, the importance of which has been originally outlined within the shape resonance model [3] applicable, strictly speaking, only to single crystalline objects. Our findings are important both for fundamental studies and for various nanoelectronic applications utilizing low dimensional superconducting elements.

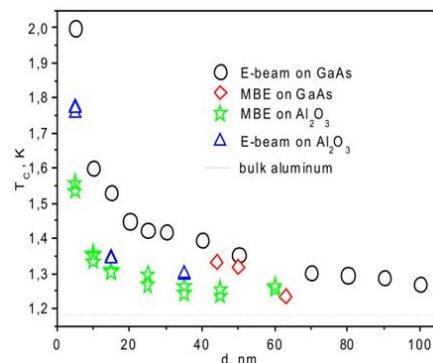


Figure 1. Critical temperature  $T_c$  vs. thickness  $d$  of aluminum films, deposited on various substrates using various methods [2].

Support by HSE University Mirror Lab project is acknowledged.

[1] K. Yu. Arutyunov et al., *Phys. Stat. Sol. RRL*, **13** (2019) 1800317.

[2] K. Yu. Arutyunov et al., *Physics of Metals and Metallography*, **1** (2023) 53.

[3] J. M. Blatt, C. J. Thompson, *Phys. Rev. Lett.*, **10** (1963) 332.

5IT-B-2

## PROXIMITY EFFECTS AT SUPERCONDUCTOR/ANTIFERROMAGNET INTERFACES

*Bobkova I.V.<sup>1</sup>, Bobkov G.A.<sup>1</sup>, Bobkov A.M.<sup>1</sup>, Kamra A.<sup>2</sup>, Chourasia S.<sup>2</sup>, Johnsen Kamra L.<sup>3</sup>, Gordeeva V.M.<sup>1</sup>, Golubov A.A.<sup>4</sup>*

<sup>1</sup> Moscow Institute of Physics and Technology, Dolgoprudny, Russia

<sup>2</sup> IFIMAC and Universidad Autonoma de Madrid, Madrid, Spain

<sup>3</sup> Center for Quantum Spintronics, Trondheim, Norway

<sup>4</sup> University of Twente, 7500 AE Enschede, The Netherlands

bobkova.iv@mipt.ru

The aim of this talk is to review the current state of the young subfield of superconducting spintronics - antiferromagnetic superconducting spintronics. It is planned to discuss the structure and properties of Néel triplet correlations induced by the proximity effect in superconductor/antiferromagnet (S/AF) heterostructures [1], mechanisms of superconductivity suppression in S/AF bilayers [2], the dependence of the critical temperature of S/AF bilayers on the width of the AF layer and the relation of these theoretical findings to the existing experiments [3-5]. The proximity effect at S/AF interfaces with canted antiferromagnets is also considered [6]. A unique effect of anisotropic enhancement of proximity-induced triplet correlations by spin-orbit coupling and its perspectives for superconducting spintronics are discussed.

The support by RSF project No.22-22-00522 is acknowledged.

[1] G. A. Bobkov et al., *Phys. Rev. B*, **106** (2022) 144512.

[2] G. Bobkov, I. V. Bobkova, A. M. Bobkov, arXiv:2303.14225.

[3] C. Bell et al., *Phys. Rev. B*, **68** (2003) 144517.

[4] M. Hubener et al., *Journal of Physics: Condensed Matter*, **14** (2002) 8687.

[5] B. L. Wu et al., *APL*, **103** (2013) 152602.

[6] S. Chourasia et al., arXiv:2303.18145.

## COMPOSITE MAGNETIC EXCITATIONS IN SUPERCONDUCTOR/MAGNET HETEROSTRUCTURES

*Bobkov A.M.<sup>1</sup>, Bobkova I.V.<sup>1,2</sup>, Sorokin S.A.<sup>2</sup>, Kamra A.<sup>3</sup>, Belzig W.<sup>4</sup>*

<sup>1</sup> Moscow Institute of Physics and Technology, Dolgoprudny, Russia

<sup>2</sup> Higher School of Economics, Moscow, Russia

<sup>3</sup> IFIMAC and Universidad Autonoma de Madrid, Madrid, Spain

<sup>4</sup> Universitat Konstanz, Konstanz, Germany

bobkov.am@mipt.ru

The ability to control the dispersion law of spin waves is one of the most important requirements for the engineering of magnonic devices. We show that thin-film hybrid structures consisting of a ferromagnetic (F) or antiferromagnetic (AF) insulator and a superconductor (S) or normal metal (N) have broad prospects in this field. Structures with topological superconductors are also touched upon. Due to the presence of a surface exchange interaction between the magnetic insulator and the metal, an effective exchange field is induced in the latter, which repeats the profile of the magnetization of the magnet, including the magnon. This leads to the appearance of spin polarization of the quasiparticles in the superconductor and the generation of triplet Cooper pairs in it. Moreover, the spin polarization of quasiparticles is not co-directed with the local exchange field (the effect of dynamic delay), and therefore creates a rotational moment that acts on the magnetization of the magnet. In addition, a magnon with a nonzero wave vector creates around itself a cloud of triplet Cooper pairs of electrons with equal spins, which dress it, increasing its effective mass and screening its spin.

In structures with a ferromagnet and an antiferromagnet, due to the difference in their characteristic frequencies (GHz for ferromagnets and THz for antiferromagnets), the processes described above play a different role and the effect of a superconductor on a magnet looks different. In a typical ferromagnet, spin-triplet pairs exert the main influence. They dress the magnon, increase its mass, and screen the spin. The resulting composite particle was called magnon-Cooparon [1]. For structures with an antiferromagnetic insulator, the renormalization of the magnon spectrum involves both the polarization of quasiparticles and spin-triplet pairs. Unlike a ferromagnet, the spectrum of magnons in an antiferromagnet contains two modes, which for an easy-axis antiferromagnet are degenerate in energy at zero applied magnetic field. Interaction with a superconductor leads to the removal of this degeneracy [2]. One of the interesting practical results of our work is the proposal of a method for direct measurement of the exchange field induced by a magnet in a superconductor (or a normal metal, which is considered as the limiting case of a superconductor at high temperature).

The support by RSF project No. 22-42-04408 is acknowledged.

[1] I. V. Bobkova et al., *Communications Materials*, **3** (2022) 95.

[2] A. M. Bobkov, S. A. Sorokin, I. V. Bobkova, arXiv:2212.01831

5OT-B-4

## LOW-DIMENSIONAL MAGNETIC CENTERS IN HTSC YBCO FILM ON STEEL-276 INDUCED BY GAMMA-QUANTA AND ELECTRON BEAM

*Ibragimova E.M.<sup>1</sup>, Shodiev A.A.<sup>1</sup>, Mussaeva M.A.<sup>1</sup>, Kurbanov U.T.<sup>1</sup>, Abrorova S.<sup>1</sup>, Novikov M.S.<sup>2</sup>, Tyutyunnikov S.P.*

<sup>1</sup> Institute of Nuclear Physics (INP), Tashkent, Uzbekistan

<sup>2</sup> Joint Institute for Nuclear Researches (JINR), Dubna, Russian Federation  
ibragimova@inp.uz

Applications of HTSC for magnetic focusing and accelerating particle beam were mentioned 30 years ago and are actual now [1]. The structure of YBCO is multilayer, where Cooper pairs form 2D-vortices lattice melting above  $T_c=90$  K or  $H_c$ . The goal is to pin the vortices at 1D defects (columnar). Earlier we irradiated YBCO single crystals with 1 MeV electrons to dose  $2 \cdot 10^{19}$  e/cm<sup>2</sup> and got the maximal critical current density  $J_{mc}=2.4$  A/cm<sup>2</sup> at  $H=3$  Tesla, and the following  $\gamma$ -irradiation at 70 R/s 77 K increased  $J_{mc}$  and shifted its maximum to 4 Tesla [2]. Industrial tapes of SuperOx-1-YBCO (produced by S-Innovations in RF) were irradiated with 5 MeV electrons in air at 273 K at 400 nA to dose  $5 \cdot 10^{14}$  e/cm<sup>2</sup> (beam was  $\perp$  tape surface) and 1.17 and 1.33 MeV <sup>60</sup>Co  $\gamma$ -quanta (flux convergent to the cylinder axis  $\parallel$  tape) at 77 K to dose  $10^6$  R ( $\sim 10^{16}$  q/cm<sup>2</sup>) at the dose rate 65 R/s. Magnetization was measured with Gaussmeter at 77 K and confirmed Meissner effect at  $H=900$  G, which increased after electron irradiations. Magnetoresistance was measured at  $H=0.56$  T at Hall system (Figure 1). Log-scale was used to see strong temperature dependencies and big radiation induced changes after the irradiations. Gamma-irradiation at 77 K generated strong paramagnetic centers annealed above 250 K. Pinning centers in superconducting CuO plane are molecular oxygen bipolarons  $O_2^{3-}$  - hole trapping centers, immobile below 200 K. Oxygen divacancies in Cu-O chains trap 2 electrons (spin 0 or 1). Bose-Einstein condensation at  $>200$ K may result in biexciton superconductivity (Cu-O chain) Rydberg resonance 0.097 eV. Within 80-300 K the tape is in mixed magnetic states of YBCO and steel substrate, thereby providing effective flux pinning by highly correlated non- superconducting state.

Support by Research Program President Decree #4526 is acknowledged.

[1] I.V. Kulikov et al., *Supercond. Science & Technol.* **33** (2020) 015001.

[2] E.M. Ibragimova and M.A. Kirk, *Mat. Res. Soc. Symp. Proc.* **659** (2001) II7.8.1-6.

5IR-B-5

## DIOD EFFECT IN SUPERCONDUCTOR-FERROMAGNET STRUCTURES

*Uspenskaya L.S.*

ISSP RAS, Chernogolovka, Russia

uspenska@issp.ac.ru

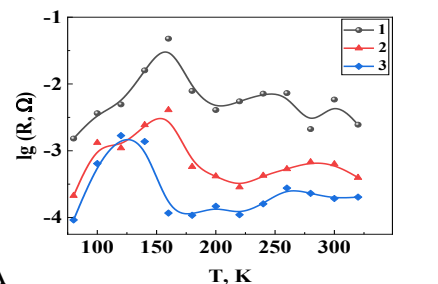
In recent decades, much attention has been paid to the development of cryogenic electronics, including those based on superconducting materials [1,2]. In particular, spin valves are implemented on the basis of superconductor-magneto-soft and magneto-hard ferromagnets structures [3,4], magnetoresistive switches are implemented on ferromagnet-superconductor structures [5,6] that is the superconductor resistance switching by a magnetic field. Currently, the possibilities of field-free switching of hybrid structures are being intensively investigated [7,8].

Recent results of study of transport properties of aluminium and niobium films and structures fabricated on single-crystal  $Y_3Fe_5O_{12}$  films with (111) and (100) orientations in a wide temperature range from 300 K to 4 K are presented by this report.

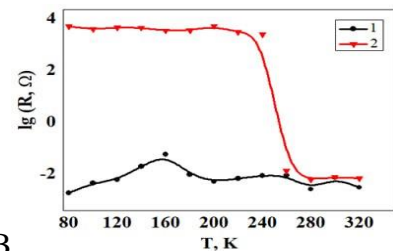
It is shown in this report that the decrease in the temperature of the superconducting transition and its expanding are more significant at (111) orientation of the films, despite the fact that numerous magnetic domain boundaries localized under the superconductor should enhance the superconductivity.

It is shown that the dependence of the superconductor resistance on the mutual direction of magnetization and current is observed only in narrow and thin stripes of niobium and disappears with their thickening. The rotation of the planar magnetic field makes it possible to effectively switch the resistance of such structures in the region of an expanded superconducting junction only. The effect is as large as 100 %.

A scheme for obtaining a diode effect based on  $Y_3Fe_5O_{12}/Al$  and  $Y_3Fe_5O_{12}/Nb$  structures is proposed and implemented. The 25% variation in the resistance is achieved by inverting a relatively low current.



A



B

Figure 1. Magnetic resistance of YBCO tapes: 1- non-irradiated, 2- irradiated: A—electrons, B— $\gamma$ -rays, 3- repeated run.

Support by ISSP RAN is acknowledged. We are thankful to G. Penzyakov for technical assistance in experiments at the initial stage of research and S. Bozhko for AFM of the film surface, to Yu. Proshin, N. Pugach and O. Tikhomirov for helpful discussion of the results.

- [1] A. Sidorenko, *Functional Nanostructures and Metamaterials for Superconducting Spintronics. NanoScience and Technology* (Springer, Cham., 2018).
- [2] A.S. Mel'nikov et al., *Phys. Usp.*, **65** (2020) 1248–1289.
- [3] R.G. Deminov et al., *J. Magn. Magn. Mater.*, **373** (2015) 16-17.
- [4] D. Stamopoulos et al., *Supercond. Sci. Technol.* **20** (2007) 1205.
- [5] L.N. Karelina et al., *JETP Lett.*, **112** (2020) 705–709.
- [6] D. Suri et al., *Appl. Phys. Lett.*, **121** (2022) 102601.
- [7] Ja. Santamaria, *Nature Materials*, **21** (2022) 993.
- [8] S.S. Ustavshikov et al., *JETP*, **135** (2022) 226–230.

## QUASIPARTICLES IN THE SYK t-J MODEL

*Kumar A.<sup>1</sup>, Sachdev S.<sup>2</sup>, Tripathi V.<sup>1</sup>*

<sup>1</sup> Department of Theoretical Physics, Tata Institute of Fundamental Research, Mumbai, India

<sup>2</sup> Department of Physics, Harvard University, Cambridge MA, USA

vtripathi@theory.tifr.res.in

The t-J model is a frequent starting point for the study of a variety of fractionalization phenomena and emergent excitations in the cuprate superconductors. We report here our study [1] of stability and change in nature of different quasiparticles upon increasing the hole doping in an SYK-like disordered t-J model as a localization phenomenon in the many-body Hilbert space. This approach, based on a scaling treatment of the quasiparticle support size in the many-body Hilbert space, was originally proposed [2] in the context of Landau quasiparticle lifetimes in disordered interacting quantum dots, and two of us recently generalized [3] the approach to disorder-free quantum spin systems. We find that away from critical doping, some stable quasiparticles are always present. In the magnetically ordered underdoped phase, apart from the spin-1 magnons, (natural excitations of a magnetic state), a very different emergent quasiparticle – essentially a Jordan-Wigner (JW) fermion – is also shown to be stable, but Landau quasiparticles are not. We believe these JW excitations likely play a significant role in determining some of the properties of underdoped cuprates such as an anomalously large thermal Hall conductivity even in the presence of collinear magnetic order, reminiscent of the Kitaev materials. In the overdoped regime, we find that Landau quasiparticles are stable but magnons and JW fermions are not. At a certain critical hole doping, we find the none of the quasiparticles is stable, which is the expectation for a strange metal phase. The JW quasiparticles we found are inherently nonlocal in the microscopic (spinful fermion) degrees of freedom, and their emergence would not be easy to capture using other contemporary local numerical approaches such as those based on the dynamical mean-field theory. Our analysis requires the evaluation of a large number of excited states, for which we have used the FEAST exact diagonalization technique.

[1] A. Kumar, S. Sachdev, V. Tripathi, *Phys. Rev. B*, **106** (2022) L081120.

[2] B. L. Altshuler et al., *Phys. Rev. Lett.*, **78** (1997) 2803.

[3] A. Kumar, V. Tripathi, *Phys. Rev. B*, **102** (2020) 100401(R).

**July 5**

11:00 – 13:00

Wednesday

ORAL  
SESSIONS I

Section C  
**Multiferroics**

## SPIN-RESOLVED POINT-LIKE CONTACT MODEL & ITS APPLICATIONS

Useinov A.<sup>1,2</sup>

<sup>1</sup> International College of Semiconductor Technology,

<sup>2</sup> National Yang-Ming Chiao-Tung University, Hsinchu, Taiwan ROC

artu@nctu.edu.tw

Present topic is focused for the basic formulation of the electron transport model for the point-like contact (PC) and demonstration its applications. The theory represents a solution, utilizing the semi-classical transport equations for a charge current with quantum boundary conditions at the interface, accounting the second order derivatives of the related quasi-classical Green functions along the transport direction. This theoretical approach allows to create  $I$ - $V$  model for the embedded object (device) into the central contact area, where the initial parameters and energy barrier profile must be well defined. The model's approach includes diffusive, quasi-ballistic, ballistic and tunneling regimes of the spin dependent transport conditions [1,2]. For example, tunneling approach of the model was utilized for  $I$ - $V$  curve modelling in the non-magnetic/magnetic tunnel junctions with spin filtering barriers such as MgO, as well as with ferroelectric multi-(mono-) domain dielectric barriers such as  $\text{Hf}_{0.5}\text{Zr}_{0.5}\text{O}_2$ , these junctions are promising devices for the computer memory and memristors. Moreover, PC model demonstrates not only it's consistency in the simulation of the ballistic magnetoresistance in ferromagnetic nanojunctions, but also explains the reason of anomalous tunnel magnetoresistance in magnetic tunnel junctions with embedded nanoparticles.

Keynote application of the spin-resolved PC model is the simulation of the resistance for the single domain wall (DW) in the magnetic nanowires (NWs) with a nano-constriction (defect), which is working as a pinning center for DW [3]. The obtained result demonstrates a few orders rapid reduction of the DW resistance, which is accompanied by its possible deviations versus the NW's diameter growth, ranging from 1.2 nm to 15.2 nm. The origin of these deviations, which are also denoted as oscillations, is related with the nonuniform electron scattering in the DW due to the intermixing electron scattering conditions: ballistic for one conductive channel and quasi-ballistic for other one with opposite spin direction. It takes place when the DW width by value is approximately in between two lengths: mean free path with the spin down ( $l_{\downarrow}$ ) and spin up ( $l_{\uparrow}$ ). A few experimental points in range of diffusive transport conditions are perfectly fitted by theoretical curve of the developed model. The ratios  $l_{\uparrow}/l_{\downarrow}$  and  $k_{F\uparrow}/k_{F\downarrow}$  ( $k_F$  – Fermi wavenumber) are most important parameters for this system as well as for spin-resolved PC theory in general. Noteworthy, the developed PC model has a potential of its application in the fields of Andreev spectroscopy and Kondo physics-based devices.

NSTC 111-2221-E-A49-120- is acknowledged.

[1] A. Useinov, H.-H. Lin, N. Useinov et al., *Data in Brief.*, **32** (2020) 106233.

[2] A. Useinov, H.-H. Lin et al., *J. Magn. Magn. Mater.*, **508** (2020) 166729.

[3] A. Useinov, *Spin*, **12(1)** (2022) 215003.

5IT-C-2

## CHIRALITY-INDUCED SPIN POLARIZATION AND ENHANCED X-RAY DICHHROISM IN A COLLINEAR ANTIFERROMAGNET

*Okamoto J.,<sup>1</sup> Wang R.-P.,<sup>2</sup> Chu Y. Y.,<sup>1</sup> Shiu H. W.,<sup>1</sup> Singh A.,<sup>1</sup> Huang H. Y.,<sup>1</sup> Mou C. Y.,<sup>3</sup> Teh S.,<sup>3</sup> Jeng H. T.,<sup>3</sup>  
Du K.,<sup>4</sup> Xu X.,<sup>4</sup> Cheong S.-W.,<sup>4</sup> Du C. H.,<sup>5</sup> Chen C. T.,<sup>1</sup> Fujimori A.,<sup>1,3,6</sup> and Huang D. J.<sup>3,7</sup>*

<sup>1</sup> National Synchrotron Radiation Research Center, Hsinchu, Taiwan

<sup>2</sup> Department of Physics, University of Hamburg, Hamburg, Germany

<sup>3</sup> Department of Physics, National Tsing Hua University, Hsinchu, Taiwan

<sup>4</sup> Department of Physics and Astronomy, Rutgers University, Piscataway, NJ, USA

<sup>5</sup> Department of Physics, Tamkang University, Tamsui, Taiwan

<sup>6</sup> Department of Physics, University of Tokyo, Bunkyo-Ku, Tokyo, Japan

<sup>7</sup> Department of Electrophysics, National Yang Ming Chiao Tung University, Hsinchu, Taiwan  
fujimori@phys.s.u-tokyo.ac.jp

Structurally chiral molecules and crystals exhibit x-ray natural circular dichroism (XNCD), which is orders of magnitude weaker than x-ray magnetic circular dichroism (XMCD) observed for ferromagnetic and ferrimagnetic materials. Collinear antiferromagnetic materials do not show any XMCD because of the fully compensated spin moments (except for “altermagnetic” materials, in which effective time-reversal symmetry is broken [1]).

We report on the observation of a new type of strong x-ray circular dichroism (XCD) at the Ni  $L_3$  edge of the structurally chiral, collinear antiferromagnet  $\text{Ni}_3\text{TeO}_6$  [2], although the material has effective time-reversal symmetry in the ground state and hence should not exhibit sizeable XCD. To explain the enhanced XCD, we propose a mechanism involving heat transport by magnons through the chiral crystal structure, in analogy to chirality-induced spin selectivity for electric current in a chiral crystal [3]. The coupling of the spin to the crystal chirality causes the accumulated spin polarization and hence the observed enhancement of XCD.

Support by the National Science and Technology Council of Taiwan, the Japan Society for the Promotion of Science and the Ministry of Education of Taiwan is gratefully acknowledged.

[1] A. Hariki, L. Smejkal et al., arXiv:2305.03588.

[2] X. Wang, S.-W. Cheong et al., *APL Mater.*, **3** (2015) 076105.

[3] A. Inui, Y. Togawa et al., *Phys. Rev. Lett.*, **124** (2020) 166602.

## MULTIFERROICS IN MESO-LIKE DEVICES

*Gareeva Z.V.*<sup>1,2</sup>, *Shulga N.V.*<sup>1</sup>, *Doroshenko R.A.*<sup>1</sup>, *Zvezdin K.A.*<sup>3</sup>, *Zvezdin A.K.*<sup>3</sup>

<sup>1</sup> Institute of Molecule and Crystal Physics, Subdivision of the Ufa Federal Research Centre of the Russian Academy of Sciences, Ufa, Russia

<sup>2</sup> Physico-Technical Institute, Ufa University of Science and Technology, Ufa, Russia

<sup>3</sup> Prokhorov General Physics Institute of the Russian Academy of Sciences, Moscow, Russia  
zukhrazzv@yandex.ru

The development of new computing technologies has given a new stimulus in the study of multiferroics (MFs). The use of MFs allows the realization of competitive energy efficient scalable logic and storage devices as an alternative to traditional CMOS technology. The low - power consumption in MESO logics and MRAM components is provided by magnetoelectric switching in multiferroic - based systems by a low-energy electric field. [1].

Our work concerns the modelling of the magnetoelectric (ME) - spin orbit (SO) logic with a focus on the ME component responsible for low power consumption. We consider the principle of operations of MESO-based logic devices; discuss the physical mechanisms, responsible for converting charge into spin in ME input and spin to charge in SO output; and simulate magnetization reversal processes in ME component of MESO.

To address this, we develop a model of magnetization switching in ME heterostructures, which leverage MFs to control magnetic states in a ferromagnetic (FM) layer via electric field. Representing the system in a form FM(1)-FM(2)-MF with a top layer of a soft ferromagnet FM(1) and a bottom layer of MF separated by a pinning layer FM(2), we explore the magnetic states in the top FM (1) at different ME states in MF [2, 3]. Based on the exchange bias effect, the processes of magnetization reversal are studied and the exchange bias fields are estimated for different ferroelectric states in the MF, which makes it possible to analyze the magnetization response of the system for different paths of polarization switching. In this study, we consider BiFeO<sub>3</sub> as a MF component, but the model is also applicable to other MF-based multilayers, in which MF is antiferromagnet with coupled ferroelectric and magnetic order parameters.

The use of the proposed approach makes it possible to analyze the influence of 1) dimensional factors (film thicknesses, transverse dimensions, sample shape) that affect the magnetic states of MF - based nanoelements; 2) the presence of several phases in composite MFs, such as interface boundaries and account for interphase interactions (magnetic anisotropy and interlayer exchange); 3) energy-efficient external influences that allow switching magnetic states using magnetic fields; 4) polarization switching in MF induced by an external electric field or strains.

Z.V.Gareeva., N.V. Shulga acknowledge the Support by Russian Science Foundation №23-22-00225, K.A. Zvezdin, A.K. Zvezdin acknowledge the Support by Ministry of Education of Russian Federation, Agreement № 075-11-2022-04.

[1] S. Manipatruni et al., *Nature*, **565** (2019) 35-42.

[2] A.A. Bersin, D.L. Vinokurov, A.I. Morozov, *Phys. Sol. State*, **58(11)** (2016) 2237-2241.

[3] Z. V. Gareeva, A.F. Popkov, S.V. Soloviov, A.K. Zvezdin, *Phys. Rev. B*, **87(21)** (2013) 214413.

## PHASE TRANSITIONS DRIVEN BY MAGNETOELECTRIC AND INTERFACIAL DZYALOSHINSKII-MORIYA INTERACTION

*Sharafullin I.F.<sup>1</sup>, Yuldasheva A.R.<sup>1</sup>, Kizirgulov I.R.<sup>1</sup>, Baisheva A.Kh.<sup>1</sup>, Diep H.T.<sup>2</sup>*

<sup>1</sup> Ufa University of Science and Technologies, Ufa, Russia

<sup>2</sup> CY Cergy Paris University, Cergy-Pontoise cedex, France

SharafullinIF@yandex.ru

Magnetic skyrmions are prime candidates for the next generation of spintronic devices. Skyrmions are topologically protected magnetic structures, skyrmions and skyrmion lattices are known to be stabilized by the Dzyaloshinskii-Moriya interaction that occurs when the inversion symmetry is broken in thin films and heterostructures. On the one hand, skyrmions can be used to store, transmit, and manipulate information with high efficiency in terms of energy consumption due to their topologically protected textures [2]. On the other hand, magnetic skyrmions form lattices in antiferromagnetic, synthetic antiferromagnetic and compensated ferrimagnetic materials – it represents an exciting state of matter [3,4]. Here, we show by steepest-descent method and Monte-Carlo calculations that metastable skyrmionic states can also be found in nominally symmetric multilayered systems. We demonstrate that this is correlated with the large enhancement of the DMI strength due to the presence of local defects. In particular, we find that metastable skyrmions can occur in multiferroic multilayers without external magnetic fields and can be stable even near room temperature conditions. We study properties of a skyrmion lattices, phase diagrams and conditions of their stability in a multiferroic bilayer with Heisenberg spin model. Considering magnetoelectric interface interaction between ferroelectric and antiferromagnetic layer and weak in-plane Dzyaloshinskii – Moriya interaction in this frustrated magnetic layer, we calculate the energy and the order parameters and layer magnetizations as functions of temperature up to the two different disordered phases.

The dependence of order parameters versus temperature shows the existence of stable skyrmion lattice branch which causes a low surface magnetization. We show that magnetoelectric interaction give rise to a stable phase of skyrmion lattices at zero temperatures and can stabilize skyrmions in antiferromagnetic layer at zero external field ant spin-polarisation current at low temperatures. We calculate the transition temperature and show that it depends strongly on the magnetoelectric coupling. Results agree with existing experimental observations on the stability of skyrmion structure in thin films and on the insensitivity of the transition temperature with the film thickness. We also study effects of various parameters such as surface exchange and anisotropy interactions.

Support by the State assignment of Russian Federation for the implementation of scientific research by laboratories (# 075-03-2021-193/5 30.09.2021).

[1] H.T. Diep, *Theory of magnetism* (Singapore: World Scientific, 2014)

[2] T.A. Shaikhulov et al., *JETP Letters*, **17** (2023) 1-6.

[3] S. El Hog et al., *J. of Magn. and Magn. Mat.*, **563** (2023) 169920-169929.

[4] X. Zhang et al., *J. Magn. Soc. of Japan*, **47** (2023) 20-27.

5IR-C-5

**TOPOLOGY IN FERROELECTRICS VS TOPOLOGY IN MAGNETISM:  
FOUNDATIONS***Lukyanchuk I.*University of Picardie, Amiens, France  
lukyanc@ferroix.net

The past decade marked breakthrough discoveries of novel topological polarization structures in nanostructured ferroelectrics. The observed polarization structures have been interpreted in terms of the real-space vector field topology as multiple combinations of vortices, skyrmions, merons, and other topological formations, previously observed in magnetic systems. However, this visible analogy misses ferroelectricity's cornerstone, the dominant role of the long-range electrostatic forces. In this talk, we present a generic topological foundation of ferroelectricity arising from its electrostatic essence and discuss from this viewpoint the recent trends in the field. We review the observed polarization topological structures and show that unlike in magnetic systems, their variety can be exhaustively described by the fundamental formations, vortices, and Hopfions. Remarkably, the emergence of the latter provides the chirality of the confined ferroelectric systems. We focus on insights into the topological origin of the chirality in the nanostructured ferroelectrics, bringing new controllable functionalities. We pay special attention to novel developments enabling tunability and manipulating the chiroptical response in ferroelectric nanoparticles and nanodots.

**July 5**

Wednesday

11:00 – 13:15

ORAL  
SESSIONS I

Section D

**Soft and Hard  
Magnetic Materials**

5OT-D-1

## INVESTIGATION OF RARE-EARTH MAGNETISM IN HARD MAGNETIC MATERIALS

*Kostyuchenko N.V.*<sup>1</sup>, *Tereshina I.S.*<sup>2</sup>, *Surdin O.M.*<sup>3,4</sup>, *Kudasov Yu.B.*<sup>3,4</sup>, *Zvezdin A.K.*<sup>5</sup>

<sup>1</sup> Moscow Institute of Physics and Technology, Dolgoprudny, Moscow Region, Russia

<sup>2</sup> Lomonosov Moscow State University, Moscow, Russia

<sup>3</sup> Russian Federal Nuclear Center – All-Russian Research Institute of Experimental Physics, Sarov, Russia

<sup>4</sup> Sarov Institute of Physics and Technology NRNU MEPhI, Sarov, Russia

<sup>5</sup> Prokhorov General Physics Institute RAS, Moscow, Russia

[nvkost@gmail.com](mailto:nvkost@gmail.com)

In the last years, investigations for searching new multicomponent rare-earth compounds is especially relevant in order to improve the properties of existing permanent magnets [1,2]. This is facilitated, among other things, by the development of new experimental techniques, that make it possible to find new features of magnetic properties of hard magnetic materials based on rare-earth. This allows us to get closer to understanding the processes occurring in the rare earth sublattice, since its behaviour plays a major role in high magnetic fields. So, that means to improve a model in order to take into account all the nuances of the rare-earth magnets properties.

In this work, we theoretically and experimentally studied the high-field behaviour of rare-earth intermetallic compounds of various types, their hydrides and complex-modified compounds (in which one rare-earth ion is replaced by another) [3,4]. When studying the above materials, a combination of analytical and numerical methods (including the quantum theory of the crystal electric field) was used as well as unique experimental data including measurements in ultrahigh magnetic fields [4,5,6].

To create magnetic fields with maximum induction values of ~600 T, we used a “small” magnetocumulative generator of the MK-1 type [4,5]. Powder samples were cooled to 5 K in a helium flow cryostat. Ultrahigh field magnetization curves were measured up to 300 T. We estimate the critical fields’ values, which allows us to clarify the magnetization behavior in the region of the magnetic transitions and predict exact magnetic field of transition to the forced-ferromagnetic state.

An important aspect of the studies that have been carried out is the ability to significantly improve the accuracy of the exchange and crystal-field parameters values using experimental data obtained in megagauss magnetic fields, and hence to get closer to understanding the processes occurring in rare-earth intermetallic compounds. This will make it possible to approach the prediction of new rare-earth permanent magnets with desired properties.

This work was supported by the Ministry of Science and Higher Education of the Russian Federation (No. FSMG-2021-0005).

[1] M.D. Coey, *Magnetism and Magnetic Materials* (Cambridge, England: Cambridge University Press, 2010).

[2] O. Gutfleisch et al., *Adv. Mater.*, **23**(7) (2011) 821.

[3] N.V. Kostyuchenko et al., *Intermetallics*, **124** (2020) 106840.

[4] N.V. Kostyuchenko et al., *Crystals*, **12** (2022) 1615.

[5] M.I. Dolotenko, *Magnetocumulative generators MK-1 of superstrong magnetic fields* (Sarov, RFNC-VNIIEF, 2015).

[6] S. Takeyama et al., *J. Phys. E*, **21** (1998) 1025.

## MAGNETOCALORIC EFFECT AND MAGNETOSTRICTION OF (Er,Y,Sm)Fe<sub>2</sub> COMPOUNDS

*Pankratov N.Yu.<sup>1</sup>, Karpenkov A.Yu.<sup>2</sup>, Umkbaeva Z.S.<sup>3</sup>, Tereshina I.S.<sup>1</sup>*

<sup>1</sup> Lomonosov Moscow State University, Faculty of Physics, Moscow, Russia

<sup>2</sup> Tver State University, Tver, Russia

<sup>3</sup> Ibragimov Complex Institute, Russian Academy of Sciences, Grozny, Russia

<sup>4</sup> Chechen State University, Grozny, Russia

pankratov@phys.msu.ru

It is known that intermetallic compounds of rare-earth metals with 3d-transition metals are in a magnetically ordered state in a certain range of temperatures. Compounds of light rare earth and 3d-transition metals are characterized by ferromagnetic ordering of magnetic moments; and compounds based on heavy rare-earth metals, by ferrimagnetic ordering. RFe<sub>2</sub> compounds (R – rare-earth metals) have both simple crystal (Laves phase C15 type) and magnetic structures. They also have fairly high Curie temperatures in range of 500 - 800 K. The ordered state of magnetic moments is found in RFe<sub>2</sub> due to exchange interactions. Three types of exchange interaction can be distinguished in a rare-earth magnetic: 3d-3d, 4f-4f, and 3d-4f. The dependence of exchange interactions on distances between atoms and magnetic state results in certain features on the thermal expansion, magnetostriction, and temperature dependence of magnetocaloric effect. The study of the magnetic and elastic properties of rare-earth intermetallic compounds is topical in modern materials science for the search for new high-performance function materials suitable for use in the room temperature range.

The aim of our work was to investigate the magnetothermal and magnetoelastic properties of ferrimagnetic compounds, including composition with a compensated magnetic moment. This kind of compounds can be obtained by mixing light and heavy rare earth in RR'Fe<sub>2</sub> compounds and/or by replacing light rare-earth metals with non-magnetic yttrium. The magnetocaloric effect and magnetostriction of (Er,Y)<sub>0.8</sub>Sm<sub>0.2</sub>Fe<sub>2</sub> were studied. The temperatures of the spin-reorientation transitions were determined from the features in the temperature dependences of the magnetostriction. The value of magnetocaloric effect near Curie temperature was obtained by an indirect method from calculation from magnetization curves. The temperature dependencies of magnetocaloric effect in the range of 100-320 K were investigated by direct method.

It was found that peculiarity on the temperature dependences of the anisotropic magnetostriction and the magnetocaloric effect correspond to the temperatures of magnetic phase transitions. It is shown that the presence of spin-reorientation transitions in the (Er,Y)<sub>0.8</sub>Sm<sub>0.2</sub>Fe<sub>2</sub> system is determined primarily by the contribution of samarium. It is shown that an increase in the concentration of yttrium ions in the studied system leads to a decrease in the temperatures of spin-reorientation transition and the magnitude of magnetostriction as a result of the weakening of the 3d-4f exchange interaction. A significant contribution of the single-ion magnetostriction of the rare-earth sublattice was found. A decrease in the magnitude of the magnetocaloric effect in the region of magnetic compensation was fixed. The magnetic phase diagram was constructed.

The research was supported by project no. 22-22-00313 from the Russian Science Foundation, <https://rscf.ru/project/22-22-00313/>.

## MAGNETIC TOMOGRAPHY OF AMORPHOUS MAGNETIC MICROWIRES: IMPEDANCE-BASED APPROACH

*Alekhina Yu.A.<sup>1,2</sup>, Kolesnikova V.G.<sup>1,2</sup>, Andreev N.V.<sup>3</sup>, Rodionov V.V.<sup>2</sup>, Rodionova V.V.<sup>2</sup>, Panina L.V.<sup>3</sup>, Perov N.S.<sup>1,2</sup>*

<sup>1</sup> Lomonosov Moscow State University, Moscow, Russia

<sup>2</sup> REC SMBA, Immanuel Kant Baltic State University, Kaliningrad, Russia

<sup>3</sup> National University of Science and Technology “MISiS”, Moscow, Russia  
Ya.alekhins@physics.msu.ru

Micromagnetic structure of the material has a crucial role for its response on the applied magnetic field. Numerous approaches to the determination of magnetization distribution in the volume of the materials, including various microtomography techniques [1-2] have been developed; however, the presented methods have strong size limitations and thus can hardly be applied to the class of amorphous magnetic microwires.

This work presents the results of the study of the magnetic properties and micromagnetic structure of amorphous microwires and structures based on them, as well as the method of magnetic tomography of amorphous microwires. The proposed technique consists in reconstruction of the permeability distribution on the basis of information on frequency dependence of the wire impedance [3-4]. The interpretation of the results was supported by the micromagnetic simulation using OOMMF software package. The criteria for applicability of the model are determined, which consisted in the absence of inhomogeneous magnetization reversal processes, as well as the negligibility of the contributions of the field and frequency dependences of the permeability.

The distributions of permeability were calculated for two series of microwires based on Co-Fe alloy with near-zero magnetostriction, including samples with different types of domain structures. It is shown that the distribution of permeability has a maximum in the region of the assumed position of the domain wall between axially magnetized core and near-surface shell. It has been found that for wires with a predominance of the radial type of anisotropy, inhomogeneous magnetization processes can distort calculation results. It was also found that the relaxation of mechanical stresses during post-processing leads to a change in the shape of the radial dependence of the permeability, including those appearing due to a change in the magnetization reversal processes.

The obtained experimental data were supported by the results of the micromagnetic modeling.

It was also shown that helical structures based on amorphous microwires can exhibit controlled anisotropic properties, as well as an asymmetric giant magnetic impedance effect, which is characteristic of materials with helicoidal anisotropy when a bias field or current is applied.

The approach proposed is promising for the development of non-destructive testing systems and new types of sensors.

The research was financially supported by RSF grant 22-22-00606. Alekhina Yu.A. acknowledges the financial support of the Grants of the President of Russian Federation Foundation.

- [1] C. Donnelly et al., *Nature*, **574** (2017) 328–331.
- [2] C. Donnelly et al., *New Journal of Physics*, **20(8)** (2018) 083009.
- [3] I. Alekhina et al., *Nanomaterials*, **11(2)** (2021) 1–16.
- [4] I. Alekhina et al., *J. Magn. Magn. Mat.*, **573** (2021) 168155.

## ENGINEERING OF MAGNETIC PROPERTIES OF Co-RICH MICROWIRES BY PROCESSING

González-Legarreta L.<sup>1</sup>, Zhukova V.<sup>1,2,3</sup>, Corte-Leon P.<sup>1,2</sup>, Ipatov M.<sup>1,2</sup>, Blanco J. M.<sup>2</sup>, Zhukov A.<sup>1,2,3,4</sup>

<sup>1</sup> Dept. Polymers and Advanced Materials, Univ. Basque Country, UPV/EHU, San Sebastian, Spain

<sup>2</sup> Dept. Appl. Phys., EIG, Univ. Basque Country, UPV/EHU, San Sebastian, Spain

<sup>3</sup> EHU Quantum Center, University of Basque Country, UPV/EHU, Spain

<sup>4</sup> IKERBASQUE, Basque Foundation for Science, Bilbao, Spain  
valentina.zhukova@ehu.es

Amorphous glass-coated microwires can present excellent magnetic properties such as magnetic bistability, enhanced magnetic softness and Giant Magnetoimpedance (GMI) effect and fast domain wall dynamics. Excellent magnetic softness and GMI effect have been reported for Co-rich microwires [1]. We present our recent experimental results on influence of stress- annealing on magnetic softness and GMI effect in Co- rich glass-coated microwires.

The influence of post-processing (annealing and stress-annealing) on the magnetic softness, Giant magnetoimpedance (GMI) effect and domain wall dynamics of  $\text{Fe}_{3.6}\text{Co}_{69.2}\text{Ni}_1\text{B}_{12.5}\text{Si}_{11}\text{Mo}_{1.5}\text{C}_{1.2}$  glass-coated microwires is studied.

As-prepared Co-rich glass-coated microwire presents linear hysteresis loops and rather higher magnetoimpedance ratio with double-peak dependence, typical for materials with transverse magnetic anisotropy.

Considerable magnetic hardening and transformation of linear hysteresis loop with low coercivity ( $H_c \approx 4$  A/m) into rectangular with  $H_c \approx 90$  A/m upon annealing without stress is observed (see Figure 1a). A single domain wall propagation is observed in annealed Co-rich microwires exhibiting such magnetic bistability effect. In spite of rectangular hysteresis loop form, we observed remarkable MI effect improvement at certain annealing conditions in such Co-rich microwires.

Stress-annealing of studied microwire allows considerable magnetic softening (see Figure 1a), GMI ratio (Figure 1b) and even domain wall velocity increasing. Additionally, remanent magnetization growth and coercivity decrease are generally observed upon stress annealing. Frequency dependence of maximum GMI ratio for as-prepared and annealed samples is evaluated. The obtained frequency dependence of the maximum GMI ratio allows determination of the optimal GMI measurement conditions for each sample. The origin of observed stress-induced anisotropy and related changes in magnetic properties are discussed considering the internal stresses relaxation and “back-stresses”.

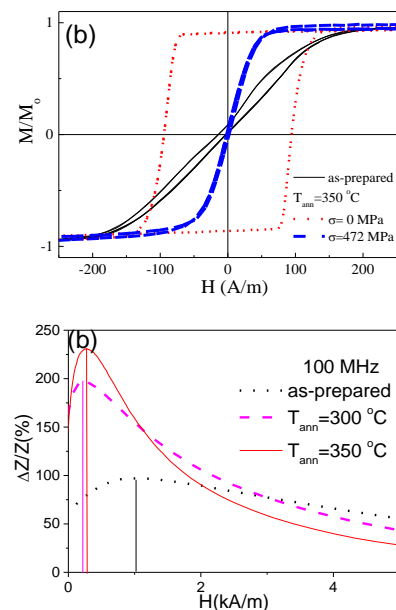


Figure 1. Effect of annealing on hysteresis loops (a), GMI effect (b)

[1] A. Zhukov, M. Ipatov and V. Zhukova, *In Handbook of Magnetic Materials* (Elsevier, 2015).

## MULTIMAGNETIC CORE/SHELL MICROWIRES FOR BIOMEDICAL APPLICATIONS: EXPERIMENT AND SIMULATIONS

*Kolesnikova V.G.<sup>1</sup>, Sadovnikov A.V.<sup>2</sup>, Baraban I.A.<sup>1,3</sup>, Martysbkin A.A.<sup>2</sup>, Sobolev K.V.<sup>1</sup>, Vázquez M.<sup>4</sup>, Rodionova V.V.<sup>1</sup>*

<sup>1</sup> Immanuel Kant Baltic Federal University, Kaliningrad, Russia

<sup>2</sup> Saratov State University, Saratov, Russia

<sup>3</sup> Department of Physics, Drexel University, Philadelphia, USA

<sup>4</sup> Institute of Materials Science of Madrid, CSIC, Madrid, Spain  
VGKolesnikova1@kantiana.ru

Magnetism of wires is relevant because of their specific geometry characterized by a cylindrical symmetry and large length to diameter aspect ratio. That implies strong shape anisotropy, which in addition to anisotropy contribution from magnetostrictive deformations confer a unique magnetic behavior that makes microwires ideal systems for fundamental studies on the magnetization process and very suitable for technological applications [1,2].

In the present work, we introduce a novel family of biphasic glass-coated microwires with two original innovations: i) the external shell is asymmetric; and ii) the external shell is sputtered directly onto the glassy coating so, the process is simplified in comparison to the commonly used electrochemical growth of the shell where an intermediate sputtered tiny metallic nanotube is in addition needed. Particularly, we focus on soft/soft and soft/hard bimagnetic microwires composed by a soft magnetostrictive nucleus out of Fe-based amorphous alloy, and an outer layer either with soft (e.g., NiFe) or harder (e.g., Co) magnetic behavior. The final goal has been twofold: firstly, the synthesis of such asymmetric bimagnetic microwires and the achievement of an asymmetric magnetic response to applied magnetic fields, as well as the identification of the magnetic contribution from each magnetic phase. In addition, we simulatively and experimentally inspect the influence of that asymmetry in their magnetoelastic properties for sensing applications, particularly in the magnetostrictive effect experienced by the spontaneously bent microwire under the application of static magnetic fields. A numerical model has been developed based on the finite element method (FEM) realized making use of Comsol Multiphysics software [3]. The calculation of elastic deformations caused by an external magnetic field was carried out for biphasic microwires with either Co- or FeNi shell. A self-consistent Multiphysics model was developed to describe the field dependence of the microwire bending and the distribution of the magnetostrictive deformation inside the microwire.

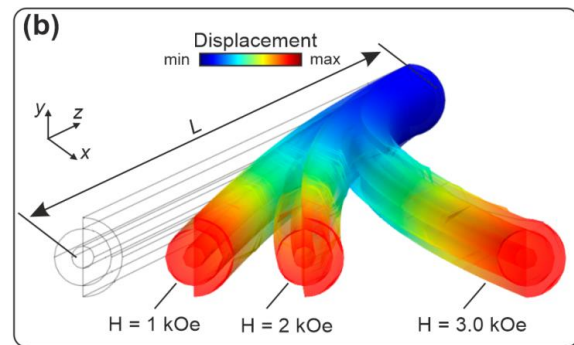


Figure 1. Model of the field dependence of the microwire bending.

particularly in the magnetostrictive effect experienced by the spontaneously bent microwire under the application of static magnetic fields. A numerical model has been developed based on the finite element method (FEM) realized making use of Comsol Multiphysics software [3]. The calculation of elastic deformations caused by an external magnetic field was carried out for biphasic microwires with either Co- or FeNi shell. A self-consistent Multiphysics model was developed to describe the field dependence of the microwire bending and the distribution of the magnetostrictive deformation inside the microwire.

The project was supported by the Ministry of Science and Higher Education of the Russian Federation (agreement no. 075-02-2023-934)

[1] J. Alam et al., *J. Magn. Magn. Mater.*, **513** (2020) 167074.

[2] M. Vazquez, *Magnetic Nano- and Microwires* (Woodhouse Publ., 2020).

[3] COMSOL Multiphysics® v. 5.6. www.comsol.com. COMSOL AB, Stockholm, Sweden.

5OT-D-6

## HIGH-TEMPERATURE SPONTANEOUS SPIN MAGNETIZATION OF DONOR CONDUCTION ELECTRONS IN HIGHLY DILUTED MAGNETIC SEMICONDUCTORS

*Govorkova T.E.<sup>1</sup>, Okulov V.I.<sup>1</sup>, Pamyatnykh E.A.<sup>2</sup>, Vaulin A.A.<sup>1</sup>, Gaviko V.S.<sup>1</sup>, Surikov V.T.<sup>3</sup>*

<sup>1</sup> M.N. Mikheev Institute of Metal Physics UB RAS, Yekaterinburg, Russia

<sup>2</sup> Ural Federal University, Yekaterinburg, Russia

<sup>3</sup> Institute of Solid State Chemistry of UB RAS, Yekaterinburg, Russia

govorkova@imp.uran.ru

In the given report there are presented the results of a detailed study of high-temperature impurity ferromagnetism of a new type in a highly dilute magnetic semiconductor (HDMS) based on  $\text{Hg}_{1-x}\text{Fe}_x\text{Se}$  ( $x < 0.01$ ). The electronic structure of the systems under study is a gapless crystalline matrix and a conduction band filled with donor electrons of the impurity atoms. In such systems, spontaneous spin magnetism can manifest itself at low temperatures [1-2].

The aim of the work has been a detailed study of this new effect - the spontaneous spin magnetism of donor conduction electrons in semiconductors at high temperatures. This effect is observed in the case of extremely low concentration of d-impurities ( $< 0.01$ ). In this case, in the conduction band of the crystal matrix one is formed a low-concentration system of donor electrons, the states of which, under the action of a strong exchange interaction, depending on the spin, with the initial polarization of electrons of impurity atoms, produce a complete spontaneous spin polarization of such a system. In this case, the impurity states are hybridized with the states of the conduction band, which is also a necessary condition for the appearance of a special type of spontaneous polarization.

The study of high-temperature impurity magnetization was carried out on a SQUID-magnetometer MPMS-5-XL at  $T=300$  K in magnetic fields  $H=\pm 50$  kOe (in the FC mode,  $H \parallel \langle 001 \rangle$ ) on bulk single crystals: HgSe (undoped) and  $\text{Hg}_{1-x}\text{Fe}_x\text{Se}$  ( $x=0.0006$ ). From the experimental dependence  $M_{exp}(H) = M_H + \chi_d H$  (where  $M_{exp}(H)$  is the total magnetization,  $M_H$  is the impurity magnetization,  $\chi_d H$  is the diamagnetic part), there was obtained the impurity contribution  $M_H(H)$ , which saturates with increasing magnetic field strength, characteristic for ferromagnets. The parameters of the magnetization curve were determined: the saturation field  $H_S \sim 15.6$  kOe and the saturation magnetization  $M_S \sim 3.4 \cdot 10^{-5}$  emu/g, which characterize the features of the new mechanism of magnetic ordering due to the exchange interaction of electrons in hybridized states. It has been established that the appearance of the magnetization of the system of donor conduction electrons in the HDMS-structure based on  $\text{Hg}_{1-x}\text{Fe}_x\text{Se}$  ( $x < 0.01$ ) at  $T=300$  K, as well as at low temperatures ( $T=5$  K), is associated with the same effect – the hybridization of the impurity states and the conduction band of the crystal.

In solving the actual problem there were obtained the results, reflecting phenomenal electron properties of the semiconductor structures studied, in which spontaneous spin magnetism is observed at high temperatures up to room one.

The study was supported by the Russian Science Foundation grant No. 23-22-00126, <https://rscf.ru/project/23-22-00126/>.

[1] T.E. Govorkova, V.I. Okulov, K.A. Okulova, *Low Temp. Physics*, **45** (2019) 234-240.

[2] T.E. Govorkova, V.I. Okulov, *Physics of the Solid State*, **64** (2022) 58-61.

## SOFT MAGNETIC FILMS WITH THE Fe+ZrN NANOCOMPOSITE STRUCTURE

*Tedzhetov V.A., Sheftel E.N., Harin E.V., Usmanova G.Sh.*

Baikov Institute of Metallurgy and Materials Science RAS, Moscow, Russia  
vtedzhetov@imet.ac.ru

Films characterized by nanocomposite structure  $\alpha\text{Fe} + \text{Me}_{\text{IV}}\text{X}$  ( $\text{Me}_{\text{IV}} = \text{Ti, Zr, Hf}$ ;  $\text{X} = \text{C, N, O, B}$ ) are considered as promising materials capable to provide a combination of high saturation magnetization  $B_S$  and low coercive field  $H_C$  for soft magnetic application [1]. The above nanocomposite structure can be formed in the films of the alloying system Fe-Zr-N containing equilibrium concentration region with two-phase structure  $\alpha\text{Fe} + \text{ZrN}$  and eutectic crystallization (quasi-binary system Fe-ZrN). The report presents the results of Fe-Zr-N alloying system film investigations aimed at finding of the composition range and the magnetron deposition conditions followed by annealing providing the nanocomposite structure  $\alpha\text{Fe} + \text{ZrN}$ . The dependence of the film static magnetic properties on their structural state is investigated as well.

The  $\text{Fe}_{92-78}\text{Zr}_{3-11}\text{N}_{5-12}$  films were prepared by DC and RF magnetron deposition on glass substrates and subsequent 1-hour annealing at temperatures of 300-600°C [2,3]. The film phase composition and structure were studied by XRD, TEM methods. Static magnetic properties were measured by VSM method. Metastable phase composition is formed in the deposited films. It is presented by one or few following phases: supersaturated solid solution  $\alpha\text{Fe}(\text{Zr,N})$ ,  $\text{Fe}_4\text{N}/\text{Fe}_3\text{N}$  or  $\text{ZrN}$  and amorphous phases. As Zr and N content in the films increases the supersaturation of  $\alpha\text{Fe}(\text{Zr,N})$  phase by these elements increases and the phase grain size decreases from 14 nm to 5 nm depending on the film composition. The volume fraction of an amorphous phase increases when Zr and N content in the film increases and when the rate of the film cooling during its growth on the substrate increases. Complete amorphization of the studied films is not achieved. The annealing of the films leads to the crystallization of the amorphous phase providing a formation of new grains of the phases  $\alpha\text{Fe}(\text{Zr,N})$ ,  $\text{Fe}_3\text{N}/\text{Fe}_4\text{N}$ ,  $\text{ZrN}$  in addition to the ones formed during deposition and to a decrease in supersaturation of the solid solution  $\alpha\text{Fe}(\text{Zr,N})$ . The  $\alpha\text{Fe}(\text{Zr,N})$  grain size doesn't change during annealing up to 500°. The high compressive macrostresses  $\sigma$  (up to 1.5 GPa) are formed in all deposited films. As the annealing temperature increases,  $\sigma$  decrease reaching zero at 300-500°C depending on the composition. Further increase in the annealing temperature leads to a transformation of the compressive macrostresses to tensile ones. High microstrain in  $\alpha\text{Fe}(\text{Zr,N})$  phase grain  $\varepsilon_{\alpha\text{Fe}(\text{Zr,N})}$  (2,6 %) formed in deposited films decreases after annealing (1,7 %).

The  $B_S$  and  $H_C$  values of the films as-deposited depending on the composition are 1.3-2.1 T and 0.08-1.0 kA/m respectively. The annealing leads to decrease of  $B_S$  (up to 1.2-1.9 T) due to additional nonferromagnetic phase formation and to the decrease of  $H_C$  (to 25-26 A/m) after annealing at 400-500°C. The decrease of  $H_C$  after annealing is explained by the decreasing of  $\sigma$  and  $\varepsilon_{\alpha\text{Fe}(\text{Zr,N})}$ . The physicochemical concept of a purposeful choice of compositions and producing conditions of super soft magnetic FeZrN films with a nanocomposite structure ( $\alpha\text{Fe} + \text{ZrN}$ ) and high  $B_S$  is formulated.

The study was supported by the Russian Science Foundation (project no. 23-23-00434).

[1] E.N. Sheftel, *Inorganic Materials: Applied Research*, **1(1)** (2010) 17-24.

[2] E.N. Sheftel et al., *Materials*, **15** (2022) 137.

[3] E.N. Sheftel et al., *Thin Solid Films*, **748** (2022) 139146.

## TUNING THE BAND STRUCTURE OF HEUSLER FERROMAGNETS FOR SPINTRONIC AND THERMOELECTRIC APPLICATIONS

*Kimura A.*

Graduate School of Advanced Science and Engineering &  
International Institute for Sustainability with Knotted Chiral Meta Matter (WPI-SKCM),  
Hiroshima University, Hiroshima, Japan  
akiok@hiroshima-u.ac.jp

Transverse thermoelectric conversion, known as the anomalous Nernst effect (ANE), holds significant potential for the development of future thermoelectric devices. Recently, Co-based Heusler alloys and related binary alloys have emerged as promising ANE materials, exhibiting a thermopower more than two orders of magnitude larger than that of pure Fe, for instance. This implies that the Berry curvature, generated by multiple 3d bands forming a “nodal web” is responsible [1-3]. Understanding the origin of this significant Nernst thermopower requires a careful inspection of the band structure, as the Berry curvature varies quite sensitively depending on the position of the Fermi level. However, experimental investigations of the band structure have been hindered by the difficulty of cleaving bulk crystals.

Here, we demonstrate that the utilization of a vacuum suitcase enables the direct observation of the spin-resolved band structure for in-situ grown ordered Co<sub>2</sub>MnGa (L21) and Fe<sub>3</sub>Ga (D03) thin films through spin- and angle-resolved photoelectron spectroscopy (spin-ARPES) with synchrotron radiation. By performing soft X-ray ARPES to observe the half-metallic band structure of a Co<sub>2</sub>MnGe bulk crystal, we have identified a band crossing in the majority spin channel far below the Fermi level [4]. Upon replacing Ge atoms with Ga atoms, the topological band crossing is precisely positioned at the Fermi level, resulting in a high Berry curvature. Through a close comparison of the iso-energy surfaces of Co<sub>2</sub>MnGa and Co<sub>2</sub>MnGe, we have verified the validity of the rigid-band picture, indicating the potential for fine carrier tuning by replacing Ga with Ge to maximize anomalous Nernst conductivities [5].

Furthermore, we have employed the spin-ARPES technique on an ordered Fe<sub>3</sub>Ga thin film [6]. The observed energy dispersions crossing the Fermi level are found to be of the minority spin. By comparing the experimental results with the calculated band structure, we have determined that the two bands intersecting near the L point under finite spin-orbit coupling play a crucial role as the source of Berry curvature leading to substantial ANE. Consequently, it is concluded that the intrinsic nature of significant ANE in ordered Fe<sub>3</sub>Ga has been established. These findings provide valuable insights for optimizing Nernst thermopower.

- [1] A. Sakai et al., *Nat. Phys.*, **14** (2018) 1119.
- [2] H. Nakayama et al., *Phys. Rev. Mater.*, **3** (2019) 114412.
- [3] A. Sakai et al., *Nature*, **581** (2020) 53.
- [4] T. Kono and AK et al., *Phys. Rev. Lett.*, **125** (2020) 216403.
- [5] T. Kono and AK et al., *Phys. Rev. B*, **104** (2021) 195112.
- [6] K. Ohwada, AK et al., submitted.

**July 5**

Wednesday

15:00 - 16:30

ORAL  
SESSIONS II

Section A  
**Miscellaneous**

## THE FERROMAGNETIC PROPERTIES OF EUROPIUM AND GADOLINIUM ATOMS IN SILICON

*Zikrillaev N.F.<sup>1</sup>, Mavlonov G.H.<sup>1</sup>, Isamov S.B.<sup>1</sup>, Abduganiev Y.A.<sup>1</sup>, Kushiev G.A.<sup>1</sup>, Nematov O.S.<sup>2</sup>*

<sup>1</sup>Tashkent State Technical University, Tashkent, Uzbekistan

<sup>2</sup>Samarkand State University named after Sharof Rashidov, Samarkand, Uzbekistan  
yoldoshaliabduganiyev2@gmail.com

Based on the results of research conducted by scientists and specialists on the formation of compounds of elements belonging to the lanthanides group in monocrystalline silicon, the possibilities of obtaining modern materials that can be used to create modern magnetic devices (magnetic sensors, hard disks and spintronic devices) and magnetoelectronic devices have been revealed. The reason for the interest in this field is not only the creation of the technology for obtaining new materials, but also the study of their basic physical properties that still remains a current issue in the physics of semiconductors. Based on the scientific analysis of the literature, the observation of ferromagnetism state in silicon with dopants of lanthanide elements is explained by the parallel arrangement of the magnetic moments of the dopant atoms in the solid volume. Since metals have a high concentration of electrons, it is relatively easy to control their spins. Semiconductor materials, particularly silicon, are diamagnetic materials. It was shown in work [1-2] that it is possible to change the magnetic properties of primary silicon by introducing the elements belonging to the lanthanides group with high spin ordering into silicon. The magnetic moments of lanthanide metal ions, particularly europium and gadolinium, are given in the table below. As dopant atoms of 99.999% (the product of Hebei Suoyi New Material Technology Co., Ltd.) chemically pure europium (EuO) and gadolinium (Gd) metallic elements selected as dopant atoms were diffused from the gaseous state into the initial n-type silicon. The obtained results were viewed using the MFM (FM-NANOVIEW 1000 AFM) device to see the ferromagnetic properties of the domain boundaries (Figure 1). It is scientific and practical importance to study the magnetic properties of silicon by adding dopant atoms of EuO and Gd.

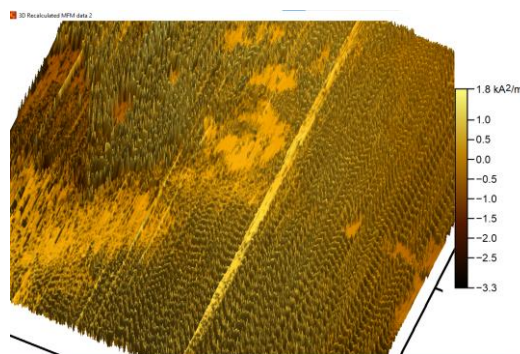


Figure 1. 3D view of domains of Si,P<Eu> atoms (2 $\mu$ m $\times$ 2 $\mu$ m).

Table.1. The magnetic moments of lanthanide metal ions.

Ion	Condition	g	$g[J(J+1)]^{1/2}$	$\mu_{\text{eff}}, \mu_B$
Eu <sup>2+</sup> , Gd <sup>3+</sup>	$4f^7, {}^8S_{7/2}$	2	7,9	7,9

[1] M.A. Ruderman, C. Kittel. *Phys. Rev.*, **96** (1954) 99–102.

[2] F. Formisano et al., *J. Magn. Magn. Mat.*, **502** (2020) 166429.

## ANISOTROPIC MAGNETORESISTANCE OF GaMnAs:Be

*Parchinskiy P.B., Gazizulina A.S., Nasirov A.A., Yuldashev Sh.U.*

National University of Uzbekistan, Tashkent, Uzbekistan

p.parchinskiy@nuu.uz

GaMnAs one of the most promising materials for spintronics application. Among the other properties of GaMnAs, magnetic anisotropy is one of the most important for successful realization of the spintronics devices. It is known, that the anisotropy parameters of GaMnAs epilayers can be modified by co-doping with a nonmagnetic impurity [1,2]. In this context, we present the results of investigation of magnetic anisotropy in GaMnAs co-doped with Be.

GaMnAs:Be samples were obtained by low-temperature molecular beam epitaxy on a semi-insulating GaAs (001) substrate. Concentration of Mn and Be in the samples was 1.41 and 0.1 at.%, respectively. More information about samples is given elsewhere [2]. In this work, the magnetic anisotropy was investigated by using anisotropic magnetoresistance (AMR), defined as  $\Delta R = R_p - R_n$ , where  $R_p$  is magnetoresistance values measured under magnetic field applied along the current and  $R_n$  is magnetoresistance seen for fields applied perpendicular to the current. AMR value were determinate for both in-plane and out-of-plane field orientation.

Figure 1 shows the AMR(H) value, determinate along different crystal axes in the field region up to 3000 Oe. It can be seen from the presented dependences that the AMR value depends both on the crystal axis and on the magnetic field orientation relative to the axis. The maximum value of AMR is observed along the  $[1\bar{1}0]$  axis at the normal orientation of the magnetic field. The minimum of the AMR values is observed along the  $[110]$  axis under parallel field orientation. It is notable that for the  $\langle 110 \rangle$  direction, the AMR value determinate for equivalent  $[110]$  and  $[1\bar{1}0]$  axes is significantly different both for normal and parallel H orientations, whereas for the  $\langle 100 \rangle$  direction under normal field orientation the differences in the AMR value along  $[100]$  and  $[010]$  axes are less pronounced, and for the parallel orientation of H practically disappears.

According to [3] obtained results indicate that the easy axis has both in-plane component oriented along the  $[1\bar{1}0]$  direction and a significant component in the direction perpendicular to the film plane. It is known that in GaMnAs epilayers under compressive strain, the easy axis prefers to in-plane orientation, while in GaMnAs under tensile strain the easy axis is oriented in out-of-plane direction. As far as Be has a smaller ionic radius compared to Mn and Ga, the out-of-plane component of easy axis in GaMnAs:Be can be associated with a decrease in compressive strains in the epitaxial layer due to co-doping with Be impurity.

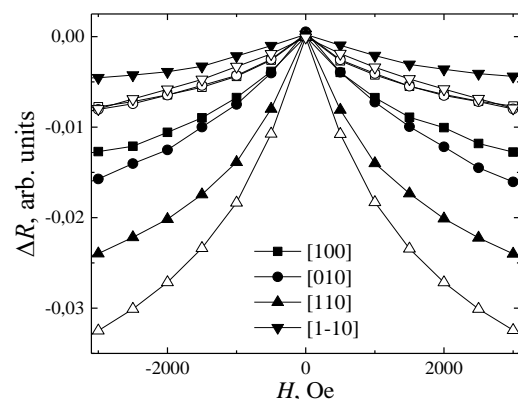


Figure 1. AMR of GaMnAs:Be determinate at 20 K. Open symbols – parallel field orientation, closed symbols – normal field orientation.

[1] J. Chang et al., *J. Cryst. Growth.*, **512** (2019) 112-118.

[2] P.B. Parchinskiy, A.S. Gazizulina, A.A. Nasirov, *Rus. Phys. J.*, **65** (2023) 1732-1737.

[3] D.Y. Shin, S.J. Chung, S. Lee, *Phys. Rev. B*, **76** (2007) 035327.

## HALL EFFECT IN AMORPHOUS FERROMAGNETIC ALLOYS

*Kuvandikov O., Subkhankulov I., Razhabov R.M., Khomitov Sh.A., Bakaev G.S.*

Samarkand State University named after Sharof Rashidov, Samarkand, Uzbekistan

subhonqulov1955@gmail.com

The study of the temperature dependence of the Hall effect in amorphous ferromagnets makes it possible to estimate the sign and concentration of charge carriers, to establish a relationship between the anomalous Hall coefficient  $R_S$ , electrical resistivity  $\rho$ , and saturation magnetization  $J_S$ . This makes it possible to obtain useful information about the nature of galvanomagnetic phenomena in amorphous ferromagnetic alloys depending on their composition and structure, as well as to establish regularities in the change in the main parameters associated with electrotransport and during the transition to the crystalline state. The purpose of this work is to experimentally study the temperature dependences of the Hall coefficient  $R_H$ , electrical resistivity  $\rho$ , and saturation magnetization  $J_S$  in ferromagnetic alloys based on iron group metals in the amorphous and crystalline states and to establish the relationship between these parameters. The Hall resistivity  $\rho_H$  is given by:

$$\rho_H = R_0 B + 4\pi J_S R_S \quad (1)$$

The value of the anomalous Hall coefficient is usually much larger in metals and alloys that are in the amorphous state than in the crystalline state. This is probably a direct consequence of the high electrical resistance in the amorphous state. It follows from expression (1) that the study of the dependence  $\rho_H = f(B)$  makes it possible to experimentally separate the normal  $R_0$  and anomalous  $R_S$  components of the Hall coefficient. In a certain temperature range characteristic of each alloy, a linear relationship between  $R_S$  and the square of the magnetization  $J_S^2$  is performed, which can be represented as:

$$\Delta R_S = R_S(T) - R_S(T_H) = \alpha [J_S^2(T_H) - J_S^2(T)] \quad (2)$$

Where  $R_S(T)$  and  $J_S(T)$  are, respectively, the anomalous Hall coefficient and the magnetization at  $T < T_c$ ;  $R_S(T_H)$  and  $J_S(T_H)$  values of the anomalous Hall coefficient and magnetization at the initial temperature  $T_H$ . Equation (2) characterizes the ferromagnetic fraction of the anomalous Hall coefficient  $R_S$  in a certain temperature range, depending on the saturation magnetization  $J_S$ .

The main reason for the difference in the temperature dependences of the anomalous Hall effect in amorphous and crystalline alloys of identical composition is the difference in the scattering mechanisms, which is determined by the feature of the short-range order structures. In magnetic crystals, phonon scattering, impurity scattering, and scattering caused by thermal fluctuations of spins contribute to the total electrical resistance  $\rho$ .

At  $T < T_c$  for crystalline ferromagnetic alloys, the relation is fulfilled:

$$R_S = a\rho + b\rho^2 \quad (3)$$

The first term in equation (3) is determined by the asymmetric scattering of current carriers under the influence of its own periodic spin-orbit interaction, and the second is mainly associated with the mechanism of lateral displacement of carriers of the anomalous Hall effect under the influence of spin-orbit interaction. For all the alloys under study, the values of the first term of equation (2) is much less than the second. The value of  $R_S$  is determined by the detailed dependence of the structure factor, pseudo potentials on the wave vector and is very sensitive to the microstructure of the alloys. Differences in the values of the coefficients  $a$  and  $b$  of equation (3) for the amorphous and crystalline states of ferromagnetic alloys indicate a partial transformation of the electronic spectrum during amorphization, leading to partial localization of charge carriers.

Thus, the main reason for the difference in the temperature dependence of the anomalous Hall effect in crystalline and amorphous ferromagnetic alloys is the difference in scattering mechanisms due to structural disordering.

## MAGNETO-OPTIC FARADAY EFFECT OF CoFe<sub>2</sub>O<sub>4</sub> BASED FERROFLUIDS

*Kuvandikov O.K., Razhabov R.M., Imamnazarov D.H., Salakbitdinova M.K., Kirgizov S.E.*  
Samarkand State University named after Sharof Rashidov, Samarkand, Uzbekistan  
quvandikov@rambler.ru

The magnetic nanocomposites are special intelligent materials with many applications in biosensors, magneto – optical devices, medicine and photonics. In turn, these applications depends on the magneto-optical properties of magnetic fluids. High and quick magneto-optic response or Faraday rotation to external magnetic field is fundamental requirement for magneto-optic sensing. Researchers have synthesized a lot of films, crystals, and glasses with Faraday effects.

An effective way for realizing the magneto-optic sensing is to use liquid-phase systems, where the bonding energy is smaller and the molecular order of the structure can be easily modified using external magnetic field. These materials are known as ferrofluids. Ferrofluids are colloidal suspensions of magnetic (MFe<sub>2</sub>O<sub>4</sub>, M-3d metals) nanoparticles that have both characteristics: the fluidity of liquids and the magnetism of solid magnetic materials which find many applications. Among such nanoparticles, CoFe<sub>2</sub>O<sub>4</sub> is distinguished by its strong magnetic properties.

CoFe<sub>2</sub>O<sub>4</sub> nanoparticles were synthesized by chemical co-precipitation method and magnetic fluid was prepared. Figure 1 is elemental analysis by X-ray fluorescence of CoFe<sub>2</sub>O<sub>4</sub> nanoparticles. The mass concentration of sample analyzed by Fundamental Parameters method.

Faraday rotation of CoFe<sub>2</sub>O<sub>4</sub> based ferrofluid (at 0.25% volume concentration) shown in Figure 2.

### Analyzed result(FP method)

No.	Component	Result	Unit	Stat. Err.	LLD	Element line	Intensity(cps/μA)
1	Fe	61,7	mass%	0,0372	0,0039	M:Fe-Kα	312,63410
2	Ni	0,144	mass%	0,0052	0,0136	M:Ni-Kα	0,40497
3	Co	38,1	mass%	0,0260	0,0170	M:Co-Kα	279,11786

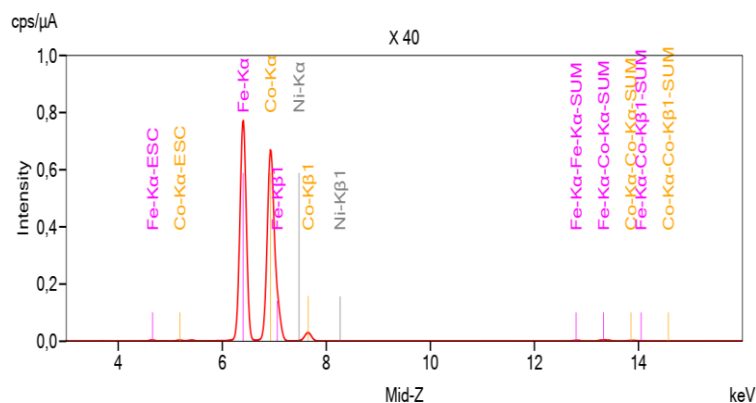


Figure 1. Elemental X-ray fluorescence of CoFe<sub>2</sub>O<sub>4</sub> nanoparticles.

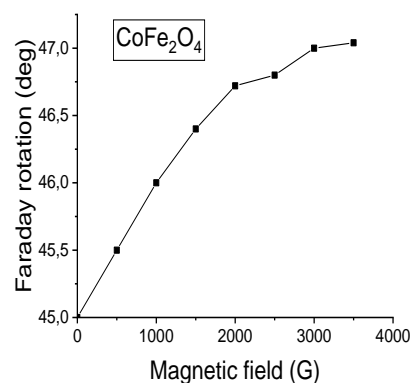


Figure 2. Faraday rotation of CoFe<sub>2</sub>O<sub>4</sub> based ferrofluid.

Despite the small volume concentration, it was found the Faraday effect is strongly manifested in CoFe<sub>2</sub>O<sub>4</sub> based ferrofluids. The results show that, the faraday rotation of CoFe<sub>2</sub>O<sub>4</sub> ferrofluids is highly than pure Fe<sub>3</sub>O<sub>4</sub> and other metal oxide composite based magnetic fluids by volume concentration of magnetic nanoparticle [1,2].

[1] N.A. Yusuf, A.A. Rousan, H.M. El-Ghanem. *J. Magn. Magn. Mat.*, **65** (1989) 282-284.

[2] M. Dai, S.L. Pu. *Advances in materials Physics and Chemistry*, **5** (2015) 344-349.

## TRANSPORT PROPERTIES OF IRON-SILICON DIOXIDE-COMPENSATED SILICON HYBRID STRUCTURES

*Arzikulov E.U., Salakbitdinov F.A., Nurimov A.D., Ashirov U.A., Sharafova T.S., Usanov R.M.*

Samarkand State University named after Sharof Rashidov, Samarkand, Republic of Uzbekistan  
eshkuvata@gmail.com

In the last ten years, a lot of scientific papers have appeared on the technology of obtaining and the physical properties of structures of the Metal/Oxide/Semiconductor type under various conditions. This is due to the discovery of a number of interesting and previously undiscovered effects in them, such as giant magneto-impedance and positive magnetoresistance, large positive magnetoresistance induced by light, giant lateral photoeffect, etc. The above effects indicate the prospect of using such hybrid structures as the element base of spintronics, optoelectronics and photovoltaics applications.

A literature review of the work carried out showed that in the studied structures, low-resistance, 7.5  $\Omega\cdot\text{cm}$  and 4.5  $\Omega\cdot\text{cm}$ , respectively, for n- and p-types of conductivity, single-crystal silicon wafers were mainly used as substrates. At the same time, there is no justification for the choice of substrate material, however, there are a number of studies regarding the influence of the type of substrate conductivity on their photoelectric properties. In this case, interest arises in the use of compensated (C), highly compensated (HC) and over compensated (OC) samples of single-crystal silicon doped with various impurities by high-temperature diffusion as a substrate in such structures. Совершенная технология получения компенсированного кремния дает еще один степень свободы управления параметров таких гибридных структур и наблюдаемых физических явлений. It is known that C, HC and OC silicon samples have unique physical properties, namely, high photosensitivity both in the impurity and intrinsic regions of the spectrum, infra-low-frequency oscillations of the photocurrent with a large amplitude, recombination waves, large positive and negative magnetoresistance, deep temperature and infrared quenching of photoconductivity, etc.

In this paper, we present the results of studying obtaining technology and studying the magnetotransport properties of  $\text{Fe}/\text{SiO}_2/\text{p-Si}\langle\text{B,Mn}\rangle$  and  $\text{Fe}/\text{SiO}_2/\text{n-Si}\langle\text{B,Mn}\rangle$  hybrid structures. Samples for research were made as follows. Firstly, samples of both n - and p - types of conductivity and different electrical resistivity were obtained using standard high-temperature diffusion technology. Then, tunneling thin  $\text{SiO}_2$  oxide layers of the order of  $\sim 1,5$  nm were obtained chemically. After that, thin metal layers of iron were obtained by vacuum thermal and electron-beam evaporation methods. As a result, perfect hybrid structures  $\text{Fe}/\text{SiO}_2/\text{p-Si}\langle\text{B,Mn}\rangle$  and  $\text{Fe}/\text{SiO}_2/\text{n-Si}\langle\text{B,Mn}\rangle$  with different electrical resistivities of the HC substrate were obtained.

## EFFECT OF MAGNETIC FIELD ON EXCITATION CONDITIONS AND CURRENT AUTO-OSCILLATION PARAMETERS IN SILICON DOPED WITH SELENIUM ATOMS

*Zikrillaev N.F.<sup>1</sup>, Shoabdurakhimova M.M.<sup>1</sup>, Bobonov D.<sup>2</sup>, Nematov O.S.<sup>3</sup>*

<sup>1</sup> Tashkent State Technical University (TSTU), Tashkent, Uzbekistan

<sup>2</sup> Jizzakh Polytechnic Institute (JPI), Jizzakh, Uzbekistan

<sup>3</sup> Samarkand State University named after Sharof Rashidov, Samarkand, Republic of Uzbekistan  
shoabduraximova.m@gmail.com

The influence of the magnetic field on excitation conditions and parameters of auto-oscillation current in silicon doped with selenium atoms was studied in weak magnetic fields. The condition  $(\mu/s)H \ll 1$ , where:  $\mu$  is the mobility of charge carriers,  $c$  is the speed of light,  $H$  is the magnetic field strength [1, 2].

Till now the influence of the magnetic field on excitation conditions and auto-oscillation parameters was investigated in works which showed, that transversal magnetic field influences on threshold characteristics of slow recombination waves (RW) in silicon of n conductivity type, compensated by zinc atoms. However, we were the first to investigate the influence of magnetic field on the excitation conditions and parameters of low-frequency auto-oscillation currents of temperature and electrical instability (TEI) type. The studies were carried out in a special cryostat, which allows the creation of magnetic field strengths up to values  $H \leq 25$  kEr in both longitudinal and transverse directions of the magnetic field relative to the current direction.

The results showed that the magnetic fields regardless of direction have almost the same effect on the excitation threshold and the parameters of auto-oscillation current. It was found that with increasing the value of the magnetic field the threshold of current auto-oscillation linearly increases, and with increasing resistivity of silicon samples doped with impurity atoms of selenium this dependence is expressed more strongly. At some critical value of magnetic field ( $H_{cr}$ ) regardless of the direction, auto-oscillation of the current in the circuit breaks, i.e. there was a place of magnetic damping of auto-oscillation of the current. We also found that the critical value of the magnetic field of auto-oscillation quenching can be shifted by controlling the illumination and temperature of silicon samples doped with selenium atoms.

The magnetoresistance ( $\rho_l$ ) was measured in Si<Se> silicon samples to find out the reasons for changing the excitation conditions and the parameters of the auto-oscillation current. The results showed that in all the samples the value of  $\rho_l$  significantly exceeded the conventional magnetoresistance values and practically did not depend on the magnetic field direction. The magnetoresistance was stronger in the Si<Se> samples with high resistivity.

Experimental results and studies are well explained taking into account the heterogeneity of the material, indicating a real heterogeneous distribution of impurity selenium atoms, regardless of their location in the crystal lattice of silicon. In addition, these studies show the possibility of creating magnetosensitive devices based on low-frequency auto-oscillation currents in silicon samples doped with selenium atoms.

[1] M. K. Bakhadyrchanov et al., *Surf. Eng. and Appl. Electrochem.*, **49(4)** (2013) 308.

[2] Yu.N. Parkhomenko et al., *Semiconductors*, **38(5)** (2004) 572-575.

**July 5**

Wednesday

15:00 - 16:45

ORAL  
SESSIONS II

Section B

**Magnetism and  
Superconductivity**

## APPROXIMATE APPROACH TO THE THEORY OF THE PROXIMITY EFFECT OF A SUPERCONDUCTOR/CHIRAL FERROMAGNET CONTACT

*Tumanov V.A., Proshin Yu.N.*

Kazan Federal University, Kazan, Russia  
yurii.proshin@kpfu.ru

This research addresses the proximity effect of a superconductor with a chiral ferromagnetic metal. We theoretically study the effect of skyrmions on a critical temperature of superconductor/ferromagnet (S/F) heterostructure. In contrast to the previously discovered micron-scale spin vortices, recently observed nanoscale structures [1] can have a significant effect on the critical temperature of the superconducting transition. Based on the Usadel equations for inhomogeneous magnetization obtained in [2] we started with rotation of the matrix Usadel function in spin space. The rotation matrix is chosen in such a way that in the transformed equation the term responsible for the interaction with localized spins becomes diagonal. After transformation the gradient transforms into the extended derivative in the Usadel equations and boundary conditions. Self-consistency equation is invariant under such transformations and has conventional form. For complex spin textures, such as spin vortices and domain walls, the Usadel equation does not reduce to an equation with constant coefficients after the unitary rotation. However, the transformed Usadel function phase changes much weaker along the SF boundary. This allows us to use an approximate approach to solve boundary value problem by neglecting some terms in the Usadel equation for the ferromagnetic layer. This approach allowed us to obtain a quantitative estimation of the effect on the superconducting critical temperature for almost any spin texture.

As expected, the impact on critical temperature near the magnetic inhomogeneity is determined by its scale compared to the superconducting coherence length. According to our calculations, the described effect is very sensitive to the thickness of the superconducting layer and the border transparency. By special choice of layer thicknesses, it is possible to achieve that superconductivity occurs only in the spin vortex localization region. In this case the critical temperature is about 10-20% of the bulk superconductor critical temperature [3]. The significant effect of nanoscale spin vortices on the critical temperature, combined with topological stability and low current density required for their movement, makes it possible to use such systems as superconducting spin valves. An island of superconductivity tied to a skyrmion can be placed between the superconducting shores as a movable bridge for supercurrent (see Figure 1).

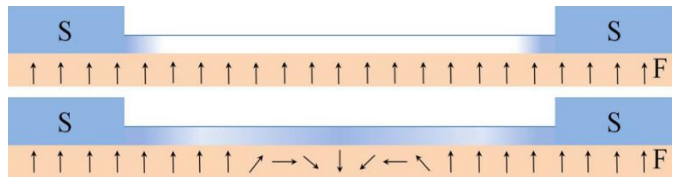


Figure 1. Schematic image of the spin valve based on an increase in the critical temperature of the superconductor in the skyrmion localization domain. The fill intensity of the superconducting layer indicates the density of Cooper pairs. Displacement of the vortex in the region between the contacts provides the conditions for superconducting current between the superconducting edges (at the bottom).

Support by Strategic Academic Leadership Program of the Kazan Federal University.

[1] A.O. Leonov *et al*, *New J. Phys.*, **18** (2016) 065003.

[2] Y.V. Fominov, A.F. Volkov, K.B. Efetov, *Physical Review B*, **75** (2007) 104509.

[3] V.A. Tumanov, V.E. Zaitseva, Yu.N. Proshin, *JETP Letters*, **116** (2022) 449–455.

## PROXIMITY EFFECTS AT SUPERCONDUCTING AND FERROMAGNETIC HETEROSTRUCTURES

*Zhaketov V.D.*

Joint Institute for Nuclear Research, Dubna, Russia  
zhaketov@nf.jinr.ru

Nowadays studying of proximity effects at the interface between two media are in focus of view [1-4]. In particular hybrid heterostructures comprising superconducting (S) and ferromagnetic (F) layers are currently attracting great attention due to a diverse set of proximity effects. Manifestations of the influence of ferromagnetism on the superconducting properties of S/F heterostructures include phase changes of the superconducting wave function (“ $\pi$ -phase superconductivity”) and spin-triplet Cooper pairing. Converse proximity effects in which superconductivity influences ferromagnetism have received less attention. These magnetic proximity effects (MPEs) are expected in systems where the F and S transition temperatures,  $T_F$  and  $T_C$ , are comparable, including for instance cuprate high- $T_C$  superconductors and ferromagnetic manganates.

The requirement, among other things, for such systems is that the thicknesses of ferromagnetic layers should be on the order of the correlation length of superconductivity in ferromagnetic  $\xi_F \sim 1 \div 5$  nm [4]. To reduce the exchange interaction, alloys of ferromagnetic materials with non-magnetic materials are used. When making structures with given parameters, the structures are heterogeneous, clusters with a diameter of  $\xi_{cl} = 5 \div 10$  nm are formed. Clusters interact with each other. This condition is known in the literature as super-spin glass [5]. The effect of the superconducting transition on the super-spin glass state in various types of heterostructures was investigated: V/FeV/V (Cr)/FeV/Nb, Nb/CuNi [1].

Promising systems for study of MPEs are S/F heterostructures comprised of niobium and rare-earth (RE) materials. First of all high transparency of S/F interface is reported for such RE/Nb systems as Gd/Nb which simplifies penetration of superconducting correlations in F system [2]. Second, the REs are characterized by weak ferromagnetism, which equalize energies of both interactions and make MPEs easier. Last, but not least many REs such as Dy and Ho are known rare-earth ferromagnets with helimagnetic non-collinear structure allowing for generation of long-range triplet superconductivity. Taking into account all these considerations, RE/Nb structures potentially interesting for search of magnetic proximity effects.

One of the most effective methods for studying the magnetism of thin films is polarized neutron reflectometry, which allows to obtain isotope and magnetic profiles to the depth of the structure with nanometer resolution. Polarized neutron reflectometer REMUR, located on the 8th channel of the IBR-2 pulse reactor (Dubna), is one of the most luminous reflectometers in the world with a neutron flux on the sample  $\Phi = 3 \cdot 10^5 \text{ n} \cdot \text{s}^{-1} \cdot \text{cm}^{-2}$ . This reflectometer is time-of-flight with an operating neutron wavelength range of  $\lambda \approx 1 - 15 \text{ \AA}$ . Low-temperature studies of proximity effects in superconducting-ferromagnetic systems [1-2] and rare-earth films with non-trivial magnetic ordering were carried out on the REMUR reflectometer [3].

- [1] V.D. Zhaketov et al., *JETP*, **129(2)** (2019) 258-276.
- [2] Yu.N. Khaydukov et al., *Phys. Rev. B*, **99(14)** (2019) 140503.
- [3] D.I. Devyaterikov et al., *Journal of Surface Investigation*, **16(5)** (2022) 839-842.
- [4] A.I. Buzdin, *Reviews of Modern Physics*, **77(3)** (2005) 935.
- [5] S. Sahoo, *Journal of Physics: Condensed Matter*, **14** (2002) 6729-6736.

## PROGRESS IN RFTES DETECTOR TECHNOLOGY

*Shitov S.V.*<sup>1,2</sup>

<sup>1</sup> Kotelnikov IRE RAS, Moscow, Russia

<sup>2</sup> National University of Science and Technology “MISIS”, Moscow, Russia  
sergey3e@gmail.com

The new Radio Frequency Transition Edge Sensor technology aims to demonstrate the fusion of the best features of mature technologies such as TES, MKID and HEDD. The operation near the critical temperature of the superconducting film is taken from the TES technology, the Q-factor control of the micro-resonator is taken from the MKID technology, and the heating of the micro-absorber with electron gas, which volume determines the detector sensitivity, is taken from the HEDD technology. The fundamental advantages of RFTES technology can be defined as the extremely high sensitivity, which originates from a countable number of electrons, along with the convenience of integrating such detectors into FDM imaging arrays with readout frequencies of  $\sim 1$  GHz, which are suitable for fundamental studies of the Universe, including from space observatories. .

To date, a number of important properties and new approaches to the development and study of RFTES detectors have been demonstrated: the fabrication of thin (50–80 nm) disordered hafnium films with a critical temperature in the range of 200–400 mK; bridges made of such a material are technologically compatible with niobium micro-resonators and can control their quality factor with a typical value of  $\sim 10^4$ , exhibiting a nonlinear microwave impedance similar to a superconducting transition; a low thermal conductivity of the heated electron subsystem was obtained, which exhibits the properties of an electron gas in the temperature range of 100–400 mK; experimental detectors for the 550–750 GHz range have been demonstrated with their NEP practically equal with theoretical predictions for the currently record-breaking HEDD detectors. All these inspire optimism for obtaining  $NEP \sim 10^{-20}$  W/ $\sqrt{\text{Hz}}$  using the RFTES technology [1].

From a methodological point of view, several new approaches to measuring the intrinsic noise and dynamic characteristics of RFTES have been developed and demonstrated [2]. A new concept of an active superconducting terahertz detector for imaging array applications has been developed, which is based on combining two devices in an integrated circuit: an RFTES bolometer and a microwave preamplifier based on a DC SQUID. An electromagnetic model of the practical structure of an active detector is developed, which is suitable for RFTES, MKID and other detectors using high-Q superconducting cavities, which provides the maximum, theoretically possible, signal transmission from the sensor to the amplifier.

All this makes the RFTES technology an interesting topic in the field of applied superconductivity.

[1] A.V. Merenkov et al., *Ph. Sol. State*, **64(10)** (2022) 1404.

[2] T.M. Kim, S.V. Shitov, *Pis'ma v Zhurn. Teor. Fiz.*, **47(24)** (2021) 13-16.

## ELECTRONIC STRUCTURE AND EXCHANGE INTERACTIONS OF QUASI-LOW-DIMENSIONAL $\text{Cu}_3\text{TeO}_3(\text{SO}_4)_2$ AND $\text{PbCu}(\text{SeO}_4)(\text{OH})_2$

*Pchelkina Z.V.*

M.N. Mikheev Institute of Metal Physics UB RAS, Yekaterinburg, Russia  
pchelkzl@mail.ru

The crystals incorporating transition metal ions tend to experience the long range magnetic order at decreasing temperature. This trend is opposed by the frustration of exchange interactions and the reduced dimensionality of the magnetic subsystem. Here we investigate electronic structure and exchange interactions of two recently synthesized compounds:  $\text{Cu}_3\text{TeO}_3(\text{SO}_4)_2$  [1] and  $\text{PbCu}(\text{SeO}_4)(\text{OH})_2$  [2]. The crystal structure of anhydrous copper tellurite-sulfate  $\text{Cu}_3\text{TeO}_3(\text{SO}_4)_2$  is formed by hexamers  $[\text{Cu}_6\text{O}_{22}]$  of  $\text{CuO}_x$  polyhedra interconnected into a three dimensional framework by tellurite and sulfate groups. DFT (Density Functional Theory) calculation taking into account correlation effects for  $3d$  Cu shell within DFT+U approach results in the insulating ground state. The calculated exchange interactions within hexamer (Figure 1) and between hexamers show that one third of  $\text{Cu}^{2+}$  ions form magnetically silent dimers with  $J_1=439$  K, while antiferromagnetic long-range order with  $T_N=13$  K is due to weaker interactions between hexamers. Thus,  $\text{Cu}_3\text{TeO}_3(\text{SO}_4)_2$  evidences rare coexistence of spin singlets and long-range magnetic order, both being represented by copper ions.

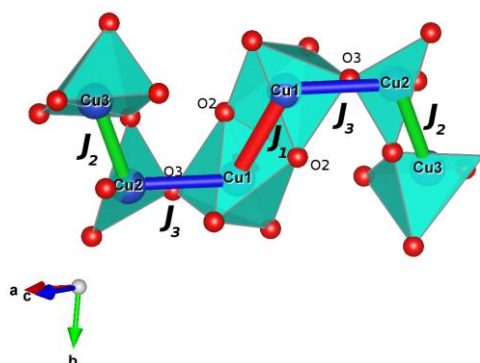


Figure 1.  $\text{Cu}_6\text{O}_{12}$  hexamer in crystal structure of  $\text{Cu}_3\text{TeO}_3(\text{SO}_4)_2$  in polyhedral representation. Solid lines represent principal intra-hexamer exchange interactions paths  $J_1$ - $J_3$ .

The second compound,  $\text{PbCu}(\text{SeO}_4)(\text{OH})_2$ , hosts well separated spin  $\frac{1}{2}$  chains of  $\text{Cu}(\text{OH})_2$  units. In such a chain competing FM nearest-neighbor  $J_{nn}$  and AFM next-nearest-neighbor  $J_{nnn}$  exchange interactions could lead to different exotic ground states depending on the ratio  $J_{nnn}/J_{nn}$ , like the Majumdar-Ghosh ground state which is expected as superposition of spin singlets for  $J_{nnn}/J_{nn} = 0.5$ . Withing DFT+U approach the following values of exchange interactions were calculated:  $J_{nn}=-103$  K,  $J_{nnn}=54$  K putting  $\text{PbCu}(\text{SeO}_4)(\text{OH})_2$  very close to the Majumdar-Ghosh critical point. There are also weak interchain interactions ( $\sim 6$  K) which lead to the long-range magnetic order at  $T_N=4.3$  K. We will also discuss formation of 1D chains in perovskite-based structures on example of  $\text{Pb}_2\text{CuMoO}_6$ .

Support by the Russian Science Foundation through project 22-22-00023 and project 23-42-00069 is acknowledged.

[1] A. F. Murtazoev et al., to be published.

[2] M. Markina et al., *Materials*, **15** (2022) 7860—7869.

5IT-B-11

## **HIGH-TEMPERATURE SUPERCONDUCTIVITY OF HYDRIDES: ROLE OF QUANTUM DEFECTS**

*Morosov A.I., Sigov A.S.*

MIREA - Russian Technological University, Moscow, Russian Federation

Formation of high-temperature superconducting phases of some hydrides with the superconducting transition temperature exceeding 200 K requires high pressure of the order of several hundred gigapascals, which causes a crystal lattice compression and correspondingly an exponential increase to values of the order of 100 K of the tunneling matrix element describing the probability of tunneling of the hydrogen atom between equivalent interstitial sites. At low temperatures, vacancies in the hydrogen sublattice completely occupied at zero temperature and stoichiometric conditions as well as hydrogen atoms in the interstitial sublattice absolutely vacant at zero temperature and stoichiometric conditions are quantum defects (defectons) and their band motion may take place. As the temperature decreases, the clustering of defects inevitably occurs due to the alternating nature of the long-range interaction between them, which is the sum of the elastic interaction and the interaction through Friedel oscillations of the electron density. In some cases, this produces a two-level systems (TLS). The interaction of electrons with either free defectons or TLS contributes to their Cooper pairing. The contribution of defectons to the superconductivity of hydrides is estimated and it is shown that it can become decisive at large widths of the defecton zone (large values of the TLS tunnel matrix element).

**July 5**

15:00 - 16:00

Wednesday

ORAL  
SESSIONS II

Section C  
**Multiferroics**

## HIERARCHY OF INTERACTIONS IN DZYALOSHINSKII-MORIYA HELIMAGNETS AND SKYRMION LATTICE

*Grigoriev S.V.<sup>1,2</sup>*

<sup>1</sup> Petersburg Nuclear Physics Institute, NRC „Kurchatov institute“, Gatchina, Russia

<sup>2</sup> Saint-Petersburg State University, Saint Petersburg, Russia

grigoryev\_sv@pnpi.nrcki.ru

The cubic noncentrosymmetric structure of the B20 compounds produces the helical (homochiral) structure with the wave vector  $k_s = D/J$  balanced by the competition of two interactions: the ferromagnetic (FM) exchange interaction  $J = A/S$  with the spin wave stiffness  $A$  and spin  $S$  and antisymmetric Dzyaloshinskii-Moriya (DM) interaction with the constant  $D$  (Bak-Jensen model) [1]. The application of the magnetic field  $H$  transforms the helix into cone structure that is collapsed into the field induced ferromagnet at  $H_{C2}$ . This field is defined by the interaction hierarchy through  $g\mu_B H_{C2} = Ak_s^2$ . The small angle neutron scattering experiments and SQUID measurements were performed on the series of the Dzyaloshinskii-Moriya helimagnets  $Mn_{1-x}Fe_xSi$  and  $Fe_{1-x}Co_xSi$ . The experiments provided the values of helix wave vector  $k_s$ , the critical field  $H_{C2}$  and the spin value  $S$ . The direct measurements of the spin wave stiffness  $A$  have experimentally confirmed the validity of the Bak-Jensen model on the quantitative level [2-4]. Moreover, we show that Bak-Jensen model is applicable to the archetypical compound MnSi in the whole temperature range from 0 to  $T_C$ . Particularly, the DM constant for the whole set of the samples of  $Mn_{1-x}Fe_xSi$  and  $Fe_{1-x}Co_xSi$  compounds is equal to  $D \approx a_0/\mu_B$ . As soon as the spin wave stiffness  $A$  and the spin  $S$  of the system is known then the main parameters of the magnetic system, such as helix wave vector  $k_s$  and the critical field  $H_{C2}$ , can be directly estimated.

The wave vector of the Skyrmion Lattice (SkL) practically equal to that of the helix  $k_s$  showing that the SkL is built on the same hierarchy of interactions [5,6]. The SkL is realized under applied magnetic field within the narrow field corridor [ $H_{A1}$ ,  $H_{A2}$ ] and close to  $T_C$  only. It is shown that SkL is energetically favourable as compare to the conical structure close to  $H_A = 0.4 H_{C2}$ . We propose the model for the appearance and stability of the SkL. It is dipole interaction and the demagnetization field that makes the SkL more favourable as compared to the conical phase. The model is validated experimentally on the series of the helimagnetic compounds  $Mn_{1-x}Fe_xSi$  and  $Fe_{1-x}Co_xSi$ .

Thus it is experimentally confirmed that the whole (H-T) phase diagram in the helimagnets with DM interaction can be drawn on the basis of the hierarchy of interactions determining the energy landscape of the magnetic system: the FM exchange interaction, DM interaction as well as dipole interaction, important for stability of SkL.

- [1] P. Bak, M.H. Jensen, *J. Phys. C*, **13** (1980) L881.
- [2] S.V. Grigoriev et al., *Phys. Rev. B*, **92** (2015) 220415(R).
- [3] S.V. Grigoriev et al., *Phys. Rev. B*, **97** (2018) 024409.
- [4] S.V. Grigoriev et al., *Phys. Rev. B*, **100** (2019) 094409.
- [5] S. Muhlbauer et al., *Science*, **323** (2009) 915.
- [6] S.V. Grigoriev et al., *JETP Letters*, **100(3)** (2014) 238-243.

## THE IRON GARNET STRIPE DOMAIN STRUCTURE “REFRACTION” EFFECT AT THE ELECTRODE LOCATION

*Nikolaeva E.P., Podkletnova A.A., Kolyushenkov M.A., Kaminskiy A.S., Pyatakov A.P.*

Lomonosov Moscow State University, Moscow, Russia

nikolaevaep@physics.msu.ru

The surface energy of magnetic domain walls is one of the major factors determining the size and shape of magnetic domains. In magnetoelectric media its value depends not only on exchange stiffness and anisotropy like in classical theory [1], but also on the electric polarization in the medium [2] as well as its topography [3].

Recently the refraction-like behavior of domain walls on the step-like topography defect was reported [3] in magnetoelectric compound  $\text{Cr}_2\text{O}_3$  that was ascribed to the local changes in the surface energy of the domain wall.

In this report the analogous domain wall refraction effect on the stripe electrode is demonstrated (Figure 1): in contrast to the case of [3] it can be controlled by electric voltage applied to the electrode.

The required geometry of the problem, i.e. the stripe domain structure directed at various angles to the stripe electrode was realized in the orthorhombic anisotropy (210)  $(\text{BiLu})_3(\text{FeGa})_5\text{O}_{12}$  film with the electrode deposited approximately at the right angle to the stripe domain structure: the “angle of incidence” can be varied by application the in plane magnetic field. The domain wall structure was magneto-optically visualized in Faraday geometry.

The results of the measurements of incidence and refraction angles ( $\theta_1$ ,  $\theta_2$  in the inset of Figure 1) show the following features of the effect:

1) the Snell's law is confirmed in the range of angles up to 30 degrees.

2) the effective “refractive index” is the linear function of electric voltage applied to the electrode (see Figure 1 graph).

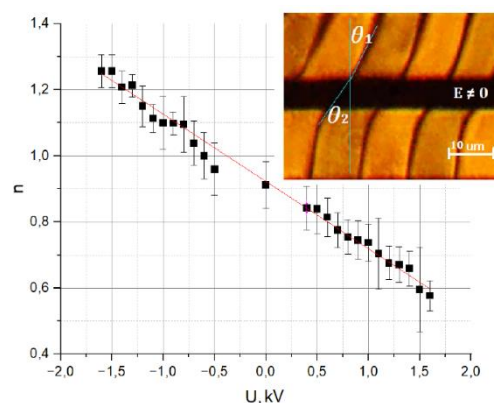


Figure 1. The effect of “domain wall refraction”: the dependence of “refraction index” on the electric voltage applied to the electrode (the example of a typical magneto-optical image is presented in the inset).

The support by Russian Science Foundation grant #23-22-00162 is acknowledged.

[1] L. D. Landau et al., *Electrodynamics of Continuous Media* (Amsterdam: Pergamon, 1984).

[2] A.P. Pyatakov et al., *Topics in Applied Physics*, **138** (2021) 129-136.

[3] N. Hedrich et al., *Nature Physics*, **17** (2021) 574–577

## MAGNETOELECTRIC EFFECT IN A COMPOSITE STRUCTURE PVDF-MAGNETOSTRICTIVE FIBER COMPOSITE BASED ON AMOPRHOUS MICROWIRES

*Savelev D.V., Fetisov L.Y., Musatov V.I., Fetisov Y.K.*

MIREA – Russian Technological University, Moscow, Russia  
dimsav94@gmail.com

Magnetolectric (ME) effect in multiferroic materials manifests itself as a change of polarization in external magnetic field. The highest values of ME coefficients were observed in flexible composite structures consisting of mechanically coupled piezoelectric (PE) and ferromagnet (FM) layers [1]. One of the promising materials for FM layers of such structures is a magnetostrictive fiber composite (MFC). MFC represents as a set of parallel magnetostrictive fibers placed close to each other in a polymer matrix [2]. In this work, ME effect in a flexible composite structure comprising layers of piezopolymer PVDF and MFC based on amorphous magnetic alloy microwires was studied.

PVDF layer had in-plane dimensions  $25 \text{ mm} \times 13 \text{ mm}$  and thickness of  $100 \text{ }\mu\text{m}$ . MFC consisted of wires of an amorphous magnetic alloy FeCoSiB (ELIRI®, Moldova) covered with glass. Total diameter of wires was  $71 \text{ }\mu\text{m}$ . MFC had in-plane dimensions  $20 \text{ mm} \times 13 \text{ mm}$ . The composite structure (see the inset in Figure 1) was rigidly fixed at one end and placed in a permanent magnetic field  $H$  up to 100 Oe directed along the fiber axis, created by Helmholtz coils. The second pair of coils created an alternating magnetic field  $h\cos(2\pi ft)$  parallel to the permanent one with an amplitude  $h$  up to 3 Oe in the frequency range 0.1-100 kHz. The dependences of the ME voltage on the permanent field  $H$  and amplitude and frequency of excitation field were measured.

Figure 1 shows the dependence of the ME voltage on the permanent field measured at the resonance frequency  $f = 2.2 \text{ kHz}$ . The highest ME coefficient  $\alpha_E \approx 23 \text{ V}/(\text{Oe cm})$  was observed in the field  $H_m \approx 18.2 \text{ Oe}$ , corresponding to the maximum value of the piezomagnetic modulus. In the field region up to 6 Oe, a slow increase in the ME voltage was observed. Such a dependence was also observed for the piezomagnetic modulus of the MFC. The obtained values of the ME coefficients exceed those for similar structures in which the layer of an amorphous Metglas alloy or MFC based on nickel was used as the FM layer [2, 3]. Nonlinear ME effect of the second harmonic generation was also observed.

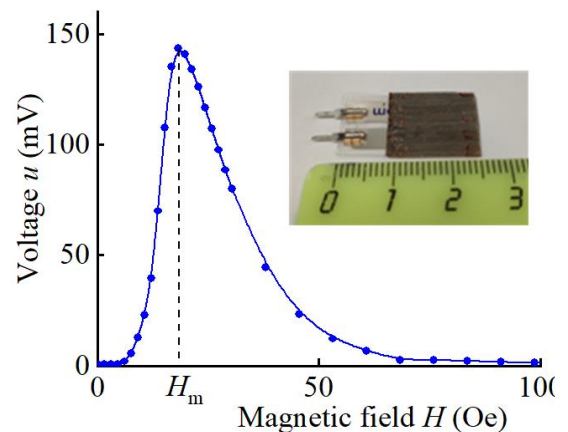


Figure 1. ME voltage vs magnetic field dependence for PVDF-MFC structure.

The work was supported by Ministry of Science and High Education of Russian Federation (State task for the University #FSFZ-2023-005).

[1] X. Liang et al., *IEEE. Trans. Mag.*, **57**(8) (2021) 400157.

[2] L. Fetisov et al., *APL*, **119**(25) (2021) 252904.

[3] L. Fetisov et al., *JMMM*, **441** (2017) 628-634.

# Author Index

Abduganiev Y.A. ....	209, 312	Ashirov U.A.....	316
Abdulkadirova N.Z. ....	176	Askarov S.....	99, 120
Abduvaitov A.A. ....	205	Attanasio C. ....	140
Abe S.....	284	Avdeev M.V.....	189
Absanov A.....	230	Avdeev P.Yu.....	46, 49, 220, 221
Abuova A. ....	35	Averkiev N.S. ....	39, 42, 43, 144, 210
Ahrorova S. ....	293	Averyanov D.V.....	154
Akhmedzhanov F.H. ....	216, 217	Babachanakh A. ....	160
Akhmetova A.A. ....	123	Badelin A.G. ....	203, 206
Akhtamov J.Sh. ....	202, 212	Baigutlin D.R.....	30
Alam J. ....	15	Baisheva A.Kh.....	300
Albino M.....	95	Bakaev G.S. ....	314
Alekhina Yu.A. ....	25, 260, 305	Bakhtiarov A.V.....	261
Aleksandrov I.A. ....	86	Balabanov V. ....	160
Alekseeva O.A. ....	195	Balaev D.A.....	121
Aleroev A.-R.A.....	184	Bălășoiu M.....	254
Alexandrov A. ....	142	Baraban I.A.....	307
Ali N.....	185	Baranov N.V. ....	16, 73, 84, 124, 268
Aliev A.M. ....	32, 176, 177	Barsukov I.....	271
Alisultanov Z.Z. ....	177	Baryshev A.V.....	150
Altynbaev E.V.....	54	Bataev D.S. ....	182
Ambarov A.V.....	26	Batdalov A.B. ....	32
Amelchenko M.D.....	223	Batulin R.G. ....	102, 105, 109, 172, 265, 281
Amelichev V.A. ....	285	Baulin R.A. ....	98
Amirov A.A. ....	74, 183	Bazrov M.A. ....	45
Amonov B.....	226	Beginin E.N. ....	50
Andreev G.Yu. ....	281, 284	Belotelov V.I.....	131, 149, 163, 170, 171
Andreev N.V.....	272, 305	Belskaya N.A. ....	208
Andreev S.V.....	72, 274	Belyaev V.K.....	95, 103, 152, 153, 252
Andreeva M.A.....	98	Belzig W. ....	292
Andryushchenko T.A. ....	173	Berzhansky V.N.....	83, 170, 171
Angelopoulos S. ....	276	Bessonov V.D. ....	244
Anikin A.A. ....	95, 252	Bezvikonny N. ....	46
Antipova V.....	25	Bezymiannykh D.G. ....	290
Antonets I.V. ....	224	Blanco J. M. ....	14, 306
Antonov G.I. ....	47	Bobkov A.M. ....	187, 191, 291, 292
Antonov V.A.....	45	Bobkov G.A.....	187, 291
Ari-Gur P.....	31	Bobkova I.V.....	159, 187, 191, 291, 292
Aronzon B.A. ....	63	Bobonov D.....	317
Arslanov A. ....	213	Bobrovskii S.Y.....	71
Artemov V.V.....	195	Bogach A.V. ....	35, 82
Artemova A.V.....	69	Bogomolova A.V.....	204
Arutyunov K.Yu.....	290	Boltaev Kh.Kh. ....	205
Arzikulov E.U. ....	316	Bondarev I.A.....	145

Borovkova O. ....	163	Doroshenko R.A. ....	299
Bostrem I.G. ....	64, 100, 117	Drokina T.V. ....	211
Buchelnikov V.D. ....	30, 33, 178	Du C. H. ....	298
Bugaev A.S. ....	136	Du K. ....	298
Bunkov Yu.M. ....	131	Du L. ....	245
Burdin D. ....	193	Dubenko I. ....	185
Buryakov A.M. ....	46, 49, 220, 221	Duncan J. ....	185
Buznikov N. ....	106	Dzhumanov S. ....	161, 190
Bychkov I.V. ....	36, 101, 136, 168	Dzhun I.O. ....	12
Campo J. ....	11, 132	Edel'man V.S. ....	283
Caprara S. ....	157	Ekomasov E.G. ....	47, 100, 101, 117
Casals B. ....	140	Ekonomov N. ....	193
Castro G. ....	247	Elboeva M.I. ....	216
Chashin D. ....	193, 194	Elfimova E.A. ....	26, 91, 92, 93, 257
Chatterjee R. ....	35	Erager K.R. ....	178
Chechenin N.G. ....	12	Eremin E.V. ....	200, 208
Chen C. T. ....	298	Eremin M.V. ....	172
Chen Y.-J. ....	247	Eremina R.M. ....	102, 109, 110, 265
Cheong S.-W. ....	269, 298	Ermolaeva O.L. ....	288
Cherkasskii M. ....	271	Ernst A. ....	19, 247
Chernoglazov K.Y. ....	144	Ershov P. ....	25
Chernov A.I. ....	20, 171	Eshkulov A.A. ....	227, 232
Chernov I.E. ....	167	Estemirova S.Kh. ....	203, 206
Chernyshov A. ....	119	Evseev A.A. ....	250
Cherosov M.A. ....	102, 172, 265, 284	Farle M. ....	271
Chichkov M.V. ....	180	Fedina A.D. ....	66
Chilom C.G. ....	254	Fedulov F. ....	194
Chirkova A.M. ....	34	Fedyanin A.A. ....	153
Chmelenin D.N. ....	195	Felici R. ....	247
Chourasia S. ....	291	Feshchenko A.A. ....	107
Chu Y. Y. ....	298	Fetisov L.Yu. ....	193, 194, 327
Chupakhina T.I. ....	105, 265	Fetisov Yu.K. ....	193, 194, 327
Cirillo C. ....	140	Feyer V. ....	247
Corte-Leon P. ....	14, 306	Ficai D. ....	254
Creanga D. ....	254	Figueiredo Neto A.M. ....	22
Damatopoulou T. ....	276	Filimonov D.F. ....	71
Danilova E.A. ....	228	Filippov M.A. ....	123
Davydov A.B. ....	63	Filippova V.V. ....	47
Deeva Yu.A. ....	105, 265	Fominov Ya.V. ....	158
Demidov V.V. ....	60	Foshin V.A. ....	286
Demin G.D. ....	66, 67	Fraerman A.A. ....	143
Demin V.A. ....	144	Frolov D.S. ....	42
Derzhavin I.M. ....	206	Frolov K.V. ....	195
Devyaterikov D.I. ....	104	Fujimori A. ....	298
Diep H.T. ....	300	Gabrielyan D.A. ....	48, 51
Djabbarov I. ....	207	Gaibov A.G. ....	227
Djuzhev N.A. ....	66, 67	Gamzatov A.G. ....	32, 176, 177
Dobroserdova A.B. ....	86	Gan'shina E.A. ....	98, 144, 169, 174, 286
Dolmatov A.V. ....	275	García-Santiago A. ....	140
Doludenko I.M. ....	121	Gareev R.R. ....	146

Gareeva Z.V. ....	299	Hämäläinen S.J. ....	146
Garif'yanov N.N. ....	158, 188	Iafarova A.F. ....	281, 283
Garifullin I.A. ....	158, 188	Ianovskaia A.S. ....	191
Garshin V.V. ....	174	Ibragimova B. ....	99
Gaviko V.S. ....	308	Ibragimova E.M. ....	287, 293
Gazizulina A.S. ....	313	Ignatov A.A. ....	87
Geck J. ....	247	Ignatyeva D.O. ....	170, 171
Geidorf M. ....	267	Ilina T.S. ....	34
Gerasimov E.G. ....	127	Imamnazarov D.Kh. ....	80, 179, 315
Gerevenkov P.I. ....	244	Inerbaev T.M. ....	35
Gilmutdinov I.F. ....	284	Ipatov M. ....	14, 306
Gladyshev I.V. ....	169, 174	Isaev D.A. ....	260
Glazkov V.N. ....	281	Isaev M.Sh. ....	232
Gokhfeld Yu.S. ....	208	Isamov S.B. ....	209, 312
Golovnia O.A. ....	274	Islamov B.Kh. ....	233, 234
Golubov A.A. ....	159, 187, 291	Ivankov A. ....	254
González C. ....	140	Ivanov A.O. ....	93, 257
Gonzalez-Legarreta L. ....	306	Ivanov A.S. ....	24
Gorbatova A.V. ....	49, 220, 221	Ivanov P.A. ....	222
Gordeeva V.M. ....	187, 291	Jagga D. ....	196
Gorlach M.A. ....	50	Jeng H. T. ....	298
Gorshenkov M.V. ....	82, 272	Jeon Y.S. ....	111, 113
Goto T. ....	151	Jeong E. ....	111, 113
Govorkova T.E. ....	308	Jin X. ....	10
Grabar V.A. ....	39	Johnsen Kamra L. ....	291
Grachev A.A. ....	50	Jovanović S. ....	252
Granovsky A.B. ....	144, 169, 174, 185, 286	Jumabaev A. ....	230
Gridneva G.T. ....	199	Jurayev Y.T. ....	231
Grigoriev S.V. ....	54, 325	Kadirbardeev A.T. ....	176
Grilli M. ....	157	Kadirov Sh.A. ....	231
Grishin S.V. ....	204, 223	Kalashnikova A.M. ....	8, 146, 167, 244
Gritsenko Ch.A. ....	103, 152	Kalinin Yu.E. ....	286
Grunin A.A. ....	153	Kalish A. ....	163
Gudim I.A. ....	195, 200, 208	Kaluzhnaya D.A. ....	27
Gudkov V.V. ....	210	Kalyabin D.V. ....	48, 51, 60, 61, 285
Gulenko A.S. ....	40	Kamantsev A.P. ....	36, 160
Gusev N.A. ....	170	Kamashev A.A. ....	158, 188
Gusev N.S. ....	143, 288	Kaminskaya T.P. ....	77
Gusev S.A. ....	288	Kaminskiy A.S. ....	249, 326
Guskov A.A. ....	164	Kamra A. ....	291, 292
Han X.F. ....	130, 238	Kamzin A.S. ....	108
Harin E.V. ....	309	Kantorovich S.S. ....	86, 88, 89, 94, 259
Heinemann A. ....	54	Karabassov T. ....	159
Helbig S. ....	259	Karashtin E.A. ....	143
Hernández J.M. ....	140	Karateev I.A. ....	154
Holikulov U. ....	230	Karpasyuk V.K. ....	203, 206
Hristoforou E. ....	276	Karpenkov A.Yu. ....	304
Huang D. J. ....	298	Karpenkov D.Yu. ....	82, 273
Huang H. Y. ....	298	Karpukhin D.A. ....	36, 160
Hushvaktov H. ....	230	Karshiboyev Sh.E. ....	231

Kataev V. ....	158	Kostyuchenko N.V. ....	303
Kats V.N. ....	154	Kotov L.N. ....	224
Kaul A.R. ....	285	Kozhevnikova P.Y. ....	77
Kazak N.V. ....	208	Kozlov A.G. ....	52, 56, 113, 115
Kazenwadel D.L. ....	146	Kozlov G.G. ....	166
Khaidarov X.S. ....	231	Kozlov V.O. ....	166
Khairullaev B.A. ....	212	Kramarenko E.Yu. ....	258
Khamraev N.S. ....	179	Kravtsov E.A. ....	107
Kharlamova A.M. ....	77	Krichevsky D.M. ....	170, 171
Khasanov Kh.B. ....	202, 212	Krinitcina T.P. ....	104
Khasanov M.A. ....	231	Kudasov Yu.B. ....	303
Khashirova S. ....	74	Kudyukov E.V. ....	107
Khaydarov A.A. ....	228	Kugel K.I. ....	38, 63
Khokhlov N.E. ....	244	Kuklin A. ....	254
Khomitov Sh.A. ....	179, 314	Kulesh N.A. ....	34
Khomskii D.I. ....	38	Kulevoy T.V. ....	70
Khovaylo V.V. ....	35, 82	Kulikova D.P. ....	150
Khudaigulova E.F. ....	165	Kulmatova G. ....	207
Khudayberdiev Z.S. ....	161	Kumar A. ....	295
Kichin G.A. ....	55, 147	Kurbaniyazov A.S. ....	229
Kiiamov A.G. ....	172, 284	Kurbaniyazov S.Kh. ....	229
Kilmetova I.V. ....	70	Kurbanov B.I. ....	228
Kim G.W. ....	113	Kurbanov J.O. ....	217
Kim Y.K. ....	111, 113	Kurbanov U.T. ....	161, 293
Kimura A. ....	310	Kurlyandskaya G.V. ....	77, 78, 106
Kirgizov S.E. ....	315	Kushchev S.B. ....	286
Kirilenko D.A. ....	146	Kushiev G.A. ....	209, 312
Kiselev D.A. ....	34	Kuvandikov O.K. ...	58, 81, 179, 202, 212, 226, 287, 314, 315
Kizirgulov I.R. ....	300	Kuzikova A.V. ....	167
Klimov A. ....	51	Kuzmichev A.N. ....	131
Knyazev G.A. ....	131	Kuzmin D.A. ....	36, 101, 136, 168
Knyazev Yu.V. ....	208	Kuznetsov A.A. ....	88, 259
Ko M.J. ....	113	Kuznetsov A.S. ....	36, 180, 181
Kokurin I.A. ....	43	Kuznetsova M.A. ....	52
Koledov V.V. ....	31, 36, 160, 180	Kvashnin D.G. ....	269
Kolesnikov E.A. ....	82	Lagarkov A.N. ....	69, 71
Kolesnikova V.G. ....	25, 74, 103, 260, 305, 307	Laliena V. ....	11, 132
Kolesov K.A. ....	36, 180, 181	Larrañaga A. ....	77
Kolosvetov A. ....	171	Lebedeva E.D. ....	49, 220, 221
Kolyushenkov M.A. ....	326	Leiko G.A. ....	118
Komanicky V. ....	152	Lepalovskij V.N. ....	106, 107
Komarov I.V. ....	69	Letushev M.E. ....	45
Komarova V.A. ....	84	Levada K.V. ....	25, 95, 252
Komlev A.S. ....	34, 273	Levchenko S.V. ....	105
Komleva E. ....	267	Lifshits M.B. ....	39
Komogortsev S.V. ....	121	Likerov R.F. ....	110
Korableva S.L. ....	281, 283, 284	Lim S. ....	269
Koshkid'ko Yu.S. ....	36, 185	Litvinova L.S. ....	252
Koskov M.A. ....	24	Lobanov D.A. ....	261
Kostishin V.G. ....	15, 275		

Lobanov N.D.	218	Mironov V.L.	288
Lobkova M.D.	53	Mirzaev S.Z.	216
Logunov M.V.	60	Mishina E.D.	46, 49, 164, 220, 221
Lorenzana J.	157	Mitetelo N.V.	164
Lryukhin V.	160	Mitrofanov T.	103
Lukshina V.A.	78	Mohseni K.	247
Lukyanchuk I.	301	Molokeev M.S.	208
Lukyanenko A.V.	145	Mondal R.	271
Luzanov V.A.	285	Morchenko A.T.	15
Lyaschenko S.A.	114, 173	Morosov A.I.	323
Maccari I.	157	Morozov I.	267
Macià F.	140	Morozov O.A.	281, 283, 284
Madiligama A.	31	Morozova M.M.	218, 219
Maekawa S.	126	Moshkina E.M.	102, 119
Maiti T.	265	Moskalev M.E.	107
Makagonov V.A.	286	Mostarac D.	259
Makar R.A.	34, 260, 273	Motorzhina A.V.	95, 252
Makarova L.A.	25, 260	Mou C. Y.	298
Makharov N.M.	217	Mozgovykh S.N.	84
Maklakov S.A.	71	Mukhtarov A.P.	122
Maklakov S.S.	69, 71, 275	Münzenberg M.	146
Maltseva V.	72	Murtazin A.A.	35
Maltseva V.E.	79, 274	Murzin D.V.	74, 103, 152, 153
Mamin R.F.	188	Musabirov I.I.	181
Mantsevich V.N.	42	Musatov V.I.	194, 327
Markeev A.M.	219	Mushnikov N.V.	127
Markelova M.N.	285	Musikhin A.Yu.	255, 257
Martin N.	54	Musov I.	74
Martyshkin A.A.	307	Musov Kh.	74
Mashirov A.V.	36, 83, 180, 181	Mussaeva M.A.	293
Maslova N.S.	42	Naboko A.S.	71
Matsumoto K.	284	Naletova V.A.	28, 90
Matveev A.A.	60, 65	Namsaraev Zh.Zh.	45, 111
Matveev O.V.	218, 219	Nasirov A.A.	213, 313
Matyunina M.V.	33	Nasyrova M.I.	172
Mavlonov A.	120	Naumova L.I.	104
Mavlonov G.H.	312	Nebesniy A.	213
Mavlyanov A.	99, 120	Nedopekin O.V.	250
Maximov F.M.	167	Nematov O.S.	312, 317
Maximova O.A.	114, 173	Nemirovich M.	15
Mayinova U.K.	190	Nikitin S.I.	108, 172
Mazitova D.I.	105	Nikitov S.A.	48, 51, 60, 61, 65, 129, 219, 285
Mekhiya A.B.	63	Nikolaev A.V.	41
Melnikov G.Yu.	78, 106	Nikolaev S.N.	144
Melnikov N.B.	40	Nikolaeva E.P.	326
Merkulov D.I.	206	Nizyamova A.R.	198
Meyerheim H.L.	247	Norjigitov A.	231
Mikhashenok N.V.	200	Norkulov A.	230
Milyaev M.A.	104	Nosova N.M.	73, 124, 268
Mirkamilova M.S.	234	Novak E.	94

Novikau I.S. ....	89	Piyanzina I.I. ....	250
Novikov M.S. ....	293	Podkletnova A.A. ....	326
Nurimov A.D. ....	316	Pokholok K.V. ....	71
Nuzhina D.S. ....	284	Politova G.A. ....	184
Ofitserova N. Yu. ....	210	Polozov V.I. ....	71
Ogloblichev V.V. ....	124	Polulyakh S.N. ....	83, 170
Ognev A.V. ....	45, 111, 113, 115, 118	Polyakov A. ....	247
Ognev N.A. ....	118	Popov D.V. ....	102, 109, 110, 265
Ogrin F. Yu. ....	223	Popov Z.I. ....	269
Okamoto J. ....	298	Preobrazhensky V. ....	46, 193
Okulov V.I. ....	308	Prilepskii I.V. ....	170
Oli A. ....	185	Pripechenkov I.M. ....	98, 169, 174
Omelyanchik A.S. ....	25, 74, 112, 272	Prisyazhnyuk A.V. ....	170
Orelovich O. ....	254	Proglyado V.V. ....	104
Orlova A.N. ....	288	Prokunin A.V. ....	36
Orshulevich M.A. ....	182	Proshin Yu.N. ....	189, 319
Osinskaya N.S. ....	228	Prudkoglyad V.A. ....	63
Osipov A.V. ....	69, 71	Pshenichnikov S.E. ....	95, 252
Otrokov M.M. ....	18	Pugach N.G. ....	156, 290
Ovchenkov E. ....	267	Pyanzina E. ....	94
Ovchinnikov A.S. ....	64, 100, 117, 268	Pyatakov A.P. ....	164, 249, 326
Ovchinnikov S.G. ....	114, 173, 208	Radushnov D.I. ....	91
Oveshnikov L.N. ....	63	Rakhmanov A.L. ....	266
Ovsianikov A.K. ....	197	Rautskii M.V. ....	145
Pakhomov A.S. ....	20	Razhabov R.M. ....	179, 314, 315
Pamyatnykh E.A. ....	308	Reser B.I. ....	40
Pan Sh. ....	269	Ritschel T. ....	247
Panina L.V. ....	15, 95, 121, 252, 305	Rodionov V.V. ....	25, 305
Pankratov N. Yu. ....	184, 304	Rodionov Ya.I. ....	63
Parchinskiy P.B. ....	313	Rodionova V.V. 25, 74, 87, 95, 103, 112, 152, 153, 252, 260, 272, 305, 307	
Parfenov O.E. ....	154	Rogachev A. ....	254
Parkin S.S.P. ....	7, 247	Rogachev K.A. ....	111
Pashen'kin I. Yu. ....	49, 143, 220, 221	Romanenko D.V. ....	204
Pasynkova A.A. ....	78	Romanova I.V. ....	281, 283, 284
Patsaev T.D. ....	144	Rosenberg M. ....	259
Pavlov V.V. ....	135, 154	Rovirola M. ....	140
Pavlova A. Y. ....	104	Rozanov K.N. ....	69, 71, 222, 275
Pavlovskii M. ....	119	Rozhansky I.V. ....	42
Pchelkina Z.V. ....	322	Rozhkov A.V. ....	266
Peddis D. ....	264	Rubio-Zuazo J. ....	247
Pelevina D.A. ....	28, 90	Rusalina A.S. ....	104
Perov N.S. ....	34, 75, 260, 305	Rusanov M.S. ....	92
Perova N.N. ....	286	Ryapolov P.A. ....	27
Pertsev N.A. ....	146	Rylkov V.V. ....	144
Petrov A.O. ....	36	Ryzhikov I.A. ....	71
Petrov A.V. ....	108, 172	Ryzhov I.I. ....	166
Petrov D.A. ....	69, 222, 275	Sabirov L.M. ....	231
Petrov P.E. ....	131	Sachdev S. ....	295
Pisarev R.V. ....	167	Sadovnikov A.V. ....	50, 307
Piskunov Yu.V. ....	124		

Sadykov A.S.....	124	Shitov S.V.....	321
Safin A.R.....	48, 51, 57, 60, 61, 65, 285	Shiu H. W. ....	298
Salakhitdinov F.A. ....	316	Shoabdurakhimova M.M. ....	317
Salakhitdinova M.K. ....	207, 287, 315	Shodiev A.A.....	293
Saliyeva Sh.....	99, 120	Shodiev Z.M. ....	202, 212
Salnikov V.D.....	112	Shukurova D. ....	120
Samardak A.S.....	45, 111, 113, 115, 118	Shulga N.V.....	299
Samardak A.Yu.....	111, 113, 118	Shvanskaya L.....	267
Sangregorio C. ....	95, 279	Sidorenko A. ....	139
Sapozhnikov M.V. ....	49, 143, 220, 221	Sidorova E.V.....	195
Sarychev M.N. ....	210	Sigov A.S.....	323
Savelev D.V. ....	194, 327	Simdyanova M.A. ....	169, 174
Savochkin I.V.....	131	Singh A. ....	298
Sboychakov A.O. ....	266	Sinityn VI.E.....	64, 100, 117
Scherbakov A.V. ....	146	Siraev F.M. ....	189
Sedov E.A. ....	290	Sitnikov A.V.....	98, 144, 286
Seleznev D.V. ....	156	Sizov V.E.....	60
Seleznev M.S. ....	34	Skachkov V.S.....	70
Selezneva N.V.....	16, 73, 84, 124, 268, 274	Skanchenko D.O. ....	54
Selivanov Yu.G.....	63	Skidanov V.A.....	169
Semakin A.S.....	284	Skirdkov P.N.....	20, 53, 55, 147
Semenov S.V.....	121	Smirnov A.I. ....	283
Semisalova A.S. ....	271	Smirnova E.S. ....	195
Seredina M.A. ....	35, 82	Sobirov M.I.....	111, 118
Sergeeva O.S.....	70	Sobolev K.V.....	25, 272, 307
Sgibnev E.M.....	150	Socolovsky L.M.....	248
Shafikova A.E.....	110	Sofronova S.....	119
Shaikhulov T.A. ....	60, 61, 285	Sogomonyan K.L.....	28
Shalygina E.E.....	77	Sokolov E.A.....	27
Shapaeva T.B. ....	165	Sokolovskiy V.V.....	30, 33, 178
Shaposhnikov A. ....	171	Sokolsky S.A. ....	93
Shapovalov V.A. ....	211	Soldatov T.A.....	283
Shapovalov V.V.....	211	Solonetsky R.V. ....	123, 198
Sharafova T.S.....	316	Solovyova A.Yu.....	91, 93, 257
Sharafullin I.F. ....	300	Somov S.A.....	24
Sharipov B.....	99, 120	Sorokin S.A.....	292
Sharova O.A.....	28, 90	Sorokin T.A. ....	195
Shatilov V.S. ....	115	Sosin S.S. ....	281, 283
Shavrov V.G....	31, 36, 83, 101, 136, 160, 180, 181	Stadler S. ....	185
Sheftel E.N. ....	309	Stebliy M.E. ....	45
Shel'deshova E.V. ....	27	Stepanov G.V.....	261
Shelaev A.V. ....	150	Stepanov M.A. ....	164
Shelukhin L.A. ....	146, 154, 167	Stolbov O.V. ....	87
Sherokalova E.M.....	16, 84, 124, 268	Stolyar S.....	254
Sherstyuk D.P.....	75	Storchak V.G. ....	154
Shevtsov D.V. ....	114, 173	Storozhenko P.A. ....	261
Shilov N.R.....	272	Streltsov S.V. ....	38, 267, 269
Shipkova E.D. ....	75	Strugatsky M.B. ....	48
Shiryaev A.O.....	69, 275	Subbotin I.M. ....	257
		Subkhankulov I. ....	179, 314

Suess D.....	259	Tyutyunnikov S.I. ....	293
Sukhanova E.V.....	269	Ubukata K.....	284
Suleimanov O.A.....	81	Umirzakov B.E. ....	205
Sun Sh. ....	253	Umkhaeva Z.S. ....	304
Surdin O.M.....	303	Urakova F.E. ....	209
Surikov V.T.....	308	Urzhumtsev A.N. ....	72, 79
Suslov D.A. ....	36, 83	Usachev P.A.....	154
Svalov A.V.....	106	Usanov R.M.....	316
Svec P.....	276	Usanov Sh.....	81
Tagirov L.R.....	108	Usarov U.T.....	58, 81
Tagirov M.S. ....	284	Useinov A. ....	196
Talapatra S. ....	185	Useinov A.N. ....	59, 297
Taldenkov A.N.....	144, 154	Useinov N.Kh. ....	59
Tananaev P.N.....	150	Ushakov A.V. ....	269
Tarasenko S.A.....	242	Usik M.O. ....	136, 168
Tarasov A.S.....	145	Usmanov O.V. ....	197
Tarasov E.V. ....	56	Usmanova G.Sh. ....	309
Tashmukhamedova D.A.....	205	Uspenskaya L.S. ....	294
Taskaev S.V. ....	36, 82, 83, 182	Ustinov A.....	138
Tatarskiy D.A.....	288	Ustinov V.V.....	104, 237
Tayurskii D.A.....	250	Utarbekova M.V. ....	36, 182
Tedzhetov V.A. ....	309	Vahabov Q.I.....	227
Teh S. ....	298	Vakhitov R.M. ....	123, 198, 199
Telegin A.V.....	244	Vakhobov K.I.....	233, 234
Temiryazeva M.P.....	60, 61, 285	Validov A.A.....	158, 188
Temnikov F.....	38	Valkov V.I. ....	211
Temnov V.V.....	134, 136	van Dijken S.....	146
Teplov V.S. ....	244	Varnakov S.N.....	114, 145, 173
Terentyev Yu.....	160	Vas'kovskiy V.O. ....	107
Tereshchenko A.A. ....	64	Vasenko A.S. ....	159
Tereshina I.S. ....	184, 303, 304	Vashchenkova A.R. ....	34
Tian H. ....	245	Vasilchikova T.....	267
Tiercelin N. ....	46, 51	Vasilev A.L.....	144
Timofeeva A.V.....	78	Vasiliev A.N. ....	267
Titova V.R.....	200	Vaulin A.A.....	308
Tkachenko I.A.....	56	Vázquez M.....	278, 307
Tlegenov R.....	60	Vedyayev A. ....	142
Tokmachev A.M. ....	154	Velikanov D.A.....	119, 208
Tretiakov O.A. ....	241	Venditti G. ....	157
Tripathi V.....	295	Vetoshko P.M. ....	131
Trushin A.S.....	147	Vetoshko V.V. ....	83
Tsvyashenko A.....	54	Vinnik D.A.....	75
Tsyrulnikova L.A. ....	57	Vinogradova A.S. ....	28
Tumanov V.A.....	319	Vivchar V.I. ....	262
Turchenko V. ....	254	Volegov A.S.....	34, 72, 73, 79, 84, 274
Turkin Ya.V. ....	156	Volkov D.A.....	48, 51, 60
Turkov V.A. ....	90	Volkov N.V.....	145
Turniyazov R.K.....	229	Volkova O.....	267
Turpak A.A. ....	52, 56	von Gratowski S.....	160
Tusche C. ....	247	Vorobyeva A.....	267

Vorontsov S.....	74	Zagrebin M.A.....	30, 33
Vorotynov A.M.....	211	Zaikina A. ....	267
Walowski J.....	146	Zakharov K. ....	267
Wang K. ....	269	Zapasskii V.S.....	166
Wang R.-P.....	298	Zavornitsyn R.S. ....	104
Wang S.....	245	Zayats P.A.....	124
Xu L. ....	253	Zbarsky V. ....	146
Xu X.....	298	Zenkevich A.....	214
Xudoyqulov J. ....	213	Zezyulina P.A. ....	71
Yagovtsev V.O.....	156	Zhaketov V.D.....	320
Yakovlev I.A. ....	145, 173	Zhandun V.S. ....	62
Yamamoto K.....	243	Zhang R.....	253
Yankovskii G.M.....	150	Zhang T.....	130
Yashin M.M. ....	169, 174	Zhelezniy M.V.....	273
Yasyulevich I.A. ....	237	Zhevstovskikh I.V.....	210
Yatsyk I.V. ....	105, 109, 265	Zhong J. ....	253
Yemelyanov A.V. ....	144	Zhukov A. ....	14, 306
Yerin C.V.....	262	Zhukova V. ....	14, 306
Yudanov N.A. ....	15	Zhuravlev M.Ye.....	41, 142
Yuldashev Sh.U. ....	213, 313	Zikrillaev N.F.....	209, 312, 317
Yuldasheva A.R. ....	300	Zobkalo I.A. ....	197
Yumaguzin A.R. ....	199	Zubarev A.Yu. ....	23, 255
Yurasov A.N. ....	169, 174	Zverev V.I.....	34
Yurin I.A. ....	183	Zverev V.S.....	26, 88, 92, 94
Yurlov V.V.....	20	Zvezdin A.K.....	170, 299, 303
Yusupov R.V.....	108, 172	Zvezdin K.A.....	20, 47, 53, 55, 147, 299
Zagorskiy D.L. ....	121		

Available online  
Copyright SISM-2023

ISBN 978-5-00202-320-2

